Determining the Zone of Influence for High Energy Arcing Faults Using Fire Dynamics Simulator

Draft for public comment

U.S. Nuclear Regulatory Commission
Office of Nuclear Regulatory Research
Washington, D.C. 20555-0001

Electric Power Research Institute
3420 Hillview Avenue
Palo Alto, CA 94304-1338

Disclaimer

Legally binding regulatory requirements are stated only in laws, NRC regulations, licenses, including technical specifications, or orders; not in Research Information Letters (RILs). A RIL is not regulatory guidance, although NRC's regulatory offices may consider the information in a RIL to determine whether any regulatory actions are warranted.

Determining the Zone of Influence for High Energy Arcing Faults using Fire Dynamics Simulator

Draft for Public Comment

Technical Report, April 2022
NRC Research Information Letter

U.S. Nuclear Regulatory Commission
Office of Nuclear Regulatory Research (RES)
Washington, D.C. 20555-0001

U.S. NRC-RES Project Manager
M. H. Salley

Electric Power Research Institute (EPRI)
3420 Hillview Avenue
Palo Alto, CA 94304-1338

EPRI Project Manager
M. Randelovic

All or a portion of the requirements of the EPRI Nuclear Quality Assurance Program apply to this product.

YES NO

ELECTRIC POWER RESEARCH INSTITUTE
3420 Hillview Avenue, Palo Alto, California 94304-1338 ▪ PO Box 10412, Palo Alto, California 94303-0813 ▪ USA
800.313.3774 ▪ 650.855.2121 ▪ askepri@epri.com ▪ www.epri.com

DISCLAIMER OF WARRANTIES AND LIMITATION OF LIABILITIES

THIS DOCUMENT WAS PREPARED BY THE ORGANIZATIONS NAMED BELOW AS AN ACCOUNT OF WORK SPONSORED OR COSPONSORED BY THE ELECTRIC POWER RESEARCH INSTITUTE, INC. (EPRI). NEITHER EPRI, ANY MEMBER OF EPRI, ANY COSPONSOR, THE ORGANIZATIONS BELOW, NOR ANY PERSON ACTING ON BEHALF OF ANY OF THEM:

(A) MAKES ANY WARRANTY OR REPRESENTATION WHATSOEVER, EXPRESS OR IMPLIED, (I) WITH RESPECT TO THE USE OF ANY INFORMATION, APPARATUS, METHOD, PROCESS, OR SIMILAR ITEM DISCLOSED IN THIS DOCUMENT, INCLUDING MERCHANTABILITY AND FITNESS FOR A PARTICULAR PURPOSE, OR (II) THAT SUCH USE DOES NOT INFRINGE ON OR INTERFERE WITH PRIVATELY OWNED RIGHTS, INCLUDING ANY PARTY'S INTELLECTUAL PROPERTY, OR (III) THAT THIS DOCUMENT IS SUITABLE TO ANY PARTICULAR USER'S CIRCUMSTANCE; OR

(B) ASSUMES RESPONSIBILITY FOR ANY DAMAGES OR OTHER LIABILITY WHATSOEVER (INCLUDING ANY CONSEQUENTIAL DAMAGES, EVEN IF EPRI OR ANY EPRI REPRESENTATIVE HAS BEEN ADVISED OF THE POSSIBILITY OF SUCH DAMAGES) RESULTING FROM YOUR SELECTION OR USE OF THIS DOCUMENT OR ANY INFORMATION, APPARATUS, METHOD, PROCESS, OR SIMILAR ITEM DISCLOSED IN THIS DOCUMENT.

REFERENCE HEREIN TO ANY SPECIFIC COMMERCIAL PRODUCT, PROCESS, OR SERVICE BY ITS TRADE NAME, TRADEMARK, MANUFACTURER, OR OTHERWISE, DOES NOT NECESSARILY CONSTITUTE OR IMPLY ITS ENDORSEMENT, RECOMMENDATION, OR FAVORING BY EPRI.

THE FOLLOWING ORGANIZATIONS PREPARED THIS REPORT:

Electric Power Research Institute (EPRI)

U.S. Nuclear Regulatory Commission, Office of Nuclear Regulatory Research

Fleischer Consultants, LLC

Jensen Hughes

National Institute of Standards and Technology

THE TECHNICAL CONTENTS OF THIS PRODUCT WERE **NOT** PREPARED IN ACCORDANCE WITH THE EPRI QUALITY PROGRAM MANUAL THAT FULFILLS THE REQUIREMENTS OF 10 CFR 50, APPENDIX B. THIS PRODUCT IS **NOT** SUBJECT TO THE REQUIREMENTS OF 10 CFR PART 21.

NOTE

For further information about EPRI, call the EPRI Customer Assistance Center at 800.313.3774 or e-mail askepri@epri.com.

ABSTRACT

This report documents the development of zones of influence (ZOIs) using Fire Dynamics Simulator (FDS) for equipment subject to the effects of a high energy arcing fault (HEAF). This effort consisted of three stages: the development of an approach to use the computational fluid dynamics (CFD) model FDS to predict the thermal exposure of targets in the vicinity of a HEAF, the validation of the FDS HEAF analysis, and the application of the analysis approach to a matrix of HEAFs that encompasses a broad range of HEAF events.

FDS simulations of HEAFs were performed for three classes of equipment: low-voltage switchgear, medium-voltage switchgear, and non-segregated bus ducts. Simulation variables include fault current magnitude and duration, location, electrode composition, and type of equipment. The end result of the FDS analysis is a detailed tabulation of ZOIs for each simulation in the matrix. These ZOIs will be used to develop guidance for modeling HEAF events in PRA. This PRA guidance is expected in a separate EPRI/NRC report.
The work performed as part of this effort provided a number of important findings, including differences between electrode material, range of ZOI estimate that both exceed and are bounded by existing ZOI guidance [1], effect of bus duct housing material, ZOI sensitivities to orientation. All of these findings are based on the current state-of-knowledge that has been significantly advanced though collaborative research efforts between the NRC-RES and EPRI.

Keywords
Arcing fault
Electrical explosion hazard
Fire probabilistic risk assessment
High energy arcing fault (HEAF)
Zone of influence (ZOI)

CONTENTS

LIST OF FIGURES

LIST OF TABLES

EXECUTIVE SUMMARY

PRIMARY AUDIENCE: Fire protection, electrical, and probabilistic risk assessment (PRA) engineers conducting or reviewing fire risk assessments related to high energy arcing faults (HEAFs).

SECONDARY AUDIENCE: Engineers, reviewers, utility managers, and other stakeholders who conduct, review, or manage fire protection programs and need to understand the underlying technical basis for the hazards associated with HEAFs.

KEY RESEARCH QUESTION

At what distance from an electrical enclosure or non-segregated bus duct that experiences a HEAF will targets be exposed to conditions that exceed their failure threshold criteria?

RESEARCH OVERVIEW

The U.S. Nuclear Regulatory Commission (NRC) Office of Nuclear Regulatory Research and the Electric Power Research Institute (EPRI) HEAF working group (WG) has been tasked with improving the methodology for assessing the HEAF hazards at nuclear power plants. A major part of this effort includes updating the zone of influence (ZOI) used to determine target sets assumed failed in fire PRA scenarios. Hazard modeling with Fire Dynamics Simulator (FDS) is used in conjunction with target fragility limits to determine the ZOI of failed equipment. There were three parts to this research effort:

1. The development of the geometric models, key assumptions, and input data used in FDS to predict the thermal exposure of targets in the vicinity of a HEAF.
2. The benchmarking and validation of the analysis approach using data from full-scale testing and operational experience (OE).
3. The application of the analysis approach to a matrix of HEAF simulations that encompasses a broad range of HEAF events.

FDS simulations of HEAFs were performed for three classes of equipment: low-voltage switchgear, medium-voltage switchgear, and medium-voltage non-segregated bus ducts. Simulation variables included fault current magnitude and duration, arc location, electrode composition, and type of equipment. The result of the FDS analysis is a detailed tabulation of the ZOIs predicted by FDS for each HEAF simulation. These ZOIs will be used to develop PRA guidance on the modeling of HEAF events in PRA and provided in a separate EPRI/NRC report. The resulting HEAF ZOI ranges are summarized in Table ES-1 for medium-voltage switchgear, Table ES-2 for low-voltage switchgear, and Table ES-3 for non-segregated bus ducts.

Table ES-1
Summary of medium-voltage switchgear ZOI ranges

Switchgear Enclosure Face	ZOI (m) for 15 MJ/m² Target Fragility	ZOI (m) for 30 MJ/m² Target Fragility
Back	0 – 1.13	0 – 0.76
Left	0 – 1.24	0 – 0.92
Right	0 – 1.24	0 – 0.92
Top	0 – 1.01	0 – 0.58
Front	0 – 1.31	0 – 0.97

Table ES-2
Summary of low-voltage switchgear ZOI ranges

Switchgear Enclosure Face	ZOI (m) for 15 MJ/m² Target Fragility	ZOI (m) for 30 MJ/m² Target Fragility
Back	0 – 0.17	0
Left	0	0
Right	0 – 0.9	0 – 0.59
Top	0 – 0.84	0 – 0.53
Front	0	0

Table ES-3
Summary of non-segregated bus duct ZOI ranges

Non-Segregated Bus Duct Enclosure Face	ZOI (m) for 15 MJ/m² Target Fragility	ZOI (m) for 30 MJ/m² Target Fragility
Back	0 – 1.32	0 – 0.86
Front	0 – 1.32	0 – 0.86
Right	0.41 – 1.31	0.21 – 0.84
Above	0 – 1.39	0 – 0.93
Below	0 – 1.37	0 – 0.92

KEY FINDINGS

This research resulted in a number of findings based on the current state-of-knowledge related to the HEAF hazard phenomena. These are summarized as follows:

- The difference between ZOIs from HEAFs with aluminum electrode and HEAFs with copper electrode is not significant for all equipment classes (Sections 6.1.3.3, 6.2.2.2, and 6.3.2.2).

- The dominant parameter affecting the HEAF ZOIs in medium-voltage switchgear was the total arc energy. A secondary parameter for the medium-voltage switchgear was the switchgear type (vertical-lift breaker style or horizontal draw-out style) (Section 6.1.3.3).
- The side ZOIs are lower for vertical-lift breaker style switchgear as compared to horizontal draw-out breaker style breaker switchgear. In addition, for vertical-lift breaker style switchgear in the supply configuration, there is no vertical (top) ZOI component. The load configuration vertical-lift breaker style switchgear and the horizontal draw-out style switchgear have comparable top ZOIs (Section 6.1.3.3).
- The ZOIs for low-voltage switchgear were smaller than those postulated in the existing guidance in Appendix M of NUREG/CR-6850 EPRI 1011989 EPRI/NRC-RES *Fire PRA Methodology for Nuclear Power Facilities.* The ZOIs for low-voltage switchgear HEAF simulations are documented in Table 6-2 for 15 MJ/m² and 30 MJ/m² target fragilities (Section 6.2.2.2).
- The ZOIs for medium-voltage switchgear and bus ducts were smaller than the existing guidance for some configurations and directions, but larger for others. The ZOIs for medium-voltage switchgear HEAF simulations are documented in Table 6-1 for 15 MJ/m² and 30 MJ/m² target fragilities. Similarly, the ZOIs for non-segregated bus duct HEAF simulations are documented in Table 6-3 for 15 MJ/m² and 30 MJ/m² target fragilities (Section 6.3.2.2).
- The composition of bus duct housing (steel versus aluminum) had a significant impact on the ZOIs; HEAFs in aluminum ducts had ZOIs that were, on average, about 0.15 m larger than those in steel ducts (Section 6.3.2.2).
- ZOIs for low- and medium-voltage switchgear were sensitive to equipment geometry and orientation. Bus ducts, with comparatively simply geometries, were not. (Sections 6.1.3.3, 6.2.2.2, and 6.3.2.2).

WHY THIS MATTERS

This report provides ZOI information to assist researchers, analysts, and stakeholders to evaluate the HEAF hazard and the adequacy of current approaches. The conclusions provided will support advances in the method, tools, and data to assess the HEAF hazard in nuclear facilities.

HOW TO APPLY RESULTS

Engineers and scientists advancing hazard and fire PRA methods should focus on the tabulated summaries of ZOIs in sections 6.1.3.3, 6.2.2.2, and 6.3.2.2.

LEARNING AND ENGAGEMENT OPPORTUNITIES

Users of this report may be interested in periodic stakeholder engagement opportunities with EPRI and/or NRC on this topic.

EPRI CONTACTS: Marko Randelovic, Principal Technical Leader, mrandelovic@epri.com

NRC CONTACT: Kenneth Hamburger, Fire Protection Engineer, Kenneth.Hamburger@nrc.gov

PROGRAM: Nuclear Power, P41; and Risk and Safety Management, P41.07.01

IMPLEMENTATION CATEGORY: Reference – Technical Basis

CITATIONS

This report was prepared by the following:

U.S. Nuclear Regulatory Commission
Washington, D.C. 20555-0001

Principal Investigators
K. Hamburger

Under contract to NRC:

Sandia National Laboratories
1515 Eubank SE
Albuquerque, NM 87123

Principal Investigators
C. LaFleur
A. Glover
P. Clem

National Institute of Standards and Technology
100 Bureau Dr.
Gaithersburg, MD 20899

Principal Investigator
K. McGrattan

Electric Power Research Institute
3420 Hillview Avenue
Palo Alto, CA 94304

Principal Investigators
M. Randelovic
T. Short
A. Lindeman

Under contract to EPRI:

Jensen Hughes
3610 Commerce Drive, Suite 817
Baltimore, MD 21227

Principal Investigators
J. Floyd
D. Lovelace
S. Hunt

Fleischer Consultants, LLC
Lansdale, PA 19446

Principal Investigator
K. Fleischer

This report describes research sponsored jointly by the U.S. Nuclear Regulatory Commission's (NRC's) Office of Nuclear Regulatory Research (RES) and the Electric Power Research Institute (EPRI) performed under a formal Memorandum of Understanding (MOU).

This publication is a corporate document that should be cited in the literature in the following manner:

Determining the Zone of Influence for High Energy Arcing Faults using Fire Dynamics Simulator. U.S. Nuclear Regulatory Commission, Office of Nuclear Regulatory Research (RES), Washington, DC, and Electric Power Research Institute (EPRI), Palo Alto, CA: 2022.

ACRONYMS

CFR	Code of Federal Regulations
CT	current transformer
CVT	current voltage transformer
DNS	direct numerical simulation
EDS	electrical distribution system
EPRI	Electric Power Research Institute
FCT	fault clearing time
FEDB	Fire Events Database
FDS	Fire Dynamics Simulator
GE	General Electric
HEAF	high energy arcing fault
IEEE	Institute of Electrical and Electronics Engineers
KEMA	Keiring van Ekektrotechnische Materialen te Arnhem
LES	large eddy simulation
LV	low-voltage
MOU	memorandum of understanding
MV	medium-voltage
NEA	Nuclear Energy Agency
NIST	National Institute of Standards and Technology
NPP	nuclear power plant
NRC	Nuclear Regulatory Commission
NSBD	non-segregated bus duct
OB	open box (low-voltage)
OBMV	open box (medium-voltage)
OE	operational experience
OECD	Organisation for Economic Cooperation and Development
PCCBB	primary cable compartment bus bar
PRA	probabilistic risk assessment
RES	NRC's Office of Nuclear Regulatory Research

RIL	Research Information Letter
SEM	scanning electron microscopy
SNL	Sandia National Laboratories
SWGR	switchgear
TCC	time current characteristic
TP	thermoplastic
TS	thermoset
UAT	unit auxiliary transformer
VLES	very large eddy simulation
WG	working group
ZOI	zone of influence

1
INTRODUCTION

1.1 Background

High energy arcing faults (HEAFs) are hazardous events in which an electrical arc leads to the rapid release of energy in the form of heat, vaporized metal, and mechanical force. The existing methodology for modeling switchgear and load center HEAFs in fire probabilistic risk assessment (PRA) is documented in Appendix M of NUREG/CR-6850 [1]. The methodology for HEAFs in bus ducts and iso-phase bus ducts is contained in Section 7 of NUREG/CR-6850 Supplement 1, *Fire Probabilistic Risk Assessment Methods Enhancements* [2]. Both reports provide zone of influence (ZOI) estimates based on well-documented United States nuclear power plant (NPP) operational experience (OE).

Under a memorandum of understand (MOU), the Nuclear Regulatory Commission (NRC) Office of Research (NRC-RES) and the Electric Power Research Institute (EPRI) have collaborated and formed a joint HEAF working group (WG) to advance the state of practice. The HEAF WG is chartered to update the methods, tools, and data to support realistic estimates of HEAF risk in industry fire PRAs based on experimental data, operating experience, and engineering judgment.

To develop an updated analysis approach, several intermediate steps were necessary to determine the ZOI and fire PRA guidance, including:

- Survey the U.S. nuclear fleet to determine presence of aluminum and fault clearing times. Insights from this effort are documented in EPRI 3002020692 [3].

- Perform small, medium, and full-scale physical tests. Small-scale testing characterized the morphology and oxidation states of aluminum particles (see Appendix D). Medium-scale “open box” experiments characterized the spectral emission of the arc and conductivity of the arc ejecta [4]. Full-scale experiments provided data on enclosure breach time, and pressure effects, and serve as a benchmark against the computational fluid dynamics (CFD) model Fire Dynamics Simulator (FDS) [5-9].

- Evaluate target fragility (i.e., the HEAF fragilities). This was a two-part effort that involved physical testing and analysis to determine the conditions when targets external to the HEAF are likely to be damaged [10].

- Identify and validate the CFD model FDS for simulating HEAF effects (the subject of this report). The purpose of this model is to calculate the incident energy at target locations with respect to a HEAF across a wide variety of configurations (e.g., fault duration, arc voltage, arcing fault current, equipment geometry, and electrode composition).

- PRA analysis approach development. This step combines the insights developed in preceding efforts and provides an approach that the analyst can follow to model HEAFs

in the fire PRA (forthcoming report). This task includes an evaluation of the United States nuclear power plant (NPP) operating experience, updated fire ignition frequencies and manual non-suppression probabilities, and provides the structure to model the potential outcomes of a HEAF given the ignition sources and location within the electrical distribution system (EDS).

1.2 Overview of HEAF Zones of Influence

The HEAF ZOIs provided in NUREG/CR-6850 and NUREG/CR-6850 Supplement 1 are a single ZOI for electrical enclosures, a single ZOI for non-segregated bus ducts, and a single ZOI for isophase bus ducts. These ZOIs were not based on testing and were not tied to HEAF-specific fragility criteria, but rather were estimates of the ZOI based on a review of the OE for HEAF events [11]. This set of one-size-fits all ZOIs does not account for arc duration, arc power, or the impact of arc location and enclosure configuration.

During the development of HEAF fragilities [10], a detailed review of the EPRI survey of industry fault clearing times [3], more recent HEAF events [12], and data from testing [4-9] was done. From that review, it was clear to the HEAF WG that the exposure to a target is dependent on the duration, power, and location of an arc. It was not clear, however, if the electrode composition (e.g., copper or aluminum) was a significant factor in determining target exposure.

While the various full-scale testing efforts have provided a wealth of data for generating insights, the limited number of tested configurations (geometries, initial conditions, material type) and the limited instrumentation per test (for the objective of determining a ZOI), means that CFD modeling is needed to provide ZOIs for the configurations that have not been tested but are present in the majority of the NPPs in the U.S. [3].

1.3 Objective

The objective of this report is to document a three-part effort for developing estimates of the ZOI for HEAF events. First, the report documents the development of an approach to use the CFD model Fire Dynamics Simulator (FDS) [13–17] to calculate the thermal exposure seen by targets exposed to a HEAF. Second, the report documents validation of that analysis approach. Lastly, the report documents the application of that analysis approach to a large matrix of simulations that vary HEAF duration, power, location, electrode composition, and type of equipment. The end result of the analysis approach is a detailed tabulation of ZOIs for each simulation in the matrix.

1.4 Scope

The scope of the ZOI modeling task is to develop a dataset of ZOIs that encompasses a broad range of HEAF events with representative conditions and configurations. These ZOIs are used as input to develop guidance for modeling HEAFs in the fire PRA. This guidance is expected in a forthcoming EPRI/NRC report.

2
HEAF DESCRIPTION AND FDS CAPABILITIES

The purpose of this section is to give a brief description of a HEAF event and a brief overview of FDS and its capabilities to model HEAF events. The review of the HEAF events is performed for the identification of the major phenomena and initial/boundary conditions impacting the modeling of HEAF events. The FDS overview is given to review the basic capabilities and assumptions in FDS for the development an analysis approach that can be used to model HEAFs.

2.1 HEAF Event Description

A HEAF begins with a weakness in the electrical distribution system components that results in a fault that persists until it is cleared by the removal of the power source. For the purpose of modeling the hazard created by a HEAF with FDS, the only relevant detail of the initiating event that plays an important role is the specific physical location where the HEAF occurs. The HEAF will continue until either the current feeding the HEAF is terminated by tripping overcurrent protection (breakers, fuses, etc.) or the arc self-extinguishes which can result from decay in current and/or voltage feeding the HEAF or an inability to sustain an arc given the specific geometric and material configuration present in the faulting equipment. The HEAF location and the arc power profile are not phenomena that FDS can predict.

When the arc first initiates, there is a pressure wave that results from the sudden release of energy from the arc. In OE and in testing, this pressure wave has opened enclosure access doors and opened doors to the fire compartment containing the faulting equipment. As discussed in the next section, this pressure wave cannot be modeled by FDS and is not in the scope of this report. The impacts of the pressure wave on the fire risk have been assumed by the HEAF WG as having negligeable impact on PRA targets; therefore, the lack of FDS capability to model the pressure wave is considered acceptable by the HEAF WG.

As an electromagnetic phenomenon, the electromagnetic fields present in the faulted equipment and associated bus bars may result in the arc moving from its initiating location. This is not a phenomenon that FDS can predict. The location of the arcs (replicated from the OE) in the FDS model has been selected to provide representative incident energies; therefore, the lack of FDS capability to model the relocation of the arcs is considered acceptable by the HEAF WG.

The main hazard of a HEAF event is the energy that is released by the arc, which is dominated by thermal radiation and to a lesser extent oxidation of the vaporized bus bar metal. This has two primary effects that impact the hazard for targets outside the enclosure.

First, at the location where the arc attaches to the electrodes inside the enclosure, temperatures can exceed the boiling point of the electrode metal. This will lead to electrode mass loss in the form of metal vapor and droplets of molten metal. The high temperatures that evolve inside the enclosure and resistive heating from current flow will act to further increase the electrode temperature and mass loss rates may increase over time. Prior to a HEAF event, the electrodes would be coated with a thin layer of metal oxide. The release of metal vapor and liquid metal droplets will expose unoxidized metal in a configuration with a high surface area. When exposed to oxygen, the metal will undergo exothermic oxidation reactions which will add to the energy of

HEAF event. The fraction of metal that oxidizes is a function of the droplet size and the fraction of metal that goes to vapor.

Second, within the electrical enclosure, the energy from the arc will rapidly increase the internal temperature of the enclosure. The resulting thermal expansion will result in outflow from any available vent path, including fixed vent openings present for normal heat dissipation as well as leakage through any gaps in the enclosure's external bolted covers. Over time, the high internal gas temperature and direct radiation from the arc will heat the external walls of the enclosure. If the arcing fault duration is long enough, portions of the external walls may fail due to melting and/or tearing from loss of yield strength. Once there is a breach in the enclosure walls, outflow of the arcing jet will occur through the opening. Targets near the opening may be enveloped by the high temperature outflow. Targets with a direct line of site through the opening to the arc will be directly exposed to thermal radiation from the arc.

The HEAF hazard does not terminate immediately after the arc terminates. Outflow leaving the enclosure will take time to dissipate. Additionally, the remaining enclosure surfaces near the arc location will be very hot and serve as a source of radiant heat that will continue to expose targets. Both of these will rapidly decay following the arc termination in the period immediately after an arc.

2.2 Fire Dynamics Simulator Capabilities Applicable to HEAF Events

FDS is a computational fluid dynamics (CFD) model that has been under development for approximately 30 years by a multinational team led by the National Institute of Standards and Technology (NIST) [13-17]. FDS was developed for the purpose of modeling fires in the structures. The physical sub-models within FDS and the overall solution approach taken within FDS were developed to support modeling fires within enclosures. However, FDS is a general purpose CFD model, and its use is not restricted to fires alone. FDS has undergone extensive verification and validation [15,16,18] for a wide range of fire-related applications though these applications do not include modeling the effects of HEAFs.

A CFD model numerically solves the Navier-Stokes equations. The Navier-Stokes equations are a set of coupled, partial differential equations that describe the three-dimensional mass, momentum, and energy conservation of fluids over time. Except for some simple cases, the Navier-Stokes equations do not have an analytic solution and CFD models often make some simplifying assumptions to reduce the computational expense of solving the equations. Since the Navier-Stokes equations only describe fluid motion, a CFD fire models needs other physical sub-models for combustion, radiation, surface heat transfer, and other fire-related phenomena.

2.2.1 Primary Relevant FDS Assumptions

FDS has two primary assumptions that underlie all uses of FDS. The first assumption is that the equation of state (relationship between temperature, pressure, and density) is the ideal gas law. This means that FDS cannot model the flow of fluids in the liquid state, only the gaseous state. The second is the assumption of low-speed flow. A key component of numerically solving the Navier-Stokes equations is determining the pressure field, as pressure gradients drive fluid flow. High-speed flows (i.e., flows having a Mach number over 0.3) introduce compressibility effects such as shock waves. This assumption means that FDS cannot model explosions or other events where pressure waves must be resolved as the low-speed assumption means that pressure waves are filtered out of the equations solved by FDS. Numerically modeling those effects can be computationally expensive. Although fire driven flows are normally considered low-speed flow in terms of compressibility effects, flows associated with HEAFs may have velocities that are comparable to the FDS low-speed limit. However, pressure waves (shocks)

and compressibility effects are assumed to be minor given the target exposure is dominated by thermal radiation and, to a lesser extent, the surrounding gas temperatures, which justifies the use of the low-speed flow assumption.

Another major assumption in FDS is the mode of operation. FDS can run in two primary modes: direct numerical simulation (DNS) and large eddy simulation (LES). For DNS, the grid size needs to be small enough to directly resolve turbulence and the diffusion of gas species into and out of combusting regions. This requires grid sizes of a millimeter or less and is not practical for engineering scale calculations. With LES (FDS has three selectable variants of LES depending on grid scale), larger grid cells can be used and the effects of turbulence occurring at smaller length scales are determined using a turbulence model. Although the use of the LES method may introduce uncertainty with regard to the turbulence structure and momentum transport as compared to a DNS method, this uncertainty is assumed to be minor given the target exposure is dominated by thermal radiation and, to a lesser extent, the surrounding gas temperatures.

2.2.2 Key FDS Sub-models Relevant to HEAF

FDS contains a number of sub-models necessary to enable FDS to predict fire specific behavior. Key sub-models relevant to HEAF events are discussed in the subsections that follow. A very brief description is provided to give some basic context for the Section 3 development of the analysis approach for using FDS to model HEAF events. Full details on the sub-models can be found in Volume 1 of the FDS Technical Reference Guide [14].

2.2.2.1 Combustion

FDS uses a turbulent batch reactor model to predict the energy release and production/destruction of species due to combustion. For this model, each grid cell is treated as if it were a combustion chamber where fuel and air are introduced and react. The heat release rate is determined by two factors: how quickly fuel and air can mix inside the chamber (i.e., the grid cell) and how quickly chemical reactions take place once mixing occurs.

The rate at which mixing occurs is a function of the grid size. At very small length scales where species gradients in the flame are being resolved, mixing is simply given by diffusion times. For very coarse grid cells mixing is driven by buoyant acceleration or (for extremely large cells) the need to burn fuel within a single grid cell. At intermediate scales, as expected for a HEAF within an electrical enclosure as well as the HEAF arc-jet regions, the mixing is driven by the modeled sub-grid turbulence.

Combustion reactions are complex. Something as simple as the combustion of methane to water vapor and carbon dioxide actually involves dozens of intermediate reactions and chemical species. The rate at which each of those reactions occurs is a function of temperature and the concentrations of species present. Modeling at this level of detail is only possible if the temperature and species concentrations are being resolved at flame thickness (~1 mm) length scales. For practical engineering applications, FDS considers just the single total reaction of fuel plus air producing products plus heat. As long as a reaction is taking place, temperatures should be high enough that the reaction rates are faster than the hydrodynamic timestep. Under these conditions, the assumption of fast chemistry can be used where the heat release rate is determined by how quickly fuel and air mix and consuming all of the limiting species that mixes (i.e., if there is more fuel than air, only that fuel that has enough air is allowed to burn).

FDS also contains an extinction model. This model looks at the conditions in a grid cell and determines if the mixed fuel and air is allowed to burn. For a flame to sustain itself, the flame

must produce enough heat such that, after convective and radiative losses from the flame, there is still enough heat present to keep a high reaction rate. If this is not the case, the heat losses drop the flame temperature which drops the reaction rate and quickly leads to extinction of the flame. If temperature-dependent reaction rates are being used the model is not necessary; however, with fast chemistry fuel and air will always burn unless an extinction model prevents it. For typical fuels in pre-flashover compartments, extinction will occur once oxygen levels drop below 12 to 15%.

2.2.2.2 Radiation

FDS has a sub-model for the transport of thermal radiation from a fire. The approach FDS uses is a finite volume calculation method where radiation is transported along a finite number of angular directions. In the radiation transport model, each grid cell emits and absorbs radiation where both terms are a function of the cell temperature and the gas species present in the cell. The gas-phase radiative properties used in FDS are based on a small number of fuel types: water vapor, soot, carbon dioxide, and carbon monoxide for temperatures in the approximate range of 300 to 2,500 K and for pressures near atmospheric pressure. However, the properties for carbonaceous soot can be replaced with properties of other species, including aluminum oxide. For radiating species that are not defined within FDS, one can select among existing species to be used as a surrogate.

Radiative emissions are proportional to the temperature of the emitting item to the fourth power. For hot surfaces and hot gas layers, the surface or gas temperature is appropriate to use directly. In cells with combustion, however, unless the grid is very refined, the grid cell temperature will represent some average of the temperature of the flame in the grid cell and the temperature of the remaining volume of the grid cell. To avoid underpredicting radiative emission from a fire, FDS allows the user to specify a radiant fraction and, in cells with combustion, FDS ensures that at least the radiant fraction is emitted.

2.2.2.3 Solid-Phase

Solid-phase refers to the treatment of solid surfaces, such as the walls of an electrical enclosure, within an FDS simulation. As discussed in Section 2.2.1, a key phenomenon during a HEAF event is breach of the enclosure. The breach time and the size of the resulting opening have a significant impact on heat flux seen by targets outside of the enclosure. Predicting this phenomenon requires predicting the temperature of the solid and predicting failure of the material.

In most cases, solid-phase temperatures in FDS are predicted using one-dimensional heat transfer; that is, every wall cell in an FDS model has its own heat transfer solution that treats that wall cell as a one-dimensional surface. This means that FDS is not modeling conduction between wall cells. FDS does have some three-dimensional heat transfer capabilities, but this currently only operates on the same numerical mesh as the hydrodynamic solver, which limits its application. In the case of a HEAF event, the centimeter-scale grid cells needed to cover the domain size means the three-dimensional model would not be suitable for the bus bars which have centimeter-scale cross-sections or the enclosure face which have millimeter-scale thicknesses. For a surface like a bus duct or switchgear enclosure, the one-dimensional approximation is sufficient when the area being exposed is significantly larger than the material thickness. Since the total electrode width (defines the area being exposed) is tens of centimeters, and the enclosure wall thickness is a few millimeters, the one-dimensional approximation is considered sufficient.

2.2.3 HEAF Phenomena not Present in FDS

As a fire model, FDS lacks physical sub-models for some HEAF-related phenomena:

- FDS does not model the dissociation of molecules at high temperatures or the formation of plasma. At very high temperatures, there will be some errors in the FDS temperature prediction due to unaccounted enthalpy changes associated with dissociation and ionization. The impact of this is primarily inside the enclosure in the arc volume where the highest temperatures are seen. There is likely a minor impact on target exposures since overall energy is still being conserved and since the source term for the arc used a predefined radiant fraction.
- FDS does not have equations for the electric and magnetic field. The impacts of voltage fields on ionized gas cannot be accounted for. This means that FDS cannot predict movement of the arc due to voltage fields. Movement of the arc, however, can be scripted in FDS inputs should subject matter experts assess it is important for a specific HEAF.
- An alternating current, 3-phase arc is very dynamic with the arc jumping from phase to phase as the current in each phase crosses zero. The sudden, rapid changes in local power this represents would introduce rapidly cycling and large local changes in the pressure or flow divergence. This is not compatible with the low-speed flow assumption and a fully dynamic arc cannot be specified.

3
APPROACH FOR APPLYING FDS TO DETERMINE THE HEAF ZOI

This section describes the analysis approach for applying FDS to model HEAFs for the purpose of defining the ZOI. Validation of this analysis approach is presented in Section 4 and the results of FDS simulations used by the HEAF WG to determine the ZOIs are presented in Section 6. The sections that follow detail specific categories of FDS inputs and the basis for the manner in which they were specified. The analysis approach developed in this section evolved over the period of time from December 2019 through September of 2021. The development of this approach began with initial scoping calculations to assess if there was any merit to the concept of applying FDS. This was followed by a combination of increasing the level of detail and complexity of the analysis approach along with some minor enhancements to FDS.

3.1 Simulation Time

The model simulation time is the time over which the HEAF effects are evaluated in FDS. This time needs to be long enough to capture the key target effects from the HEAF modeled. Given the computational cost of running the model, the simulation time also should not be extended excessively beyond the period over which the HEAF can affect the target. Because targets will still be exposed to convective and radiative heat flux after extinguishment of the arc, the simulation time needs to extend for a period after the fault is cleared. This time may be estimated through consideration of the rate at which the temperatures and heat fluxes decay as well as observations from test data of the total incident energy at target locations.

Figure 3-1 plots the incident energy over time for a typical plate thermometer (PTC) used in a medium-voltage (MV) switchgear (SWGR) scale test [6]. This test involved a 4 s arc, which is expected to have a longer decay stage relative to a shorter arc since there is a larger amount of energy to dissipate. The PTC shows a rapid increase in temperature during the 4 s arc due to a high incident heat flux. Within a couple of seconds of the end of the arc, the temperature rise has slowed significantly. From 8 s post arc to 12 s post arc, 2% or less additional energy deposition is recorded.

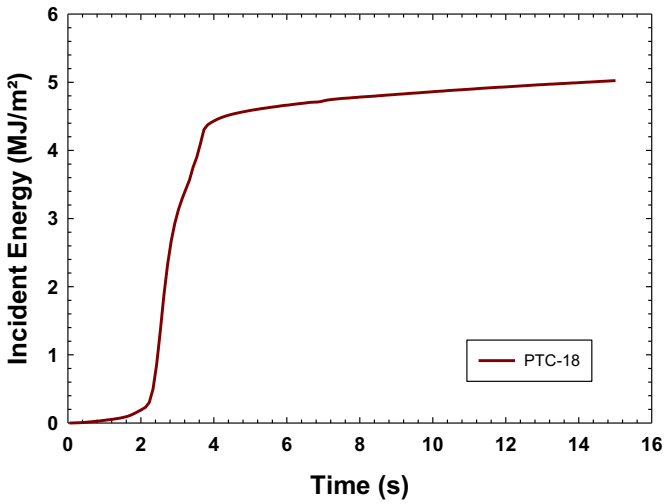

Figure 3-1
Incident energy for a typical plate thermometer (PTC-18) measured during MV SWGR Test 2-21 [6]

Figure 3-2 shows the FDS-predicted heat flux and incident energy for the plate thermometer shown in Figure 3-1. The FDS simulation for this test was run long enough to cover the period of time over which data was processed in the test report (see Section 4.2). Within a couple of seconds after the arc ends, the heat flux to the plate thermometer has dropped by at least a factor of 15 from the peak value. The flux continues to decay with the highest locations dropping over 15% from 5 s to 6 s. Extrapolating that decay rate out 8 s after the arc would add approximately 2% incident energy. For 12 s after the arc, the value would be 3% incident energy or an increase of 1% more. This is in line with the measured data shown in Figure 3-2.

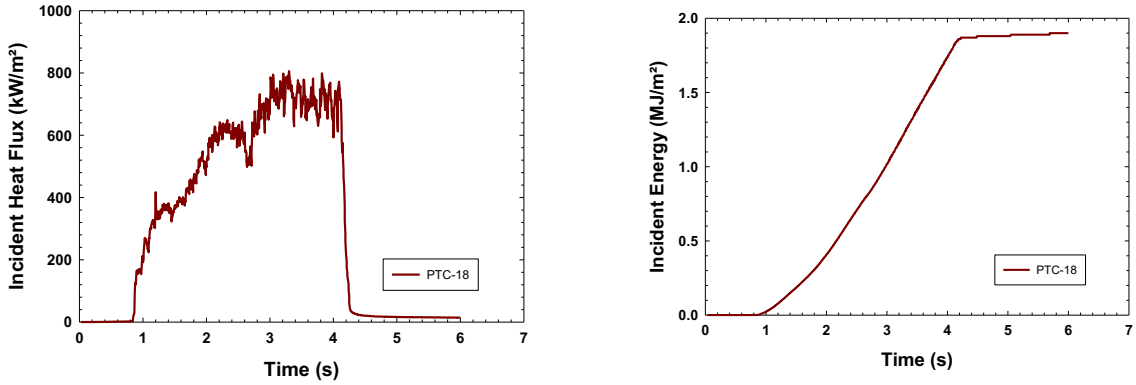

Figure 3-2
FDS-predicted heat flux at PTC-18 for MV SWGR Test 2-21 [6]

Both the data and the FDS validation show that by 8 s following the end of the arc that a target in a high flux zone (where one could reach the fragility criteria) will accumulate little additional incident energy. Based upon these observations, FDS simulations were run the fault duration plus 8 s.

3.2 Gas properties

FDS requires a number of gas-phase thermophysical properties. These consist of the molecular weight, specific heat, viscosity, and diffusivity. Given the computational grids selected (Section 3.4), the default very large eddy simulation (VLES) mode of operation for FDS was used. As a large eddy simulation (LES) approach, a turbulence model is employed which means that the molecular viscosity and diffusivity (i.e., the values one finds tabulated in references) are not directly used in the transport equations. Instead, values derived from the sub-grid turbulence model are used with the molecular values setting a lower bound. This approach is appropriate for simulations where the resolvable length scales are at least an order of magnitude greater than those appropriate for direct numerical simulation (DNS) calculation methods, which is the case for the HEAF models. Specific heat is used at any length scale as this is used to determine the enthalpy present at a given temperature.

As a fire model, FDS had been developed to support thermophysical data up to 5,000 K. This was a programming decision for setting array sizes for temperature based thermophysical data. To support HEAF applications, an FDS modification was made to allow a user-definable upper limit for the temperature arrays. This enabled defining extended specific heat values for nitrogen, carbon dioxide, and oxygen (up to 20,000 K, the maximum values in the NASA polynomials used in FDS [19]). Specific heat data for Cu vapor, Al vapor, and Al_2O_3 was taken from NIST-JANAF tables [20] for each of those species. Detailed specific heat data was not located for Cu_2O, and a constant specific heat of 0.7 kJ/(kg·K) was used. Lennard-Jones data used to determine viscosity, diffusivity, and conductivity for gas-phase metallic species were taken from Cressault et al. [21, 22].

3.3 Radiation

FDS uses a finite volume calculation method for solving the radiation transport equation. This approach subdivides the unit sphere into a series of solid angles which define the directions used for radiation transport. The default number of angles is 100, which is generally adequate for typical usage of FDS in fire protection engineering. For HEAF events, the arc occupies a much smaller volume than the flame volume of a typical design fire. This condition requires additional resolution. Scoping calculations indicated that 500 angles provided a reasonable level of realism and computational resources and are used in the FDS HEAF models.

The radiation solver uses the NIST RADCAL program [23] to define the absorptivity of a grid cell based on the species present in the grid cell. There is an option to replace the radiative properties of soot aerosols with the radiative properties of Al_2O_3 aerosols. This option was selected. It was assumed that the Al_2O_3 properties were more applicable for Cu_2O than those for soot and this option also applied to Cu_2O aerosols. Although this reflects an inherent limitation of the state of knowledge for the copper oxide radiant properties, the FDS results indicated the dominant factor was the distance between the target and the arc (the radiant heat flux directly from the arc). Uncertainty in the radiant heat flux from the heated gases due to this assumption is expected to be a secondary effect that is addressed through bias adjustments for the model predictions.

As discussed in Section 2.2.2.2, at typical engineering length scales the flame temperature and flame species are not resolved well enough to use those values directly for the radiation source term. Instead, a radiative fraction is used to define a minimum amount of radiation from the flame volume of a fire. A similar approach was taken for the HEAF simulations. As discussed in Section 3.8, the arc input power was applied as a volumetric heat source. A radiative fraction was applied for the source. The fraction was based upon research by Cressault et al. [24]. This research measured the radiant fraction from vertically oriented, cylindrical electrodes, and

testing varied the electrode metal and the arc power. Figure 3-3 shows the measured data from Cressault et al. [24] and a power law fit to the data. This power law fit was used to define the radiant fraction input for each HEAF simulation discussed in sections 4 and 5.

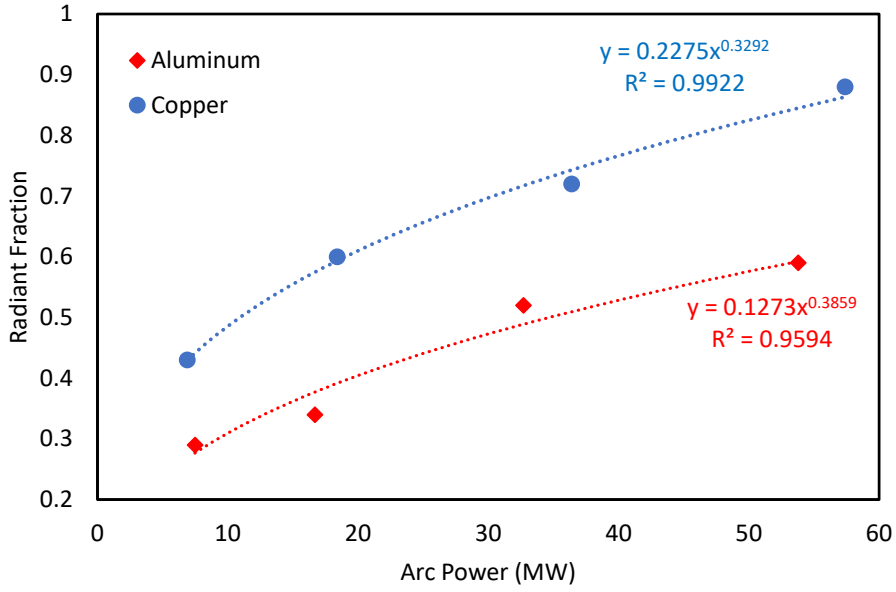

Figure 3-3
Arc power versus radiant fraction data of Cressault [24]

3.4 Computational Grid

For the MV SWGR and low-voltage (LV) SWGR cases, a grid resolution of 0.0762 m was used. This puts at least a dozen grid cells between the face of the enclosure and the ZOIs in NUREG/CR-6850 and allows for some resolution of flow dynamics at closer distances to the enclosure. Given the physical size of these enclosures, smaller grid resolutions would significantly add to the expense of the simulations given the number of simulations being performed.

For the non-segregated bus duct (NSBD) cases, a grid resolution of 0.02 m was used. The NSBD modeled is significantly smaller in cross-section than the two SWGR enclosures, and a finer grid was needed to avoid only having a few grid cells across the span of the NSBD.

For all geometries, the grid was extended 1.5 to 2 m from the face of the enclosure. Based on the data from testing and from scoping calculations, this distance was expected to fully contain the ZOI.

3.5 Combustion

Combustion was modeled for the oxidation of metal vapor (see Section 3.7 for discussion of vapor addition). This is either aluminum to aluminum oxide (Al_2O_3) releasing 31,100 kJ/kg of aluminum or copper to copper oxide (Cu_2O) releasing 1,340 kJ/kg of copper. The heats of combustion are taken from NIST-JANAF data [20]. Given the multiple centimeter grid cell size, fast chemistry was used. Given the very high temperatures seen in HEAF events, Arrhenius-based rates are expected to be essentially instantaneous compared to timestep sizes. The FDS extinction mode was disabled. This extinction model prevents combustion based on the local cell temperature and oxygen concentration. The inputs for this model are only well known for

typical organic materials and not for metal oxidation. Additionally, the very high temperatures would likely allow for near complete consumption of oxygen in grid cells with metal vapor.

3.6 Enclosure breach

In the large-scale testing, metal enclosures containing a HEAF are observed to breach within 1 s [4, 6]. Typical enclosure wall thicknesses are a couple of millimeters. Given the intense heat fluxes from the HEAF, this thin metal thickness will quickly heat to the melting point. In the FDS model, the metal enclosure walls were modeled using a phase change material. This is a material with a single-step reaction that occurs at a threshold temperature (i.e., the melting point). For steel a melting point of 1,300°C and a heat of fusion of 250 kJ/kg of steel was used. For aluminum a melting point of 650°C and a heat of fusion of 320 kJ/kg of aluminum was used. Note that the melting points for both steel and aluminum are set slightly below (about 10 – 70°C) the actual melting point temperatures for these materials to account for enclosure failure due to dynamic forces tearing the metal before it actually melts.

3.7 Electrode Mass Loss

As described in Section 2.1, during a HEAF event the electrodes lose mass due to melting and sublimation of the electrodes. The rate at which mass loss occurs for the different events and the resulting amount of metal oxidation both have an impact on the ZOI. FDS inputs are required for both of these. The FDS simulations use a single electrode material; the feasibility of using two electrode materials (e.g., an arc starting in one material and migrating to another) was not assessed in this effort.

3.7.1 Electrode Mass Loss Rate

The total mass lost from the electrodes was measured in the open box tests [4] and the MV SWGR tests [6] as summarized in Table 3-1. Measurements of the actual time dependence of the mass loss are not available. Prior research by Stanback [25], established a function relationship for the electrode mass loss rate, $\dot{m}_{\text{Bus Bar}}(t)$ in kg/s over all three phases, as a function of the arc current, $I(t)$ in amps, and electrode composition. This is shown in equations 3-1 and 3-2 respectively for copper and aluminum.

Copper:

$$\dot{m}_{\text{Electrode}}(t) = 3.18 \times 10^{-7}\, I(t)^{1.5} \tag{3-1}$$

Aluminum:

$$\dot{m}_{\text{Electrode}}(t) = 2.016 \times 10^{-7}\, I(t)^{1.5} \tag{3-2}$$

These equations were used to predict the total mass loss from the open box tests. The results compared with the measured mass loss are shown in Figure 3-4. While data for the low-voltage (OB) and medium-voltage (OBMV) open box tests are reasonably predicted by the Stanback equations, the full-scale MV SWGR tests performed with aluminum electrodes are not. Based on these results, the HEAF WG consensus was to use the Stanback equations for determining the mass loss rate of low-voltage HEAF events (due to the low-voltage open box data) and bus duct events (where a breached bus duct is more geometrically similar to the open box configuration than the full-scale MV SWGR configuration) and develop an alternative treatment for the MV SWGR.

Table 3-1
Summary of 2019 open box tests [4] and the 2018 medium-voltage full-scale switchgear tests used to assess electrode mass loss [6]

Test	Electrode	System Voltage (kV)	Current (kA)	Arcing Fault Duration (s)	Arc Energy (MJ)	Test Type	Electrode Mass Loss (kg)
OB01(a)	Copper	1.03	1.05	2.01	0.2	Open Box	0.0245
OB01(b)	Copper	1.03	1.03	2.02	0.7	Open Box	
OB02	Copper	1.01	14.02	2.02	12.0	Open Box	0.762
OB03	Copper	1.01	13.80	3.03	20.0	Open Box	1.328
OB04	Copper	1.06	27.79	1.03	12.4	Open Box	0.789
OB05	Aluminum	1.03	1.02	2.01	0.8	Open Box	Not measured
OB06	Aluminum	1.01	11.96	2.02	12.7	Open Box	0.74
OB07	Aluminum	1.01	12.95	1.52	10.3	Open Box	0.552
OB08	Aluminum	1.06	24.87	1.02	20.1	Open Box	0.597
OB09	Copper	1.03	4.79	2.01	2.2	Open Box	0.213
OB10	Aluminum	1.03	4.87	2.01	4.1	Open Box	0.175
OBMV1	Aluminum	6.9	14.3	3.18	37.5	Open Box	1.324
OBMV2	Aluminum	6.9	29.1	1.12	21.4	Open Box	0.945
OBMV3	Aluminum	6.9	14.4	5.05	55.7	Open Box	2.296
OBMV4	Copper	6.9	14.3	5.08	51.8	Open Box	3.252
OBMV5	Copper	6.9	28.6	2.32	43.5	Open Box	3.216
OBMV6	Aluminum	6.9	14.6	2.05	22.7	Open Box	0.727
2-19	Aluminum	6.9	25.76	2.05	39.3	Full-Scale	0.458
2-21	Aluminum	6.9	26.57	4.11	100.7	Full-Scale	1.966
2-22	Aluminum	6.9	31.97	2.07	51.3	Full-Scale	0.894
2-24	Aluminum	6.9	29.84	4.15	121.8	Full-Scale	2.573

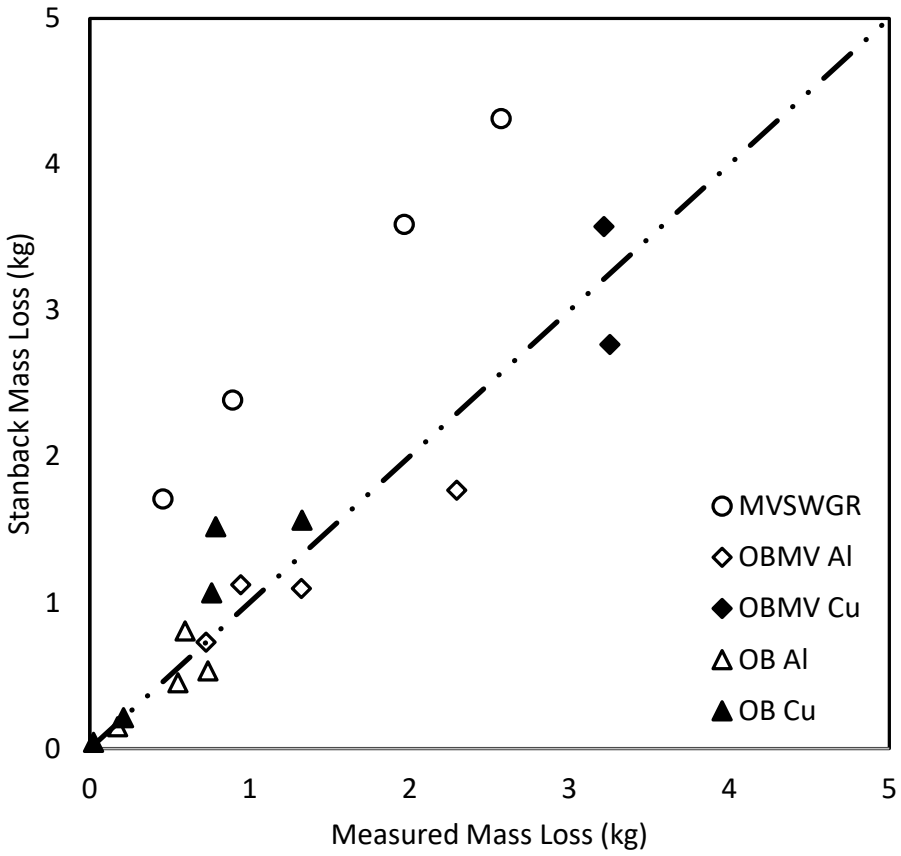

Figure 3-4
Predicted versus measured electrode mass loss for the open box [4] and MV SWGR [6] tests. Symbol shape indicates test series (OB is open box, OBMV is medium-voltage open box, and MV SWGR is full-scale medium-voltage switchgear with aluminum electrodes), and shading indicates aluminum (hollow) or copper (filled)

For the full-scale MV SWGR tests an alternative approach was sought for specifying the mass loss rate. The total measured mass loss $m_{\text{Electrode}}$ was plotted as the function shown in Equation 3-3:

$$m_{\text{Electrode}} = a\, E^{b} \tag{3-3}$$

where E is the total energy dissipated over the test for different values of the exponent b (1, 1.5, and 2). Results are shown in Figure 3-5 for different function parameters.

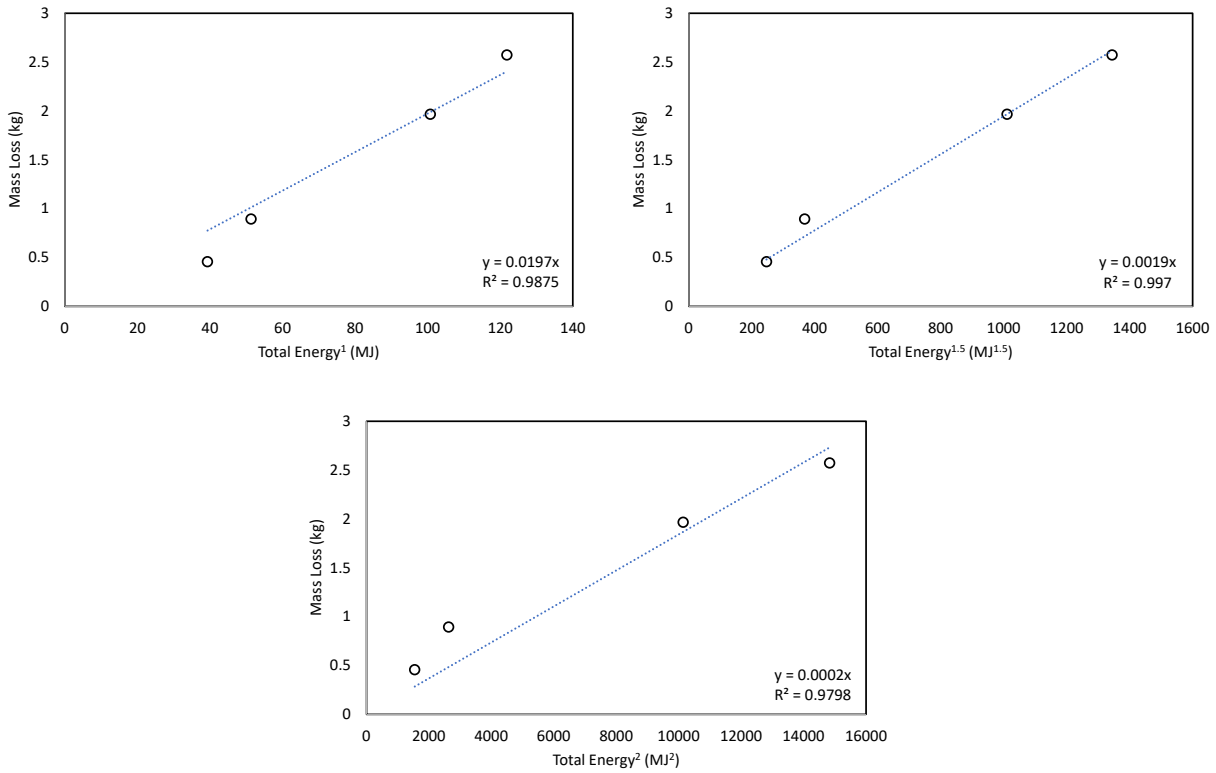

Figure 3-5
Results of fitting Equation 3-3 using different exponents to the MV SWGR mass loss data

The best fit was obtained with an exponent of 1.5, and the HEAF WG consensus was to use that exponent for determining the mass loss rate. All of the MV SWGR tests used aluminum electrodes. The HEAF WG consensus was to assume that the same ratio of copper to aluminum mass loss in the Stanback equations (1.58) applied to the MV SWGR test. The end results are equations 3-4 and 3-5 for the mass loss for copper and aluminum electrodes, respectively. The mass loss rate used in the FDS model was obtained by taking the time derivative of the equations.

Copper:

$$m_{\text{Electrode}}(t) = 1.58 \times 0.019\, E(t)^{1.5} \quad (3\text{-}4)$$

Aluminum:

$$m_{\text{Electrode}}(t) = 0.019\, E(t)^{1.5} \quad (3\text{-}5)$$

3.7.2 Electrode Mass Loss Particle Size Distribution and Oxidation

The mass lost from the electrodes during a HEAF consists of vaporized metal and various sized metal drops, all of which may oxidize to some extent during or after the HEAF. Because oxidation will potentially add to the incident energy seen by targets, the treatment of the electrode mass loss in the FDS model considers this process.

3.7.2.1 Electrode Mass Loss Particle Size Distribution

A review of particle data collected during the 2018 MV SWGR HEAF tests [6] shows both nanoscale particles (which were likely condensed metal vapor) and small metal droplets. Relative masses of the particles collected were not provided, and particles were only collected at locations away from the enclosure where large droplets would not be expected.

To improve knowledge of particle size distributions, Sandia National Laboratories (SNL) performed small-scale testing of HEAF-type events. Sandia replicated the conditions of the 2018 MV SWGR tests at a reduced scale where the voltage and current density was preserved in the electrodes. The particles collected included nanoscale material, which was likely condensed metal vapor, small droplets, and large droplets as expected. This effort is summarized in detail in Appendix D.

Table 3-2 shows that nanoscale particles, which represent the vaporized metal, have a negligible mass fraction. Large drops, characterized as those with diameters over 15 microns, represent the majority of the electrode mass

Table 3-2.
Particle size distribution for mass lost from different electrodes (see Appendix D)

Electrode	Mass Fraction		
	Nanoscale Particles (Condensed Metal Vapor)	**Small drops (~ 2 – 15 microns)**	**Large drops (Over 15 microns)**
Aluminum	~ 0.0	0.10	0.90
Copper	~ 0.0	0.08	0.92

3.7.2.2 Electrode Oxidation

Metal vapor and metal droplets generated by a HEAF that are around 10 microns or smaller in diameter will eventually see complete or near complete oxidation and they will be transported within the outflow from an enclosure. Larger droplets (around 100 microns or more) will only see limited oxidation over the timescale of interest. The thickness of the oxide layer that can develop on this timescale is on the order of several microns since 10 micron drops are nearly completely oxidized. If the oxide layer is 3 microns, then 93% of the mass of a 10 micron diameter drop mass would be oxidized, whereas only 17% of a 100 micron diameter drop would be oxidized. Additionally, larger droplets will more quickly fall out of outflow. As a result, electrode mass lost to larger droplets will not significantly contribute to the ZOI as they will have significantly less oxidation and that oxidation will occur at locations that do not determine the ZOI.

The 2018 MV SWGR full-scale tests noted that roughly between 30 – 75% of aluminum drops oxidized, which provides some confirmation of the estimated oxidation levels. The small-scale testing performed by Sandia considered the oxidation levels for specific particle size ranges. The results of these tests are as summarized below (see Appendix D).

- Aluminum electrode: 75% oxidation for micron sized particles (small drops).

- Copper electrode: 25% oxidation for micron sized particles (small drops).

3.7.2.3 FDS Model Treatment of Electrode Particles

Particles are included in the FDS model primarily to account for the oxidation process. The incorporation of the energy associated with melting and vaporizing the electrode metal in the FDS model is described in Section 3.8.

Based on the observations of the particle size mass distribution and oxidation fraction, the following approach is adopted:

1. Nanoscale particles, which represent the portion of the electrode that is converted to metal vapor, are ignored. They represent a near zero mass fraction and the energy budget associated with vaporization and transport of these particles is negligible.
2. Small diameter particles, with characteristic diameters between about 2 – 15 microns represent a non-negligible mass fraction of the electrode mass and will have high levels of oxidation; therefore, the particles are included in the FDS model.
3. Large diameter particles, with characteristic diameters greater than about 15 microns, are ignored. These particles do not significantly oxidize or absorb significant energy in the areas of interest and tend to fall out of the outflow and do not influence the ZOI.

The particles included in the FDS model are introduced using a uniform diameter that is representative of the small diameter drops with diameters between 2 – 15 microns. Oxidation of these particles is incorporated through a pyrolysis model where the oxidation process occurs in the vapor phase but represents surface oxidation. Thus, the energy required to vaporize the metal is not included in the model.

This approach is implemented in the FDS model as described below.

- 10-micron particles were injected into the FDS domain in the arc volume. This particle diameter is within the small droplet range observed in the Sandia tests and represents all particles in this range. The particles were injected into the domain using three spray nozzles, with one nozzle at each bus bar location. A 120° cone with a particle velocity of 10 m/s [26] was used. The cone was oriented to face the largest expected breach. The mass flow rate was set following the discussion in Section 3.7.1.
- The particles were defined with a simple pyrolysis model involving a constant reaction rate. That rate was set such that the particles emitted 75% or 25% for aluminum or copper, respectively, of their mass as metal vapor over 0.3 s. This represents surface oxidation; therefore, the energy associated with the vaporization process was not included in the model. The metal vapors that are pyrolyzed combust as soon as they mix with oxygen in the FDS model, thus guaranteeing the correct amount of oxidative heat release. The pyrolysis (oxidation) time of 0.3 s is the approximate time needed for particles to move past the instrument racks and past the ZOI in the 2018 MV SWGR simulations and thus forces oxidation in the areas of interest. This is expected to result in a slight overestimate of the energy released between the arc and the target as it is likely some surface oxidation occurred later in time after particles move past the instrumentation racks.
- The particles were defined with a surface temperature of the respective melting point of the metal. The energy needed to melt the metal and form the particles is described in Section 3.8.2 and is not directly associated with the modeling of the particles. In addition, the heat transfer coefficient and emissivity were set to zero for the particles. This means the vapor from the particle oxidation model is injected at high temperature, but the particles themselves are neutral in terms of the gas-phase heat exchange. In the volume

of space defining the ZOI, gas temperatures are generally much higher than the melting point and the droplets or solid particles act as heat sinks within that volume. Therefore, not including heat transfer between the particles and the surroundings results in an overestimate of the gas temperatures.

3.8 Arc Power Input

3.8.1 Arc Power Profiles

Three generic arc power profiles were used: two that were applied to MV SWGR and NSBD HEAFs and one applied to LV SWGR HEAFs. These arc power profiles were selected after a review of HEAF operational experience as described in Section 5.1 and Appendix A. Appendix A provides a detailed review and summary of the arc profiles and the corresponding HEAF simulations developed using these arc power profiles. The generic profiles are briefly summarized below.

1. A constant-current arcing fault (stiff-source). The current was 30 kA and the arc line-to-line voltage (V_{L-L}) was 650 V_{L-L} resulting in a maximum three-phase arc power of 33.8 MW. This was implemented in the FDS model with a 0.1 s ramp up and down at the start and end of the arc to avoid numerical instabilities that could arise when a large heat source is imposed instantaneously. This arc power profile was used to model MV SWGR and NSBD HEAFs.
2. Generator-fed faults (constant-current arc followed by 15 s of decaying arc current). The constant-current arc portion of this arc power profile was characterized in the same way as the constant-current arc power profile. The decay portion was characterized with a 20 kA starting current, 650 V_{L-L} arc voltage, and an exponential decay profile estimated from operational experience (see Appendix A). A 1 s ramp from the stiff current to the decaying current was used provided some consistency with the exponential decay profile used on the generator-fed fault portion. This arc power profile was used to model MV SWGR and NSBD HEAFs (see Figure 3-6, Figure 3-7, and Figure 3-8).
3. A two-stage, constant-current arc. This arc power profile was based on FEDB 50935 [12] and is implemented by a 20 s constant initial arc current followed by a 21 s constant reduced arc current, both at 375 V_{L-L} as described in Appendix A. This arc power profile was used to model LV SWGR HEAFs (Figure 3-9).

The generic profiles were used to construct different HEAF model simulations primarily by changing to the constant-current acing fault duration. Appendix A provides plots of the arc power profiles used to develop the HEAF ZOIs.

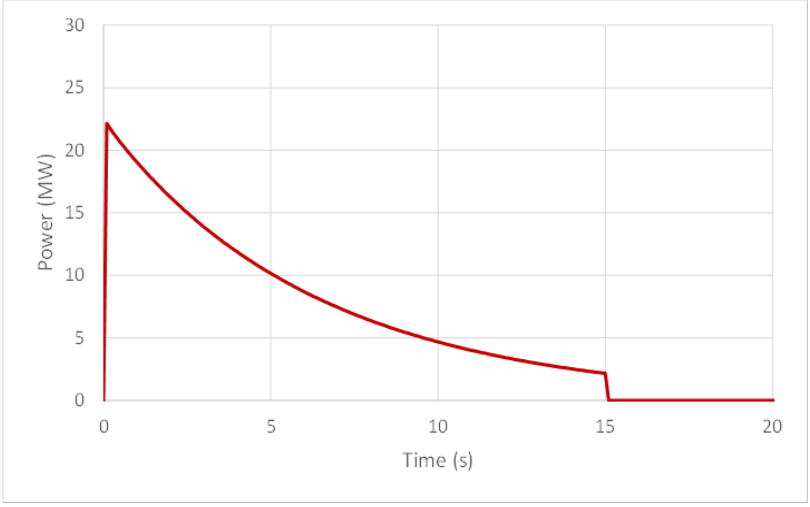

Figure 3-6
Power curve for a 0 s stiff and 15 s decay HEAF

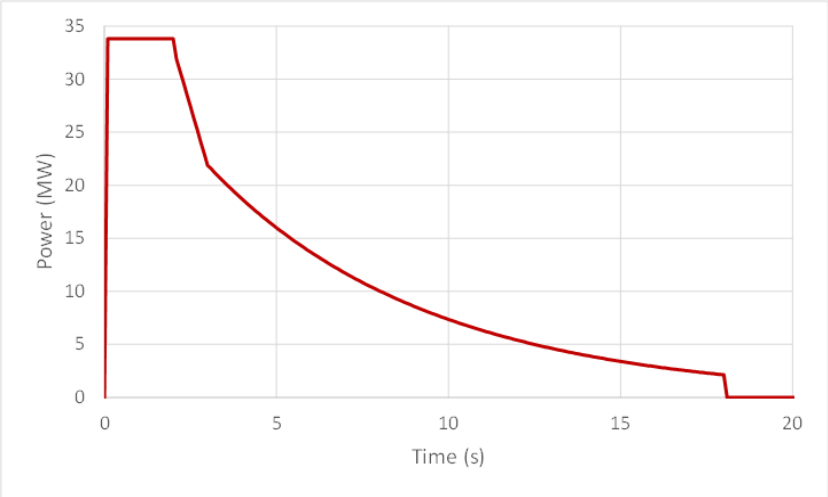

Figure 3-7
Power curve for a 3 s stiff and 15 s decay HEAF

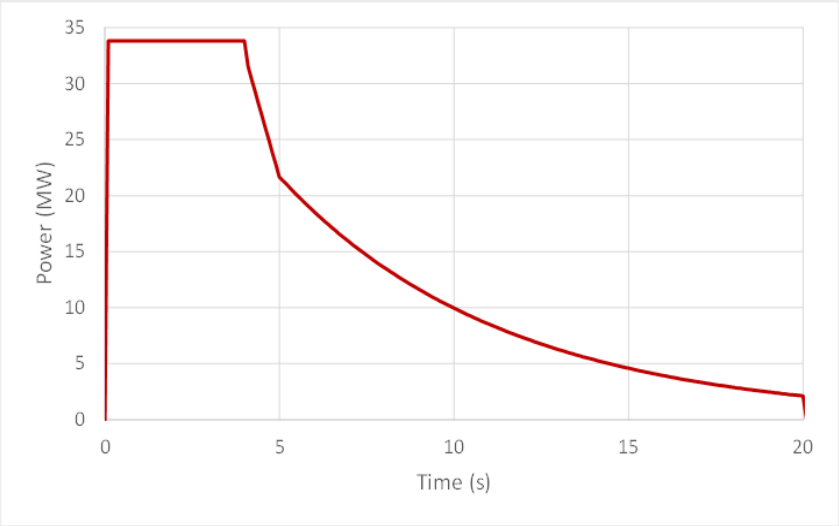

Figure 3-8
Power curve for a 5 s stiff and 15 s decay HEAF

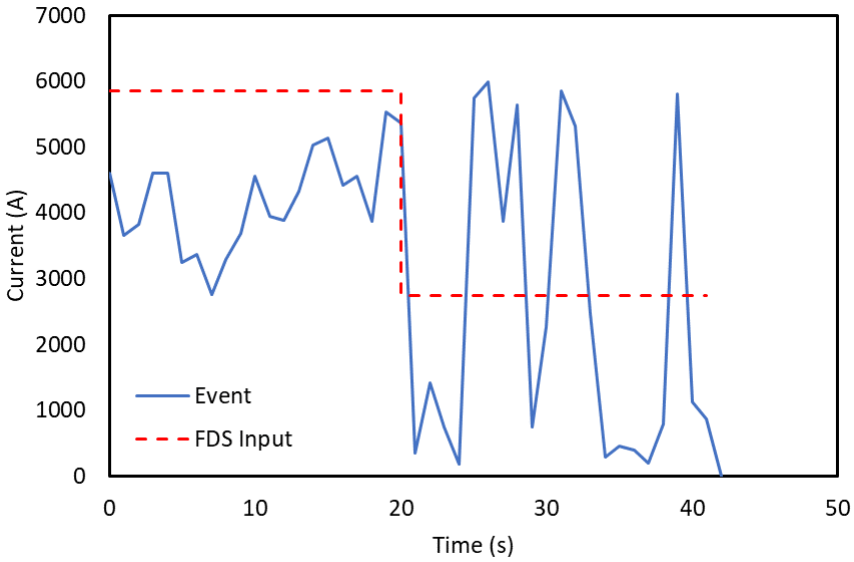

Figure 3-9
Low voltage HEAF current profile

3.8.2 Power Input for FDS Simulations

For the FDS simulation, the electrical power dissipated inside the enclosure is given as an input. The actual power dissipation for a HEAF is the heating, melting, and vaporization of the bus bars and the convective and radiative energy released by the arc (some of which goes into the electrodes). Within FDS, the heating, melting, and vaporization of the electrode metal was not modeled directly; therefore, the energy needed to accomplish this is not present in the FDS model as an energy sink. Based on the discussion in Section 3.7.2.3, the mass fraction of vaporized metal is negligible and is not considered when determining the power dissipation. In addition, the energy associated with heating melted drops is conservatively ignored as described in Section 3.7.2.3. The FDS model only considers the energy required to melt the electrodes. This is the energy it takes to heat the metal up to its melting point and then the energy needed to change the phase from solid to liquid. Using the NIST JANAF data [20], this

energy, ΔE_{melt}, is 1.063 MJ/kg for aluminum and 0.695 MJ/kg for copper assuming an initial temperature of 25°C. The time dependent arc power input used for FDS, $\dot{E}_{\text{FDS}}(t)$ in MJ/s is shown in Equation 3-6:

$$\dot{E}_{\text{FDS}}(t) = \dot{E}(t) - \Delta E_{\text{melt}}\, \dot{m}_{\text{Electrode}}(t) \qquad (3\text{-}6)$$

where $\dot{E}(t)$ in MJ/s is the HEAF-dependent power discussed in Section 3.8.1 and $\dot{m}_{\text{Bus Bar}}$ is the mass loss rate of the electrodes as discussed in Section 3.7.1. This adjustment is applied only to the MV SWGR arc power profiles.

The FDS input power was applied to a volumetric heat release rate defined in a fixed volume in the enclosure where the volume was located at the arc location for that HEAF. The volume covered the width occupied by the electrodes plus a small number of grid cells perpendicular to the plane of the electrodes and along the electrodes. The volumetric heat release was assigned a fixed radiant fraction per the discussion in Section 3.3. To avoid numerical instabilities by instantaneously introducing an extreme volumetric heat release rate, the arc power was ramped up to its initial value over a period of 0.1 s using a linear ramp.

3.9 Input File Generation

Over 100 FDS simulations were performed as part of the ZOI definition effort (see Section 5.2). This large number of simulations posed some issues. First, multiple sets of simulations where each set involves a series of inputs with minor input-to-input changes introduces a significant likelihood of user error if input files were edited manually. Second, after running through the entire HEAF simulation matrix for the first time, there was a possibility of noticing an issue with one or more of the input assumptions and approaches discussed above that had not been revealed in the smaller set of HEAF simulations used for validation. Having to manually re-edit a large number of inputs would also introduce a significant likelihood of user error. Third, the long-term maintenance of that number of input files introduces its own risk. Over time, institutional knowledge on what changes are made for what files can be lost if not documented in an appropriate fashion. Also, as FDS continues to evolve there may be a desire to update inputs files to reflect new FDS capabilities which would again bring the risk of user error when editing the entire suite of files by hand.

To reduce the risk of user error and support the long-term maintenance of the inputs, an algorithmic approach was used to develop the input files. The FDS repository contains a Python utility called `swaps.py`. This utility reads a comma-delimited file called `paramfile.csv`. This file has the format:

`template, param`$_1$`, param`$_2$`, …, param`$_n$

`file01.fds, val`$_{1,01}$`, val`$_{2,01}$`,… val`$_{n,01}$

`file02.fds, val`$_{1,02}$`, val`$_{2,02}$`,… val`$_{n,02}$

…

`filem.fds, val`$_{1,m}$`, val`$_{2,m}$`,… val`$_{n,m}$

On the first line `template` is the name of a template FDS file that serves as the baseline input file, each `param` is a unique text string, and each `val` is a text string (the text string can be a number). For each of the following lines, FDS creates the input file `filem.fds` and in that file it replaces each `param` with its corresponding `val`. For example, if a template file called `template.fds` had the contents:

```
&MESH ID='meshname',XB=x1,x2,0,1,0,1,IJK=ival,jval,kval/
```

and the `paramfile.csv` contained:

```
template.fds, meshname, x1, x2, ival, jval, kval
scenario1.fds, Mesh1, -1, 2, 20, 10, 10
```

then `swaps.py` would create the file `scenario1.fds` with the contents:

```
&MESH ID='Mesh1',XB=-1,2,0,1,0,1,IJK=20,10,10/
```

With this approach, all of the FDS input file editing is done by the python code. There is a single file to review that contains a tabulation of all the scenarios and the input changes needed. If some future change to FDS meant that some input needed to be changed, only the template file would need to be updated with the scenario files then regenerated again by the python script.

For this effort, a template file and a parameter file were created for each geometry type. The template files were reviewed. The parameter files were created using Excel. One sheet of the Excel file contained a series of columns containing the variables being permutated (electrode composition, arc location, fault current magnitude, duration, etc.) and all of the parameters in the parameter files. Other sheets contained lookup tables for items like arc location. Logical formulas were defined for each parameter to autogenerate its value based on the specific permutation for the HEAF simulation. File names were also autogenerated based on the specific variable permutation. This approach meant adding or removing a HEAF simulation was a simple process of adding or removing rows and ensuring the correct permutations were defined.

3.10 Outputs and Output processing

Data from testing, observations of test videos, and the results of FDS simulations indicate that the highest exposures occur where targets are immersed in outflow from the enclosure or where targets have a direct line of site to the arc. FDS simulations were instrumented with planes of devices measuring the FDS output quantity of `GAUGE HEAT FLUX GAS` in units of kW/m² integrated over time, resulting in a total exposure energy output quantity in units of MJ/m². The planes were located where outflow was expected to occur either due to a fixed vent opening in the enclosure or openings expected as a result of enclosure failure. Figure 3-10 shows an example of the FDS instrumentation for a General Electric (GE) Magne-Blast series of breakers with an arc in the main bus bar compartment (see Section 4.1 and Section 5.4.1 for more details).

The planes are implemented as line devices in FDS, where a starting point and end point are given along with a number of devices to place between the two points including the start and end. In this case, devices were defined as a line normal to the enclosure face starting at the first grid cell with devices in every grid cell moving outward along the normal. A plane of such devices was defined at each fixed vent opening and in locations where enclosure failure was expected. The inputs were grouped in the FDS input file such that all line devices for a particular enclosure face were together.

The `GAUGE HEAT FLUX GAS` output quantity inserts a massless particle at the device location (i.e., each green dot in Figure 3-10) and the particle is treated as a virtual water-cooled heat flux gauge. The particle is given an `ORIENTATION` input which defines the normal vector to the particle used to determine the radiative flux. The local velocity and temperature are used to predict the convective flux. This approach of measuring the target exposure as the exposure to a cold wall is consistent with how target fragilities have been defined for both fire exposures [1] and HEAF exposures [10]. The device outputs were further defined to integrate the heat flux over the simulation time.

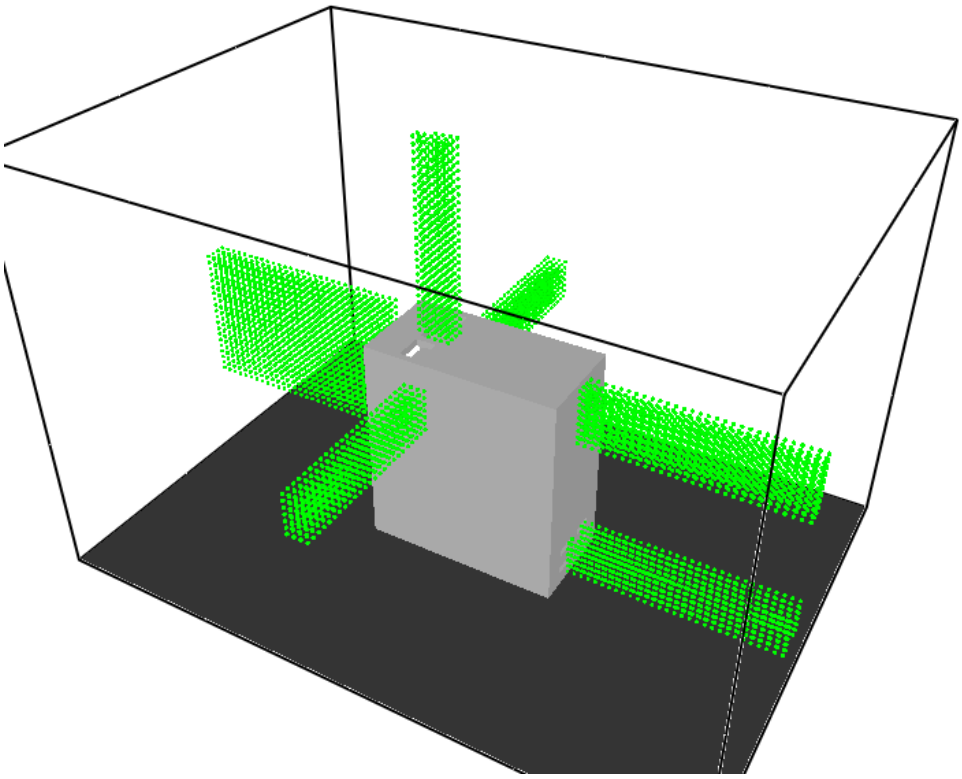

Figure 3-10
FDS output devices (green dots) for the GE Magne-Blast geometry with the arc in the main bus bar compartment

At the end of an FDS simulation, there is a comma separate variable (`csv`) file containing a column for each line device where the first row is the identity of the device, and the remaining rows are the output for each point along the line. Since points were defined in each grid cell normal to the enclosure, each row is simply one more grid cell away from the enclosure. This makes it simple to query the output file and determine for each face of the enclosure what the maximum exposure was as a function of distance.

For determining the ZOI for each face for each HEAF simulation, the FDS-predicted exposures were adjusted to account for the FDS bias discussed in Section 4.1.3. This process is depicted in Figure 3-11 shows the back face exposure for a GE Magne-Blast enclosure with aluminum bus bar power flow in the load configuration with a 4 s stiff (constant power) arc located in the primary cable compartment. The plot shows the predicted FDS exposure, the bias adjusted exposure, the 95% confidence interval, and the 15 MJ/m² and 30 MJ/m² target fragility criteria. The bias adjusted distance versus exposure data was used to determine the ZOI with the ZOI distance obtained using linear interpolation and the fragility criteria. In this specific case, this results in a 15 MJ/m² target fragility ZOI of 0.97 m (0.76 to 1.20 m 95% confidence interval) and a 30 MJ/m² target fragility ZOI of 0.63 m (0.46 to 0.82 m 95% confidence interval).

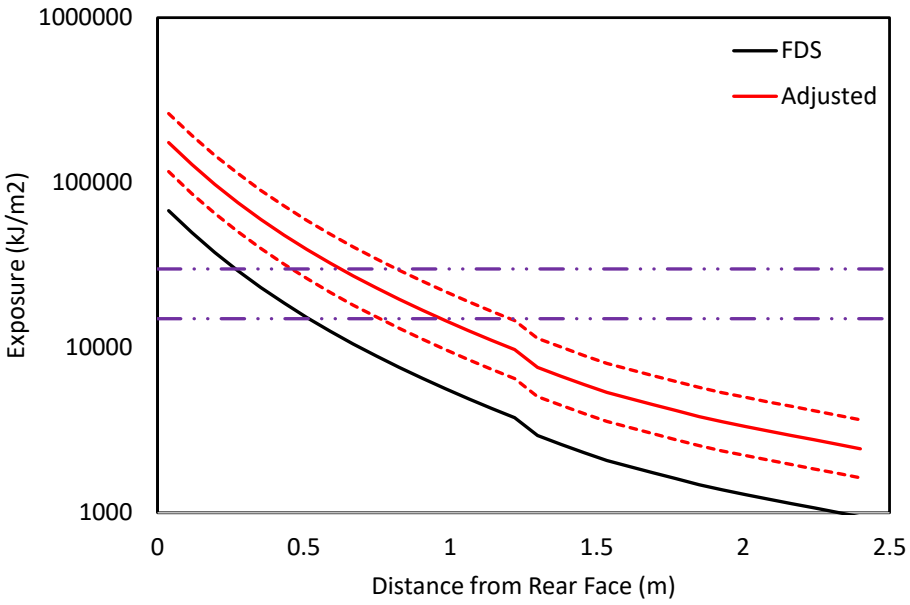

Figure 3-11
Depiction of the adjustment of FDS results for the bias and error (Section 4.1.3). Dotted lines are 95% confidence and dot-dot-dash lines are 15 MJ/m² and 30 MJ/m² target fragility criteria

4
VALIDATION OF THE FDS ANALYSIS APPROACH

This section documents the validation of the FDS analysis approach described in Section 3. Validation consists of the 2018 MV SWGR tests, a LV SWGR event, a NSBD event in an elbow, and a full-scale test replicating a NSBD event in a straight segment of bus duct.

4.1 2018 Medium Voltage Switchgear Tests

4.1.1 Summary of Experiments

The MV SWGR experiments used General Electric Type M-36 enclosures for Magne-Blast circuit breakers (see Figure 4-1). The enclosures were previously used and refurbished. The four enclosures used in testing were identical except for some differences in components attached to the front door. However, those components do not play a significant role in the thermal environment generated by the HEAF induced on the bus bars in the primary cable compartment. The enclosure is 202 cm (79 in.) long, 91 cm (36 in.) wide, 229 cm (90 in.) tall. The bus bars in all experiments were aluminum. Further details of the enclosure construction are contained in the test report [6].

Figure 4-1
GE Type M-36 enclosure

Instrumentation consisted of five racks of instrumentation. Two racks (Rack 1 and Rack 4) were placed 0.91 m from the sides of the bus bar location, two racks were placed at 0.91 m (Rack 2) and 1.82 m (Rack 3) from the back face of the cabinet where the bus bars are located, and a

fifth rack (Rack 5) was placed 0.91 m above the top of the cabinet. Each rack contained a number of measurement devices including ASTM copper slug calorimeters (ASTM), plate thermometers (P_{TC}), tungsten slug calorimeters (T), as well as cut segments of electrical cables or cable coupons (CCn). Gauge construction is discussed in the test report. Instrumentation layouts are shown in Figure 4-2.

All four experiments used aluminum bus bars and initiated the arc in the primary cable compartment (at the upper left where the bus bars bend 90° in the left image in Figure 4-1). A summary of the test conditions is given in Table 4-1.

Table 4-1
Summary of 2018 medium-voltage switchgear experiments [7]

Experiment	Electrode	Voltage (kV)	Current (kA)	Duration (s)	Energy[1] (MJ)	Power[2] (MW)	Electrode Mass Loss (kg)
2-19	Aluminum	6.9	25.8	2.05	39.3	19.2	0.458
2-21	Aluminum	6.9	26.6	4.11	101	24.5	1.97
2-22	Aluminum	6.9	32.0	2.07	51.3	24.8	0.894
2-24	Aluminum	6.9	29.8	4.15	122	29.3	2.57

[1]Arc energy estimated from energy at generator. [2]Average, determined by dividing arc energy by the arc duration.

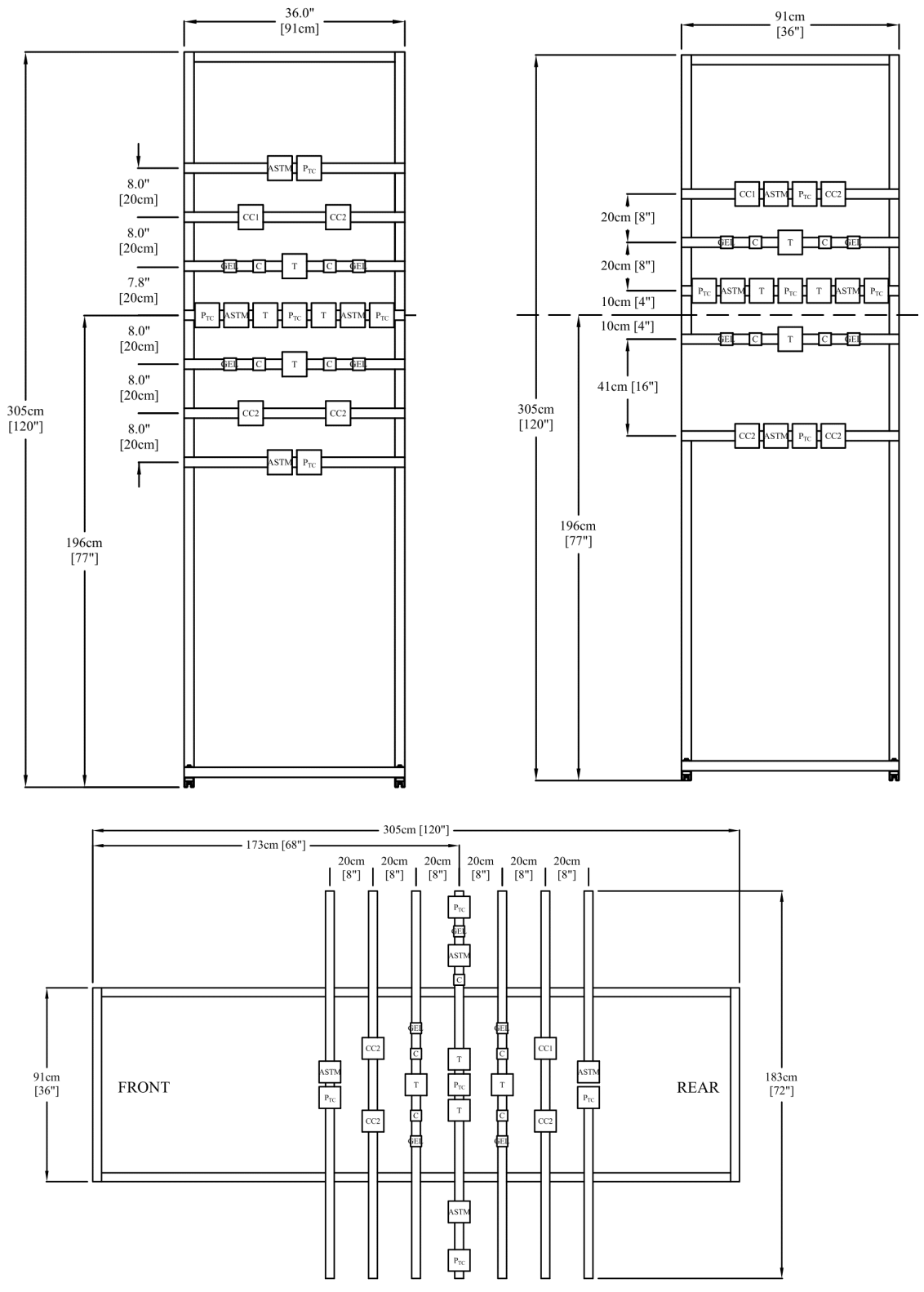

Figure 4-2
MV SWGR instrumentation racks (top left racks 1,2, and 4; top right rack 3; bottom rack 5) [6]

4.1.2 Discussion of FDS Inputs

The FDS input geometry and other simulation parameters were identical to those described in Section 5.3.1. The exceptions were the definition of outputs, the arc power, and the simulation duration.

FDS outputs were defined to model the devices used to measure the heat flux and incident energy that were made during the test using FDS particles, with a unique particle class associated with each device type. The thermal response of the particles was evaluated by FDS by solving the one-dimensional heat condition equation at the appropriate device locations and orientations (see Figure 4-2). Figure 4-3 shows the FDS geometry with the device locations modeled. These particle classes were defined with the specific construction of each instrument. The particle classes were defined as follows:

- The plate thermometer particle class was defined as a cartesian surface with an 0.79 mm plate of Inconel backed by a 2.54 cm layer of ceramic fiber.
- The ASTM slug calorimeter particle class was defined as a cartesian surface with a 1.6 mm copper plate, a 9.7 mm air-gap, a 3.4 mm red board plate backed by a 2.54 cm layer of marinate board.
- The tungsten slug calorimeter particle class was defined as a cartesian surface with a 1.5 cm tungsten plate backed by a backed by a 1.7 cm layer of marinate board.

Note that for validation purposes, it is better to replicate the physical measurement being made rather than quantities derived from the physical measurement (i.e., heat flux).

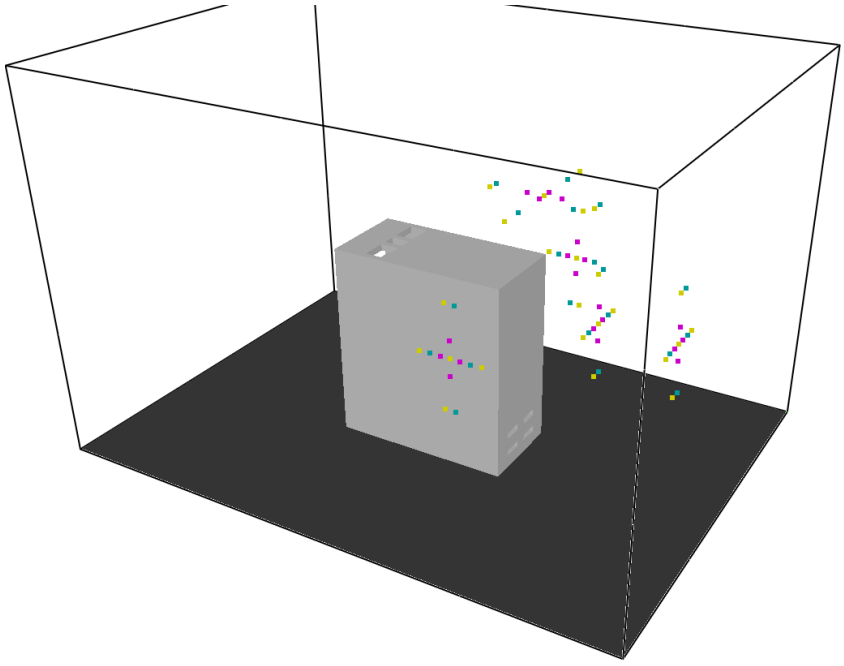

Figure 4-3
FDS geometry showing particles used for instrumentation (magenta is a tungsten slug calorimeter, yellow is a plate thermocouple, and teal is an ASTM copper slug calorimeter)

The arc power was defined using the power indicated in Table 4-1 with adjustments to account for the electrode mass loss per the discussion in Section 3.7. The mass loss equation in Section 3.7.1 was used instead of the measured mass loss to validate the overall FDS analysis approach.

The four simulations were all run for 6 s. For each experiment, this was sufficient time to capture the peak temperatures seen in the various gauges. As discussed in Section 4.1.3, the temperature rise of each gauge (which is proportional to the total exposure) was used to assess the performance of FDS.

4.1.3 Results of FDS Simulations

There are three experiment results considered for FDS validation. The first is the enclosure breach times. PRA targets outside of an enclosure do not see significant exposures from a HEAF unless they have a direct line of sight to the arc or can be engulfed in outflow from the enclosure. For a given HEAF duration, the breach time determines how long targets can see significant exposure. The second is the amount of damage to the enclosure. The size of holes in the enclosure defines the view factor that a target has of the volume inside the initiating enclosure (arc location). The third is the maximum temperature achieved by the plate or slug calorimeter during the experiment. This represents the actual target exposure and is the primary quantity of interest for defining ZOIs.

Table 4-2 shows the breach time estimated from videos of the experiment and the breach time predicted by FDS. Also shown is the highest exposure measured during the experiment. Breach times are overestimated for all experiments with larger errors for shorter experiments (tests 2-19 and 2-22) and lower arc current experiments (tests 2-19 and 2-21). For the 2 s experiment, while the breach times result in 0.21 – 0.57 second over-predictions in the breach time, these experiments had exposures of 1.4 MJ/m² and 2.1 MJ/m^2 or less compared to the 15 MJ/m² target fragility criteria which corresponds to thermoplastic (TP) cables or aluminum bus ducts [10]. The ZOIs for these experiments are small and predictive errors for small ZOIs are unlikely to have a large risk significance given that there is generally clearance around MV SWGR to support operation and maintenance activities. For the 4 s experiments, the difference in the predicted and observed breach time is less than 0.2 s for both cases. Note that part of the differences between measured and predicted breach times is due to the 0.1 s time FDS uses to increase the arc energy from zero to its full value.

Table 4-2
FDS versus observed breach times for the 2018 MV SWGR experiments [6]

Experiment	Experiment duration (s)	Experiment current (kA)	Breach time (s)		Post-breach time difference[1] (s)	Largest exposure at 0.9 m (MJ/m²)
			Experiment video	FDS		
2-19	2.05	25.8	0.53	1.1	– 0.57	1.4
2-21	4.11	26.7	0.65	0.82	– 0.17	7.0
2-22	2.07	32.0	0.60	0.81	– 0.21	2.1
2-24	4.15	29.8	0.61	0.73	– 0.12	15[2]

[1]Experimental result relative to the predicted value.

[2]Fragility report estimate using 2-24 Rack 3 data at 1.8 m and relative ratio of Rack 2 and Rack 3 for other tests [10].

Figure 4-4 through Figure 4-7 show the final enclosure condition of the four experiments. For experiment 2-19, FDS predicts small holes on the sides and a larger hole on the back enclosure face. During the experiment, only a back breach occurred; the hole size is similar. For experiment 2-21 holes are seen on both sides and the back face with FDS predicting similar hole sizes. FDS also predicts a hole on the top. The post-arc test photos for this experiment show that the top face was not breached in this experiment [6]. For experiment 2-22 and experiment 2-24 FDS also predicts hole sizes similar to those observed in the experiments.

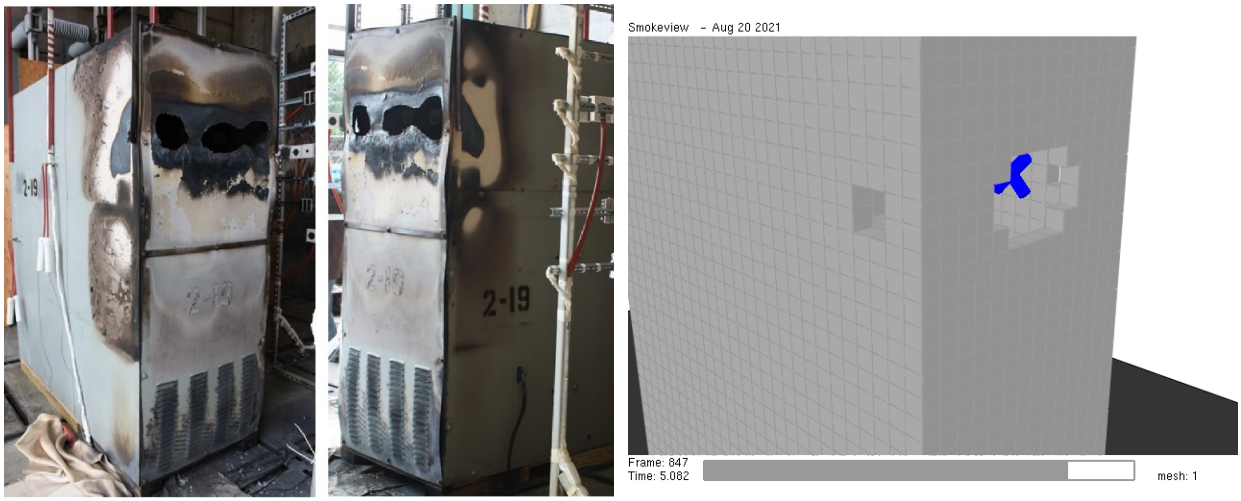

Figure 4-4
Enclosure condition post-HEAF for experiment 2-19

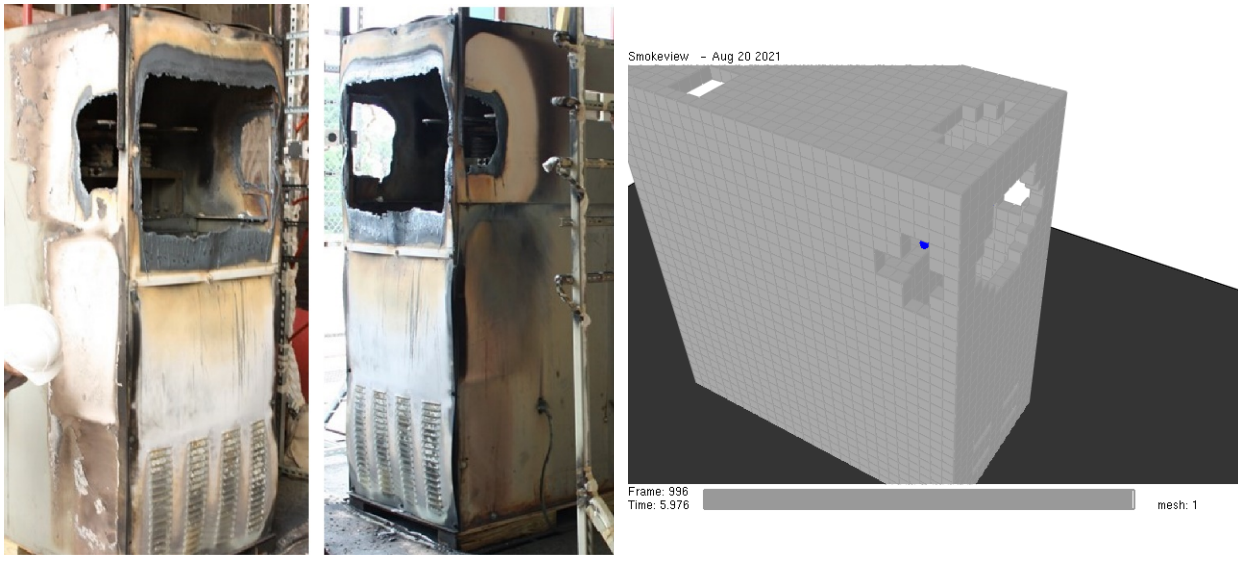

Figure 4-5
Enclosure condition post-HEAF for experiment 2-21

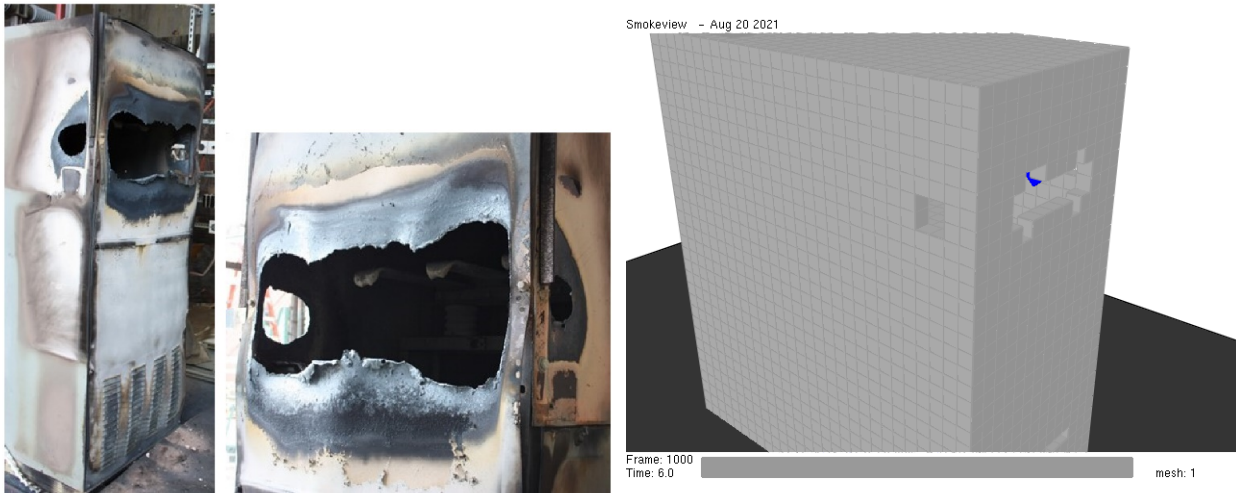

Figure 4-6
Enclosure condition post-HEAF for experiment 2-22

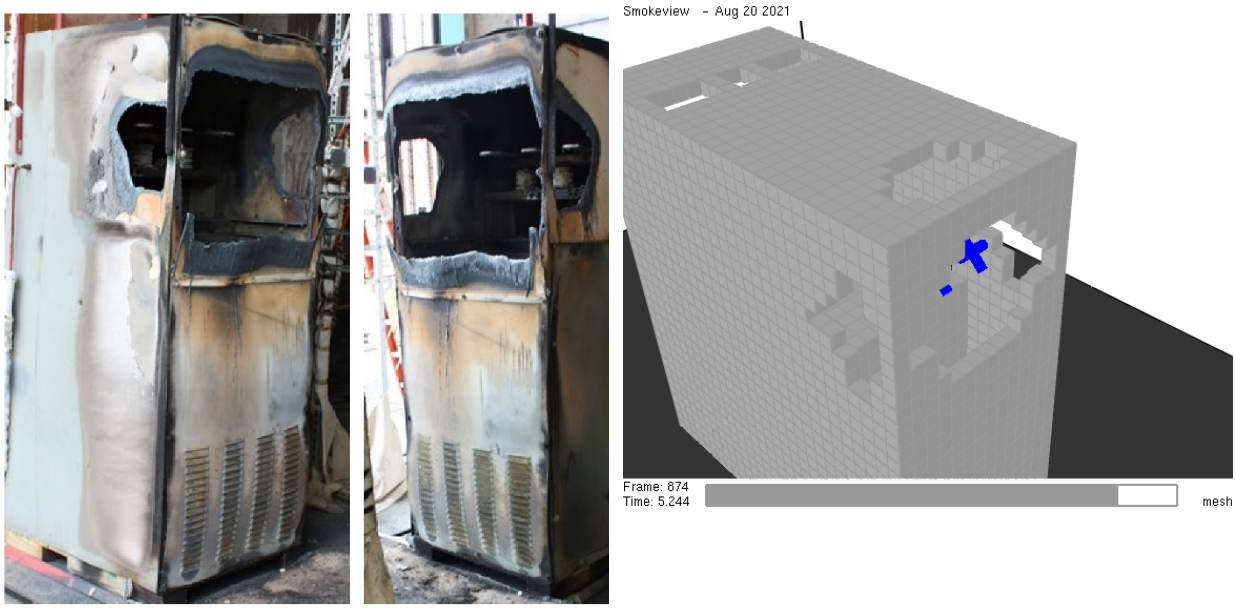

Figure 4-7
Enclosure condition post-HEAF for experiment 2-24

Figure 4-8 shows the measured and predicted temperature rise for each instrument gauge for the four MV SWGR experiments. There is a tendency for FDS to underpredict the values for Racks 1 and 4 (combined) and for Rack 5. During the experiments, the internal pressure of the enclosure increased and caused the enclosure exterior panels to bulge outward slightly. This opened small gaps along the edges of the panels where outflow occurred. These gaps are not included in the FDS model. This is likely a significant factor in the observed performance. The locations with the largest under predictions are also locations with the lower temperature rises. It is the highest temperature location at a given distance from the enclosure that determines the ZOI, and data corresponding to those locations are better predicted for Racks 1 and 4

(combined) and for Rack 5. Racks 2 and 3, oriented facing the large hole in the back of the enclosure, are much better predicted by FDS.

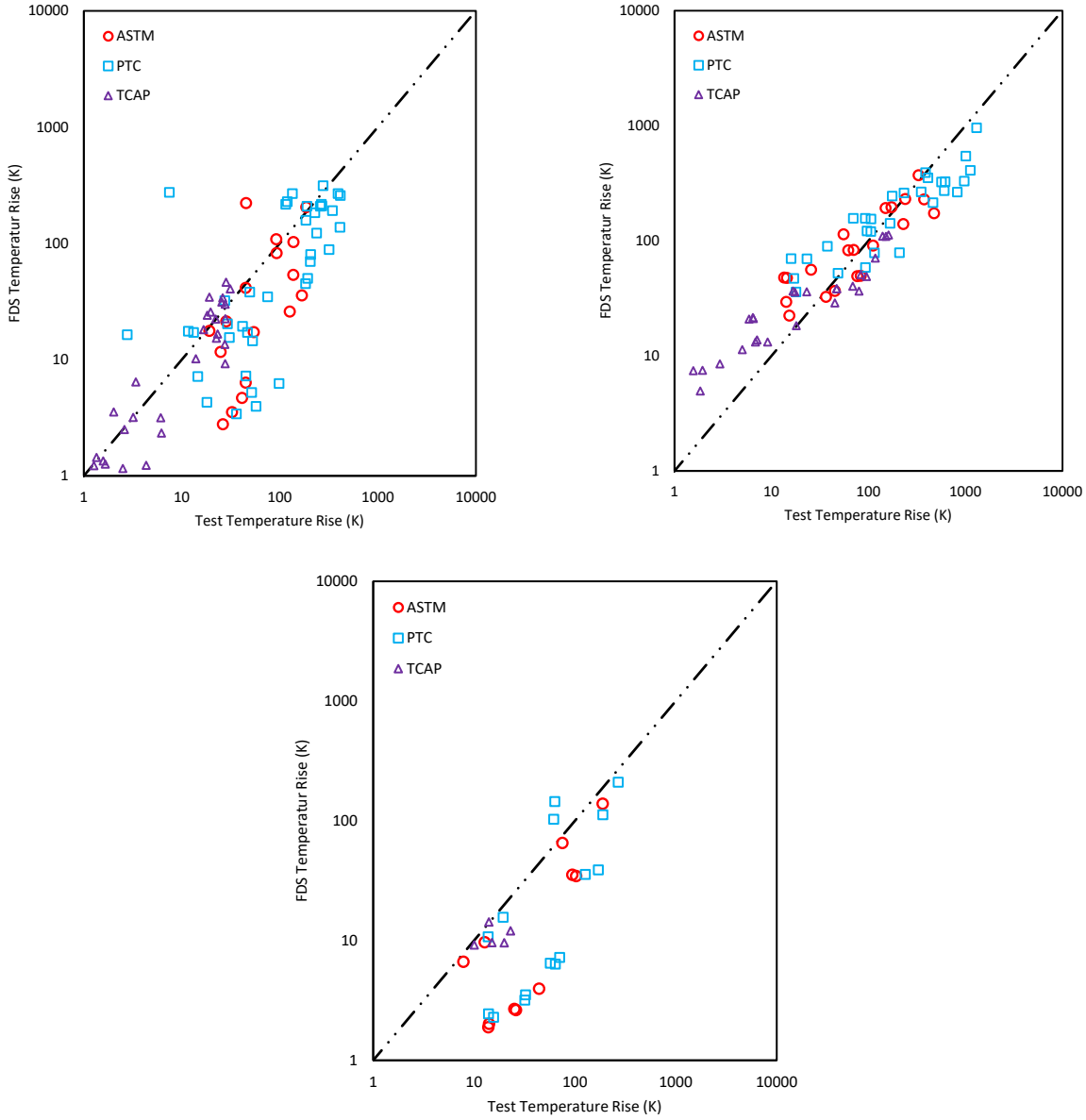

Figure 4-8
Scatterplot of measured versus FDS-predicted temperature rise for all 2018 MV SWGR experiments. Top left – Racks 1 and 4 (enclosure side), top right – Racks 2 and 3 (enclosure back), bottom – Rack 5 (enclosure top). Symbol type indicates gauge type

The process outlined in the FDS Validation Guide [16] is used to assess the FDS bias and relative standard deviation (uncertainty). The relative standard deviation represents the degree of scatter and the bias represents the tendency to over or under predict the data. In statistical terms, if the expected (true) measured value is μ, then the expected FDS value, M, would be $M = \mu \times \delta$ where δ is the bias. That expected FDS value would have a normal distribution with a relative deviation of σ. The relative standard deviation and bias for Racks 1 and 4 (combined) and Rack 5 are 1.06 and 0.28, respectively. For Racks 2 and 3 the respective values are 0.91

and 0.84. In both cases, the experimental measurement and input uncertainty was conservatively assumed to be 0.2 based on the FDS Validation Guide [16]. The calculated bias for these cases suggests that on average, Racks 2 and 3 are 16% underpredicted and Racks 1 and 4 (combined) and Rack 5 are 72% underpredicted.

The FDS-predicted temperature rise is sensitive to enclosure breach times. The readings of the various gauges see rapid increase in the heat flux exposure once a breach occurs. Since FDS was slightly delayed in predicting breach time, this effect will be much more significant for the 2 s experiments than the 4 s experiments. As an example, if the breach time was 0.5 s, and FDS predicted 0.8 s, then for a 2 s experiments, that would be a change from 1.5 s to 1.2 s of post-breach exposure, which is a 27% reduction. For the 4 s experiments, it would only be 11%. Data from the 2 s MV SWGR experiments indicate the ZOI on all faces is relatively close to the enclosure and within the ZOI of NUREG/CR-6850. Data from the 4 s experiments indicate the ZOI is on the order of the ZOI in NUREG/CR-6850. As discussed in Section 5.1, there are potential HEAFs with longer durations and higher total energies than the 2018 experiments. HEAFs with the largest ZOIs are expected to pose the highest risk. To ensure that the ZOIs for those events are well characterized, the 2018 test data was reevaluated using just the 4 s experiments. As seen in Figure 4-8, the FDS performance for just the 4 s experiment is significantly better than that for the 2 s experiments. In large part, this is due to the 4 s experiments failing both the top and bottom of the enclosure making leakage around gaps less important to the total exposure. Similar performance is observed on all racks; the relative standard deviation and bias of the two 4 s experiments are 0.71 MJ/m² and 0.57, respectively, based on Racks 1 – 4 with an assumed experimental measurement and input uncertainty of 0.2 as previously noted. These results are applicable to all racks and are used to adjust the FDS predictions when defining the HEAF ZOIs. FDS output data was adjusted for bias and relative standard deviation. The bias adjusted measurement is given by M/δ and the 95% confidence interval is given as $(M/\delta)/(1+2\sigma)$ to $(M/\delta)\times(1+2\sigma)$.

4.2 FEDB 50935

4.2.1 Summary of Event

In 2011, a HEAF occurred in a breaker cubicle of low-voltage switchgear (FEBD 50935 [12]). The event started at the breaker stabs and the arc moved into the bus bar compartment. No damage occurred to cables or equipment outside the switchgear. The cubicle containing the breaker stabs (where the HEAF initiated) and one other breaker were damaged in the event. The event reports and supporting information do not report any detailed discussion of the damage to the enclosure other than the breaker and bus bars. Figure 4-9 shows the cabinet where the HEAF initiated (right-side of the figure) and details of the backside where the bus bars are located (left side of the figure). In the left photo, the arc failed the partition between the breakers and the bus bar compartment. The photo of the rear compartment shows a region of discolored paint in the location opposite the breaker location on the front. There may have been some damage to the partition between the bus bar and runback compartments.

Figure 4-9
Backside of initiating breaker (left) showing damaged bus bars and backside of low-voltage switchgear (right) showing smoke stains and discolored paint behind arc location (brown stain at the mid-height of the middle section) [34]

This event is the basis for the FDS LV SWGR ZOI simulations in Section 5. The event lasted 41 s and had two distinct periods: a 20 s period of fluctuating current at a higher average (4,167 A) followed by a 21 s period at a lower average (2,512 A), as recorded in the current profile in Appendix A.

4.2.2 Discussion of FDS Inputs

The FDS model geometry for this LV SWGR event is based on the Westinghouse DS metal clad switchgear (Section 5.3.2). Validation for this event uses the FDS simulation for the arc at the breaker at the enclosure mid-height.

4.2.3 Results of FDS Simulation

Results of the FDS simulations are shown in Figure 4-10. The FDS geometry included a single DS enclosure with two columns of breakers. The FDS simulation predicts more extensive damage to the separation between the breakers and bus bar compartment than observed in post-event photos. The FDS model predicts small holes in the sides of the bus bar and breaker enclosure compartment which were not reported in the event documentation; however, the FDS model did not include the mounting rails for the breaker or the enclosure panels. The FDS model shows a small hole between the bus bar compartment and the runback compartment. This was not mentioned in the event report, but it may be consistent with the discolored paint on the rear compartment panel.

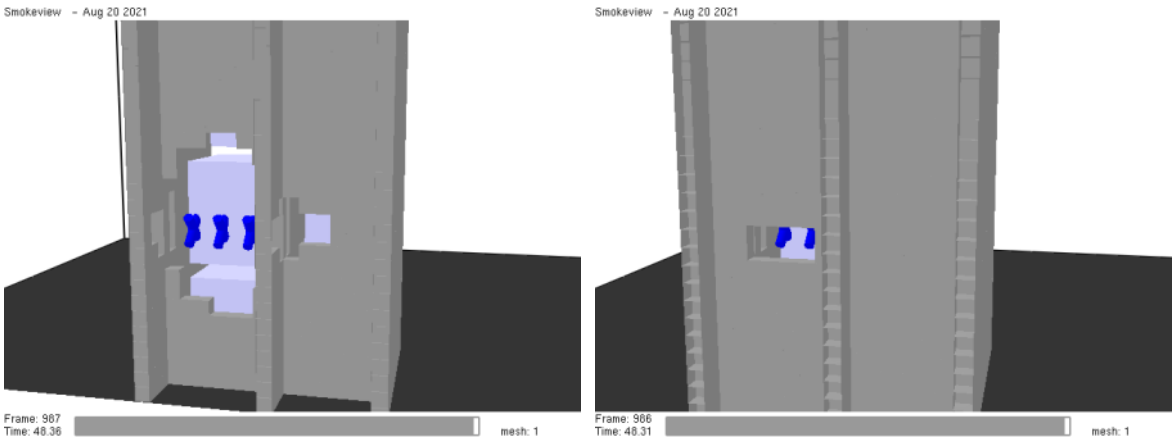

Figure 4-10
FDS-predicted damage for FEDB 50935. Left image clips the back of the enclosure to show the panel separating the breaker cubicles from the bus bar compartment. Right image clips the back face of the enclosure to show the partition between the bus bar compartment and rear connection compartment

4.3 Full-Scale Test of FEDB 51764

The NRC did not conduct any usable laboratory testing of bus duct HEAFs and there is little data against which to compare the FDS modeling results. The EPRI/NRC working group identified two events that could be modeled to support benchmarking: the first was a non-segregated bus duct HEAF that occurred in a U.S. nuclear power plant and was later replicated in full-scale testing at CESI (Keiring van Ekektrotechnische Materialen te Arnhem (KEMA)) laboratories. The second was a generator-fed non-segregated bus duct HEAF that occurred at a different U.S. nuclear power plant.

4.3.1 Summary of Event

On January 17th, 2017, a HEAF occurred in a non-segregated bus duct (FEDB 51764). The event was replicated in a full-scale test on October 3, 2017. The test apparatus consisted of two parallel bus ducts, one located 0.3 m above the other, supported by a frame. The upper duct ("ESST") housing was constructed of 3.2 mm thick steel on the top and sides, however the bottom was a removable cover constructed of aluminum. The ESST duct was 0.64 m wide and 0.42 m high. The lower duct ("SSST") housing was constructed of aluminum. Both ducts contained insulated aluminum bus bars with Glastic bus bar supports every 0.91 m. The ESST bus bars measured 0.015 m wide and 0.15 m high, spaced 0.17 m apart on center. The ends of the ESST duct were 86% covered, leaving an opening of 14%, or approximately 0.036 m².

The arcing fault was initiated at the bottom of the bus bars in the ESST duct. A small area of insulation was removed adjacent to the center bus bar support, and a 3.2 mm hole was drilled near the bottom of each bus bar. A 24-gauge bare tinned copper wire was strung across all three phases to initiate the fault.

The electrical energy delivered to the ESST duct had the following properties:

- 4,500 volts (line-to-line voltage of 650 volts)
- 14,700 amps
- 1.02 s

4.3.2 Discussion of FDS Inputs

A simplified model of the test apparatus was constructed in FDS (Figure 4-11). The model included the ESST duct housing, the ESST bus bars, and the SSST duct housing. The model did not include the frame where the ducts were resting, the bus bars of the SSST duct, or the Glastic bus bar supports, as they are assumed to have no impact on the simulated quantities of interest.

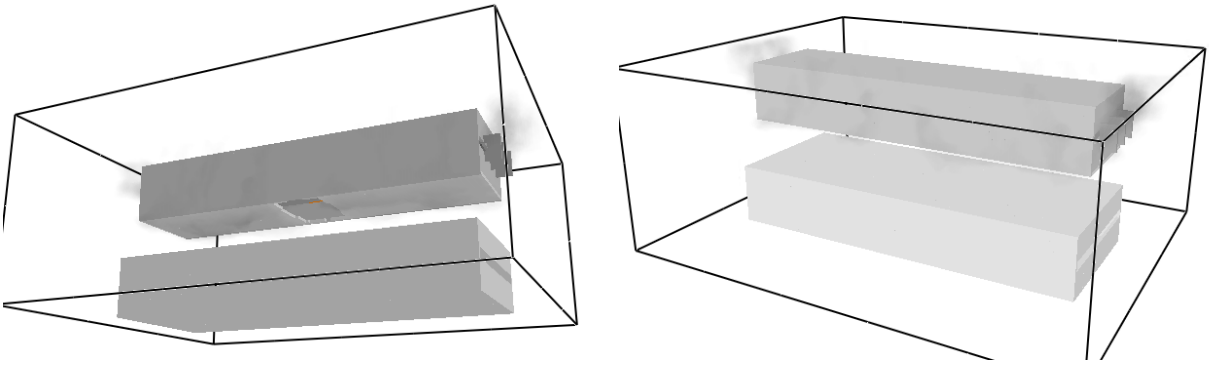

Figure 4-11
FDS-predicted holing in the NSBD test showing bottom of top duct (left) and top of bottom duct (right)

The FDS model relies on several additional assumptions, including:

- Liquid droplets from molten metal do not significantly impact the results and are neglected. (This does not include gaseous particles that oxidize and release energy.)
- The duct housing, while melted, does not participate in any oxidation, or contribute to any heat release. This is because the FDS model was developed to simulate a multi-phase bus bar fault rather than a ground-fault to the aluminum duct housing. For this bus bar fault model, the underlying assumption is the housing would tend to melt in large sections rather than generate significant amounts of oxidizing particles, and this source of energy is not included.
- The fraction of the mass of aluminum bus bar lost that is converted to vapor is 7.5%.
- The bus bar vaporization begins 0.2 s after arc initiation and ends 0.2 s after arc extinguishment.

The report of test states that 0.3 kg of aluminum was lost across all three phases. Using the assumed 7.5% vapor fraction, a total of 0.0225 kg of aluminum vapor was injected into the computational domain using three nozzles located at the arc initiation point on each bus bar to simulate the contribution of oxidizing aluminum.

The total electrical energy delivered to the fault is calculated as:

$$E = \sqrt{3} \times V_{\mathrm{L-L}} \times I_{\mathrm{t}} = \sqrt{3} \cdot 650 \cdot 14700 \cdot 1.02 = 16.88 \text{ MJ}$$

The radiative fraction of the arc energy for an aluminum bus bar is given by Cressault [24] as 0.573. The 16.88 MJ of energy was introduced into the computational domain by specifying a volumetric heat release rate in a volume comparable to that of the arc volume. To avoid numerical instabilities, the heat release rate was ramped up and down over 0.1 s. The heat

release rate volume was biased slightly downward from the center of the duct to replicate the arc initiation location at the bottom of the bus bars.

4.3.3 FDS Simulation Results

The laboratory testing did not include instrumentation to measure temperature, heat flux, or incident energy. The goal of the testing was to investigate whether a fault in the upper duct would impair the lower duct. Accordingly, the benchmark relies on similar qualitative observations. Two points of comparison were used: the time from arc initiation to breach of the duct housings and the size of the duct housing breach.

The bottom aluminum panel of the upper duct was first observed to breach at 0.28 s after the initiation of the arc in the laboratory experiment. FDS predicts an initial breach of the same panel at 0.39 s. This 40% overprediction of time-to-breach is consistent with the results of the MV SWGR modeling.

The size of the breach in the bottom panel is described in the test report as 0.28 m long and 0.58 m wide (0.17 m²) FDS predicts a final breach size of 0.18 m², representing an 11.5% overprediction.

Although there were no measurements of temperature, heat flux, or incident energy taken around the duct in the experiment, there was no observable damage to the steel sides and top of the upper duct, nor the steel housing of the lower duct, which provides some data about the maximum thermal conditions outside the duct. Consistent with these experimental observations, FDS-predicted no damage to any of the steel panels on either of the ducts, though the aluminum panel on the top duct was damaged.

4.4 Bus Duct Event in an Elbow (FEDB 51765)

4.4.1 Summary of Event

A generator-fed HEAF occurred at a vertical elbow in a NSBD with aluminum bus bars and an aluminum duct housing (FEDB 51765) [35]. The HEAF lasted for 15 s until the generator decay resulted in arc extinguishment. A solid-bottom cable tray was located approximately 10 in below the bottom of the elbow, with 5 in of overhang in the horizontal plane. Post event photos show charred cables and molten aluminum slag from the bus bars and duct covers on the cables and in the tray (Figure 4-12). The plant reported that the cables experienced jacket damage and exposed insulation but remained functional. The cables in this tray were Kerite, which can have a fragility threshold between the thermoplastic and thermoset limits depending on the specific formulation [37].

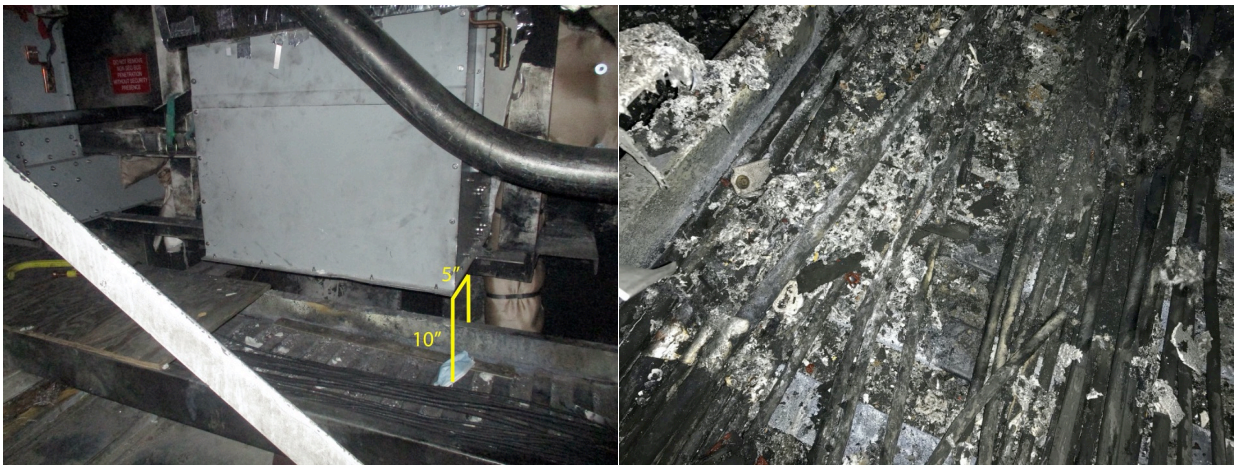

Figure 4-12
Repaired NSBD from the HEAF event showing cable tray location (left), aluminum metal and charred cables in cable tray (right)

4.4.2 Discussion of FDS Inputs

A simplified model of the vertical elbow was constructed in FDS (Figure 4-13). In addition to the arrays of incident energy measurement devices located orthogonally to the faces of the duct near the elbow, an extended array of measurement devices was placed in the region of the cable tray.

Because of the high degree of similarity between this event and the comparably configured ZOI model (elbow geometry, aluminum bus bars, aluminum duct housing, 0 s stiff-source duration, 15 s generator decay duration), the working group elected to use the nominal duct dimensions from the ZOI models: 0.4 m tall, 0.56 m wide and with a duct housing thickness of 3.2 mm, corresponding to 11-gauge sheet metal.

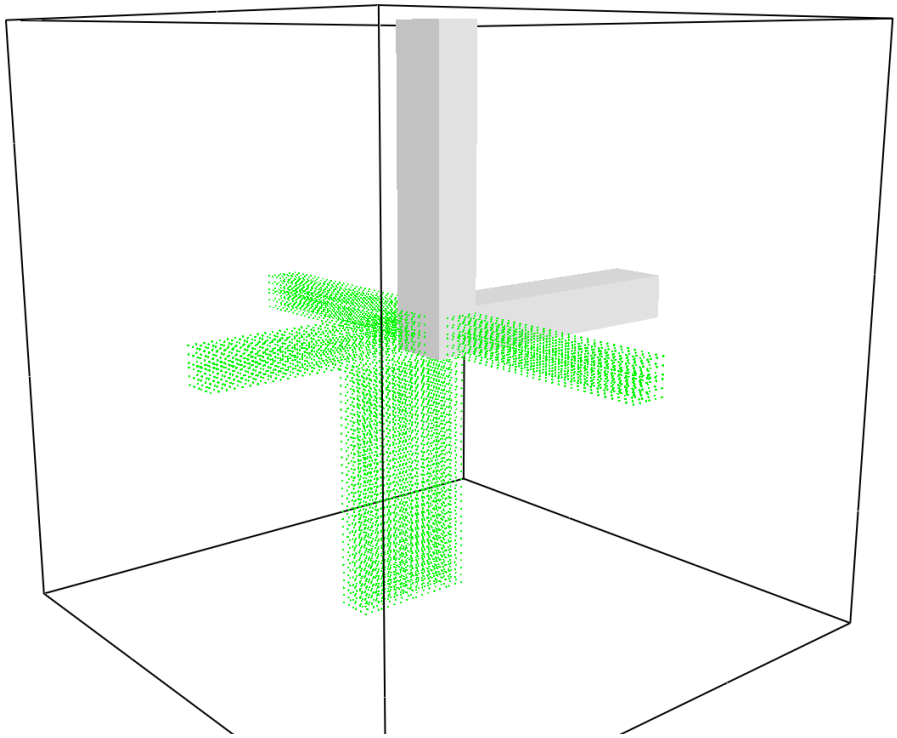

Figure 4-13
FDS model of NSBD vertical elbow. Incident energy measurement devices shown as green dots

The FDS model relies on several assumptions, including:

- The arc is modeled as stationary, despite evidence that during the actual event, the arc initiated several inches away from the elbow in the horizontal portion of the duct and moved towards the elbow. Modeling the Lorentz forces that push the arc along the bus bars is beyond the scope of this effort. Accordingly, the model results are expected to overpredict the incident energies in the region of the cable tray.
- Though the radiative fraction of the arc given by Cressault [24] is dependent upon arc power, a single, static radiative fraction corresponding to the initial arc power is sufficient for generator-fed faults.
- Liquid droplets from molten metal do not significantly impact the results and are neglected. (This does not include gaseous particles that oxidize and release energy.)
- The duct housing, while melted, does not participate in any oxidation nor contribute to any heat release.
- The ends of the duct are open to the computational boundary, i.e., the hot gases that pass through the ends of the duct are no longer accounted for. The computational boundary is sufficiently far from the location of the fault and targets that this is not expected to affect the results.

4.4.3 FDS Simulation Results

A contour plot of the total incident energy in the central plane of the bus duct predicted by FDS is shown in Figure 4-14. The 15 MJ/m² and 30 MJ/m² target fragility thresholds are outlined in magenta and are applicable to the cable targets. The cables in the cable tray are predicted to experience incident energies ranging from 20 MJ/m² to 50 MJ/m² depending on their location within the tray.

Given that the fragility for the Kerite cables should lie between 15 MJ/m² and 30 MJ/m², depending on the formulation, one would expect to see loss of cable functionality across most, if not all, of the cable tray. However, in the actual event, the arc did not start at the elbow; it initiated several inches away in the horizontal segment of the duct and moved towards the elbow. Because the FDS model places the arc at the elbow for the entire duration of the HEAF (due to the generator decay, 30% of the arc energy is released in the first 2 s), some overprediction of incident energy is expected. Considering this overprediction and the near-failure state (damaged jacket, exposed insulation) of the cables in the tray, the results of the simulation are reasonable.

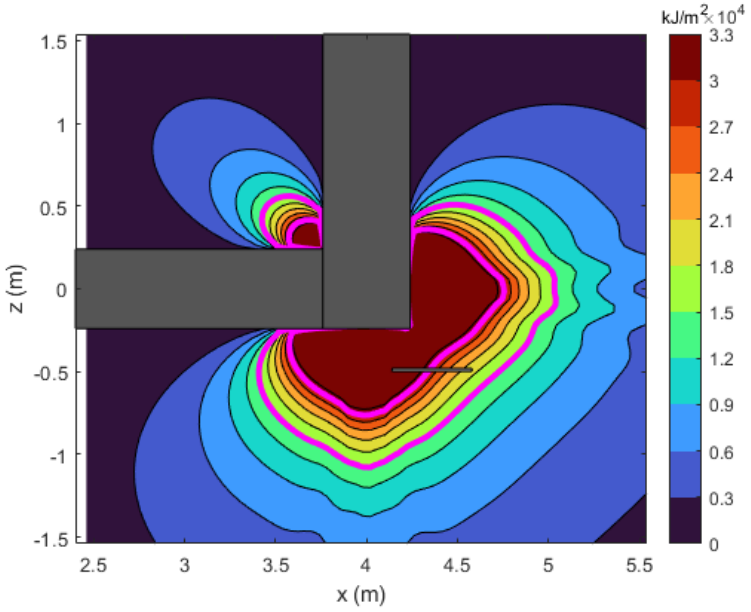

Figure 4-14
Contour plot of the FDS simulation for a 0 s stiff, 15 s decay arc at a NSBD elbow. Approximate location of cable tray for this event shown below bus duct elbow. Magenta contours are the 15 MJ/m² and 30 MJ/m² target fragility thresholds applicable to thermoplastic (TP) and thermoset (TS) cables

4.5 Summary of FDS Validation for Modeling HEAF Events

The validation of the FDS HEAF analysis is based on the following:

- The 2018 MV SWGR experiments [6]
- A LV SWGR event
- A full-scale experiment replicating a NSBD event [7]
- A HEAF event at a NSBD elbow (FEDB 51765)

The 2018 MV SWGR experiments were used to assess FDS for predicting enclosure breach, the extent of the enclosure damage, and the gauge temperature at a fixed location (i.e., target exposure). Overall, the predicted breach time are reasonably well predicted, though there are significant differences in some situations with small predicted external ZOI. Generally, the extent of damage predicted by FDS is comparable to the observed damage extent for the tests considered. Finally, FDS is shown to underpredict the gauge temperature, likely due to differences in the actual versus predicted breach time.

Three of the 2018 MV SWGR experiments are considered in the validation effort and were used to develop the overall relative standard deviation (σ) and bias (δ) applied to the predicted exposure. The resulting relative standard deviation and bias were based on the 4 s switchgear tests given these experiments resulting in the failure of the top and bottom of the enclosure, making leakage around the gaps less important to the total exposure. The resulting relative standard deviation and bias as determined from these FDS predictions and experimental results were 0.71 MJ/m² and 0.57, respectively; however, the relative standard deviation and bias was similar for all instrument locations and tests. The bias is a measure of the under- or over-prediction of FDS is used to adjust the predicted output quantity by M/δ and the 95% confidence interval is given as $(M/\delta)/(1+2\sigma)$ to $(M/\delta)\times(1+2\sigma)$.

The LV SWGR event (FEDB 50935) was used to assess the overall ability of FDS to predict the damage extent. The FDS geometry for the LV SWGR event included a DS enclosure with two columns of breakers. The FDS simulation shows more extensive damage to the separation between the breakers and bus bar compartment than seen in post-event photos.

The NSBD full-scale test was used to assess the capability of FDS to predict the breach time and damage extent. FDS-predicted a longer breach time and comparable damage extent on all sides for this configuration. The HEAF at the NSBD elbow (FEDB 51765), was used to assess the exposure predictions of the FDS analysis approach. In this case, FDS overpredicts the exposure and the damage potential to the target cables when characterized using the 15 MJ/m² target fragility criterion. However, the target cables were Kerite, which could have an intermediate damage threshold between TP and TS cables, depending on the Kerite formulation [37], and some overprediction was expected due to the stationary placement of the arc. As such, it is concluded that the FDS analysis approach was reasonable for this configuration.

From the metrics analyzed for the NSBD benchmarks, the predictive capabilities of FDS are comparable for NSBDs and switchgear enclosures. Because high-quality heat flux data only exists for switchgear enclosures, the HEAF WG chose to use the same bias factor when evaluating the results of the NSBD ZOI simulations.

5
DEVELOPEMNT OF THE HEAF SIMULATION MATRIX

This section discusses the approach for defining HEAFs to be modeled by FDS and used to determine the ZOIs for the MV SWGR, LV SWGR, and NSBDs. Insights into the HEAF ZOI have been obtained from full scale testing, including the OECD and KEMA tests described in Section 4. However, due to the cost of these testing efforts, only a limited number of tests have been performed [7, 27]. With limited full-scale testing, only a small number of the possible configurations and boundary conditions can be tested. While past testing programs yielded insights on important variables that impact the dimensions of the ZOIs, the U.S. OE [11, 12] and the EPRI survey [3] indicated that the U.S. industry has significant variations of these important variables that must be accounted for in the simulations to derive the most realistic ZOIs. The following sections include detailed discussions on the derivation of important variables and the set of simulations combining these variables to account for different physical, equipment, and electrical configurations.

5.1 Development of HEAF Model Simulations

The review of the limited full-scale test results, the open box tests [4–9] and the relevant U.S. OE clearly underlined the importance of variables such as 1) arc energy, 2) the geometry and the electrical physical configuration of the faulted equipment, 3) the location of the arcing fault in relation to the electrical distribution system (which affects the arcing fault duration), and 4) fault origination inside the faulted equipment in determining the level of damage of the faulted equipment and therefore the ZOIs. In addition to the test results that were reviewed, an EPRI survey [3], and insights from HEAF operating experience [12] are used to define the most predominant equipment design, equipment materials (conductor and enclosure), expected fault durations, arcing fault currents and fault locations.

As there are many different equipment designs and electrical configurations across the NPP fleet, the HEAF WG's main objective is to develop ZOIs that could be used for general NPP electrical distribution system design, specific equipment manufacturer and type, and electrical protection scheme characteristics. A large number of plant-specific variables resulted in a significant number of parameter and equation combinations for modeling in FDS to calculate true plant-specific ZOIs. Since the effort is not be economically viable, or possible from a computational resource perspective, the HEAF WG defined a minimum number of HEAF simulations encompassing the most predominant configurations and characteristics. The HEAF WG acknowledges the differences that may exist between actual plant design and the FDS modeled configuration; however, this minimum number of HEAF simulations provide sufficient data to determine the ZOIs for each specific equipment type and electrical distribution alignment.

The purpose of the following sections is to provide the rationale for the selection of the important variables used to develop representative HEAF model simulations for the MV SWGR (Section 5.1.1), LV SWGR (5.1.2), and NSBDs (5.1.3).

5.1.1 Medium Voltage Switchgear

Based on OE events [12] and survey results [3], the HEAF parameters that have the highest impact on the ZOI are listed below.

- Bus bar material: copper or aluminum
- Switchgear manufacturer/models typically found in the NPPs, and used during the full-scale testing/FDS validation[1]:
  - GE Magne-Blast (vertical-lift breaker)
  - ABB HK (horizontal draw-out)
- Fault initiation location:
  - Circuit Breaker
    - Stab connection to the primary cable compartment bus bars or risers
    - Stab connection to main bus bars
    - Circuit breaker internal poles
  - Primary cable compartment bus bars (PCCBBs) or risers (also referred to as a riser compartment)
  - Main bus bars
- Power flow (bus supply or load circuit breaker)
- Energy level (fault current, fault durations and arc voltage):
  - Best estimate fault current of 30 kA
  - Arc fault durations
    - Arcing fault duration of 2 to 5 s for simulating arcing faults with constant-current. The expected range of 2 to 5 s is obtained from transformer back-up fault clearing time provided in the EPRI survey results [3]
    - Generator-fed faults of up to 15 s in duration, with generator current decay during the coast-down immediately after a unit trip
  - Arc voltage was set at 650 V_{L-L}, value derived from the full-scale testing (see Appendix A)

5.1.1.1 Bus Bar Material

The EPRI survey [3] found that almost half of the US NPP fleet has MV SWGR bus bar material made from aluminum and the other half is copper. From the HEAF testing program, it was not clear if the electrode composition (e.g., copper versus aluminum) was a significant factor in determining target exposure and the associated ZOI. Therefore, both materials are considered in the FDS modeling of bus bar faults (main bus bars or the riser/primary compartment bus bars). Only copper was used to simulate faults occurring at the circuit breaker connections, since aluminum is not used for the construction of the current carrying portions of circuit breakers in U.S. NPP switchgear.

5.1.1.2 Switchgear Type and Breaker Orientation

The EPRI survey that collected the MV SWGR manufacturer/model designs revels that 89% of the switchgear that contain aluminum in the U.S. fleet are either GE Magne-Blast, ABB/ITE HK,

[1]There are other types and designs of the MV SWGR in the U.S. fleet. Subsection 5.2.1.2 explains the difference between the designs and provides justification on why modeling only these two types and designs is adequate for defining the ZOIs for similar types/designs.

or Westinghouse DHP switchgear. The remaining 11% (other) is comprised of Gould, Siemens Type 3AH, and Allis Chalmers switchgear (see Figure 5-1).

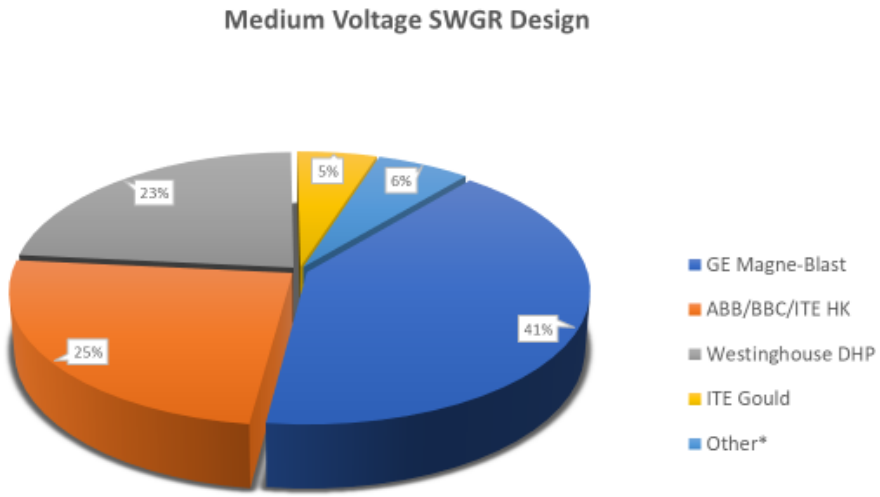

Figure 5-1
MV SWGR designs with aluminum

As for the configurations, the EPRI survey indicates that there are two circuit breaker/switchgear orientation styles of MV SWGR: horizontal draw-out and vertical-lift breaker. Identifying the configuration style of MV SWGR is important in the understanding how that particular configuration can influence the HEAF arc jet direction and time to cabinet breach. Per the EPRI survey results, 55% of the GE Magne-Blast MV SWGR are horizontal draw-out style and 45% are vertical-lift breaker style. Since all other MV SWGR manufacturers used in U.S. NPPs produce only horizontal draw-out style, the GE Magne-Blast vertical-lift breaker switchgear represents 17% of the entire population of MV SWGR containing aluminum (see Figure 5-2).

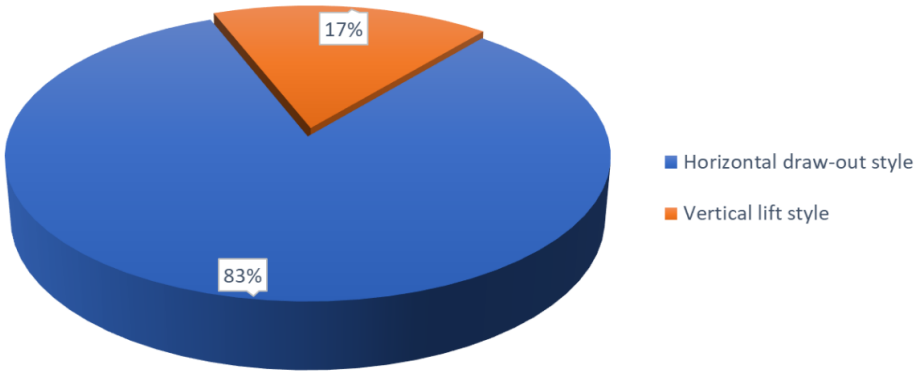

Figure 5-2
Breaker orientation for MV SWGR designs with aluminum

The three common switchgear manufacturer/models and orientations (vertical-lift breaker versus horizontal draw-out) are further reviewed to compare similarities between the internal compartment design and location of various current carrying subcomponents. Simplified cross sections of the switchgear are in Figure 5-3 through Figure 5-5.

The configurations of the internal compartments are observed to be relatively similar, particularly when comparing the horizontal style circuit breaker switchgear (Westinghouse DHP, GE Magne-Blast and ABB HK). The internal compartments in general have similar physical dimensions and the number of barriers necessary to result in external cabinet breach are also similar.

The difference identified most likely to have an effect on the ZOI is whether the SWGR is the vertical-lift breaker style or the horizontal draw-out style. The two different switchgear styles result in similar fault locations for horizontal distances from the cabinet sides and rear compartments; however, for faults occurring in the circuit breaker or at the circuit breaker stab connections, the configuration of the horizontal style switchgear has the mass of the circuit breaker between the fault locations and the front of the switchgear cabinet. The circuit breaker will provide a barrier at the front of the switchgear that will shield a large portion of the HEAF energy, limiting the exposure to the targets outside of the cabinet. The vertical-lift breaker style switchgear does not have the breaker between the front of the cabinet and circuit breaker stab connections where arcing can occur. This shielding effect necessitates the modeling of the breaker mass in evaluating the differences between these two switchgear styles.

The following two MV SWGR designs are modeled in FDS for the representative HEAF simulations: GE Magne-Blast (vertical-lift breaker) and ABB HK (horizontal draw-out). The full-scale tests on the MV SWGR also used the GE Magne-Blast (vertical-lift breaker), used for benchmarking and validation purposes. Small variations in equipment geometry do not significantly impact the ZOIs.

For plants that have horizontal draw-out switchgear other than ABB HK (such as Westinghouse DHP, Gould, Siemens Type 3AH, and Allis Chalmers), the use of the resulting ZOIs is justified based on the similarity of the most important features of the horizontal draw-out breaker designs with respect to the FDS model geometry. Both switchgear designs configurations have similar locations for the circuit breaker in relation to the circuit breaker stabs. Different horizontal draw-

out SWGR have sufficiently similar layout and, therefore, the ZOIs will not differ significantly across manufacturers.

Observed and potential fault locations on the selected SWGR designs (GE Magne-Blast and ABB HK) are shown as the red circles on Figure 5-3 and Figure 5-4 based on U.S. HEAF OE and the HEAF WG investigations. To reduce the number of FDS simulations (while preserving the overall fault locations), additional insights from early sensitivity analyses and WG expertise were considered.

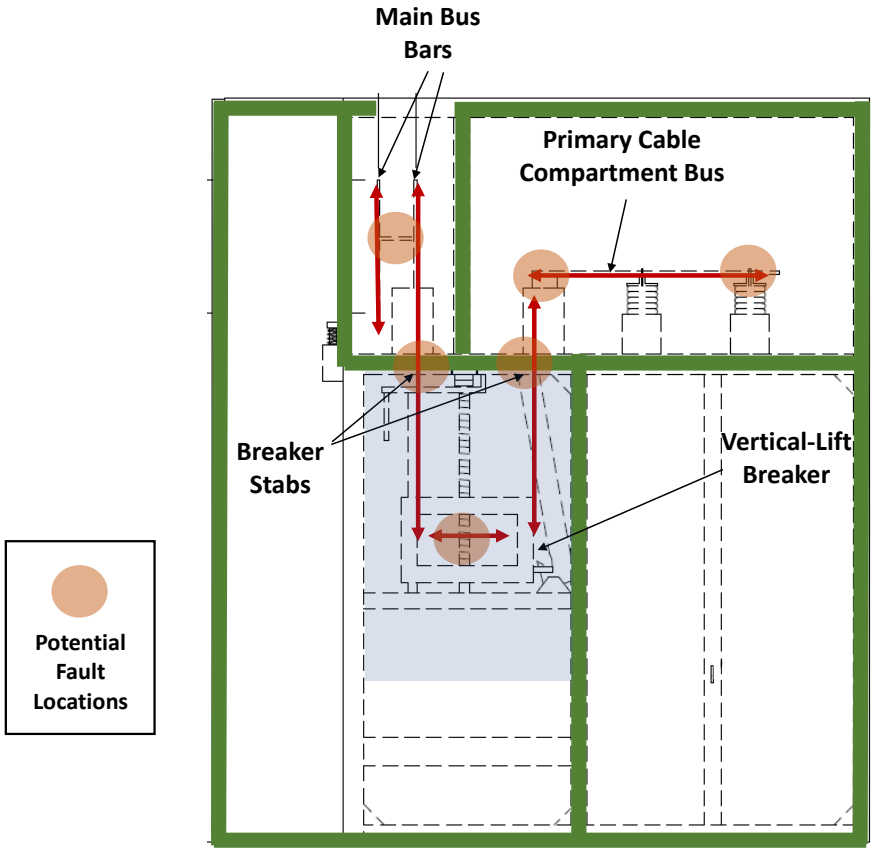

Figure 5-3
GE Magne-Blast vertical-lift breaker switchgear

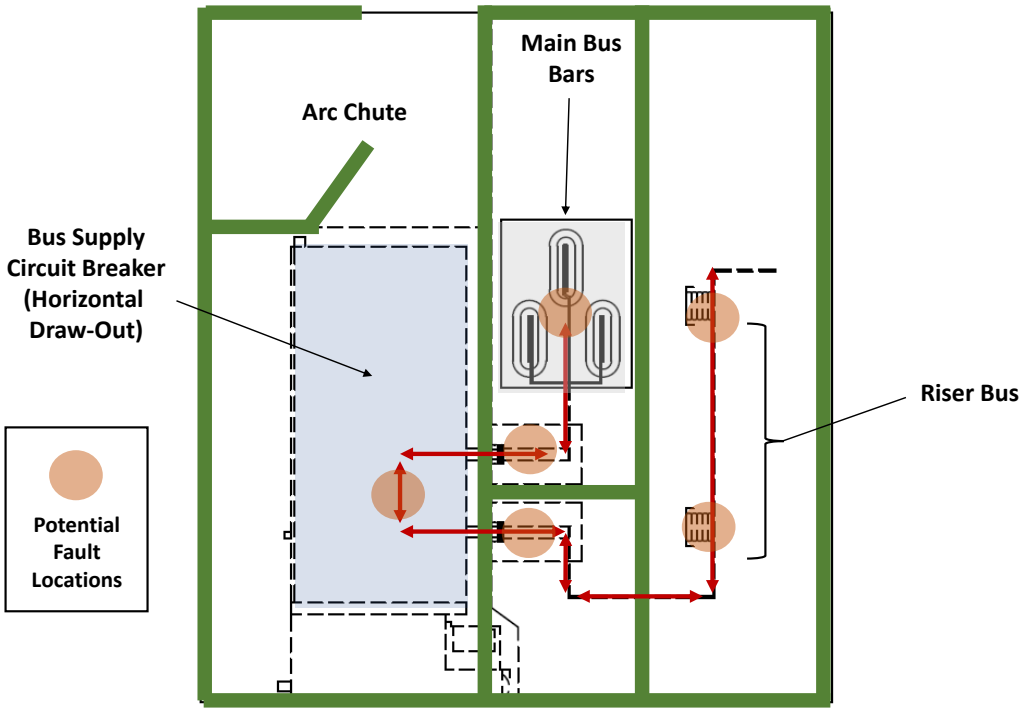

Figure 5-4
ABB/ITE HK horizontal draw-out switchgear

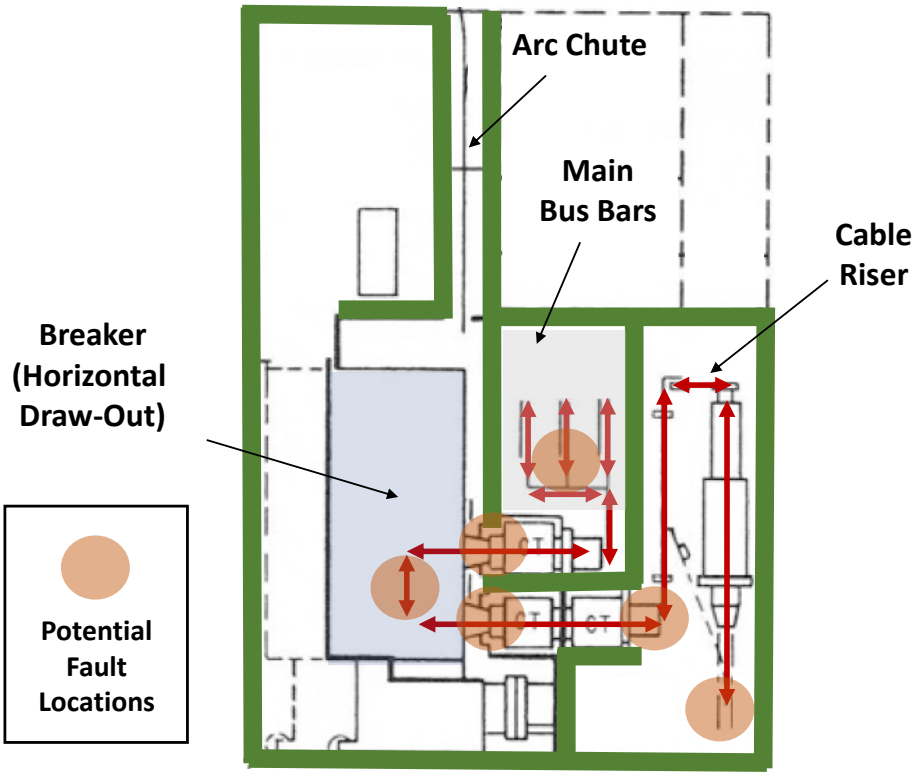

Figure 5-5
Westinghouse DH-P horizontal draw-out switchgear

5.1.1.3 Fault Location and Power Flow

The fault locations are representative of the U.S. HEAF operating experience [12]. Of the seven US MV SWGR HEAF events, four originated at the circuit breakers for the switchgear bus supply due to either high resistance connections at the circuit breaker cubicle stabs or as a result of internal circuit breaker failures. Three of the four events occurred during or immediately following a switching demand associated with a bus transfer. Each event resulted in a generator-fed HEAF due to the failure of the single circuit breaker to isolate the residual rotating energy from the tripped generator. The remaining three events occurred outside the switchgear circuit breaker cubicle as follows:

- One HEAF occurred where the incoming power supply cable faulted at the switchgear enclosure entry
- One HEAF was a result of the main bus bar failure
- One HEAF was a result of insulation failure on the switchgear primary cable compartment bus

Figure 5-6 illustrates the location of the breaker stabs, primary compartment bus bars and main bus bars from the GE Magne-Blast vertical-lift breaker SWGR design.

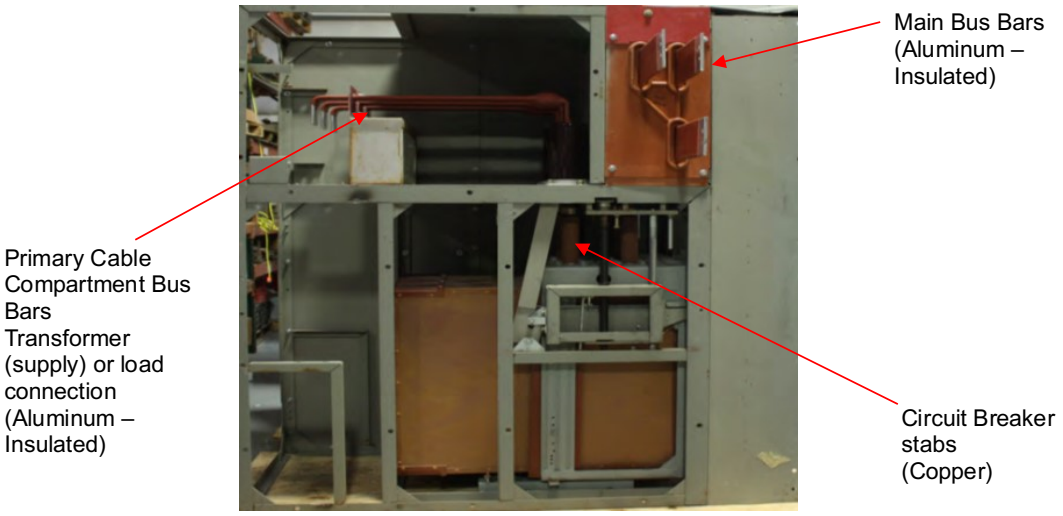

Figure 5-6
GE Magne-Blast vertical-lift breaker SWGR showing location of breaker stabs, primary compartment bus bars, and the main bus bars

FDS models the energy from the arc in a volumetric space. For small volumes, such as the circuit breaker or at the circuit breaker stab connections, the model ZOI results are expected to be similar provided these locations are in the same general area. Therefore, the fault locations of the load and line side breaker stab connections were consolidated with the circuit breaker fault location, eliminating two variables in the fault location.

The load and supply circuit breaker power flow are not a direct input variable considered in FDS; however, it is a variable in the expected directionality of the arc since magnetic forces will push the arc along the conductor until impeded. In reviewing the horizontal draw-out style switchgear (Figure 5-4 and Figure 5-5**),** the configuration of the switchgear vertical riser bus section in the supply (current flow from the riser/primary compartment bus to the breaker) or load (current flows from the main bus to the breaker) does not affect the distance of the fault location with respect to the back face of the switchgear, which means the ZOIs will be the same.

For the vertical-lift breaker switchgear, the primary cable compartment bus (upper right compartment shown in Figure 5-3) utilizes a horizontal run bus bar. For faults in the supply configuration, the arc will be pushed to the end of the bus bar. For the load configurations the arc will be pushed to the closet point on the bus bar towards the rear cabinet wall.

Figure 5-7 and Figure 5-8 show the final configurations of switchgear breaker orientation types and fault locations modeled in FDS.

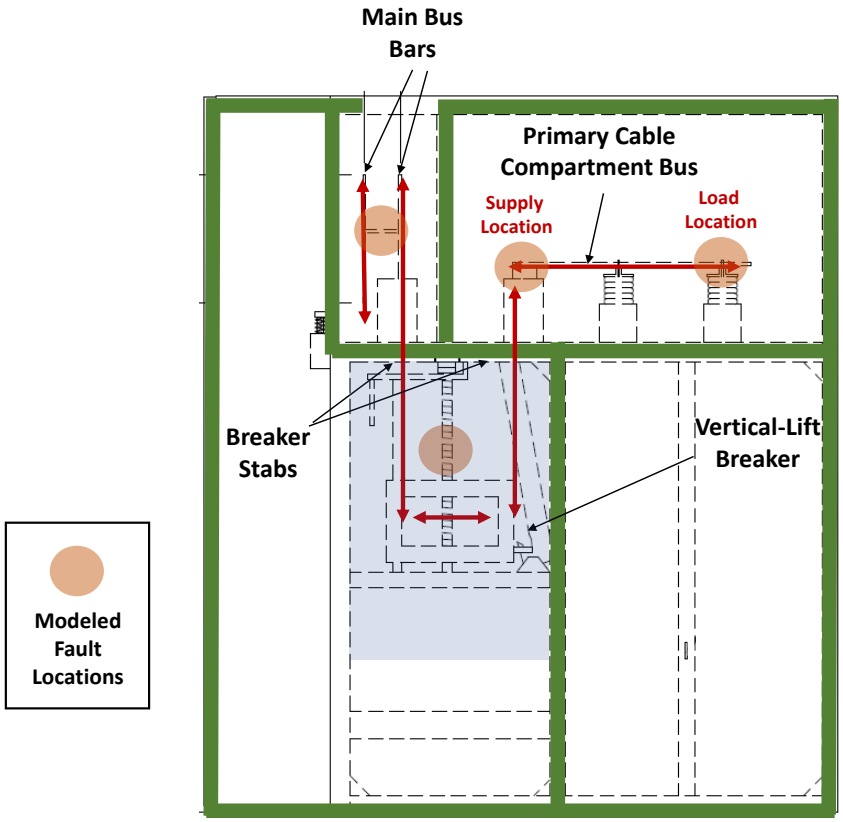

Figure 5-7
Vertical-lift breaker switchgear with consolidated fault locations

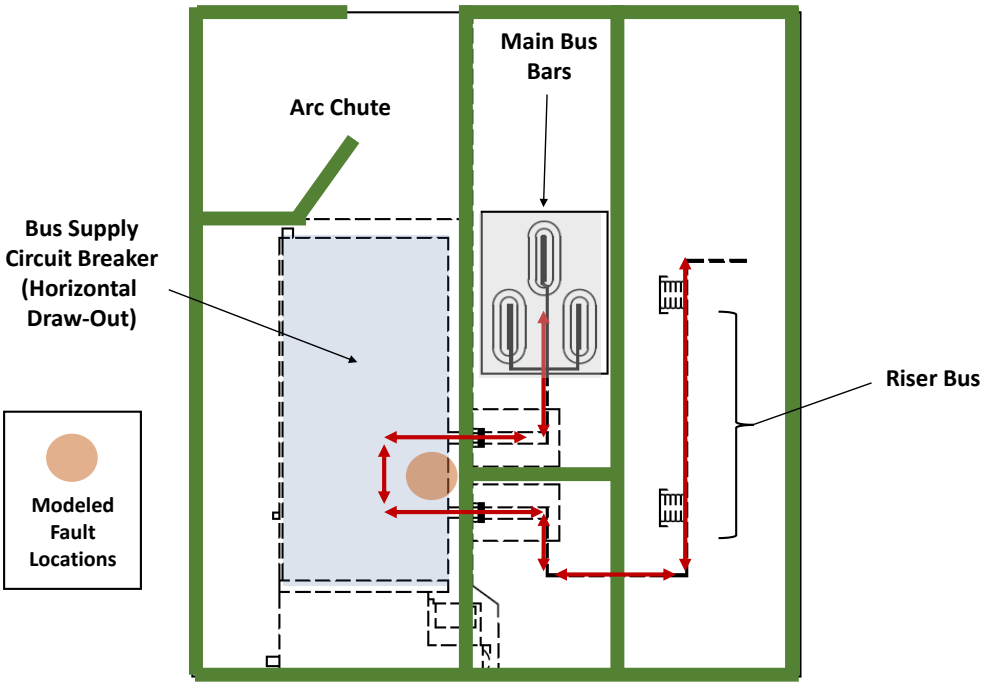

Figure 5-8
Horizontal draw-out switchgear with consolidated fault locations

5.1.1.4 Arc Current and Voltage

A constant arc voltage of 650 V_{L-L} is used for the for the MV SWGR regardless of the system voltage. This value was derived from the available HEAF testing data as explained in Appendix A.

For arcing faults with a stiff-source (constant-current and voltage) simulating a three-phase low impedance fault, the arcing current is constant until the overcurrent protective device trips and isolates the faulted equipment. The arcing current depends on multiple parameters such as bolted fault current, system voltage, grounding types, enclosure type, and other variables that are not always readily available and known. Determining the arcing fault current for each MV SWGR is not a trivial exercise. For this analysis, the fault current will be selected based on observed values from U.S. MV SWGR operating experience [12]. The range of fault currents varied from 28 kA to 32 kA. The middle of the range, 30 kA, is used for the arc energy calculation. See Appendix A for a list of HEAF events with known fault currents.

As for generator-fed faults, the arc voltage for the arc energy calculation is the same as above with the exception that the arc current is no longer constant but rather decays with time. The arcing current decays exponentially based on the time it takes the generator to coast down to a voltage level at which the arc fault can no longer be sustained. The current decay profile of a generator-fed HEAF event is discussed and shown in Appendix A. This decaying current profile is simulated in FDS for the generator-fed HEAFs.

5.1.1.5 Arcing Fault Duration

The arcing fault duration is a significant factor in determining the arc energy level during a HEAF. The fault durations are determined by the overcurrent protective element settings in the NPP's electrical distribution system. It has been observed in U.S. HEAF OE [12] that HEAF

events generally involve a failure of the circuit breaker or time over-current protection and relied on the upstream or back-up time over-current protection to clear the fault, or in cases of generator-fed faults, there is no back-up overcurrent protection or circuit breaker to clear the fault.

EPRI conducted a survey [3] in which the U.S. NPPs provided the fault clearing time (FCT) of the back-up time overcurrent protection for the auxiliary transformers. This data set along with a review of coordination calculations for a sampling of plants, indicated that the expected duration of the fault clearing time is typically 2 s, but can last up to 5 s. This fault clearing time is applicable for the constant-current faults (stiff-source). Testing demonstrated that arc faults in MV switchgear under a 2 s duration do not have sufficient energy reach HEAF thresholds. A minimum threshold of 2 s is sufficient to bound arc faults at 2 s and under. The arcing fault duration for the constant-current faults simulated in FDS is selected as a low (2 s), a mid (4 s), and a high point (5 s). The selection of these values allowed a curve fit against a power trendline.

Generator-fed faults in historical U.S. HEAF OE [12] have little data available as to the actual duration of the arcing fault. Data from a recent HEAF event (FEDB 51765) summarized in Section 4.5.1 was used to characterize the generator-fed fault energy and duration. In this event, the generator tripped within several cycles of the fault; however, the residual energy of the generator continued to feed the fault for an additional 15 s. The current decay profile over the 15 s duration is shown in Appendix A. There is a potential for generator-fed arc faults to occur outside the instantaneous differential fault protection zone in which a time over-current device wis relied on to trip the generator. This delay causes the energy profile to be that of a constant-current fault followed by the generator decay profile after the generator is tripped (via generator protection). The delay times selected include 0 s, 3 s, and 5 s, all with a subsequent generator decay profile. Theses profiles are seen in Appendix A.

5.1.1.6 Arc Energies

The arc energies considered for the medium-voltage switchgear constant-current arc faults are calculated as:

$$\text{Arc Energy} = \text{Arc Current} \cdot \text{Line-to-Line Arc Voltage} \cdot \text{Arcing fault Duration} \cdot \sqrt{3}$$

This equates to energies of 68 MJ for the 2 s constant arc fault, 135 MJ for the 4 s constant arc fault, and 169 MJ for the 5 s constant arc fault as seen in Table 5-1.

The generator-fed faults are the summation of the delay time in the above equation and an additional 131 MJ of energy based on the generator decay profile associated with a generator-fed fault (see Figure A-1 through Figure A-5 in Appendix A for the resulting arc power profiles).

This equates to energies of 131 MJ for the 2 s constant arc fault followed by a 15 s generator-fed fault, 232 MJ for a 4 s constant arc fault followed by a 15 s generator-fed fault, and 300 MJ for a 5 s constant arc fault followed by a 15 s generator-fed fault as seen in Table 5-1.

5.1.1.7 Medium Voltage Switchgear FDS Simulation Matrix

Sections 5.1.1.1 through 5.1.1.6 provide details on the important parameters for the MV SWGR ZOIs. The resulting minimum number of FDS HEAF simulations developed from these parameters by the WG is summarized in Table 5-1. The overall results of these FDS MV SWGR HEAF simulations are used by the HEAF WG to derive the ZOIs.

Table 5-1.
FDS MV SWGR HEAF simulations

HEAF ID	Encl. Material	Bus Bar Material	Switch-gear Type	Breaker Orien-tation	Fault Location	Power Config-uration	Arc Voltage (V_{L-L})	Arc Current (kA)	Power (MW)	Stiff (s)	Decay (s)	Arc Energy (MJ)
MV-GE-33	Steel	Copper	GE Magne-Blast	Vertical	Riser/Primary Compartment Bus Bars	Load	650	30	23	0	15	131
MV-GE-11	Steel	Aluminum	GE Magne-Blast	Vertical	Riser/Primary Compartment Bus Bars	Load	650	30	23	0	15	131
MV-GE-32	Steel	Copper	GE Magne-Blast	Vertical	Main Bus Bars	Supply/ Load	650	30	23	0	15	131
MV-GE-10	Steel	Aluminum	GE Magne-Blast	Vertical	Main Bus Bars	Supply/ Load	650	30	23	0	15	131
MV-GE-31	Steel	Cu (Breaker)	GE Magne-Blast	Vertical	Circuit Breaker	Supply/ Load	650	30	23	0	15	131
MV-ABB-4	Steel	Cu (Breaker)	ABB/ITE HK	Hori-zontal	Circuit Breaker	Supply/ Load	650	30	23	0	15	131
MV-GE-21	Steel	Copper	GE Magne-Blast	Vertical	Riser/Primary Compartment Bus Bars	Load	650	30	33.8	2	0	68
MV-GE-2	Steel	Aluminum	GE Magne-Blast	Vertical	Riser/Primary Compartment Bus Bars	Load	650	30	33.8	2	0	68
MV-GE-20	Steel	Copper	GE Magne-Blast	Vertical	Main Bus Bars	Supply/ Load	650	30	33.8	2	0	68
MV-GE-1	Steel	Aluminum	GE Magne-Blast	Vertical	Main Bus Bars	Supply/ Load	650	30	33.8	2	0	68
MV-GE-19	Steel	Cu (Breaker)	GE Magne-Blast	Vertical	Circuit Breaker	Supply/ Load	650	30	33.8	2	0	68

HEAF ID	Encl. Material	Bus Bar Material	Switch-gear Type	Breaker Orien-tation	Fault Location	Power Config-uration	Arc Voltage (V_{L-L})	Arc Current (kA)	Power (MW)	Stiff (s)	Decay (s)	Arc Energy (MJ)
MV-ABB-1	Steel	Cu (Breaker)	ABB/ITE HK	Hori-zontal	Circuit Breaker	Supply/ Load	650	30	33.8	2	0	68
MV-GE-37	Steel	Copper	GE Magne-Blast	Vertical	Riser/Primary Compartment Bus Bar	Load	650	30	33.8	3	15	232
MV-GE-14	Steel	Aluminum	GE Magne-Blast	Vertical	Riser/Primary Compartment Bus Bar	Load	650	30	33.8	3	15	232
MV-GE-36	Steel	Copper	GE Magne-Blast	Vertical	Main Bus Bars	Supply/ Load	650	30	33.8	3	15	232
MV-GE-13	Steel	Aluminum	GE Magne-Blast	Vertical	Main Bus Bars	Supply/ Load	650	30	33.8	3	15	232
MV-GE-35	Steel	Cu (Breaker)	GE Magne-Blast	Vertical	Circuit Breaker	Supply/ Load	650	30	33.8	3	15	232
MV-ABB-5	Steel	Cu (Breaker)	ABB/ITE HK	Hori-zontal	Circuit Breaker	Supply/ Load	650	30	33.8	3	15	232
MV-GE-25	Steel	Copper	GE Magne-Blast	Vertical	Riser/Primary Compartment Bus Bar	Load	650	30	33.8	4	0	135
MV-GE-5	Steel	Aluminum	GE Magne-Blast	Vertical	Riser/Primary Compartment Bus Bar	Load	650	30	33.8	4	0	135
MV-GE-24	Steel	Copper	GE Magne-Blast	Vertical	Main Bus Bars	Supply/ Load	650	30	33.8	4	0	135
MV-GE-4	Steel	Aluminum	GE Magne-Blast	Vertical	Main Bus Bars	Supply/ Load	650	30	33.8	4	0	135
MV-GE-23	Steel	Cu (Breaker)	GE Magne-Blast	Vertical	Circuit Breaker	Supply/ Load	650	30	33.8	4	0	135

HEAF ID	Encl. Material	Bus Bar Material	Switch-gear Type	Breaker Orien-tation	Fault Location	Power Config-uration	Arc Voltage (V_{L-L})	Arc Current (kA)	Power (MW)	Stiff (s)	Decay (s)	Arc Energy (MJ)
MV-ABB-2	Steel	Cu (Breaker)	ABB/ITE HK	Hori-zontal	Circuit Breaker	Supply/ Load	650	30	33.8	4	0	135
MV-GE-29	Steel	Copper	GE Magne-Blast	Vertical	Riser/Primary Compartment Bus Bar	Load	650	30	33.8	5	0	169
MV-GE-41	Steel	Copper	GE Magne-Blast	Vertical	Riser/Primary Compartment Bus Bar	Load	650	30	33.8	5	15	300
MV-GE-8	Steel	Aluminum	GE Magne-Blast	Vertical	Riser/Primary Compartment Bus Bar	Load	650	30	33.8	5	0	169
MV-GE-17	Steel	Aluminum	GE Magne-Blast	Vertical	Riser/Primary Compartment Bus Bar	Load	650	30	33.8	5	15	300
MV-GE-28	Steel	Copper	GE Magne-Blast	Vertical	Main Bus Bars	Supply/ Load	650	30	33.8	5	0	169
MV-GE-40	Steel	Copper	GE Magne-Blast	Vertical	Main Bus Bars	Supply/ Load	650	30	33.8	5	15	300
MV-GE-7	Steel	Aluminum	GE Magne-Blast	Vertical	Main Bus Bars	Supply/ Load	650	30	33.8	5	0	169
MV-GE-16	Steel	Aluminum	GE Magne-Blast	Vertical	Main Bus Bars	Supply/ Load	650	30	33.8	5	15	300
MV-GE-27	Steel	Cu (Breaker)	GE Magne-Blast	Vertical	Circuit Breaker	Supply/ Load	650	30	33.8	5	0	169
MV-GE-39	Steel	Cu (Breaker)	GE Magne-Blast	Vertical	Circuit Breaker	Supply/ Load	650	30	33.8	5	15	300
MV-ABB-3	Steel	Cu (Breaker)	ABB/ITE HK	Hori-zontal	Circuit Breaker	Supply/ Load	650	30	33.8	5	0	169

HEAF ID	Encl. Material	Bus Bar Material	Switch-gear Type	Breaker Orien-tation	Fault Location	Power Config-uration	Arc Voltage (V_{L-L})	Arc Current (kA)	Power (MW)	Stiff (s)	Decay (s)	Arc Energy (MJ)
MV-ABB-6	Steel	Cu (Breaker)	ABB/ITE HK	Hori-zontal	Circuit Breaker	Supply/ Load	650	30	33.8	5	15	300
MV-ABB-34	Steel	Copper	GE Magne-Blast	Vertical	Riser/Primary Compartment Bus Bar	Supply	650	30	23	0	15	131
MV-GE-12	Steel	Aluminum	GE Magne-Blast	Vertical	Riser/Primary Compartment Bus Bar	Supply	650	30	23	0	15	131
MV-GE-22	Steel	Copper	GE Magne-Blast	Vertical	Riser/Primary Compartment Bus Bar	Supply	650	30	33.8	2	0	68
MV-GE-3	Steel	Aluminum	GE Magne-Blast	Vertical	Riser/Primary Compartment Bus Bar	Supply	650	30	33.8	2	0	68
MV-GE-38	Steel	Copper	GE Magne-Blast	Vertical	Riser/Primary Compartment Bus Bar	Supply	650	30	33.8	3	15	232
MV-GE-15	Steel	Aluminum	GE Magne-Blast	Vertical	Riser/Primary Compartment Bus Bar	Supply	650	30	33.8	3	15	232
MV-GE-26	Steel	Copper	GE Magne-Blast	Vertical	Riser/Primary Compartment Bus Bar	Supply	650	30	33.8	4	0	135
MV-GE-6	Steel	Aluminum	GE Magne-Blast	Vertical	Riser/Primary Compartment Bus Bar	Supply	650	30	33.8	4	0	135
MV-GE-30	Steel	Copper	GE Magne-Blast	Vertical	Riser/Primary Compartment Bus Bar	Supply	650	30	33.8	5	0	169

HEAF ID	Encl. Material	Bus Bar Material	Switch-gear Type	Breaker Orien-tation	Fault Location	Power Config-uration	Arc Voltage (V_{L-L})	Arc Current (kA)	Power (MW)	Stiff (s)	Decay (s)	Arc Energy (MJ)
MV-GE-9	Steel	Copper	GE Magne-Blast	Vertical	Riser/Primary Compartment Bus Bar	Supply	650	30	33.8	5	15	300
MV-GE-42	Steel	Aluminum	GE Magne-Blast	Vertical	Riser/Primary Compartment Bus Bar	Supply	650	30	33.8	5	0	169
MV-GE-18	Steel	Aluminum	GE Magne-Blast	Vertical	Riser/Primary Compartment Bus Bar	Supply	650	30	33.8	5	15	300

5.1.2 Low Voltage Switchgear

Based on OE events [12], survey results [3], and the insights from the full-scale testing [5], the HEAF parameters that have the highest impact on the ZOI are listed below:

- Bus bar material: copper or aluminum
- Switchgear manufacturer/models/geometry typically found in the NPPs, and used during the full-scale testing/FDS validation
- Fault initiation location: circuit breaker connection to cubicle switchgear bus stabs

Per the HEAF OE [12], only two LV SWGR HEAF events occurred in the United States. FEDB 50935 [12] reported information with respect to the arc current and the arcing fault duration. These values are used to determine the arc energy simulated in FDS and used as a surrogate arc energy for all LV SWGR HEAF ZOIs. Discussion and justifications are provided in Appendix A.

- Energy level (fault current, fault durations and arc voltage):
    - The arcing current profile of 5.85 kA for 20 s and 2.75 kA for 21 s is used as a surrogate for the LV SWGR HEAF events modeled in FDS
    - Arc voltage was set at 375 V_{L-L}, (derived from the full-scale testing)

5.1.2.1 LV SWGR Type and Arc Initiation Location

EPRI survey results [3] determined that 86% of the LV switchgear designs that contain aluminum in the U.S. nuclear fleet are either ABB/ITE K Line, GE AKD, or Westinghouse Type DS. The remaining 14% are: Westinghouse DB, Allis Chalmers, Powell Nelson, LVME, Sorgel, ABB RLN, or LMAZ-LK-32 C-IC.

The three most common types of LV SWGR containing aluminum were compared to highlight any major difference in design (geometry, free volume, barrier usage, etc.). The main bus compartment arrangements of these LV SWGRs are similar between manufacturers (i.e., vertically stacked circuit breakers connected to a vertical bus for each load center tower, with each adjacent load center tower connected by horizontal main bus bars). For the supply circuit breaker, the incoming bus is typically horizontal and is powered by the LV SWGR transformer. Finally, short sections of bus connecting the line side of the circuit breaker to the vertical main bus bars are commonly referred to as the jumper bus. Although some bus bar spacing and dimensional differences exist between manufacturers, the overall geometry, free volume, bus bar arrangements, and lack of arc trapping barriers of the three major U.S. types of LV SWGR are evaluated and are similar. Similarity between the LV SWGR designs reduces the number of simulations in FDS since the ZOIs are expected to be similar for all major LV SWGR designs.

The majority of the LV HEAF testing was performed using the Westinghouse Type DS cabinet design (Figure 5-9). For most of these tests, the fault was initiated at the bus bars in the main bus bar middle compartment where the aluminum bus is located. For most LV tests performed with the Westinghouse Type DS (with the fault location at the bus bars), the arc self-extinguished before reaching the intended test duration. Although many tests were performed with the arc initiated at the main compartment bus bars, very limited data from the LV SWGR testing was used for the FDS benchmarking and validation due to the lack of arc sustainability; and as such, there was no cabinet breaching and, therefore, no ZOIs.

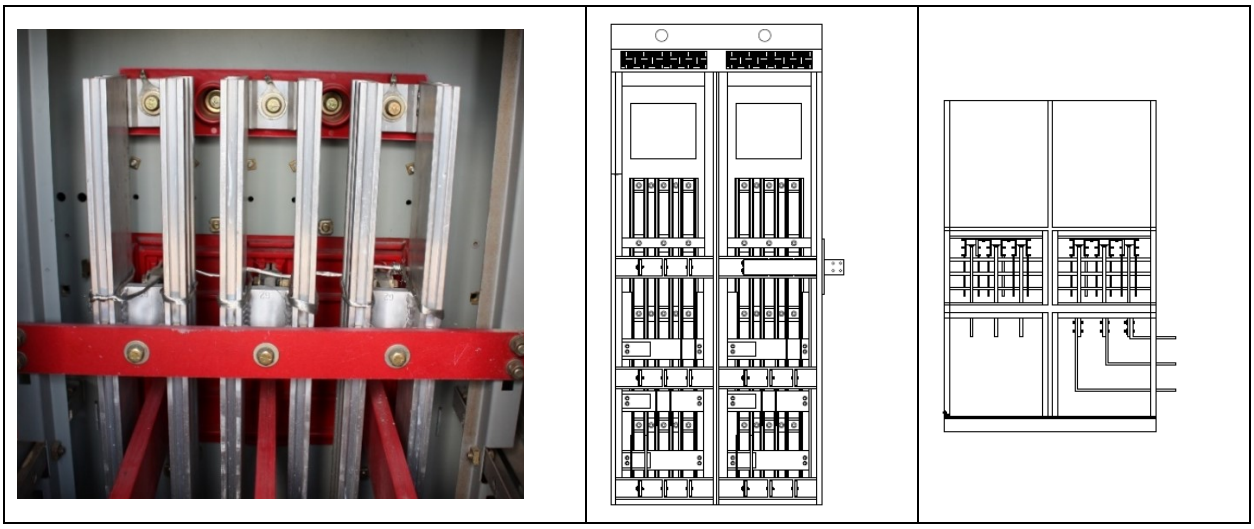

Figure 5-9
Westinghouse DS electrical cabinet and arc test location [5]

Due to the limited number of the HEAF events in OE [12] and the lack of directly applicable test data from the HEAF testing program, several fault locations were modeled in FDS to determine the impact on the ZOIs. LV HEAF testing highlighted the lack of sustainability at the bus bars located on the back of the cabinet, therefore this location was not selected for the FDS simulations. Based on this, arcs were simulated at the breaker and mid compartment (jumper bus). Arc relocation between the breaker and the aluminum bus bars, as observed in the FEDB 50935, was also simulated.

5.1.2.2 Bus Bar Material

The EPRI survey results [3] show that almost 60% of US NPPs have LV SWGR with aluminum bus bars while the other 40% have copper bus bars. From the HEAF testing program it was not conclusive if the electrode composition (i.e., copper versus aluminum) was a significant factor in determining target exposure and the associated ZOI. Both aluminum and copper bus bar materials are considered in the FDS modeling of the fault locations that initiate in the mid-main bus bar compartment or arc migration from the breaker to the mid compartment.

Arcs that initiate at the breaker stabs involve copper electrode materials given the breaker stabs use copper. Although there are no configurations with aluminum, arcs that initiate in the breaker stabs are evaluated with both copper and aluminum to further assess the differences in the ZOIs as a result of the electrode material. In addition, the arc simulations that are representative of FEDB 50935 in which the arc begins at the breaker stabs and migrates to the bus bar compartment use aluminum rather than copper since aluminum electrodes have the potential for a larger ZOI and will bound the uncertainty in the transition time from one compartment to the other.

5.1.2.3 Arc Current, Voltage, and Duration

The arcing current profile of 5.85 kA for 20 s and 2.75 kA for 21 s is selected to simulate FEDB 50935. The arc voltage of 375 V_{L-L} is selected. The profiles for arcing current and arc power documented in Appendix A. Sensitivity studies are performed to compare a larger fault of 21.5 kA on a low-voltage switchgear with various durations of 2 s, 4 s, and 6 s.

5.1.2.4 Low Voltage Switchgear FDS Simulation Matrix

Section 5.1.2.1 through 5.1.2.3 provide details on the important parameters for the LV SWGR ZOIs. The resulting minimum number of FDS LV SGWR HEAF simulations developed from these parameters by the WG is summarized in Table 5-2. The analysis of the overall results allows the HEAF WG to determine the ZOIs.

Table 5-2
FDS LVSWGR HEAF Simulations

HEAF ID	Enclosure Material	Bus Bar Material	Fault Location	Elevation	Arc Voltage (V_{L-L})	Arc Current (kA)	Power (MW)	Duration (s)	Arc Energy (MJ)
LV-BASE-1	Steel	Aluminum	Breaker	Mid	375	5.85/2.75	3.8/1.8	41	90
LV-BASE-2	Steel	Aluminum	Breaker	Top	375	5.85/2.75	3.8/1.8	41	90
LV-BASE-3	Steel	Aluminum	Mid	Mid	375	5.85/2.75	3.8/1.8	41	90
LV-BASE-4	Steel	Aluminum	Mid	Top	375	5.85/2.75	3.8/1.8	41	90
LV-BASE-5	Steel	Aluminum	Breaker to Mid	Mid	375	5.85/2.75	3.8/1.8	41	90
LV-BASE-6	Steel	Aluminum	Breaker to Mid	Top	375	5.85/2.75	3.8/1.8	41	90
LV-BASE-7	Steel	Copper	Breaker	Mid	375	5.85/2.75	3.8/1.8	41	90
LV-BASE-8	Steel	Copper	Breaker	Top	375	5.85/2.75	3.8/1.8	41	90
LV-BASE-9	Steel	Copper	Mid	Mid	375	5.85/2.75	3.8/1.8	41	90
LV-BASE-10	Steel	Copper	Mid	Top	375	5.85/2.75	3.8/1.8	41	90
LV-SENS-1	Steel	Aluminum	Breaker	Mid	375	21.5	14	2	28
LV-SENS-2	Steel	Aluminum	Breaker	Top	375	21.5	14	2	28
LV-SENS-3	Steel	Aluminum	Mid	Mid	375	21.5	14	2	28
LV-SENS-4	Steel	Aluminum	Mid	Top	375	21.5	14	2	28
LV-SENS-5	Steel	Copper	Breaker	Mid	375	21.5	14	2	28
LV-SENS-6	Steel	Copper	Breaker	Top	375	21.5	14	2	28
LV-SENS-7	Steel	Copper	Mid	Mid	375	21.5	14	2	28
LV-SENS-8	Steel	Copper	Mid	Top	375	21.5	14	2	28
LV-SENS-9	Steel	Aluminum	Breaker	Mid	375	21.5	14	4	56
LV-SENS-10	Steel	Aluminum	Breaker	Top	375	21.5	14	4	56

HEAF ID	Enclosure Material	Bus Bar Material	Fault Location	Elevation	Arc Voltage (V_{L-L})	Arc Current (kA)	Power (MW)	Duration (s)	Arc Energy (MJ)
LV-SENS-11	Steel	Aluminum	Mid	Mid	375	21.5	14	4	56
LV-SENS-12	Steel	Aluminum	Mid	Top	375	21.5	14	4	56
LV-SENS-13	Steel	Copper	Breaker	Mid	375	21.5	14	4	56
LV-SENS-14	Steel	Copper	Breaker	Top	375	21.5	14	4	56
LV-SENS-15	Steel	Copper	Mid	Mid	375	21.5	14	4	56
LV-SENS-16	Steel	Copper	Mid	Top	375	21.5	14	4	56
LV-SENS-17	Steel	Aluminum	Breaker	Mid	375	21.5	14	6	84
LV-SENS-18	Steel	Aluminum	Breaker	Top	375	21.5	14	6	84
LV-SENS-19	Steel	Aluminum	Mid	Mid	375	21.5	14	6	84
LV-SENS-20	Steel	Aluminum	Mid	Top	375	21.5	14	6	84
LV-SENS-21	Steel	Copper	Breaker	Mid	375	21.5	14	6	84
LV-SENS-22	Steel	Copper	Breaker	Top	375	21.5	14	6	84
LV-SENS-23	Steel	Copper	Mid	Mid	375	21.5	14	6	84
LV-SENS-24	Steel	Copper	Mid	Top	375	21.5	14	6	84

5.1.3 Non-Segregated Bus Ducts

Based on OE events [12] and survey results [3], the HEAF parameters that have the highest impact on the ZOI are listed below.

- Orientation of the bus duct as observed in the HEAF OE events [12]:
  - Straight run
    - Horizontal
    - Vertical
  - Elbow
  - Tee
- NSBD construction type based on voltage class type:
  - Bus duct (insulated or non-insulated bus bars with air-gap spacing)
  - Armor clad busway (insulated bus bars with no air-gap spacing – low voltage only)
- Bus bar material: copper or aluminum
- Enclosure material: steel or aluminum

For MV bus ducts, the arc current and voltage are the same as MV SWGR (Section 5.1.1.4). For the arcing fault durations, smaller HEAF durations were investigated in addition to the durations used for the MV SWGR. The bus duct breach time can be shorter than MV SWGR, which necessitated the development at resolutions less than 2 s. A summary of the energy variables for NSBD considered are as listed below.

- Energy level (fault current, fault durations and arc voltage):
  - Best estimate fault current of 30 kA as observed in medium voltage HEAF events [12]
  - Arc fault durations
    - Arcing fault duration of 1 to 5 s with constant-current. The expected range of 1 to 5 s is documented in the EPRI survey results and operating experience [3].
    - Generator-fed faults of 15 s duration, with generator voltage/current decay during the coast-down immediately after a unit trip.
    - Arc voltage was set at 650 V_{L-L}, derived from full-scale testing (see Appendix A).

5.1.3.1 Orientation

From a review of typical bus duct configurations and bus duct HEAF operating experience [12], it was determined that the arcing fault can breach the end of a bus duct when the fault occurs near the edge of a segmented transition. This applies to bus duct configurations such as tee and elbow. Arcing faults in straight runs tend to breach perpendicular to the bus duct. Due to the limited number of NSBD HEAF tests, the impact of the bus duct orientation on the ZOIs remains unknown; therefore, all three orientations (straight run, elbow, and tees) are modeled in FDS.

5.1.3.2 NSBD Type

Bus ducts in HEAF OE [12] have either flat facing or edge facing bus bars (single set of bars or multiple sets in parallel). An example of an edge facing bus bar duct is shown in Figure 5-10 below. Although other bus bar configurations, such as square tubes exist, the configuration in Figure 5-10 is used for the FDS simulations.

From the EPRI survey results [3] and HEAF OE [12], arc faults occurred on low-voltage armor-clad busways. This configuration consists of bus bars with smaller gap spacing, due to an insulating material used instead of an air gap. This smaller gap spacing lowers the expected arc voltage. This specific NSBD type used on the low-voltage side was not modeled in FDS; instead, a typical bus duct configuration and associated energies yield ZOIs that bound the ZOIs from the low-voltage busway with smaller arc energies.

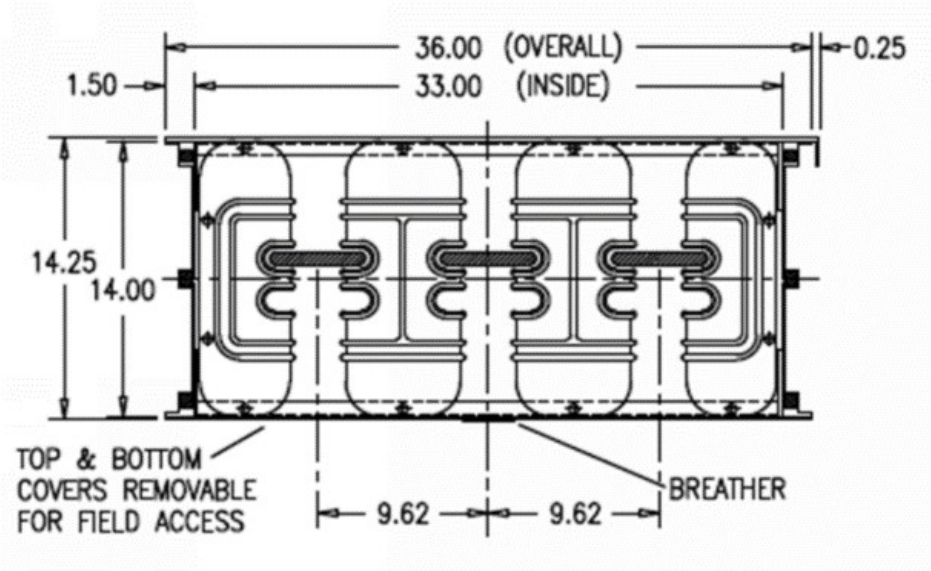

Figure 5-10
Example of a non-segregated bus duct configuration

5.1.3.3 Arc Current, Voltage, and Duration

Medium voltage NSBDs rely on similar over-current protective schemes as MV switchgear and are subject to approximately the same available fault current. An arcing current of 30 kA is also used for bus ducts. A predominant factor in determining arc voltage is the gap spacing between conductors. Minor differences are expected in the gap spacing of bus bars between switchgear and bus ducts; however, the difference is not large enough to have a significant impact on the resulting ZOIs. Therefore, the same arcing voltage of 650 V_{L-L} is used for NSBDs.

Similarly, the same arcing fault durations with an additional duration of 1 s are considered for the constant-current faults. Arc durations of 1 s, 2 s, 4, s, and 5 s are modeled in FDS.

For generator-fed faults on NSBDs, the same are power profile and durations as MV SWGR are used.

5.1.3.4 Bus Bar and Bus Duct Enclosure Material

The type of material used for the construction of the NSBDs in the U.S. NPPs was collected by EPRI [3]. The survey results identified four main construction types of medium- voltage NSBDs in the U.S. fleet:

1. Aluminum bus bars with aluminum enclosure
2. Aluminum bus bars with steel enclosure

3. Copper bus bars with aluminum enclosure, and
4. Copper bus bars with steel enclosure

Figure 5-11 provides the material type breakdown for bus bars and the bus duct enclosure.

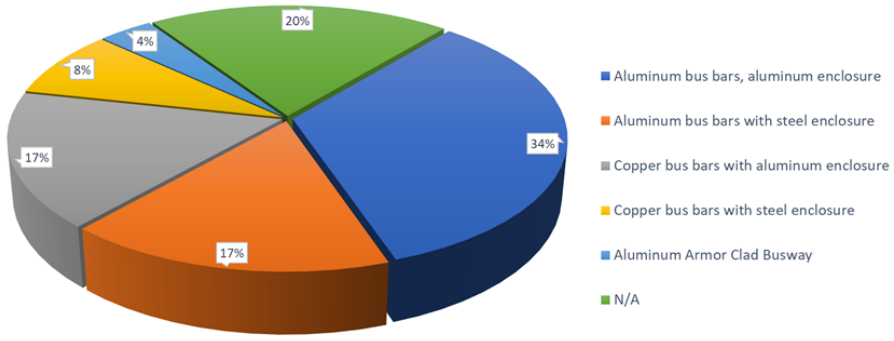

Figure 5-11
Bus bar and enclosure material type distribution

Twenty percent of U.S. NPPs do not use NSBDs and use cables instead. Four percent of U.S. NPPs reported use of Armor Clad Busway for some low-voltage NSBDs.

For FDS simulations, both materials are be used. Simulations with aluminum bus bars are be compared with a set of simulations using copper bus bars while keeping other variables the same for direct comparison.

For bus duct enclosures, the time to breach aluminum versus steel enclosures is expected to be different. Assuming the same enclosure thickness and arc energies, it takes more time to breach the steel enclosure than the aluminum enclosure. Lower or higher breaching time directly impacts the target exposure and the associated ZOIs. Based on this, simulations were run with different bus bar and enclosure materials to allow for direct comparison.

5.1.3.5 Non-Segregated Bus Duct FDS Simulation Matrix

Section 5.1.3.1 through 5.1.3.4 provide details on the important parameters for the NSBD ZOIs. The resulting minimum number of FDS HEAF simulations developed from these parameters by the WG is summarized Table 5-3. The analysis of the overall results of these NSBD HEAF simulations allow the HEAF WG to derive the ZOIs.

Table 5-3
FDS NSBD HEAF Simulations

HEAF ID	Enclosure Material	Bus Bar Material	NSBD Type	Orientation	Fault Location	Arc Voltage (V_{L-L})	Arc Current (kA)	Power (MW)	Stiff (s)	Decay (s)	Arc Energy (MJ)
NSBD-18	Steel	Copper	Typical	Straight-Horizontal	Bus Bar	650	30	23	0	15	131
NSBD-5	Steel	Aluminum	Typical	Straight-Horizontal	Bus Bar	650	30	23	0	15	131
NSBD-19	Steel	Copper	Typical	Straight-Horizontal	Bus Bar	650	30	33.8	3	15	232
NSBD-6	Steel	Aluminum	Typical	Straight-Horizontal	Bus Bar	650	30	33.8	3	15	232
NSBD-20	Steel	Copper	Typical	Straight-Horizontal	Bus Bar	650	30	33.8	5	15	300
NSBD-7	Steel	Aluminum	Typical	Straight-Horizontal	Bus Bar	650	30	33.8	5	15	300
NSBD-14	Steel	Copper	Typical	Straight-Horizontal	Bus Bar	650	30	33.8	1	0	34
NSBD-1	Steel	Aluminum	Typical	Straight-Horizontal	Bus Bar	650	30	33.8	1	0	34
NSBD-15	Steel	Copper	Typical	Straight-Horizontal	Bus Bar	650	30	33.8	2	0	68
NSBD-2	Steel	Aluminum	Typical	Straight-Horizontal	Bus Bar	650	30	33.8	2	0	68
NSBD-16	Steel	Copper	Typical	Straight-Horizontal	Bus Bar	650	30	33.8	4	0	135
NSBD-3	Steel	Aluminum	Typical	Straight-Horizontal	Bus Bar	650	30	33.8	4	0	135
NSBD-17	Steel	Copper	Typical	Straight-Horizontal	Bus Bar	650	30	33.8	5	0	169

HEAF ID	Enclosure Material	Bus Bar Material	NSBD Type	Orientation	Fault Location	Arc Voltage (V_{L-L})	Arc Current (kA)	Power (MW)	Stiff (s)	Decay (s)	Arc Energy (MJ)
NSBD-4	Steel	Aluminum	Typical	Straight-Horizontal	Bus Bar	650	30	33.8	5	0	169
NSBD-43	Steel	Copper	Typical	Tee	Bus Bar	650	30	23	0	15	131
NSBD-31	Steel	Aluminum	Typical	Tee	Bus Bar	650	30	23	0	15	131
NSBD-44	Steel	Copper	Typical	Tee	Bus Bar	650	30	33.8	3	15	232
NSBD-32	Steel	Aluminum	Typical	Tee	Bus Bar	650	30	33.8	3	15	232
NSBD-45	Steel	Copper	Typical	Tee	Bus Bar	650	30	33.8	5	15	300
NSBD-33	Steel	Aluminum	Typical	Tee	Bus Bar	650	30	33.8	5	15	300
NSBD-40	Steel	Copper	Typical	Tee	Bus Bar	650	30	33.8	2	0	68
NSBD-28	Steel	Aluminum	Typical	Tee	Bus Bar	650	30	33.8	2	0	68
NSBD-41	Steel	Copper	Typical	Tee	Bus Bar	650	30	33.8	4	0	135
NSBD-29	Steel	Aluminum	Typical	Tee	Bus Bar	650	30	33.8	4	0	135
NSBD-42	Steel	Copper	Typical	Tee	Bus Bar	650	30	33.8	5	0	169
NSBD-30	Steel	Aluminum	Typical	Tee	Bus Bar	650	30	33.8	5	0	169
NSBD-25	Aluminum	Copper	Typical	Straight-Horizontal	Bus Bar	650	30	23	0	15	131
NSBD-58	Aluminum	Aluminum	Typical	Straight-Horizontal	Bus Bar	650	30	23	0	15	131

HEAF ID	Enclosure Material	Bus Bar Material	NSBD Type	Orientation	Fault Location	Arc Voltage (V_{L-L})	Arc Current (kA)	Power (MW)	Stiff (s)	Decay (s)	Arc Energy (MJ)
NSBD-26	Aluminum	Copper	Typical	Straight-Horizontal	Bus Bar	650	30	33.8	3	15	232
NSBD-12	Aluminum	Aluminum	Typical	Straight-Horizontal	Bus Bar	650	30	33.8	3	15	232
NSBD-27	Aluminum	Copper	Typical	Straight-Horizontal	Bus Bar	650	30	33.8	5	15	300
NSBD-13	Aluminum	Aluminum	Typical	Straight-Horizontal	Bus Bar	650	30	33.8	5	15	300
NSBD-21	Aluminum	Copper	Typical	Straight-Horizontal	Bus Bar	650	30	33.8	1	0	34
NSBD-8	Aluminum	Aluminum	Typical	Straight-Horizontal	Bus Bar	650	30	33.8	1	0	34
NSBD-22	Aluminum	Copper	Typical	Straight-Horizontal	Bus Bar	650	30	33.8	2	0	68
NSBD-9	Aluminum	Aluminum	Typical	Straight-Horizontal	Bus Bar	650	30	33.8	2	0	68
NSBD-23	Aluminum	Copper	Typical	Straight-Horizontal	Bus Bar	650	30	33.8	4	0	135
NSBD-10	Aluminum	Aluminum	Typical	Straight-Horizontal	Bus Bar	650	30	33.8	4	0	135
NSBD-24	Aluminum	Copper	Typical	Straight-Horizontal	Bus Bar	650	30	33.8	5	0	169
NSBD-11	Aluminum	Aluminum	Typical	Straight-Horizontal	Bus Bar	650	30	33.8	5	0	169
NSBD-49	Aluminum	Copper	Typical	Tee	Bus Bar	650	30	23	0	15	131
NSBD-37	Aluminum	Aluminum	Typical	Tee	Bus Bar	650	30	23	0	15	131

HEAF ID	Enclosure Material	Bus Bar Material	NSBD Type	Orientation	Fault Location	Arc Voltage (V_{L-L})	Arc Current (kA)	Power (MW)	Stiff (s)	Decay (s)	Arc Energy (MJ)
NSBD-50	Aluminum	Copper	Typical	Tee	Bus Bar	650	30	33.8	3	15	232
NSBD-38	Aluminum	Aluminum	Typical	Tee	Bus Bar	650	30	33.8	3	15	232
NSBD-51	Aluminum	Copper	Typical	Tee	Bus Bar	650	30	33.8	5	15	300
NSBD-39	Aluminum	Aluminum	Typical	Tee	Bus Bar	650	30	33.8	5	15	300
NSBD-46	Aluminum	Copper	Typical	Tee	Bus Bar	650	30	33.8	2	0	68
NSBD-34	Aluminum	Aluminum	Typical	Tee	Bus Bar	650	30	33.8	2	0	68
NSBD-47	Aluminum	Copper	Typical	Tee	Bus Bar	650	30	33.8	4	0	135
NSBD-35	Aluminum	Aluminum	Typical	Tee	Bus Bar	650	30	33.8	4	0	135
NSBD-48	Aluminum	Copper	Typical	Tee	Bus Bar	650	30	33.8	5	0	169
NSBD-36	Aluminum	Aluminum	Typical	Tee	Bus Bar	650	30	33.8	5	0	169
NSBD-46	Aluminum	Aluminum	Typical	Elbow	Bus Bar	650	30	33.8	2	0	68
NSBD-47	Aluminum	Aluminum	Typical	Elbow	Bus Bar	650	30	33.8	4	0	135
NSBD-48	Aluminum	Aluminum	Typical	Elbow	Bus Bar	650	30	33.8	5	0	169
NSBD-49	Aluminum	Aluminum	Typical	Elbow	Bus Bar	650	30	23	0	15	131
NSBD-50	Aluminum	Aluminum	Typical	Elbow	Bus Bar	650	30	33.8	3	15	232

HEAF ID	Enclosure Material	Bus Bar Material	NSBD Type	Orientation	Fault Location	Arc Voltage (V_{L-L})	Arc Current (kA)	Power (MW)	Stiff (s)	Decay (s)	Arc Energy (MJ)
NSBD-51	Aluminum	Aluminum	Typical	Elbow	Bus Bar	650	30	33.8	5	15	300

5.2 Details on the FDS Implementation of the HEAF Simulations

5.2.1 Medium Voltage Switchgear HEAFs

5.2.1.1 GE Vertical-Lift Breaker MV SWGR

Views of the FDS geometry for the GE MV SWGR are shown in Figure 5-12. The light purple object represents the circuit breaker, and the gray blockages represent the enclosure structure. The walls and internal partitions are modeled as 2.38 mm thick steel with the phase change model. The breaker is modeled as a 0.02 m thickness of steel without the phase change model and accounts for the breaker mass and its internal construction.

The domain uses 0.076 m grid cells. The as-modeled external dimensions of the enclosure are 2.13 m × 1.07 m × 2.36 m. The enclosure walls are one cell thick resulting in internal dimensions of 1.98 m × 0.91 m × 2.21 m. Although the enclosure boundaries are modeled as one cell thick to assist the FDS pressure solver, the thermal behavior of the enclosure is governed by the specified thickness of surface. The switchgear enclosure is centered at the base of a model domain that measures 7.01 m × 5.03 m × 4.57 m and is divided into 36 meshes. This provides 2.44 m to the front and rear of the enclosure, 1.98 m to the sides of the enclosure, and 2.21 m above the top of the enclosure. As seen in Figure 5-12, the enclosure is modeled assuming the front door is opened by the initial pressure pulse from the arc. Four arc locations are modeled in this enclosure: at the breaker stab connections, in the middle main bus bar compartment, and in the primary cable compartment for both supply and load configurations. Figure 5-13 shows the instrumentation layouts for the four configurations. The location of instrumentation to the sides identifies the location of the arc. The arc at the breaker stab connection is located just above the top of the breaker centered below the partition for the main and primary cable compartments. The arc dimensions for each simulation are 0.15 m front/back and top/bottom and 0.46 m side to side.

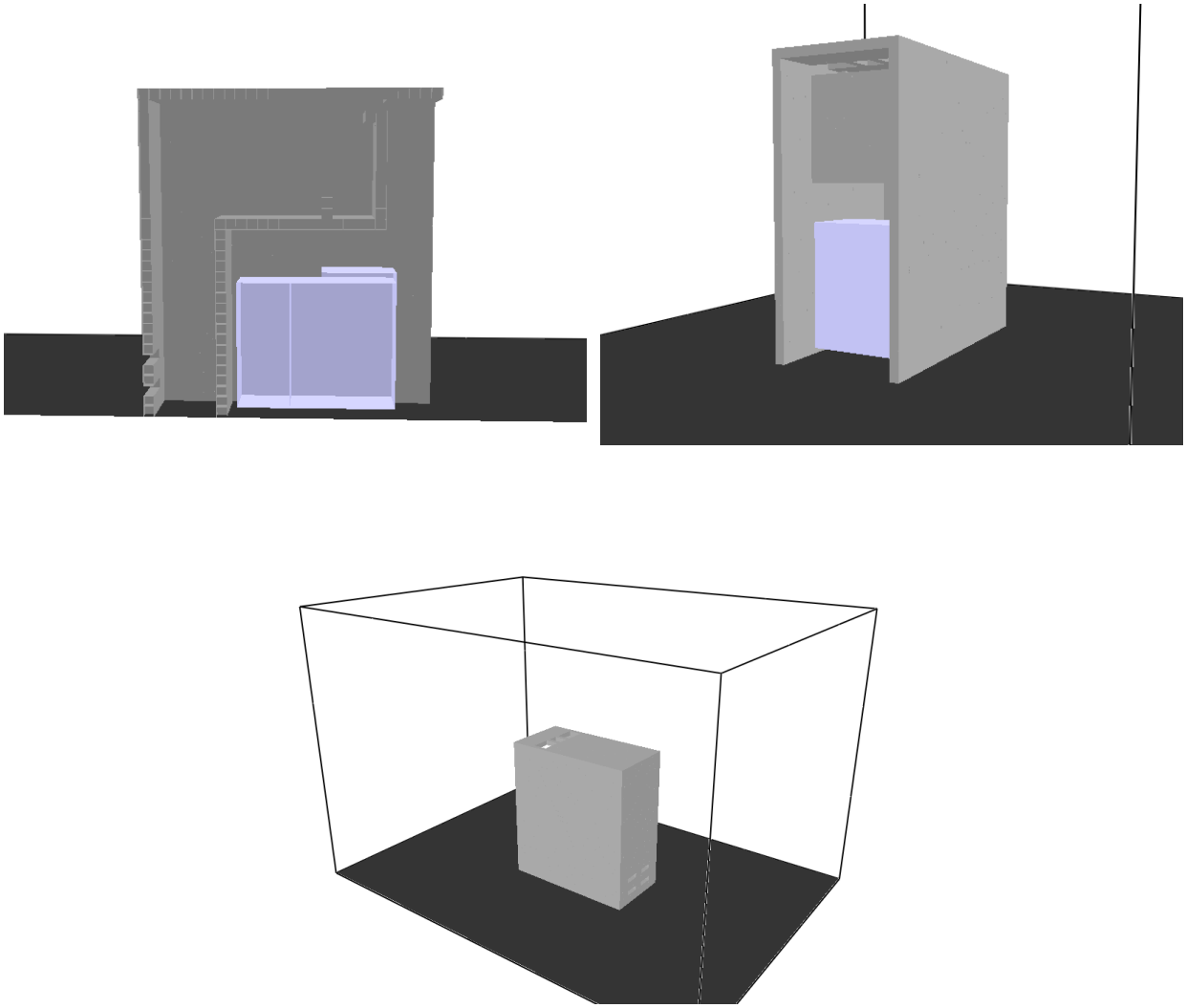

Figure 5-12
FDS model for the GE MV SWGR. Top left – view of enclosure with side clipped showing the internal layout. Top right – view of enclosure front showing open door. Bottom – Rear isometric view showing the entire FDS domain

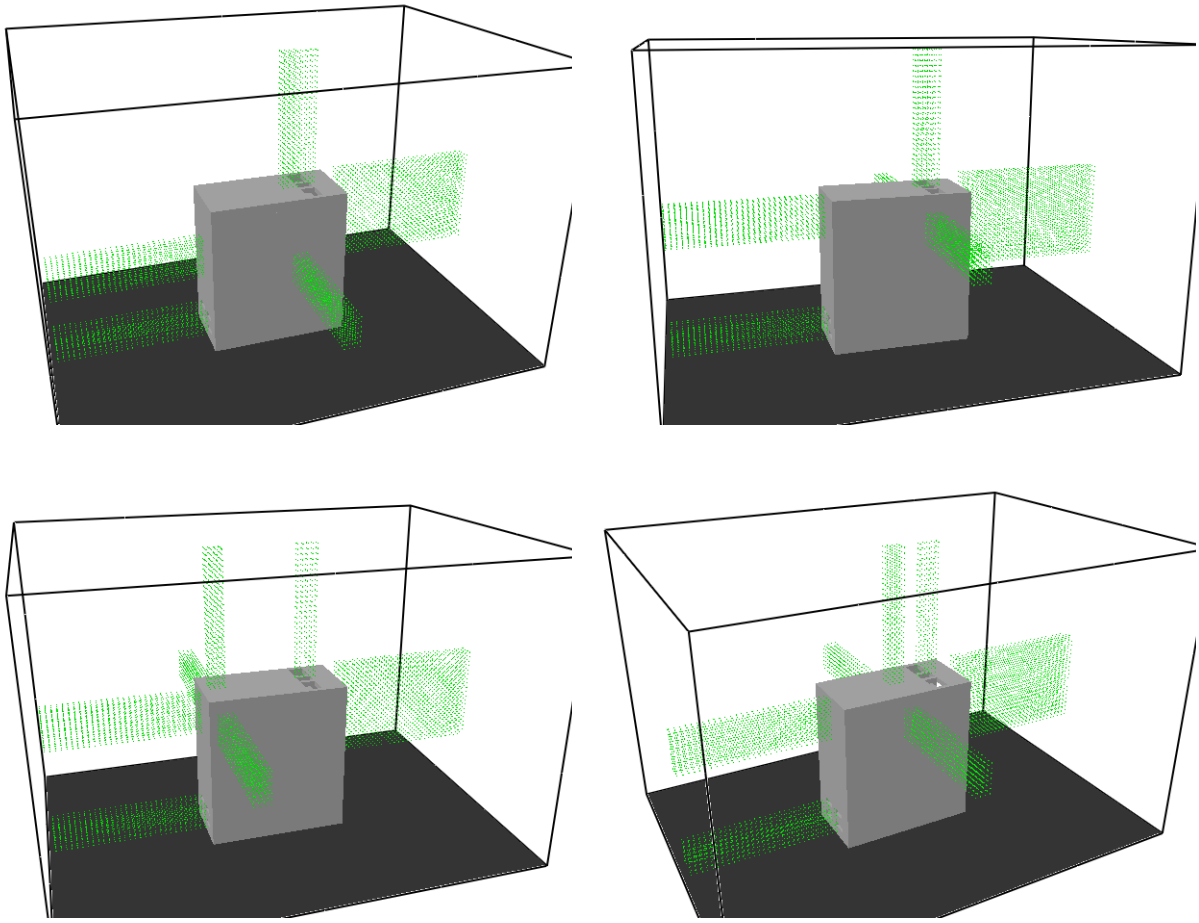

Figure 5-13
GE MV SWGR exposure measurement locations (green dots) Top left – breaker stabs. Top right – main bus bar compartment. Bottom left – primary cable compartment (load). Bottom right – primary cable compartment (supply)

5.2.1.2 ABB Horizontal Draw-Out HK Breaker MV SWGR

Views of the FDS geometry for the ABB MV SWGR are shown in Figure 5-14. The light purple object represents the breaker, and the gray blockages represent the enclosure structure. The walls and internal partitions are modeled as 2.38 mm thick steel with the phase change model. The circuit breaker is modeled as a 0.02 m thickness of steel without the phase change model and accounts for the breaker mass and its internal construction.

The domain uses 0.076 m grid cells. The as-modeled external dimensions of the enclosure are 2.06 m × 0.914 m × 2.29 m. The enclosure walls are one cell thick resulting in internal dimensions of 1.91 m × 0.762 m × 2.21 m. Although the enclosure boundaries are modeled as one cell thick to assist the FDS pressure solver, the thermal behavior of the enclosure is governed by the specified thickness of surface. The switchgear enclosure is centered at the base of a model domain that measures 7.32 m × 5.03 m × 4.57 m and is divided into 36 meshes. This provides 2.63 m to the front and rear of the enclosure, 2.06 m to the sides of the enclosure, and 2.29 m above the top of the enclosure. As seen in Figure 5-14, the enclosure is modeled assuming the front door is opened by the initial pressure pulse from the arc. The arc

location for this SWGR is modeled at the breaker stabs. Figure 5-15 shows the instrumentation layouts for the configuration. The location of instrumentation to the sides identifies the location of the arc. The arc at the breaker stab connection is located in the front center of the switchgear. The arc used for each simulation is 0.152 m front/back and top/bottom and 0.457 m side to side.

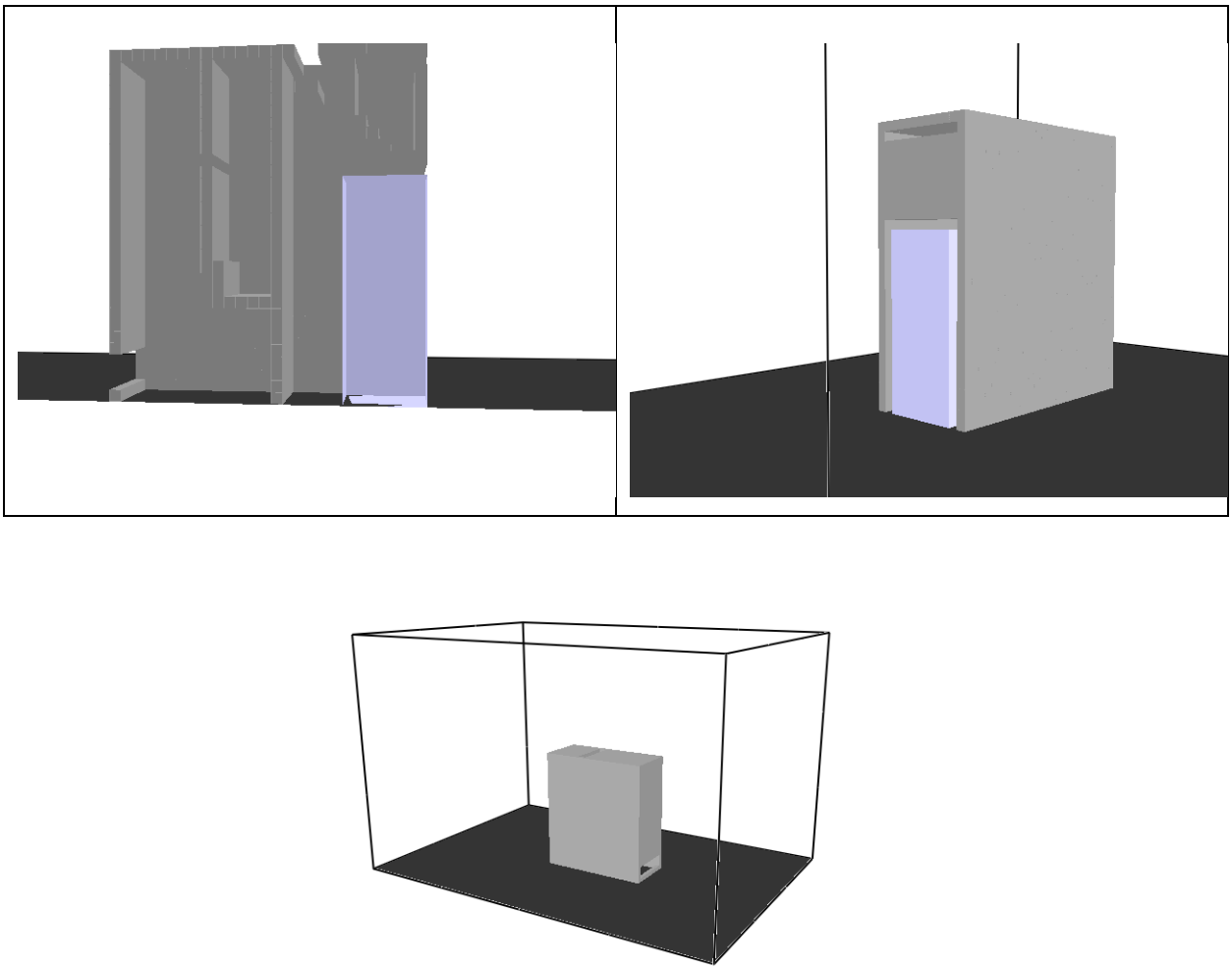

Figure 5-14
FDS model for the ABB MV SWGR. Top left – view of enclosure with side clipped showing the internal layout. Top right – view of enclosure front showing open door. Bottom – Rear isometric view showing the entire FDS domain

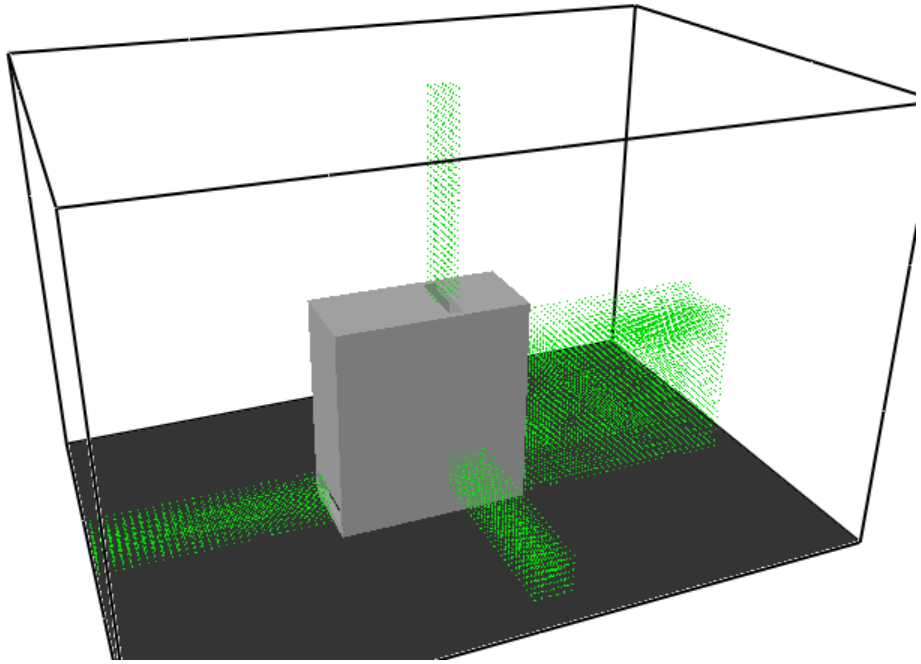

Figure 5-15
ABB MV SWGR exposure measurement locations (green dots)

5.2.2 Low Voltage Switchgear HEAFs

Views of the FDS geometry for the LV SWGR are shown in Figure 5-16. The light purple object represents the breaker, and the gray blockages represent the enclosure structure. The walls and internal partitions were modeled as 2.38 mm thick steel with the phase change model. The breaker is modeled as a 0.02 m thickness of steel without the phase change model and accounts for the breaker mass and its internal construction.

The domain uses 0.076 m grid cells. The as-modeled external dimensions of the enclosure are 1.83 m × 1.22 m × 2.44 m. The enclosure walls are one cell thick resulting in internal dimensions of 1.68 m × 1.07 m × 2.29 m. Although the enclosure boundaries are modeled as one cell thick to assist the FDS pressure solver, the thermal behavior of the enclosure is governed by the specified thickness of surface. The model domain measures 5.26 m × 5.03 m × 4.57 m and is divided into 27 meshes. This provides 1.72 m to the front and rear of the enclosure, 1.91 m to the sides of the enclosure, and 2.14 m above the top of the enclosure. As seen in Figure 5-16, the enclosure is modeled assuming the front door is open due to the initial pressure pulse from the arc. Six arc locations are modeled in this enclosure. These are as follows:

- Breaker connection stabs, mid-height location
- Breaker connection stabs, top location
- Middle main bus bar, mid-height location
- Middle main bus bar, top location
- Breaker connection stabs, migrating to the middle compartment (mid-height location)

- Breaker connection stabs, migrating to the middle compartment (top location)

The top right of Figure 5-16 shows the mid-height circuit breaker connection stab location. The barrier between the circuit breaker compartment and the middle main bus bar compartment started with a hole in it to accommodate the arc volume. Given the arc's proximity to that barrier, this is a reasonable approach since the breach time would be short. The image also shows a small hole at the top of the barrier between the bus bar compartment and the back compartment. This is added to prevent large pressure rises in a sealed space. Figure 5-17 shows the measurement locations for the LV SWGR HEAFs. One set of measurements is used for all HEAF simulations. On the arc side of the enclosure, groups of measurement devices were located to the side at the top and mid arc locations. On the non-arc side of the enclosure, only a single plane of devices is used with the devices immediately adjacent to the face. While the HEAF is capable of breaching the partition between the two columns of breaker cubicles, it is not capable of breaching the next barrier. It is too far to receive enough exposure to breach; therefore, only a single plane of devices is needed to capture the maximum exposure as there will be no ZOI on that side of the enclosure. The arc dimensions for each simulation are 0.076 m front/back, 0.15 m top/bottom, and 0.38 m side to side. For simulations where the arc moves from the circuit breaker stab connection to the mid compartment, two arc volumes of the aforementioned size are defined with only one volume active at a time.

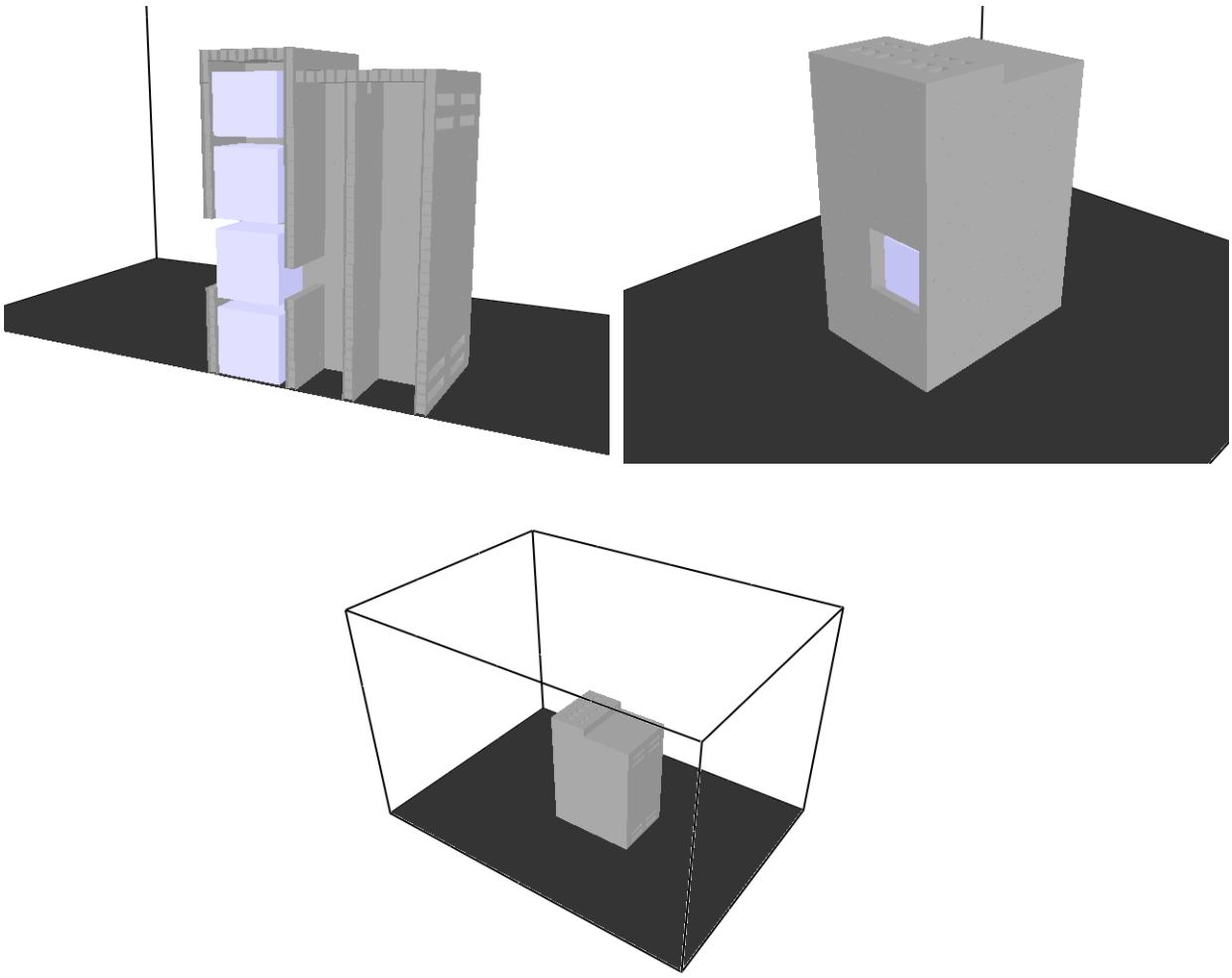

Figure 5-16
FDS model for the LV SWGR. Top left – view of enclosure with side clipped showing the internal layout. Top right – view of enclosure front showing open door. Bottom – Rear isometric view showing the entire FDS domain

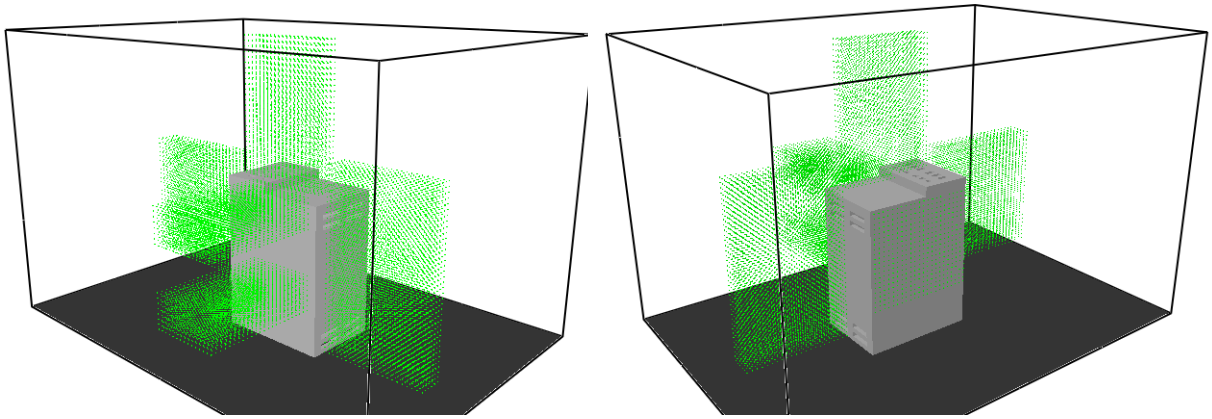

Figure 5-17
LV SWGR exposure measurement locations (green dots) Left – View of side with the arc. Right – View of non-arc side of the enclosure

5.2.3 Non-Segregated Bus Duct HEAFs

Views of the FDS geometry and the measurement locations for the NSBD HEAF simulations are shown in Figure 5-18. The duct walls are modeled as 3.18 mm steel or aluminum with the phase change model. No internal partitions are modeled in the ducts, and the FDS boundary at the edge of the domain is an open pressure boundary condition for the inside of the duct.

The domain is meshed with 0.04 m grid cells. The as-modeled cross-section of the ducts is 0.56 m × 0.48 m. The duct walls are one cell thick resulting in internal dimensions of 0.48 m × 0.40 m. Although the enclosure boundaries are modeled as one cell thick to assist the FDS pressure solver, the thermal behavior of the enclosure is governed by the specified thickness of surface. The model domain for each duct measured 6 m × 6 m × 6 m and is divided into 27 meshes. This provides 2.7 m model domain around the duct arc volume. The arc dimensions for each simulation are 0.24 m along the duct length, 0.16 m top/bottom, and 0.4 m across the duct width. The arc is centered in the straight segment and elbow. For the tee, the arc is centered in the upper branch of the tee.

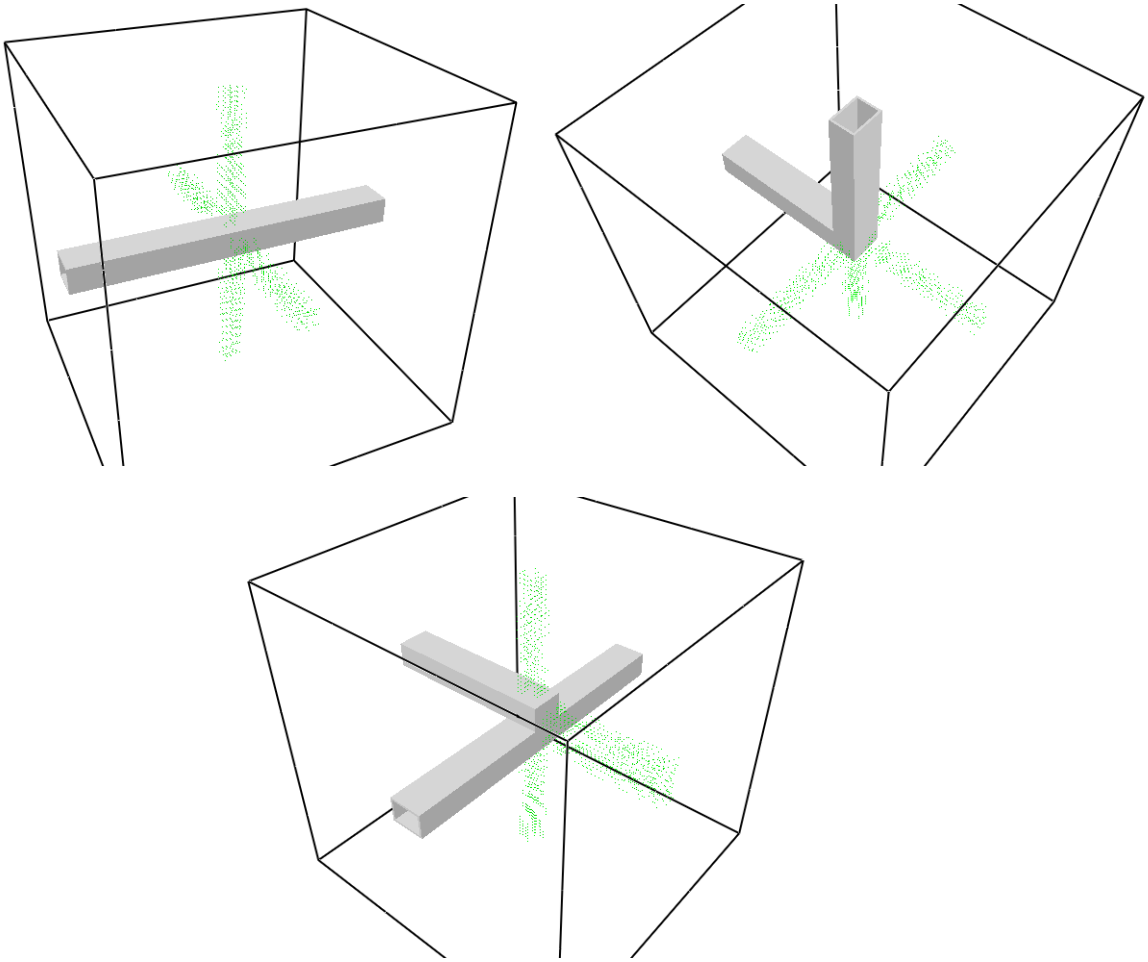

Figure 5-18
NSBD geometry and exposure measurement locations (green dots) Top Left – straight segment. Top right – elbow. Bottom – Tee

6
FDS SIMULATION RESULTS

This section provides the ZOI results of the FDS HEAF simulations. One FDS simulation for each geometry and arc location is presented in detail, including selected temperature contours and incident energy plots. The graphical results for all simulations are provided in Appendix B.

6.1 Medium Voltage Switchgear HEAF Simulations

This section provides a summary of the FDS results for the GE vertical-lift breaker and the ABB horizontal draw-out breaker MV SWGR HEAF simulations. The detailed FDS results are typical of the HEAF simulations evaluated and highlight the key predictive features of the FDS analysis. Graphical results showing the exposure as a function of distance from each face of the enclosure are provided in Appendix B.1 for the MV SWGR HEAF simulations. A general discussion of the MV SWGR results and the ZOIs are presented in Section 6.1.2.

6.1.1 Selected GE Vertical-Lift Breaker MV SWGR HEAF Simulations

The FDS results for four GE Magne-Blast vertical-lift breaker simulations are reviewed in detail:

- A HEAF at the main bus bar
- A HEAF at the breaker stab
- A HEAF at the primary cable compartment bus bar load configuration
- A HEAF at the primary cable compartment bus bar supply configuration

These HEAFs represent the four basic locations where a HEAF could occur in the GE MV SWGR geometry. The detailed FDS results review compare the same HEAF arc energy profile (226 MJ arc energy with relatively large ZOI dimensions) to highlight the effect of the HEAF location. The characteristics are as follows:

- 3 s of stiff current
- 15 s of decaying current
- Copper electrode
- 226 MJ arc energy

The arc energy power profile for this HEAF is provided in Appendix A (see Figure A-4). The detailed results include depictions of the switchgear enclosure breach, particle dispersion, the luminous thermal plume, the heat release rate per unit volume, the enclosure wall temperatures, and the exposure profiles as a function of distance for each switchgear enclosure surface.

6.1.1.1 GE Vertical-Lift Breaker MV SWGR Design with a HEAF at the Main Bus Bar

Figure 6-1 depicts the metal particle distribution about the upper portion of the GE vertical-lift breaker switchgear at various times for a HEAF located at the main bus bar. At 0 s, there are no

particles, and the switchgear enclosure is intact. The openings at 0 s are the top surface vents and the upper front below the top vents. At 0.3 s, the switchgear enclosure is still intact, but there are metal particles ejected from the top vents. The switchgear enclosure is breached at about 0.6 s, with particles ejected from the front face through portions of the switchgear enclosure that have disintegrated. At about 1.3 s, the left- and right-sides are breached, with particles ejected from the openings in the switchgear enclosure wall (note that only the right-side is shown in Figure 6-1). The front face openings continue to expand between 0.6 and 1.3 s also. At about 3.5 s, a small portion of the switchgear enclosure at the top near the vent is breached. Between 1.3 s and 3.5 s, the front- and right-sides as well as the front openings continue to grow larger as more portions of the switchgear enclosure are breached. The left- and right-side openings are the same size, and the front opening is symmetric about the vertical centerline. The openings continue to expand during the decay stage, up to about 15 s. After 20 s, the fault is cleared and nearly all particles have dispersed. The final state of the switchgear enclosure boundary is depicted at 20 s, with significant openings on the left, right, front, and top surfaces. There are no openings on the rear of the switchgear enclosure.

Figure 6-2 depicts the luminous portion of the thermal plume at 0.3 s, 1.3 s, 3.5 s, and 15 s, corresponding to the times at which the particle distributions are shown. The luminous thermal plume reaches a peak near the start of the decay phase where significant portions of the switchgear enclosure are breached.

Figure 6-3 depicts the heat release rate per unit volume at 4 s, near the beginning of the arc current decay phase. The heat release rate per unit volume shows the arc location and is largely confined to the bus bar and the immediate location around the bus bar. The openings in the front, sides, and top of the switchgear enclosure are clearly visible.

Figure 6-4 depicts the wall temperature at about 15 s, the time at which the greatest extent of the switchgear enclosure boundary is heated. Although the heated wall temperature contributes to the heat flux at a fixed location, the temperatures are relatively low, suggesting this component is relatively small compared the energy flux directly from the arc fault and gases.

The calculated total exposure energy as a function of distance is shown in Figure 6-5, which indicates that the ZOI for this simulation is less than 1 m from the sides, top, and front, and zero from the rear of the switchgear enclosure. This is consistent with the particle distribution in Figure 6-1 and the luminous plume progression depicted in Figure 6-2.

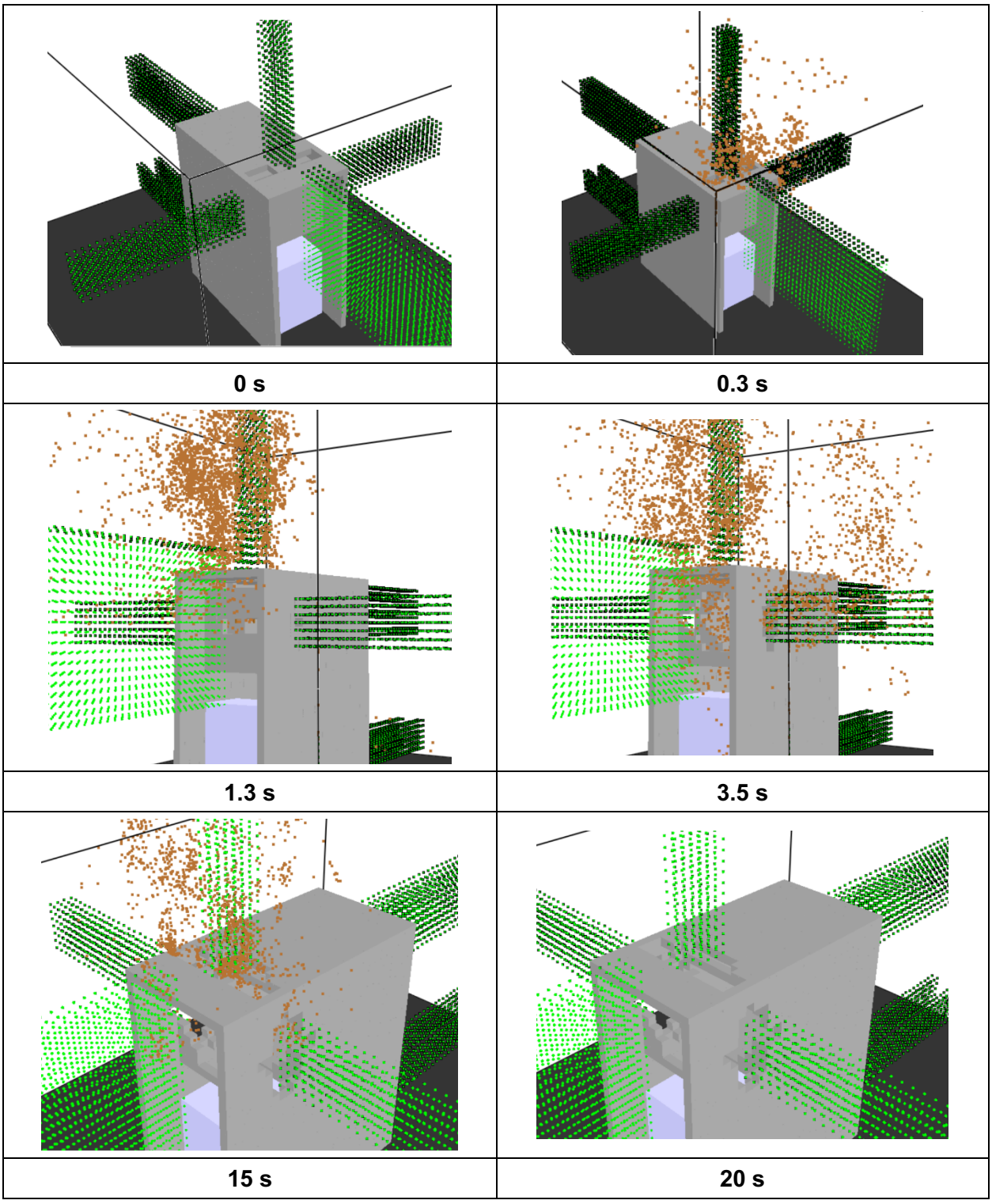

Figure 6-1
Particle distribution at various times for a 226 MJ HEAF located at the main bus bars of a vertical-lift breaker MV SWGR design

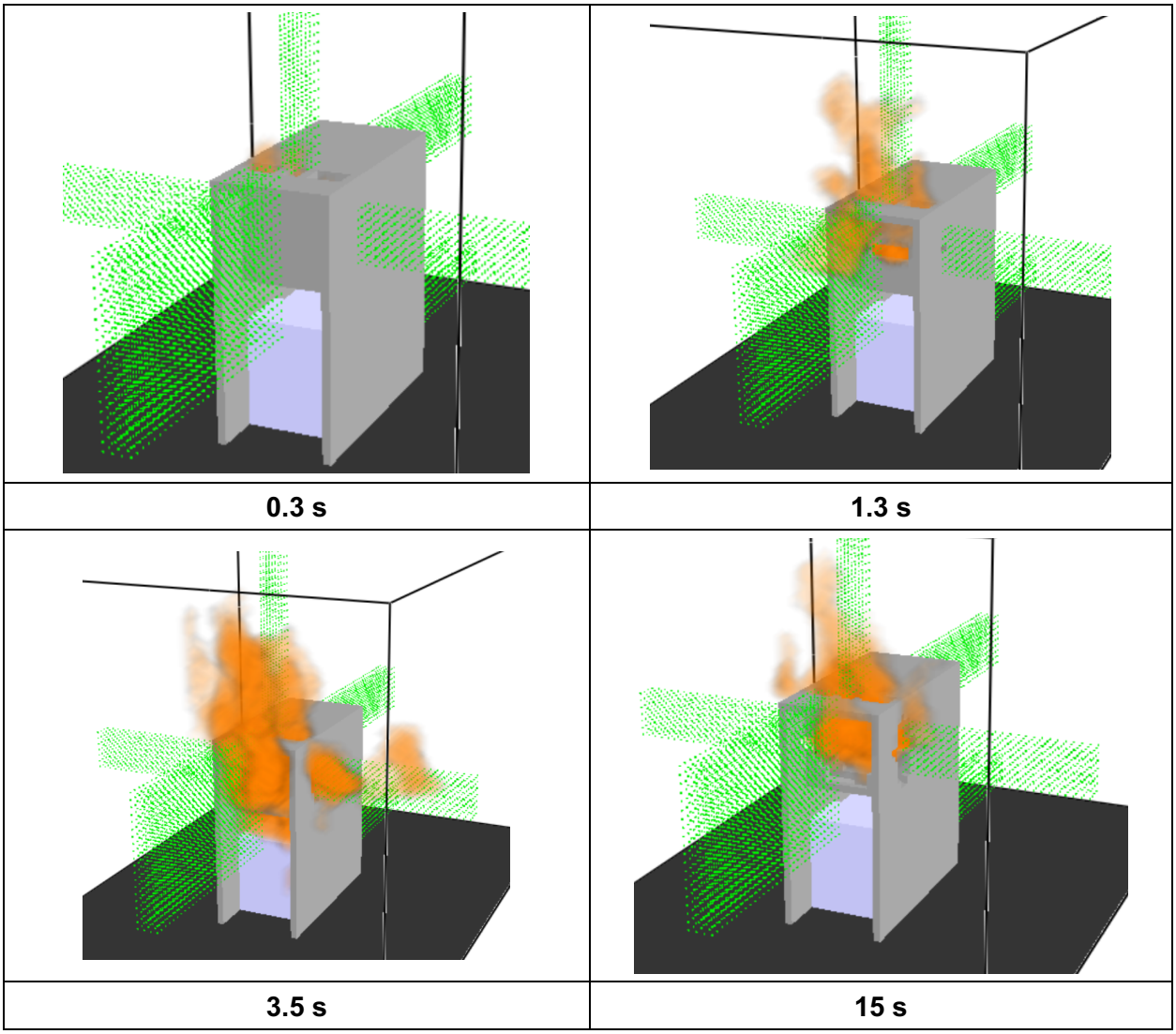

Figure 6-2
Luminous portion of the thermal plume at various times for a 226 MJ HEAF located at the main bus bars of a vertical-lift breaker MV SWGR design

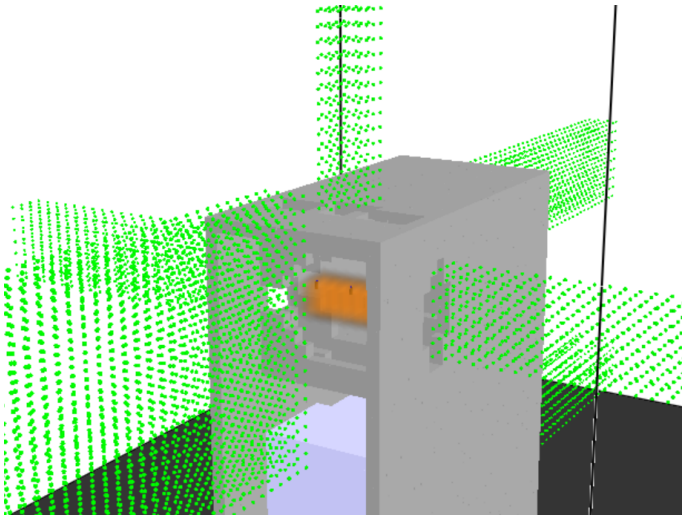

Figure 6-3
Heat release rate per unit volume at 4 s for a 226 MJ HEAF located at the main bus bars of a vertical-lift breaker MV SWGR design

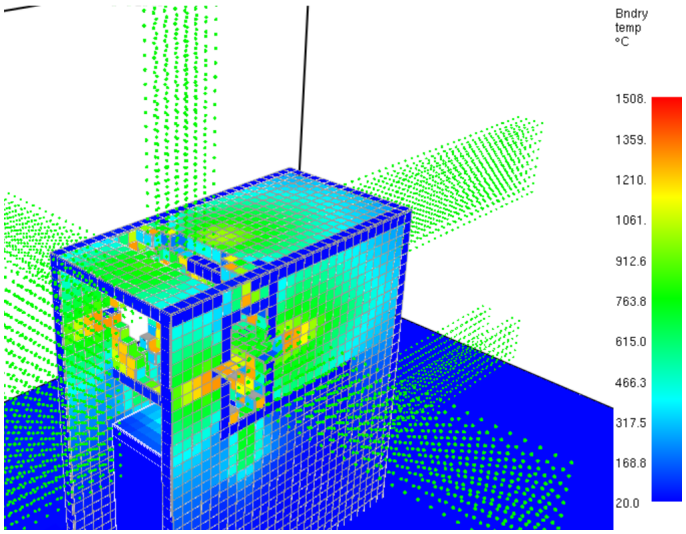

Figure 6-4
Wall temperature of the thermal plume at 15 s for a 226 MJ HEAF located at the main bus bars of a vertical-lift breaker MV SWGR design

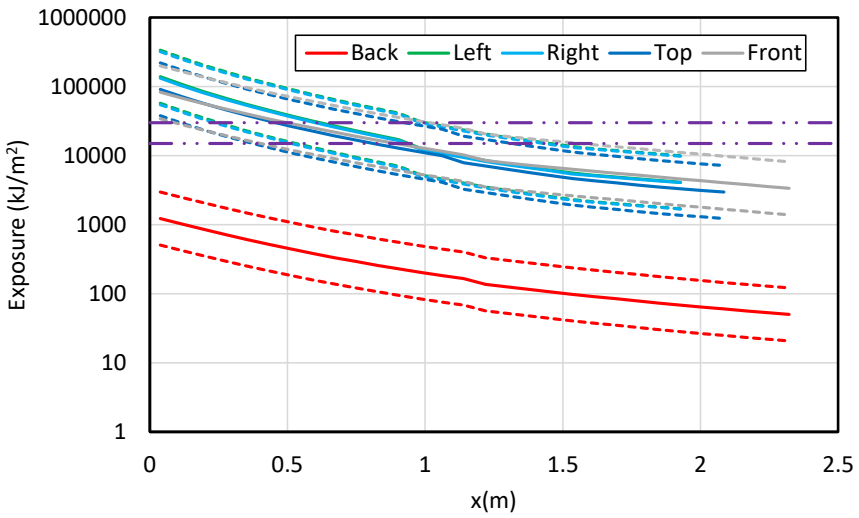

Figure 6-5
Total energy exposure as a function of distance from each face for a 226 MJ HEAF located at the main bus bars of a vertical-lift breaker MV SWGR design (HEAF simulation ID MV-GE-36). Note the results for the left- and right-sides are nearly coincident. Dashed horizontal lines correspond to the 15 MJ/m² and 30 MJ/m² target fragility thresholds

6.1.1.2 GE Vertical-Lift Breaker MV SWGR Design with a HEAF at the Beaker Stabs

Figure 6-6 depicts the metal particle distribution about the upper portion of the GE vertical-lift breaker style switchgear at various times for a HEAF at the breaker stabs. At 0 s, there are no particles and the switchgear enclosure is intact. The openings at 0 s are in the front face of the switchgear enclosure. At 0.47 s, the switchgear enclosure is still intact, but there are metal particles ejected from the front opening. The switchgear enclosure is breached at about 0.75 s, with switchgear enclosure breach on the upper surface. At about 1.85 s, the left and right switchgear enclosure faces are breached, with particles ejected from these openings (note that only the right-side is shown in Figure 6-6). The side and top switchgear enclosure openings continue to expand between 1.85 and 6.8 s, where the maximum damage to the switchgear enclosure is reached. The left and right-side openings are the same size, and the rear opening is symmetric about the vertical centerline. After 20 s, the fault is cleared and nearly all particles have dispersed. The final state of the switchgear enclosure is depicted at 20 s, with significant openings on the left, top, and right enclosure faces.

Figure 6-7 depicts the luminous portion of the thermal plume at 0.47 s, 0.75 s, 1.85 s, and 6.8 s, corresponding to the times at which the particle distributions are shown. The luminous thermal plume reaches a peak near the start of the decay phase between 1.85 s and 6.8 s where significant portions of the switchgear enclosure are breached.

Figure 6-8 depicts the heat release rate per unit volume at 4 s, near the beginning of the arc current decay phase. The heat release rate per unit volume shows the arc location and is largely confined to the electrode and the immediate location around the electrode. The openings in the sides of the switchgear enclosure are clearly visible.

Figure 6-9 depicts the wall temperature at about 15 s, the time at which the greatest extent of the switchgear enclosure boundary is heated. Although the heated wall temperature contributes to the heat flux at a fixed location, the temperatures are relatively low, suggesting this component is relatively small compared the energy flux directly from the arc fault and gases.

The calculated total exposure energy as a function of distance is shown in Figure 6-10, which indicates that the ZOI for this simulation is less than 1 m from the sides and top and nearly zero from the front and rear of the switchgear enclosure. The ZOIs for the front are slightly smaller than the sides even though the particle distribution and luminous plume (Figure 6-6 and Figure 6-7) suggest a more severe exposure. In this case, the ZOI is strongly dependent on the distance from the arc emitter, which is toward the rear of the switchgear enclosure and thus further from the front face.

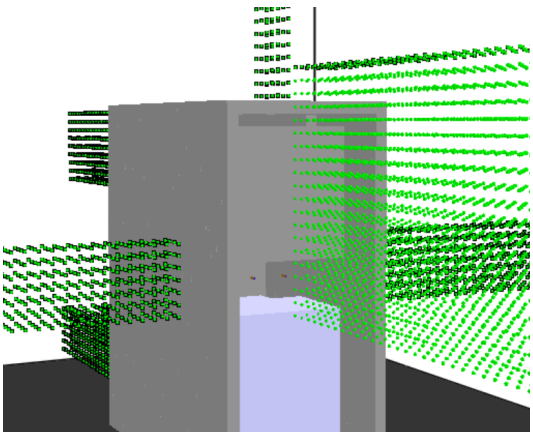

0 s

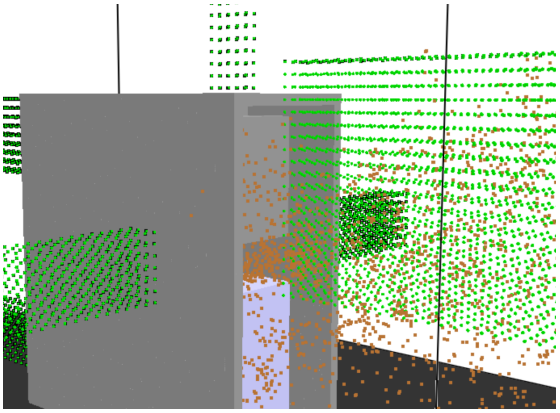

0.47 s

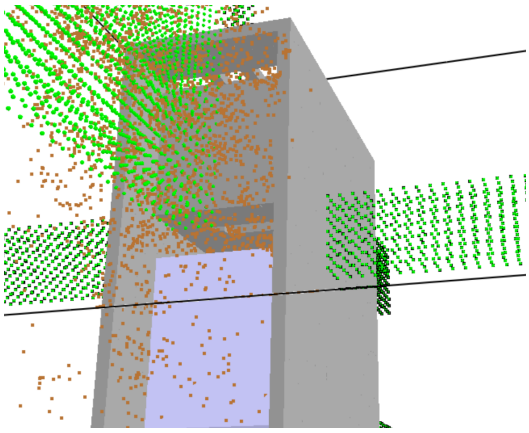

0.75 s

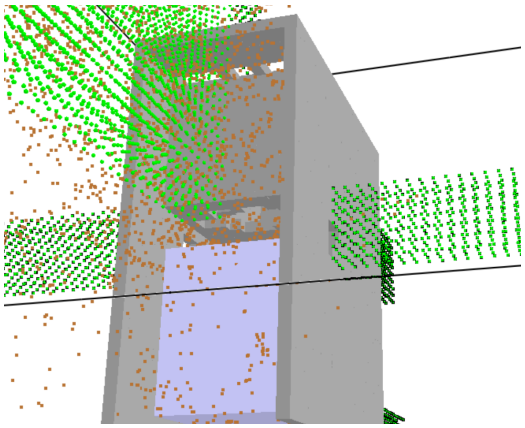

1.85 s

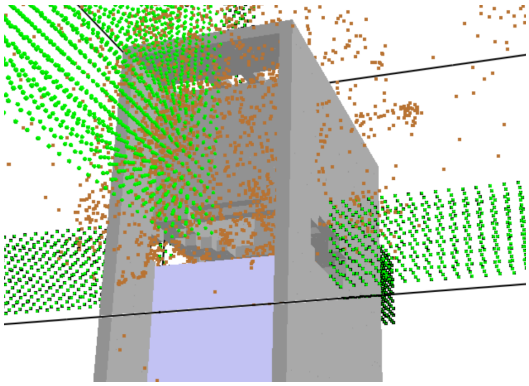

6.8 s

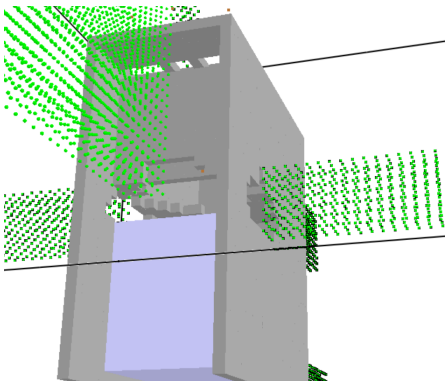

20 s

Figure 6-6
Particle distribution at various times for a 226 MJ HEAF located at the breaker stabs of a vertical-lift breaker MV SWGR design

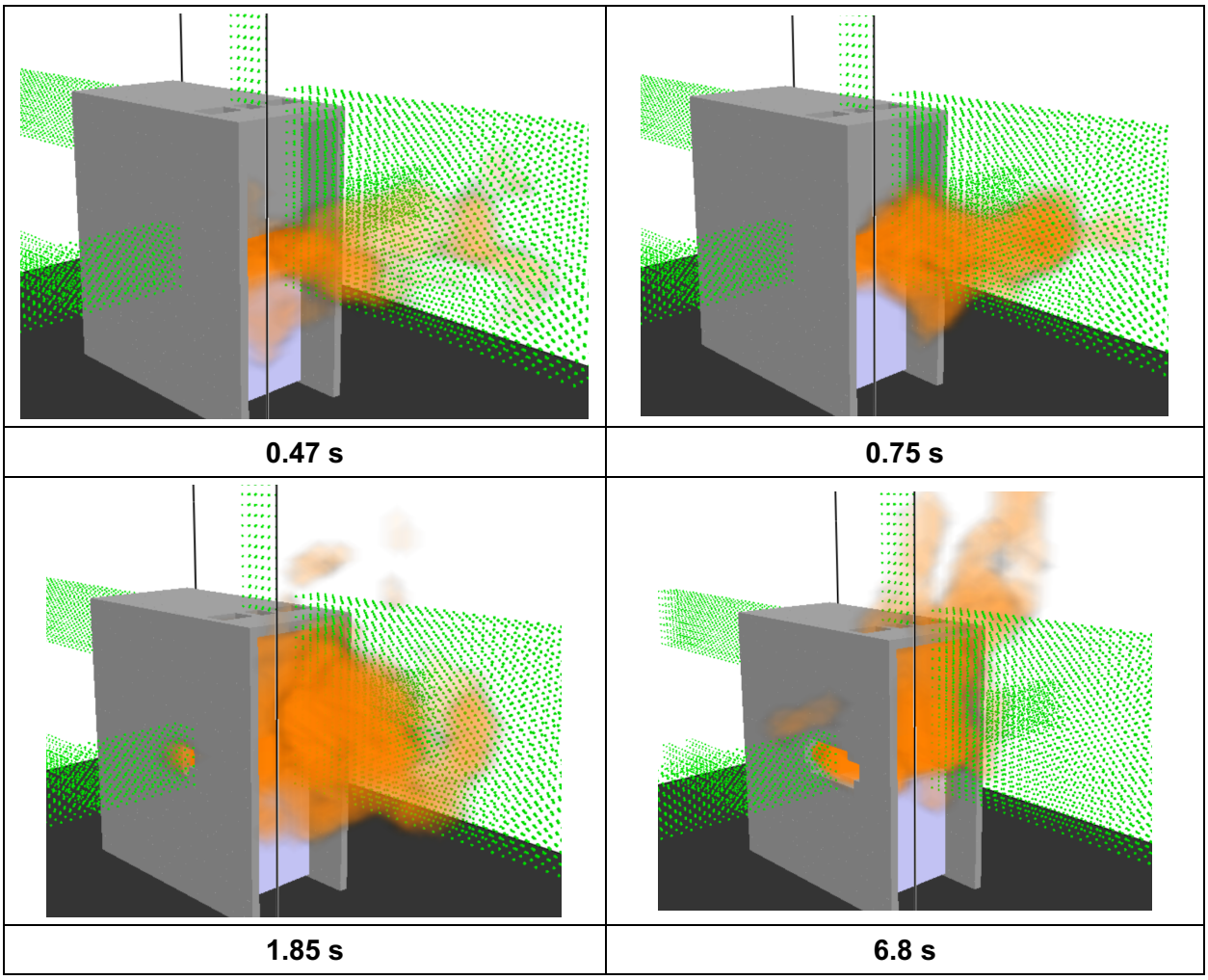

Figure 6-7
Luminous portion of the thermal plume at various times for a 226 MJ HEAF located at the breaker stabs of a vertical-lift breaker MV SWGR design

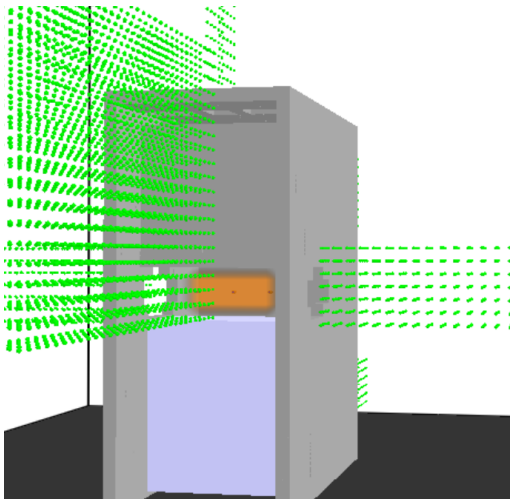

Figure 6-8
Heat release rate per unit volume at 4 s for a 226 MJ HEAF located at the breaker stabs of a vertical-lift breaker MV SWGR design

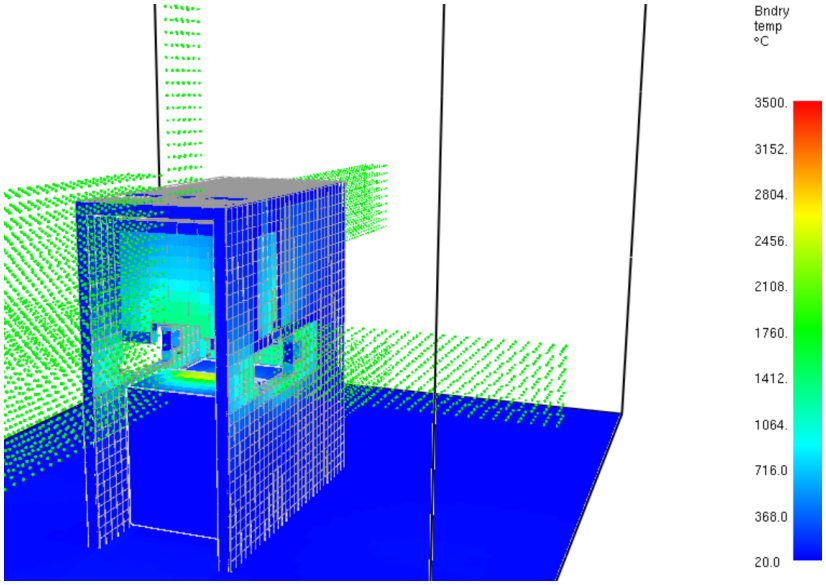

Figure 6-9
Wall temperature of the thermal plume at 15 s for a 226 MJ HEAF located at the breaker stabs of a vertical-lift breaker MV SWGR design

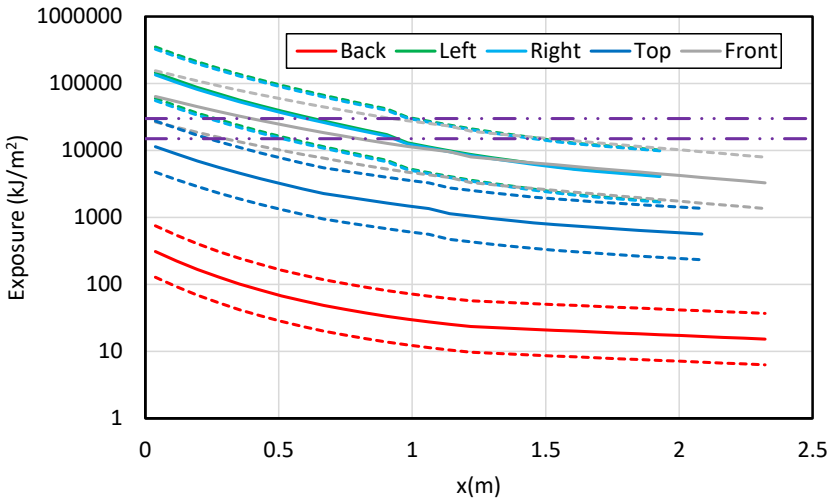

Figure 6-10
Total energy exposure as a function of distance from each face for a 226 MJ HEAF located at the breaker stabs of a vertical-lift breaker MV SWGR design (HEAF simulation ID MV-GE-35). Note the results for the left- and right-sides are nearly coincident. Dashed horizontal lines correspond to the 15 MJ/m² and 30 MJ/m² target fragility threshold

6.1.1.3 GE Vertical-Lift Breaker MV SWGR Design with a HEAF at the Primary Cable Compartment Bus Bars in the Load Configuration

Figure 6-11 depicts the metal particle distribution about the rear, side, and upper portion of the GE vertical-lift breaker switchgear at various times for a HEAF located at the primary cable compartment bus bars in the load configuration. At 0 s, there are no particles and the switchgear enclosure is intact. The openings at 0 s are front top vents, the rear top vents, and the rear bottom vents. At 0.69 s, the switchgear enclosure is still intact, but there are metal particles ejected from the three vent openings. The switchgear enclosure is breached at about 0.99 s, with initial switchgear enclosure breach on the upper rear surface near the electrode. At about 1.86 s, the left and right switchgear enclosure faces are breached, with particles ejected from these openings (note that only the left side is shown in Figure 6-11). The side and rear switchgear enclosure openings continue to expand between 1.86 and 3.43 s, when the top rear of the switchgear enclosure is breached. The switchgear enclosure openings continue to grow during the decay stage and reach a maximum at about 16.7 s (near the end of the decay stage). After 20 s (not shown in Figure 6-11), the fault is cleared and nearly all particles have dispersed. Although particles are ejected from the lower rear vents, the majority of the particles are ejected through the upper vents and later through the damaged switchgear enclosure.

Figure 6-12 depicts the luminous portion of the thermal plume at 0.69 s, 0.99 s, 1.86 s, and 3.43 s, corresponding to the times at which the particle distributions are shown. The luminous thermal plume is primarily confined to the switchgear enclosure prior to the breach of the switchgear enclosure as shown at 0.69 s and 0.99 s. After 0.99 s, the luminous thermal plume expands outside the switchgear and reaches a peak near the start of the decay phase between 1.86 s and 3.43 s where significant portions of the switchgear enclosure are breached.

Figure 6-13 depicts the heat release rate per unit volume at 4 s, near the beginning of the arc current decay phase. The heat release rate per unit volume shows the arc location and is largely confined to the electrode and the immediate location around the electrode. Some heat release rate occurs above and outside due to particle oxidation. The openings in the sides of the switchgear enclosure are clearly visible.

Figure 6-14 depicts the wall temperature at about 15 s, the time at which the greatest extent of the switchgear enclosure boundary is heated. Although the heated wall temperature contributes to the heat flux at a fixed location, the temperatures are relatively low, suggesting this component is relatively small compared the energy flux directly from the arc fault and gases.

The calculated total exposure energy as a function of distance is shown in Figure 6-15, which indicates that the ZOI for this simulation is between 0.5 – 1.2 m for the rear, side, and top faces and zero from the front face, consistent with the particle distribution and luminous plume location.

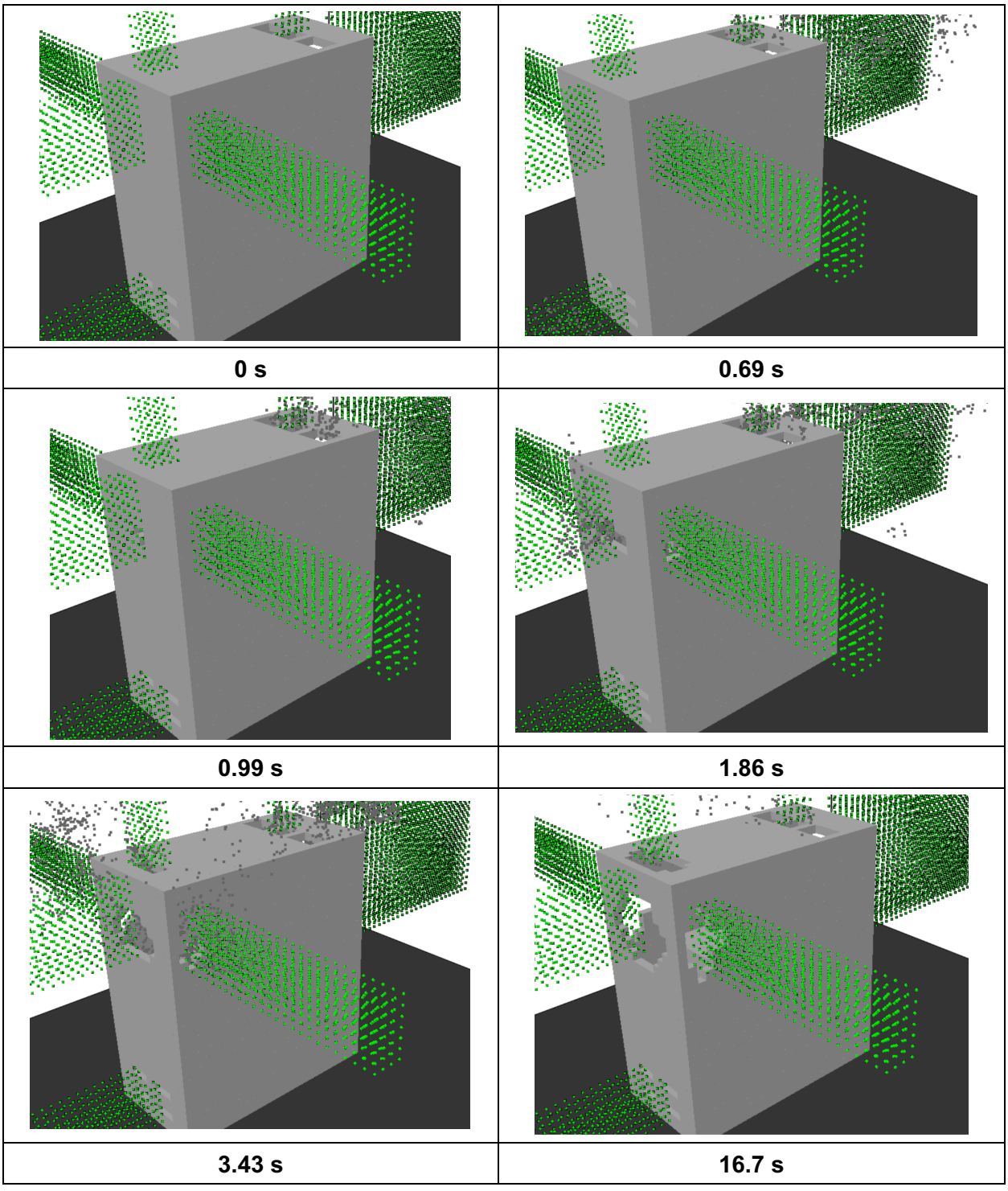

Figure 6-11
Particle distribution at various times for a 226 MJ HEAF located at the primary cable compartment bus bars in the load configuration of a vertical-lift breaker MV SWGR design

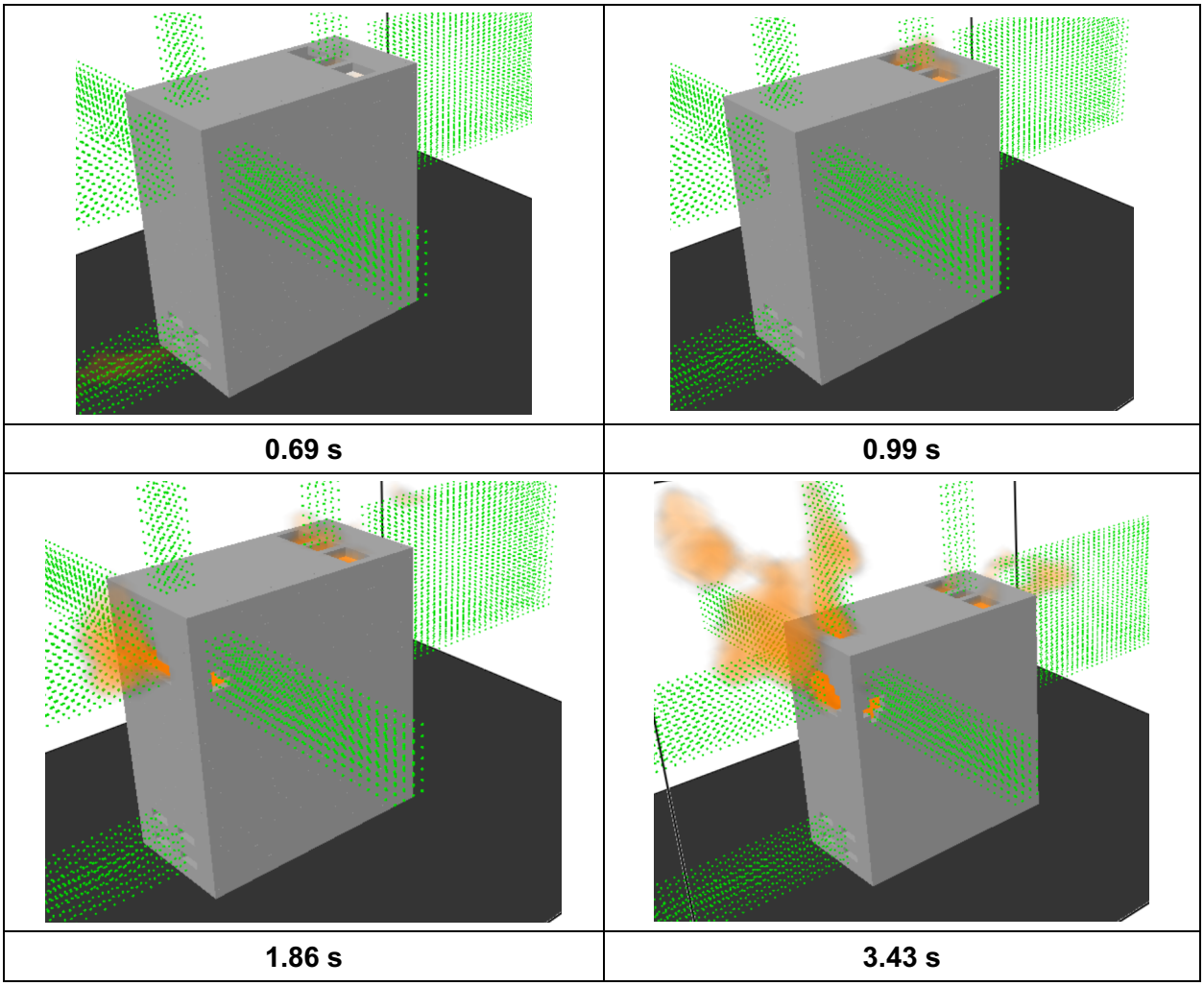

Figure 6-12
Luminous portion of the thermal plume at various times for a 226 MJ HEAF located at the primary cable compartment bus bars in the load configuration of a vertical-lift breaker MV SWGR design

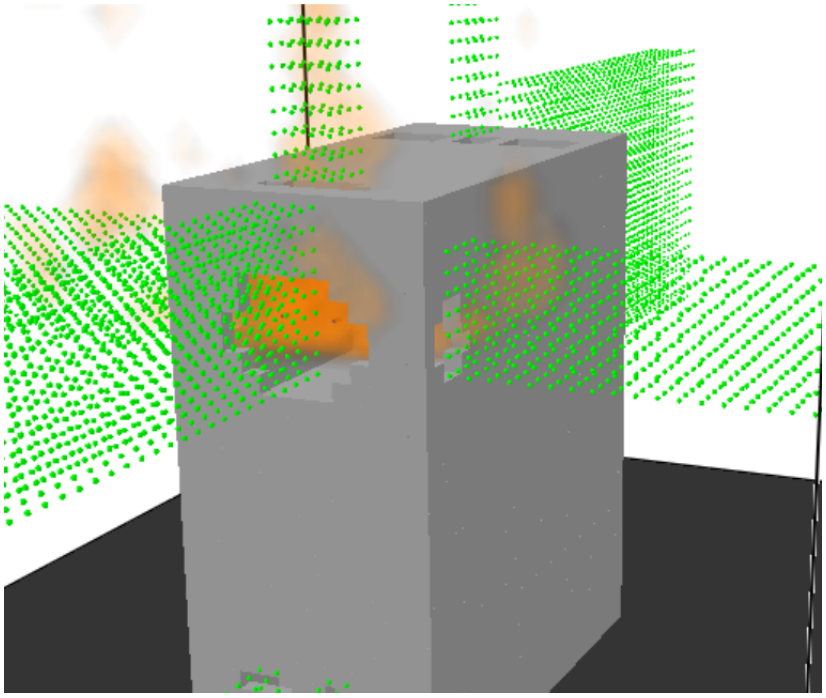

Figure 6-13
Heat release rate per unit volume at 4 s for a 226 MJ HEAF located at the primary cable compartment bus bars in the load configuration of a vertical-lift breaker MV SWGR design

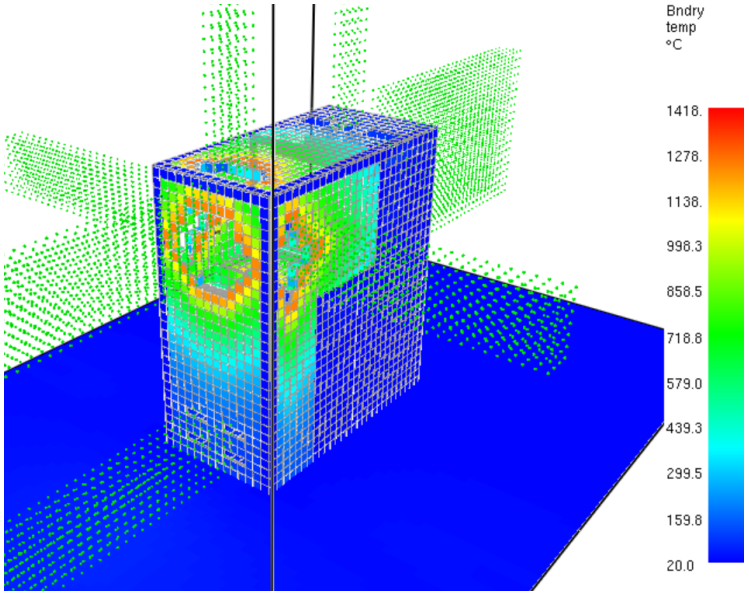

Figure 6-14
Wall temperature of the thermal plume at 15 s for a 226 MJ HEAF located at the primary cable compartment bus bars in the load configuration of a vertical-lift breaker MV SWGR design

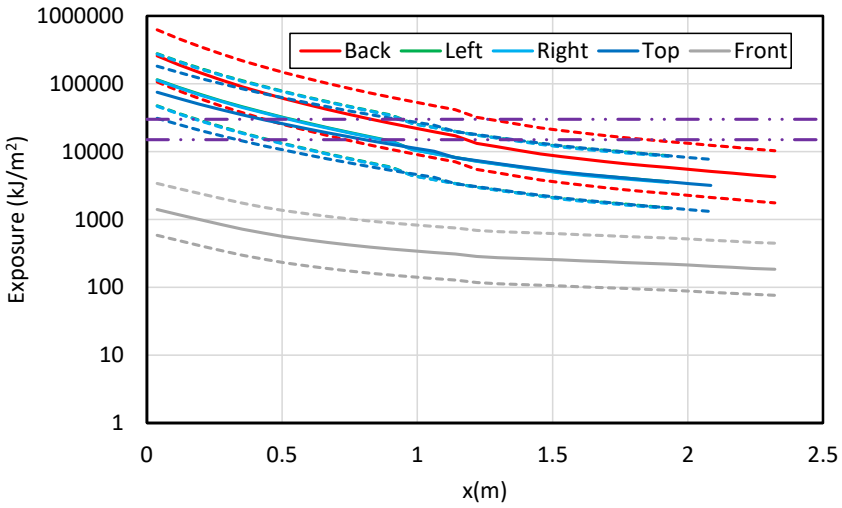

Figure 6-15
Total energy exposure as a function of distance from each face for a 226 MJ HEAF located at the primary cable compartment bus bars in the load configuration of a vertical-lift breaker MV SWGR design (HEAF simulation ID MV-GE-37). Note the results for the left- and right-sides are nearly coincident. Dashed horizontal lines correspond to the 15 MJ/m² and 30 MJ/m² target fragility threshold

6.1.1.4 GE Vertical-Lift Breaker MV SWGR Design with a HEAF at the Primary Cable Compartment Bus Bars in the Supply Configuration

Figure 6-16 depicts the metal particle distribution about the rear, side, and upper portion of the GE vertical-lift breaker switchgear at various times for a HEAF located at the primary cable compartment bus bars in the supply configuration. At 0 s, there are no particles and the switchgear enclosure is intact. The openings at 0 s are front top vents, the upper front (not shown in Figure 6-16), the rear top vent, and the rear bottom vent (not shown in Figure 6-16). At 1.52 s, the switchgear enclosure is still intact, but there are metal particles ejected from the top and, to a lesser extent, the rear vent openings. The switchgear enclosure is breached at about 1.77 s, with the switchgear enclosure breach on the upper side surfaces near the electrode. At about 3.29 s, the top of the switchgear enclosure is breached, with particles ejected from the sides and top openings (note that only the right-side is shown in Figure 6-16). The side and top switchgear enclosure openings continue to expand between 3.29 and 5.93 s, about the time the opening size growth begins to slow. The openings continue to grow slowly during the remainder of the decay stage and reach a maximum at about 16.7 s near the end of the decay stage. After 20 s (not shown in Figure 6-16), the fault is cleared and nearly all particles have dispersed. Although particles are ejected from the lower rear vent, the majority of the particles are ejected through the upper vents, and later, through the damaged switchgear enclosure.

Figure 6-17 depicts the luminous portion of the thermal plume at 1.52 s, 1.77 s, 3.29 s, and 5.93 s, corresponding to the times at which the particle distributions are shown. The luminous thermal plume is primarily confined to the switchgear enclosure prior enclosure breach as shown at 1.52 s and 1.77 s. After 1.77 s, the luminous thermal plume expands outside the switchgear enclosure and reaches a peak near the start of the decay phase between 3.20 s and 5.93 s where significant portions of the switchgear enclosure are breached.

Figure 6-18 depicts the heat release rate per unit volume at 4 s, near the beginning of the arc current decay phase. The heat release rate per unit volume shows the arc location and is largely confined to the electrode and the immediate location around the electrode. Some heat

release rate occurs above and outside due to particle oxidation. The openings in the sides of the switchgear enclosure are clearly visible.

Figure 6-19 depicts the wall temperature at about 15 s, the time at which the greatest extent of the switchgear enclosure boundary is heated. Although the heated wall temperature contributes to the heat flux at a fixed location, the temperatures are relatively low, suggesting this component is relatively small compared the energy flux directly from the arc fault and gases.

The calculated total exposure energy as a function of distance is shown in Figure 6-20, which indicates that the ZOI for this HEAF is between 0.5 – 1.0 m for the side and top faces and zero from the front and rear faces, consistent with the particle distribution and luminous plume location.

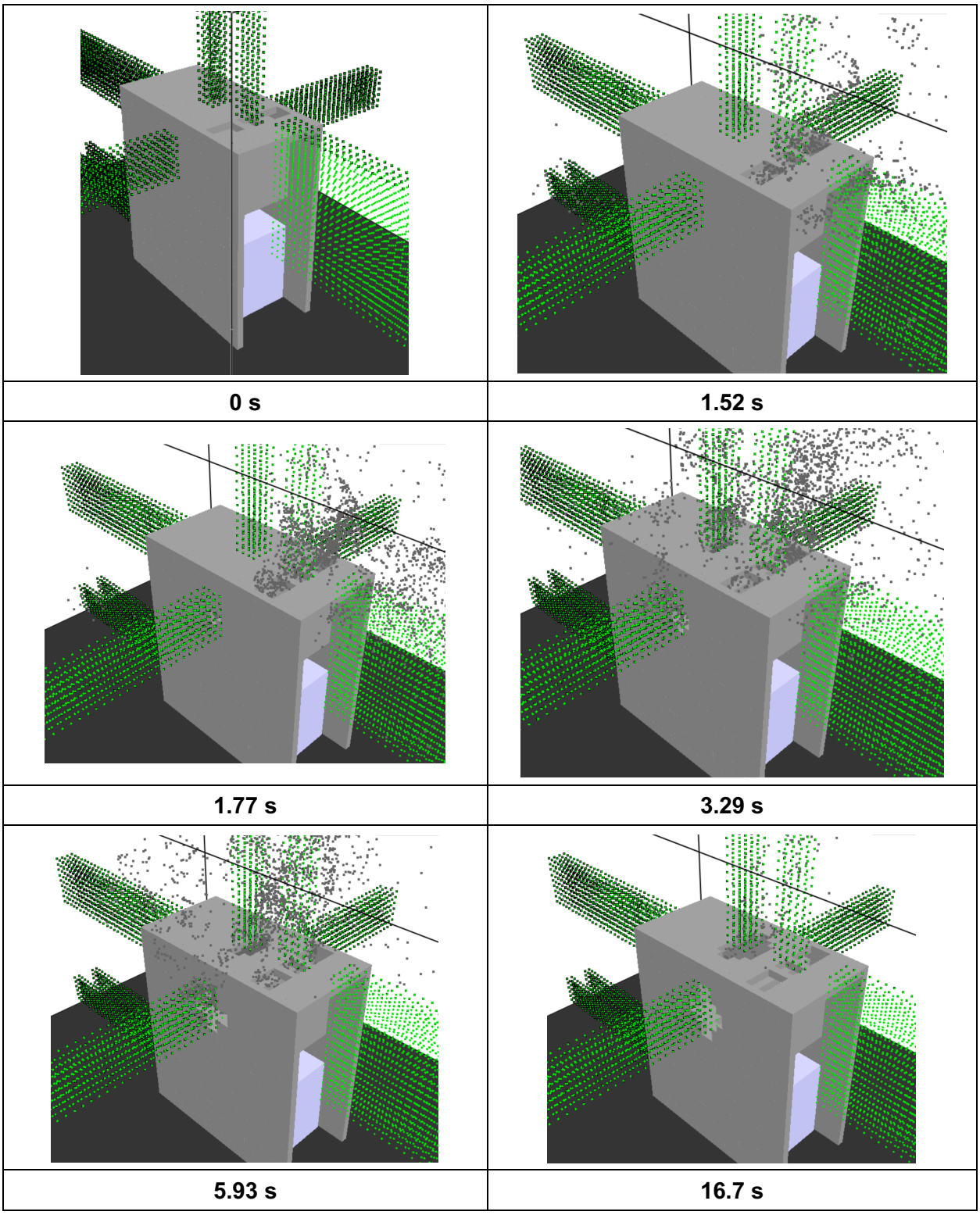

Figure 6-16
Particle distribution at various times for a 226 MJ HEAF located at the primary cable compartment bus bars in the supply configuration of a vertical-lift breaker MV SWGR design

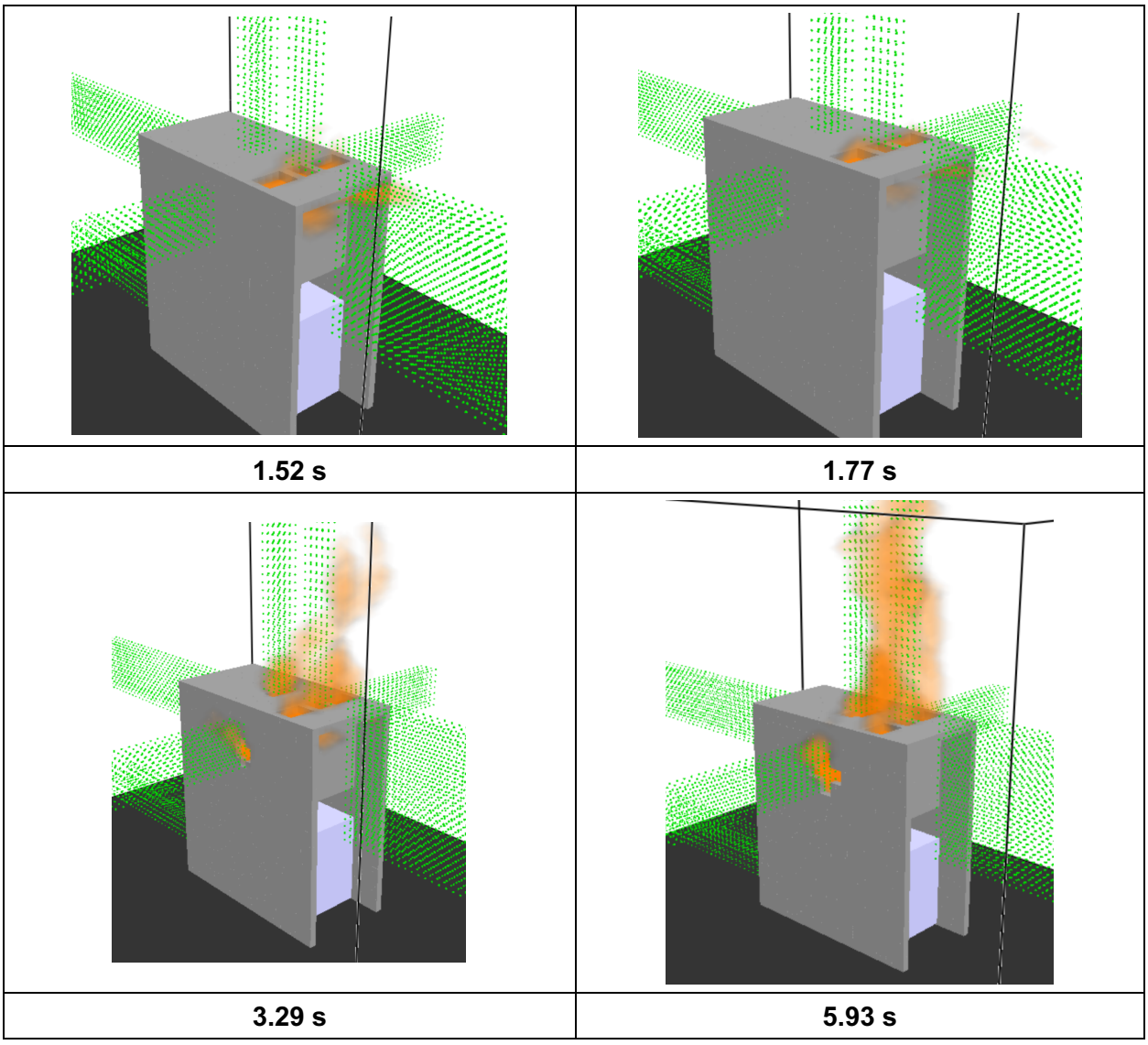

Figure 6-17
Luminous portion of the thermal plume at various times for a 226 MJ HEAF located at the primary cable compartment bus bars in the supply configuration of a vertical-lift breaker MV SWGR design

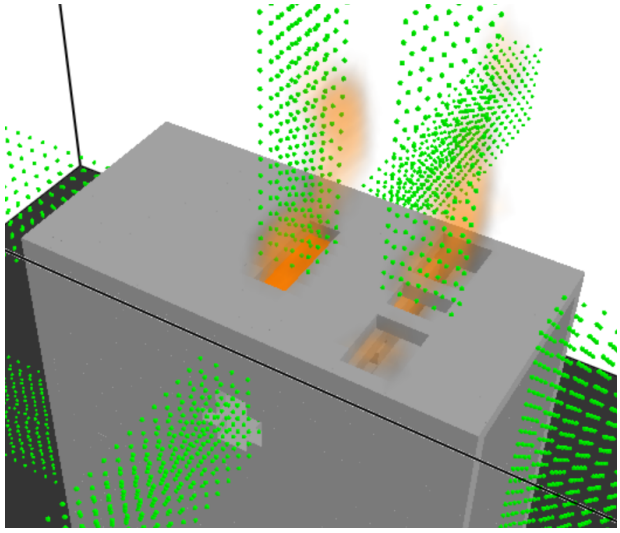

Figure 6-18
Heat release rate per unit volume at 4 s for a 226 MJ HEAF located at the primary cable compartment bus bars in the supply configuration of a vertical-lift breaker MV SWGR design

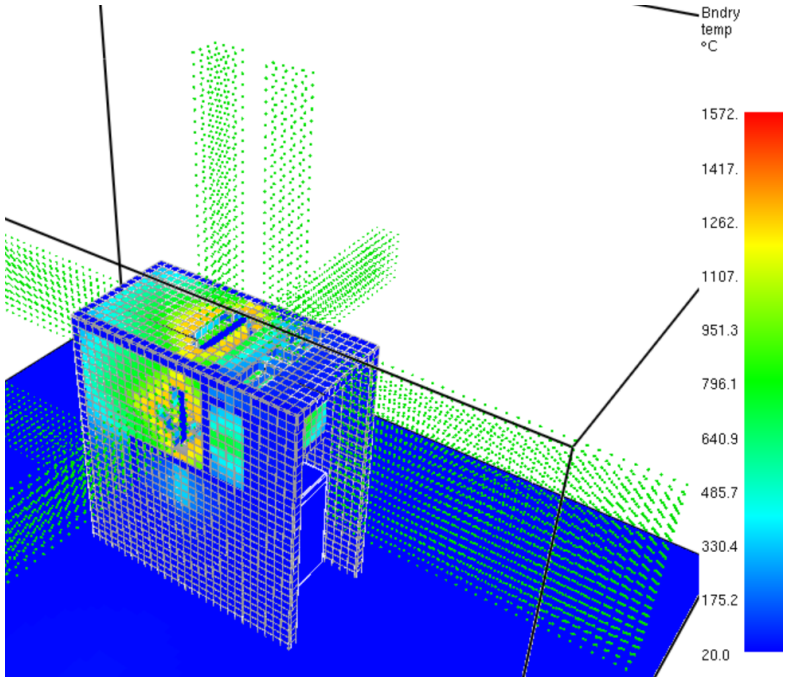

Figure 6-19
Wall temperature of the thermal plume at 15 s for a 226 MJ HEAF located at the primary cable compartment bus bars in the supply configuration of a vertical-lift breaker MV SWGR design

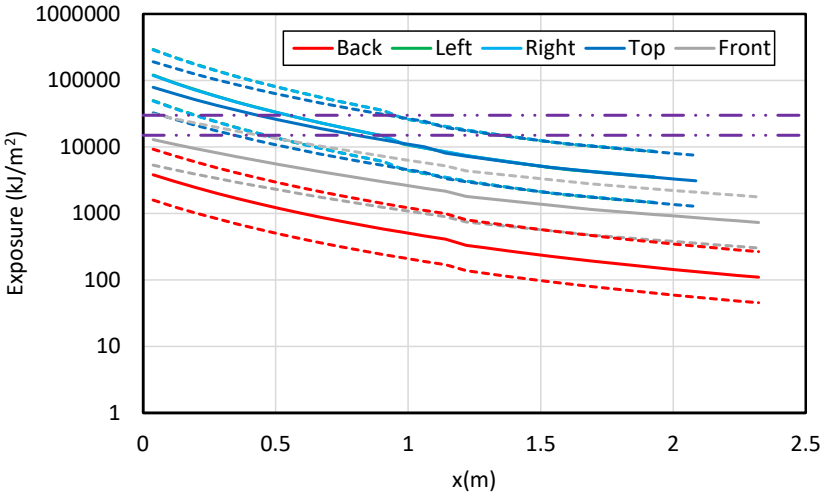

Figure 6-20
Total energy exposure as a function of distance from each face for a 226 MJ HEAF located at the primary cable compartment bus bars in the supply configuration of a vertical-lift breaker MV SWGR design (HEAF simulation ID MV-GE-38). Note the results for the left- and right-sides are nearly coincident. Dashed horizontal lines correspond to the 15 MJ/m² and 30 MJ/m² target fragility threshold

6.1.1.5 Summary of GE Vertical-Lift Breaker MV SWGR Design Results

Sections 6.1.1.1 through 6.1.1.4 present detailed FDS results for the 226 MJ HEAF in the four basic locations an arc fault is expected in the GE vertical-lift breaker MV SWGR design. The FDS results are presented in terms of the exposure severity around the switchgear enclosure, such as the particle distribution, luminous plume, the arc energy, and the switchgear enclosure boundary temperature. The exposure profiles for each switchgear enclosure face are considered, which are used to determine the ZOIs, is generally consistent with the HEAF simulation results as characterized using the particle distributions and luminous plume. In addition, the exposure is strongly dependent on the location of the HEAF. For example, HEAFs located toward the middle and front of the switchgear enclosure (i.e., the breaker stabs, the main bus bar, and the primary cable compartment main bus bar in the supply configuration) have no ZOI predicted for the rear face. Conversely, a HEAF located at the rear of the switchgear enclosure (primary cable compartment main bus bar in the load configuration) has no ZOI predicted for the front face. In all cases, the side face ZOIs are comparable given the dimensions of the arc energy and its orientation are parallel to the short switchgear enclosure face dimension. These results show the general consistency of the ZOIs and FDS model predictions with intuitive expectations.

6.1.2 ABB Horizontal Draw-Out Style MV SWGR with a HEAF at the Breaker Stabs

The FDS results for an ABB horizontal draw-out style MV SWGR with a HEAF at the breaker stabs is reviewed in detail. This HEAF is representative of HEAFs initiated in the horizontal draw-out breaker designs. The 226 MJ energy HEAF is selected (the same energy as the GE vertical lift style breaker), which corresponds to a HEAF with relatively large ZOI dimensions. This is the same HEAF energy considered for the GE vertical-lift breaker MV SWGR cabinet design HEAFs. The characteristics are as follows:

- 3 s of stiff current
- 15 s of decaying current
- Copper electrode

The arc energy power profile for this HEAF is provided in Appendix A (see Figure A-4). Similar to the HEAFs postulated on the GE vertical-lift breaker MV SWGR design, the detailed results include depictions of the switchgear enclosure breach, particle dispersion, the luminous thermal plume, the heat release rate per unit volume, the enclosure wall temperatures, and the exposure profiles as a function of distance for each switchgear enclosure surface.

Figure 6-21 depicts the metal particle distribution about the rear, side, and upper portion of the ABB horizontal draw-out style MV SWGR at various times for a horizontal draw-out breaker stab HEAF. At 0 s, there are no particles and the switchgear enclosure is intact. The openings at 0 s are front top vents, the top vents, and the lower rear vent (not shown in Figure 6-21). At 0.57 s, the switchgear enclosure is still intact, but there are metal particles ejected from the top and front vents openings. The switchgear enclosure is breached at about 0.94 s, with boundary penetration on the left- and right-sides adjacent to the electrode. The side openings continue to grow rapidly through 3.29 s. Between 3.35 s and 7.31 s, the openings grow, but less rapidly to their maximum extent. The openings continue to grow slowly during the remainder of decay stage and reach an overall maximum at about 10 s (not shown in Figure 6-21). After 19.6 s (not shown in Figure 6-21), the fault is cleared and nearly all particles have dispersed. A small number of particles are ejected from the lower rear vent before the switchgear enclosure is breached; however, the majority of the particles are ejected through the upper and front vents, and later, through the damaged switchgear enclosure walls.

Figure 6-22 depicts the luminous portion of the thermal plume at 0.57 s, 0.94 s, 3.35 s, and 7.31 s, corresponding to the times at which the particle distributions are enclosure. The luminous thermal plume extends out the top and front vents before the switchgear enclosure wall is breached as shown at t0.57 s and 0.94 s. After 0.94 s, the luminous thermal plume expands outside the cubicle sides as well as the top and front vents and reaches a peak near the start of the decay phase between 3.35 s and 7.31 s where significant portions of the switchgear enclosure are breached.

Figure 6-23 depicts the heat release rate per unit volume at 4 s, near the beginning of the arc current decay phase. The heat release rate per unit volume shows the arc location and is largely confined to the electrode and the immediate location around the electrode. The openings in the sides of the switchgear enclosure are clearly visible.

Figure 6-24 depicts the wall temperature at about 11 s, the time at which the greatest extent of the switchgear enclosure boundary is heated. Although the heated wall temperature contributes to the heat flux at a fixed location, the temperatures are relatively low, suggesting this component is relatively small compared to the energy flux directly from the arc fault and gases.

The calculated total exposure energy as a function of distance is shown in Figure 6-25. Figure 6-25 indicates that the ZOI for this simulation is between about 0.75 – 1.0 m for the side and zero from the front, top, and rear faces, consistent with the particle distribution and luminous plume location. These ZOIs are comparable to the ZOIs for the vertical-lift breaker style switchgear summarized in sections 6.1.1.1 through 6.1.1.4. One key difference is that the left and right ZOIs for the horizontal draw-out style are about 0.1 – 0.2 m greater than the vertical lift style switchgear.

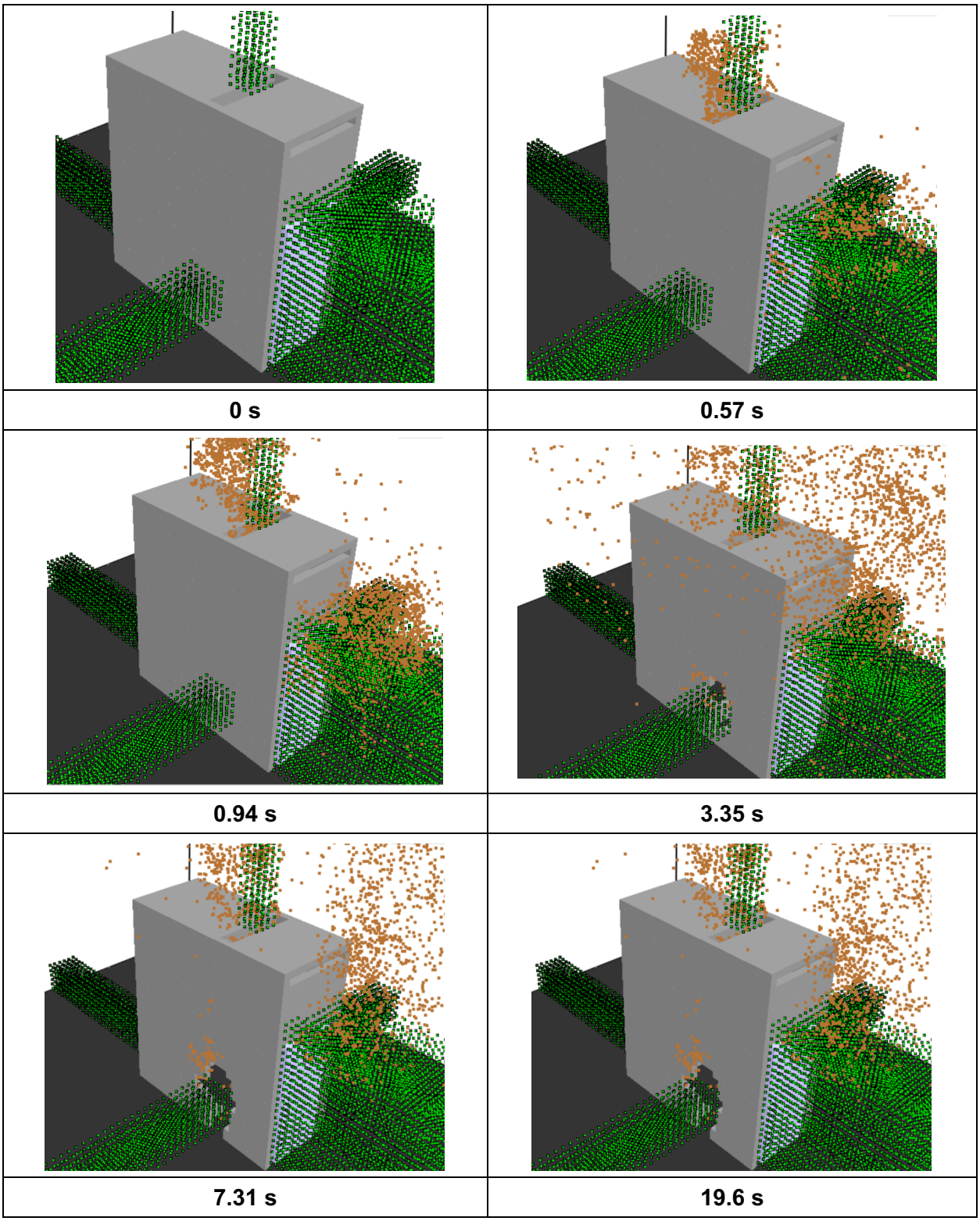

Figure 6-21
Particle distribution at various times for a 226 MJ HEAF located at the breaker stabs of the horizontal draw-out style MV SWGR

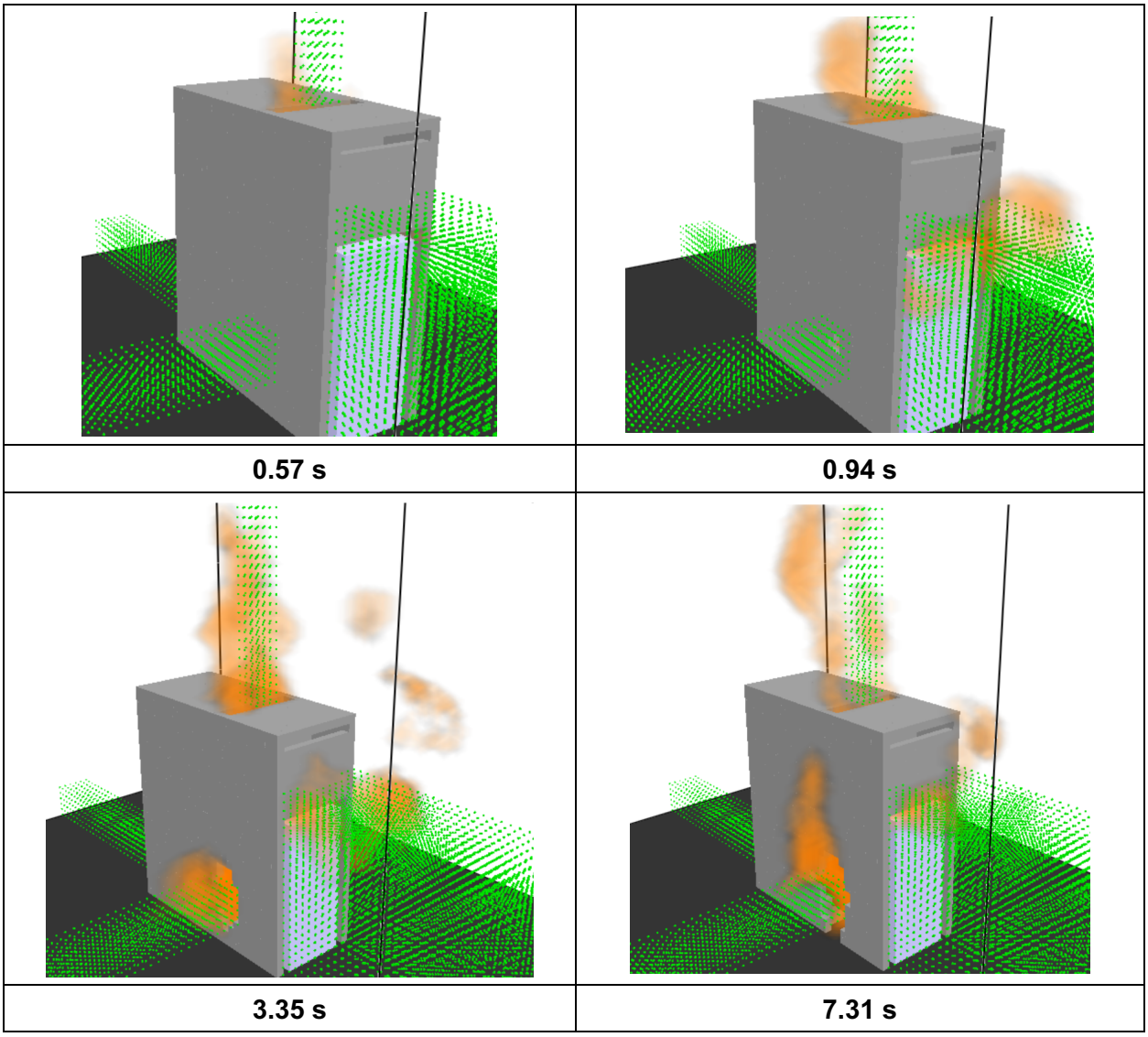

Figure 6-22
Luminous portion of the thermal plume at various times for a 226 MJ HEAF located at the breaker stabs of the horizontal draw-out style MV SWGR

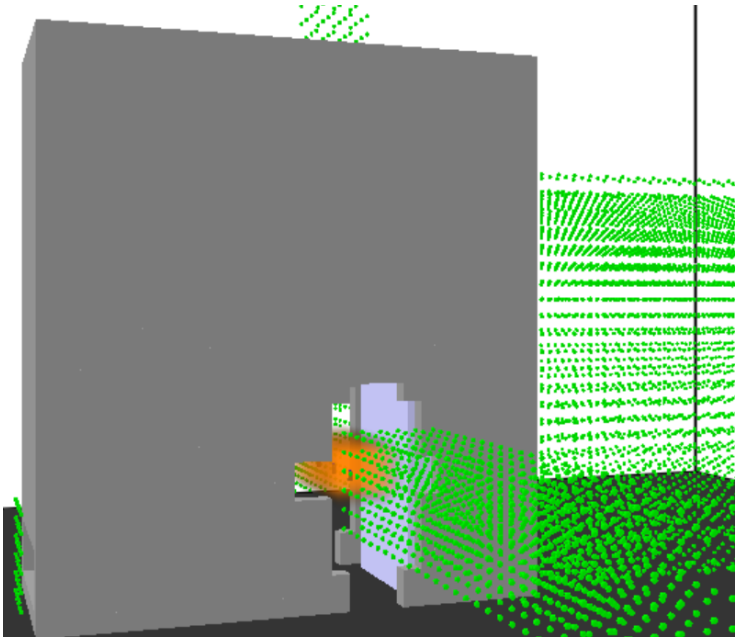

Figure 6-23
Heat release rate per unit volume at 4 s for a 226 MJ HEAF located at the breaker stabs of the horizontal draw-out style MV SWGR

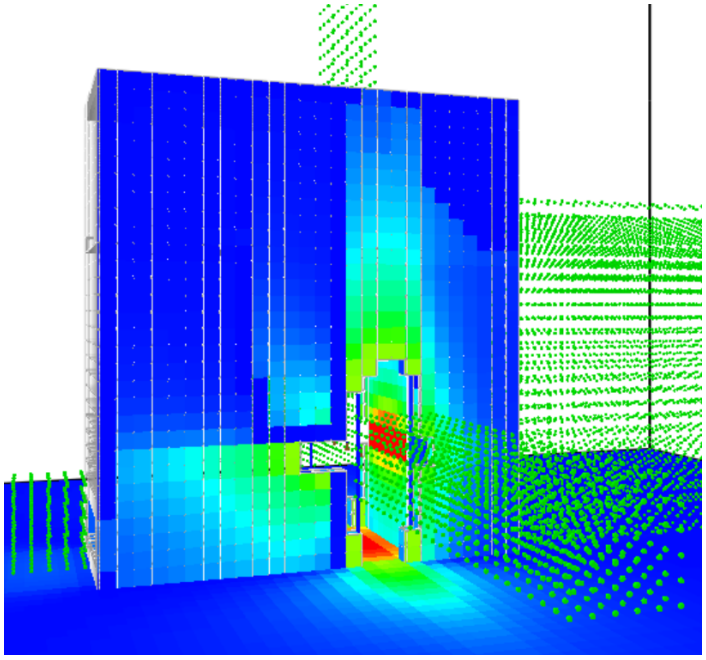

Figure 6-24
Wall temperature of the thermal plume at 11 s for a 226 MJ HEAF located at the breaker stabs of the horizontal draw-out style MV SWGR

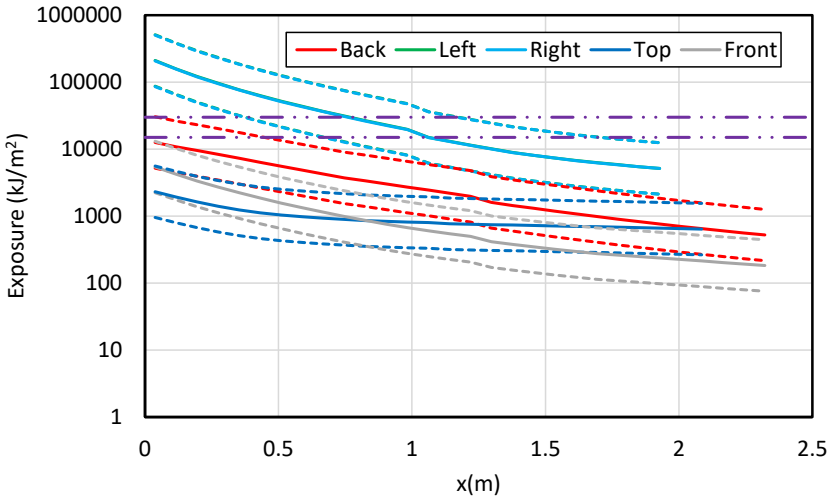

Figure 6-25
Total energy exposure as a function of distance from each face for a 226 MJ HEAF located at the breaker stabs of the horizontal draw-out style MV SWGR (HEAF simulation ID MV-ABB-5). Note the results for the left- and right-sides are nearly coincident. Dashed horizontal lines correspond to the 15 MJ/m² and 30 MJ/m² target fragility threshold

6.1.3 Summary of MV SWGR Results

6.1.3.1 ZOI Symmetry

The MV SWGR HEAFs have symmetry over the left- and right-sides of the enclosure. However, because the flow induced by the HEAF is turbulent, at any instant in time the left- and right-side flows will not be perfectly symmetric due to the random fluctuations in turbulent flow. Over time, the turbulent fluctuations should average out resulting in symmetry in the ZOIs on the left- and right-sides of the enclosure. Figure 6-26 shows the 15 MJ/m² (i.e., thermoplastic (TP) cable or aluminum bus duct) and the 30 MJ/m² (i.e., thermoset (TS) cable or steel bus duct) target ZOIs for the left- and right-sides for the MV SWGR HEAFs. For the largest ZOIs (the longest duration events) the left and ride sides are essentially equal. For the smallest ZOI (the shortest duration events) where there is insufficient time for fluctuations to average out, there is a larger amount of scatter in the left- and right-side ZOIs. Overall, the high degree of symmetry provides confidence that the simulations remained stable even though extremely high volumetric heat sources were in the domain. Numerically unstable simulations often manifest with large asymmetries.

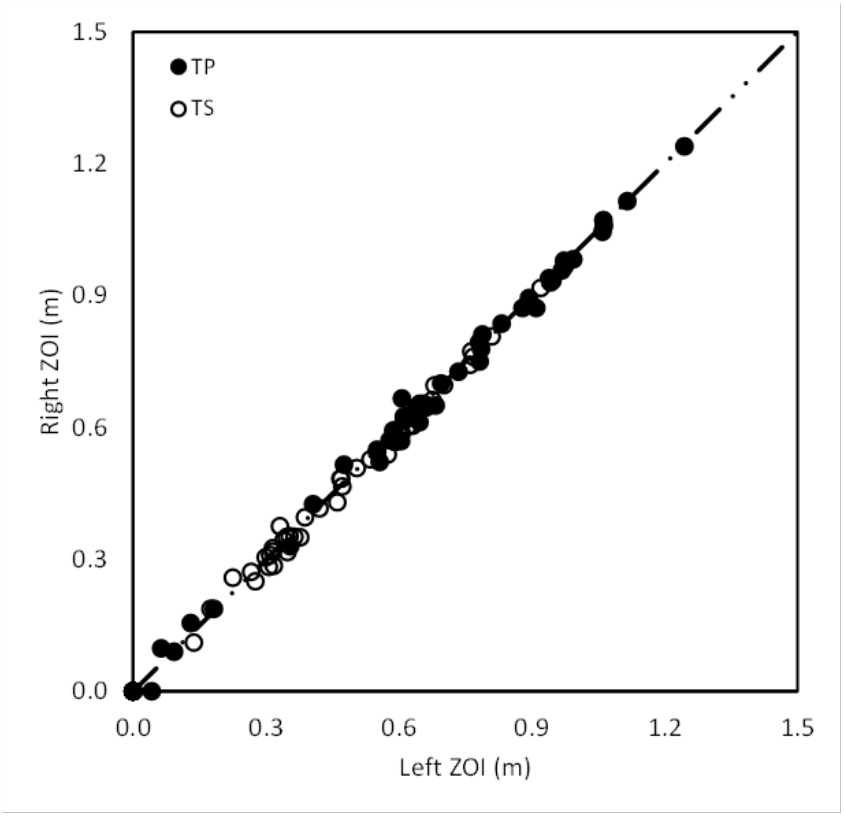

Figure 6-26
Left versus right ZOIs for all MV SWGR HEAF simulations

6.1.3.2 MV SWGR ZOI Dependencies

Figure 6-27 shows the ZOIs for the MV SWGR HEAF simulation as a function of the arc energy. The results show an increasing trend in ZOIs with respect to the arc energy and that the maximum ZOIs for 15 MJ/m² fragility targets are approximately 0.30 m larger than the maximum

ZOIs for 30 MJ/m² fragility targets. Most ZOIs are smaller than the ZOI dimensions currently used from NUREG/CR-6850 Volume 2 Appendix M [2].

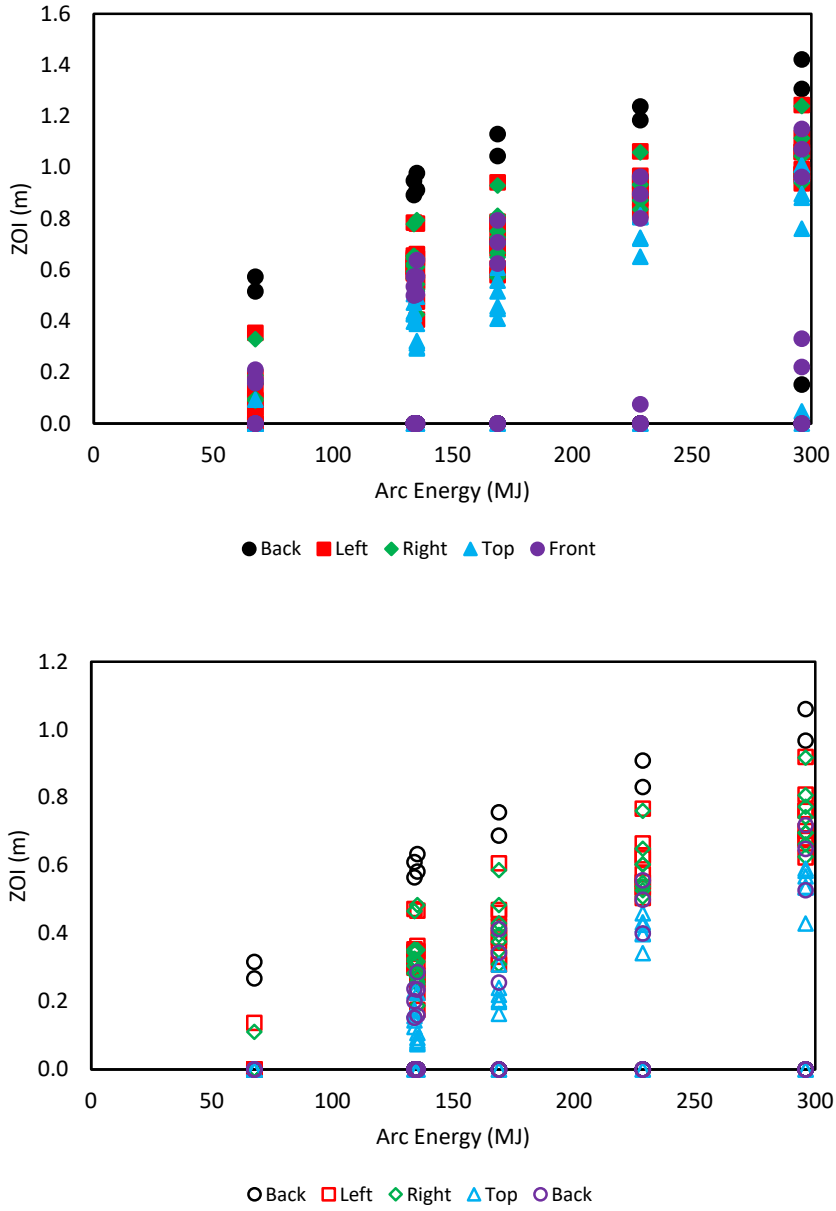

Figure 6-27
ZOIs as a function of arc energy for all MV SWGR HEAF simulations. Top – 15 MJ/m² fragility target, bottom – 30 MJ/m² fragility target. Symbol shape and color indicates the enclosure face

Figure 6-28 through Figure 6-31 show the results for each arc location.

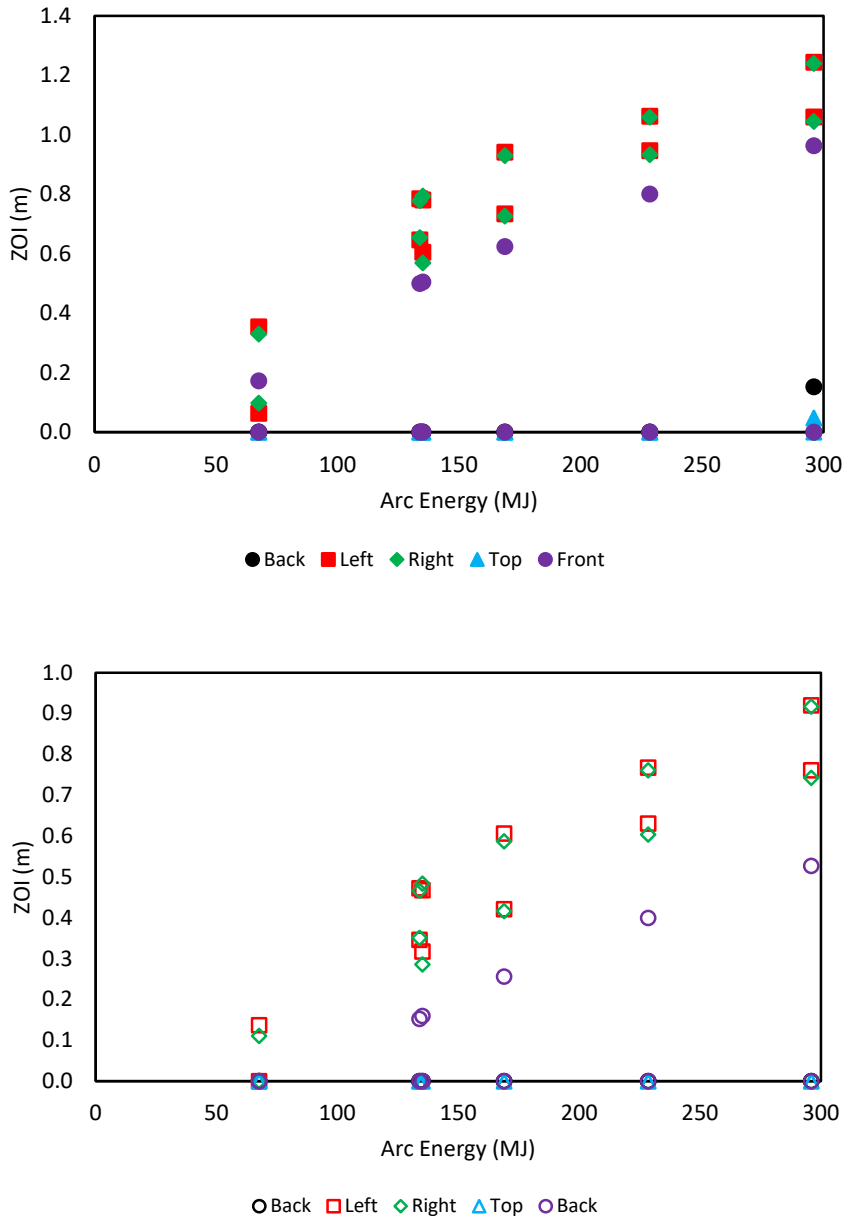

Figure 6-28
ZOIs as a function of arc energy for MV SWGR HEAF simulations with the arc initiated at the breaker stabs. Top – 15 MJ/m² fragility target, bottom – 30 MJ/m² fragility target. Symbol shape and color indicates the enclosure face

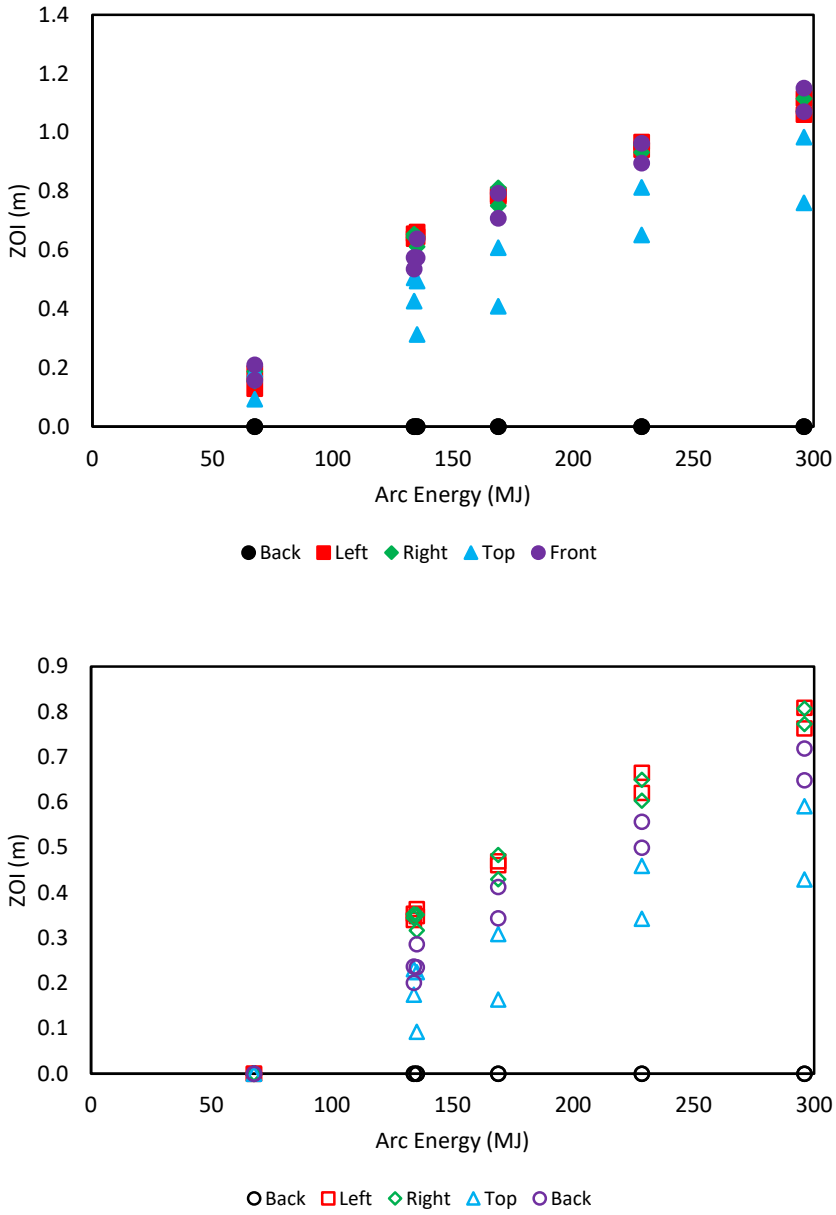

Figure 6-29
ZOIs as a function of arc energy for MV SWGR HEAF simulations with the arc initiated at the main bus bars. Top – 15 MJ/m² fragility target, bottom – 30 MJ/m² fragility target. Symbol shape and color indicates the enclosure face

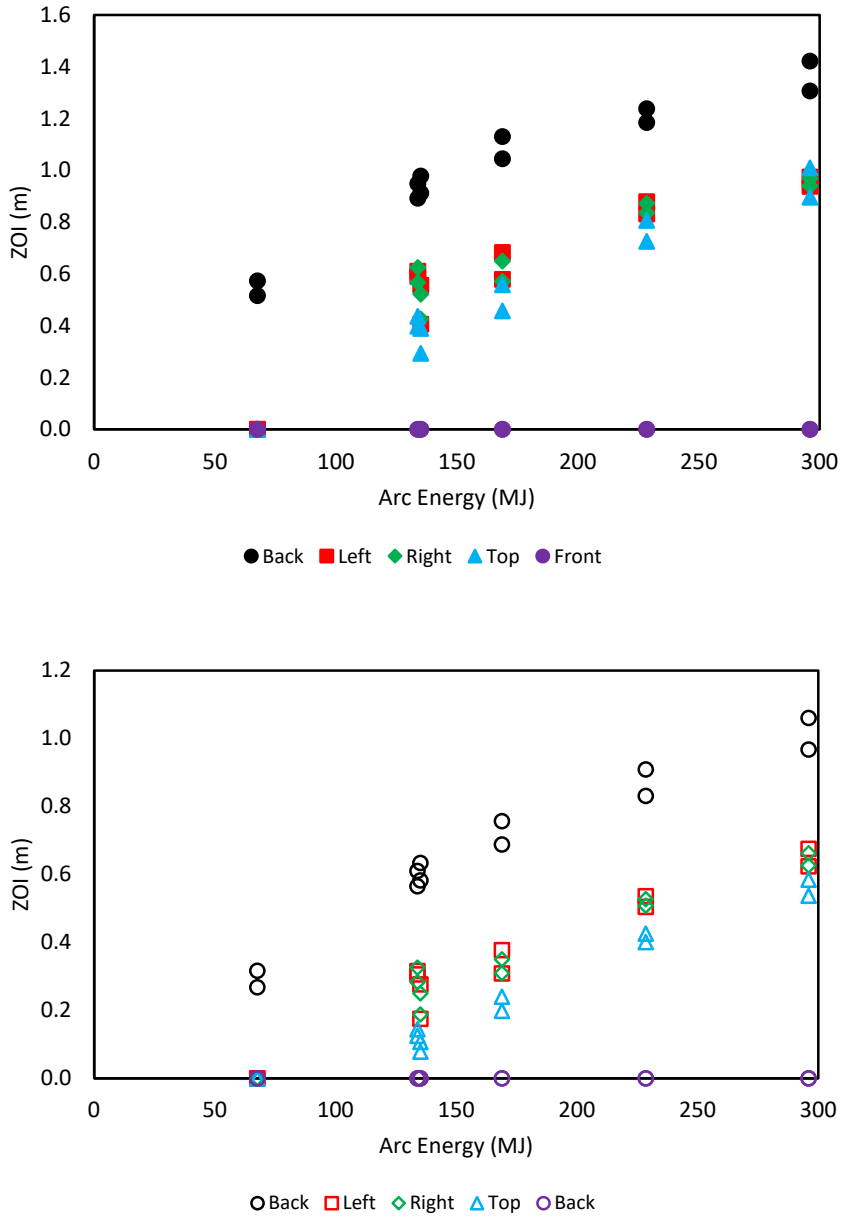

Figure 6-30
ZOIs as a function of arc energy for MV SWGR HEAF simulations with arc initiated at the primary cable compartment bus bars (PCCBB) in the load configuration. Top – 15 MJ/m² fragility target, bottom – 30 MJ/m² fragility target. Symbol shape and color indicates the enclosure face

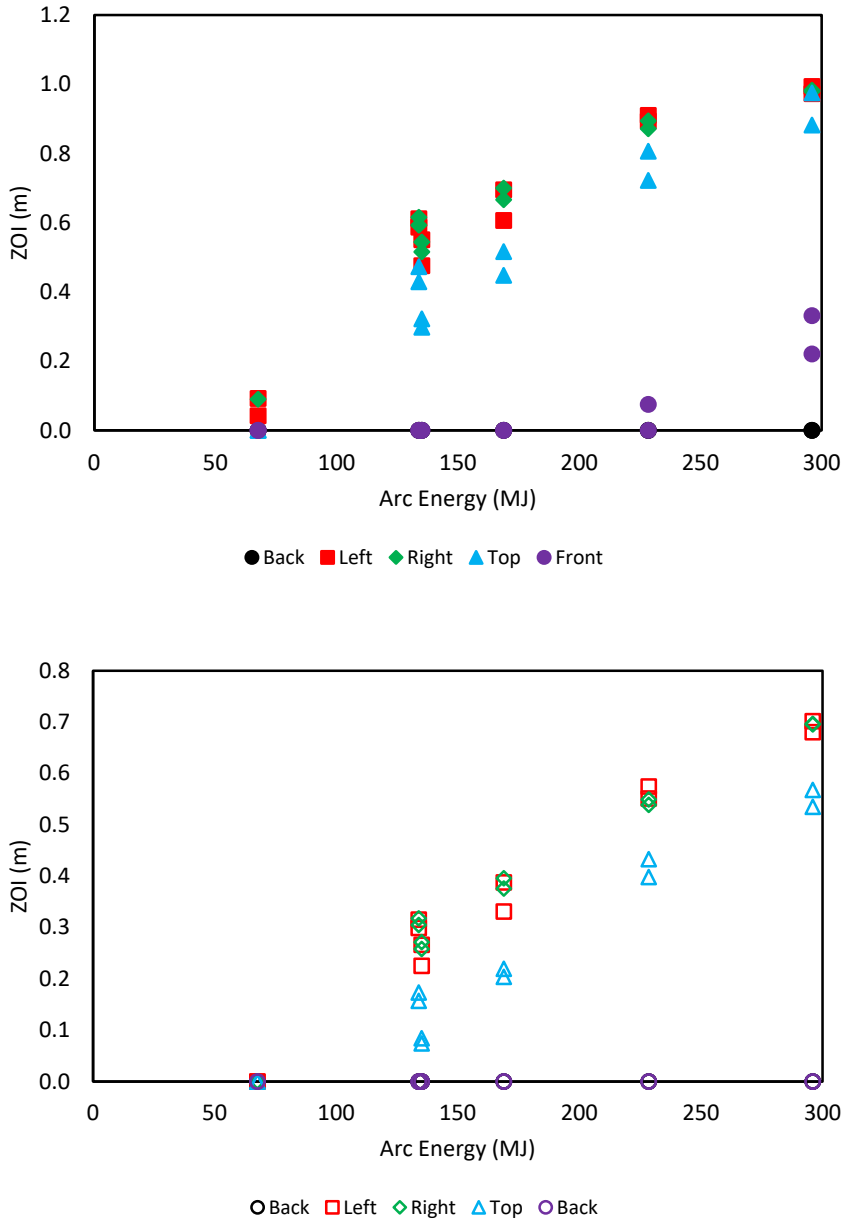

Figure 6-31
ZOIs as a function of arc energy for MV SWGR HEAFs with arc initiated at the PCCBB in the supply configuration. Top – 15 MJ/m² fragility target, bottom – 30 MJ/m² fragility target. Symbol shape and color indicates the enclosure face

Figure 6-32 compares the ZOIs for copper and aluminum bus bars for all the MV SWGR HEAF simulations except the breaker stab HEAF simulations where only copper bus bars were modeled. The comparison of copper and aluminum bus bar ZOIs shown in Figure 6-32 identify the line of perfect agreement, which indicates the copper and aluminum bus bar ZOIs are equal. There is data on each side of the line, indicating the results are not equal, but the absolute difference in the ZOIs is on the order of 0.1 m or less. As described in Section 4.1, there is a known model uncertainty with the FDS exposure predictions, and 95% confidence intervals are computed for the simulations (see Appendix B). For ZOI differentials of 0.1 m or less, the 95% confidence intervals for the copper bus bar material includes the ZOI for the aluminum bus bar material, and vice versa. This means that there is no significant difference in the aluminum and copper bus bar ZOIs for a given arc energy profile, arc location, and switchgear enclosure face. This is a significant result especially given the treatment of each electrode is different within the FDS model in terms of the energy absorbed by the bus bars, the mass consumed during the arc by the bus bars, and the oxidation of the liquid particles.

The overall results indicate that while there are differences in the treatment of the copper and aluminum in the FDS model, the resulting differences in the ZOIs are small. This is a significant conclusion demonstrated by the FDS modeling and may be illustrated further by considering the absolute ZOI differences and the model uncertainty. The aluminum bus bar material has a lower melting temperature and a greater oxidation energy, both of which nominally contribute to an increased energy flux at a fixed location. However, the dominant factor is the arc energy, and these differences in electrode behavior are minor in comparison to this.

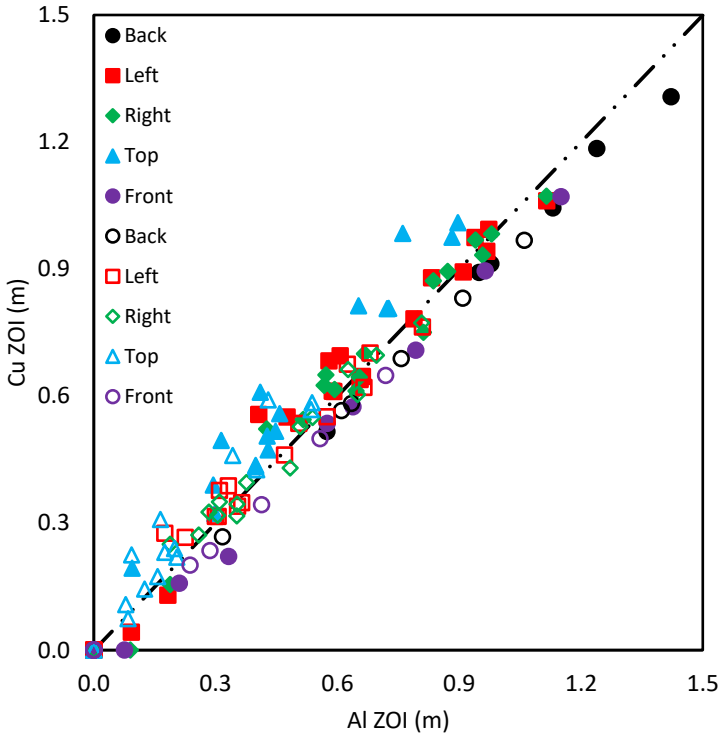

Figure 6-32
Aluminum versus copper bus bar ZOIs for all MV SWGR HEAF simulations (except for the breaker stab HEAFs which only used copper)

6.1.3.3 FDS Modeling Insights for MV SWGR

FDS modeling insights for MV SWGR HEAF simulations are as follows:

- There is no significant difference in the ZOI dimensions between copper and aluminum bus bar materials given common arc energy profile, arc location, and switchgear enclosure face. The ZOIs for each material are within the 95th percentile of the model uncertainty band as computed from the ZOI predictions for either material.
- The dominant parameter affecting the HEAF ZOIs in the MV SWGR was the total arc energy. A secondary parameter for the medium-voltage switchgear was the switchgear type (vertical-lift breaker style or horizontal draw-out breaker style).
- The largest factor affecting the ZOIs is duration and extent of the view between the arc volume and the target location. ZOIs tend to increase within increasing arc energy due to the greater damage to the switchgear boundaries.
- ZOIs are greater on the switchgear enclosure faces closest to the arc. Switchgear enclosure faces that are near the arc melt sooner, resulting in an opening that increases in size during the arc and shortly after the arc clears. This results in a larger energy flux at the target location and a larger ZOI at these sides.
- The side ZOIs are smaller for vertical-lift breaker style switchgear as compared to horizontal draw-out breaker style breaker switchgear. In addition, for vertical-lift breaker style switchgear in the supply configuration, there is no top ZOI. The load configuration vertical-lift breaker style switchgear and the horizontal draw-out breaker style switchgear have comparable top ZOIs.

These insights are consistent with overall expectations in terms of the HEAF phenomena as modeled in FDS. Since the HEAF is modeled as a high heat release rate per unit volume, the greatest exposure at a fixed location occurs when the view factor between the arc volume and the location in consideration is maximized.

6.1.3.4 Tabulated MV SWGR ZOIs

Table 6-1 shows a summary of the ZOIs for the MV SWGR HEAF simulations, including the type of enclosure, the bus bar material, the stiff current period for the arc power, the decay period for the arc power, the arc location, the total energy dissipated by the HEAF, and the ZOIs on each face of the enclosure for both 15 MJ/m² and 30 MJ/m² fragility targets.

Table 6-1
Summary of MV SWGR ZOIs

HEAF Summary						ZOI (m)									
						15 MJ/m² Target Fragility					30 MJ/m² Target Fragility				
HEAF ID[1,2]	Bus Bar Material	Stiff (s)	Decay (s)	Arc Location	Arc Energy[3] (MJ)	Back	Left	Right	Top	Front	Back	Left	Right	Top	Front
MV-GE-1	Al	2	0	Main Bus Bar	68	None	0.18	0.19	0.09	0.21	None[4]	None	None	None	None
MV-GE-2	Al	2	0	PCCBB Load	68	0.57	None	None	None	None	0.32	None	None	None	None
MV-GE-3	Al	2	0	PCCBB Supply	68	None	0.09	0.09	None	None	None	None	None	None	None
MV-GE-4	Al	4	0	Main Bus Bar	135	None	0.66	0.65	0.31	0.64	None	0.36	0.35	0.09	0.29
MV-GE-5	Al	4	0	PCCBB Load	135	0.98	0.41	0.43	0.29	None	0.63	0.17	0.19	0.08	None
MV-GE-6	Al	4	0	PCCBB Supply	135	None	0.48	0.52	0.30	None	None	0.23	0.26	0.08	None
MV-GE-7	Al	5	0	Main Bus Bar	169	None	0.79	0.81	0.41	0.79	None	0.47	0.48	0.16	0.41
MV-GE-8	Al	5	0	PCCBB Load	169	1.13	0.58	0.57	0.46	None	0.76	0.31	0.31	0.20	None
MV-GE-9	Al	5	0	PCCBB Supply	169	None	0.61	0.67	0.45	None	None	0.33	0.38	0.20	None
MV-GE-10	Al	0	15	Main Bus Bar	131	None	0.66	0.65	0.43	0.57	None	0.35	0.35	0.17	0.24
MV-GE-11	Al	0	15	PCCBB Load	131	0.95	0.59	0.57	0.40	None	0.61	0.31	0.28	0.12	None

HEAF Summary						ZOI (m)									
						15 MJ/m² Target Fragility					30 MJ/m² Target Fragility				
HEAF ID[1,2]	**Bus Bar Material**	**Stiff (s)**	**Decay (s)**	**Arc Location**	**Arc Energy[3] (MJ)**	**Back**	**Left**	**Right**	**Top**	**Front**	**Back**	**Left**	**Right**	**Top**	**Front**
MV-GE-12	Al	0	15	PCCBB Supply	131	None	0.59	0.59	0.43	None	None	0.30	0.30	0.16	None
MV-GE-13	Al	3	15	Main Bus Bar	226	None	0.97	0.96	0.65	0.96	None	0.67	0.65	0.34	0.56
MV-GE-14	Al	3	15	PCCBB Load	226	1.24	0.83	0.84	0.73	None	0.91	0.50	0.51	0.40	None
MV-GE-15	Al	3	15	PCCBB Supply	226	None	0.91	0.87	0.72	0.08	None	0.57	0.54	0.40	None
MV-GE-16	Al	5	15	Main Bus Bar	293	None	1.12	1.11	0.76	1.15	None	0.81	0.81	0.43	0.72
MV-GE-17	Al	5	15	PCCBB Load	293	1.42	0.94	0.94	0.90	None	1.06	0.62	0.63	0.54	None
MV-GE-18	Al	5	15	PCCBB Supply	293	None	0.97	0.98	0.88	0.33	None	0.68	0.70	0.54	None
MV-GE-19	Cu	2	0	Breaker Stabs	68	None	0.06	0.10	None	0.17	None	None	None	None	None
MV-GE-20	Cu	2	0	Main Bus Bar	68	None	0.13	0.16	0.19	0.16	None	None	None	None	None
MV-GE-21	Cu	2	0	PCCBB Load	68	0.52	None	None	None	None	0.27	None	None	None	None
MV-GE-22	Cu	2	0	PCCBB Supply	68	None	0.04	None	None	None	None	None	None	None	None
MV-GE-23	Cu	4	0	Breaker Stabs	135	None	0.60	0.57	None	0.50	None	0.32	0.29	None	0.16

HEAF Summary						ZOI (m)									
						15 MJ/m² Target Fragility					30 MJ/m² Target Fragility				
HEAF ID[1,2]	Bus Bar Material	Stiff (s)	Decay (s)	Arc Location	Arc Energy[3] (MJ)	Back	Left	Right	Top	Front	Back	Left	Right	Top	Front
MV-GE-24	Cu	4	0	Main Bus Bar	135	None	0.65	0.61	0.49	0.57	None	0.35	0.32	0.22	0.23
MV-GE-25	Cu	4	0	PCCBB Load	135	0.91	0.56	0.52	0.39	None	0.58	0.28	0.25	0.11	None
MV-GE-26	Cu	4	0	PCCBB Supply	135	None	0.55	0.54	0.32	None	None	0.27	0.27	0.07	None
MV-GE-27	Cu	5	0	Breaker Stabs	169	None	0.73	0.73	None	0.62	None	0.42	0.42	None	0.26
MV-GE-28	Cu	5	0	Main Bus Bar	169	None	0.78	0.75	0.61	0.71	None	0.46	0.43	0.31	0.34
MV-GE-29	Cu	5	0	PCCBB Load	169	1.04	0.68	0.65	0.56	None	0.69	0.38	0.35	0.24	None
MV-GE-30	Cu	5	0	PCCBB Supply	169	None	0.70	0.70	0.52	None	None	0.39	0.40	0.22	None
MV-GE-31	Cu	0	15	Breaker Stabs	131	None	0.65	0.65	None	0.50	None	0.35	0.35	None	0.15
MV-GE-32	Cu	0	15	Main Bus Bar	131	None	0.64	0.64	0.51	0.54	None	0.34	0.34	0.23	0.20
MV-GE-33	Cu	0	15	PCCBB Load	131	0.89	0.61	0.63	0.44	None	0.57	0.32	0.33	0.14	None
MV-GE-34	Cu	0	15	PCCBB Supply	131	None	0.61	0.62	0.47	None	None	0.32	0.32	0.17	None
MV-GE-35	Cu	3	15	Breaker Stabs	226	None	0.95	0.93	None	0.80	None	0.63	0.60	None	0.40

HEAF Summary						ZOI (m)									
						15 MJ/m² Target Fragility					30 MJ/m² Target Fragility				
HEAF ID[1,2]	**Bus Bar Material**	**Stiff (s)**	**Decay (s)**	**Arc Location**	**Arc Energy[3] (MJ)**	**Back**	**Left**	**Right**	**Top**	**Front**	**Back**	**Left**	**Right**	**Top**	**Front**
MV-GE-36	Cu	3	15	Main Bus Bar	226	None	0.94	0.93	0.81	0.90	None	0.62	0.60	0.46	0.50
MV-GE-37	Cu	3	15	PCCBB Load	226	1.18	0.88	0.87	0.81	None	0.83	0.54	0.53	0.43	None
MV-GE-38	Cu	3	15	PCCBB Supply	226	None	0.89	0.89	0.81	None	None	0.55	0.55	0.43	None
MV-GE-39	Cu	5	15	Breaker Stabs	293	None	1.06	1.05	0.05	0.96	None	0.76	0.74	None	0.53
MV-GE-40	Cu	5	15	Main Bus Bar	293	None	1.06	1.07	0.98	1.07	None	0.76	0.77	0.59	0.65
MV-GE-41	Cu	5	15	PCCBB Load	293	1.31	0.97	0.97	1.01	None	0.97	0.68	0.66	0.58	None
MV-GE-42	Cu	5	15	PCCBB Supply	293	None	0.99	0.98	0.97	0.22	None	0.70	0.70	0.57	None
MV-ABB-1	Cu	2	0	Breaker Stabs	68	None	0.35	0.33	None	None	None	0.14	0.11	None	None
MV-ABB-2	Cu	4	0	Breaker Stabs	135	None	0.78	0.79	None	None	None	0.47	0.48	None	None
MV-ABB-3	Cu	5	0	Breaker Stabs	169	None	0.94	0.93	None	None	None	0.61	0.59	None	None
MV-ABB-4	Cu	0	15	Breaker Stabs	131	None	0.79	0.78	None	None	None	0.47	0.47	None	None
MV-ABB-5	Cu	3	15	Breaker Stabs	226	None	1.06	1.06	None	None	None	0.77	0.76	None	None

HEAF Summary						ZOI (m)									
						15 MJ/m² Target Fragility					30 MJ/m² Target Fragility				
HEAF ID[1,2]	**Bus Bar Material**	**Stiff (s)**	**Decay (s)**	**Arc Location**	**Arc Energy[3] (MJ)**	**Back**	**Left**	**Right**	**Top**	**Front**	**Back**	**Left**	**Right**	**Top**	**Front**
MV-ABB-6	Cu	5	15	Breaker Stabs	293	0.15	1.24	1.24	None	None	None	0.92	0.92	None	None

[1]The MV-GE-X designation corresponds to a GE vertical-lift breaker switchgear style and the MV-ABB-X designation corresponds to an ABB horizontal draw-out switchgear style.

[2]The FDS input designator is not the same as the input file name but uniquely corresponds to a single FDS input file. Refer to Appendix B of this report for the corresponding input file nomenclature designator.

[3]Energy as input into FDS model, which include a finite time of decay from the peak power. This energy total differs slightly from the energy listed in Table 5-1 due to melting of the electrode (see Section 5.8.2).

[4]None means that there is no external ZOI.

6.2 Low Voltage Switchgear HEAF Simulations

This section provides a summary of the FDS results for the LV SWGR simulations. The detailed FDS results for FEDB 50935 [12] (as explained in Section 4.3), are the basis for the LV ZOIs. Graphical results showing the exposure as a function of distance from each face of the enclosure are provided in Appendix B.1 for variations of FEDB 50935.

6.2.1 Selected Low Voltage Switchgear HEAF Simulations

Two FDS results for the LV SWGR HEAF simulations, constructed with the Westinghouse Type DS switchgear, corresponding to FEDB 50935 are reviewed in detail. Both simulations involved a HEAF at the breaker stabs, the first simulation involved a HEAF at the middle breaker compartment and the second at a breaker compartment at the top of the switchgear enclosure. In both cases, the arc remains at the initial location for the model duration. The former simulation most closely approximates FEDB 50935. The HEAF energy profile is depicted in Figure A-8.

Similar to the MV SWGR HEAF simulations, the detailed results include depictions of the switchgear enclosure breach, particle dispersion, the luminous thermal plume, the heat release rate per unit volume, the enclosure wall temperatures, and the exposure profiles as a function of distance for each switchgear enclosure surface.

6.2.1.1 Middle-Height Cubicle HEAF

Figure 6-33 depicts the metal particle distribution about the rear, side, and upper portion of the LV SWGR at various times for a HEAF located at the breaker stabs in a middle-height cubicle. At 0 s, there are no metal particles and the switchgear enclosure is intact. The openings at 0 s are the front vent, the top vents, and the rear vents (not shown in Figure 6-33). At 1.96 s the switchgear enclosure is intact, and particles are ejected through the top and front vents with an increasing in number density. At about 8 s (not shown in Figure 6-33), small portions of the switchgear enclosure right-side is breached; however, significant quantities of particles are not ejected from these openings. After about 9.46 s, the particles reach a relatively steady density, which persists through 24.6 s and 40.38 s. Except for small openings on the switchgear enclosure face adjacent to the electrode, the switchgear enclosure remains largely intact during the entire HEAF, and particles are primarily ejected through the existing top and front vents. At 43.6 s, several seconds after the fault is cleared, nearly all particles are dispersed. Internally, the switchgear cubicle containing the HEAF is breached and exposes the adjacent internal switchgear cubicle (see Figure 6-35).

Figure 6-34 depicts the luminous portion of the thermal plume at 1.96 s, 9.46 s, 24.6 s, and 40.38 s, corresponding to the times at which the particle distributions are shown. The luminous thermal plume is relatively constant after 1.96 s and extends minimally beyond the top and front vents.

Figure 6-35 depicts the heat release rate per unit volume at 30.2 s from below. The switchgear enclosure damage is about maximized, and the electrode arc is clearly defined by the heat release rate per unit volume.

Figure 6-36 depicts the wall temperature at about 33.7 s, the time at which the greatest extent of the switchgear enclosure boundary is heated. Although the heated wall temperature contributes to the heat flux at a fixed location, the temperatures are relatively low, suggesting this component is relatively small compared the energy flux directly from the arc fault and gases.

The calculated total exposure energy as a function of distance is shown in Figure 6-37, which indicates that the ZOI for this simulation is between about 0.4 – 0.7 m for the right-side and nearly zero from all other surfaces, consistent with the particle distribution and luminous plume location.

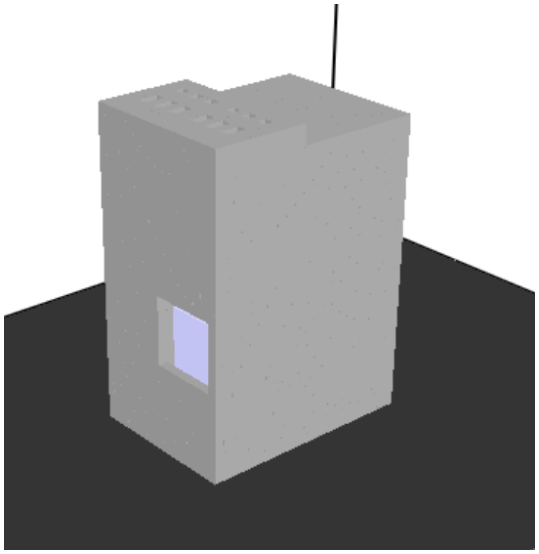

0 s

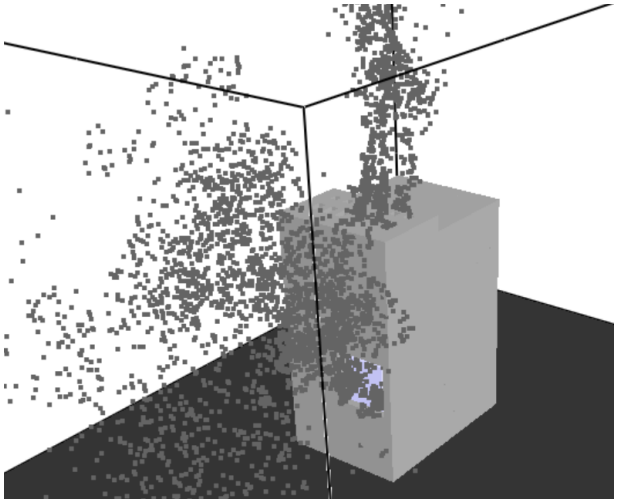

1.96 s

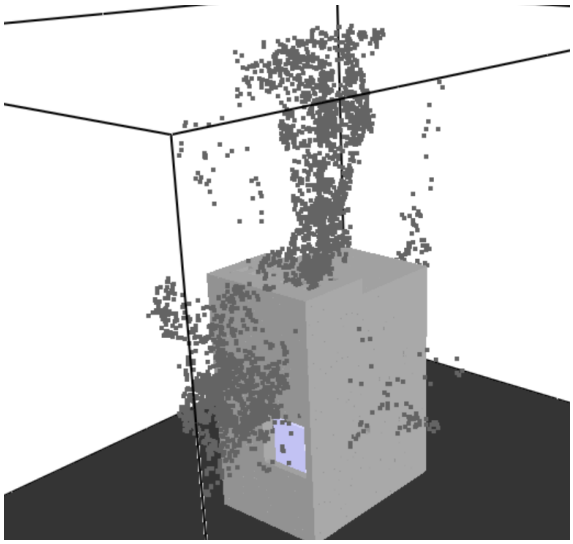

9.46 s

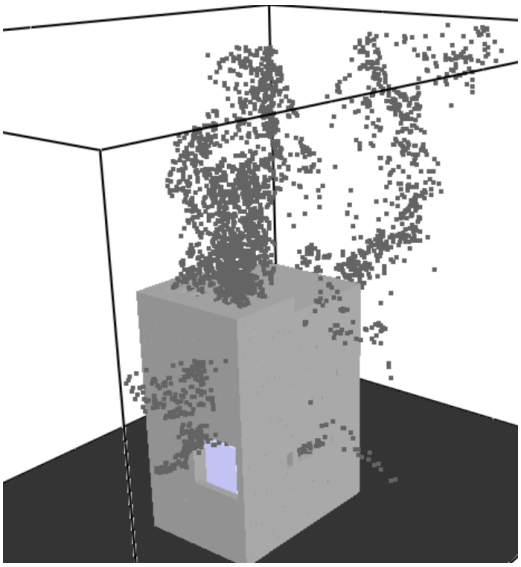

24.6 s

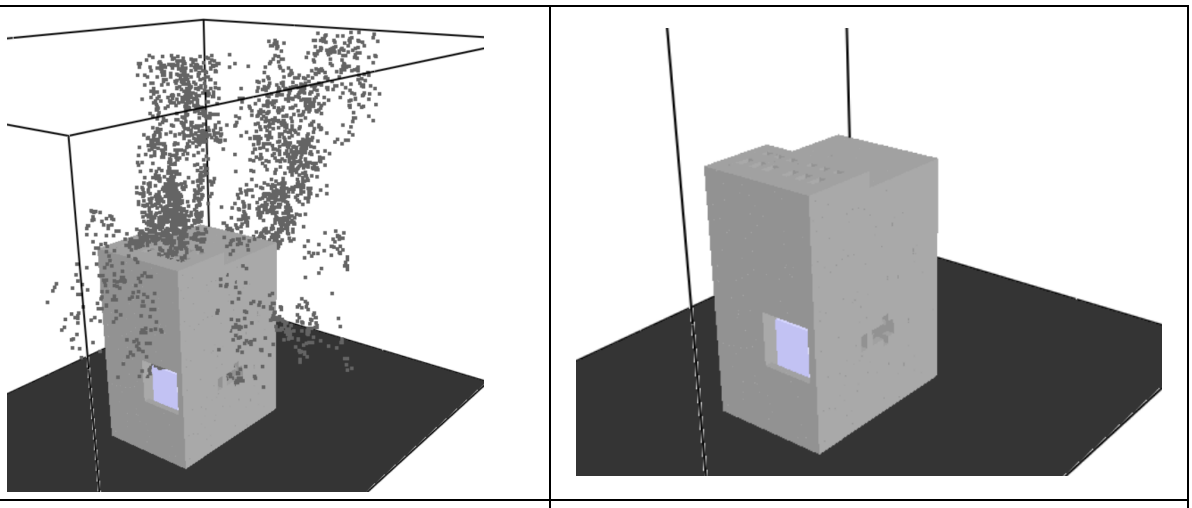

40.38 s	43.9 s

Figure 6-33
Particle distribution at various times for a LV SWGR HEAF at the cabinet middle-height cubicle with an arc energy profile based on FEDB 50935

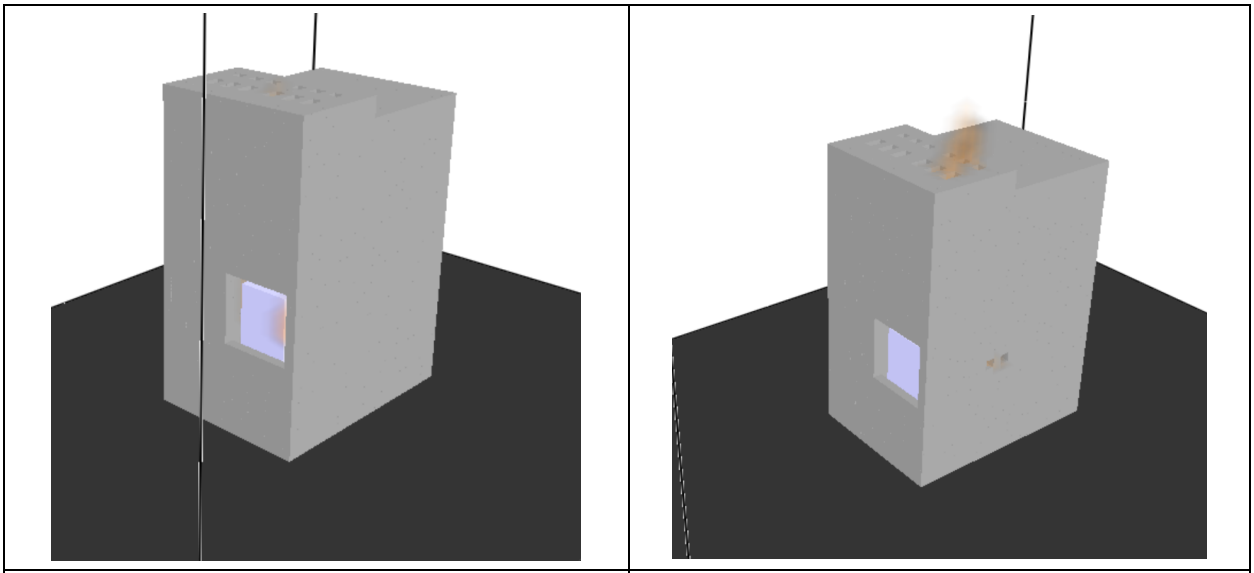

1.96 s	9.46 s

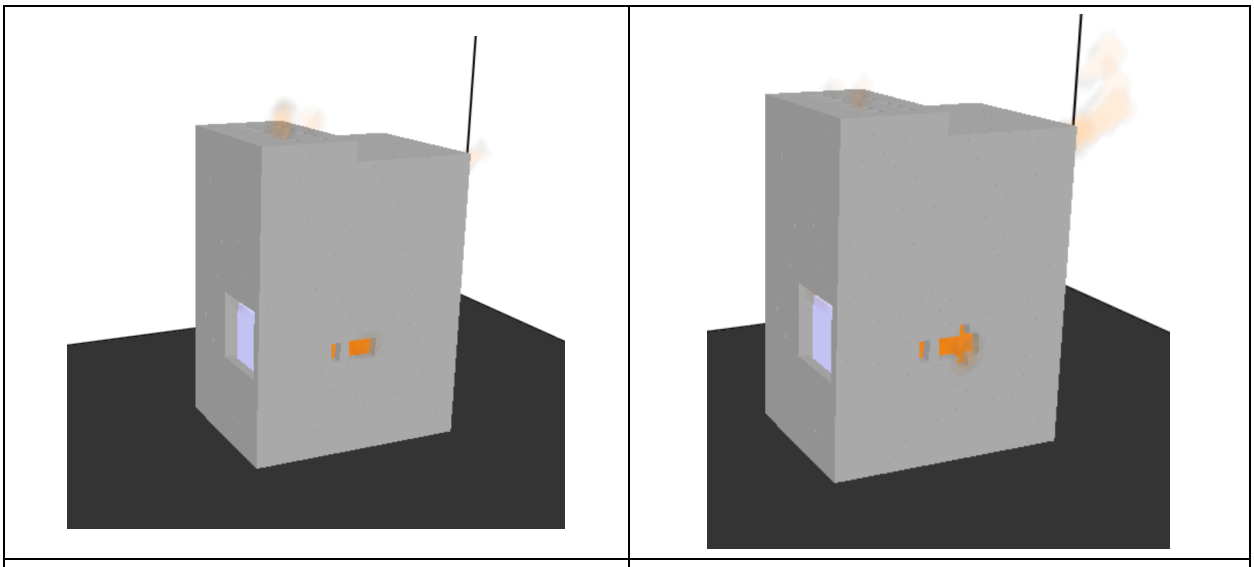

24.6 s	40.38 s

Figure 6-34
Luminous portion of the thermal plume at various times for a LV SWGR HEAF at the cabinet middle-height cubicle with an arc energy profile based on FEDB 50935

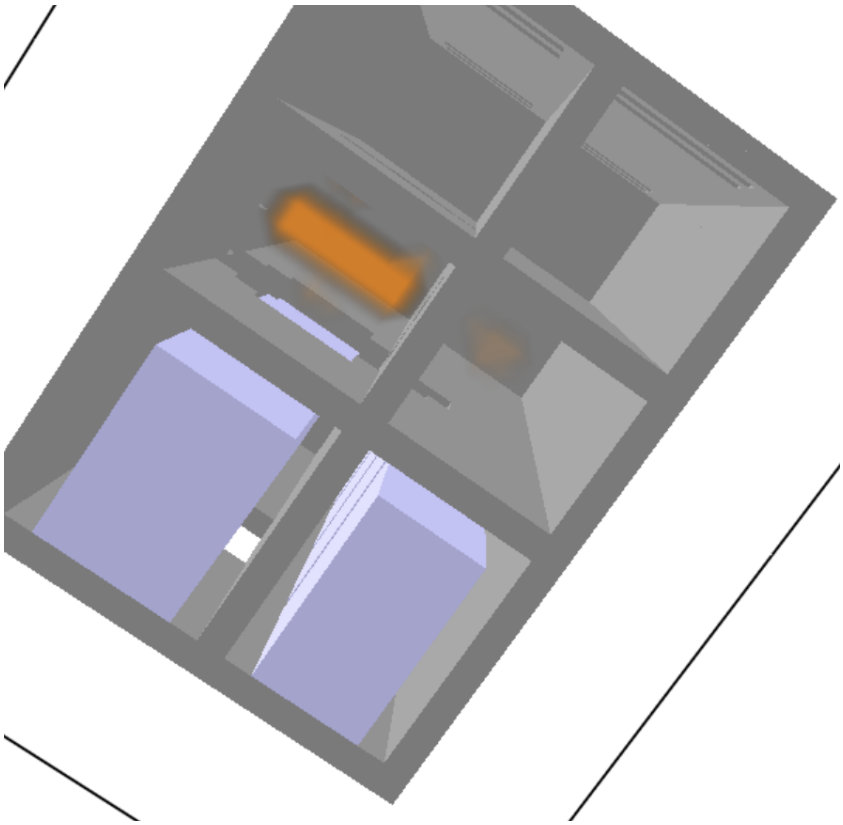

Figure 6-35
Heat release rate per unit volume at 30.2 s for a LV SWGR HEAF at the cabinet middle-height cubicle with an arc energy profile based on FEDB 50935 (viewed from below to show the arc)

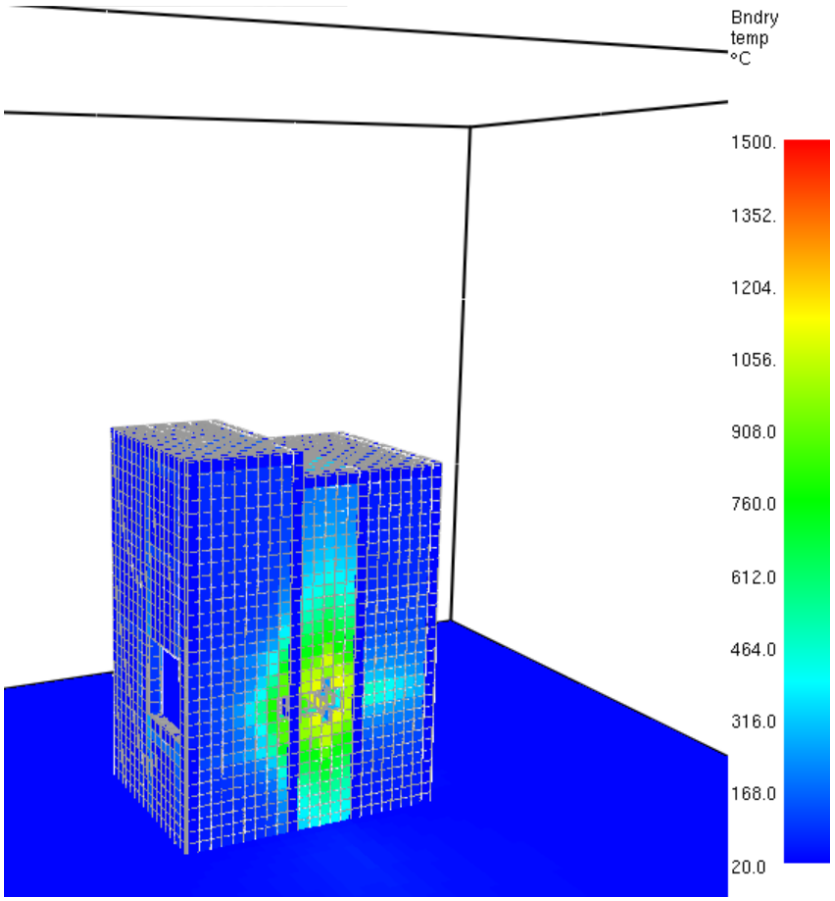

Figure 6-36
Wall temperature of the thermal plume at 33.7 s for a LV SWGR HEAF at the cabinet middle-height cubicle with an arc energy profile based on FEDB 50935

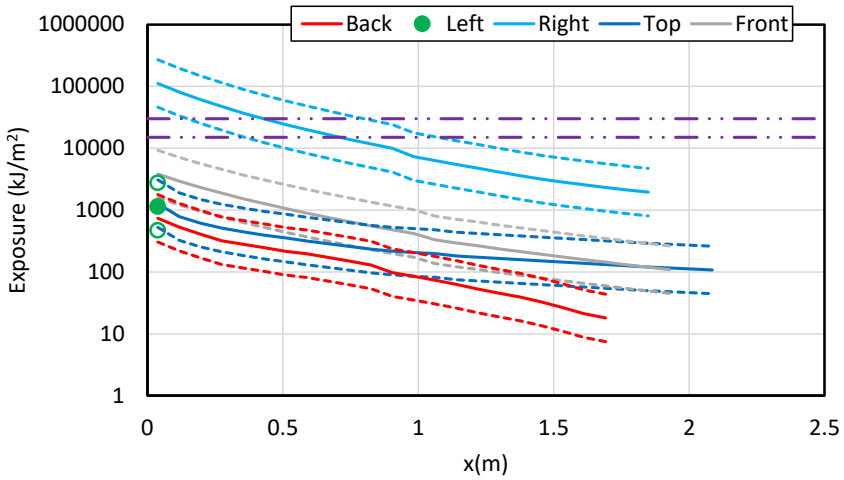

Figure 6-37
Total energy exposure as a function of distance from each face for a LV SWGR HEAF at the cabinet middle-height cubicle with an arc energy profile based on FEDB 50935 (HEAF simulation LV-BASE-5). Dashed horizontal lines correspond to the 15 MJ/m² and 30 MJ/m² target fragility threshold

6.2.1.2. Top Height HEAF

Figure 6-38 depicts the particle distribution about the rear, side, and upper portion of the LV SWGR at various times for a HEAF located at the breaker stabs at a top compartment. At 0 s, there are no metal particles and the switchgear enclosure is intact. The openings at 0 s are the front vent, the top vents, and the rear vents (not shown in Figure 6-38). At 5.78 s the switchgear enclosure is intact, and particles are ejected through the top and front vents with increasing density. At about 7.89 s, a small portion of the switchgear enclosure right-side panel is breached and at about 10 s the top is breached (not shown Figure 6-38). Between 7.89 s and 24.6 s, the openings in the top and sides increase in size and greater numbers of particles are ejected through these openings. After about 24.6 s, the openings grow slowly, and the particle number density and distribution are relatively steady. At 43.95 s, several seconds after the fault is cleared, nearly all particles are dispersed. Internally, the cubicle with the fault is breached and exposes the adjacent internal cubicle.

Figure 6-39 depicts the luminous portion of the thermal plume at 5.78 s, 7.89 s, 24.6 s, and 40.3 s, corresponding to the times at which the particle distributions are shown. The luminous thermal plume is relatively constant after 1.91 s and extends minimally beyond the top and front vents.

Figure 6-40 depicts the heat release rate per unit volume at 32.44 s from above. The switchgear enclosure damage is about maximized, and the electrode arc is clearly defined by the heat release rate per unit volume.

Figure 6-41 depicts the wall temperature at about 34.3 s, the time at which the greatest extent of the switchgear enclosure boundary is heated. Although the heated wall temperature contributes to the heat flux at a fixed location, the temperatures are relatively low, suggesting this component is relatively small compared the energy flux directly from the arc fault and gases.

The calculated total exposure energy as a function of distance is shown in Figure 6-42, which indicates that the ZOI for this simulation is between about 0.4 – 1.0 m for the right-side and top

and nearly zero from all other surfaces, consistent with the particle distribution and luminous plume location.

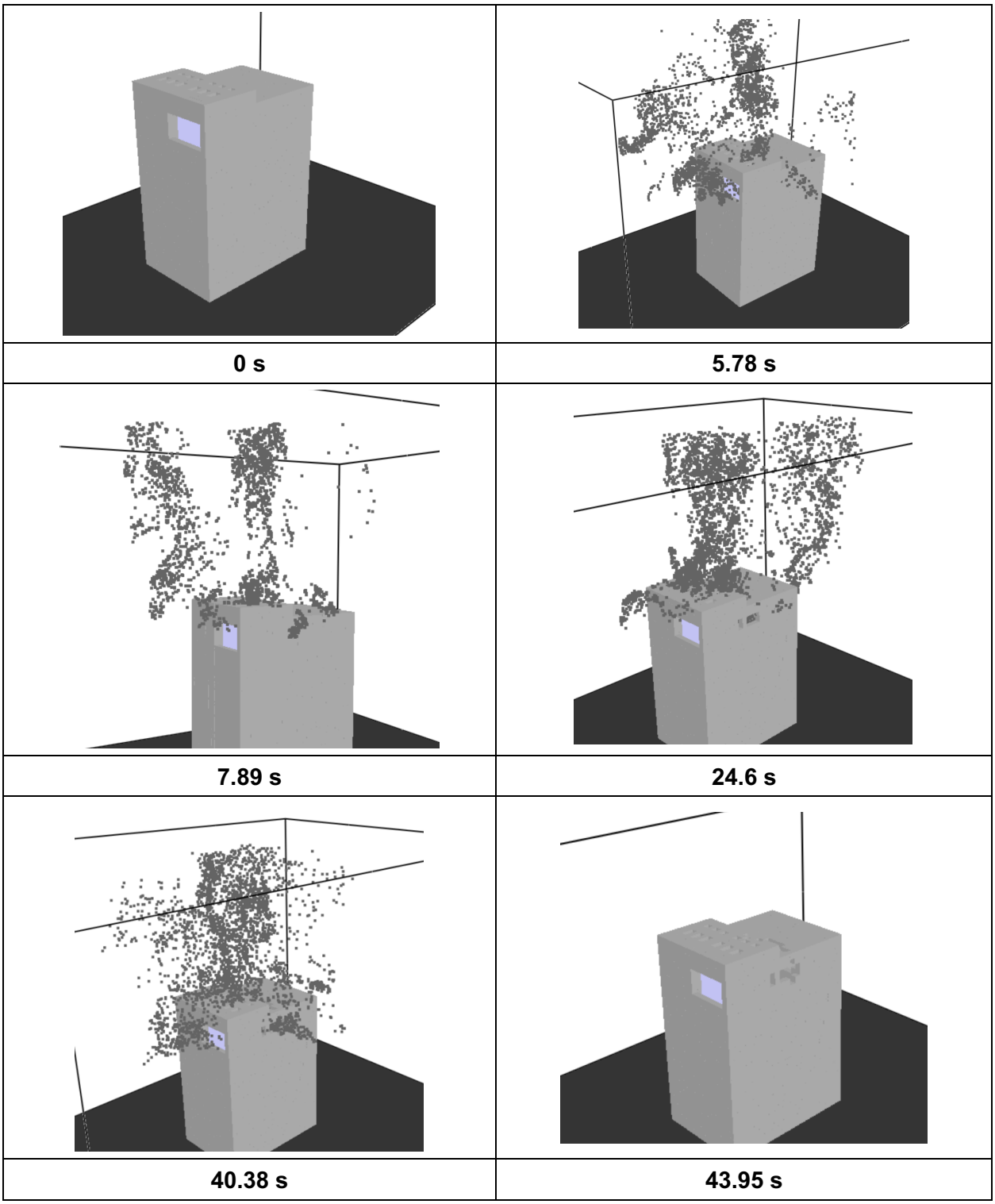

Figure 6-38
Particle distribution at various times for a LV SWGR HEAF at the cabinet top having an arc energy profile based on FEDB 50935

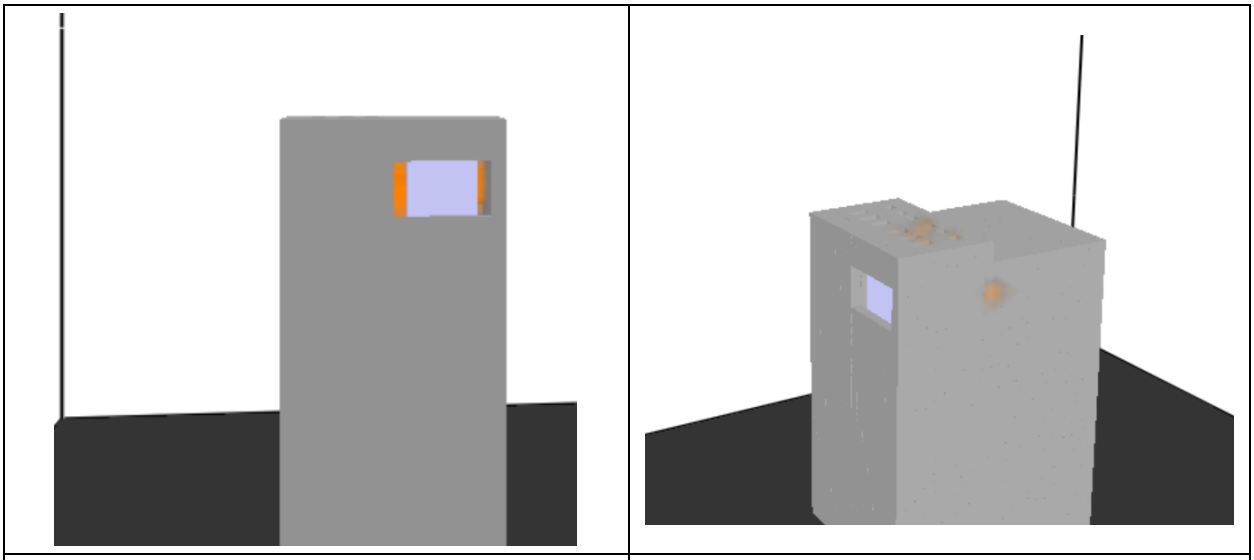

5.78 s	7.89 s
24.6 s	40.38 s

Figure 6-39
Luminous portion of the thermal plume at various times for a LV SWGR HEAF at the cabinet top with an arc energy profile based on FEDB 50935

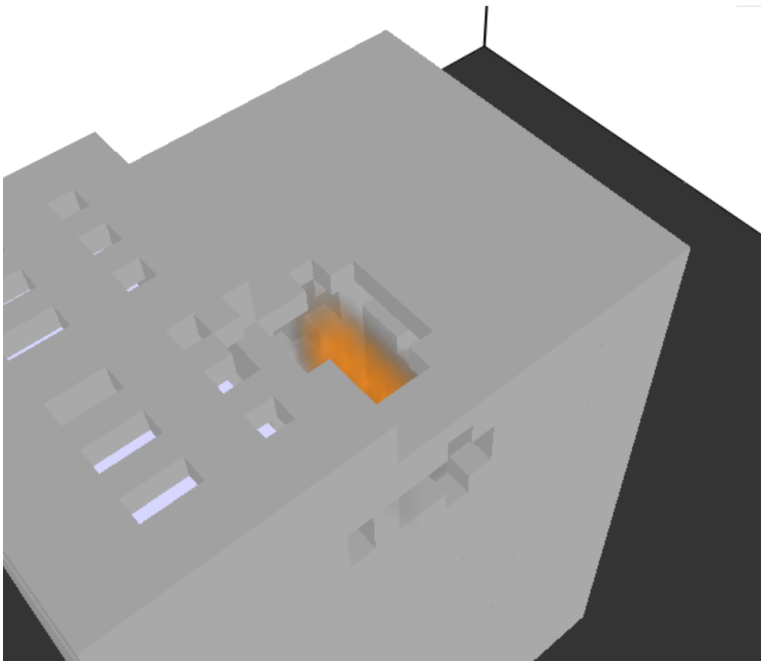

Figure 6-40
Heat release rate per unit volume at 32.44 s for a LV SWGR HEAF at the cabinet top with an arc energy profile based on FEDB 50935 (viewed from top)

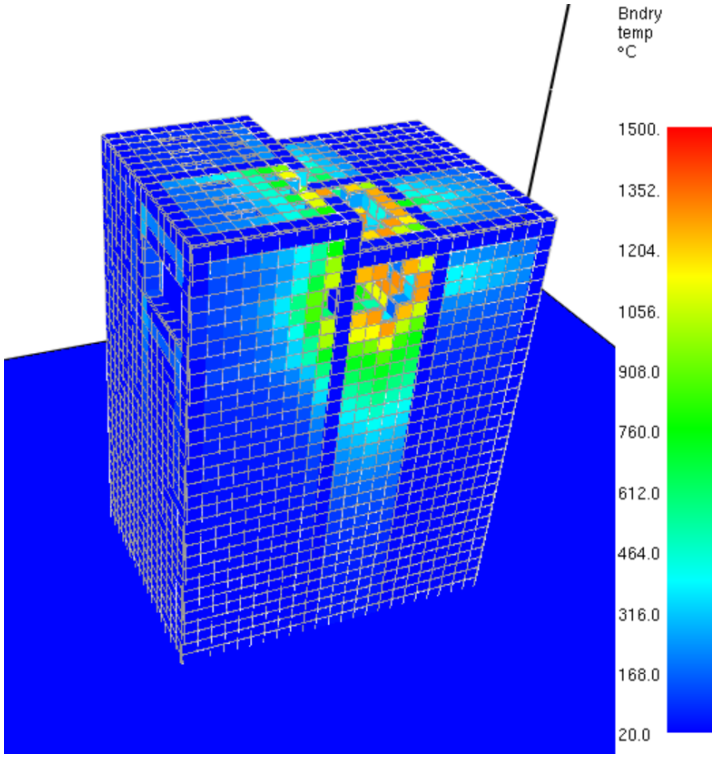

Figure 6-41
Wall temperature of the thermal plume at 34.3 s for a LV SWGR HEAF at the cabinet top with an arc energy profile based on FEDB 50935

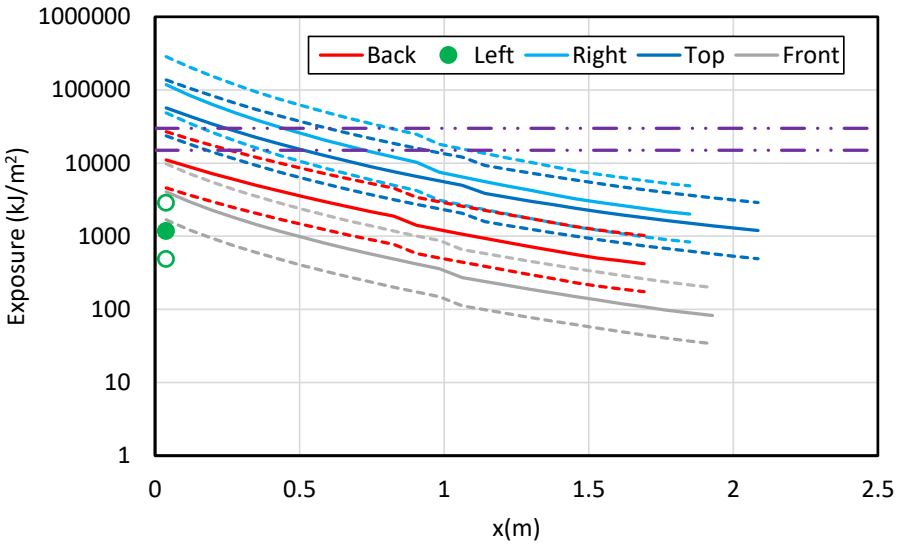

Figure 6-42
Total energy exposure as a function of distance from each face for a LV SWGR HEAF at the cabinet top with an arc energy profile based on FEDB 50935 (HEAF simulation LV-BASE-6). Dashed horizontal lines correspond to the 15 MJ/m² and 30 MJ/m² target fragility threshold

6.2.1.3 Summary of LV SWGR Results

The exposure profiles for each switchgear enclosure face considered, used to determine the ZOIs, is generally consistent with the HEAF simulation results as characterized using the particle distributions and luminous plume. The exposure is strongly dependent on the location of the HEAF. For example, both HEAFs were located in the middle of the switchgear enclosure and were not predicted to have a ZOI on the switchgear enclosure front and back. In addition, the HEAF simulation with the arc inside a middle-height cubicle did not produce a ZOI above the switchgear enclosure whereas the arc located at a top cubicle top did due to the presence of an intermediate steel boundary (cubicle enclosure). These results shown general consistency between the ZOIs and FDS model predictions with intuitive expectations.

6.2.2 Summary of Results

6.2.2.1 LV SWGR ZOI Dependencies

Figure 6-43 shows the ZOIs for each face as a function of the arc energy (90 MJ). The remaining columns correspond to sensitivity studies which use different arc energies and durations as described in Section A.3 of Appendix A. Figure 6-43 shows that the ZOIs for the FEDB 50935 energy profile bound those for the constant-current power profiles. This is due to the event having a long-duration of exposure after enclosure breach and more of the arc energy is directly visible to targets. A back ZOI was only predicted for the arc located in the bus bar compartment at the top of the enclosure. In this case, the arc burns through the partition to the back compartment and outflow is able to jet out of the ventilation openings at the back top. Breach of the partition also occurs when the arc is in the bus bar compartment at the mid-height; however, in this case there is not a direct path for the outflow, and it entrains additional air before exiting the top vent reducing the external exposure to target. Top ZOIs are only predicted for the arc at the top of the enclosure. No ZOIs are predicted out the front or out the left side. For the front, the body of the breaker blocks the line of sight to the arc. For the left

side, there is another column of breaker cubicles, and the arc does not breach the second partition. This result indicates that there is only a side ZOI if the arc has one panel to breach before exposing external targets.

Figure 6-44 shows the aluminum bus bar versus copper bus bar ZOIs for the LV SWGR HEAF simulations. There is a trend for the constant-current cases (which are not being used to determine the ZOI), that copper has overall larger ZOIs than aluminum; however, the difference is under 0.15 m except for the top face 15 MJ/m² target fragility ZOIs for the 4 s and 6 s constant-current arcs in the top of the bus bar compartment. For the FEDB event HEAF simulations, the aluminum ZOIs are slightly larger but by less than 5 cm, which is not significant compared to uncertainty or to risk.

As described in Section 4.1, there is a known model uncertainty with the FDS exposure predictions, and 95% confidence intervals have been computed for the modeled simulations (see Appendix B). For ZOI differentials of 0.15 m or less, the 95% confidence intervals for the copper bus bar material includes the ZOI for the aluminum bus bar material, and vice versa. This means that there is no significant difference in the aluminum and copper bus bar ZOIs for a given arc energy, arc location, and switchgear enclosure face. Similar to the MV SWGR, this is a significant result especially given the treatment of each electrode is different within the FDS model in terms of the energy absorbed by the bus bars, the mass consumed during the arc by the bus bars, and the oxidation of the liquid particles.

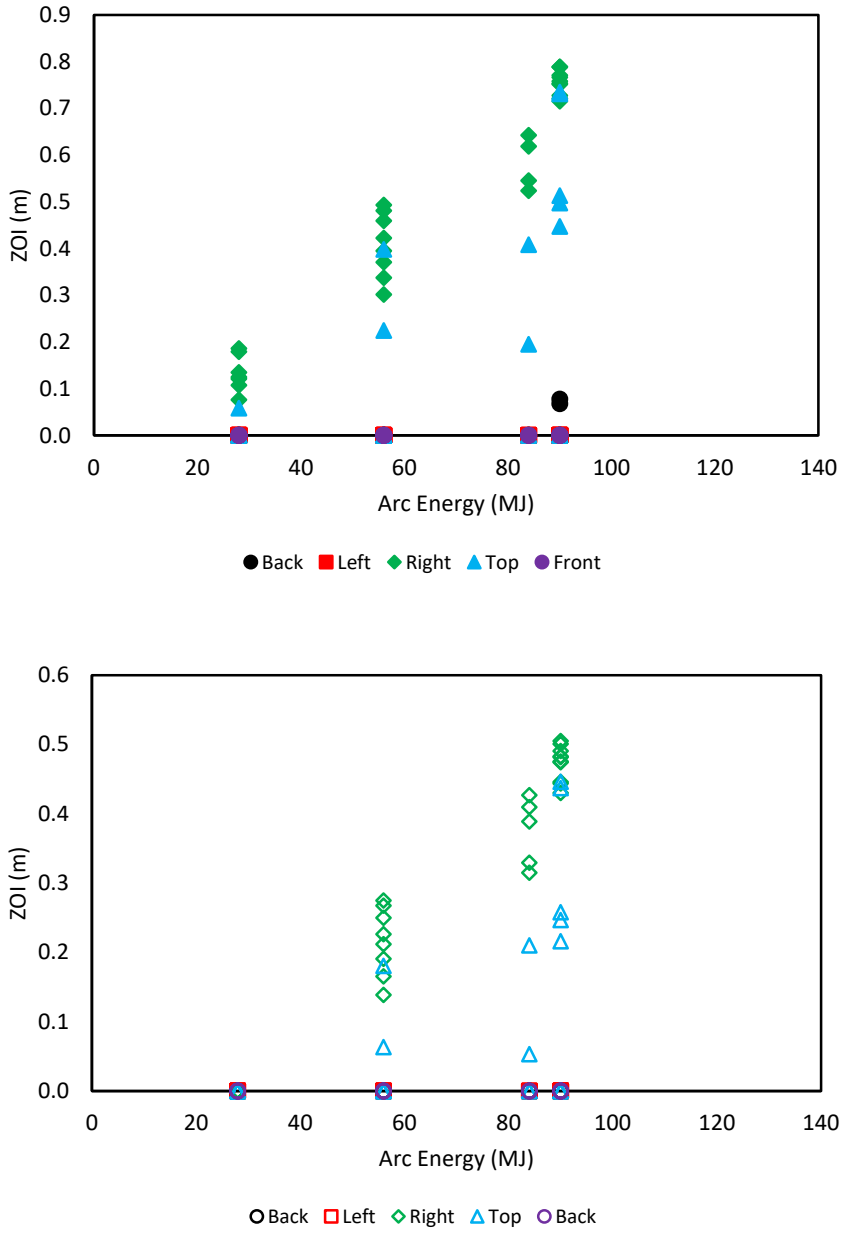

Figure 6-43
ZOIs as a function of arc energy for the LV SWGR HEAF simulations. Top – 15 kW/m² fragility target, bottom – 30 kW/m² fragility target. Symbol shape and color indicates the enclosure face

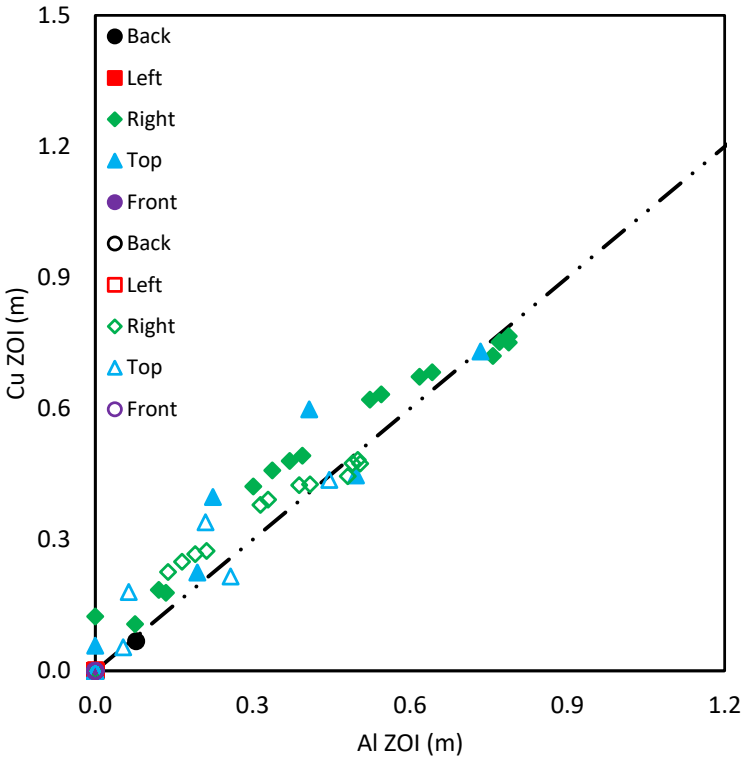

Figure 6-44
Aluminum versus copper bus bar ZOIs for all LV SWGR HEAF simulations

6.2.2.2 Modeling Insights

FDS modeling insights for LV SWGR HEAFs are as follows:

- There is no significant difference between the ZOI dimensions between copper and aluminum bus bar materials given an arc energy profile, arc location, and switchgear enclosure face. The ZOIs for each material are within the 95th percentile of the model uncertainty band as computed from the ZOI predictions for either material.
- The scenarios that represent FEDB 50935 involves an arc that begins at the breaker stabs (copper electrode) and migrates to the bus bar compartment (aluminum electrode). Aluminum was used to represent both electrodes in the FDS simulations as a conservative measure; however, given the aluminum and copper results are similar, the conservatism does not affect the ZOI results.
- The largest factor affecting the ZOIs is duration and extent of the view between the arc volume and the target location. ZOIs tend to increase within increasing arc energy due to a larger breach area switchgear enclosure.
- ZOIs are greater on switchgear enclosure faces closest to the arc. Switchgear enclosure faces that are near the arc melt sooner, resulting in an opening that increases in size during and shortly after the arc clears. This results in a larger energy flux at the target location and thus a larger ZOI at these sides.

These insights are consistent with overall expectations in terms of the HEAF phenomena as modeled in FDS. Since the HEAF is modeled as a high heat release rate per unit volume, the

greatest exposure at a fixed location will occur when the view factor between the arc volume and the location in consideration is maximized.

6.2.2.3 Tabulated LV SWGR ZOIs

Table 6-2 shows a summary of LV SWGR OIs for all of the LV SWGR simulations. A 41 s duration indicates the two-part arc power profile discussed in Section 3.8.1. Simulations with a 2 s, 4 s, or 6 s duration are sensitivity cases with a constant current of 21.5 kA.

Table 6-2
Summary of LV SWGR ZOIs

HEAF Summary						ZOI (m)									
						15 MJ/m² Target Fragility					30 MJ/m² Target Fragility				
HEAF ID[1,2]	Bus Bar Material	Arcing Fault Duration	Arc Location	Arc Elevation	Arc Energy (MJ)	Back	Left	Right	Top	Front	Back	Left	Right	Top	Front
LV-BASE-1	Aluminum	41	Breaker	Mid-Height	90	None[3]	None	0.76	None	None	None	None	0.48	None	None
LV-BASE-2	Aluminum	41	Breaker	Top	90	None	None	0.79	0.50	None	None	None	0.50	0.26	None
LV-BASE-3	Aluminum	41	Bus Bar Comp.	Mid-Height	90	None	None	0.79	None	None	None	None	0.50	None	None
LV-BASE-4	Aluminum	41	Bus Bar Comp.	Top	90	0.08	None	0.77	0.73	None	None	None	0.49	0.45	None
LV-BASE-5	Aluminum	41	Breaker to Bus Bar Comp.[4]	Mid-Height	90	None	None	0.71	None	None	None	None	0.43	None	None
LV-BASE-6	Aluminum	41	Breaker to Bus Bar Comp.[4]	Top	90	None	None	0.73	0.51	None	None	None	0.44	0.25	None
LV-BASE-7	Copper	41	Breaker	Mid-Height	90	None	None	0.72	None	None	None	None	0.45	None	None
LV-BASE-8	Copper	41	Breaker	Top	90	None	None	0.75	0.45	None	None	None	0.47	0.22	None
LV-BASE-9	Copper	41	Bus Bar Comp.	Mid-Height	90	None	None	0.77	None	None	None	None	0.48	None	None
LV-BASE-10	Copper	41	Bus Bar Comp.	Top	90	0.07	None	0.75	0.73	None	None	None	0.48	0.44	None
LV-SENS-1	Aluminum	2	Breaker	Mid-Height	28	None	None	0.12	None	None	None	None	None	None	None

HEAF Summary						ZOI (m)									
						15 MJ/m² Target Fragility					30 MJ/m² Target Fragility				
HEAF ID[1,2]	**Bus Bar Material**	**Arcing Fault Duration**	**Arc Location**	**Arc Elevation**	**Arc Energy (MJ)**	**Back**	**Left**	**Right**	**Top**	**Front**	**Back**	**Left**	**Right**	**Top**	**Front**
LV-SENS-2	Aluminum	2	Breaker	Top	28	None	None	0.13	None	None	None	None	None	None	None
LV-SENS-3	Aluminum	2	Bus Bar Comp.	Mid-Height	28	None	None	None	None	None	None	None	None	None	None
LV-SENS-4	Aluminum	2	Bus Bar Comp.	Top	28	None	None	0.08	None	None	None	None	None	None	None
LV-SENS-5	Copper	2	Breaker	Mid-Height	28	None	None	0.19	None	None	None	None	None	None	None
LV-SENS-6	Copper	2	Breaker	Top	28	None	None	0.18	None	None	None	None	None	None	None
LV-SENS-7	Copper	2	Bus Bar Comp.	Mid-Height	28	None	None	0.12	None	None	None	None	None	None	None
LV-SENS-8	Copper	2	Bus Bar Comp.	Top	28	None	None	0.11	0.06	None	None	None	None	None	None
LV-SENS-9	Aluminum	4	Breaker	Mid-Height	56	None	None	0.39	None	None	None	None	0.21	None	None
LV-SENS-10	Aluminum	4	Breaker	Top	56	None	None	0.37	None	None	None	None	0.19	None	None
LV-SENS-11	Aluminum	4	Bus Bar Comp.	Mid-Height	56	None	None	0.30	None	None	None	None	0.14	None	None
LV-SENS-12	Aluminum	4	Bus Bar Comp.	Top	56	None	None	0.34	0.22	None	None	None	0.17	0.06	None
LV-SENS-13	Copper	4	Breaker	Mid-Height	56	None	None	0.49	None	None	None	None	0.27	None	None
LV-SENS-14	Copper	4	Breaker	Top	56	None	None	0.48	None	None	None	None	0.27	None	None

HEAF Summary						ZOI (m)									
						15 MJ/m² Target Fragility					30 MJ/m² Target Fragility				
HEAF ID[1,2]	**Bus Bar Material**	**Arcing Fault Duration**	**Arc Location**	**Arc Elevation**	**Arc Energy (MJ)**	**Back**	**Left**	**Right**	**Top**	**Front**	**Back**	**Left**	**Right**	**Top**	**Front**
LV-SENS-15	Copper	4	Bus Bar Comp.	Mid-Height	56	None	None	0.42	None	None	None	None	0.23	None	None
LV-SENS-16	Copper	4	Bus Bar Comp.	Top	56	None	None	0.46	0.40	None	None	None	0.25	0.18	None
LV-SENS-17	Aluminum	6	Breaker	Mid-Height	84	None	None	0.64	None	None	None	None	0.41	None	None
LV-SENS-18	Aluminum	6	Breaker	Top	84	None	None	0.62	0.19	None	None	None	0.39	0.05	None
LV-SENS-19	Aluminum	6	Bus Bar Comp.	Mid-Height	84	None	None	0.52	None	None	None	None	0.31	None	None
LV-SENS-20	Aluminum	6	Bus Bar Comp.	Top	84	None	None	0.55	0.41	None	None	None	0.33	0.21	None
LV-SENS-21	Copper	6	Breaker	Mid-Height	84	None	None	0.68	None	None	None	None	0.43	None	None
LV-SENS-22	Copper	6	Breaker	Top	84	None	None	0.67	0.23	None	None	None	0.42	0.05	None
LV-SENS-23	Copper	6	Bus Bar Comp.	Mid-Height	84	None	None	0.62	None	None	None	None	0.38	None	None
LV-SENS-24	Copper	6	Bus Bar Comp.	Top	84	None	None	0.63	0.60	None	None	None	0.39	0.34	None

[1]The LV-BASE-X designation corresponds to FDS simulations using the FEDB 50935 arc energy profile and the LV-SENS-X designation corresponds to FDS sensitivity analysis simulations using other arc power profiles.

[2]The FDS input designator is not the same as the input file name but uniquely corresponds to a single FDS input file. Refer to Appendix B of this report for the corresponding input file nomenclature designator.

[3]None means there is no external ZOI.

[4]Fault begins at the breaker and migrates to the bus bar compartment after 20 s.

6.3 Non-Segregated Bus Duct HEAFs

This section provides a summary of the FDS results for the NSBD simulations. Forty-eight primary simulations were run with variations of bus bar material (copper, aluminum), duct housing material (aluminum, steel), duct geometry (straight, tee), and current durations (2 s stiff, 4s stiff, 5 s stiff, 0 s stiff 15 s decay, 3s stiff 15 s decay, 5 s stiff 15 s decay). Six sensitivity simulations were run with a vertical elbow geometry to determine if it was substantially different from the straight or tee duct geometries. An additional four sensitivity simulations were run with a 1 s stiff current duration to provide greater resolution into faults with short fault clearing times. In total, 58 FDS bus duct simulations were run, and are summarized in Table 6-3. One simulation—a straight duct segment with aluminum electrodes, aluminum bus duct housing, 0 s stiff current and 15 s decaying current—failed with a numerical instability and is not reported.

The bus ducts all have nominal duct dimensions of 0.4 m (15.75 inches) tall, 0.56 m (22 inches) wide and with a duct housing thickness of 0.0032 m (0.125 inches), corresponding to 11-gauge sheet metal.

6.3.1 Selected Non-Segregated Bus Duct HEAF Simulations

Three NSBD HEAF simulations are reviewed in detail. All three have the same prescribed energy input corresponding to a 3 s stiff fault, followed by a 15 s generator-fed decay, for a total of 226 MJ. The simulations are as follows:

1) Straight duct geometry with copper bus bars and steel duct housing
2) Vertical elbow duct geometry with aluminum bus bars and aluminum duct housing
3) Vertical tee duct geometry with aluminum bus bars and steel duct housing

The detailed results include depictions of the duct breach, particle dispersion, the luminous thermal plume, the heat release rate per unit volume, the duct wall temperatures, and the exposure profiles as a function of distance for each duct surface.

6.3.1.1 Non-Segregated Bus Duct Straight Section

Figure 6-45 depicts the metal particle distribution about the lower, side, and upper portion of the bus duct at various times during the HEAF. At 0 s, there are no metal particles and the duct is intact. At 2.34 s, the duct has breached on all four sides, and particles are ejected in all directions, though buoyancy causes most to exit the duct through the top opening. At 5.49 s, the size of the openings continue to grow, and the particle density has increased and reached steady state. At 10.1 s, the size of the breach reaches its approximate maximum size. Over the next several seconds, the effects of the generator decay become apparent, and there is a visible reduction in particle density.

Figure 6-46 depicts the luminous portion of the thermal plume at 1.25 s, 1.53 s, 3.09 s, and 8.94 s. From the progression shown, it is evident that early in the HEAF, when the duct is still largely intact, hot gases and particles flow through the duct and out of the computational domain. As the size of the breach grows, the duct cannot maintain pressure and the gases and particles leave primarily through the breach.

Figure 6-47 depicts the heat release rate per unit volume at 18 s. The duct damage has about reached its maximum, and the electrode arc is clearly defined by the heat release rate per unit volume.

Figure 6-48 depicts the wall temperature at 3.9 s, the time at which the greatest extent of the duct surface is heated. Although the arc continues to release heat for some time afterwards, the

duct has melted away from the arc, and the heating of the duct surface reaches steady state at about this time.

The calculated total exposure energy as a function of distance is shown in Figure 6-49, which indicates that the ZOI for this simulation is b 0.5 – 0.8 m below the duct and 0.7 – 1 m from all other surfaces, consistent with the particle distribution and luminous plume location.

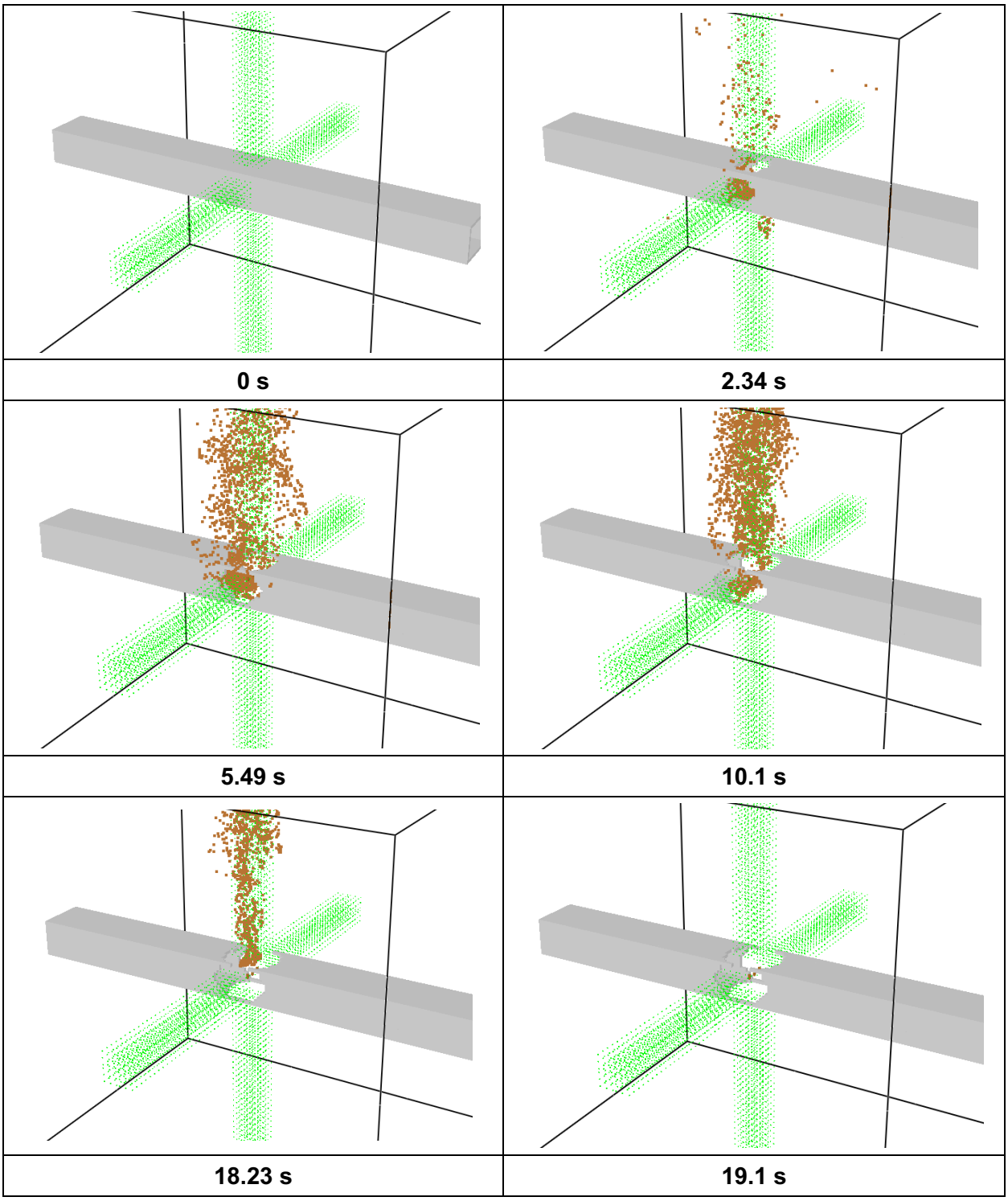

Figure 6-45
Copper particle distribution at various times for a 226 MJ NSBD HEAF in a straight duct segment with copper bus bars and steel duct housing

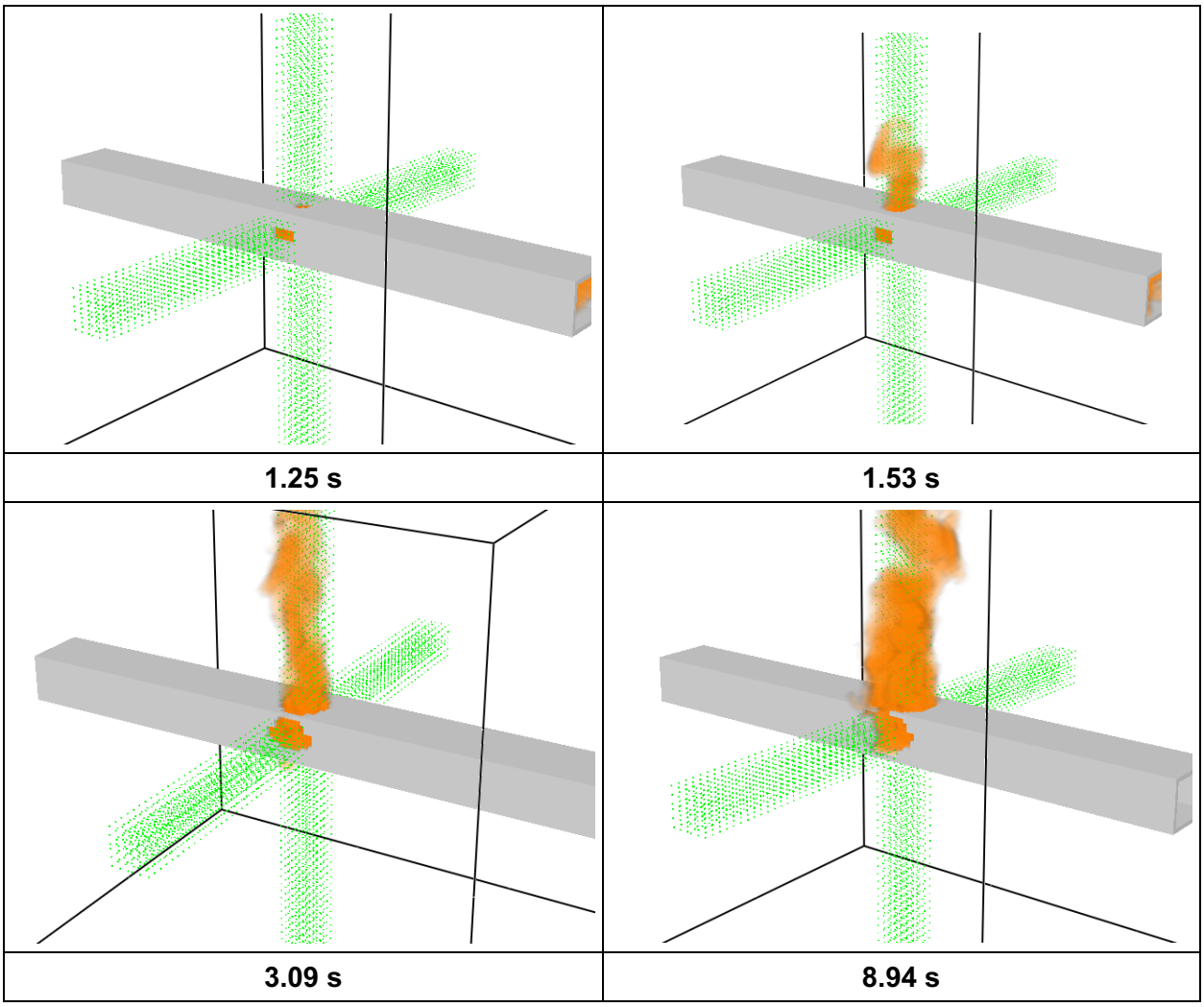

Figure 6-46
Luminous portion of the thermal plume at various times for a 226 MJ NSBD HEAF in a straight duct segment with copper bus bars and steel duct housing

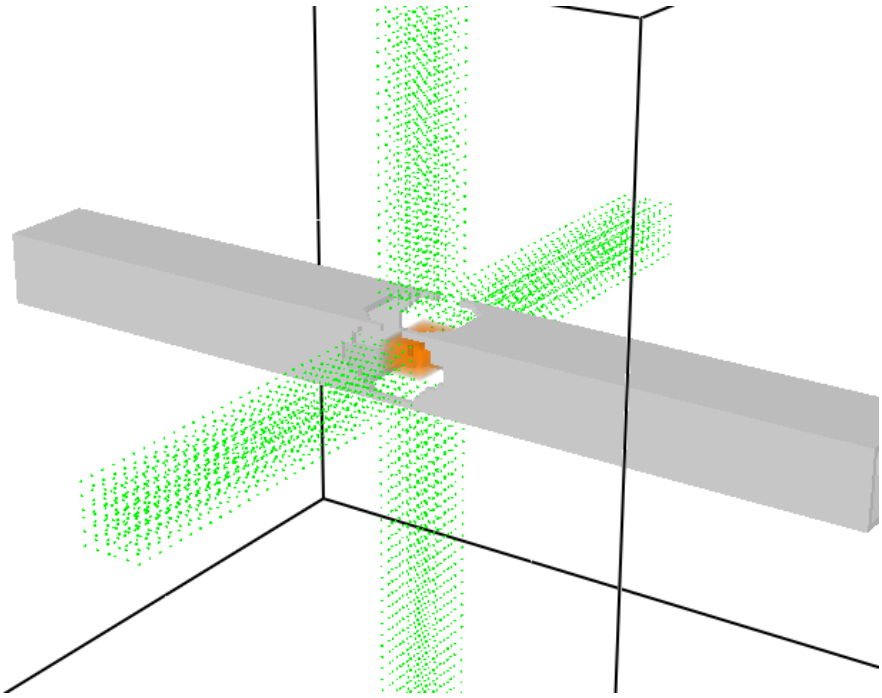

Figure 6-47
Heat release rate per unit volume at 18 s for a 226 MJ NSBD HEAF in a straight duct segment with copper bus bars and steel duct housing

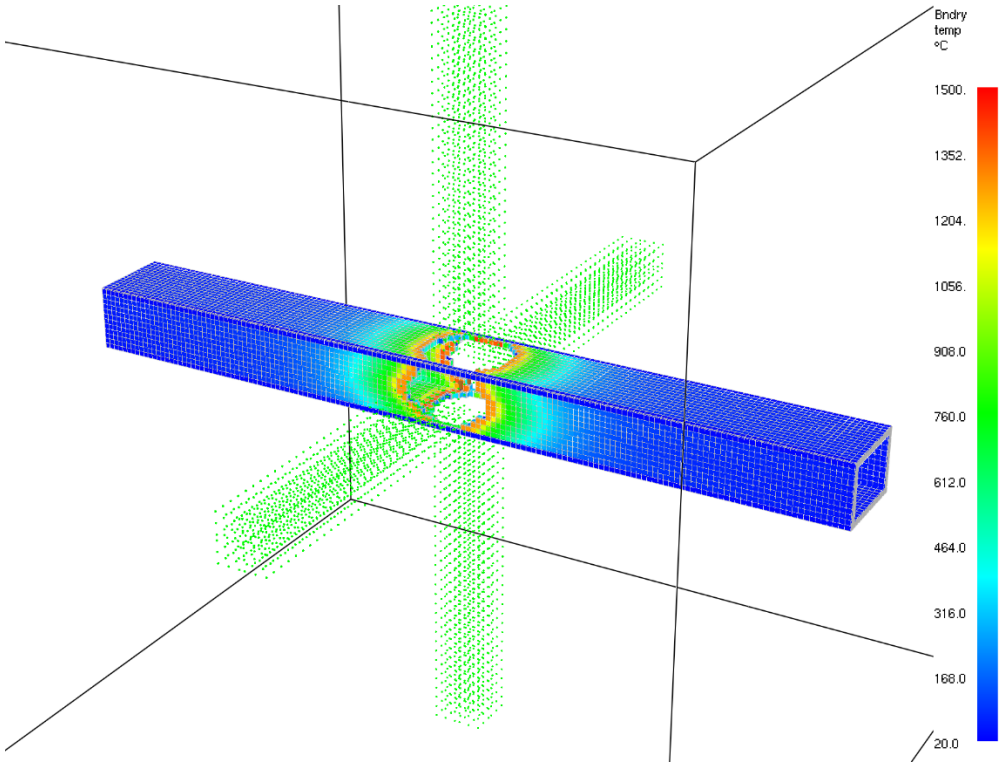

Figure 6-48
Wall temperature of the duct housing at 3.9 s for a 226 MJ NSBD HEAF in a straight duct segment with copper bus bars and steel duct housing

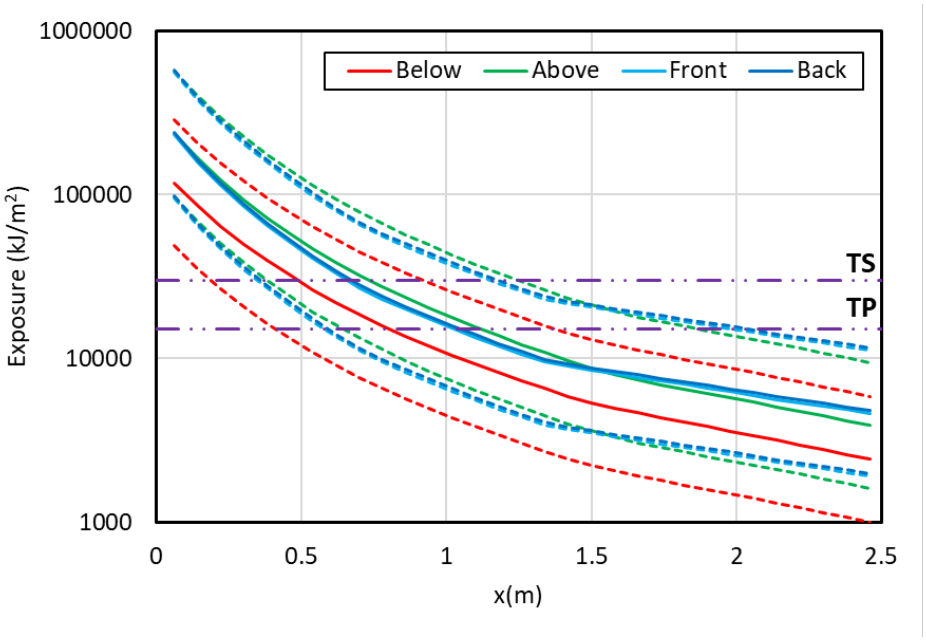

Figure 6-49
Total energy exposure as a function of distance from each face for a 226 MJ NSBD HEAF in a straight duct segment with copper bus bars and steel duct housing (HEAF simulation NSBD-19). Dashed horizontal lines correspond to the 15 MJ/m² and 30 MJ/m² target fragility threshold

6.3.1.3 Non-Segregated Bus Duct Tee

Figure 6-50 depicts the metal particle distribution about the lower, side, and upper portion of the bus duct at various times during the HEAF. At 0 s, there are no metal particles and the duct is intact. 1.14 s, the duct has breached on three sides and particles begin to escape the duct in all directions. The size of the breach grows over the next several seconds, and the particle density continues to increase. Because of the orientation of the vertical elbow, the majority of aluminum particles and hot gases travel upward through the intact duct segment. At 8.7 s, the size of the breach reaches its approximate maximum size, and the particles continue to travel upward through the duct, though there are still enough being generated that some escape through the hole on the right-side. Over the next several seconds, the effects of the generator decay become apparent, and there is a visible reduction in particle density.

Figure 6-51 depicts the luminous portion of the thermal plume at 1.04 s, 1.69 s, 2.31 s, and 7.44 s. Because of the orientation of the duct, the plume flow behaves differently than in the straight duct, i.e., early in the simulation, hot gases escape the through the holes and later in the simulation, the gases travel through the intact vertical segment.

Figure 6-52 depicts the heat release rate per unit volume at 15.5 s. The duct damage has about reached its maximum, and the electrode arc is clearly defined by the heat release rate per unit volume.

Figure 6-53 depicts the wall temperature at about 5.2 s, the time at which the greatest extent of the duct surface is heated. As with the straight duct, the duct surface melts away from the arc, bringing the duct heating to a steady state; however, it takes longer to reach steady state because significant quantities of gases are still flowing through the vertical segment after the duct melts.

The calculated total exposure energy as a function of distance is shown in Figure 6-54, which indicates that the ZOI for this simulation is 0.75 – 1.2 for all four sides, and each side sees approximately the same exposure as radiant heating on those sides is fairly consistent, and the bulk of the convective heating is directed upwards, where there is a duct and therefore no ZOI.

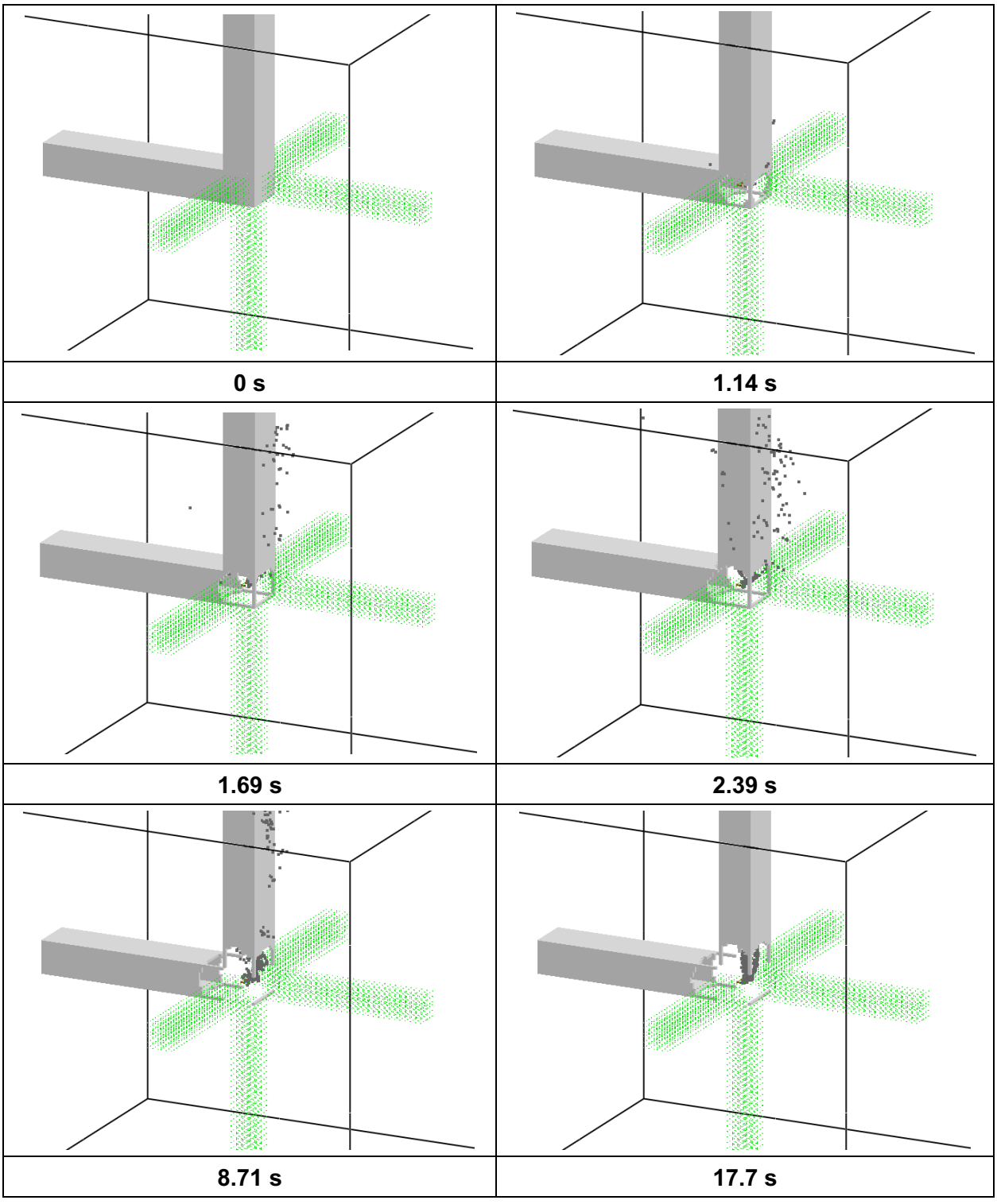

Figure 6-50
Aluminum particle distribution at various times for a 226 MJ NSBD HEAF in a vertical elbow duct segment with aluminum bus bars and aluminum duct housing

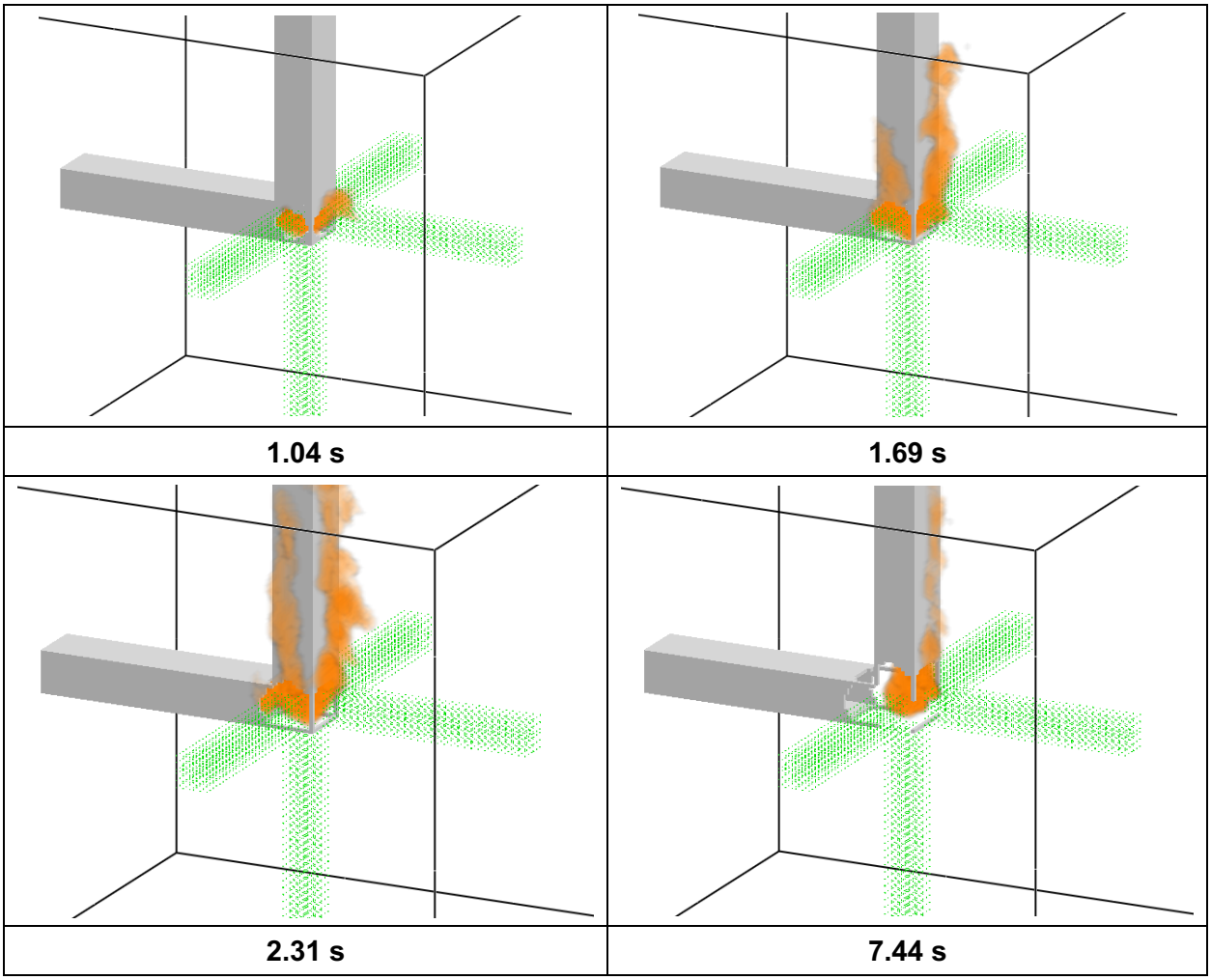

Figure 6-51
Luminous portion of the thermal plume at various times for a 226 MJ NSBD HEAF in a vertical elbow duct segment with aluminum bus bars and aluminum duct housing

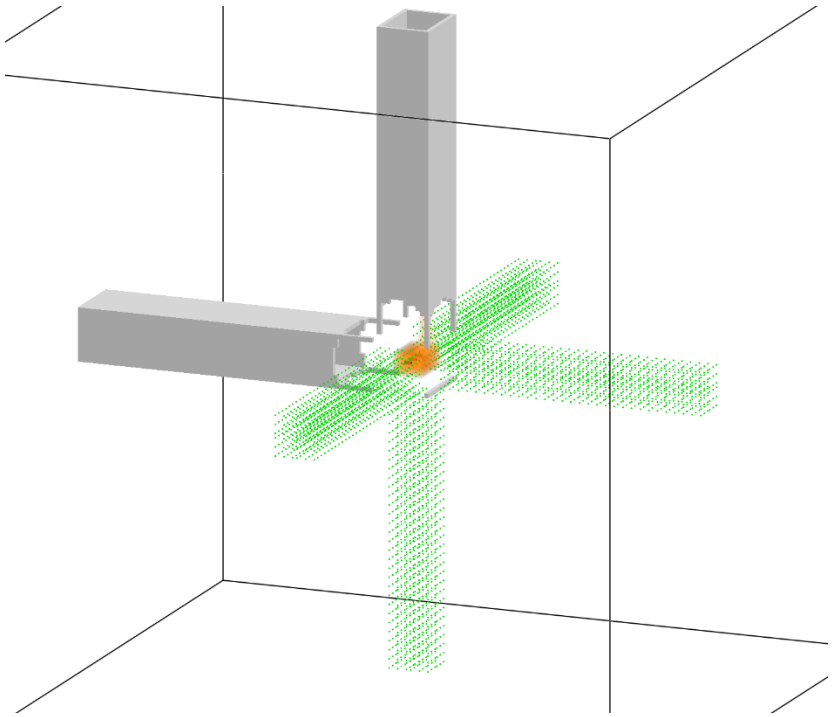

Figure 6-52
Heat release rate per unit volume at 15.5 s for a 226 MJ NSBD HEAF in a vertical elbow duct segment with aluminum bus bars and aluminum duct housing

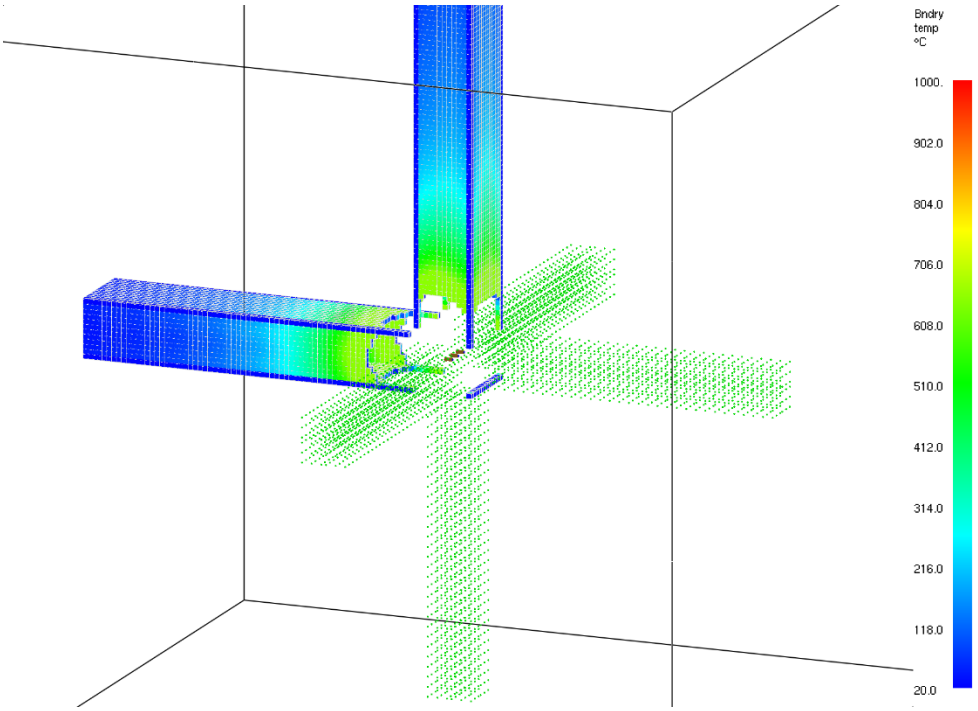

Figure 6-53
Wall temperature of the duct housing at 5.2 s for a 226 MJ NSBD HEAF in a vertical elbow duct segment with aluminum bus bars and aluminum duct housing

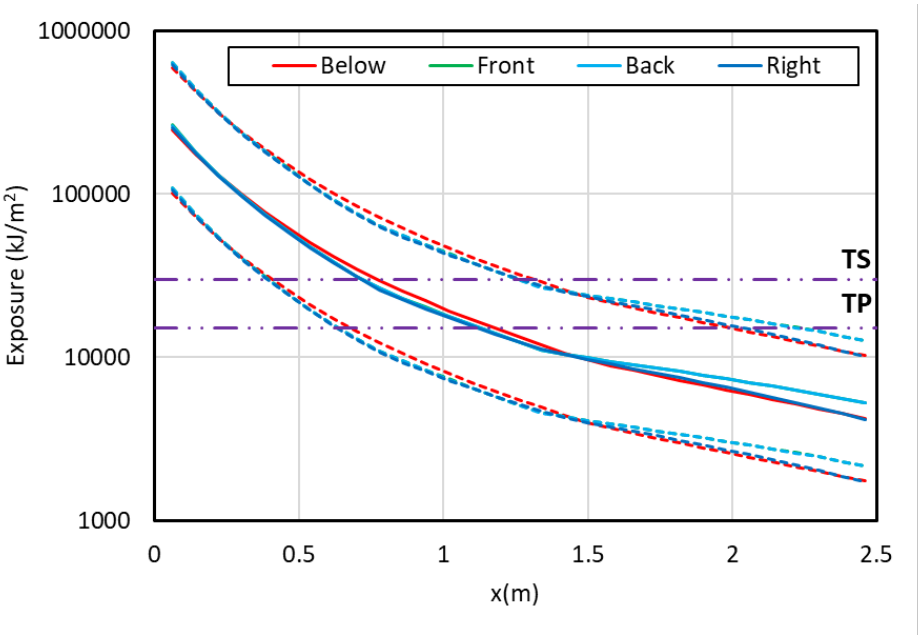

Figure 6-54
Total energy exposure as a function of distance from each face for a 226 MJ NSBD HEAF in a vertical elbow duct segment with aluminum bus bars and aluminum duct housing (HEAF simulation NSBD-57). Dashed horizontal lines correspond to the 15 MJ/m² and 30 MJ/m² target fragility threshold

6.3.1.2 Elbow Non-Segregated Bus Duct

Figure 6-55 depicts the metal particle distribution about the vertical tee intersection of the bus duct segments at various times during the HEAF. At 0 s, there are no metal particles and the duct is intact. At 1.01 s, the upper portion of the duct begins to breach on its front face. At 1.35 s, the front and top of the upper duct have breached, and holes in the sides of the upper duct are just beginning to open. Over the next 2 s, the size of the holes continues to grow, the particles trapped in the duct escape through the holes, and the flow of particles from the duct reaches steady state. At about 11.7 s, the damage to the duct is at its maximum, and particle density is decreasing due to generator decay.

Figure 6-56 depicts the luminous portion of the thermal plume at 1.04 s, 1.69 s, 2.31 s, and 7.44 s. As with the flow of particles, the thermal plume experiences a “burst” around 2.3 s, as the hot gases trapped in the relatively large duct volume escape through the holes. The lower segment of the duct in this tee acts as an energy store, and the hot gases that are initially pushed into the lower duct flow through the holes in the upper duct when they appear.

Figure 6-57 depicts the heat release rate per unit volume at 18.1 s. The duct damage has about reached its maximum, and the electrode arc is clearly defined by the heat release rate per unit volume.

Figure 6-58 depicts the wall temperature at about 7.8 s, the time at which the greatest extent of the duct surface is heated. Although the arc continues to release heat for some time afterwards, the duct has melted away from the arc, and the heating of the duct surface reaches steady state at about this time.

The calculated total exposure energy as a function of distance is shown in Figure 6-59, which indicates that the ZOI for this simulation is 0.6 – 1 m from the front and top of the duct. The

incident energy below the duct does not reach the fragility limits due to the distance between the arc and the bottom of the duct, and there is no ZOI in that direction.

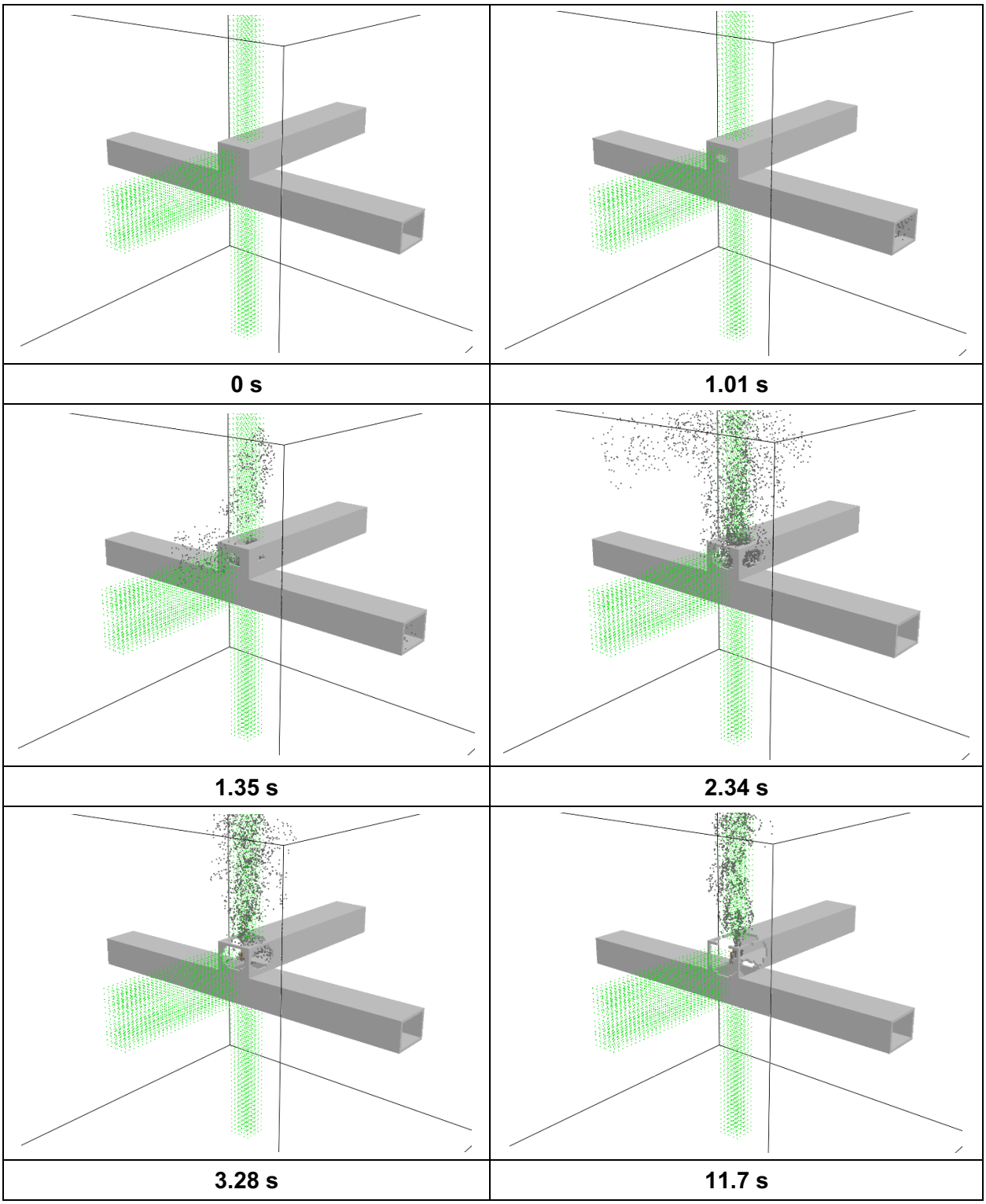

Figure 6-55
Aluminum particle distribution at various times for a 226 MJ NSBD HEAF in a vertical tee duct segment with aluminum bus bars and steel duct housing

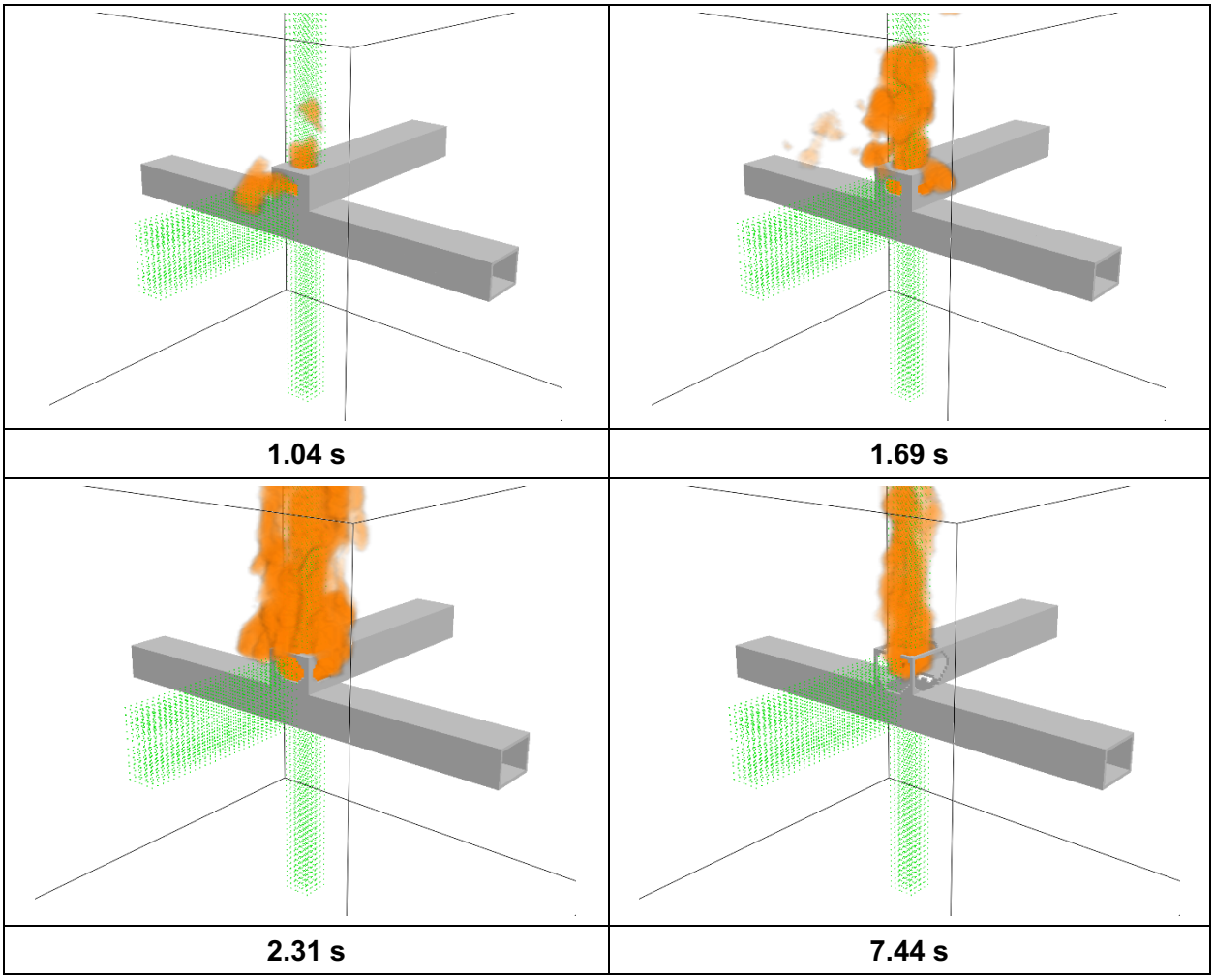

Figure 6-56
Luminous portion of the thermal plume at various times for a 226 MJ NSBD HEAF in a vertical tee duct segment with aluminum bus bars and steel duct housing

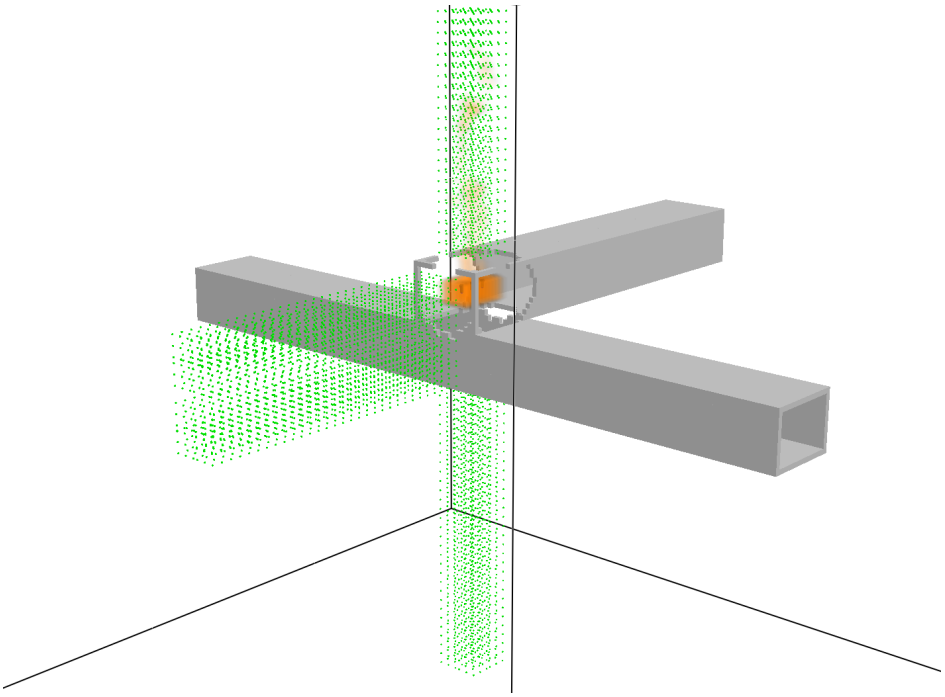

Figure 6-57
Heat release rate per unit volume at 18.1 s for a 226 MJ NSBD HEAF in a vertical tee duct segment with aluminum bus bars and steel duct housing

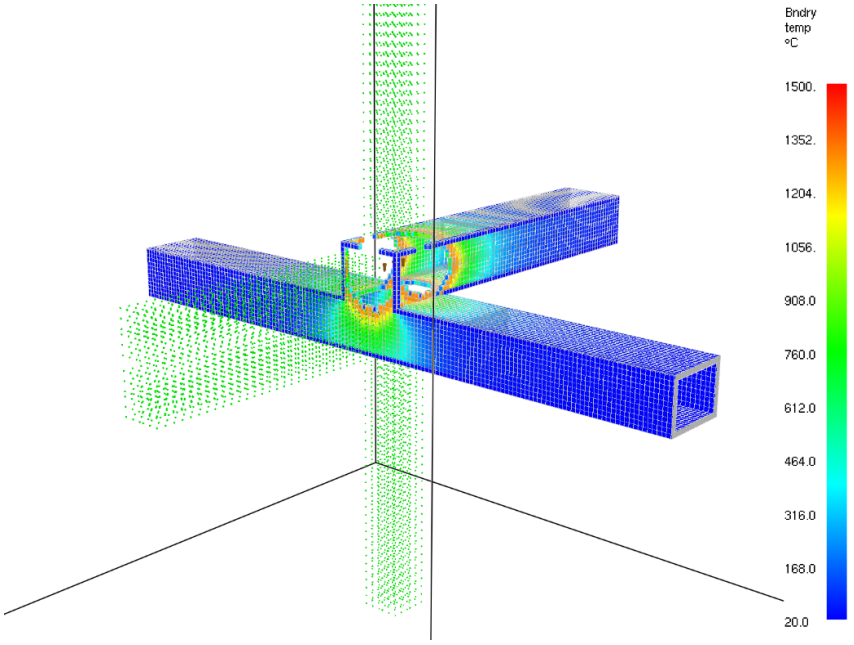

Figure 6-58
Wall temperature of the duct housing at 7.8 s for a 226 MJ NSBD HEAF in a vertical tee duct segment with aluminum bus bars and steel duct housing

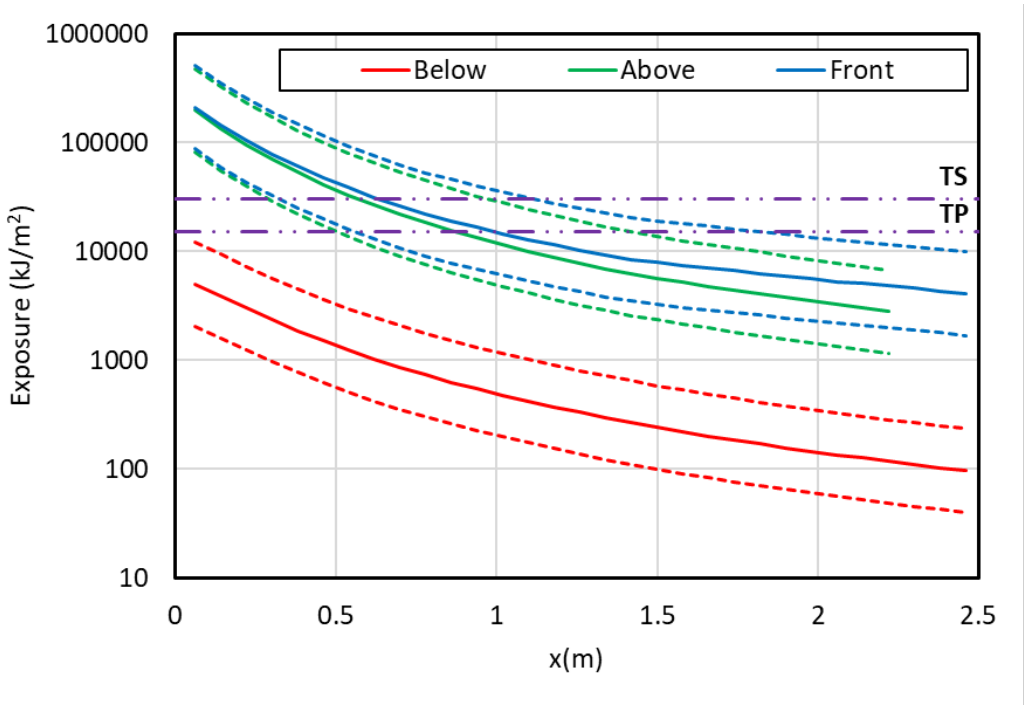

Figure 6-59
Total energy exposure as a function of distance from each face for a 226 MJ NSBD HEAF in a vertical tee duct segment with aluminum bus bars and steel duct housing (HEAF simulation NSBD-32). Dashed horizontal lines correspond to the 15 MJ/m² and 30 MJ/m² target fragility threshold

6.3.2 Summary of Results

6.3.2.1 ZOI Dependencies

Figure 6-60 shows the ZOIs for NSBD HEAF simulations. ZOIs are predicted that are larger than the current bus duct ZOIs in NUREG/CR-6850 Supplement 1 [2]. Figure 6-61 through Figure 6-63 show the ZOIs for the NSBD HEAF simulations for each geometry (straight, tee, and elbow). The elbow geometry shows less data since it was only run with aluminum duct and aluminum bus bars.

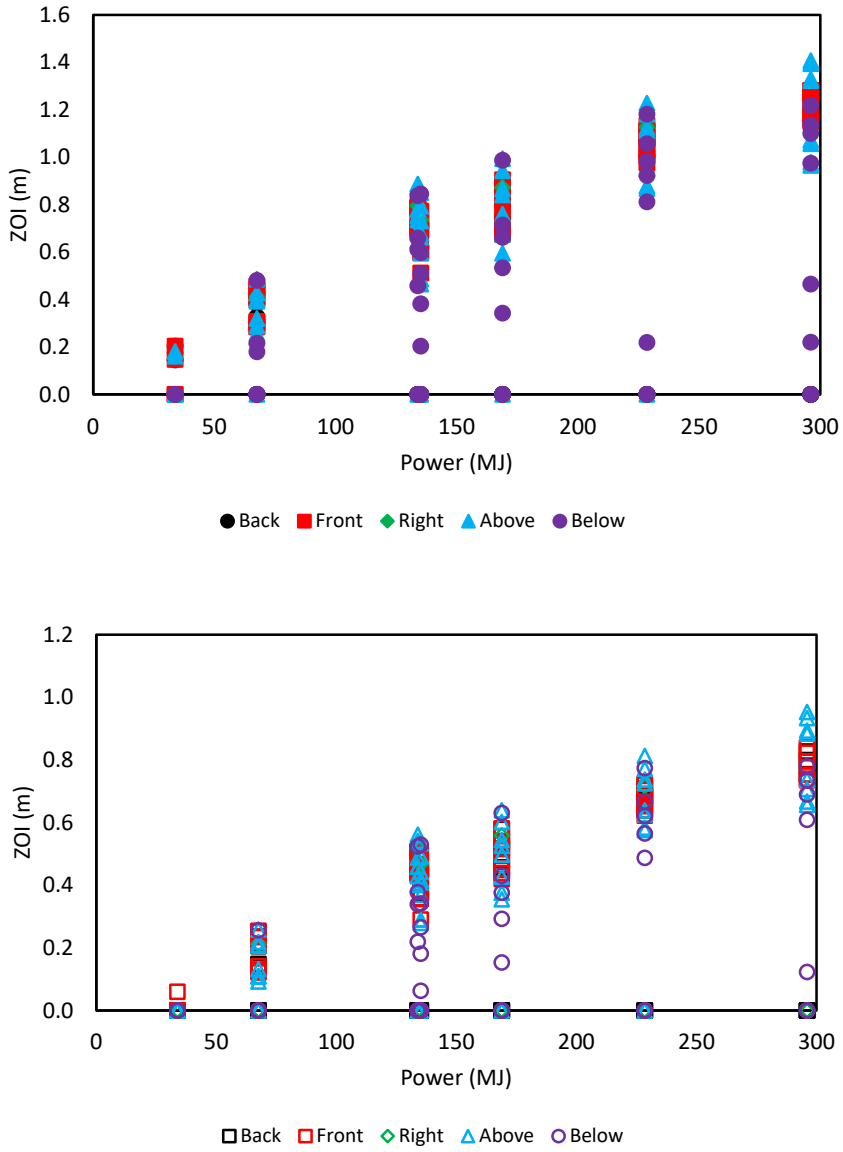

Figure 6-60
ZOIs as a function of arc energy for the NSBD HEAF simulations. Top – 15 MJ/m² fragility target, bottom – 30 MJ/m² fragility target . Symbol shape and color indicates the enclosure face. Note that sides without a ZOI component are shown with 0 m ZOI dimensions

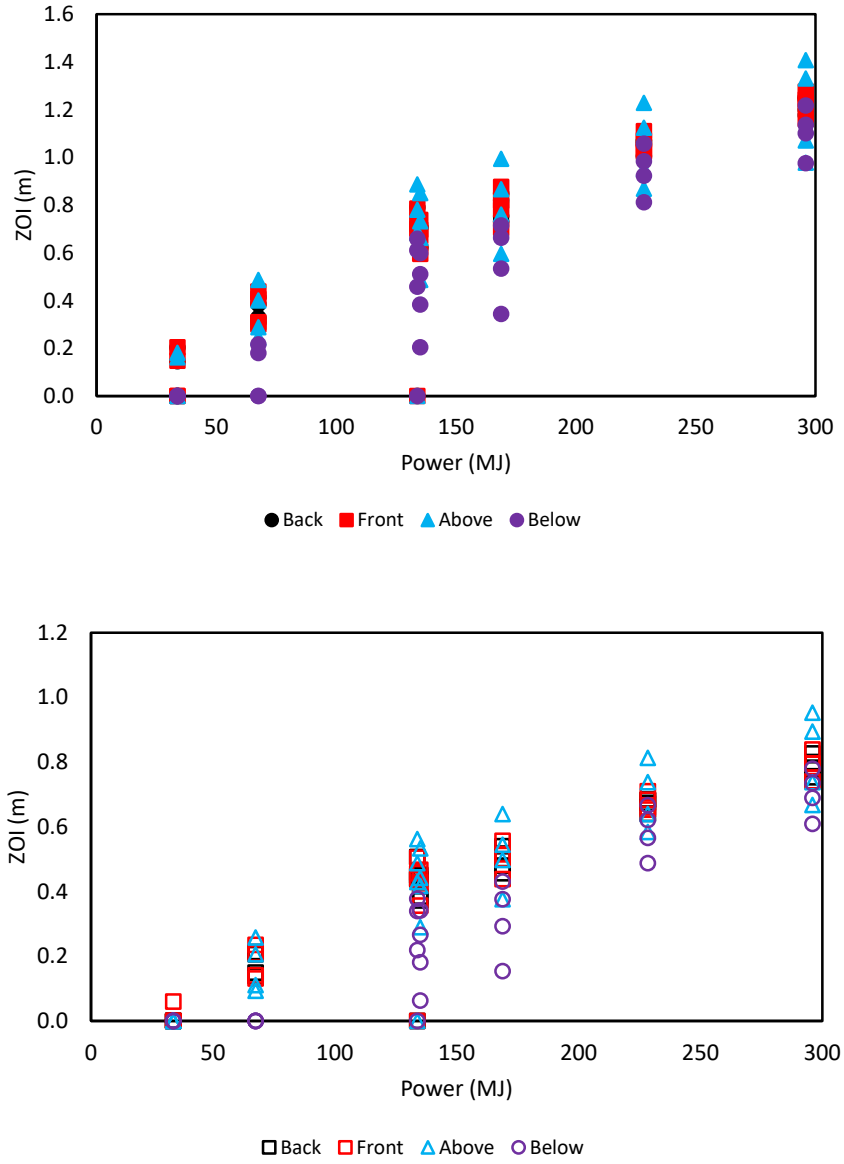

Figure 6-61
ZOIs as a function of arc energy for the NSBD straight segment HEAF simulations. Top – 15 MJ/m² fragility target, bottom – 30 MJ/m² fragility target. Symbol shape and color indicates the enclosure face

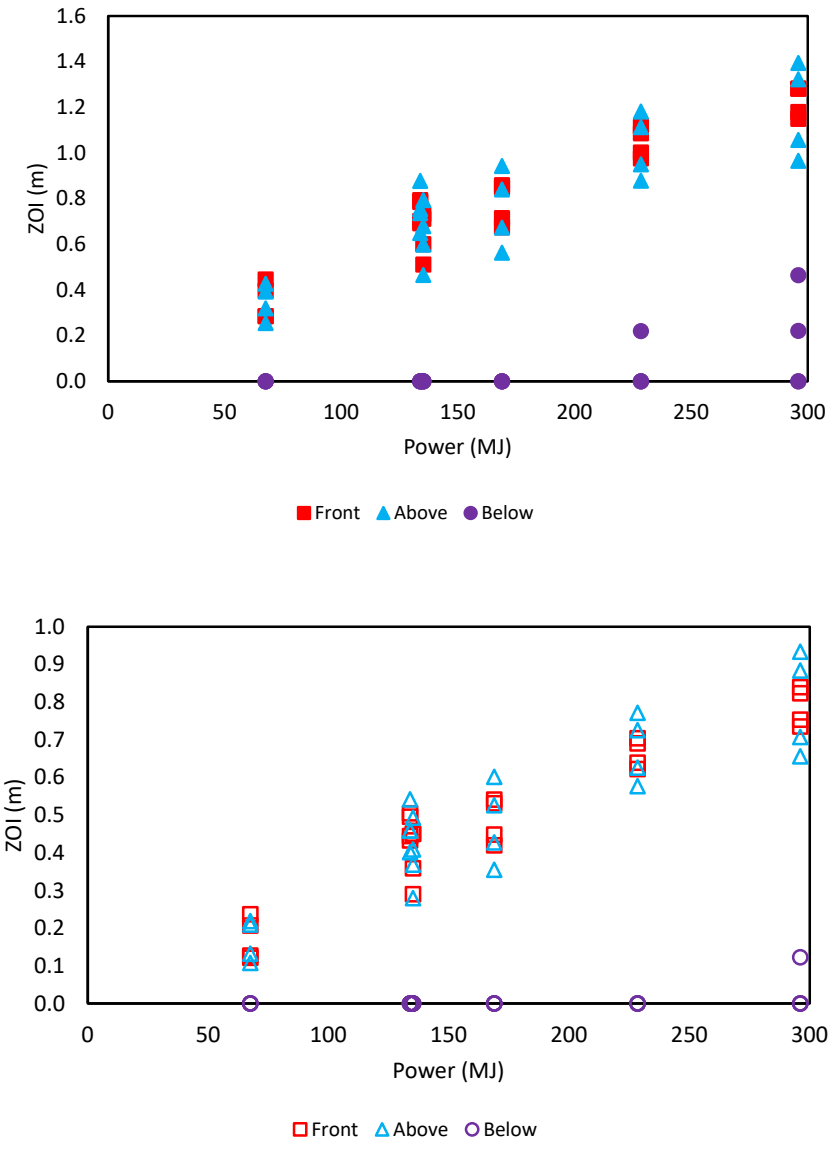

Figure 6-62
ZOIs as a function of arc energy for the NSBD tee HEAF simulations. Top – 15 kW/m² fragility target, bottom – 30 kW/m² fragility target. Symbol shape and color indicates the enclosure face

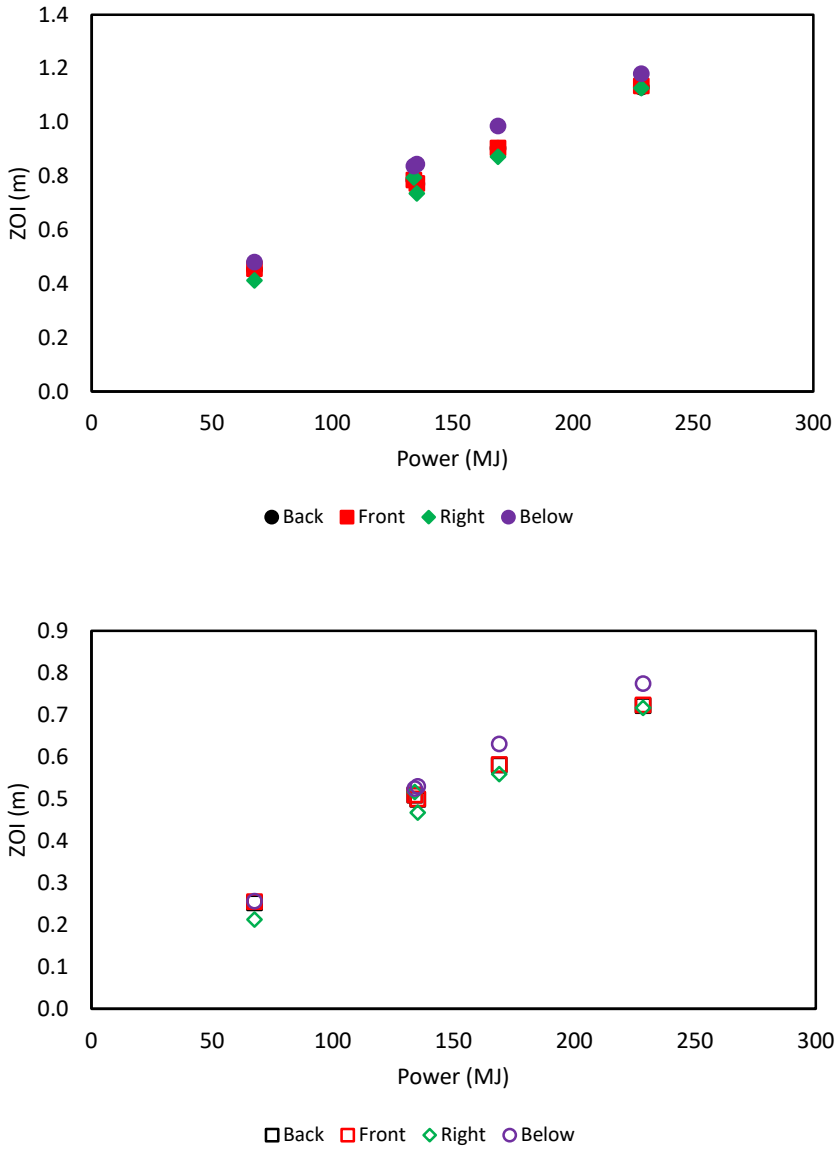

Figure 6-63
ZOIs as a function of arc energy for the NSBD elbow HEAF simulations. Top – 15 kW/m² fragility target, bottom – 30 kW/m² fragility target. Symbol shape and color indicates the enclosure face

Figure 6-64 shows the aluminum versus copper ZOIs for NSBD HEAF simulations. As observed with the MV SWGR and LV SWGR results, the results do not show that one electrode metal is more hazardous than the other. The top ZOIs for the copper electrode HEAFs tend to be larger than the aluminum electrode HEAF (green diamonds in Figure 6-64) and the bottom ZOIs tend to be larger for the aluminum electrode (blue triangles in Figure 6-64). This may be a result of the convective flow patterns that develop within the bus duct after it is breached. This pattern could be influenced by the melting temperature of the electrode via the development and path of particles generated and the energy distribution within the bus duct during the arc.

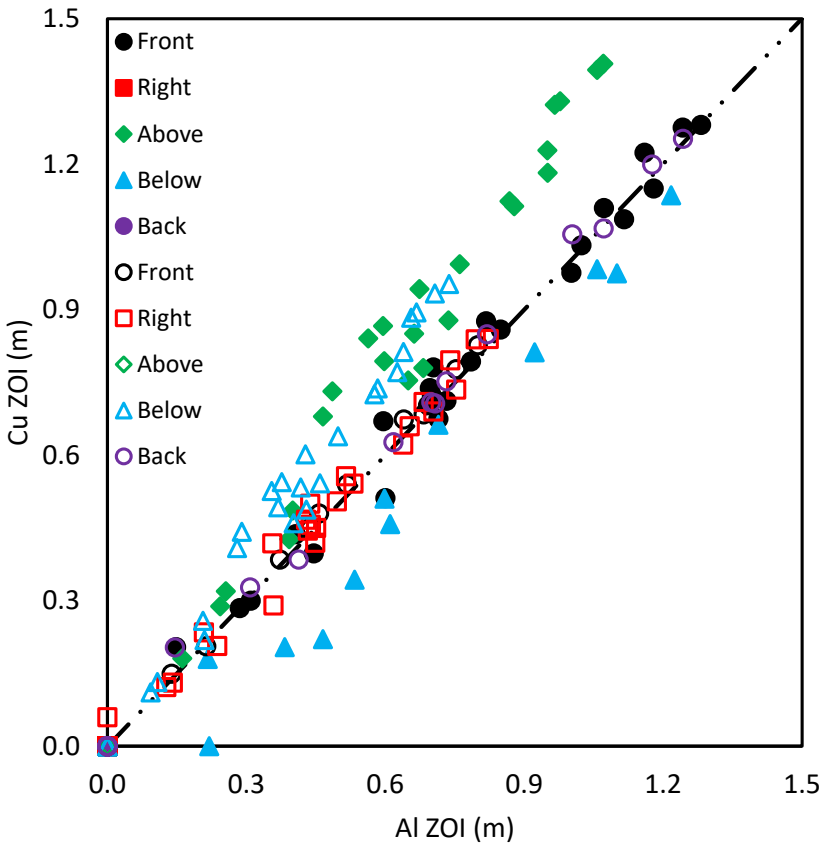

Figure 6-64
Aluminum versus copper bus bar ZOIs for all NSBD HEAF simulations. Note that the solid fill symbols indicate an aluminum bus duct and the outline symbols indicate a steel bus duct

Figure 6-65 shows the aluminum versus steel duct ZOIs for NSBD HEAF simulations. The aluminum duct shows larger ZOIs, approximately 0.15 m larger than the steel. This is due to the shorter breach time for aluminum bus ducts as compared to steel given the energy required to melt the aluminum is less than that of steel.

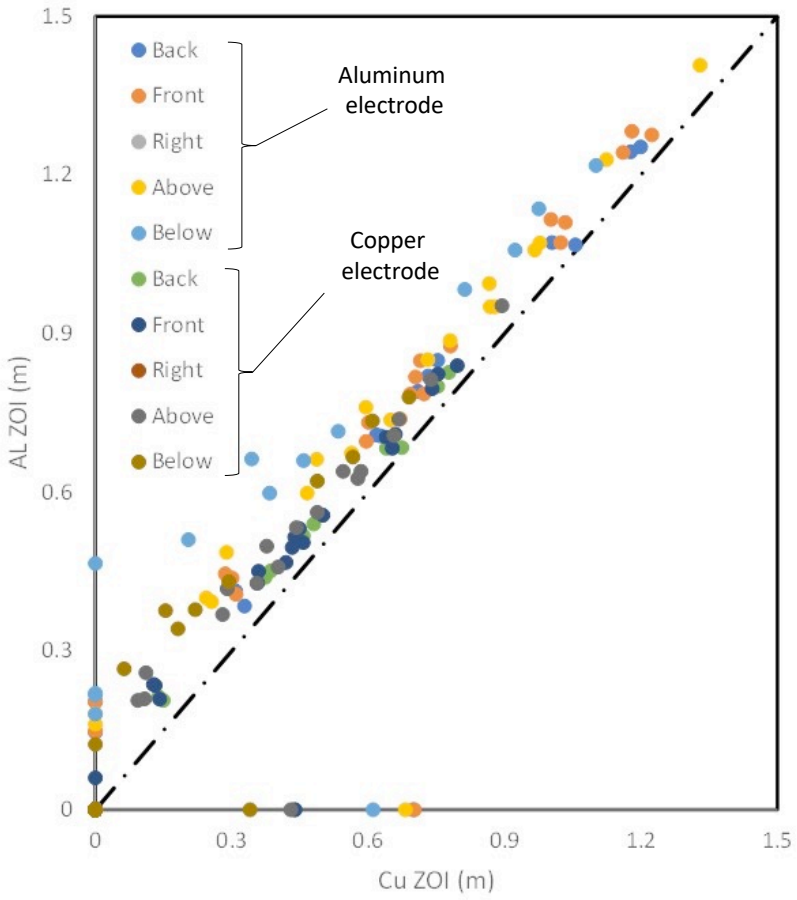

Figure 6-65
Steel duct versus aluminum duct ZOIs for all NSBD HEAF simulations.

6.3.2.2 FDS Model Insights

The NSBD results reveals a number of trends that are unique to bus ducts. Figure 6-60 through Figure 6-63 indicate that, except for the bottom of the duct, all the remaining faces see similar exposures regardless of the geometric configuration. Whereas switchgear enclosures have partitions, breakers, and vents that influence the direction of the energy, the simplistic geometry of bus ducts yields a relatively consistent distribution in all directions. Targets located below the bus duct will see lower exposures, as they are not subject to the bulk of the convective heat transfer. This is particularly noticeable for the tee geometries, where the bottom face of the bus duct is at a greater distance from the arc, which is initiated in the top segment of the tee.

The orientation of the duct (straight, elbow, or tee) has little effect on the ZOIs. Although the geometry of the duct may influence the flow of gases early in the event, once the duct is breached, targets are exposed to the same radiant flux. The geometric parameter that has the largest effect on target incident energy is the distance of the arc to the enclosure wall (i.e., how quickly the enclosure wall will breach) and the difference in this parameter across straight ducts, tees, and elbows is insignificant. This effect is most pronounced when looking at the incident energy at the bottom surface of the tee, as noted above.

Figure 6-64 indicates that, as with the switchgear enclosures, there is no significant difference in the ZOIs for bus ducts with aluminum bus bars and bus ducts with copper bus bars. Some

configurations have larger ZOIs with aluminum bus bars, others have larger ZOIs for copper bus bars.

Unlike switchgear enclosures, which are all assumed to be made of steel, bus duct housings are typically fabricated from steel or aluminum. Figure 6-65 indicates a significant difference between the two materials; HEAFs in ducts with aluminum housing have a ZOI that are, on average, 0.15 m larger than those in ducts with steel housing. Differences in specific heat and melting point between the two metals cause the aluminum duct to breach faster than the steel duct, which increased the thermal exposure of external targets.

6.3.2.3 Tabulated NSBD ZOIs

Table 6-3 shows a summary of the NSBD HEAF simulation results. The orientations of the ZOI surfaces relative to each NSBD arc location is depicted in Figure 6-66.

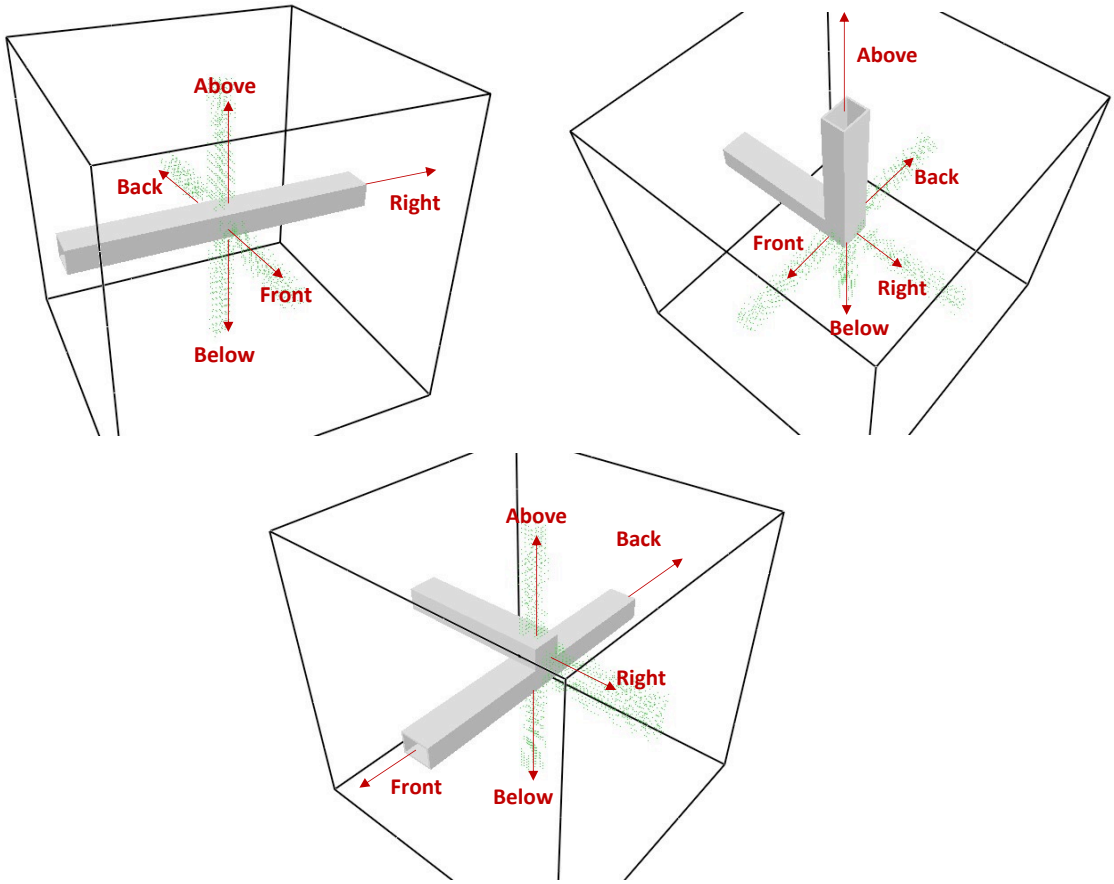

Figure 6-66
ZOI orientations for the NSBD arc locations. Straight NSBD arc location (top left), elbow arc location (top right), and tee arc location (bottom)

Table 6-3
Summary of the NSBD scenarios

HEAF Simulation Summary							ZOI (m)									
							15 MJ/m² Target Fragility					30 MJ/m² Target Fragility				
HEAF ID[1]	Duct	Bus Bar Material	Stiff (s)	Decay (s)	Arc Location	Arc Energy[2] (MJ)	Back	Front	Right	Above	Below	Back	Front	Right	Above	Below
NSBD-1	Steel	Aluminum	1	0	Straight	34	None	None	N/A[3]	None	None	None	None	N/A	None	None
NSBD-2	Steel	Aluminum	2	0	Straight	68	0.31	0.31	N/A	0.24	None	0.14	0.14	N/A	0.09	None
NSBD-3	Steel	Aluminum	4	0	Straight	135	0.62	0.60	N/A	0.49	0.38	0.37	0.36	N/A	0.29	0.18
NSBD-4	Steel	Aluminum	5	0	Straight	169	0.73	0.70	N/A	0.60	0.53	0.46	0.44	N/A	0.38	0.29
NSBD-5	Steel	Aluminum	0	15	Straight	131	0.70	0.70	N/A	0.68	0.61	0.44	0.44	N/A	0.43	0.34
NSBD-6	Steel	Aluminum	3	15	Straight	226	1.00	1.02	N/A	0.87	0.92	0.64	0.65	N/A	0.58	0.57
NSBD-7	Steel	Aluminum	5	15	Straight	293	1.18	1.16	N/A	0.98	1.10	0.75	0.74	N/A	0.67	0.69
NSBD-8	Aluminum	Aluminum	1	0	Straight	34	0.15	0.15	N/A	0.16	None	None	None	N/A	None	None
NSBD-9	Aluminum	Aluminum	2	0	Straight	68	0.41	0.41	N/A	0.40	0.22	0.21	0.21	N/A	0.21	None
NSBD-10	Aluminum	Aluminum	4	0	Straight	135	0.71	0.70	N/A	0.66	0.60	0.44	0.43	N/A	0.42	0.34
NSBD-11	Aluminum	Aluminum	5	0	Straight	169	0.82	0.82	N/A	0.76	0.71	0.52	0.52	N/A	0.50	0.43
NSBD-12	Aluminum	Aluminum	3	15	Straight	226	1.07	1.07	N/A	0.95	1.06	0.68	0.68	N/A	0.64	0.67
NSBD-13	Aluminum	Aluminum	5	15	Straight	293	1.24	1.24	N/A	1.07	1.22	0.80	0.80	N/A	0.74	0.78
NSBD-14	Steel	Copper	1	0	Straight	34	None	None	N/A	None	None	None	None	N/A	None	None
NSBD-15	Steel	Copper	2	0	Straight	68	0.33	0.30	N/A	0.29	None	0.15	0.13	N/A	0.11	None
NSBD-16	Steel	Copper	4	0	Straight	135	0.63	0.67	N/A	0.73	0.20	0.39	0.42	N/A	0.44	0.06
NSBD-17	Steel	Copper	5	0	Straight	169	0.75	0.78	N/A	0.87	0.34	0.48	0.50	N/A	0.54	0.15

HEAF Simulation Summary							ZOI (m)									
							15 MJ/m² Target Fragility					30 MJ/m² Target Fragility				
HEAF ID[1]	**Duct**	**Bus Bar Material**	**Stiff (s)**	**Decay (s)**	**Arc Location**	**Arc Energy[2] (MJ)**	**Back**	**Front**	**Right**	**Above**	**Below**	**Back**	**Front**	**Right**	**Above**	**Below**
NSBD-18	Steel	Copper	0	15	Straight	131	0.71	0.72	N/A	0.78	0.46	0.45	0.46	N/A	0.49	0.22
NSBD-19	Steel	Copper	3	15	Straight	226	1.06	1.03	N/A	1.12	0.81	0.67	0.66	N/A	0.74	0.49
NSBD-20	Steel	Copper	5	15	Straight	293	1.20	1.22	N/A	1.33	0.98	0.78	0.80	N/A	0.89	0.61
NSBD-21	Aluminum	Copper	1	0	Straight	34	0.20	0.20	N/A	0.18	None	None	0.06	N/A	None	None
NSBD-22	Aluminum	Copper	2	0	Straight	68	0.38	0.44	N/A	0.49	0.18	0.21	0.23	N/A	0.26	None
NSBD-23	Aluminum	Copper	4	0	Straight	135	0.71	0.74	N/A	0.85	0.51	0.45	0.47	N/A	0.53	0.27
NSBD-24	Aluminum	Copper	5	0	Straight	169	0.85	0.88	N/A	0.99	0.66	0.54	0.56	N/A	0.64	0.38
NSBD-25	Aluminum	Copper	0	15	Straight	131	0.79	0.79	N/A	0.89	0.66	0.51	0.50	N/A	0.56	0.38
NSBD-26	Aluminum	Copper	3	15	Straight	226	1.07	1.11	N/A	1.23	0.98	0.68	0.71	N/A	0.81	0.62
NSBD-27	Aluminum	Copper	5	15	Straight	293	1.25	1.28	N/A	1.41	1.14	0.83	0.84	N/A	0.95	0.73
NSBD-28	Steel	Aluminum	2	0	Tee	68	N/A	0.29	N/A	0.26	None	N/A	0.13	N/A	0.11	None
NSBD-29	Steel	Aluminum	4	0	Tee	135	N/A	0.60	N/A	0.47	None	N/A	0.36	N/A	0.28	None
NSBD-30	Steel	Aluminum	5	0	Tee	169	N/A	0.71	N/A	0.56	None	N/A	0.45	N/A	0.36	None
NSBD-31	Steel	Aluminum	0	15	Tee	131	N/A	0.69	N/A	0.65	None	N/A	0.43	N/A	0.40	None
NSBD-32	Steel	Aluminum	3	15	Tee	226	N/A	1.00	N/A	0.88	None	N/A	0.64	N/A	0.58	None
NSBD-33	Steel	Aluminum	5	15	Tee	293	N/A	1.18	N/A	0.97	None	N/A	0.75	N/A	0.66	None
NSBD-34	Aluminum	Aluminum	2	0	Tee	68	N/A	0.45	N/A	0.39	None	N/A	0.24	N/A	0.21	None
NSBD-35	Aluminum	Aluminum	4	0	Tee	135	N/A	0.73	N/A	0.60	None	N/A	0.45	N/A	0.37	None
NSBD-36	Aluminum	Aluminum	5	0	Tee	169	N/A	0.85	N/A	0.67	None	N/A	0.53	N/A	0.43	None

HEAF Simulation Summary							ZOI (m)									
							15 MJ/m² Target Fragility					30 MJ/m² Target Fragility				
HEAF ID[1]	Duct	Bus Bar Material	Stiff (s)	Decay (s)	Arc Location	Arc Energy[2] (MJ)	Back	Front	Right	Above	Below	Back	Front	Right	Above	Below
NSBD-37	Aluminum	Aluminum	0	15	Tee	131	N/A	0.79	N/A	0.74	None	N/A	0.50	N/A	0.46	None
NSBD-38	Aluminum	Aluminum	3	15	Tee	226	N/A	1.12	N/A	0.95	0.22	N/A	0.70	N/A	0.63	None
NSBD-39	Aluminum	Aluminum	5	15	Tee	293	N/A	1.28	N/A	1.06	0.47	N/A	0.82	N/A	0.71	0.12
NSBD-40	Steel	Copper	2	0	Tee	68	N/A	0.28	N/A	0.32	None	N/A	0.12	N/A	0.13	None
NSBD-41	Steel	Copper	4	0	Tee	135	N/A	0.51	N/A	0.68	None	N/A	0.29	N/A	0.41	None
NSBD-42	Steel	Copper	5	0	Tee	169	N/A	0.67	N/A	0.84	None	N/A	0.42	N/A	0.53	None
NSBD-43	Steel	Copper	0	15	Tee	131	N/A	0.70	N/A	0.75	None	N/A	0.44	N/A	0.46	None
NSBD-44	Steel	Copper	3	15	Tee	226	N/A	0.98	N/A	1.11	None	N/A	0.62	N/A	0.73	None
NSBD-45	Steel	Copper	5	15	Tee	293	N/A	1.15	N/A	1.32	None	N/A	0.74	N/A	0.88	None
NSBD-46	Aluminum	Copper	2	0	Tee	68	N/A	0.40	N/A	0.43	None	N/A	0.21	N/A	0.22	None
NSBD-47	Aluminum	Copper	4	0	Tee	135	N/A	0.71	N/A	0.79	None	N/A	0.45	N/A	0.49	None
NSBD-48	Aluminum	Copper	5	0	Tee	169	N/A	0.86	N/A	0.94	None	N/A	0.54	N/A	0.60	None
NSBD-49	Aluminum	Copper	0	15	Tee	131	N/A	0.79	N/A	0.88	None	N/A	0.51	N/A	0.54	None
NSBD-50	Aluminum	Copper	3	15	Tee	226	N/A	1.09	N/A	1.18	None	N/A	0.69	N/A	0.77	None
NSBD-51	Aluminum	Copper	5	15	Tee	293	N/A	1.28	N/A	1.39	0.22	N/A	0.84	N/A	0.93	None
NSBD-52	Aluminum	Aluminum	2	0	Elbow	68	0.45	0.46	0.41	N/A	0.48	0.25	0.26	0.21	N/A	0.26
NSBD-53	Aluminum	Aluminum	4	0	Elbow	135	0.77	0.77	0.74	N/A	0.85	0.50	0.50	0.47	N/A	0.53
NSBD-54	Aluminum	Aluminum	5	0	Elbow	169	0.90	0.91	0.87	N/A	0.99	0.58	0.58	0.56	N/A	0.63
NSBD-55	Aluminum	Aluminum	0	15	Elbow	131	0.79	0.79	0.80	N/A	0.84	0.51	0.51	0.52	N/A	0.52

HEAF Simulation Summary							ZOI (m)									
							15 MJ/m² Target Fragility					30 MJ/m² Target Fragility				
HEAF ID[1]	**Duct**	**Bus Bar Material**	**Stiff (s)**	**Decay (s)**	**Arc Location**	**Arc Energy[2] (MJ)**	**Back**	**Front**	**Right**	**Above**	**Below**	**Back**	**Front**	**Right**	**Above**	**Below**
NSBD-56	Aluminum	Aluminum	3	15	Elbow	226	1.13	1.14	1.13	N/A	1.18	0.72	0.72	0.72	N/A	0.77
NSBD-57	Aluminum	Aluminum	5	15	Elbow	293	1.32	1.32	1.31	N/A	1.37	0.86	0.86	0.84	N/A	0.92

[1]The FDS input designator is not the same as the input file name but uniquely corresponds to a single FDS input file. Refer to Appendix B of this report for the corresponding input file nomenclature designator.

[2]Energy as input into FDS model, which include a finite time of decay from the peak power. This energy total differs slightly from the energy listed in Table 5-3 due to melting of the electrode (see Section 5.8.2).

[3]N/A indicates that direction contains a bus duct for that HEAF simulation. For example, the straight duct HEAF simulations have the duct running left to right; therefore, right of the arc is inside the duct.

7
SUMMARY AND CONCLUSIONS

This report documents updates to the treatment of HEAFs in the fire PRA. The effort had three parts for developing estimates of the HEAF ZOIs:

- The development of an analysis approach using the CFD model FDS to calculate the thermal exposure seen by targets exposed to a HEAF event.
- The validation of the FDS analysis approach.
- The application of the FDS analysis approach to a large matrix of simulations that vary HEAF duration, location, power, electrode composition, and type of equipment.

The results of the FDS application involve tabulated ZOIs for thermoplastic and thermoset cables using damage thresholds developed under the target fragility analysis phase [10]. This dataset of ZOIs will be used by the WG to develop the final PRA guidance.

7.1 FDS Analysis Approach Summary

The FDS analysis approach was developed for use with modeling HEAFs in electrical enclosures. Key elements of the approach are as described below.

1. Simulation time – Based the MV SWGR experiments, the FDS simulations were run for 8 seconds after the termination of the arc fault to capture the effects of the gas flows and radiating boundaries.
2. Gas properties – FDS was modified to allow a user-definable upper limit for the temperature arrays. This enabled defining extended specific heat values for nitrogen, carbon dioxide, and oxygen up to 20,000 K. Material property data for Cu vapor, Al vapor, and Al_2O_3 were taken from NIST-JANAF tables [20] and Cressault et al. [21, 22].
3. Thermal radiation – A power law radiant fraction is developed using data from Cressault et al. [24]. The solution resolution was increased from a default 100 solid angles to 500 solid angles for the unit sphere used to solve the radiation transport equations.
4. Computational grid – A 0.0762 m grid is used for the MV SWGR and LV SWGR models and a 0.02 m grid is used for NSBD models. For all geometries, the grid is extended 1.5 to 2 m from the face of the enclosure.
5. Combustion – Combustion is modeled for the oxidation of metal vapor (see Section 3.7 for discussion of vapor addition). The heats of combustion are taken from NIST-JANAF data [20].
6. Enclosure breach – The metal switchgear and NSBD enclosure boundaries are modeled using a phase change material. This is a material with a single-step reaction that occurs at a threshold temperature (i.e., the melting point). A cell obstruction is removed when the metal temperature reaches the melting point, creating an opening in the enclosure boundary.

7. Electrode mass loss – The electrode mass loss rate is determined from empirical correlations between the input current and the electrode material developed by Stanback [25] for LV SWGR and NSBD HEAF events. The mass loss rate correlation for the MV SWGR is developed from the 2018 MV SWGR tests [6].
8. Particle oxidation – Particle oxidation is incorporated into the model for drop sizes in the 2 – 15 micron range. Smaller diameter particles are shown to represent a negligible bus bar mass and larger drops did not affect the ZOI. The drops are injected into the FDS model as particles with a specified pyrolysis rate that corresponded to the oxidation fraction observed.
9. Arc power – Arc energy profiles are developed for MV SWGR and NSBDs with a total energy ranging from 34 – 296 MJ. Arc energy profiles for LV SWGR range from 28 – 90 MJ, with the 90 MJ arc defined as a conservative representation of FEDB 50935 [12].
10. Input file generation – Input files were generated using a python script template to minimize input errors.

The approach required several modifications to FDS to accommodate the high temperatures involved. These changes were incorporated into several interim FDS versions, with the final simulations performed using FDS, Version 6.7.6-790. Subsequent FDS versions retained the modifications required for this effort.

7.2 FDS HEAF Validation Summary

The validation of the FDS analysis approach is based on the following cases:

- The 2018 MV SWGR tests [6]
- A LV SWGR event
- A full-scale test replicating a NSBD event (FEDB 51765) [7]
- A HEAF event at a NSBD elbow (FEDB 51765)

Three of the 2018 MV SWGR experiments are considered in the validation effort and are used to develop the overall model relative standard deviation (σ) and bias (δ) applied to the predicted exposure. The resulting relative standard deviation and bias were based on the 4 s switchgear tests given these experiments resulting in a breach of the top and bottom of the enclosure, making leakage around the gaps less important to the total exposure. The resulting relative standard deviation and bias as determined from these FDS predictions and experimental results were 0.71 MJ/m² and 0.57, respectively; however, the relative standard deviation and bias was similar for all instrument locations and tests.

7.3 FDS Results

The ZOIs predicted by the FDS are summarized in Table 6-1 for MV SWGR, Table 6-2 for LV SWGR, and Table 6-3 for NSBDs. Summaries of the ZOI ranges predicted by FDS are provided in Table 7-1 for the MV SWGR, Table 7-2 for the LV SWGR, and Table 7-3 for NSBDs.

Table 7-1
Summary of MV SWGR ZOI ranges

Switchgear enclosure face	ZOI (m) for 15 MJ/m² target fragility	ZOI (m) for 30 MJ/m² target fragility
Back	0 – 1.13	0 – 0.76
Left	0 – 1.24	0 – 0.92
Right	0 – 1.24	0 – 0.92
Top	0 – 1.01	0 – 0.58
Front	0 – 1.31	0 – 0.97

Table 7-2
Summary of LV SWGR ZOI ranges

Switchgear enclosure face	ZOI (m) for 15 MJ/m² target fragility	ZOI (m) for 30 MJ/m² target fragility
Back	0 – 0.17	0
Left	0	0
Right	0 – 0.9	0 – 0.59
Top	0 – 0.84	0 – 0.53
Front	0	0

Table 7-3
Summary of NSBD ZOI ranges

NSBD enclosure face	ZOI (m) for 15 MJ/m² target fragility	ZOI (m) for 30 MJ/m² target fragility
Back	0 – 1.32	0 – 0.86
Front	0 – 1.32	0 – 0.86
Right	0.41 – 1.31	0.21 – 0.84
Above	0 – 1.39	0 – 0.93
Below	0 – 1.37	0 – 0.92

7.4 Significant HEAF Modeling Insights

The significant modeling insights developed during this effort are summarized below.

- The difference between ZOIs from HEAFs with aluminum electrode and HEAFs with copper electrode is not significant for all equipment classes. The ZOIs for each material are within the 95th percentile of the model uncertainty band as computed from the ZOI predictions for either material.

- The dominant parameter affecting the HEAF ZOIs in the MV SWGR was the total arc energy. A secondary parameter was the switchgear type (vertical-lift breaker style or horizontal draw-out style).

- The side ZOIs are lower for vertical-lift breaker style switchgear as compared to horizontal draw-out breaker style breaker switchgear. In addition, for vertical-lift breaker style switchgear in the supply configuration, there is no vertical (top) ZOI component. The load configuration vertical-lift breaker style switchgear and the horizontal draw-out style switchgear have comparable top ZOIs

- The ZOIs for LV SWGR are smaller than those postulated in the existing guidance in Appendix M of NUREG/CR-6850 EPRI 1011989 EPRI/NRC-RES Fire PRA Methodology for Nuclear Power Facilities.

- The ZOIs for MV SWGR and bus ducts are smaller than the existing guidance for some configurations and directions, but larger for others.

- The composition of bus duct housing (steel versus aluminum) has a significant impact on the ZOIs; HEAFs in aluminum ducts had ZOIs that are, on average, 0.15 m larger than those in steel ducts.

- The ZOIs for low- and medium-voltage switchgear are sensitive to equipment geometry and orientation. Bus ducts, with comparatively simply geometries, were not.

8
REFERENCES

1. *EPRI/NRC-RES Fire PRA Methodology for Nuclear Power Facilities, Volume 2: Detailed Methodology*. Electric Power Research Institute (EPRI), Palo Alto, CA and U.S. Nuclear Regulatory Commission, Washington, DC: September 2005. EPRI 1011989 and NUREG/CR-6850.
2. *EPRI/NRC*-RES *Fire Probabilistic Risk Assessment Methods Enhancements*. Electric Power Research Institute (EPRI), Palo Alto, CA and U.S. Nuclear Regulatory Commission, Washington, DC: September 2010. EPRI 1019259 and NUREG/CR-6850 Supplement 1.
3. *Survey and Analysis of U.S. Nuclear Industry Relative to High Energy Arcing Faults in the Presence of Aluminum*. EPRI, Palo Alto, CA. May 2021. EPRI 3002020692.
4. *Report on High Energy Arcing Fault Experiments: Experimental Results from Open Box Enclosures*. U.S. Nuclear Regulatory Commission, Washington DC, National Institute of Standards and Technology, Gaithersburg, MD, and Sandia National Laboratories, Albuquerque, NM. December 2021. Research Information Letter (RIL) 2021-18, NIST TN 2198, and SAND2021-16075 R.
5. *Report on High Energy Arcing Fault Experiments: Experimental Results from Low Voltage Switchgear Enclosures*. U.S. Nuclear Regulatory Commission, Washington DC, and National Institute of Standards and Technology, Gaithersburg, MD. November 2021. RIL 2021-17 and NIST TN 2197.
6. *Report on High Energy Arcing Fault Experiments: Experimental Results from Medium Voltage Electrical Enclosures*. U.S. Nuclear Regulatory Commission, Washington DC, National Institute of Standards and Technology, Gaithersburg, MD, and Sandia National Laboratories, Albuquerque, NM. November 2021. RIL 2021-10, NIST TN 2188, and SAND2021-12049 R
7. *Report on the Testing Phase (2014-2016) of the High Energy Arcing Fault Events (HEAF) Project: Experimental Results from the International Energy Arcing Fault Research Programme*. Nuclear Energy Agency (NEA). Organisation for Economic Co-operation and Development. Paris, France. May 2017. NEA/CSNI/R(2017)7.
8. *NUREG/IA-0470, Volume 1, International Agreement Report, Nuclear Regulatory Authority Experimental Program to Characterize and Understand High Energy Arcing Fault (HEAF) Phenomena*, Regulatory Standard and Development Department, Secretariat of Nuclear Regulatory Authority (S/NRA/R), Tokyo, Japan, U.S. Nuclear Regulatory Commission, Washington, DC 20555-0001, April 2016.
9. *NUREG/IA-0470, Volume 2, International Agreement Report, Nuclear Regulatory Authority Experimental Program to Characterize and Understand High Energy Arcing Fault (HEAF) Phenomena, Basic Arc Test Experimental Data*, Regulatory Standard and Development Department, Secretariat of Nuclear Regulatory Authority (S/NRA/R), Tokyo, Japan, U.S. Nuclear Regulatory Commission, Washington, DC 20555-0001, October, 2021.

10. *Target Fragilities for Equipment Vulnerable to High Energy Arcing Faults*. Electric Power Research Institute (EPRI), Palo Alto, CA and U.S. Nuclear Regulatory Commission, Washington, DC: RIL 2022-01 / EPRI 3002023400.
11. The Updated Fire Events Database: Description of Content and Fire Event Classification Guidance. EPRI. Palo Alto, CA: 2013. 1025284.
12. Fire Events Database Update for the Period 2010–2014: Revision 1. EPRI, Palo Alto, CA: 2016. 3002005302.
13. *Fire Dynamics Simulator User's Guide,* NIST Special Publication 1019 Sixth Edition, DOI: 10.6028/NIST.SP.1019, November 2021.
14. *Fire Dynamics Simulator Technical Reference Guide, Volume 1: Mathematical Model,* NIST Special Publication 1018-1 Sixth Edition, DOI: 10.6028/NIST.SP.1018, November 2021.
15. *Fire Dynamics Simulator Technical Reference Guide, Volume 2: Verification,* NIST Special Publication 1018-1 Sixth Edition, DOI: 10.6028/NIST.SP.1018, November 2021.
16. *Fire Dynamics Simulator Technical Reference Guide, Volume 3: Validation,* NIST Special Publication 1018-1 Sixth Edition, DOI: 10.6028/NIST.SP.1018, November 2021.
17. *Fire Dynamics Simulator Technical Reference Guide, Volume 4: Software Quality Assurance,* NIST Special Publication 1018-1 Sixth Edition, DOI: 10.6028/NIST.SP.1018, November 2021.
18. *Verification and Validation of Selected Fire Models for Nuclear Power Plant Applications, Supplement 1*. EPRI, Palo Alto, CA, and U.S. Nuclear Regulatory Commission, Washington, DC, 2016. NUREG-1824 Supplement 1 and EPRI 3002002182.
19. *NASA Glenn Coefficients for Calculating Thermodynamic Properties of Individual Species*, NASA/TP-2002-211556, National Aeronautics and Space Administration, Glenn Research Center, Cleveland, OH, September 2002.
20. *NIST-JANAF Thermochemical Tables,* NIST Standard Reference Database 13, National Institute of Standards and Technology, Gaithersburg, MD, 1998. DOI: 10/18434/T42S31.
21. Cressault, Y., Hannachi, R., et. Al, "Influence of metallic vapors on the properties of air thermal plasmas," *Plasma Sources Sci. Technol.*, 17 (2008), DOI: 10.1088/0963-0252/17/3/035016.
22. Cressault, Y., Gleizes, A., and Riquel, G., "Properties of air-aluminum thermal plasmas," *J. Phys D: Appl Phys,* 45 (2012), DOI: 10.1088/0022-3727/45/26/265202.
23. W. Grosshandle, *RadCal: A Narrow Band Model for Radiation Calculations in a Combustion Environment,* NIST Technical Note 1402, National Institute of Standards and Technology, Gaithersburg, MD, 1993.
24. Cressault, Y, Bauchire, J., Hong, D., et. Al, "Radiation of long and high power arcs," *J. Phys. D: Appl. Phys.*, 48 (2015), DOI: 10.1088/0022-3727/48/41/415201.
25. Stanback, H", "Predicting Damage from 277-V Single Phase to Ground Arcing Faul"s," *IEEE Transactions on Industry Applications*, IA-13:4 (1977), DOI:10.1109/TIA.1977.4503412.
26. Siemroth, P., Laux, M., et al., "Diameter and Velocities of Droplets Emitted from the CU Cathode of a Vacuum Arc," *IEEE Transactions on Plamsa Science*, 47:8 (2019), DOI: 10.1109/TPS.2019.2912518.
27. Madjidian, D. and Wamundson, M., "Technical Services Related to Decrement Curve Testing at High Power Electrical Testing Facility Task 1: Energy Delivery Simulation Modeling," Power System Analysis, DNV GL, Sweden, April 2, 2020.

28. *Tools for the Simulation of the Effects of the Internal Arc in Transmission and Distribution Switchgear*. CIGRE, ISBN: 978-2-85873-303-3, 2014. CIGRE Standard 602.

29. *IEEE Guide for Liquid-Immersed Transformers Through-Fault-Current Duration*. Institute of Electrical and Electronics Engineers (IEEE), 1985. IEEE Standard C57.109-1985.

30. *Survey and Analysis of U.S. Nuclear Industry Relative to High Energy Arcing Faults in the Presence of Aluminum.* EPRI, Palo Alto, CA, May, 2021. Document 3002020692.

31. *Predicting High Energy Arcing Fault Zones of Influence for Aluminum Using a Modified Arc Flash Mod–I - Evaluation of a Modified Model Bias, Uncertainty, Parameter Sensitivity, and Zone of Influence Estimation*. Draft for Public Comment, (ADAMS Accession No. ML22095A236) U.S. Nuclear Regulatory Commission, Washington, D.C. 20555-0001, April, 2022.

32. *Nuclear Station Electrical Distribution Systems and High-Energy Arcing Fault Events*. EPRI, Palo Alto, CA, July, 2019. Document 300201599.

33. *IEEE Guide for Performing Arc-Flash Hazard Calculations*. IEEE, 2018. IEEE Standard 1584-2018.

34. *High Energy Arcing Fault Operating Experience Panel Discussion*. Public Workshop with NEI, EPRI, and Industry, U. S. NRC, Washington, D.C., October 20, 2021. ML21291A180.

35. *High Energy Arcing Fault (HEAF) Operating Experience (Duke Energy).* Rishel, R., Public Workshop with NEI, EPRI, and Industry, U. S. NRC, Washington, D.C., October 20, 2021. ML21293A009.

36. *Operating Experience Assessment Energetic Faults in 4.16 to 13.8 kV Switchgear and Bus Ducts That Caused Fires in Nuclear Power Plants 1986-2001.* February, 2002. Adam Package ML021290364.

37. *Kerite Analysis in Thermal Environment of FIRE (KATE-Fire): Test Results*. Sandia National Laboratories, Albuquerque, NM and U.S. Nuclear Regulatory Commission, Washington, DC, 2016. NUREG/CR-7102 and SAND2011-6548P.

A
ARC POWER AND PROFILE

This appendix details the arc power inputs and the profiles used in the modeling of the HEAFs. HEAF operating experience, various testing programs, and electrical protection schemes were reviewed. The arcing power and profile are largely dependent on where the arcing fault occurs in the electrical distribution system and the characteristics of the electrical protection system. The arc power can be divided into the arc voltage and arc current. The arc power profile represents how the arc behaves over time as observed in HEAF events.

A.1 Arc Voltage

Arc voltage is a parameter in determining the arc energy. The arc voltage is the voltage drop across an arc between the arc roots. The arc voltage is dependent on several factors such as the electrode configuration and spacing, compartment size, and pressure. The arc is purely resistive and, as such, depends on the resistivity and arc current, not necessarily the system voltage. Arc voltage is one of the inputs in determining the arc energy for the FDS model.

Arc voltage cannot be obtained directly from HEAF OE [12] and needs to be determined through testing or predicted through modeling. The U.S. NRC analyzed existing test data from full-scale tests and evaluated it against predicted values from a model based on CIGRE 602 [28] in Appendix A of ML22095A236 [31]. The analysis resulted in an estimated values of 650 V_{L-L} to use for medium-voltage equipment and 375 V_{L-L} for low-voltage equipment.

A.2 Medium Voltage Arc Energy Profiles

The energy profiles considered for both medium-voltage switchgear and non-segregated bus ducts in HEAF OE [12] and through review of U.S. NPP electrical distributions systems [32] can be broken into two distinct profiles based on where the HEAF occurs in the electrical distribution system and availability of electrical fault protection. The profiles are:

Constant-Current Arcing Fault (stiff-source).

Constant current arcing faults are ascribed to classical short circuits that are fed by an infinite source limited by the impedance of the upstream transformer(s). These faults are of constant current until interrupted by the electrical distribution system (EDS) protection scheme (e.g., differential (instantaneous) or time-overcurrent relays), which define the duration of constant current arcing faults.

For conservatism, in electrical studies the fault location is modelled as zero-impedance fault (commonly referred to as “bolted” fault). However, not all faults are zero-impedance and are referred to as “arcing” fault. For medium voltage systems, the fault current magnitude is typically 85% of a “bolted” fault. Nonetheless, they are still considered a constant current arcing fault “stiff” source for the duration of the fault.

Instantaneous protections system will limit fault duration such that the energy will not rise to the level of a HEAF (typically cycles). On the other hand, depending on fault clearing time of time

overcurrent protection system, the let-through energy can achieve that of a HEAF (typically one or more seconds depending on the equipment).

Generator-fed Faults (decaying source).

Generator-fed faults are a type of fault not modelled in classical engineering protection and coordination studies and arose out of research and investigation into several medium voltage HEAF OE events exhibiting similar characteristics. With generator-fed faults, the generator protections system will trip the switchyard circuit breakers, eliminating fault current back-feeding from the switchyard through the generator step-up (GSU) transformer. In addition, the main generator excitation field circuit breaker opens to isolate the voltage regulator/exciter from feeding the generator field (rotor). Nonetheless, some residual energy remains in the rotating generator/rotor pair resulting in an exponential generator voltage and current decay over time. With no other protective device to isolate the fault, this decaying current can feed a fault through the unit auxiliary transformer (UAT) until the rotor field voltage collapses and the arcing fault extinguishes. This is referred to as “decaying” source or fault.

Table A-1 identifies the medium-voltage HEAF OE events and whether the fault was a generator-fed fault.

Table A-1
Medium voltage HEAF events with fault currents

Event ID	Date	HEAF Location	Generator-fed Fault	Reported Fault Current
51764	1/17/2017	NSBD	No	13 kA
50910	3/28/2010	SWGR	No	28 kA
51291	12/9/2013	NSBD	Yes	Unknown
50909	3/7/2010	NSBD	No	Unknown
10584	7/27/2008	NSBD	No	Unknown
732	7/6/1988	SWGR	No	32 kA
162	8/5/2009	NSBD	Yes	Unknown
100	05/15/2000	NSBD	Yes	Unknown
678	3/2/1988	NSBD	Yes	Unknown
922	7/10/1987	NSBD	Yes	Unknown
575	3/19/1987	NSBD	Yes	Unknown
112	8/3/2001	SWGR	Yes	Unknown
106	2/3/2001	SWGR	Yes	Unknown
74	6/10/1995	SWGR	Yes	28 kA
947	1/3/1989	SWGR	Yes	Unknown

A.2.1 Medium Voltage Constant-Current Arc Profile

The energy profile of stiff-source arc faults is simply a constant arc power during the arcing fault duration. The arc power is the arc current multiplied with the line-to-line arc voltage and the $\sqrt{3}$. This indicates that both the expected arc current and fault duration are required to identify the range of arc power modeled. The HEAF events in Table A-1 are reviewed to document the arcing fault currents, if available. The review shows that for the HEAF events occurring in medium-voltage equipment (bus ducts and switchgear), the reported arcing faults were generally in the expected range (85% of typical bolted fault currents of medium-voltage). To identify a conservative best estimate, a value between the highest fault current of 32 kA and the mid-range of 28 kA was selected. 13 kA was not used as it was significantly lower than that typically associated with medium-voltage available fault current. Therefore, a 30 kA fault current is used as a surrogate value for the arcing faults in the MV portion of the electrical distribution system before the protection scheme clears the fault.

As discussed above, the stiff-source profile maintains the arcing fault current at a constant value for a set duration. This fault emulates a three-phase bolted fault that persists until cleared by an overcurrent protective device. Five of the events in Table A-1 fit this profile, identified with a “No” in the “Generator-fed fault” column. As these types of HEAF events generally transition rapidly into a three-phase bolted faults, it is expected that the available overcurrent protective devices will trip to isolate the fault. Typically, if the overcurrent protective device is an instantaneous differential or overcurrent trip, the event will not raise to the energy level of a HEAF. In order for these type of constant-current arc faults to lead to a HEAF, there is either a lack of instantaneous protection or failure of instantaneous overcurrent protection has occurred. The lack of or failure of the instantaneous protection requires the time overcurrent protection to clear the fault. The primary purpose of these time overcurrent relays is to protect the transformer or switchgear from thermal damage due to a sustained through-fault-current condition. To inform this expected duration the back-up time overcurrent fault clearing times for faults fed through the UAT and offsite power transformers for U.S. NPPs were collected in an EPRI survey [3]. For both the UAT and the offsite power transformer the range was fractions of a second to 5 seconds. The upper FCT range of 5 s found from the survey results is expected as it aligns with IEEE Std C57.109 [29] guidelines in limiting of through-fault current duration to approximately 4 to 5 s for auxiliary power transformers.

To benchmark that the range of up to 5 s is valid for arcing faults (occurring further downstream of the first medium-voltage switchgear) that may rely on the time over-current settings between supply and feeder breakers, coordination calculations and time current curves (TCCs) from a sample set of U.S. NPPs were reviewed. The maximum fault clearing time identified was 4.3 s, with the majority being centered around 2 s.

5 s was determined as the high limit for both medium-voltage switchgear and non-segregated bus ducts for stiff-source faults.

On the lower end of the fault clearing range, 2018 MV SWGR testing [6] along with review of HEAF events show that for arcing faults under 2 s, the energy is primarily contained in the switchgear. The breaching of the switchgear steel cabinet was observed to take approximately ½ to 1 s, which limits the energy seen by targets outside of the switchgear enclosure. Therefore, a minimum threshold was utilized in the FDS modeling of 2 s for medium-voltage switchgear. For bus ducts, a lower threshold of 1 s was utilized to account for the faster breaching time that bus ducts with aluminum enclosures have compared to that of bus ducts with steel enclosure.

In summary for medium-voltage switchgear, the stiff-source considered in the FDS modeling ranges from 2 to 5 s. For non-segregated bus ducts, the range is from 1 to 5 s.

A.2.2 Arc Energy Profile of the Generator-fed Fault

The HEAF WG had had limited data on how a generator-fed fault's current decays over the event duration from the historic OE HEAF events. The potential range of durations for the generator to coast down to the point where an arc cannot be sustained was historically estimated to be between 4 – 8 s [36]. However, a recent HEAF event (occurred December, 2020) had shown a generator-fed fault lasting approximately 15 s. Fault current data from the HEAF event consisted primarily of the fault current seen at the UAT secondary side (via current transformer (CT) currents) that fed the fault, for various time stamps during the arcing fault (see Table A-2). The following is performed to obtain the decaying generator-fed fault current over time as seen at the 6.9 kV NSBD:

- The primary side of the CT fault current is calculated utilizing a CT turns ratio of 400.
- The secondary fault current of the UAT is calculated utilizing the ratio of the 22 kV primary to 6.9 kV secondary.
- The power was then calculated based on an assumed arc voltage of 650 $V_{L\text{-}L}$ (as discussed Section A.1) multiplied by the secondary fault current and the $\sqrt{3}$.

Table A-2
Fault currents at various times for a generator-fed HEAF event (December 2020)

Time	Primary Fault Current (CT Secondary)	Primary Fault Current (CT Primary)	Secondary Fault Current (Amps)	Power (I*Varc) in MW
0.095	16	6400	20,348	22.91
5.5	7.1	2840	9,029	10.17
5.55	6.6	2640	8,394	9.45
5.6	6.8	2720	8,648	9.74
5.65	6.63	2652	8,432	9.49
14.35	1.72	688	2,187	2.46
14.4	1.62	648	2,060	2.32
14.45	1.7	680	2,162	2.43
14.5	1.8	720	2,289	2.58
14.55	1.68	672	2,137	2.41
14.6	1.84	736	2,340	2.63

The arcing fault current and arc power plotted over time and exponential curve fit can be seen in Figure A-1 and Figure A-2. Integration of the power curve shown in Figure A-2 over the arc time interval, $\int_{0.095}^{14.6} 23.019e^{-0.154x}$, results in a total arc event energy of 132 MJ.

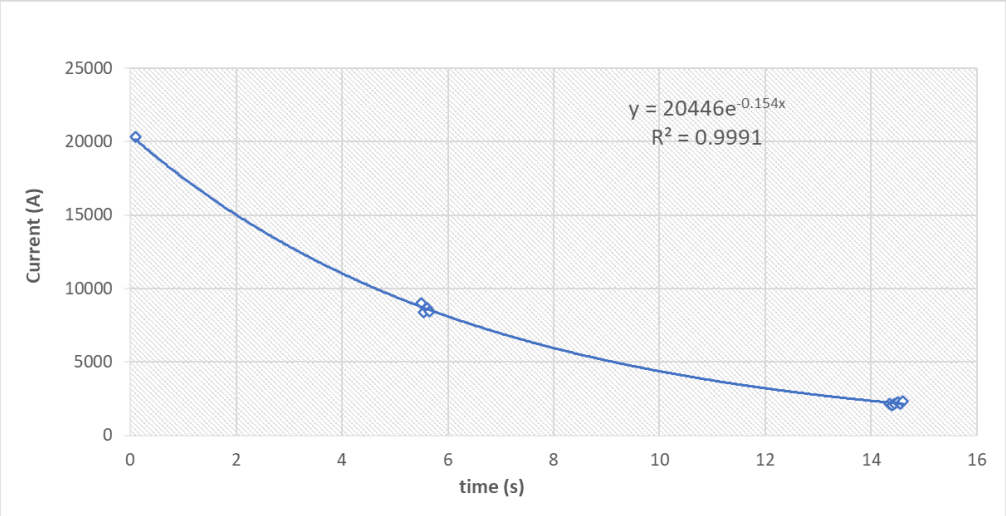

Figure A-1
Plot of the arc current for a generator-fed HEAF event (December 2020)

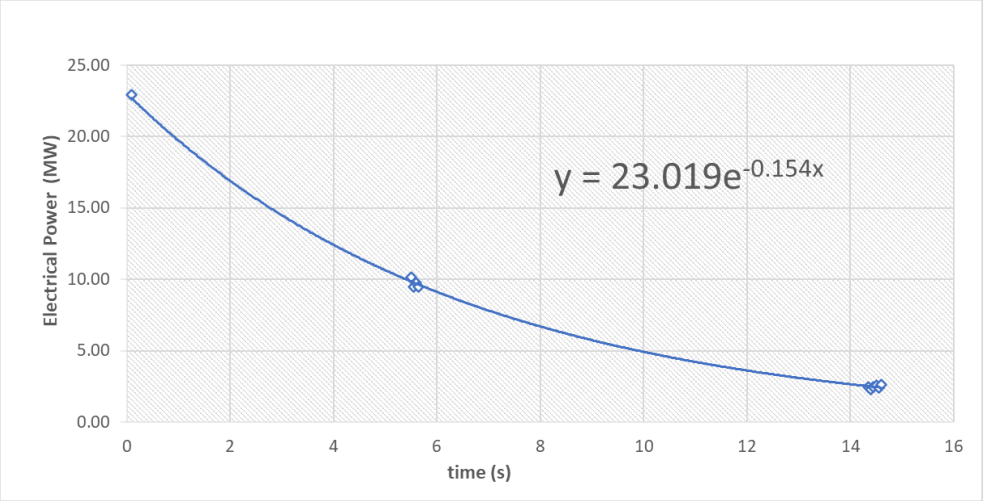

Figure A-2
Plot of the arc power for a generator-fed HEAF event (December 2020).

This exponential profile of the actual current compared favorably to the theoretical profile developed by Madjidian et al. [27] for a typical generator-fed fault. The profile comparison between the actual HEAF event and theoretical curve provided confidence that the actual decaying current can be used as a surrogate for all generator-fed faults regardless of the site-specific electrical distribution characteristics. This assumption is necessary due to the complex nature of the generator-fed faults. Site-specific prediction of the decaying fault current is extremely complex and would require additional electrical analysis. The decaying current curve and the associated arc energy calculated above is used in FDS to simulate generator-fed HEAFs.

Generator-fed HEAF events may also be preceded by a constant-current “stiff” portion that simulates the delay time overcurrent protective devices to sense the fault and trip the generator for transformer protection. The range of the constant-current portion is 0 to 5 s as discussed in

Section A.2.1 for UAT protection. The profile consists of the constant power for the first 0 to 5 s, then transitions to a “decaying” power for the next 15 s. Figure A-3 through Figure A-5 show the power profiles modeled in FDS for generator-fed HEAF events.

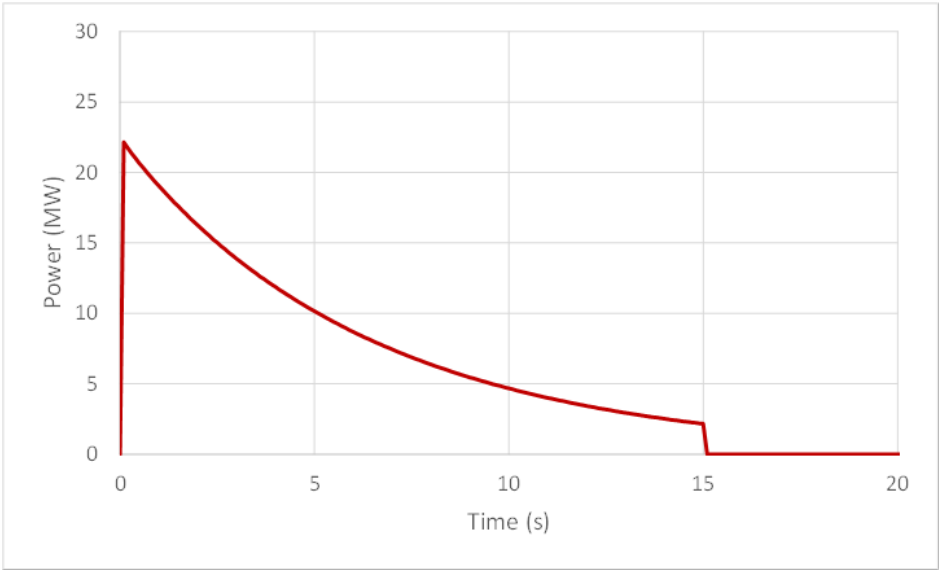

Figure A-3
Power curve for a 0 s stiff and 15 s decay HEAF

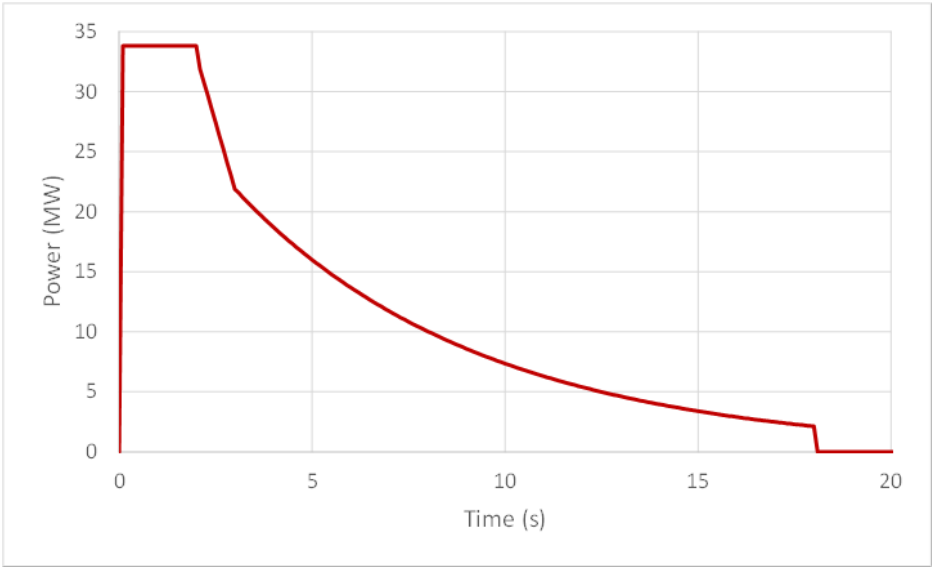

Figure A-4
Power curve for a 3 s stiff and 15 s decay HEAF

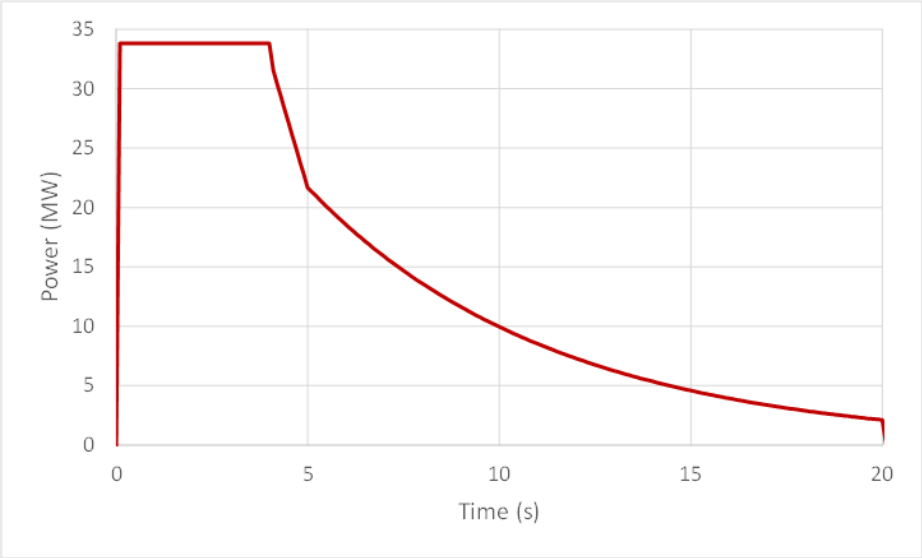

Figure A-5
Power curve for a 5 s stiff and 15 s decay HEAF

A.3 Arc Energy Profiles for Low Voltage Switchgear

Table A-3 shows that the HEAF events that occurred in low-voltage equipment (bus ducts and switchgear). Only FEDB 50935 reported the actual arcing fault current, which consisted of a single-phase arcing fault that lasted for approximately 41 s. This fault current fluctuated significantly over the duration of the event as seen in Figure A-6.

Table A-3
Low voltage HEAF events with fault currents

Event ID	Date	HEAF Location	Fault Current
434	8/2/1984	SWGR	Unknown
50935	6/7/2011	SWGR	Varied between 200 A to 6,000 A
50926	2/12/2011	NSBD	Unknown

Analysis of data from FEDB 50935 resulted in determining the approximate arc power on the secondary side of the transformer feeding the fault is shown in Figure A-6. The current is derived from the power assuming an arc voltage of 375 V_{L-L} (as discussed in Section A.1). The event shows two phases of variable current, with the first phase having a higher average overall current, and the second phase current varying from a few hundred amps (almost self-extinguishing) to 6 kA. This resulted in an overall arcing energy of approximately 90 MJ as seen in Figure A-6.

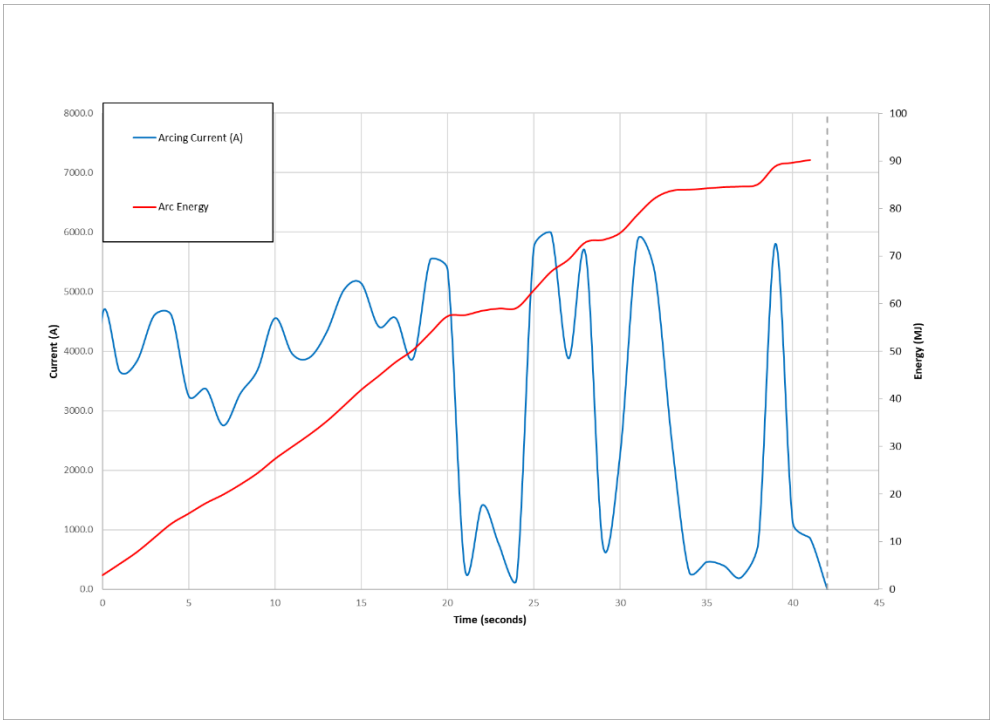

Figure A-6
FEDB 50935 energy profile

Figure A-7 shows in red the values used to approximate the current profile in the FDS simulations of the HEAF event. This approximation is necessary in order to minimize the complexity of the FDS input. The distinct phases of the event are captured by maintaining the midpoint of maximum peak current seen in the event (approximately 5.85 kA) for the first 20 s and reduced it to 2.75 kA for the next 21 s.

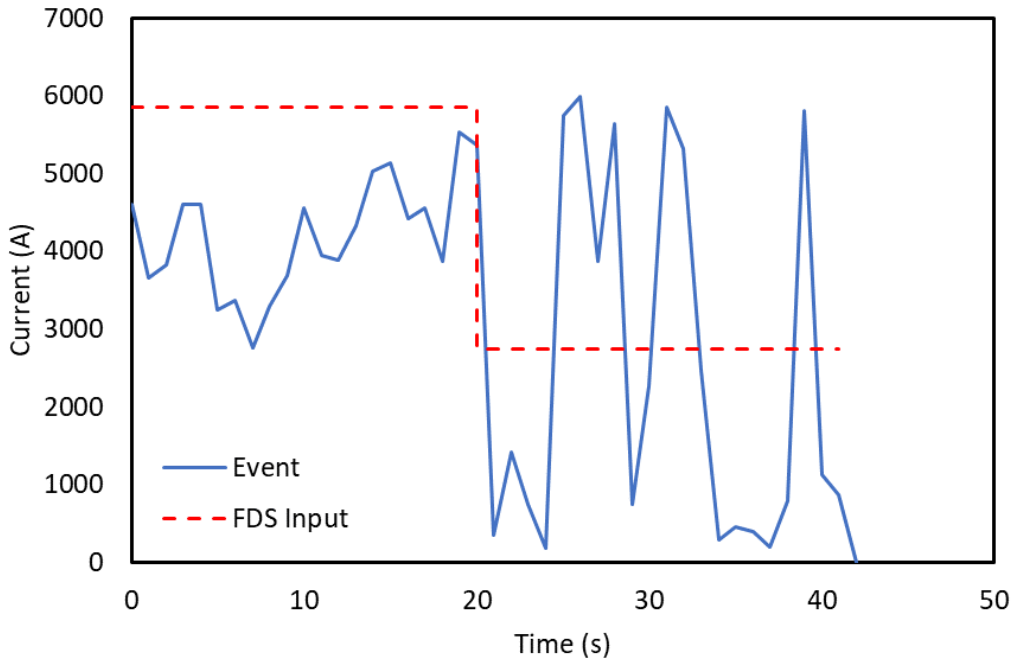

Figure A-7
Low voltage HEAF current profile

The profile in Figure A-7 represents a long-duration fault at a low fault current. The potential of a higher fault current representing a bolted fault (similar to what has been observed in medium-voltage switchgear HEAF events) is investigated to provide confidence that using the arc energy from this event is an appropriate surrogate for all LV SWGR HEAFs and associated ZOIs.

To determine if 90 MJ total arc energy from FEDB 50935 is an appropriate level for ZOI determination, several protection and coordination calculations from U.S. nuclear plants were reviewed for various load center transformer sizes. The system voltage was 480 V_{ac} and, in calculating the arcing fault energy, an arc voltage of 375 V_{L-L} is assumed. Time current characteristic (TCC) curves from the protection coordination calculations are reviewed to determine the expected fault clearing time of the load center transformer's primary side (MV SWGR) circuit breaker time overcurrent (51) relay to clear a fault on the 480 V_{ac} load center assuming the load center bus supply circuit breaker failed (stuck closed). This is done for both the zero-impedance (bolted fault) and the lower bound arcing fault current. The lower bound arcing fault current is calculated following the methodology of IEEE Standard 1584-2018 [33] in calculating the minimum arcing current. Table A-4 documents the expected energy given the fault clearing time (FCT) at the available arcing fault current and minimum fault current.

Table A-4
Sampling of low-voltage fault clearing times and fault energies

Transformer Size (kVA)	Available Fault Current (kA)	FCT at Bolted Fault (s)	Energy at Bolted Fault (MJ)	Lower Bound Arcing Fault Current (IEEE) (kA)	FCT at Lower Bound Arcing Fault (s)	Energy at Lower Bound Arcing Fault (MJ)
2,000	50	0.6	18	27	0.9	15
1,500	46	0.5	14	25	0.6	10
2,500	46	0.5	16	25	1.2	20
1,500	46	0.5	16	25	0.9	14
1,000	15	1.6	16	10	2.2	14
300	8	2.4	12	5	4.5	14
1,000	15	1.4	14	10	1.7	11
1,000	15	1.6	16	10	2.0	12
300	8	2.4	12	5	5.0	16
1,000	14	1.4	13	9	1.9	11
1,000	15	1.4	14	10	1.9	12
1,000	15	2.0	20	10	2.6	16
1,000	15	1.3	13	10	2.0	12
1,000	15	1.3	13	10	1.7	11
300	8	2.3	11	5	4.2	13
300	8	2.1	10	5	5.0	15
1,000	15	1.8	18	10	2.4	15
1,000	15	2.5	24	10	3.6	22
300	8	1.9	10	5	2.5	8
1,250	28	2.5	45	17	5.0	56
1,500	35	1.7	38	21	3.6	49
500	11	1.3	10	7	3.0	13
300	8	0.4	2	5	0.9	3
500	15	0.3	3	9	0.5	3
2,500	52	2.7	91	27	7.5	133

Transformer Size (kVA)	Available Fault Current (kA)	FCT at Bolted Fault (s)	Energy at Bolted Fault (MJ)	Lower Bound Arcing Fault Current (IEEE) (kA)	FCT at Lower Bound Arcing Fault (s)	Energy at Lower Bound Arcing Fault (MJ)
1,500	32	1.9	39	19	3.7	46
1,500	32	0.4	8	19	1.0	13
500	11	0.5	2	7	1.5	7
750	16	0.5	5	10	3.0	19
500	11	0.5	3	7	1.5	7
500	6	0.1	0	4	0.4	1
1,000	15	1.9	19	10	2.6	17
1,500	22	1.6	23	14	2.3	21
1,500	21	1.7	22	13	2.4	20
1,500	21	1.6	22	14	2.6	23
1,500	20	1.7	22	13	3.2	26
1,500	21	1.2	17	14	3.5	31
1,500	21	1.2	17	13	3.5	30
750	13	1.7	14	8	2.4	13

From the results of Table A-4, only one instance of a fault occurring at the lower bounding fault current is not bounded by the 90 MJ FEDB 50935.

In the FDS simulations, 90 MJ is modeled as a fixed power of 3.8 MW over the first 20 s followed by 21 s of 1.8 MW as shown in Figure A-8. Transitions of 0.2 s were used at the start, current change, and end of the arc.

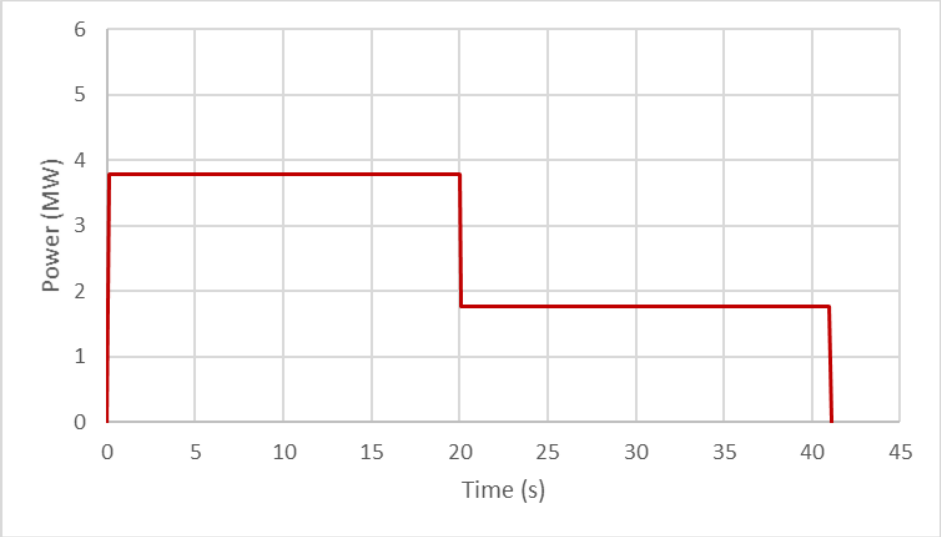

Figure A-8
Low voltage HEAF power profile

B
DETAILED FDS RESULTS

This appendix provides plots of the maximum exposure as a function of distance for each of the simulations listed in Section 5.2. The distance is measured from the face of the enclosure. The exposure, shown on a log scale, is the total exposure over the duration of the FDS simulations (arcing fault duration plus 8 s (see Section 3.1)). Each plot shows the exposed faces of the enclosure with each face in a separate color. The solid line is the bias adjusted FDS prediction (see Section 4.1.3). The dashed lines are the 95% confidence interval. The two purple dot-dot-dash lines are 15 MJ/m² and 30 MJ/m² which are the TP and TS fragility criteria [10].

B.1 Medium Voltage Switchgear

B.1.1 Vertical-Lift Breaker Design

B.1.1.1 Main Bus Bar Compartment

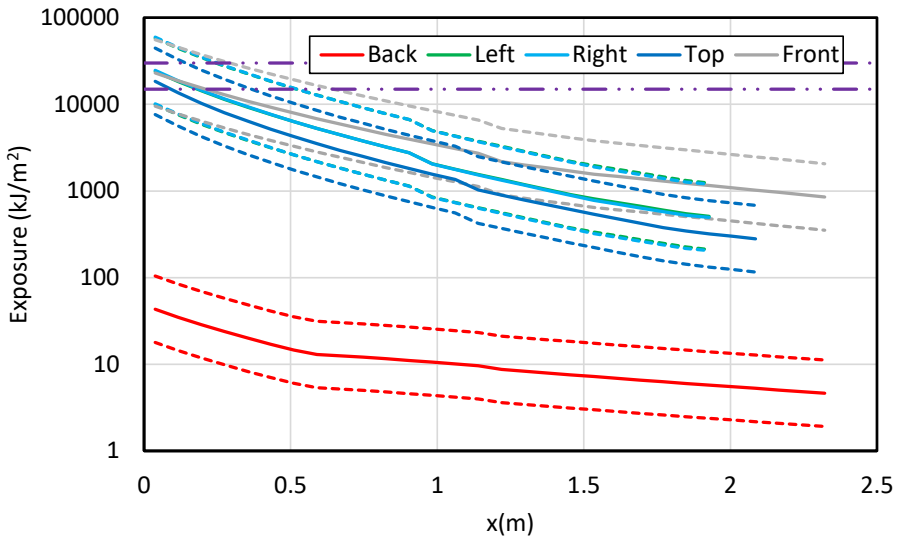

Figure B-1
Results for a vertical-lift breaker MV SWGR with an aluminum bus bar – 68 MJ HEAF located at the main bus bar (FDS Simulation MV-GE-1)

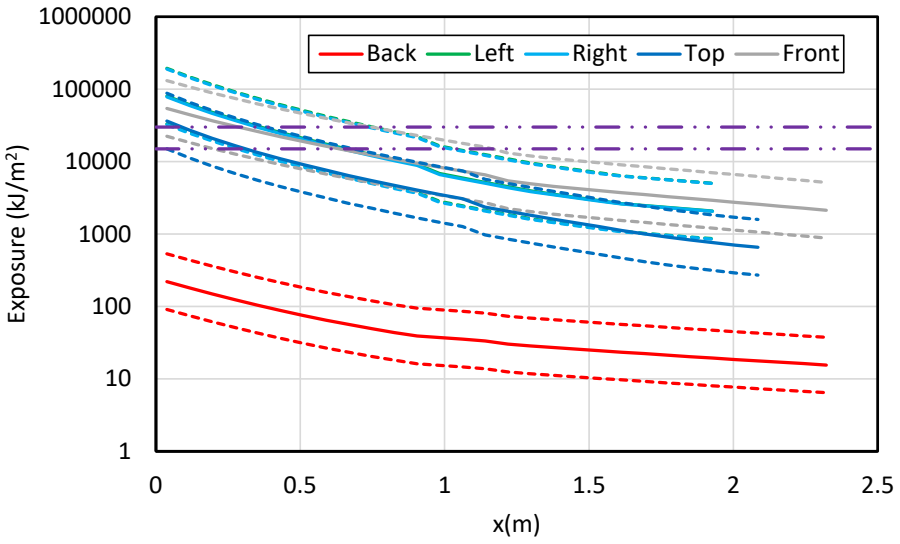

Figure B-2
Results for a vertical-lift breaker MV SWGR with an aluminum bus bar – 135 MJ HEAF located at the main bus bar (FDS Simulation MV-GE-4)

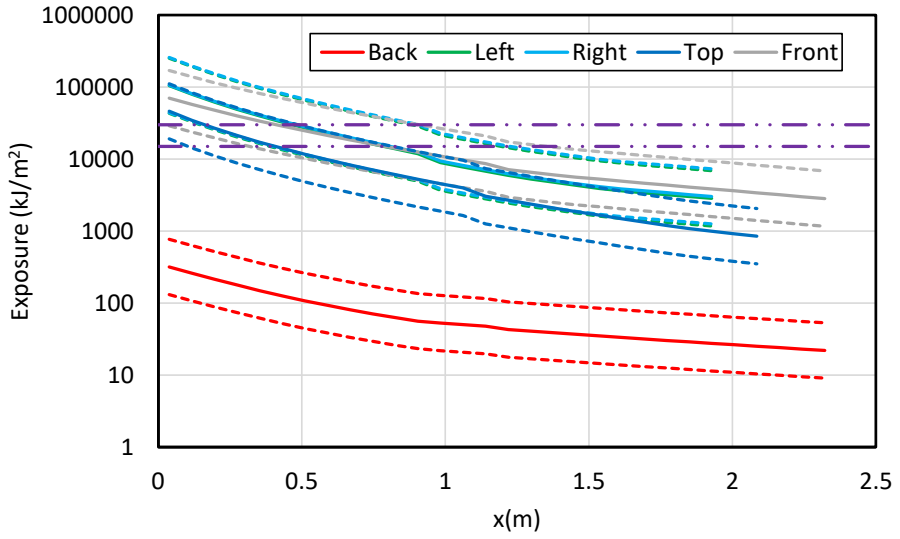

Figure B-3
Results for a vertical-lift breaker MV SWGR with an aluminum bus bar – 169 MJ HEAF located at the main bus bar (FDS Simulation MV-GE-7)

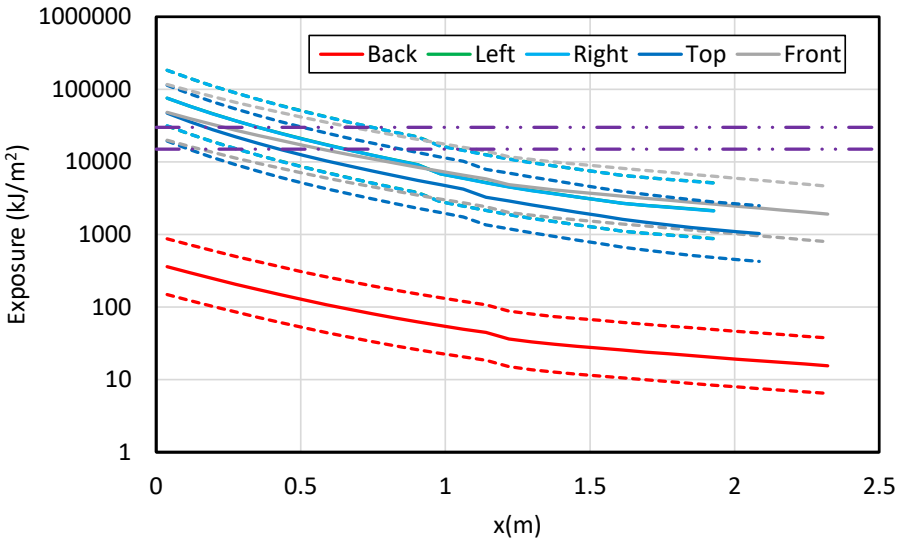

Figure B-4
Results for a vertical-lift breaker MV SWGR with an aluminum bus bar – 131 MJ HEAF located at the main bus bar (FDS Simulation MV-GE-10)

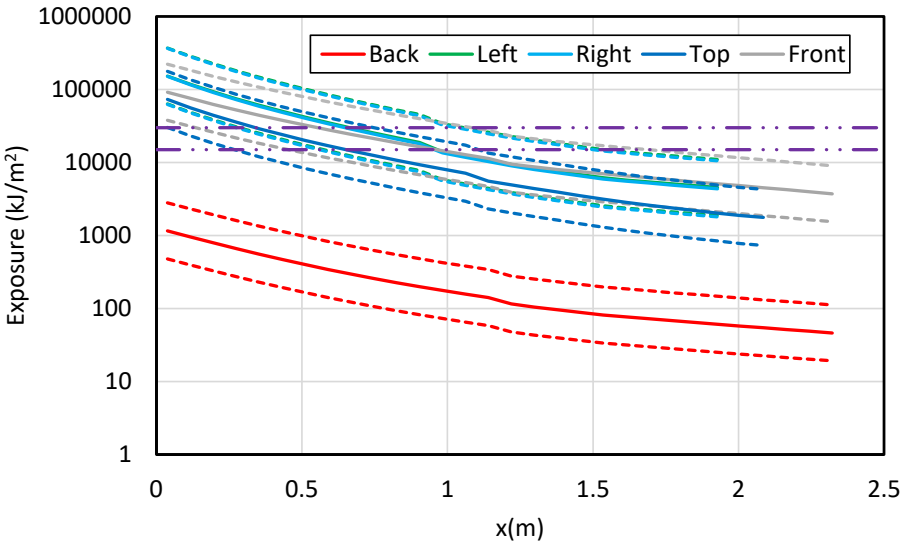

Figure B-5
Results for a vertical-lift breaker MV SWGR with an aluminum bus bar – 226 MJ HEAF located at the main bus bar (FDS Simulation MV-GE-13)

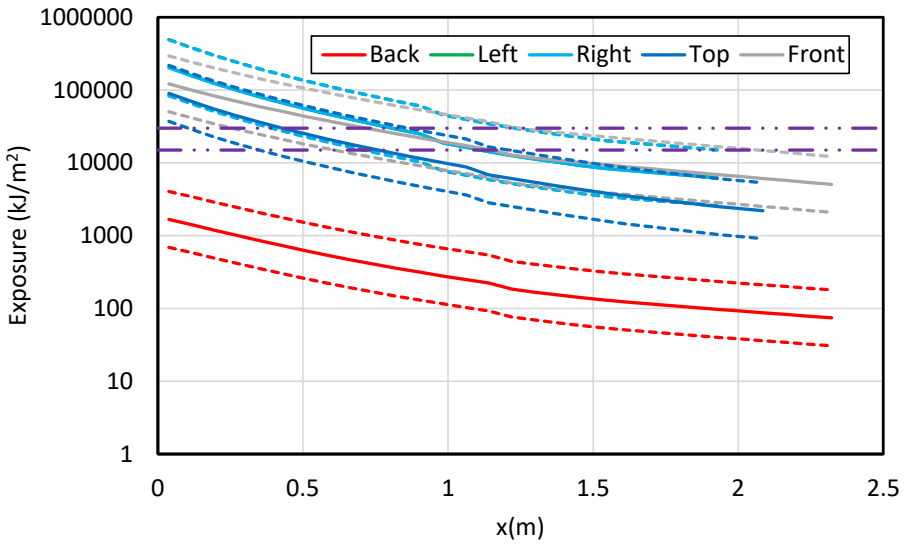

Figure B-6
Results for a vertical-lift breaker MV SWGR with an aluminum bus bar – 293 MJ HEAF located at the main bus bar (FDS Simulation MV-GE-16)

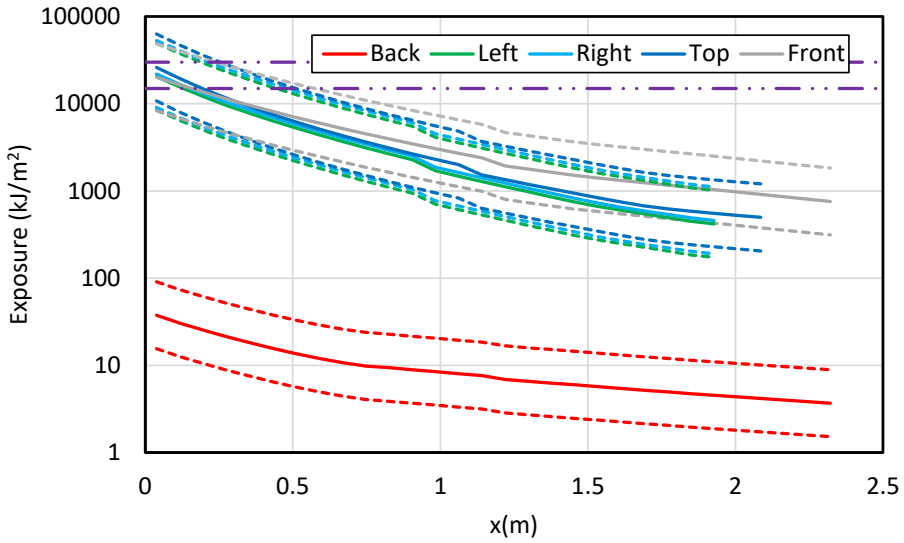

Figure B-7
Results for a vertical-lift breaker MV SWGR with a copper bus bar – 68 MJ HEAF located at the main bus bar (FDS Simulation MV-GE-20)

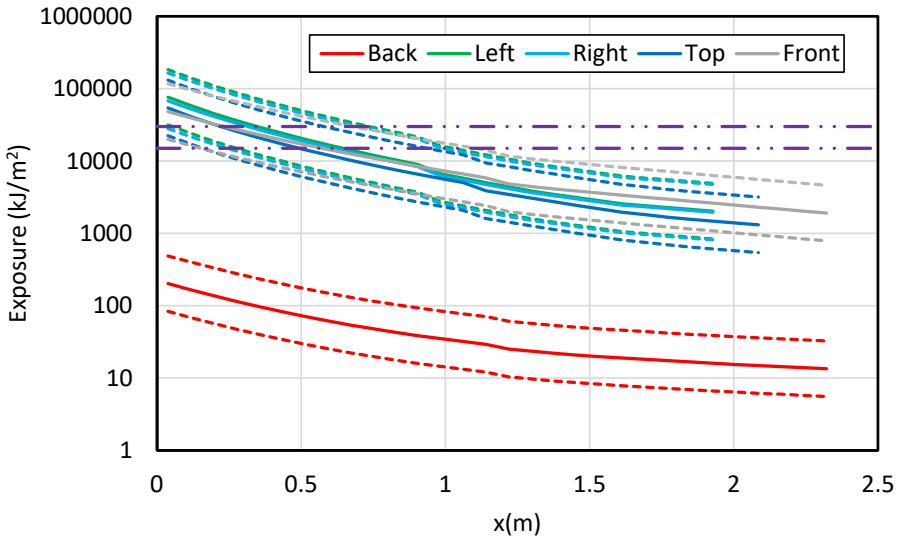

Figure B-8
Results for a vertical-lift breaker MV SWGR with a copper bus bar – 135 MJ HEAF located at the main bus bar (FDS Simulation MV-GE-24)

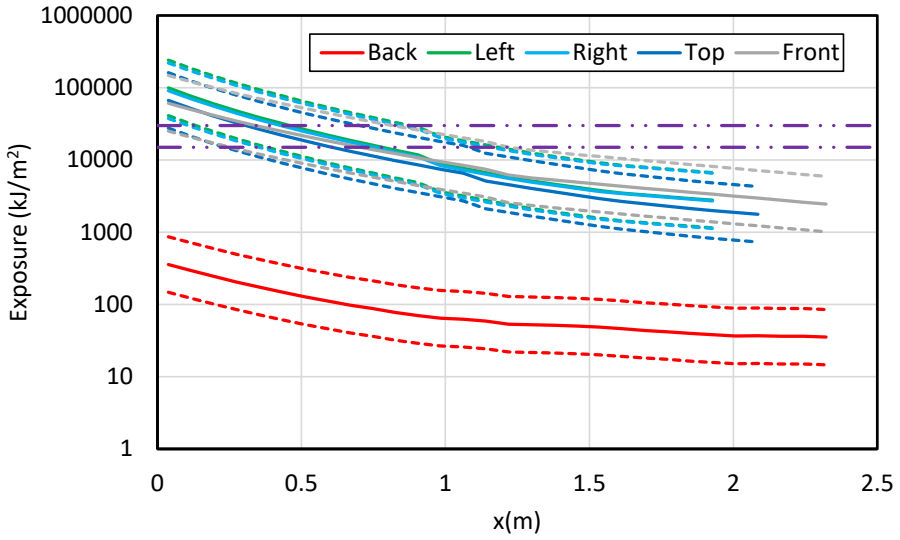

Figure B-9
Results for a vertical-lift breaker MV SWGR with a copper bus bar – 169 MJ HEAF located at the main bus bar (FDS Simulation MV-GE-28)

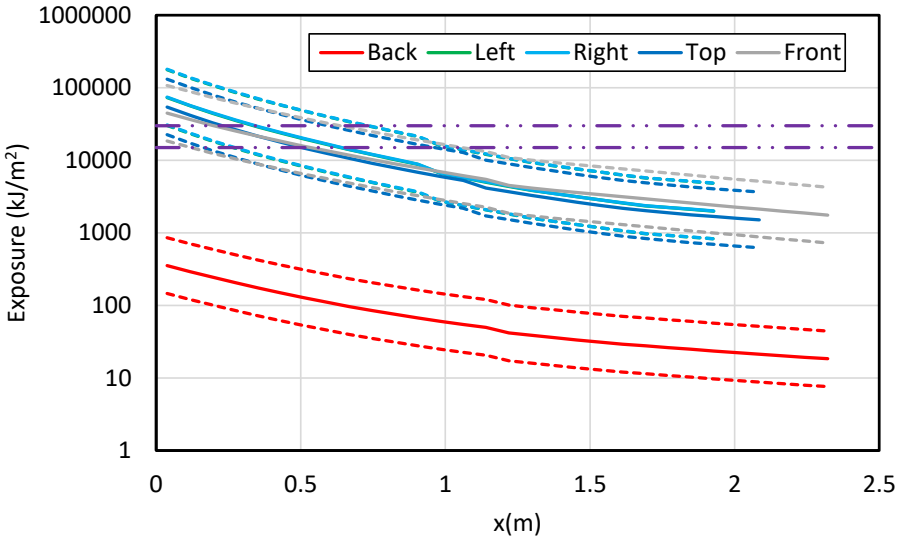

Figure B-10
Results for a vertical-lift breaker MV SWGR with a copper bus bar – 131 MJ HEAF located at the main bus bar (FDS Simulation MV-GE-32)

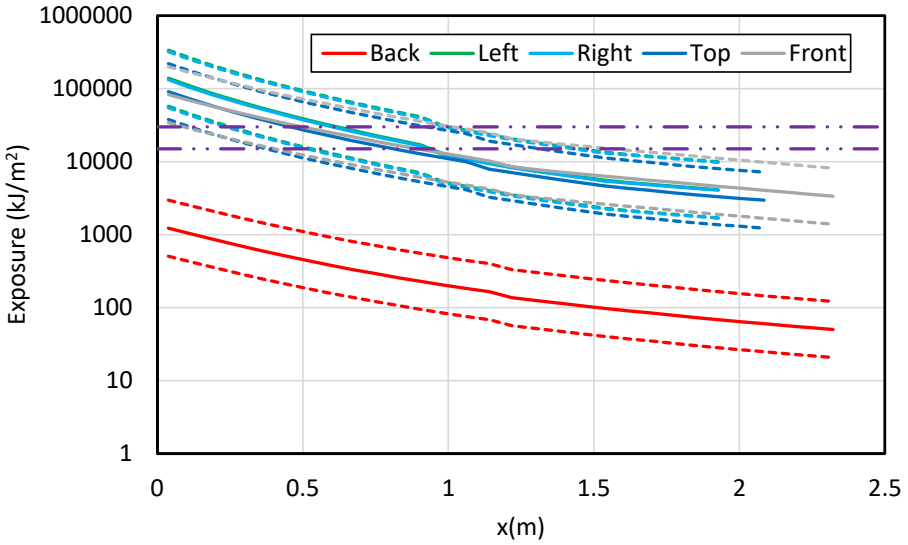

Figure B-11
Results for a vertical-lift breaker MV SWGR with a copper bus bar – 226 MJ HEAF located at the main bus bar (FDS Simulation MV-GE-36)

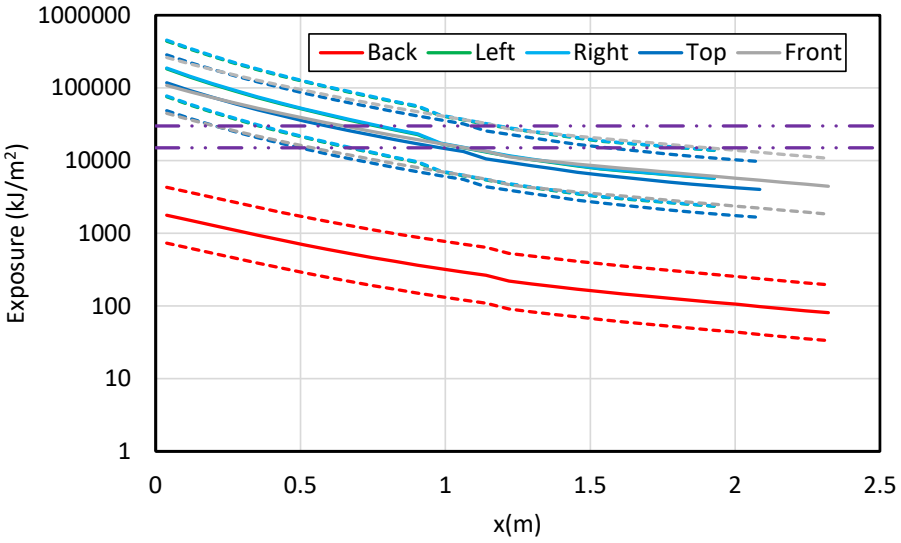

Figure B-12
Results for a vertical-lift breaker MV SWGR with a copper bus bar – 293 MJ HEAF located at the main bus bar (FDS Simulation MV-GE-40)

B.1.1.2 Breaker Stabs

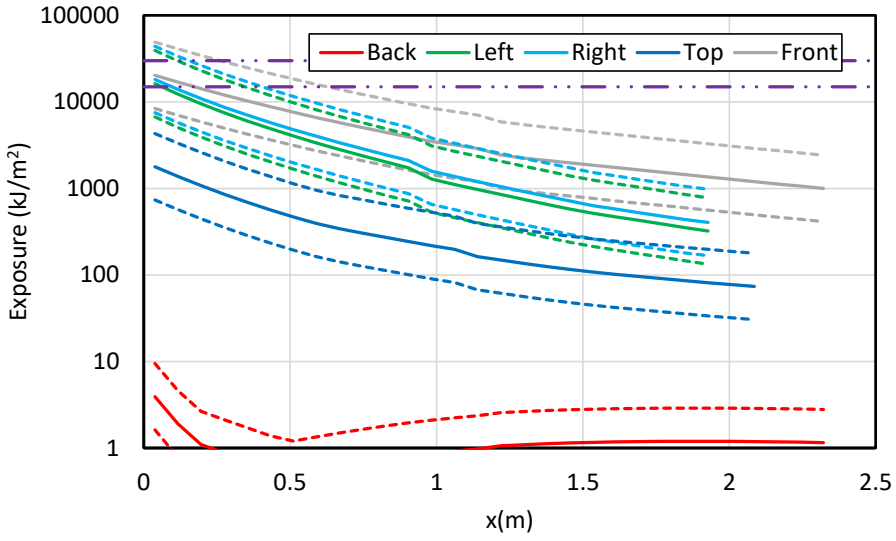

Figure B-13
Results for a vertical-lift breaker MV SWGR with copper electrodes – 68 MJ HEAF located at the breaker stabs (FDS Simulation MV-GE-19)

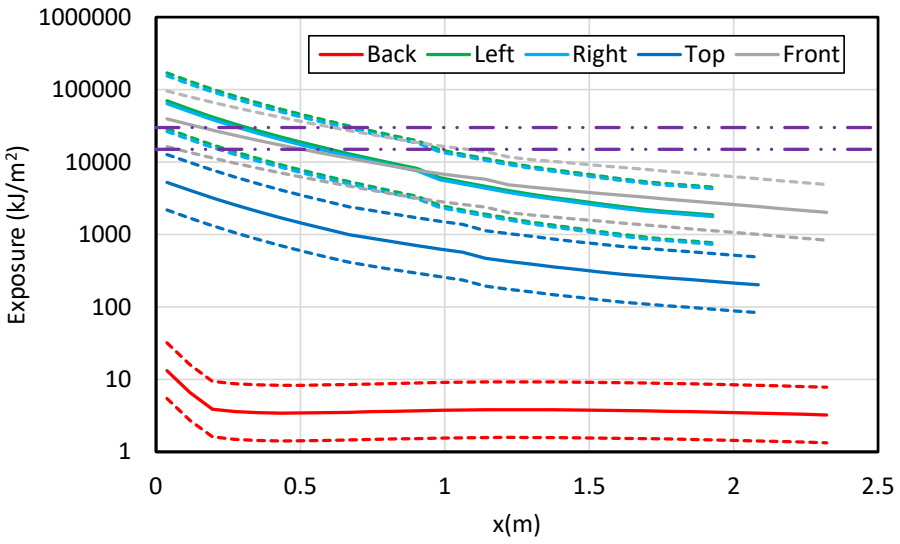

Figure B-14
Results for a vertical-lift breaker MV SWGR with copper electrodes – 135 MJ HEAF located at the breaker stabs (FDS Simulation MV-GE-23)

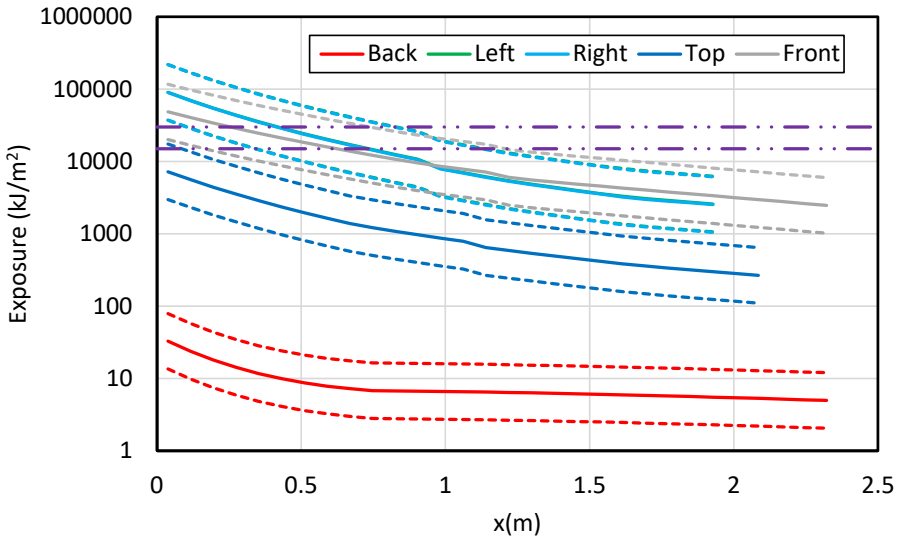

Figure B-15
Results for a vertical-lift breaker MV SWGR with copper electrodes – 169 MJ HEAF located at the breaker stabs (FDS Simulation MV-GE-27)

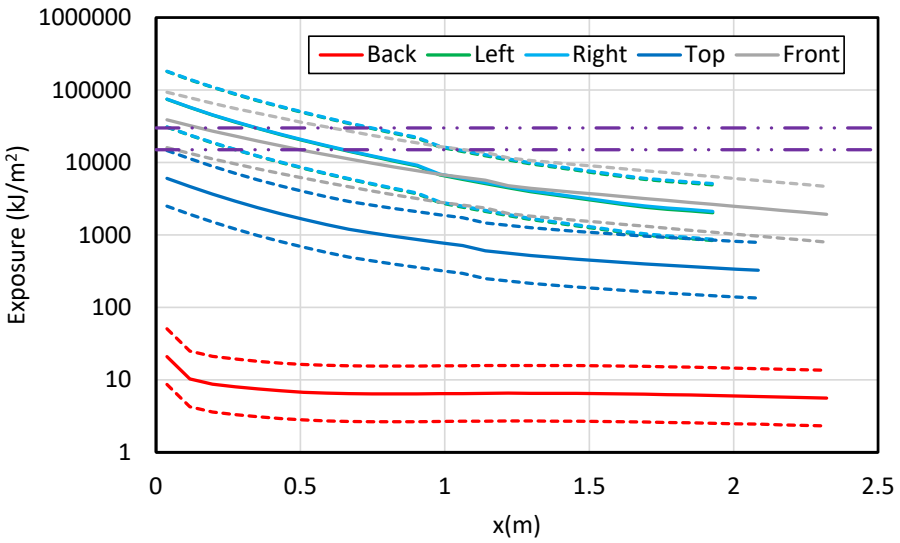

Figure B-16
Results for a vertical-lift breaker MV SWGR with copper electrodes – 131 MJ HEAF located at the breaker stabs (FDS Simulation MV-GE-31)

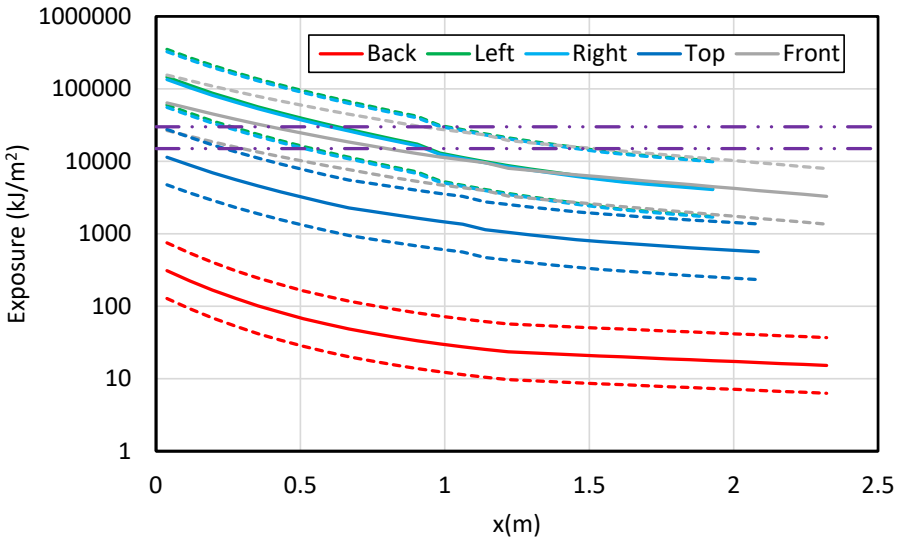

Figure B-17
Results for a vertical-lift breaker MV SWGR with copper electrodes – 226 MJ HEAF located at the breaker stabs (FDS Simulation MV-GE-35)

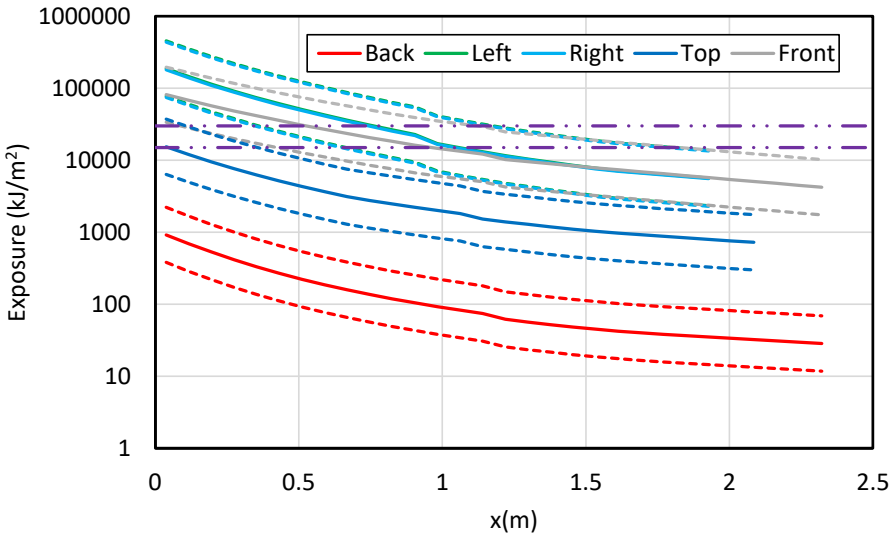

Figure B-18
Results for a vertical-lift breaker MV SWGR with copper electrodes – 293 MJ HEAF located at the breaker stabs (FDS Simulation MV-GE-39)

B.1.1.3 Primary Compartment (PCCBB) Load Configuration

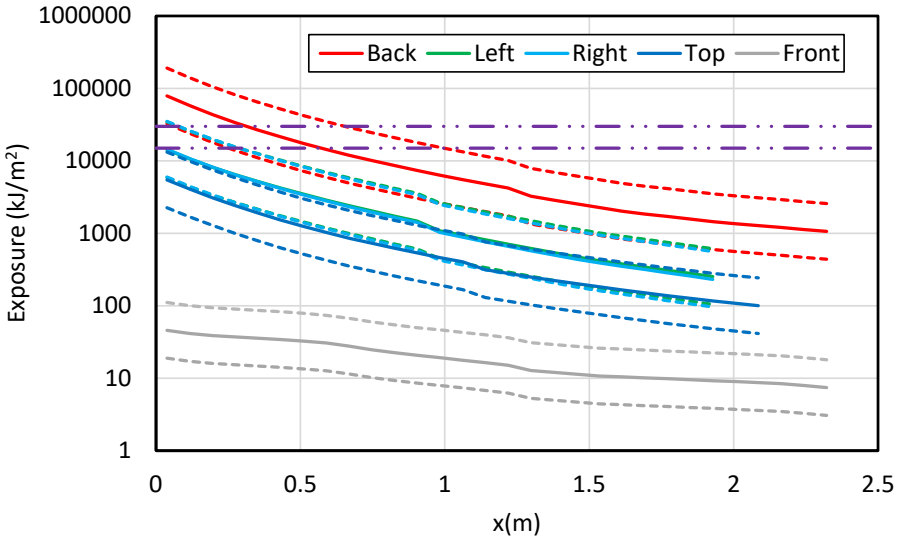

Figure B-19
Results for a vertical-lift breaker MV SWGR with an aluminum bar – 68 MJ HEAF located at the PCCBB (load configuration) (FDS Simulation MV-GE-1) (FDS Simulation MV-GE-2)

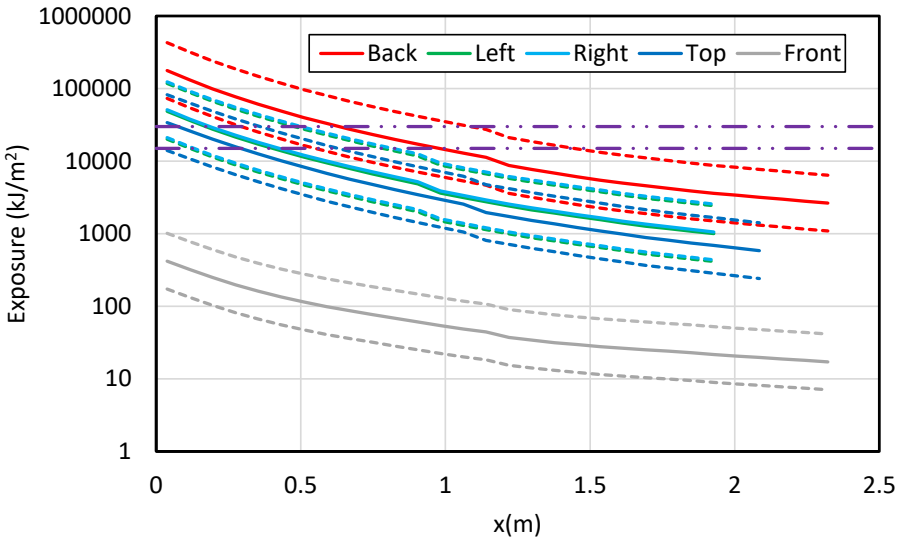

Figure B-20
Results for a vertical-lift breaker MV SWGR with an aluminum bar – 135 MJ HEAF located at the PCCBB (load configuration) (FDS Simulation MV-GE-5)

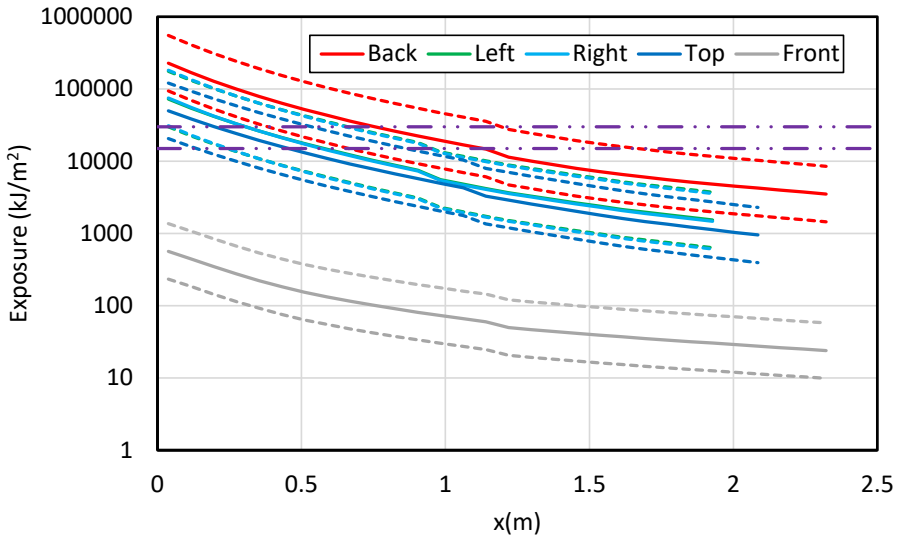

Figure B-21
Results for a vertical-lift breaker MV SWGR with an aluminum bar – 169 MJ HEAF located at the PCCBB (load configuration) (FDS Simulation MV-GE-8)

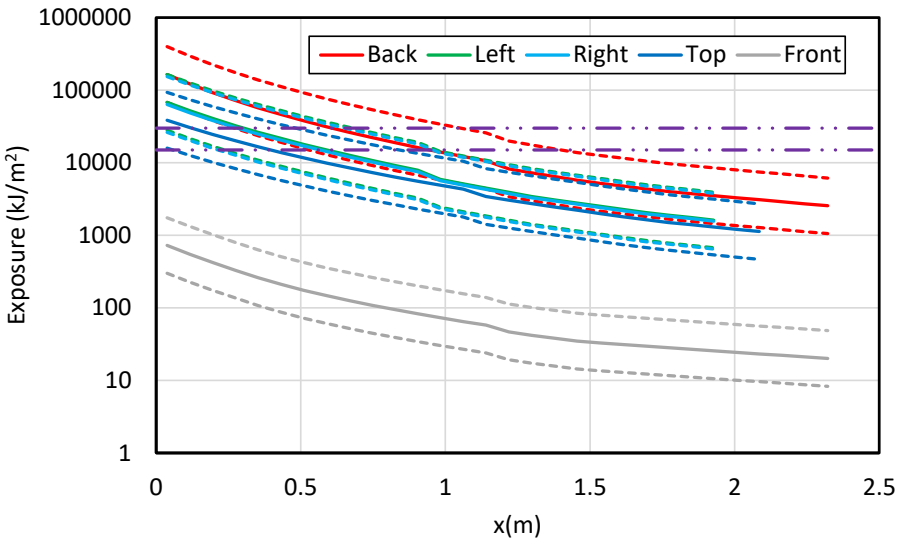

Figure B-22
Results for a vertical-lift breaker MV SWGR with an aluminum bar – 131 MJ HEAF located at the PCCBB (load configuration) (FDS Simulation MV-GE-11)

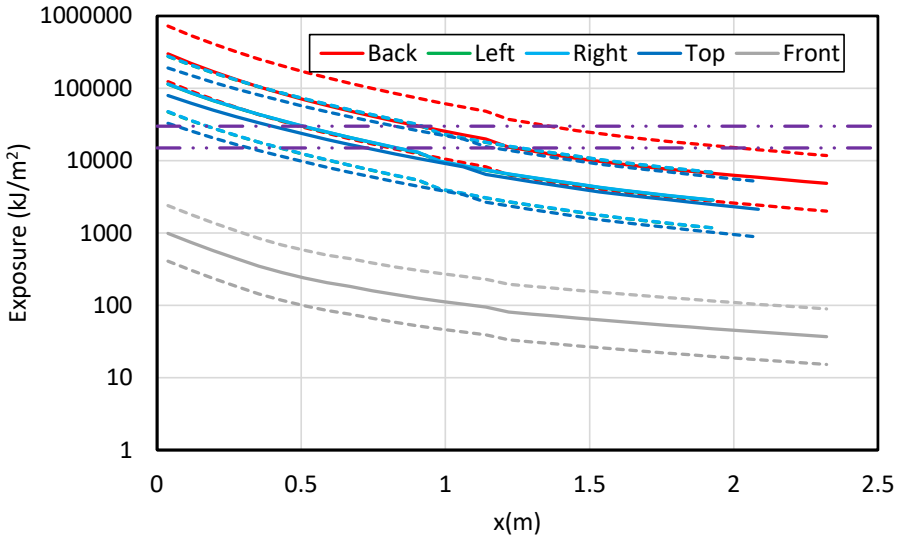

Figure B-23
Results for a vertical-lift breaker MV SWGR with an aluminum bar – 226 MJ HEAF located at the PCCBB (load configuration) (FDS Simulation MV-GE-14)

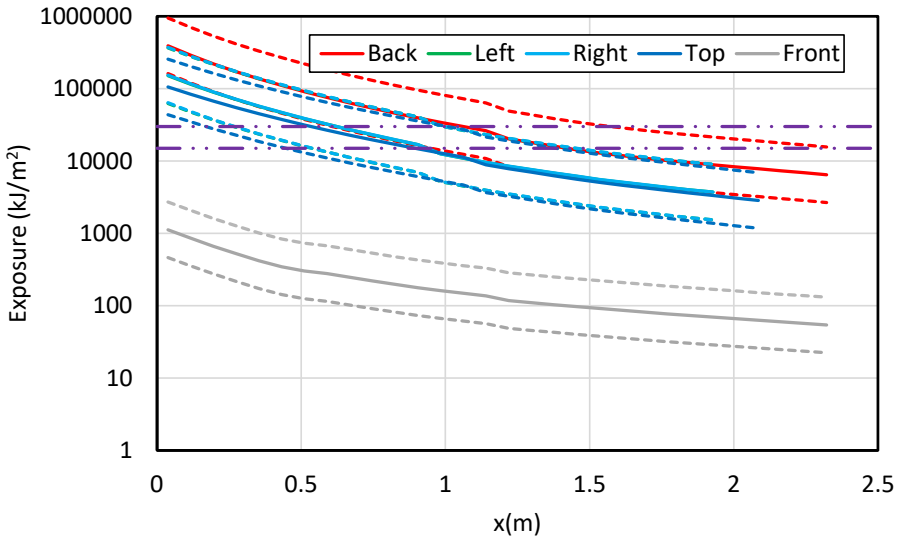

Figure B-24
Results for a vertical-lift breaker MV SWGR with an aluminum bar – 293 MJ HEAF located at the PCCBB (load configuration) (FDS Simulation MV-GE-17)

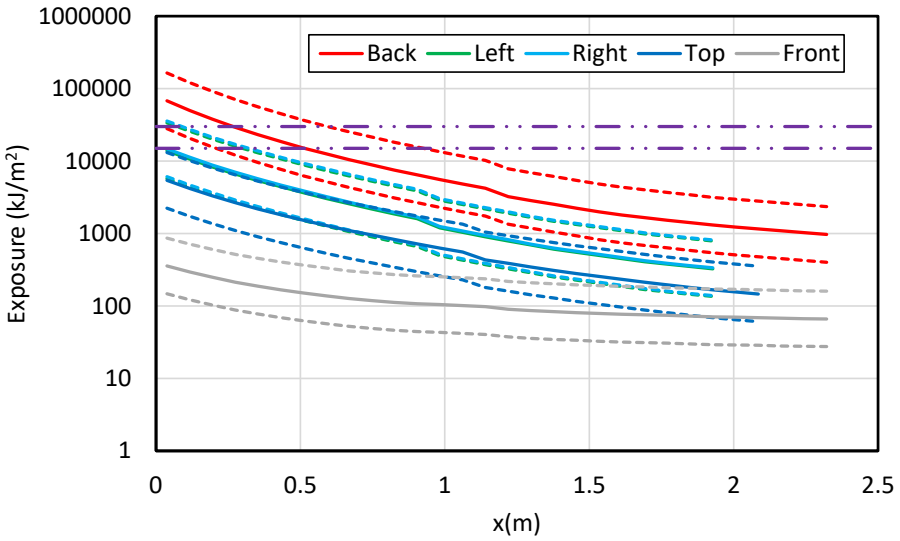

Figure B-25
Results for a vertical-lift breaker MV SWGR with a copper bar – 68 MJ HEAF located at the PCCBB (load configuration) (FDS Simulation MV-GE-21)

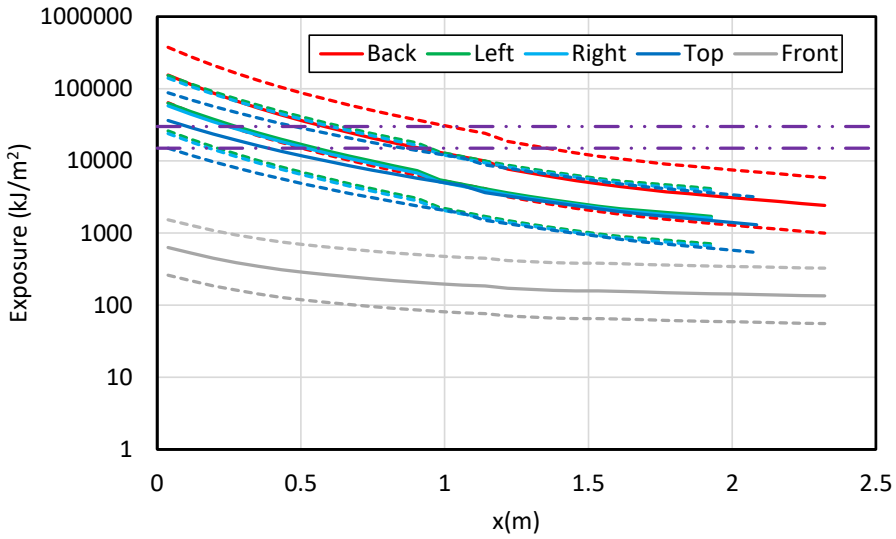

Figure B-26
Results for a vertical-lift breaker MV SWGR with a copper bar – 135 MJ HEAF located at the PCCBB (load configuration) (FDS Simulation MV-GE-25)

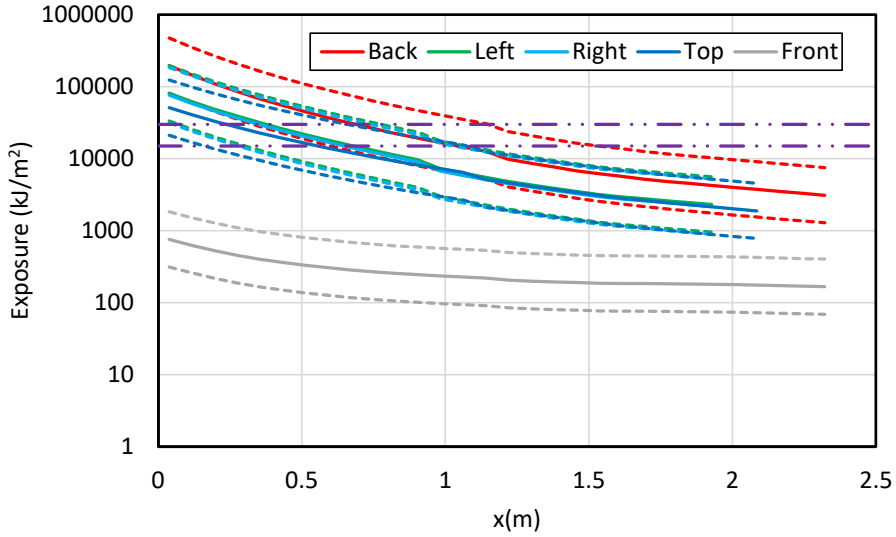

Figure B-27
Results for a vertical-lift breaker MV SWGR with a copper bar – 169 MJ HEAF located at the PCCBB (load configuration) (FDS Simulation MV-GE-29)

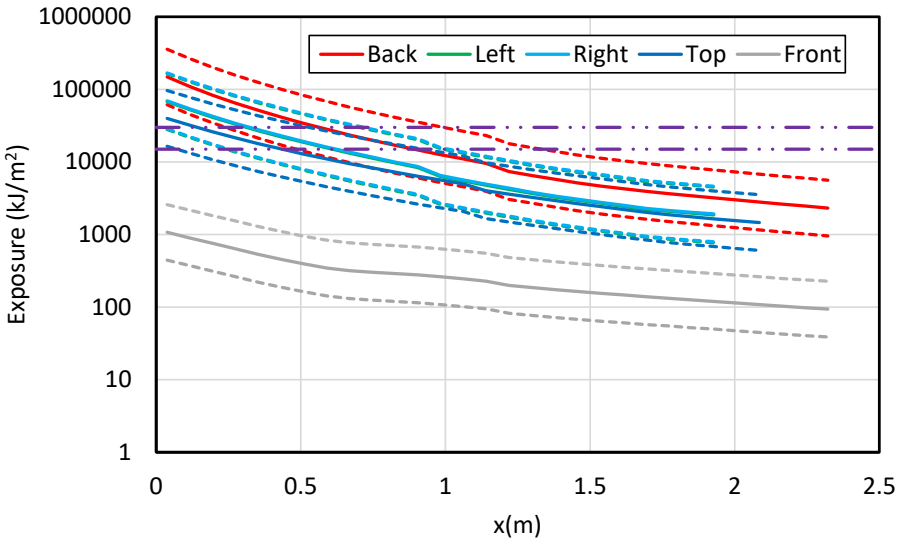

Figure B-28
Results for a vertical-lift breaker MV SWGR with a copper bar – 131 MJ HEAF located at the PCCBB (load configuration) (FDS Simulation MV-GE-33)

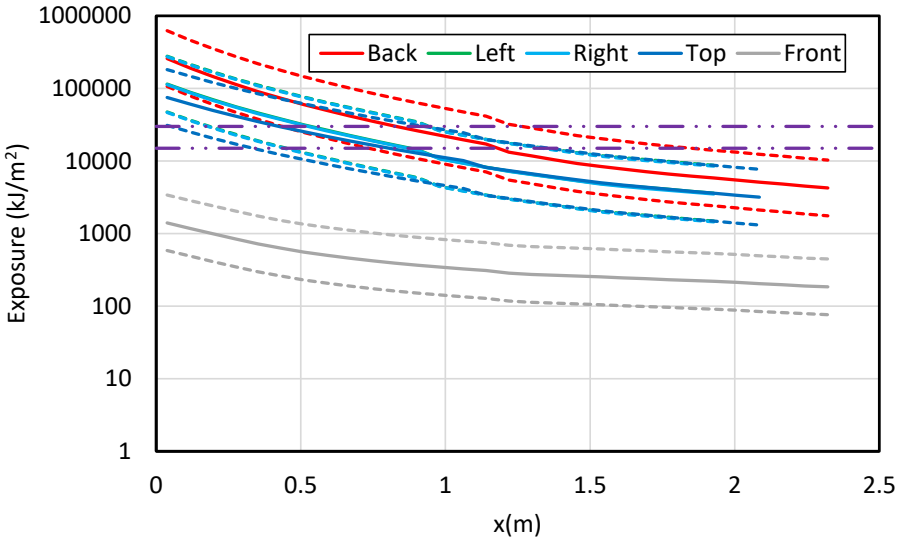

Figure B-29
Results for a vertical-lift breaker MV SWGR with a copper bar – 226 MJ HEAF located at the PCCBB (load configuration) (FDS Simulation MV-GE-37)

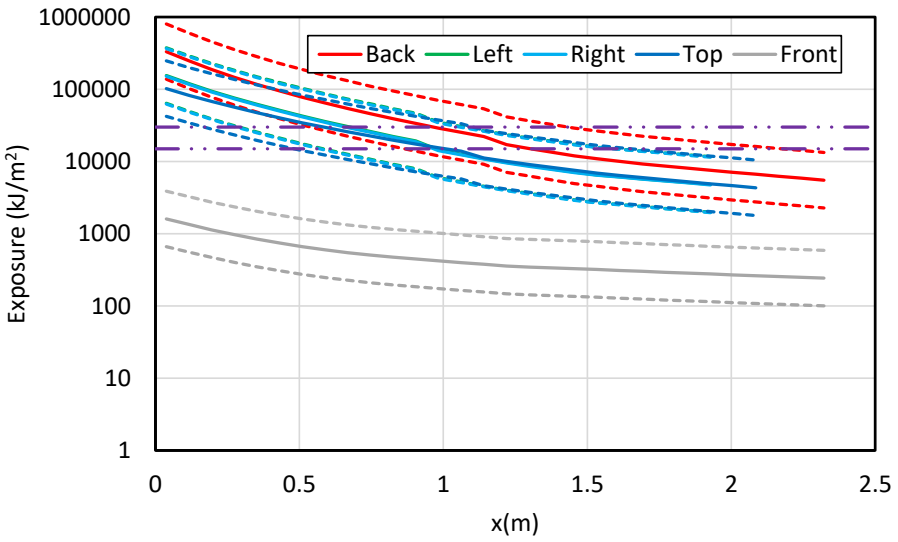

Figure B-30
Results for a vertical-lift breaker MV SWGR with a copper bar – 293 MJ HEAF located at the PCCBB (load configuration) (FDS Simulation MV-GE-41)

B.1.1.4 Primary Compartment Supply Configuration

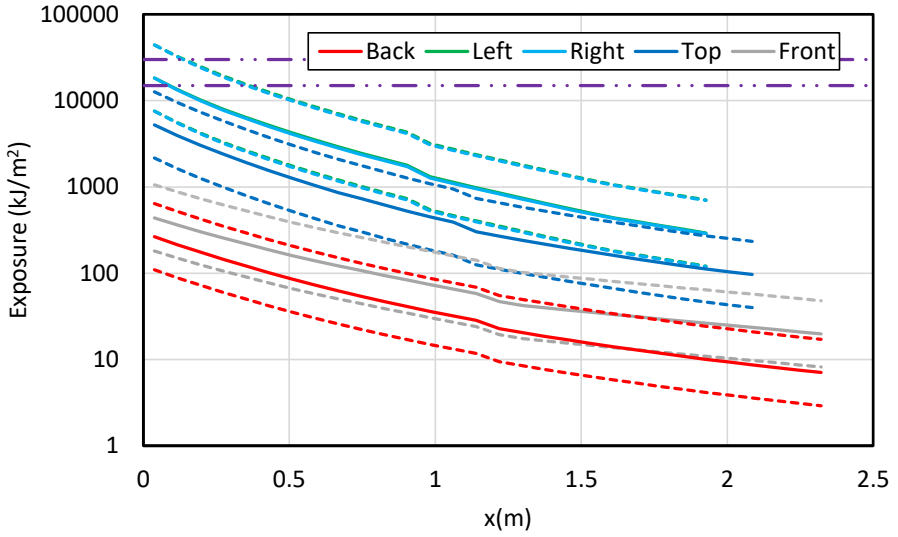

Figure B-31
Results for a vertical-lift breaker MV SWGR with an aluminum bar – 68 MJ HEAF located at the PCCBB (supply configuration) (FDS Simulation MV-GE-3)

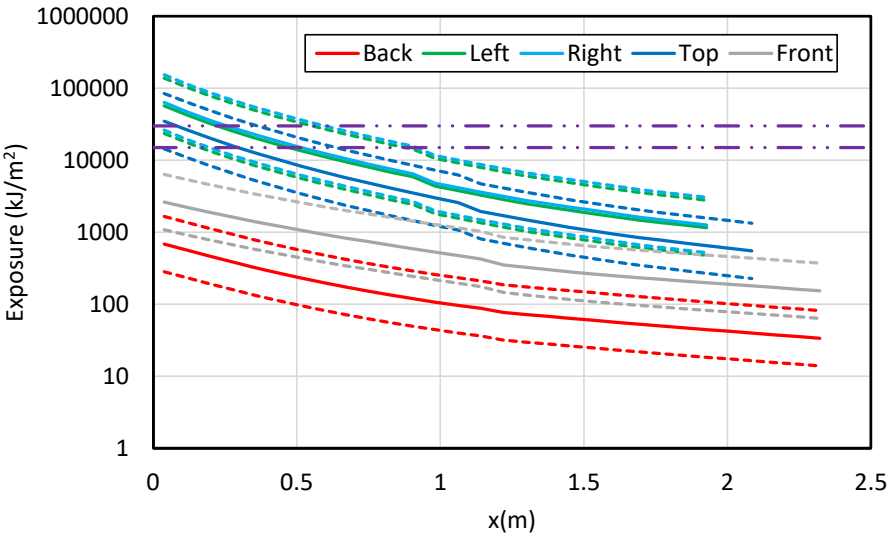

Figure B-32
Results for a vertical-lift breaker MV SWGR with an aluminum bar – 135 MJ HEAF located at the PCCBB (supply configuration) (FDS Simulation MV-GE-6)

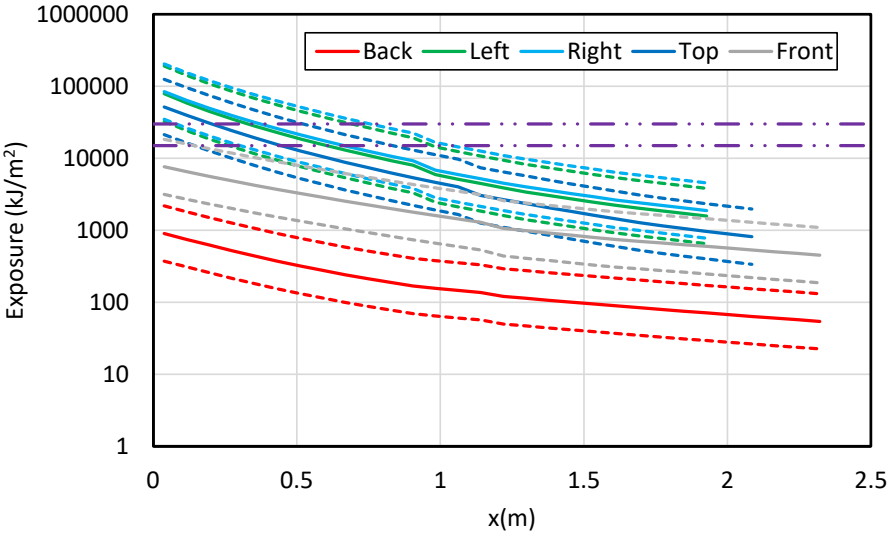

Figure B-33
Results for a vertical-lift breaker MV SWGR with an aluminum bar – 169 MJ HEAF located at the PCCBB (supply configuration) (FDS Simulation MV-GE-9)

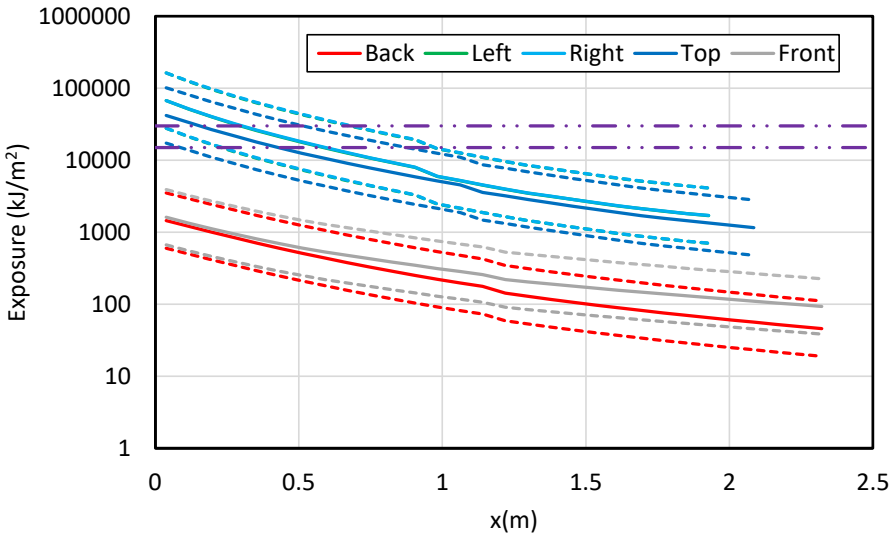

Figure B-34
Results for a vertical-lift breaker MV SWGR with an aluminum bar – 131 MJ HEAF located at the PCCBB (supply configuration) (FDS Simulation MV-GE-12)

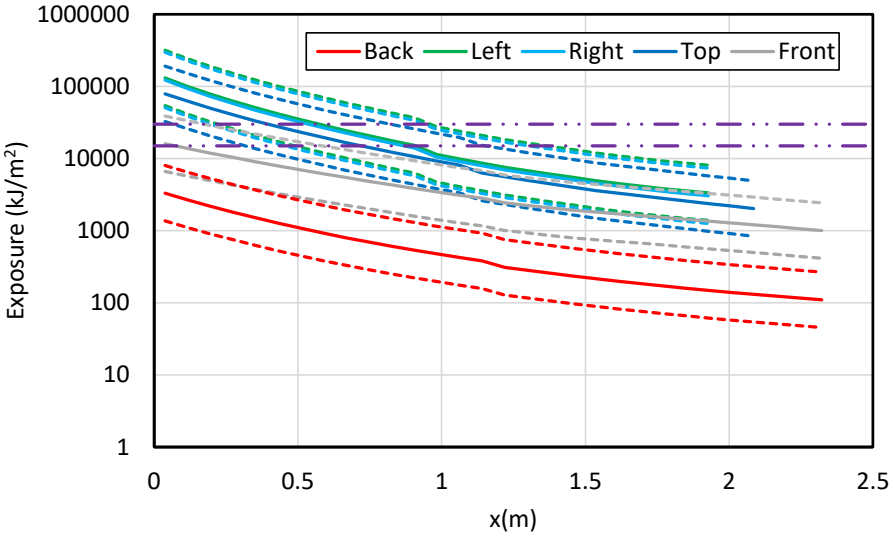

Figure B-35
Results for a vertical-lift breaker MV SWGR with an aluminum bar – 226 MJ HEAF located at the PCCBB (supply configuration) (FDS Simulation MV-GE-15)

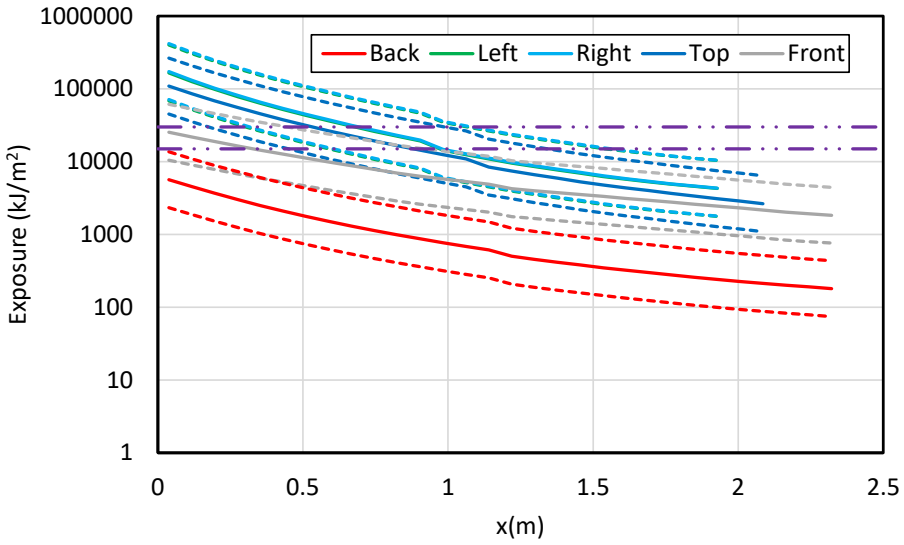

Figure B-36
Results for a vertical-lift breaker MV SWGR with an aluminum bar – 293 MJ HEAF located at the PCCBB (supply configuration) (FDS Simulation MV-GE-18)

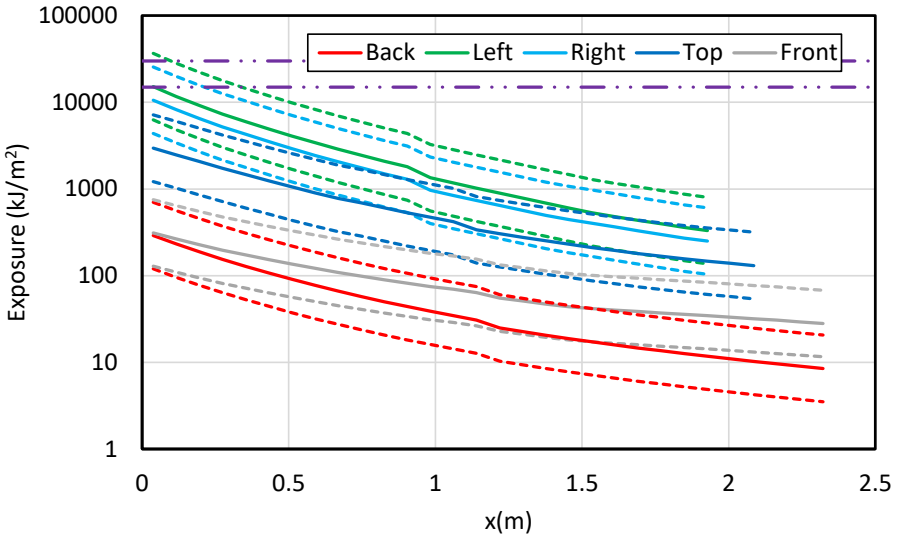

Figure B-37
Results for a vertical-lift breaker MV SWGR with a copper bar – 68 MJ HEAF located at the PCCBB (supply configuration) (FDS Simulation MV-GE-22)

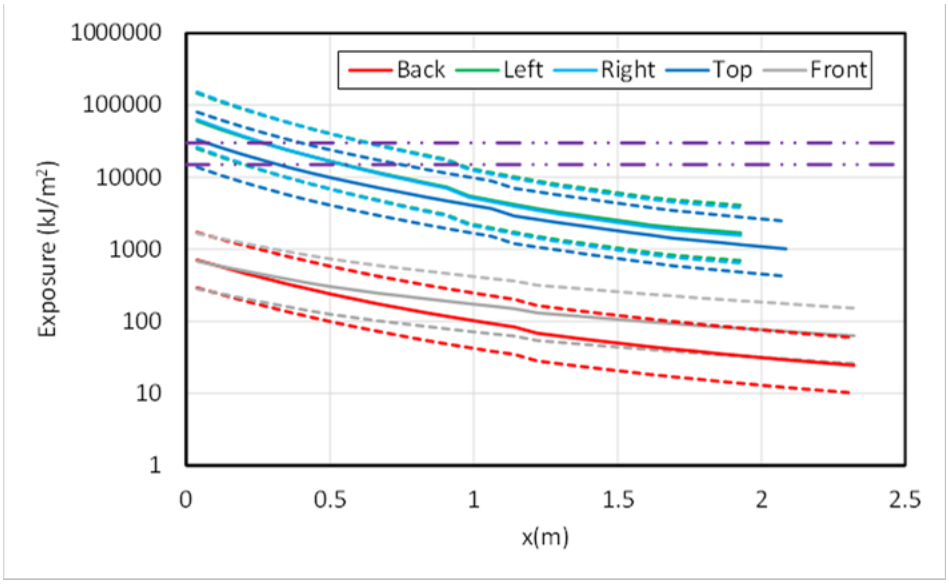

Figure B-38
Results for a vertical-lift breaker MV SWGR with a copper bar – 135 MJ HEAF located at the PCCBB (supply configuration) (FDS Simulation MV-GE-26)

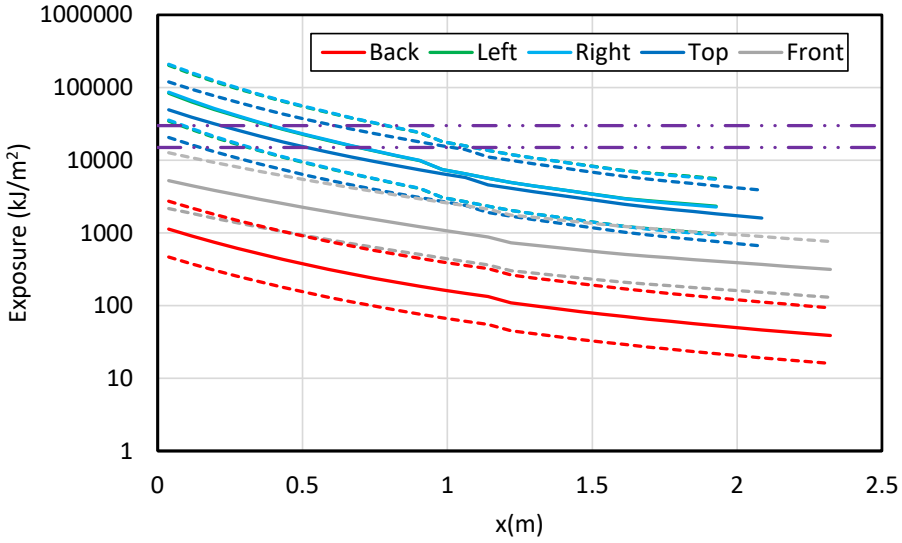

Figure B-39
Results for a vertical-lift breaker MV SWGR with a copper bar – 169 MJ HEAF located at the PCCBB (supply configuration) (FDS Simulation MV-GE-30)

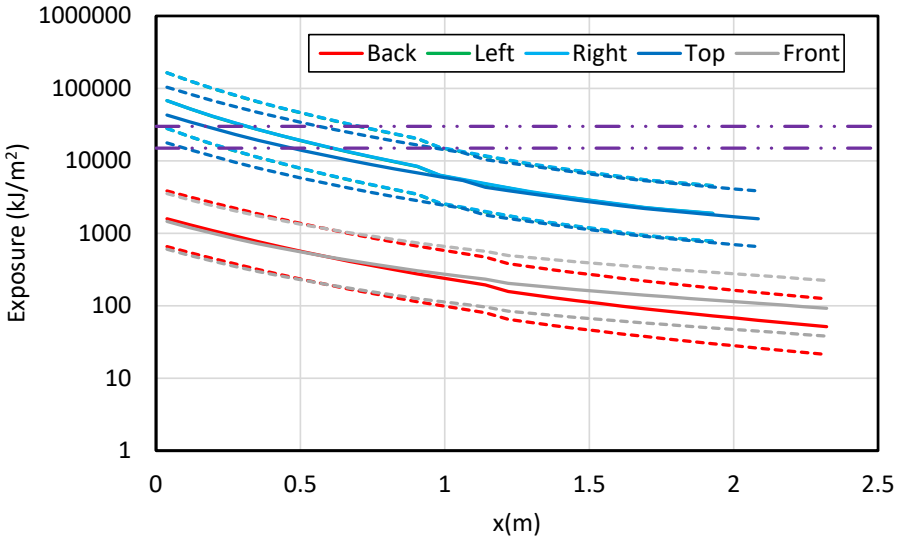

Figure B-40
Results for a vertical-lift breaker MV SWGR with a copper bar – 131 MJ HEAF located at the PCCBB (supply configuration) (FDS Simulation MV-GE-34)

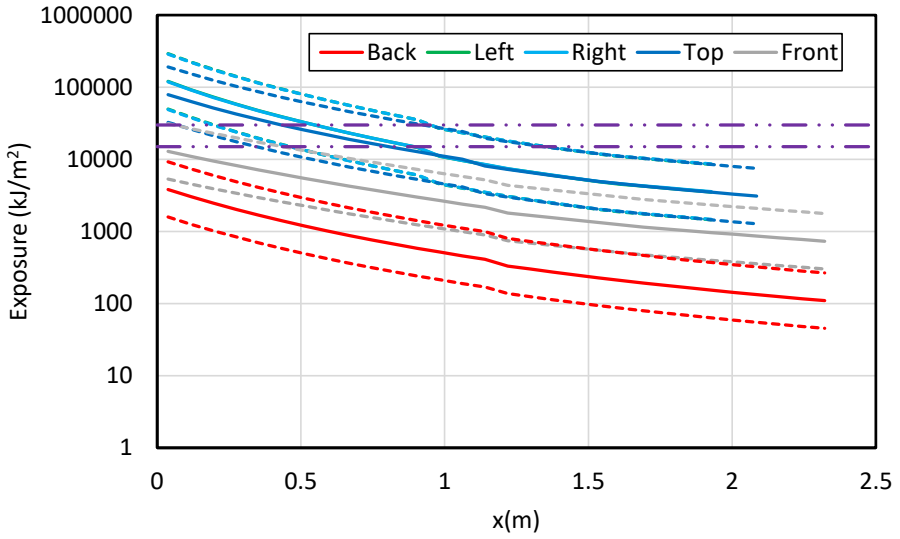

Figure B-41
Results for a vertical-lift breaker MV SWGR with a copper bar – 226 MJ HEAF located at the PCCBB (supply configuration) (FDS Simulation MV-GE-38)

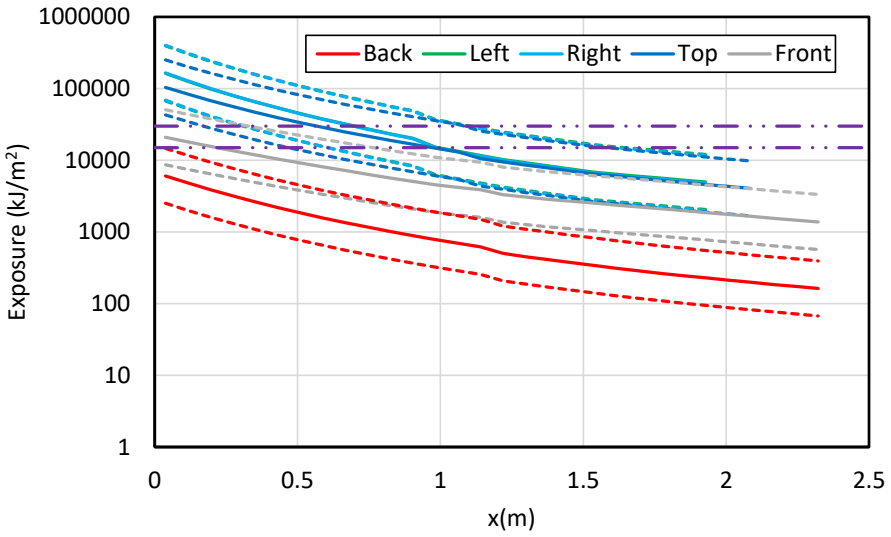

Figure B-42
Results for a vertical-lift breaker MV SWGR with a copper bar – 293 MJ HEAF located at the PCCBB (supply configuration) (FDS Simulation MV-GE-42)

B.1.2 Horizontal Draw-Out Breaker Stabs

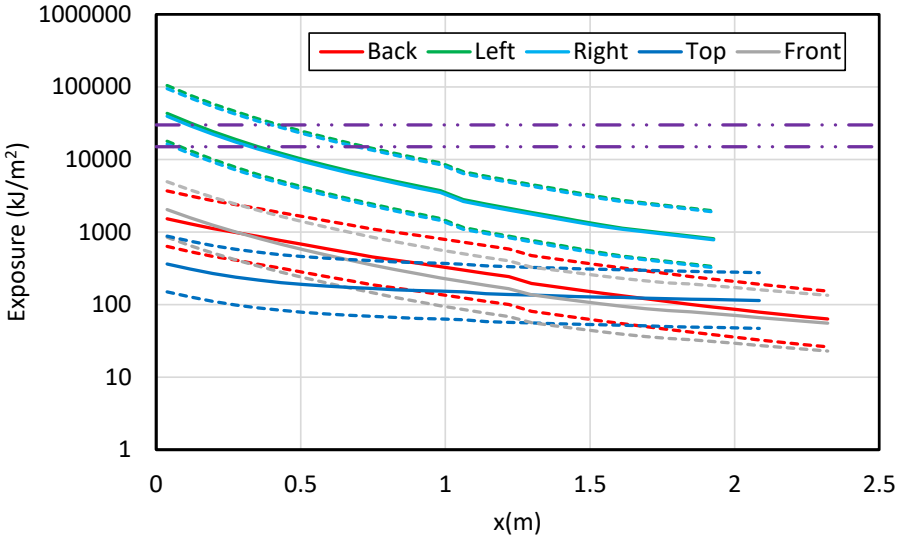

Figure B-43
Results for a horizontal draw-out MV SWGR with copper electrodes – 68 MJ HEAF located at the breaker stabs (FDS Simulation MV-ABB-1)

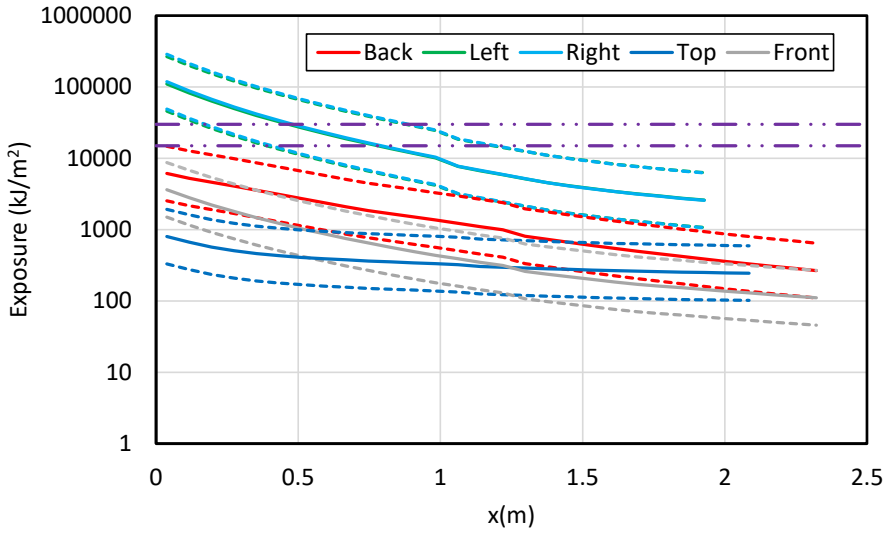

Figure B-44
Results for a horizontal draw-out MV SWGR with copper electrodes – 135 MJ HEAF located at the breaker stabs (FDS Simulation MV-ABB-2)

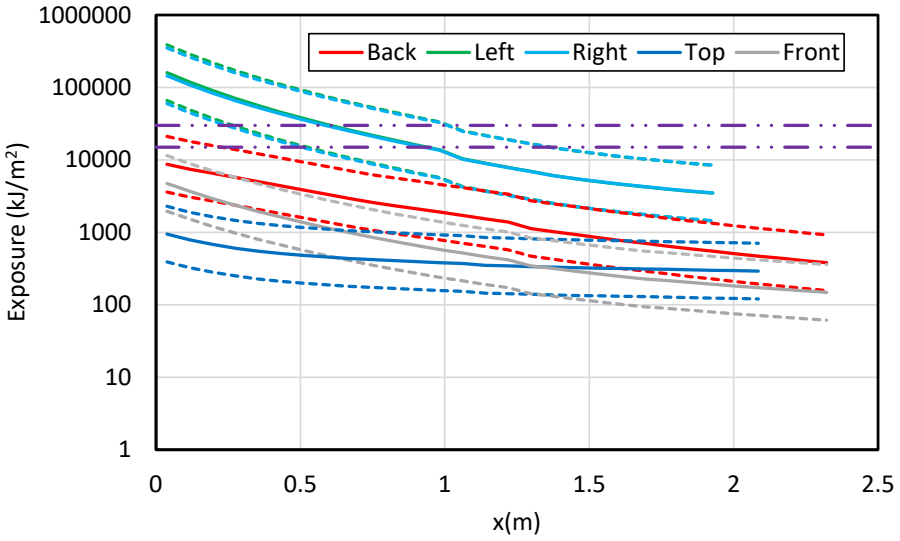

Figure B-45
Results for a horizontal draw-out MV SWGR with copper electrodes – 169 MJ HEAF located at the breaker stabs (FDS Simulation MV-ABB-3)

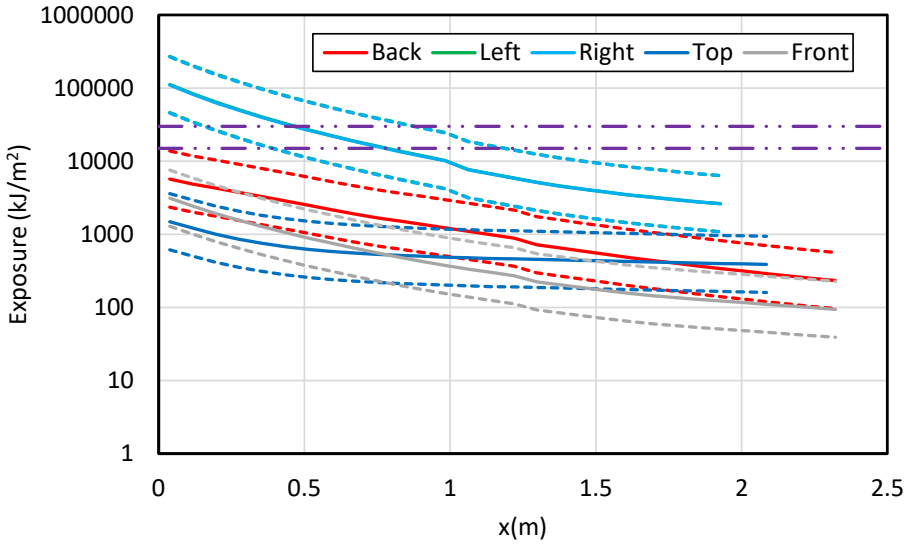

Figure B-46
Results for a horizontal draw-out MV SWGR with copper electrodes – 131 MJ HEAF located at the breaker stabs (FDS Simulation MV-ABB-4)

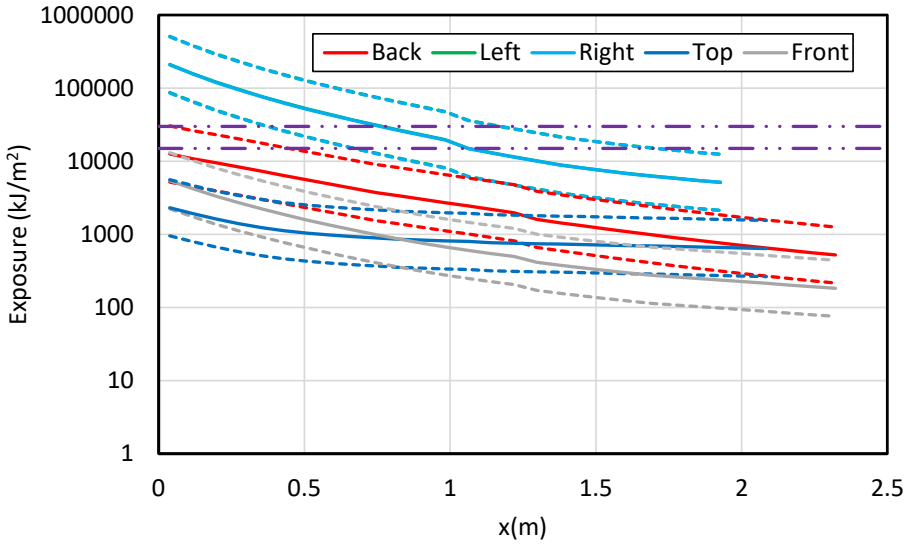

Figure B-47
Results for a horizontal draw-out MV SWGR with copper electrodes – 226 MJ HEAF located at the breaker stabs (FDS Simulation MV-ABB-5)

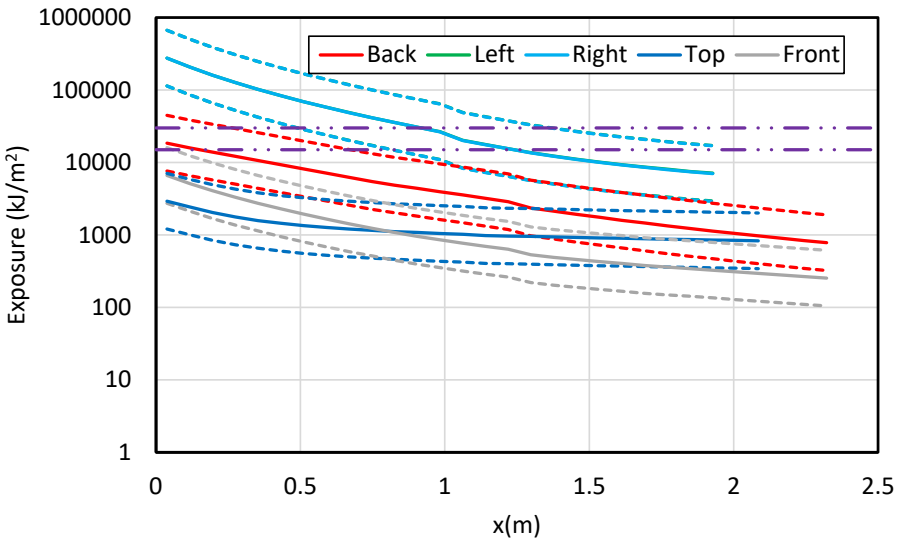

Figure B-48
Results for a horizontal draw-out MV SWGR with copper electrodes – 293 MJ HEAF located at the breaker stabs (FDS Simulation MV-ABB-6)

B.2 Low Voltage Switchgear

B.2.1 Breaker Compartment Middle-Height Cubicle

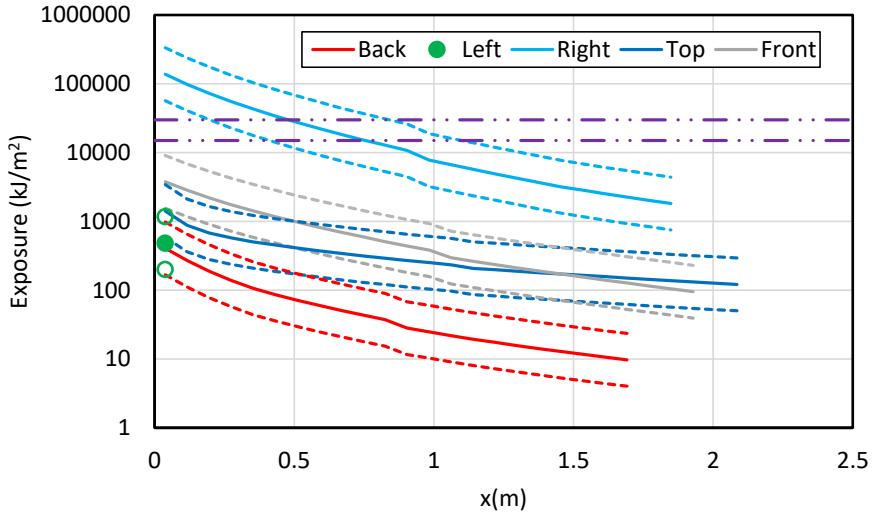

Figure B-49
Results for a LV SWGR with an aluminum bus bar with a HEAF based on FEDB 50935 – HEAF located in a middle-height breaker compartment (FDS Simulation LV-BASE-1)

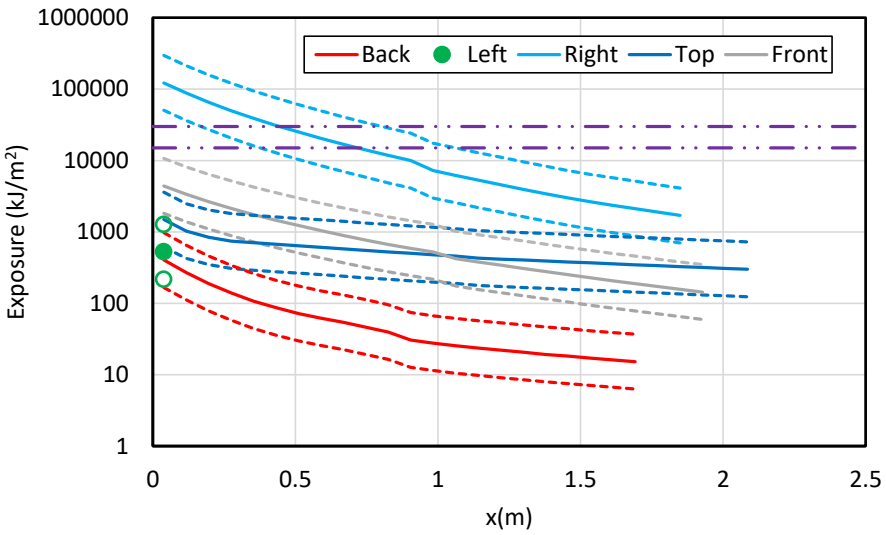

Figure B-50
Results for a LV SWGR with a copper bus bar with a HEAF based on FEDB 50935 – HEAF located in a middle-height breaker compartment (FDS Simulation LV-BASE-7)

B.2.2 Breaker Compartment Top

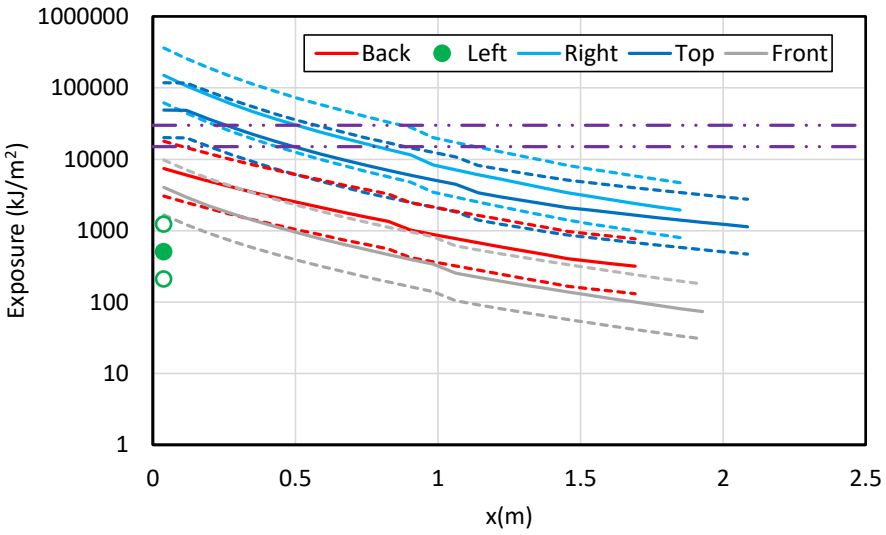

Figure B-51
Results for a LV SWGR with an aluminum bus bar with a HEAF based on FEDB 50935 – HEAF located in a breaker compartment at the top of the switchgear (FDS Simulation LV-BASE-2)

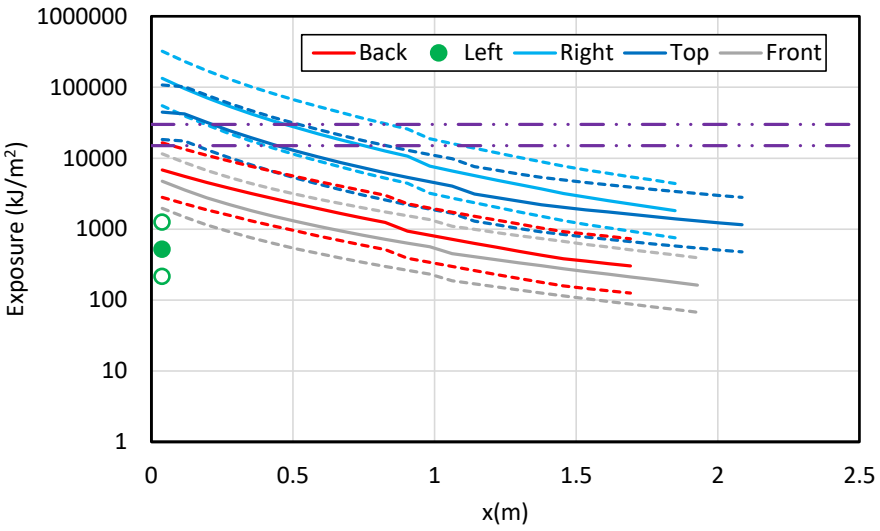

Figure B-52
Results for a LV SWGR with a copper bus bar with a HEAF based on FEDB 50935 – HEAF located in a breaker compartment at the top of the switchgear (FDS Simulation LV-BASE-8)

B.2.3 Bus Bar Compartment Middle-Height Cubicle

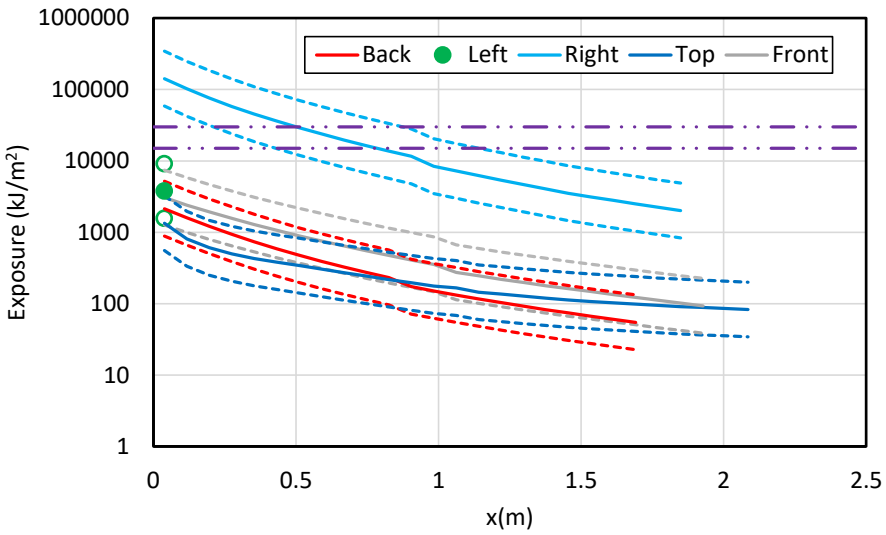

Figure B-53
Results for a LV SWGR with an aluminum bus bar with a HEAF based on FEDB 50935 – HEAF located in a middle-height bus bar compartment (FDS Simulation LV-BASE-3)

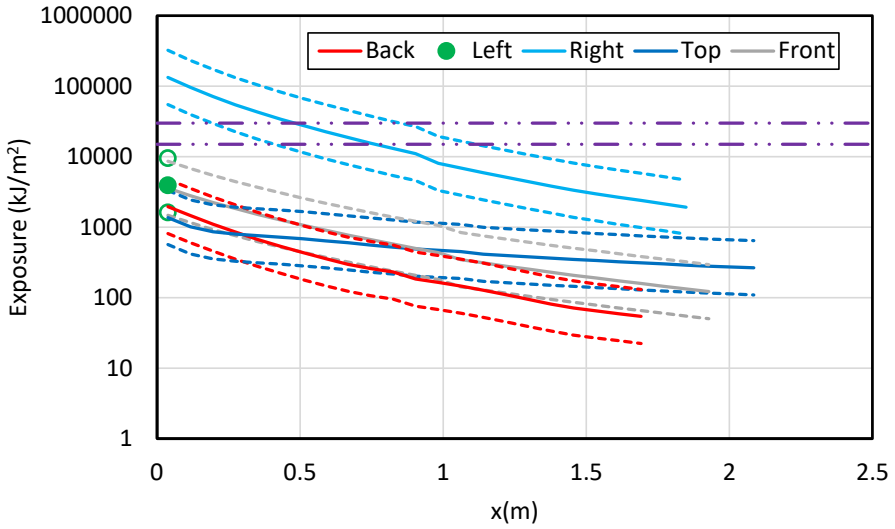

Figure B-54
Results for a LV SWGR with a copper bus bar with a HEAF based on FEDB 50935 – HEAF located in a middle-height bus bar compartment (FDS Simulation LV-BASE-9)

B.2.4 Bus Bar Compartment Top

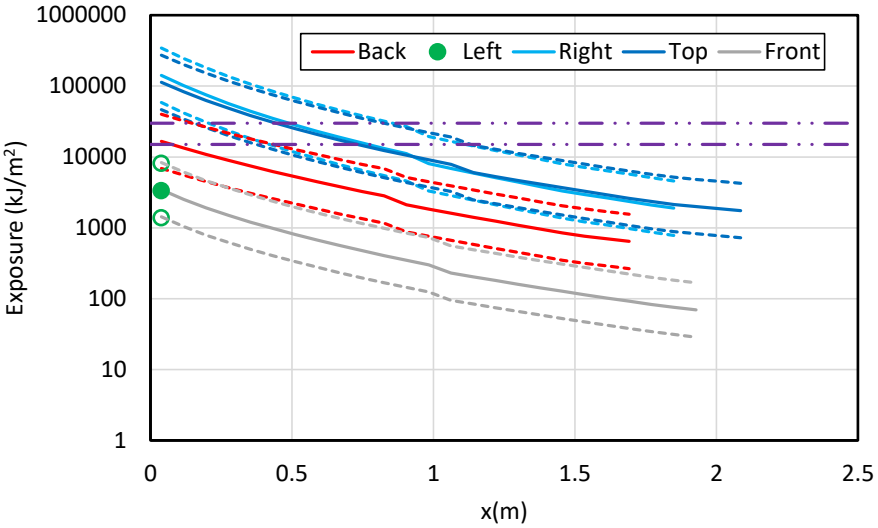

Figure B-55
Results for a LV SWGR with an aluminum bus bar with a HEAF based on FEDB 50935 – HEAF located in a bus bar compartment at the top of the switchgear (FDS Simulation LV-BASE-4)

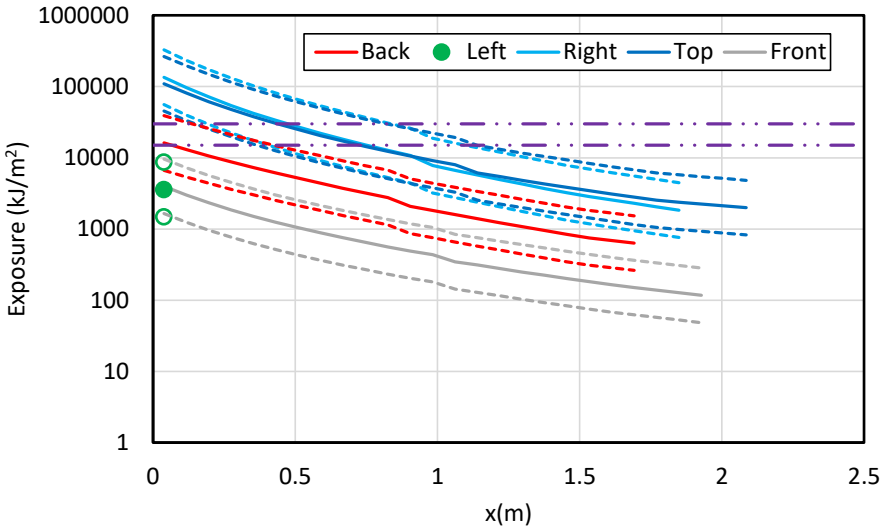

Figure B-56
Results for a LV SWGR with a copper bus bar with a HEAF based on FEDB 50935 – HEAF located in a bus bar compartment at the top of the switchgear (FDS Simulation LV-BASE-10)

B.2.5 Breaker to Bus Bar Compartment

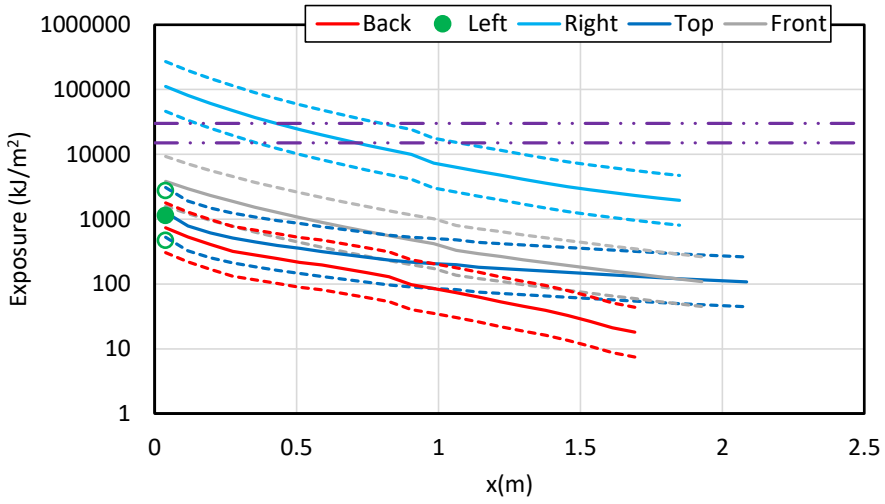

Figure B-57
Results for a LV SWGR with an aluminum bus bar with a HEAF based on FEDB 50935 – HEAF initially located in a middle-height breaker compartment and moves to the bus bar compartment at the same height (FDS Simulation LV-BASE-5)

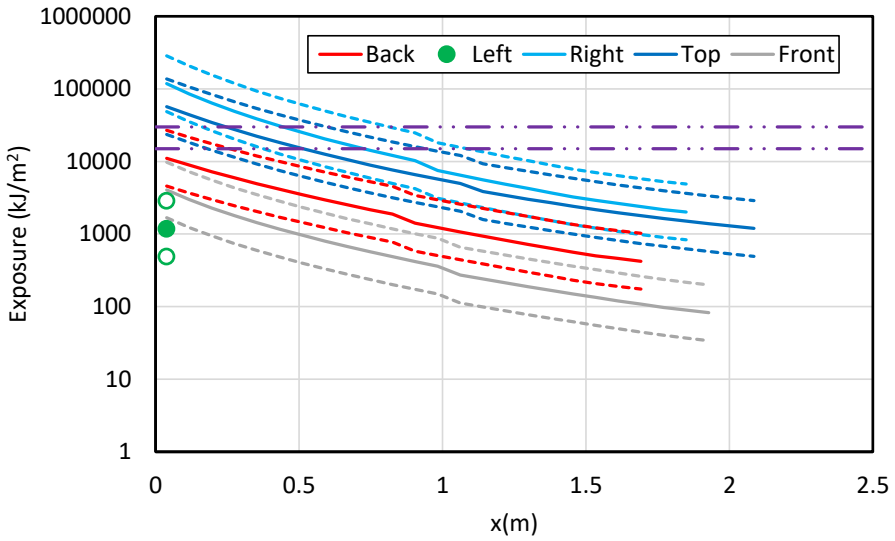

Figure B-58
Results for a LV SWGR with an aluminum bus bar with a HEAF based on FEDB 50935 – HEAF initially located in a breaker compartment at the top of the switchgear and moves to the bus bar compartment at the same height (FDS Simulation LV-BASE-6)

B.3 Non-Segregated Bus Ducts

B.3.1 Bus Duct Straight Segment

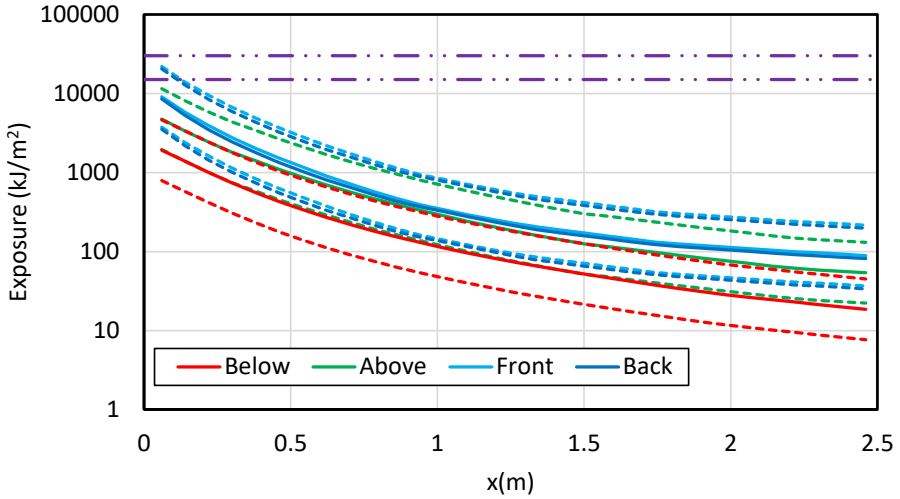

Figure B-59
Results for a straight run, steel duct NSBD with aluminum bus bars – 34 MJ HEAF (FDS Simulation NSBD-1)

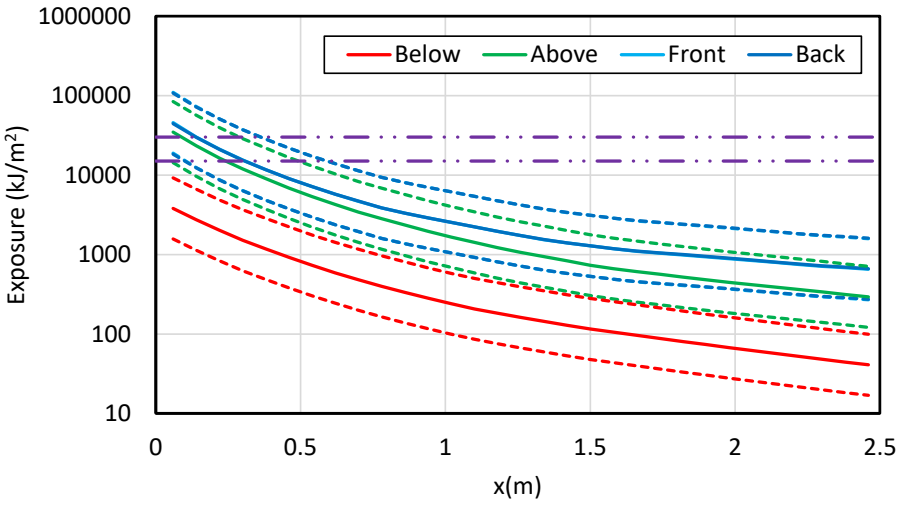

Figure B-60
Results for a straight run, steel duct NSBD with aluminum bus bars – 68 MJ HEAF (FDS Simulation NSBD-2)

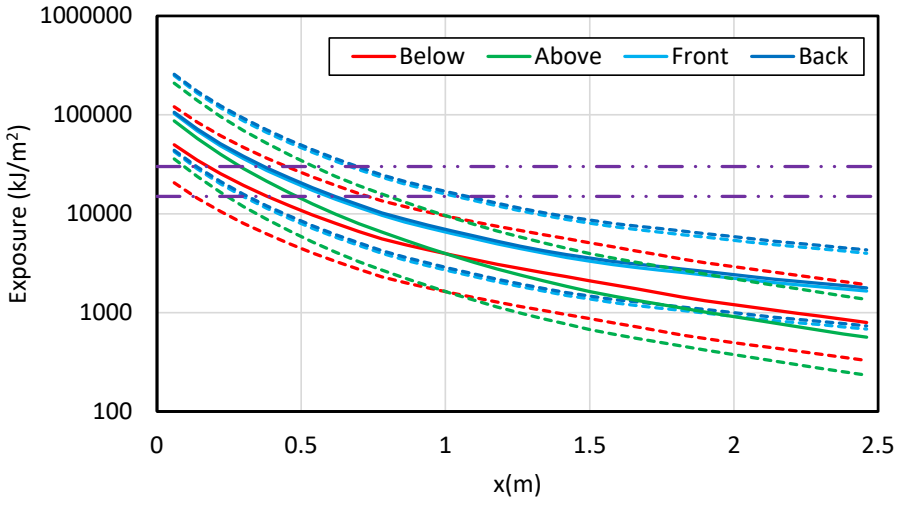

Figure B-61
Results for a straight run, steel duct NSBD with aluminum bus bars – 135 MJ HEAF (FDS Simulation NSBD-3)

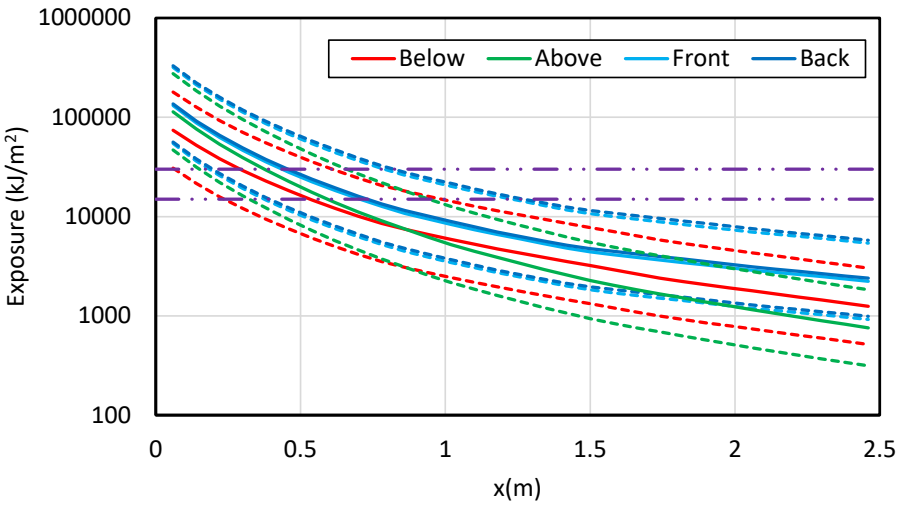

Figure B-62
Results for a straight run, steel duct NSBD with aluminum bus bars – 169 MJ HEAF (FDS Simulation NSBD-4)

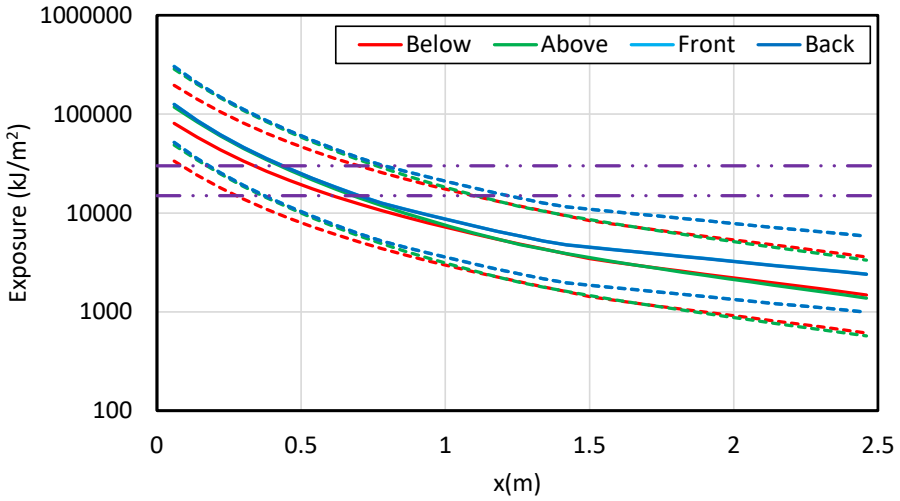

Figure B-63
Results for a straight run, steel duct NSBD with aluminum bus bars – 131 MJ HEAF (FDS Simulation NSBD-5)

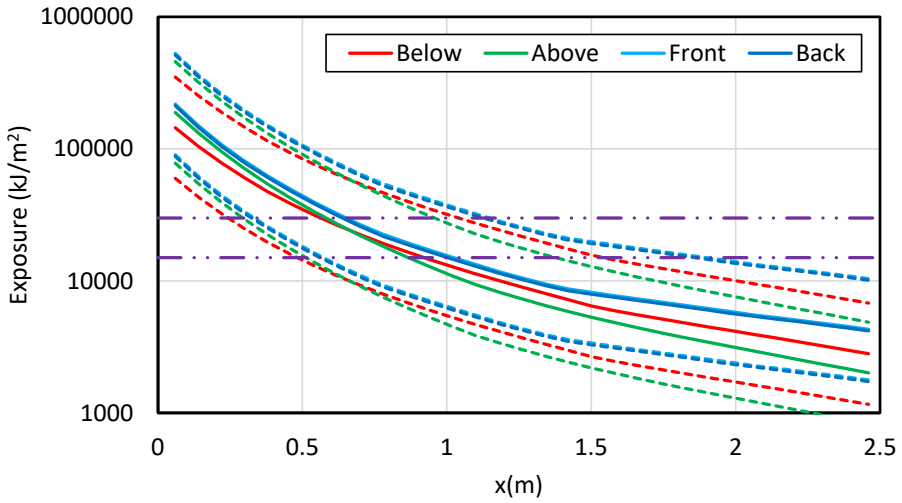

Figure B-64
Results for a straight run, steel duct NSBD with aluminum bus bars – 226 MJ HEAF (FDS Simulation NSBD-6)

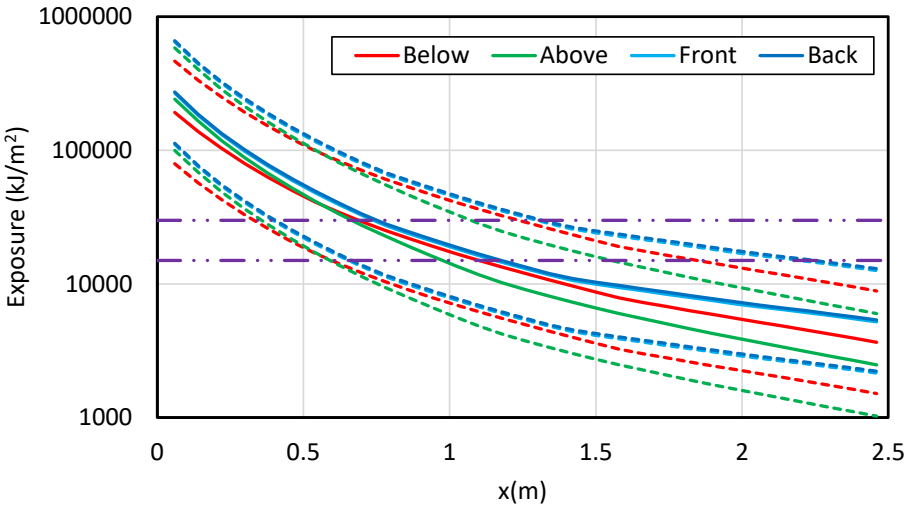

Figure B-65
Results for a straight run, steel duct NSBD with aluminum bus bars – 293 MJ HEAF (FDS Simulation NSBD-7)

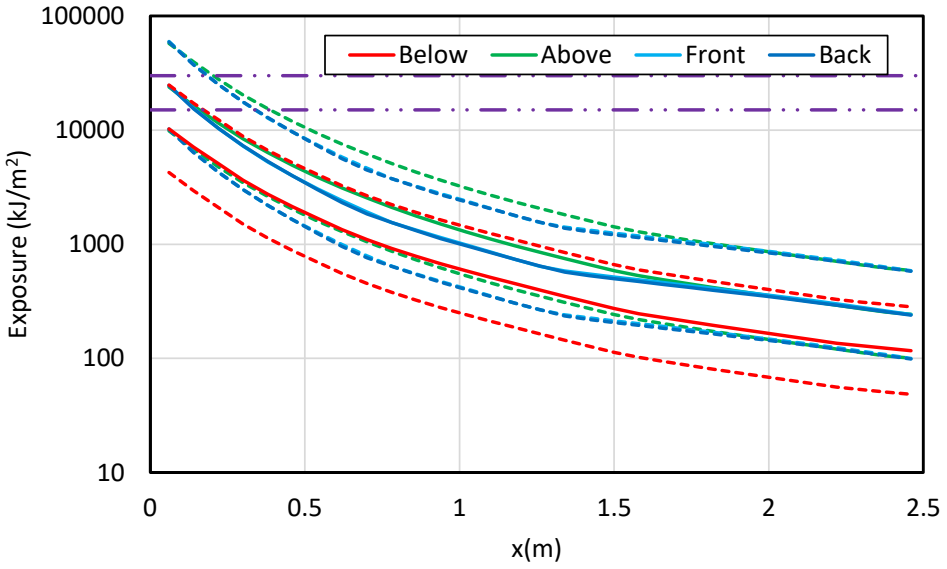

Figure B-66
Results for a straight run, aluminum duct NSBD with aluminum bus bars – 34 MJ HEAF (FDS Simulation NSBD-8)

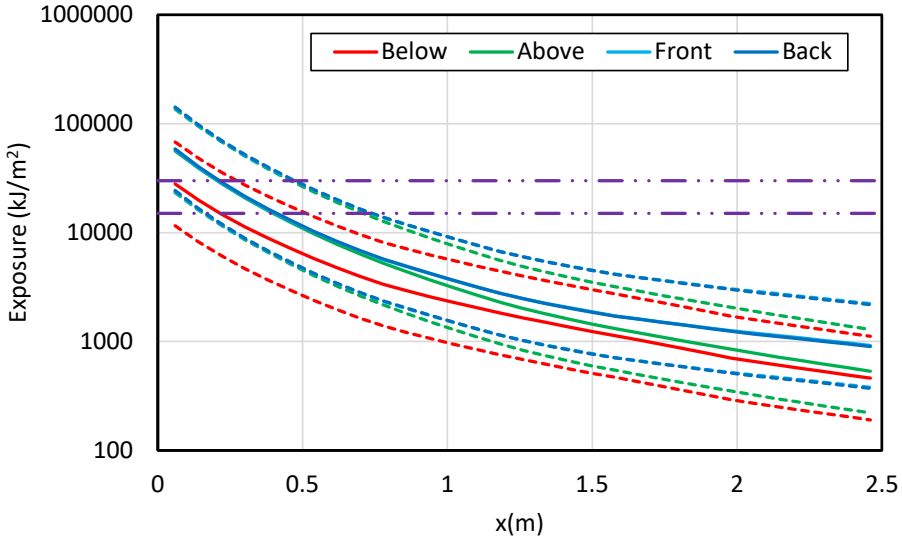

Figure B-67
Results for a straight run, aluminum duct NSBD with aluminum bus bars – 68 MJ HEAF (FDS Simulation NSBD-9)

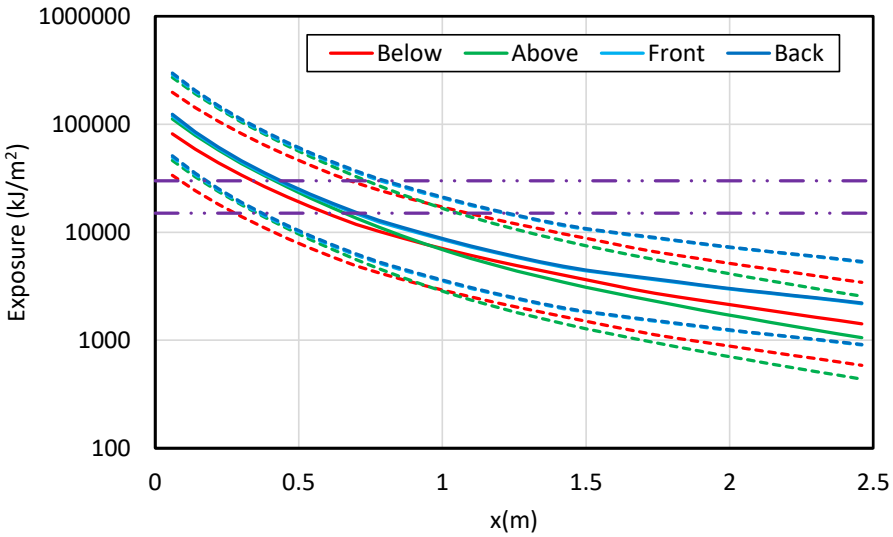

Figure B-68
Results for a straight run, aluminum duct NSBD with aluminum bus bars – 135 MJ HEAF (FDS Simulation NSBD-10)

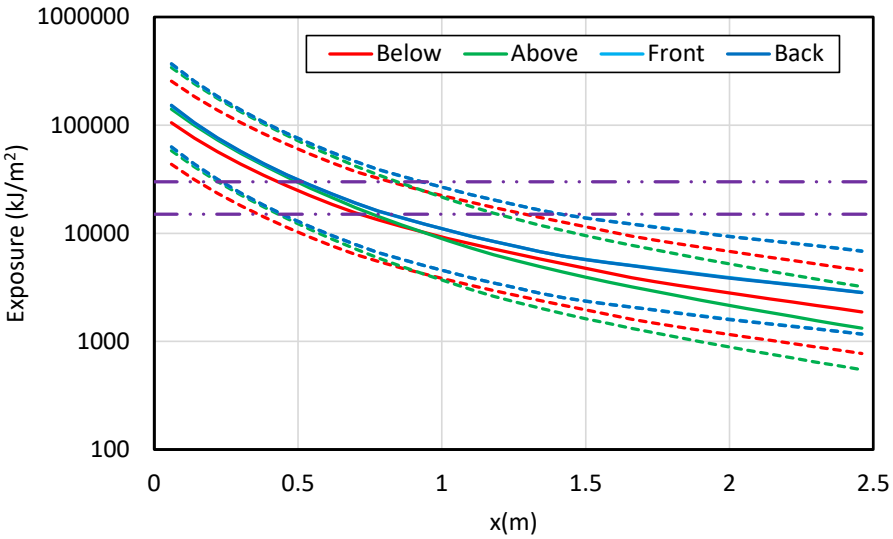

Figure B-69
Results for a straight run, aluminum duct NSBD with aluminum bus bars – 169 MJ HEAF (FDS Simulation NSBD-11)

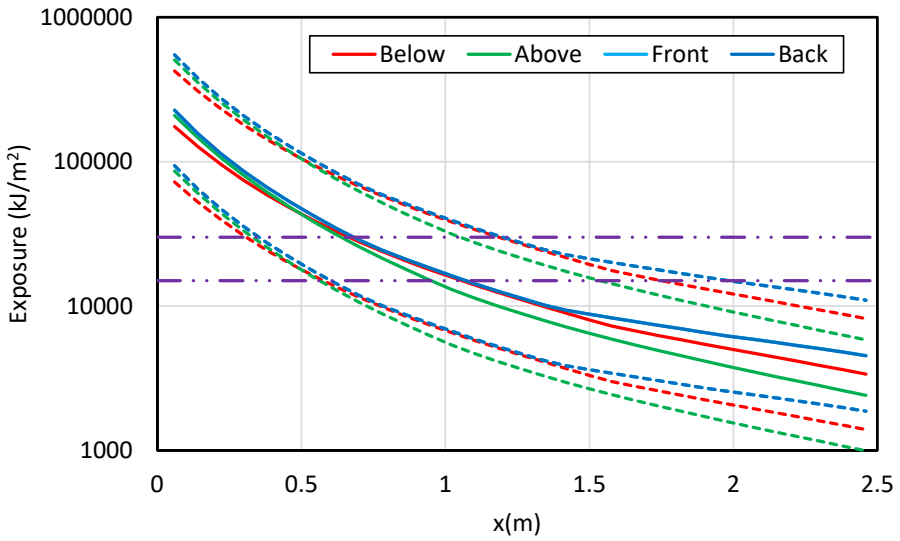

Figure B-70
Results for a straight run, aluminum duct NSBD with aluminum bus bars – 226 MJ HEAF (FDS Simulation NSBD-12)

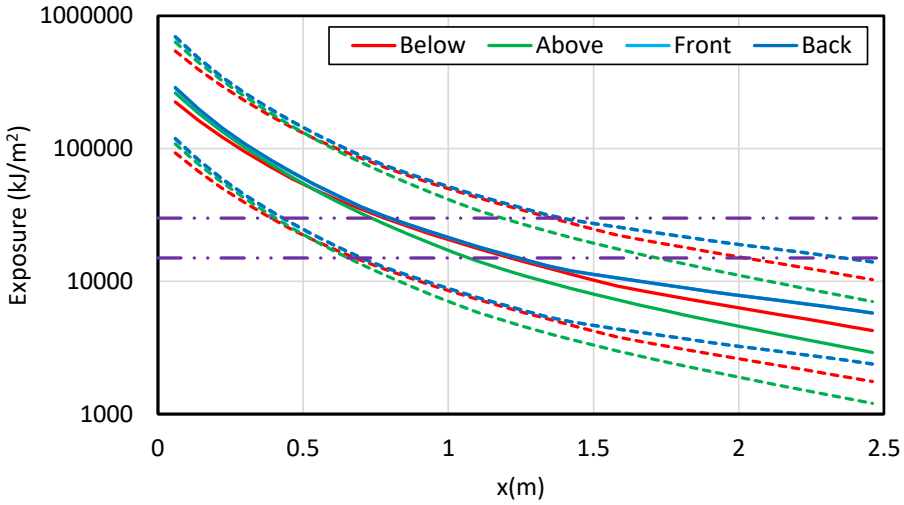

Figure B-71
Results for a straight run, aluminum duct NSBD with aluminum bus bars – 293 MJ HEAF (FDS Simulation NSBD-13)

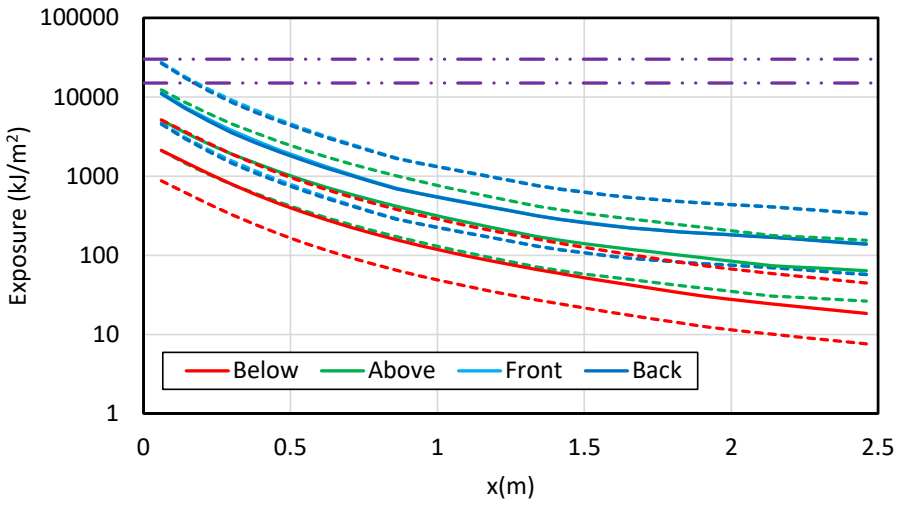

Figure B-72
Results for a straight run, steel duct NSBD with copper bus bars – 34 MJ HEAF (FDS Simulation NSBD-14)

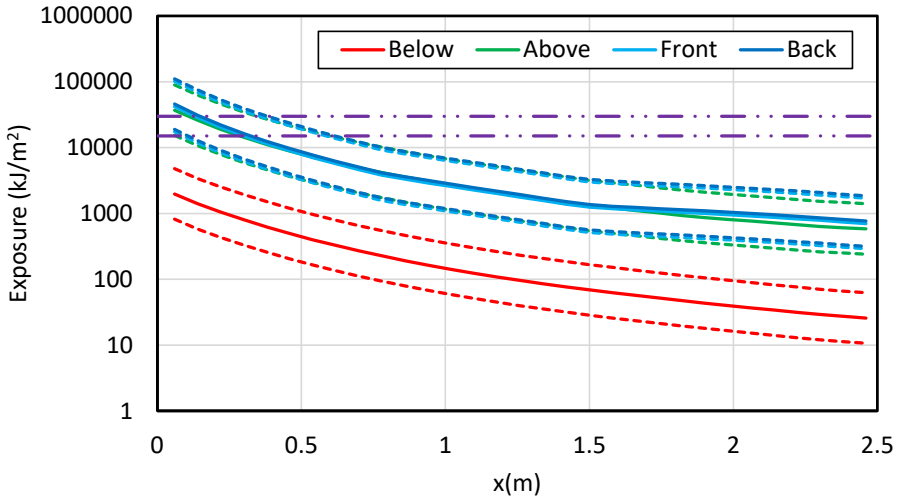

Figure B-73
Results for a straight run, steel duct NSBD with copper bus bars – 68 MJ HEAF (FDS Simulation NSBD-15)

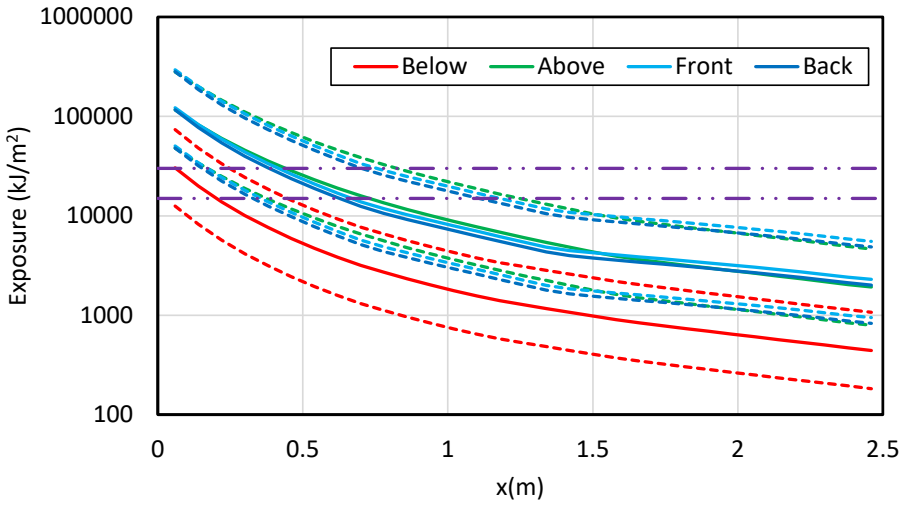

Figure B-74
Results for a straight run, steel duct NSBD with copper bus bars – 135 MJ HEAF (FDS Simulation NSBD-16)

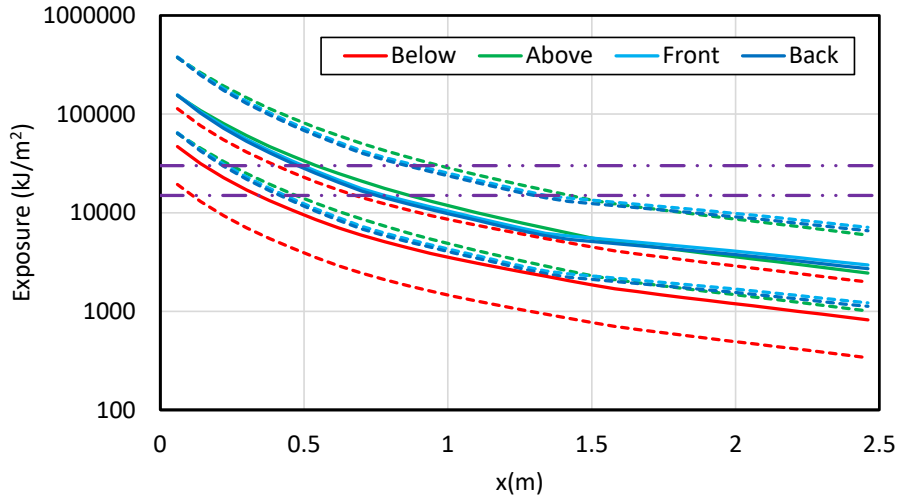

Figure B-75
Results for a straight run, steel duct NSBD with copper bus bars – 169 MJ HEAF (FDS Simulation NSBD-17)

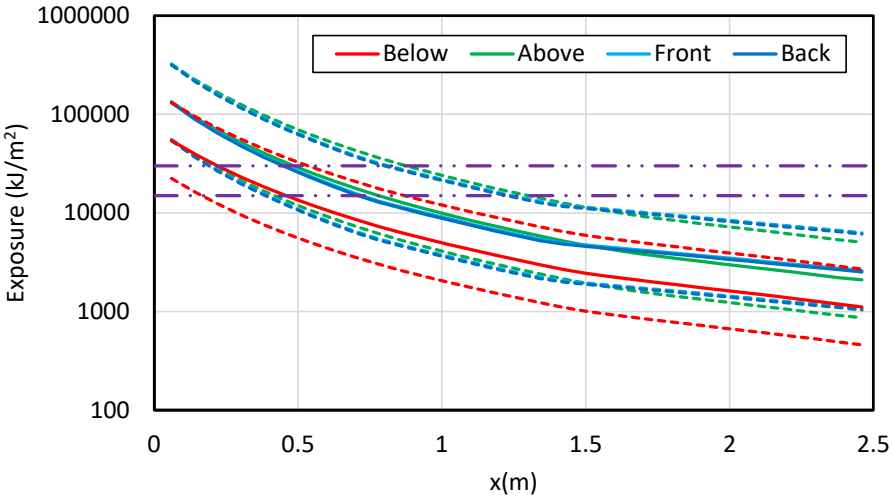

Figure B-76
Results for a straight run, steel duct NSBD with copper bus bars – 131 MJ HEAF (FDS Simulation NSBD-18)

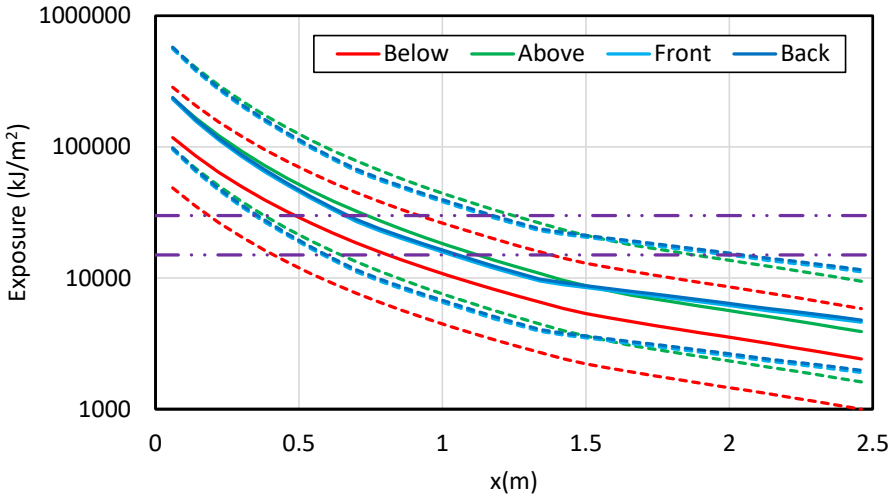

Figure B-77
Results for a straight run, steel duct NSBD with copper bus bars – 226 MJ HEAF (FDS Simulation NSBD-19)

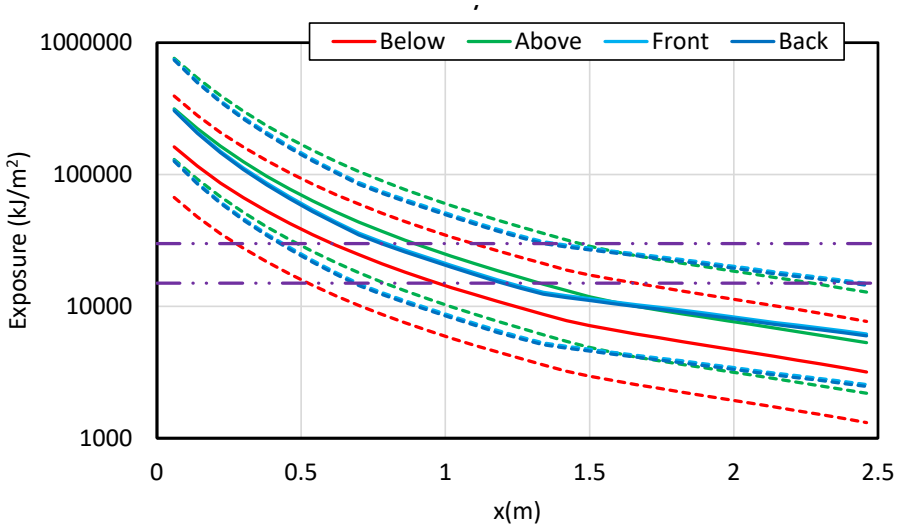

Figure B-78
Results for a straight run, steel duct NSBD with copper bus bars – 293 MJ HEAF (FDS Simulation NSBD-20)

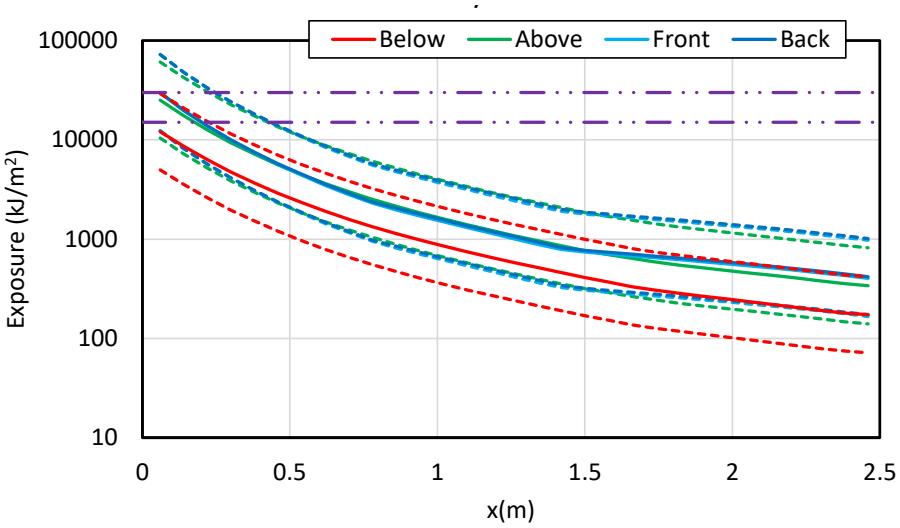

Figure B-79
Results for a straight run, aluminum duct NSBD with copper bus bars – 34 MJ HEAF (FDS Simulation NSBD-21)

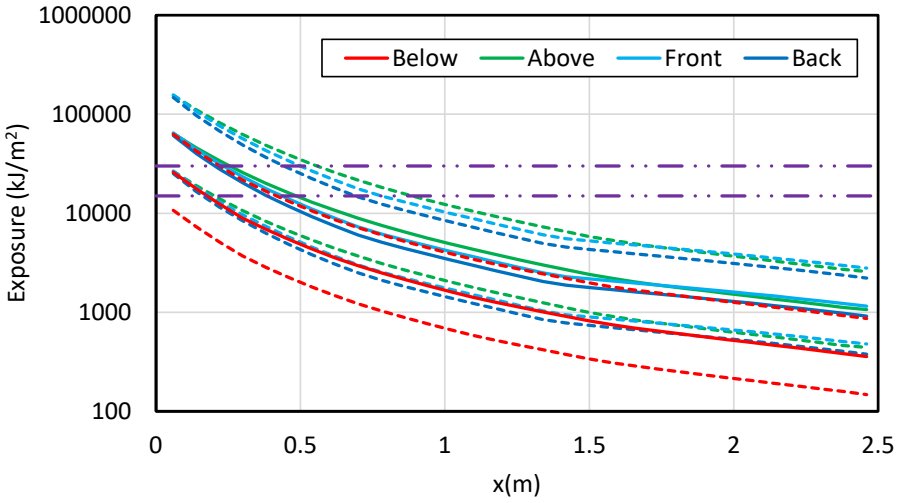

Figure B-80
Results for a straight run, aluminum duct NSBD with copper bus bars – 68 MJ HEAF (FDS Simulation NSBD-22)

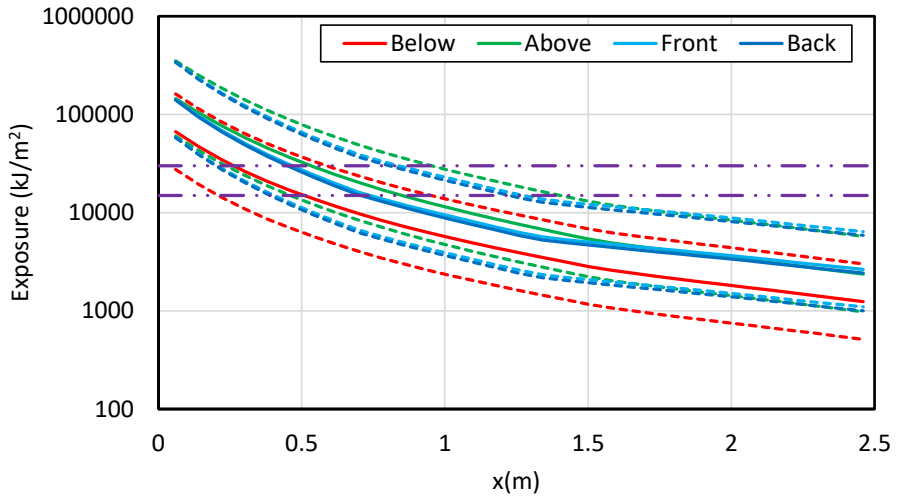

Figure B-81
Results for a straight run, aluminum duct NSBD with copper bus bars – 135 MJ HEAF (FDS Simulation NSBD-23)

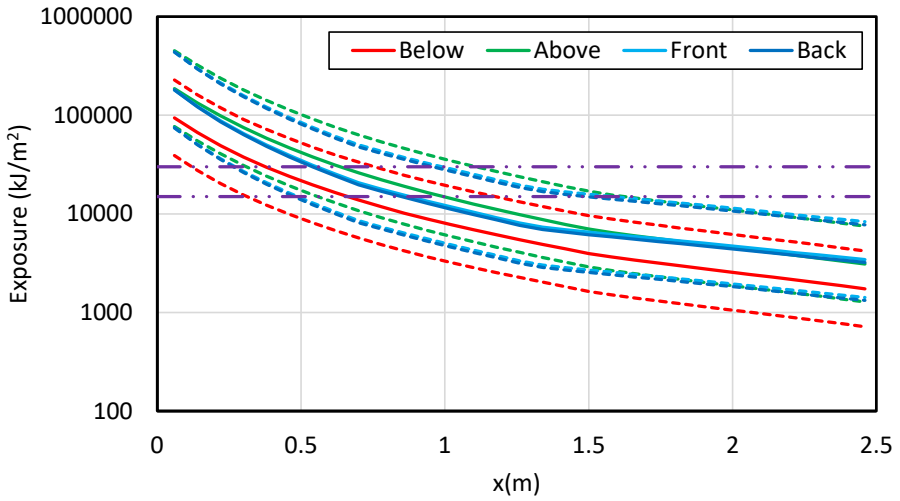

Figure B-82
Results for a straight run, aluminum duct NSBD with copper bus bars – 169 MJ HEAF (FDS Simulation NSBD-24)

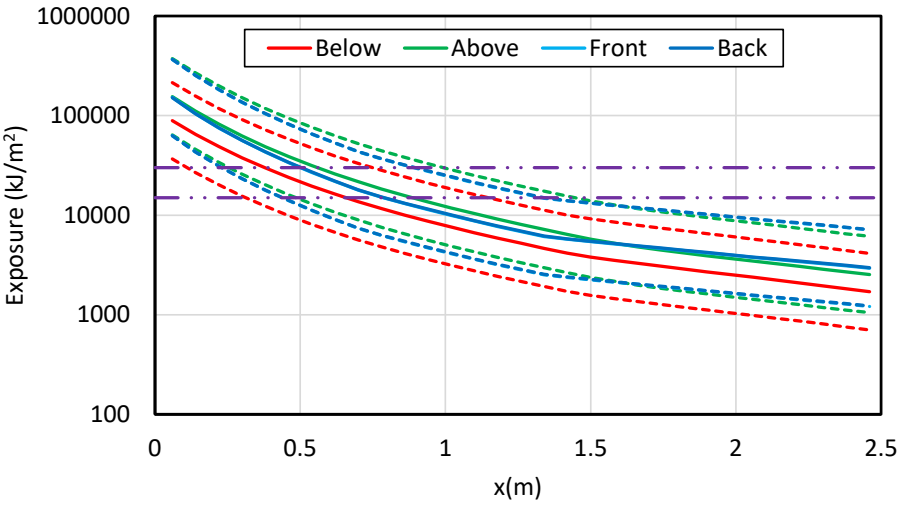

Figure B-83
Results for a straight run, aluminum duct NSBD with copper bus bars – 131 MJ HEAF (FDS Simulation NSBD-25)

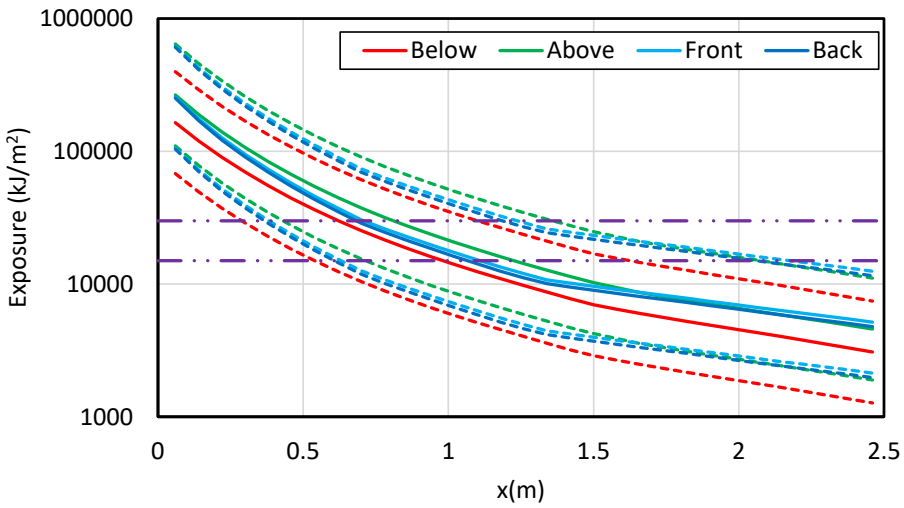

Figure B-84
Results for a straight run, aluminum duct NSBD with copper bus bars – 226 MJ HEAF (FDS Simulation NSBD-26)

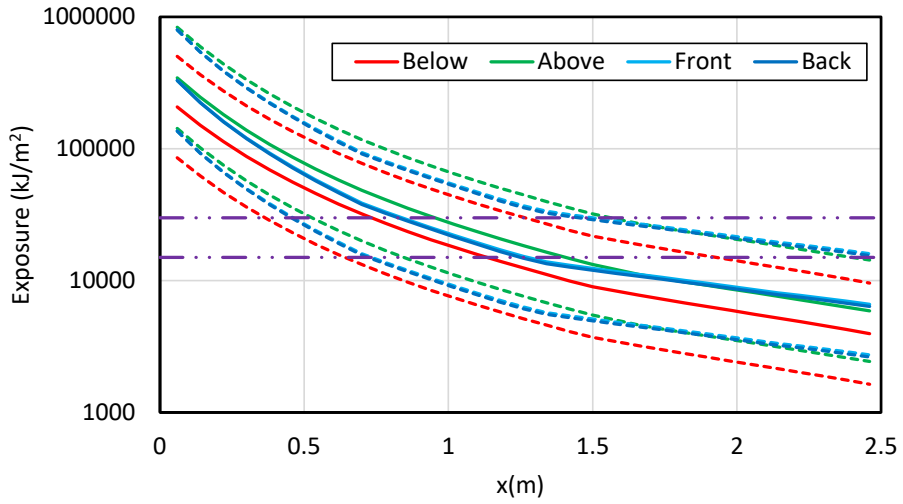

Figure B-85
Results for a straight run, aluminum duct NSBD with copper bus bars – 293 MJ HEAF (FDS Simulation NSBD-27)

B.3.2 Bus Duct Elbow

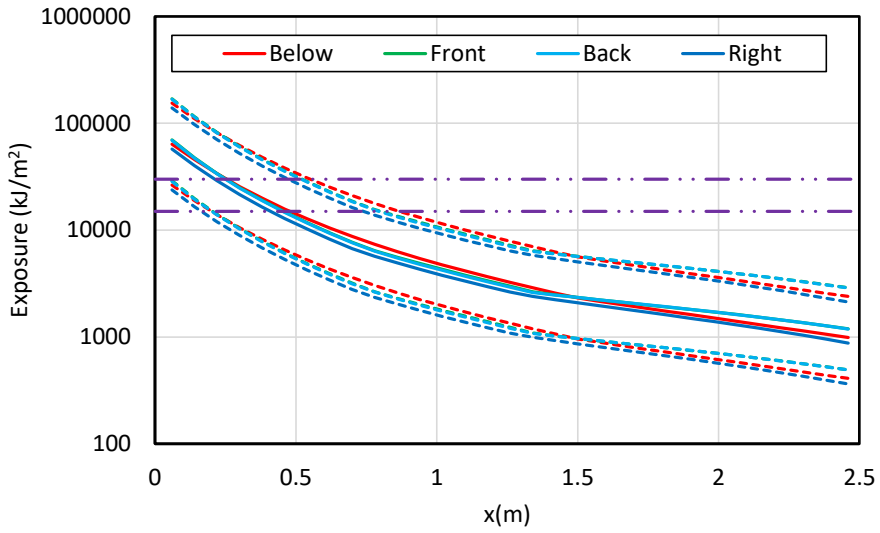

Figure B-86
Results for an aluminum duct NSBD elbow with aluminum bus bars – 68 MJ HEAF (FDS Simulation NSBD-52)

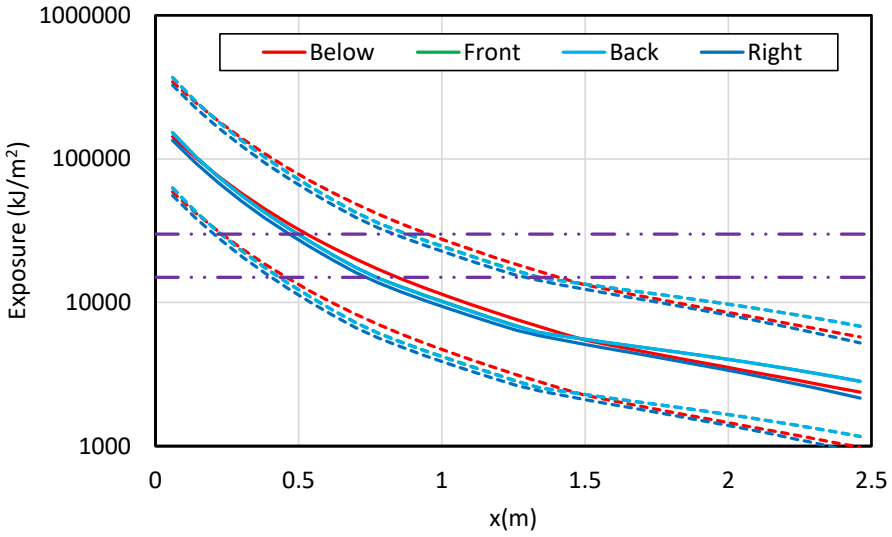

Figure B-87
Results for an aluminum duct NSBD elbow with aluminum bus bars – 135 MJ HEAF (FDS Simulation NSBD-53)

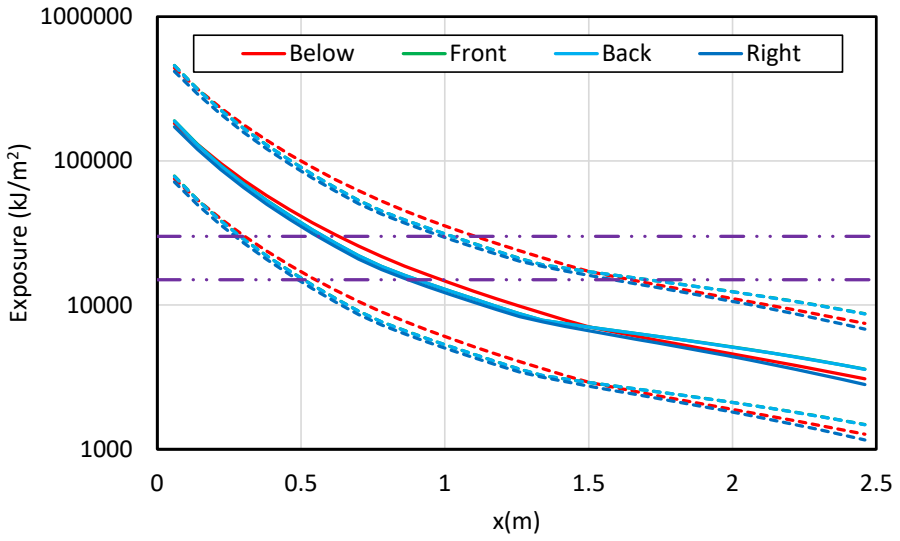

Figure B-88
Results for an aluminum duct NSBD elbow with aluminum bus bars – 169 MJ HEAF (FDS Simulation NSBD-54)

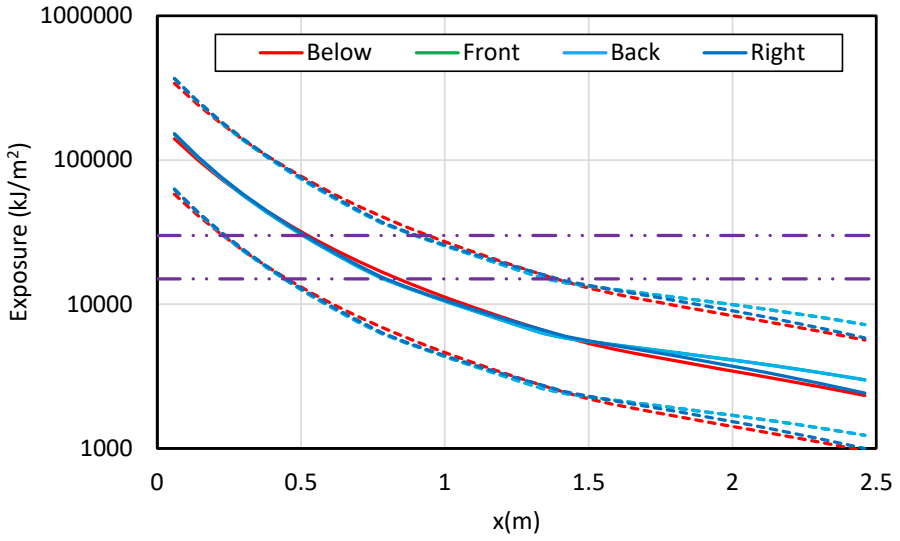

Figure B-89
Results for an aluminum duct NSBD elbow with aluminum bus bars – 131 MJ HEAF (FDS Simulation NSBD-55)

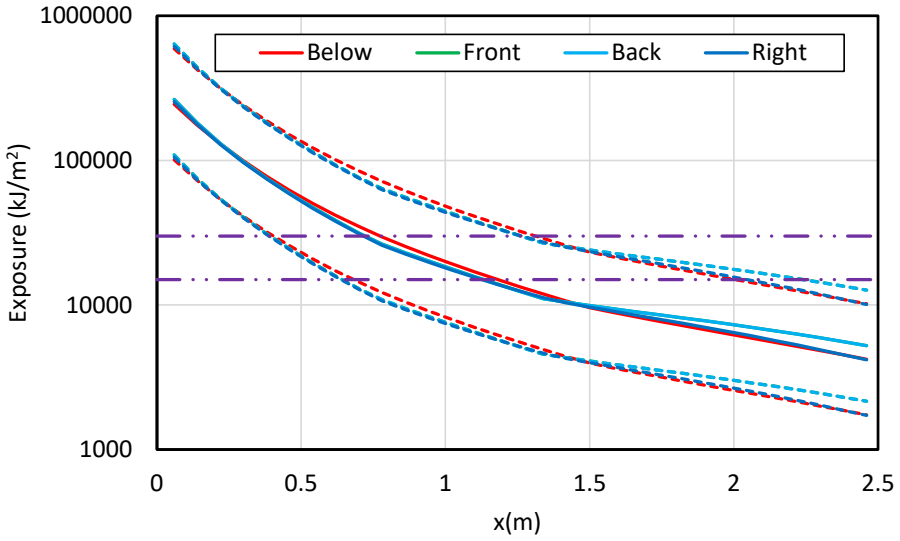

Figure B-90
Results for an aluminum duct NSBD elbow with aluminum bus bars – 226 MJ HEAF (FDS Simulation NSBD-56)

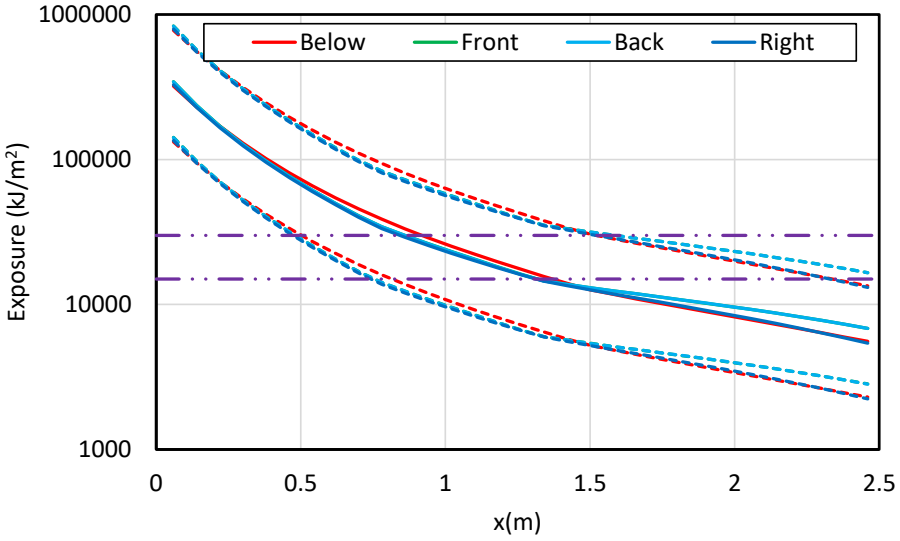

Figure B-91
Results for an aluminum duct NSBD elbow with aluminum bus bars – 293 MJ HEAF (FDS Simulation NSBD-57)

B.3.3 Bus Duct Tee

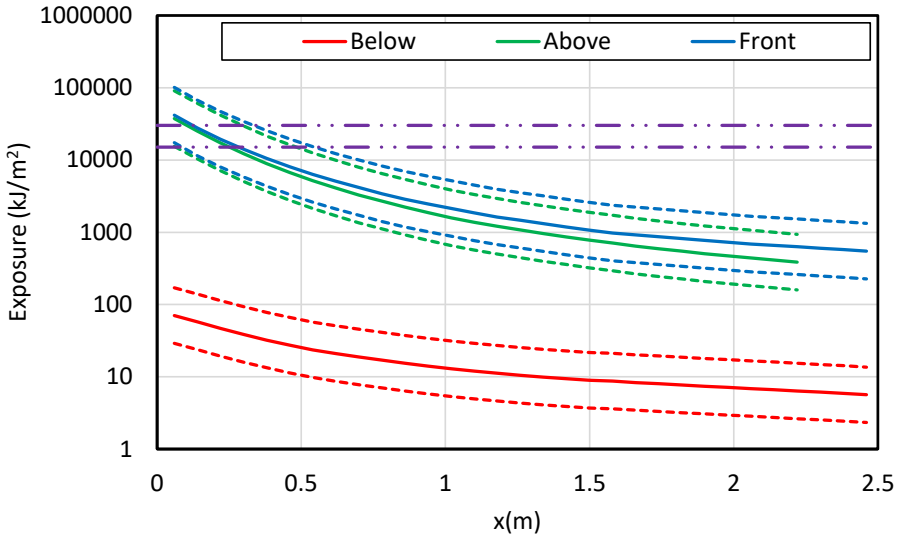

Figure B-92
Results for a steel duct NSBD tee with aluminum bus bars – 68 MJ HEAF (FDS Simulation NSBD-28)

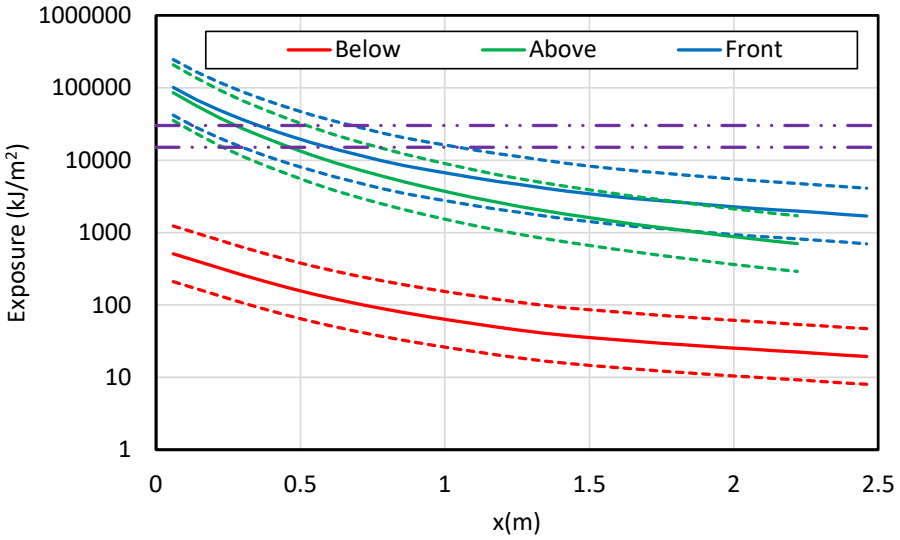

Figure B-93
Results for a steel duct NSBD tee with aluminum bus bars – 135 MJ HEAF (FDS Simulation NSBD-29)

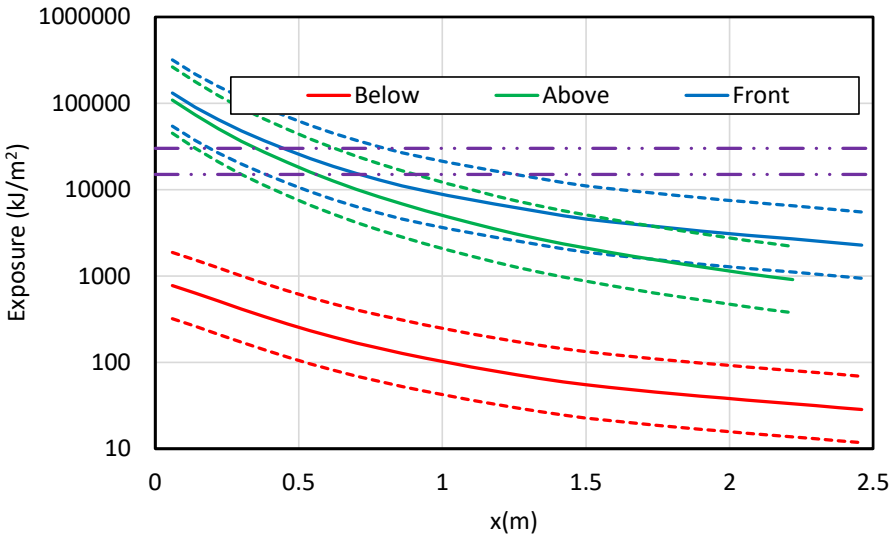

Figure B-94
Results for a steel duct NSBD tee with aluminum bus bars – 169 MJ HEAF (FDS Simulation NSBD-30)

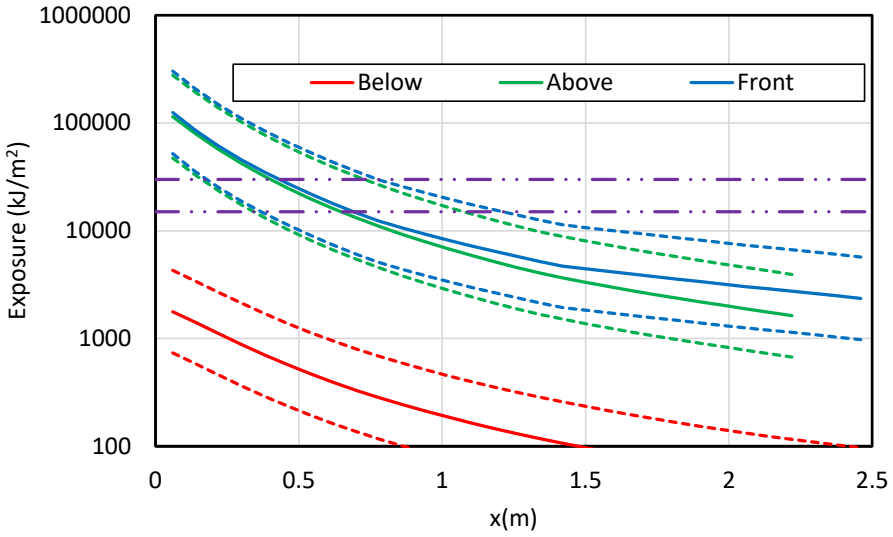

Figure B-95
Results for a steel duct NSBD tee with aluminum bus bars – 131 MJ HEAF (FDS Simulation NSBD-31)

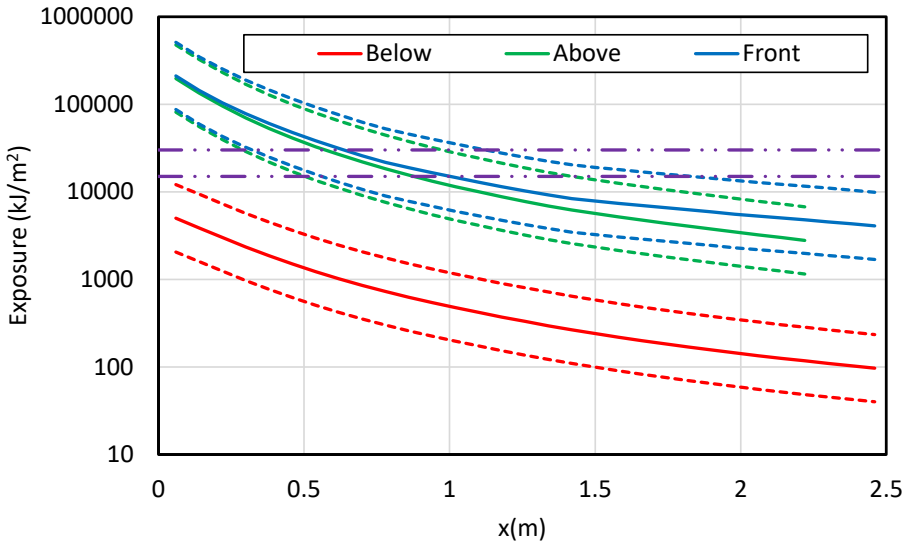

Figure B-96
Results for a steel duct NSBD tee with aluminum bus bars – 226 MJ HEAF (FDS Simulation NSBD-32)

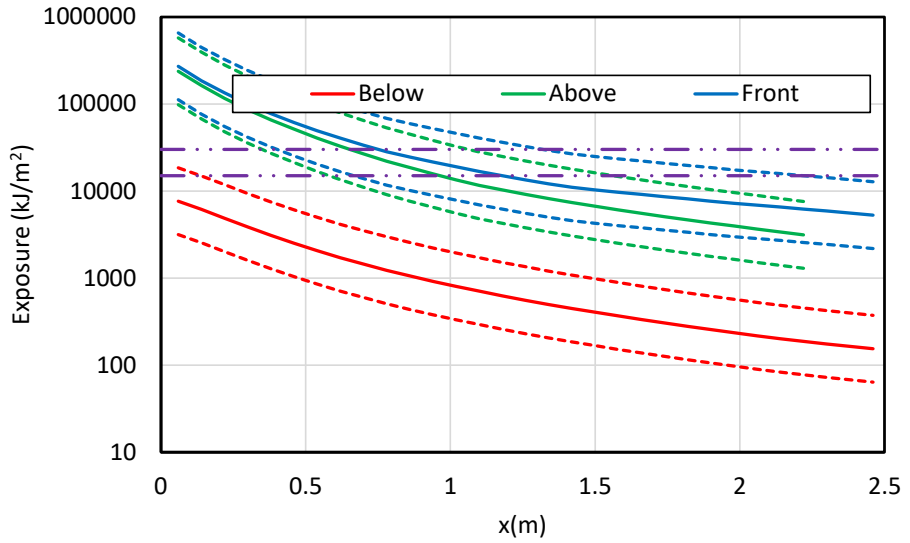

Figure B-97
Results for a steel duct NSBD tee with aluminum bus bars – 293 MJ HEAF (FDS Simulation NSBD-33)

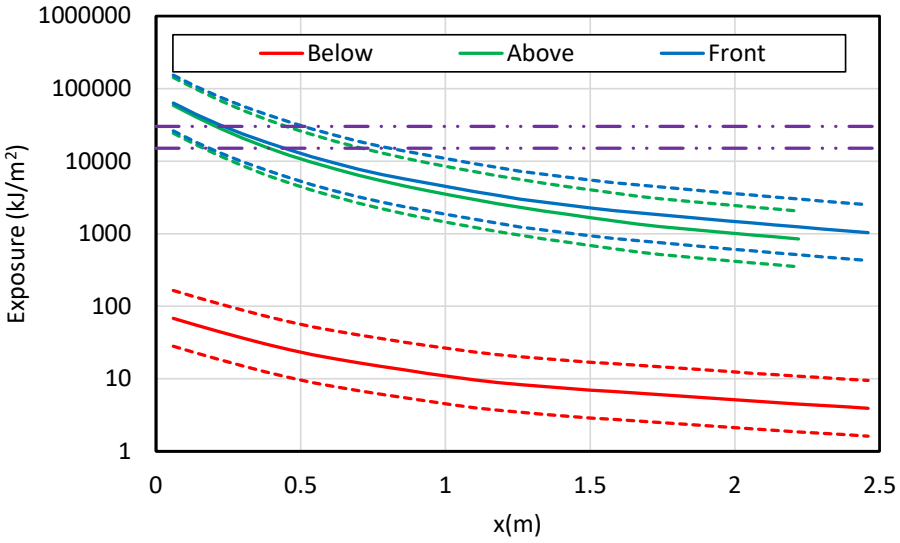

Figure B-98
Results for an aluminum duct NSBD tee with aluminum bus bars – 68 MJ HEAF (FDS Simulation NSBD-34)

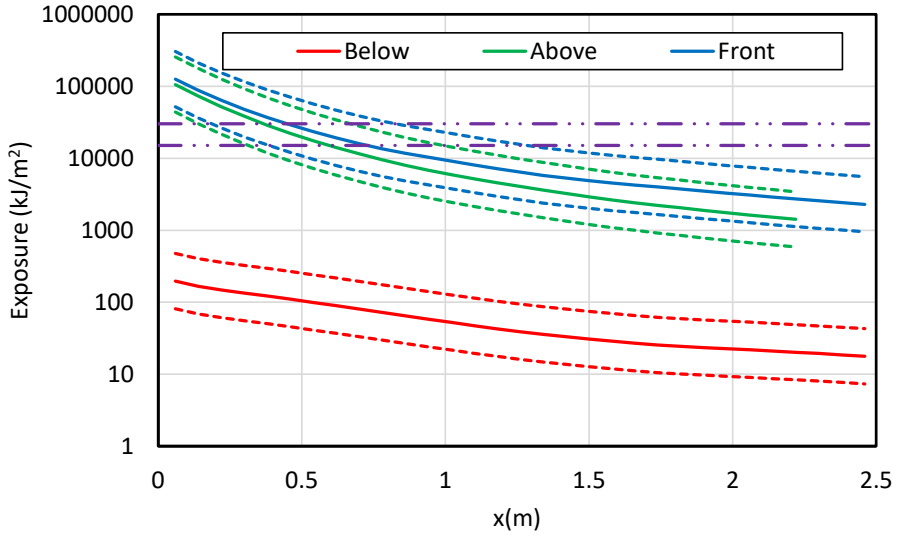

Figure B-99
Results for an aluminum duct NSBD tee with aluminum bus bars – 135 MJ HEAF (FDS Simulation NSBD-35)

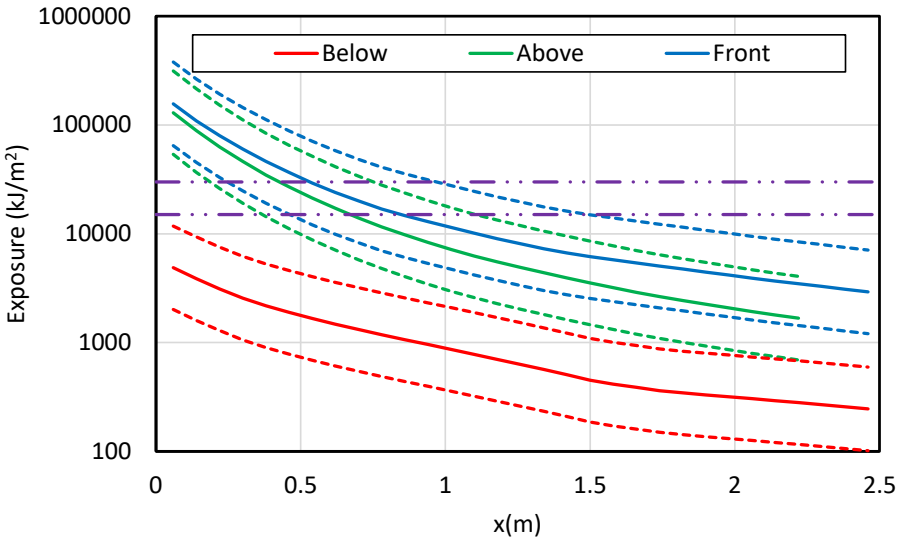

Figure B-100
Results for an aluminum duct NSBD tee with aluminum bus bars – 169 MJ HEAF (FDS Simulation NSBD-36)

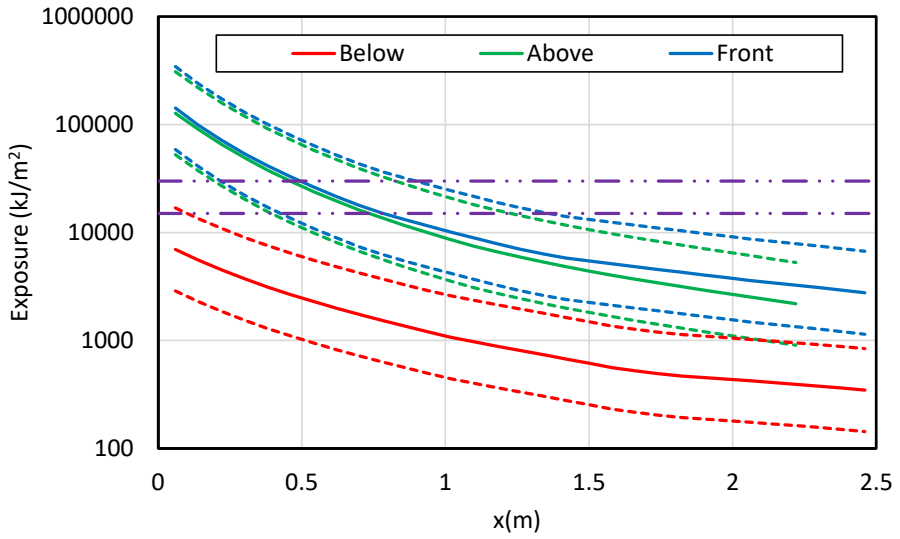

Figure B-101
Results for an aluminum duct NSBD tee with aluminum bus bars – 131 MJ HEAF (FDS Simulation NSBD-37)

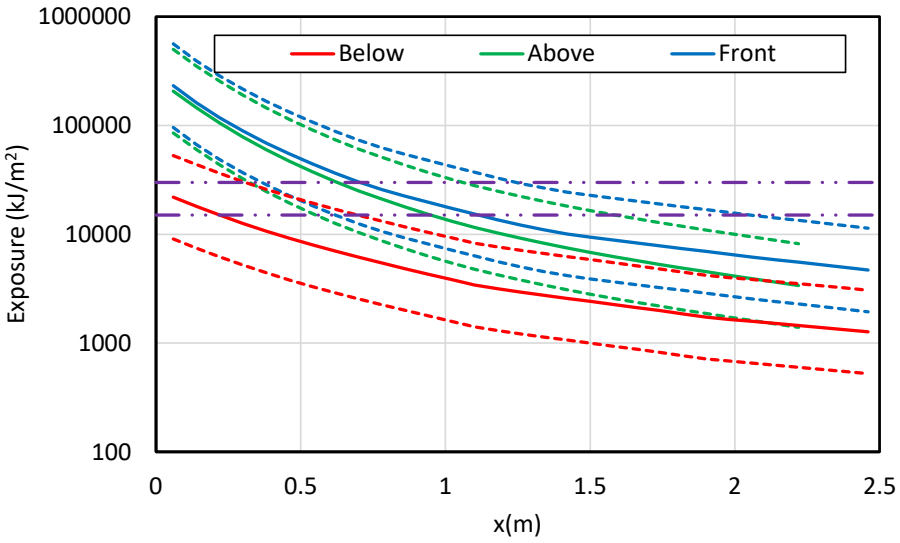

Figure B-102
Results for an aluminum duct NSBD tee with aluminum bus bars – 226 MJ HEAF (FDS Simulation NSBD-38)

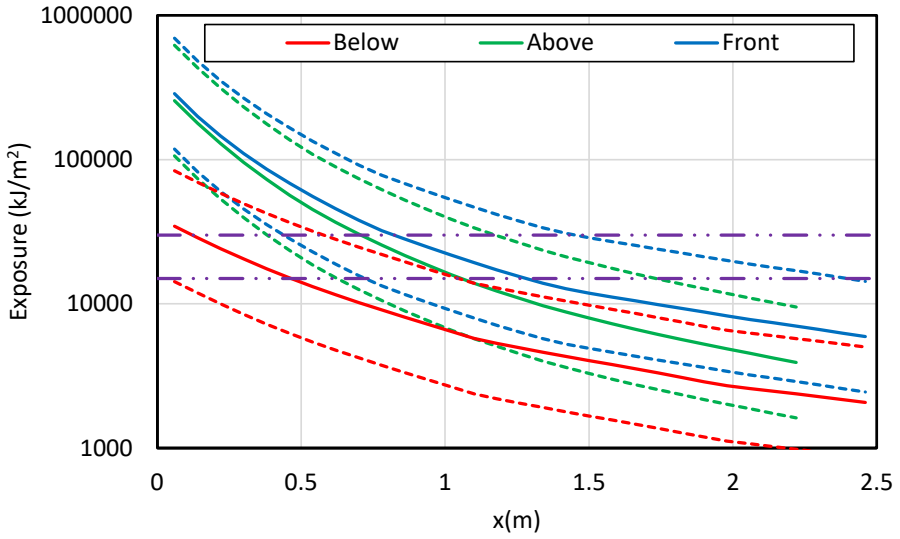

Figure B-103
Results for an aluminum duct NSBD tee with aluminum bus bars – 293 MJ HEAF (FDS Simulation NSBD-39)

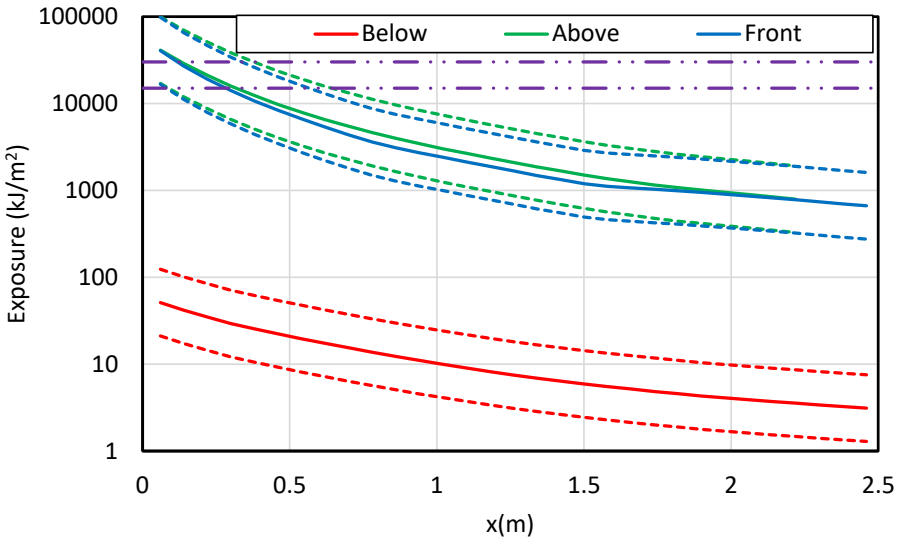

Figure B-104
Results for a steel duct NSBD tee with copper bus bars – 68 MJ HEAF (FDS Simulation NSBD-40)

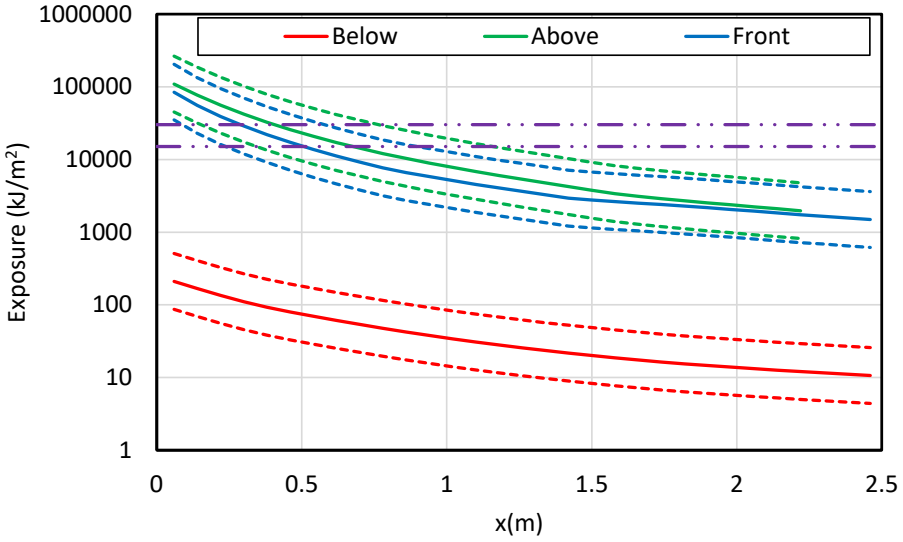

Figure B-105
Results for a steel duct NSBD tee with copper bus bars – 135 MJ HEAF (FDS Simulation NSBD-41)

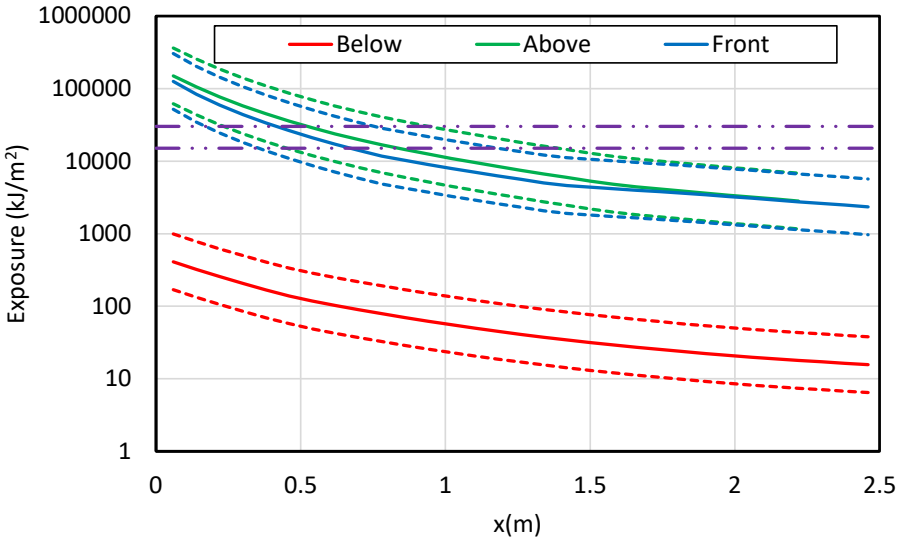

Figure B-106
Results for a steel duct NSBD tee with copper bus bars – 169 MJ HEAF (FDS Simulation NSBD-42)

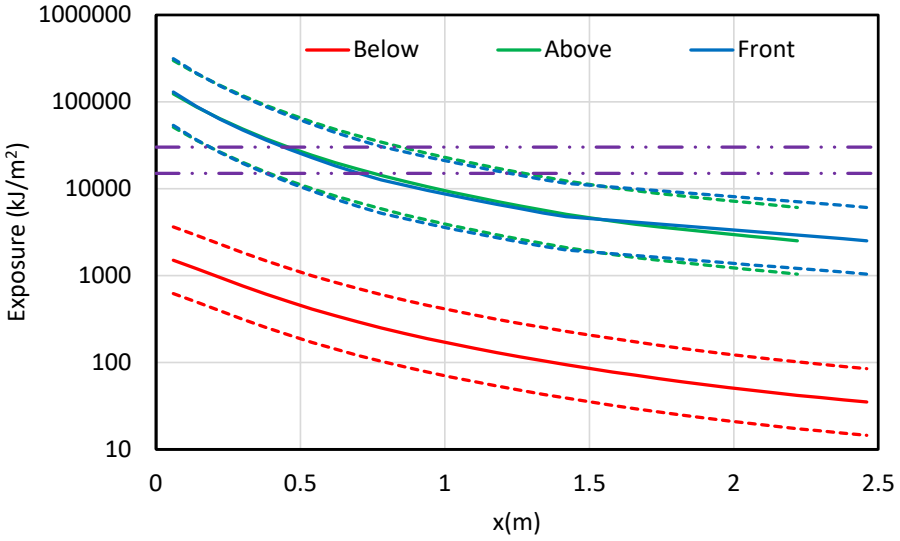

Figure B-107
Results for a steel duct NSBD tee with copper bus bars – 131 MJ HEAF (FDS Simulation NSBD-43)

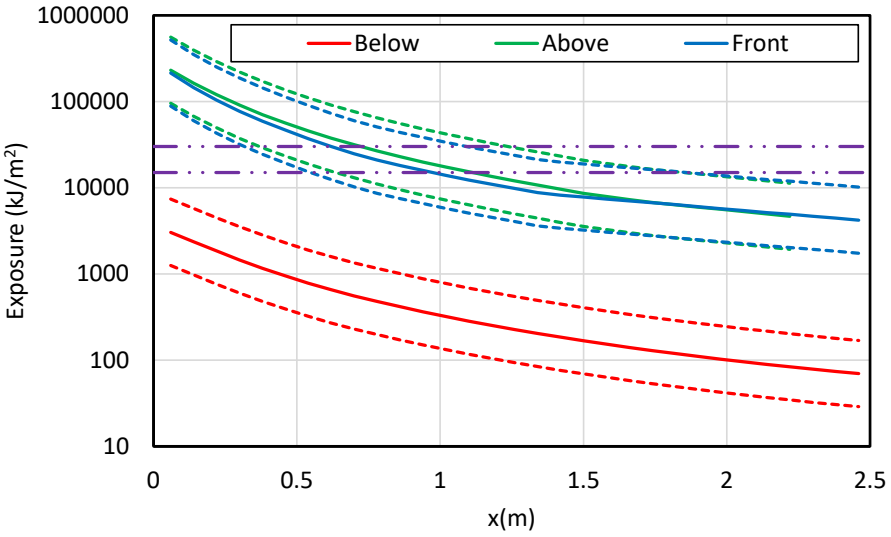

Figure B-108
Results for a steel duct NSBD tee with copper bus bars – 226 MJ HEAF (FDS Simulation NSBD-44)

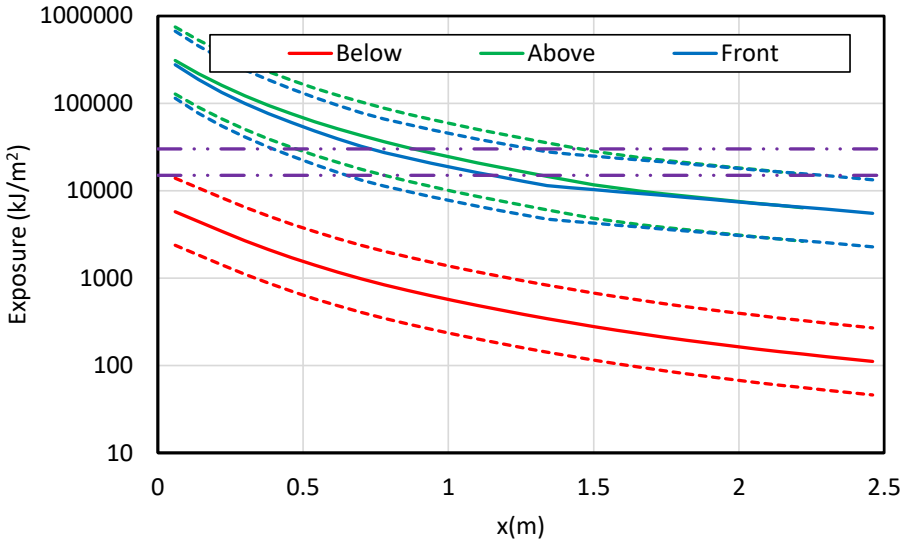

Figure B-109
Results for a steel duct NSBD tee with copper bus bars – 293 MJ HEAF (FDS Simulation NSBD-45)

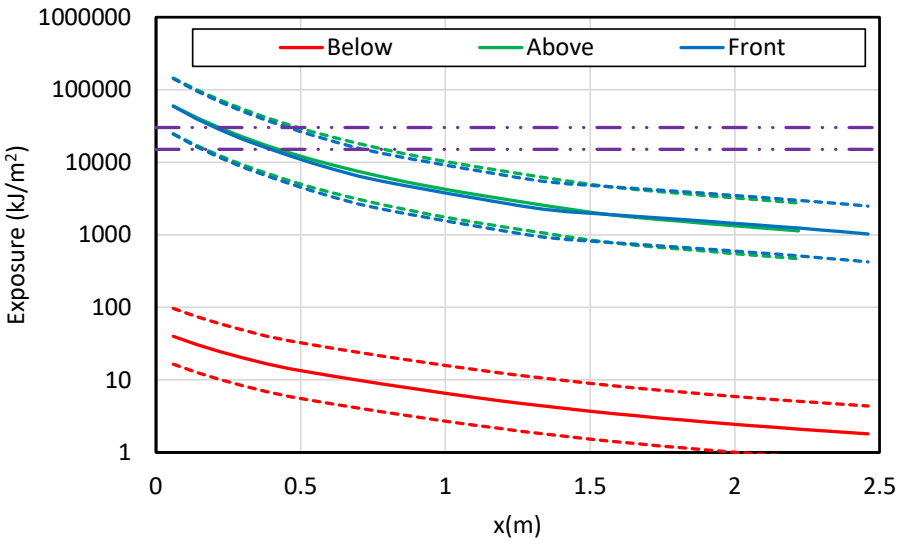

Figure B-110
Results for an aluminum duct NSBD tee with copper bus bars – 68 MJ HEAF (FDS Simulation NSBD-46)

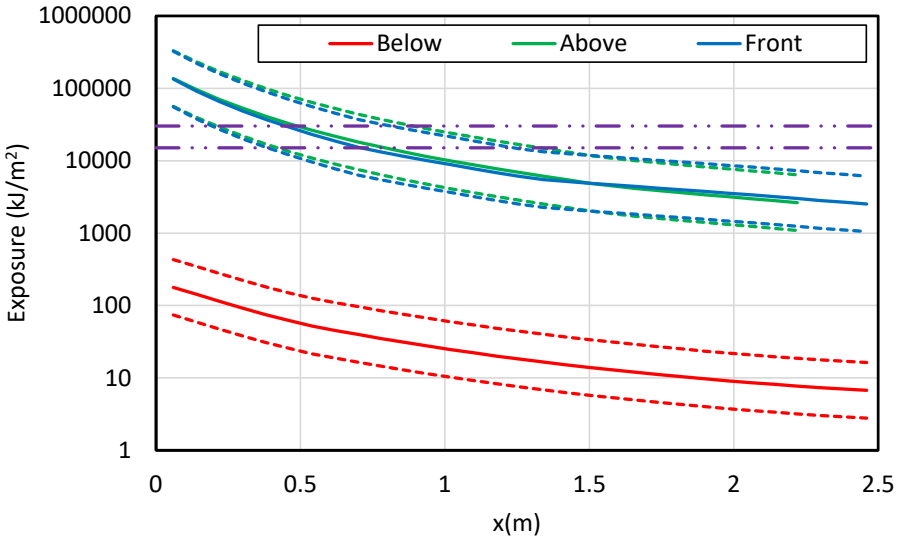

Figure B-111
Results for an aluminum duct NSBD tee with copper bus bars – 135 MJ HEAF (FDS Simulation NSBD-47)

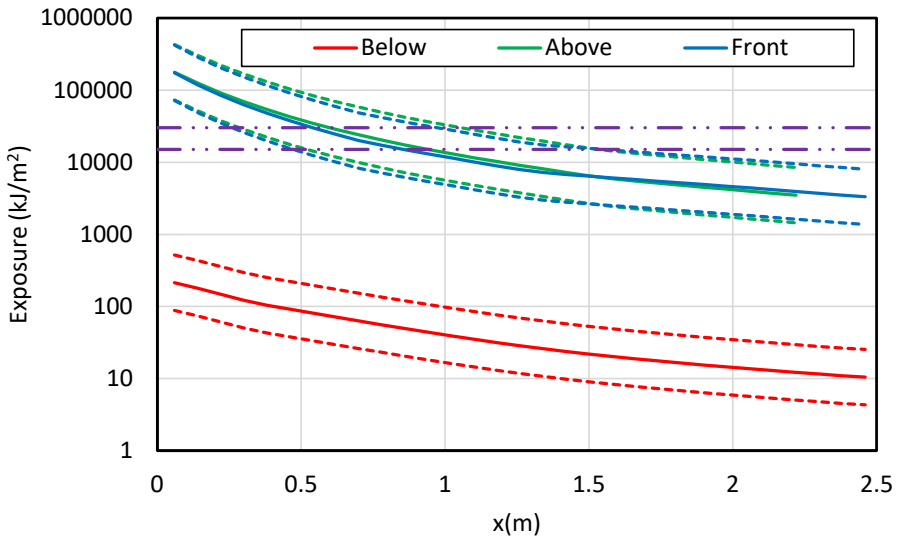

Figure B-112
Results for an aluminum duct NSBD tee with copper bus bars – 169 MJ HEAF (FDS Simulation NSBD-48)

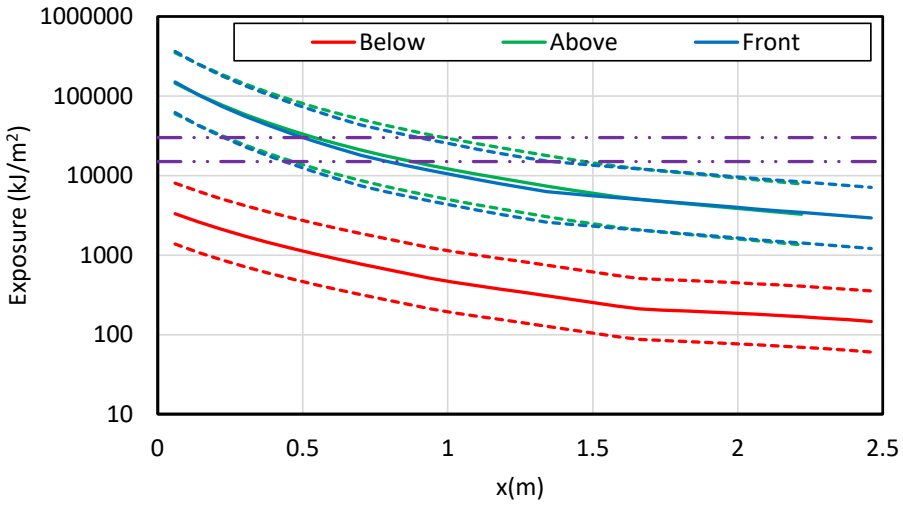

Figure B-113
Results for an aluminum duct NSBD tee with copper bus bars – 131 MJ HEAF (FDS Simulation NSBD-49)

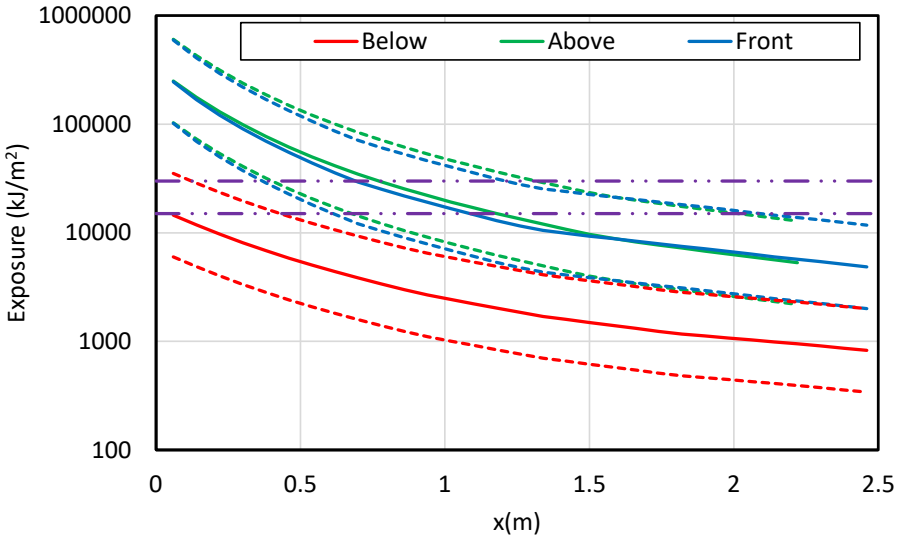

Figure B-114
Results for an aluminum duct NSBD tee with copper bus bars – 226 MJ HEAF (FDS Simulation NSBD-50)

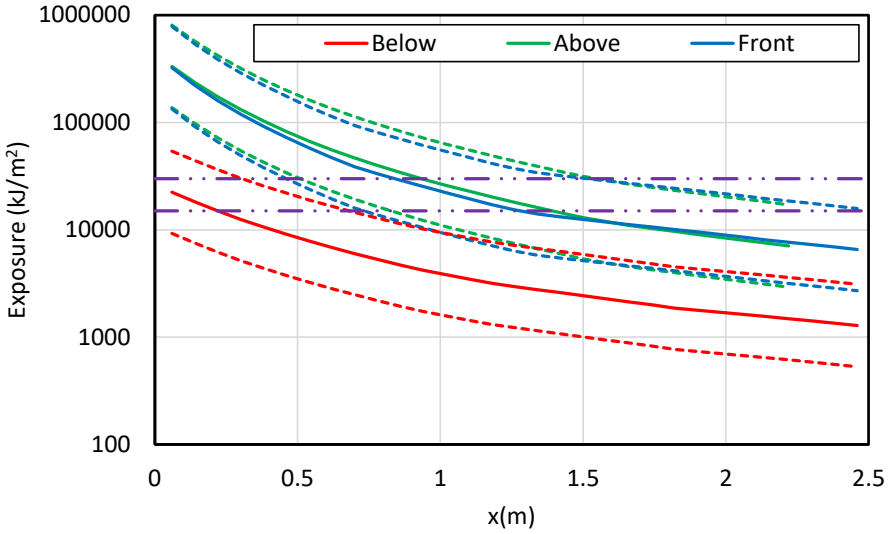

Figure B-115
Results for an aluminum duct NSBD tee with copper bus bars – 293 MJ HEAF (FDS Simulation NSBD-51)

C
FDS INPUT FILE TEMPLATES

This appendix contains the input file templates for each geometry modeled by FDS and a tabulation of the FDS input files and the specific HEAF simulations presented in Section 6 of this report.

C.1 FDS Input File Simulation Matrix

Table C-1 provides a summary of the FDS input files associated with each HEAF simulation presented in Section 6.

Table C-1
FDS input file simulation matrix

HEAF ID	Results Table	Type of HEAF	FDS Input File
MV-GE-1	6-1	MV SWGR	gemv_eAls2d0p33p8lMain.fds
MV-GE-2	6-1	MV SWGR	gemv_eAls2d0p33p8lRiser.fds
MV-GE-3	6-1	MV SWGR	gemv_eAls2d0p33p8lRiser_Supply.fds
MV-GE-4	6-1	MV SWGR	gemv_eAls4d0p33p8lMain.fds
MV-GE-5	6-1	MV SWGR	gemv_eAls4d0p33p8lRiser.fds
MV-GE-6	6-1	MV SWGR	gemv_eAls4d0p33p8lRiser_Supply.fds
MV-GE-7	6-1	MV SWGR	gemv_eAls5d0p33p8lMain.fds
MV-GE-8	6-1	MV SWGR	gemv_eAls5d0p33p8lRiser.fds
MV-GE-9	6-1	MV SWGR	gemv_eAls5d0p33p8lRiser_Supply.fds
MV-GE-10	6-1	MV SWGR	gemv_eAls0d15p33p8lMain.fds
MV-GE-11	6-1	MV SWGR	gemv_eAls0d15p33p8lRiser.fds
MV-GE-12	6-1	MV SWGR	gemv_eAls0d15p33p8lRiser_Supply.fds
MV-GE-13	6-1	MV SWGR	gemv_eAls3d15p33p8lMain.fds
MV-GE-14	6-1	MV SWGR	gemv_eAls3d15p33p8lRiser.fds
MV-GE-15	6-1	MV SWGR	gemv_eAls3d15p33p8lRiser_Supply.fds
MV-GE-16	6-1	MV SWGR	gemv_eAls5d15p33p8lMain.fds
MV-GE-17	6-1	MV SWGR	gemv_eAls5d15p33p8lRiser.fds
MV-GE-18	6-1	MV SWGR	gemv_eAls5d15p33p8lRiser_Supply.fds

HEAF ID	Results Table	Type of HEAF	FDS Input File
MV-GE-19	6-1	MV SWGR	gemv_eCus2d0p33p8lBreaker.fds
MV-GE-20	6-1	MV SWGR	gemv_eCus2d0p33p8lMain.fds
MV-GE-21	6-1	MV SWGR	gemv_eCus2d0p33p8lRiser.fds
MV-GE-22	6-1	MV SWGR	gemv_eCus2d0p33p8lRiser_Supply.fds
MV-GE-23	6-1	MV SWGR	gemv_eCus4d0p33p8lBreaker.fds
MV-GE-24	6-1	MV SWGR	gemv_eCus4d0p33p8lMain.fds
MV-GE-25	6-1	MV SWGR	gemv_eCus4d0p33p8lRiser.fds
MV-GE-26	6-1	MV SWGR	gemv_eCus4d0p33p8lRiser_Supply.fds
MV-GE-27	6-1	MV SWGR	gemv_eCus5d0p33p8lBreaker.fds
MV-GE-28	6-1	MV SWGR	gemv_eCus5d0p33p8lMain.fds
MV-GE-29	6-1	MV SWGR	gemv_eCus5d0p33p8lRiser.fds
MV-GE-30	6-1	MV SWGR	gemv_eCus5d0p33p8lRiser_Supply.fds
MV-GE-31	6-1	MV SWGR	gemv_eCus0d15p33p8lBreaker.fds
MV-GE-32	6-1	MV SWGR	gemv_eCus0d15p33p8lMain.fds
MV-GE-33	6-1	MV SWGR	gemv_eCus0d15p33p8lRiser.fds
MV-GE-34	6-1	MV SWGR	gemv_eCus0d15p33p8lRiser_Supply.fds
MV-GE-35	6-1	MV SWGR	gemv_eCus3d15p33p8lBreaker.fds
MV-GE-36	6-1	MV SWGR	gemv_eCus3d15p33p8lMain.fds
MV-GE-37	6-1	MV SWGR	gemv_eCus3d15p33p8lRiser.fds
MV-GE-38	6-1	MV SWGR	gemv_eCus3d15p33p8lRiser_Supply.fds
MV-GE-39	6-1	MV SWGR	gemv_eCus5d15p33p8lBreaker.fds
MV-GE-40	6-1	MV SWGR	gemv_eCus5d15p33p8lMain.fds
MV-GE-41	6-1	MV SWGR	gemv_eCus5d15p33p8lRiser.fds
MV-GE-42	6-1	MV SWGR	gemv_eCus5d15p33p8lRiser_Supply.fds
MV-ABB-1	6-1	MV SWGR	abbmv_eCus2d0lBreaker.fds
MV-ABB-2	6-1	MV SWGR	abbmv_eCus4d0lBreaker.fds
MV-ABB-3	6-1	MV SWGR	abbmv_eCus5d0lBreaker.fds
MV-ABB-4	6-1	MV SWGR	abbmv_eCus0d15lBreaker.fds
MV-ABB-5	6-1	MV SWGR	abbmv_eCus3d15lBreaker.fds

HEAF ID	Results Table	Type of HEAF	FDS Input File
MV-ABB-6	6-1	MV SWGR	abbmv_eCus5d15lBreaker.fds
LV-BASE-1	6-2	LV SWGR	lvswgr_eAlsFClBr_Mid-RE.fds
LV-BASE-2	6-2	LV SWGR	lvswgr_eAlsFClBr_Top-RE.fds
LV-BASE-3	6-2	LV SWGR	lvswgr_eAlsFClMid_Mid-RE.fds
LV-BASE-4	6-2	LV SWGR	lvswgr_eAlsFClMid_Top-RE.fds
LV-BASE-5	6-2	LV SWGR	lvswgr_eAlsFClBrMid_Mid-RE.fds
LV-BASE-6	6-2	LV SWGR	lvswgr_eAlsFClBrMid_Top-RE.fds
LV-BASE-7	6-2	LV SWGR	lvswgr_eCusFClMid_Mid-RE.fds
LV-BASE-8	6-2	LV SWGR	lvswgr_eCusFClMid_Top-RE.fds
LV-BASE-9	6-2	LV SWGR	lvswgr_eCusFClBr_Mid-RE.fds
LV-BASE-10	6-2	LV SWGR	lvswgr_eCusFClBr_Top-RE.fds
LV-SENS-1	6-2	LV SWGR	lvswgr_eAls2lBr_Mid.fds
LV-SENS-2	6-2	LV SWGR	lvswgr_eAls2lBr_Top.fds
LV-SENS-3	6-2	LV SWGR	lvswgr_eAls2lMid_Mid.fds
LV-SENS-4	6-2	LV SWGR	lvswgr_eAls2lMid_Top.fds
LV-SENS-5	6-2	LV SWGR	lvswgr_eCus2lBr_Mid.fds
LV-SENS-6	6-2	LV SWGR	lvswgr_eCus2lBr_Top.fds
LV-SENS-7	6-2	LV SWGR	lvswgr_eCus2lMid_Mid.fds
LV-SENS-8	6-2	LV SWGR	lvswgr_eCus2lMid_Top.fds
LV-SENS-9	6-2	LV SWGR	lvswgr_eAls4lBr_Mid.fds
LV-SENS-10	6-2	LV SWGR	lvswgr_eAls4lBr_Top.fds
LV-SENS-11	6-2	LV SWGR	lvswgr_eAls4lMid_Mid.fds
LV-SENS-12	6-2	LV SWGR	lvswgr_eAls4lMid_Top.fds
LV-SENS-13	6-2	LV SWGR	lvswgr_eCus4lBr_Mid.fds
LV-SENS-14	6-2	LV SWGR	lvswgr_eCus4lBr_Top.fds
LV-SENS-15	6-2	LV SWGR	lvswgr_eCus4lMid_Mid.fds
LV-SENS-16	6-2	LV SWGR	lvswgr_eCus4lMid_Top.fds
LV-SENS-17	6-2	LV SWGR	lvswgr_eAls6lBr_Mid.fds
LV-SENS-18	6-2	LV SWGR	lvswgr_eAls6lBr_Top.fds

HEAF ID	Results Table	Type of HEAF	FDS Input File
LV-SENS-19	6-2	LV SWGR	lvswgr_eAls6lMid_Mid.fds
LV-SENS-20	6-2	LV SWGR	lvswgr_eAls6lMid_Top.fds
LV-SENS-21	6-2	LV SWGR	lvswgr_eCus6lBr_Mid.fds
LV-SENS-22	6-2	LV SWGR	lvswgr_eCus6lBr_Top.fds
LV-SENS-23	6-2	LV SWGR	lvswgr_eCus6lMid_Mid.fds
LV-SENS-24	6-2	LV SWGR	lvswgr_eCus6lMid_Top.fds
NSBD-1	6-3	NSBD	bd_eAlhSts1d0cStraight.fds
NSBD-2	6-3	NSBD	bd_eAlhSts2d0cStraight.fds
NSBD-3	6-3	NSBD	bd_eAlhSts4d0cStraight.fds
NSBD-4	6-3	NSBD	bd_eAlhSts5d0cStraight.fds
NSBD-5	6-3	NSBD	bd_eAlhSts0d15cStraight.fds
NSBD-6	6-3	NSBD	bd_eAlhSts3d15cStraight.fds
NSBD-7	6-3	NSBD	bd_eAlhSts5d15cStraight.fds
NSBD-8	6-3	NSBD	bd_eAlhAls1d0cStraight.fds
NSBD-9	6-3	NSBD	bd_eAlhAls2d0cStraight.fds
NSBD-10	6-3	NSBD	bd_eAlhAls4d0cStraight.fds
NSBD-11	6-3	NSBD	bd_eAlhAls5d0cStraight.fds
NSBD-12	6-3	NSBD	bd_eAlhAls3d15cStraight.fds
NSBD-13	6-3	NSBD	bd_eAlhAls5d15cStraight.fds
NSBD-14	6-3	NSBD	bd_eCuhSts1d0cStraight.fds
NSBD-15	6-3	NSBD	bd_eCuhSts2d0cStraight.fds
NSBD-16	6-3	NSBD	bd_eCuhSts4d0cStraight.fds
NSBD-17	6-3	NSBD	bd_eCuhSts5d0cStraight.fds
NSBD-18	6-3	NSBD	bd_eCuhSts0d15cStraight.fds
NSBD-19	6-3	NSBD	bd_eCuhSts3d15cStraight.fds
NSBD-20	6-3	NSBD	bd_eCuhSts5d15cStraight.fds
NSBD-21	6-3	NSBD	bd_eCuhAls1d0cStraight.fds
NSBD-22	6-3	NSBD	bd_eCuhAls2d0cStraight.fds
NSBD-23	6-3	NSBD	bd_eCuhAls4d0cStraight.fds

HEAF ID	Results Table	Type of HEAF	FDS Input File
NSBD-24	6-3	NSBD	bd_eCuhAls5d0cStraight.fds
NSBD-25	6-3	NSBD	bd_eCuhAls0d15cStraight.fds
NSBD-26	6-3	NSBD	bd_eCuhAls3d15cStraight.fds
NSBD-27	6-3	NSBD	bd_eCuhAls5d15cStraight.fds
NSBD-28	6-3	NSBD	bd_eAlhSts2d0cTee.fds
NSBD-29	6-3	NSBD	bd_eAlhSts4d0cTee.fds
NSBD-30	6-3	NSBD	bd_eAlhSts5d0cTee.fds
NSBD-31	6-3	NSBD	bd_eAlhSts0d15cTee.fds
NSBD-32	6-3	NSBD	bd_eAlhSts3d15cTee.fds
NSBD-33	6-3	NSBD	bd_eAlhSts5d15cTee.fds
NSBD-34	6-3	NSBD	bd_eAlhAls2d0cTee.fds
NSBD-35	6-3	NSBD	bd_eAlhAls4d0cTee.fds
NSBD-36	6-3	NSBD	bd_eAlhAls5d0cTee.fds
NSBD-37	6-3	NSBD	bd_eAlhAls0d15cTee.fds
NSBD-38	6-3	NSBD	bd_eAlhAls3d15cTee.fds
NSBD-39	6-3	NSBD	bd_eAlhAls5d15cTee.fds
NSBD-40	6-3	NSBD	bd_eCuhSts2d0cTee.fds
NSBD-41	6-3	NSBD	bd_eCuhSts4d0cTee.fds
NSBD-42	6-3	NSBD	bd_eCuhSts5d0cTee.fds
NSBD-43	6-3	NSBD	bd_eCuhSts0d15cTee.fds
NSBD-44	6-3	NSBD	bd_eCuhSts3d15cTee.fds
NSBD-45	6-3	NSBD	bd_eCuhSts5d15cTee.fds
NSBD-46	6-3	NSBD	bd_eCuhAls2d0cTee.fds
NSBD-47	6-3	NSBD	bd_eCuhAls4d0cTee.fds
NSBD-48	6-3	NSBD	bd_eCuhAls5d0cTee.fds
NSBD-49	6-3	NSBD	bd_eCuhAls0d15cTee.fds
NSBD-50	6-3	NSBD	bd_eCuhAls3d15cTee.fds
NSBD-51	6-3	NSBD	bd_eCuhAls5d15cTee.fds
NSBD-52	6-3	NSBD	bd_eAlhAls2d0cElbow.fds

HEAF ID	Results Table	Type of HEAF	FDS Input File
NSBD-53	6-3	NSBD	bd_eAlhAls4d0cElbow.fds
NSBD-54	6-3	NSBD	bd_eAlhAls5d0cElbow.fds
NSBD-55	6-3	NSBD	bd_eAlhAls0d15cElbow.fds
NSBD-56	6-3	NSBD	bd_eAlhAls3d15cElbow.fds
NSBD-57	6-3	NSBD	bd_eAlhAls5d15cElbow.fds
NSBD-58	6-3	NSBD	bd_eAlhAls0d15cStraight.fds

C.2 Medium Voltage Switchgear

C.2.1 Vertical-Lift Breaker Style

```
&HEAD CHID='fileid'/

! 3 in. resolution. Approximately 2 m to each side, 2 m above, and 2.4 m front and
back.

&MESH ID='Cabinet',IJK=23,22,20,XB=-2.4384,-0.6858,-2.5146,-
0.8382,0.0000,1.5240,MULT_ID='M1'/ 3 in. resolution
&MULT ID='M1',I_UPPER=3,DX=1.7526,J_UPPER=2,DY=1.6764,K_UPPER=2,DZ=1.5240/

&VENT MB='ZMAX',SURF_ID='OPEN'/
&VENT MB='YMAX',SURF_ID='OPEN'/
&VENT MB='XMAX',SURF_ID='OPEN'/
&VENT MB='YMIN',SURF_ID='OPEN'/
&VENT MB='XMIN',SURF_ID='OPEN'/

! I_MAX_TEMP=35000 ensures property arrays are high enough for the CLIP values.
! AEROSOL_AL2O3 replaces default SOOT radiative properties with those for AL2O3

&MISC AEROSOL_AL2O3=T,I_MAX_TEMP=35000 /

! SMOKE3D_SPEC_ID sets the species used by Smokeview to visualize smoke

&DUMP SMOKE3D_SPEC_ID='3dsmoke',SUPPRESS_DIAGNOSTICS=F,MASS_FILE=T/

! Turns off the extinction model. Default values in the model may not be appropriate
for metal oxidation
&COMB SUPPRESSION=F /

! 0.01 kg/m3 greatly limits clipping of density.
&CLIP MINIMUM_DENSITY=0.01, MAXIMUM_TEMPERATURE=35000.,CLIP_DT_RESTRICTIONS_MAX=0 /

! These cases a very challenging for the pressure solver. The selected values seem to
give enough pressure iterations to
! drop the velocity error down to a plateau value.

&PRES MAX_PRESSURE_ITERATIONS=30, VELOCITY_TOLERANCE=0.001,
SUSPEND_PRESSURE_ITERATIONS=F/

! For ZOI runs suggest T_END = arc time + 8 s

&TIME T_END=tend, DT=0.001,WALL_INCREMENT=1 /
```

```
&RADI NUMBER_RADIATION_ANGLES=500 /

! 1 cell thick OBST to help out pressure solver.

&OBST XB=0.0000,0.0762,-0.4572,0.4572,0.4572,2.2860,SURF_ID='CABINET'/
&OBST XB=0.0000,0.0762,-0.4572,0.4572,0.0000,0.1524,SURF_ID='CABINET'/
&OBST XB=0.0000,0.0762,-0.4572,0.4572,0.2286,0.3810,SURF_ID='CABINET'/
&OBST XB=0.0000,0.0762,-0.4572,-0.3048,0.1524,0.2286,SURF_ID='CABINET'/
&OBST XB=0.0000,0.0762,-0.0762,0.0762,0.1524,0.2286,SURF_ID='CABINET'/
&OBST XB=0.0000,0.0762,0.3048,0.4572,0.1524,0.2286,SURF_ID='CABINET'/
&OBST XB=0.0000,0.0762,-0.4572,-0.3048,0.3810,0.4572,SURF_ID='CABINET'/
&OBST XB=0.0000,0.0762,-0.0762,0.0762,0.3810,0.4572,SURF_ID='CABINET'/
&OBST XB=0.0000,0.0762,0.3048,0.4572,0.3810,0.4572,SURF_ID='CABINET'/
&OBST XB=0.0000,1.5240,-0.4572,0.4572,2.2860,2.3622,SURF_ID='CABINET'/
&OBST XB=1.5240,1.7526,-0.1524,-0.0762,2.2860,2.3622,SURF_ID='CABINET'/
&OBST XB=1.5240,1.7526, 0.0762, 0.1524,2.2860,2.3622,SURF_ID='CABINET'/
&OBST XB=1.7526,2.1336,-0.4572,0.4572,2.2860,2.3622,SURF_ID='CABINET'/
&OBST XB=0.0000,2.1336,-0.5334,-0.4572,0.0000,2.3622,SURF_ID='CABINET'/
&OBST XB=0.0000,2.1336,0.4572,0.5334,0.0000,2.3622,SURF_ID='CABINET'/
&OBST XB=0.5334,1.7526,-0.4572,0.4572,1.3716,1.4478,SURF_ID='CABINET'/
&OBST XB=1.2954,1.3716,-0.4572,0.4572,1.4478,2.2098,SURF_ID='CABINET'/
&OBST XB=1.2954,1.3716,-0.4572,-0.3810,2.2098,2.2860,SURF_ID='CABINET'/
&OBST XB=1.2954,1.3716,0.3810,0.4572,2.2098,2.2860,SURF_ID='CABINET'/
&OBST XB=1.6764,1.7526,-0.4572,0.4572,1.4478,2.2098,SURF_ID='CABINET'/
&OBST XB=1.2954,1.5240,-0.4572,0.4572,2.1336,2.2098,SURF_ID='CABINET'/
&OBST XB=1.6002,1.7526,-0.4572,0.4572,2.1336,2.2098,SURF_ID='CABINET'/
&OBST XB=0.5334,0.6096,-0.4572,0.4572,0.0000,1.3716,SURF_ID='CABINET'/
&OBST XB=0.6858,1.8288,-0.3810,0.3810,0.0762,0.9906,SURF_ID='BREAKER'/
&OBST XB=1.2954,1.8288,-0.3810,0.3810,0.9906,1.0668,SURF_ID='BREAKER'/

! RADCAL_ID='SOOT' makes the SPEC use the SOOT radiation properties which the MISC
line has changed to those for AL2O3
! RAMPs used instead of built in cp data for N2, CO2, and O2 to extend temperature to
20,000 K

&SPEC ID='WET NITROGEN',BACKGROUND=T,SPEC_ID='NITROGEN','CARBON DIOXIDE','WATER
VAPOR',MASS_FRACTION=1,0.000775,0.007792/FDS Default AIR without O2
&SPEC ID='NITROGEN', LUMPED_COMPONENT_ONLY=T,RAMP_CP='N2 C'/
&SPEC ID='CARBON DIOXIDE', LUMPED_COMPONENT_ONLY=T,RAMP_CP='CO2 C'/
&SPEC ID='WATER VAPOR', LUMPED_COMPONENT_ONLY=T /
&SPEC ID='OXYGEN', MASS_FRACTION_0=0.230997,RAMP_CP='O2 C' /
alspec1 ID='ALUMINUM',FORMULA='Al',RAMP_CP='AL
C',SIGMALJ=2.655,EPSILONKLJ=2750.,PR_GAS=1/
alspec2 ID='ALUMINUM
OXIDE',MASS_EXTINCTION_COEFFICIENT=3000,FORMULA='Al2O3',RAMP_CP='AL2O3
C',SIGMALJ=3.186,EPSILONKLJ=557.449,PR_GAS=1,RADCAL_ID='SOOT'/
cuspec1 ID='COPPER',FORMULA='Cu',RAMP_CP='CU
C',SIGMALJ=5.058,EPSILONKLJ=2983.,PR_GAS=1/
cuspec2 ID='COPPER
OXIDE',MASS_EXTINCTION_COEFFICIENT=3000,FORMULA='Cu2O',SPECIFIC_HEAT=0.7,SIGMALJ=5.403
,PR_GAS=1,RADCAL_ID='SOOT'/C from JANAF, LJ take as CuO

alreac FUEL='ALUMINUM', SPEC_ID_NU='ALUMINUM','OXYGEN','ALUMINUM OXIDE', NU=-2,-1.5,1,
HEAT_OF_COMBUSTION=31100. / Al -> AL2O3
cureac FUEL='COPPER',SPEC_ID_NU='COPPER','OXYGEN','COPPER OXIDE',NU=-2,-
0.5,1,HEAT_OF_COMBUSTION=1340./ Cu->Cu2O

&MATL ID='CONCRETE', DENSITY=2400, CONDUCTIVITY=1.6, SPECIFIC_HEAT=0.75,
EMISSIVITY=0.95 /

! Non-melting steel
&MATL ID='INERT STEEL', DENSITY=7800., SPECIFIC_HEAT_RAMP='STEEL C',
CONDUCTIVITY_RAMP='STEEL K', EMISSIVITY=0.85/
```

```
! Melting steel
&MATL ID='STEEL', DENSITY=7800., SPECIFIC_HEAT_RAMP='STEEL C',
CONDUCTIVITY_RAMP='STEEL K', EMISSIVITY=0.85,
      THRESHOLD_TEMPERATURE=1300., THRESHOLD_SIGN=1, HEAT_OF_REACTION(1)=250.,
PCR(1)=T, A(1)=0.6, E(1)=0., N_S(1)=0., N_T(1)=1. /

! Eurocode values
&RAMP ID='STEEL C',T=20,F=0.440/
&RAMP ID='STEEL C',T=600,F=0.760/
&RAMP ID='STEEL C',T=700,F=1.008/
&RAMP ID='STEEL C',T=720,F=1.388/
&RAMP ID='STEEL C',T=725,F=1.666/
&RAMP ID='STEEL C',T=730,F=2.291/
&RAMP ID='STEEL C',T=735,F=5.000/
&RAMP ID='STEEL C',T=740,F=2.525/ BCC -> FCC Transition
&RAMP ID='STEEL C',T=745,F=1.818/
&RAMP ID='STEEL C',T=750,F=1.483/
&RAMP ID='STEEL C',T=800,F=0.803/
&RAMP ID='STEEL C',T=900,F=0.650/

&RAMP ID='STEEL K',T=20,F=53.3/
&RAMP ID='STEEL K',T=800,F=27.3/

&SURF ID='BREAKER', MATL_ID='INERT STEEL', THICKNESS=0.02,
RGB=204,204,255,CELL_SIZE_FACTOR=0.05,STRETCH_FACTOR=1 /
&SURF ID='CABINET', MATL_ID='STEEL', THICKNESS=0.002381,  COLOR='GRAY 60',
BURN_AWAY=.TRUE.,CELL_SIZE_FACTOR=0.05,STRETCH_FACTOR=1 /
&SURF ID='FLOOR', MATL_ID='CONCRETE', THICKNESS=0.15, RGB=50,50,50, DEFAULT=T /

!The block below defines particles that emit vapor for aluminum.
!The particles are initialized at the melting point.
!The PROP MASS_FLOW_RATE is the maximum liquid production rate divided by the number
of electrodes
!NU_SPEC and NU_MATL are set to get the 75 % oxidation for Al and 25 % for Cu. The
second MOLTEN AL2 and CU2 species have a modified density to preserve diameter.
!A and E are set to give the vapor over 0.3 s.

almatl1 ID='MOLTEN
AL',DENSITY=2375,CONDUCTIVITY=100.,SPECIFIC_HEAT=1.177,EMISSIVITY=0,A=3.333,E=0,
N_REACTIONS=1,HEAT_OF_REACTION=0,HEAT_OF_COMBUSTION=0,MATL_ID(1,1)='MOLTEN
AL2',SPEC_ID(1,1)='ALUMINUM',NU_MATL(1,1)=0.25,NU_SPEC(1,1)=0.75/
almatl2 ID='MOLTEN
AL2',DENSITY=593.75,SPEC_ID='ALUMINUM',NU_SPEC=1,CONDUCTIVITY=100.,SPECIFIC_HEAT=1.177
/

alsurf1 ID='AL DROP',MATL_ID='MOLTEN AL',GEOMETRY='SPHERICAL',THICKNESS=5.E-
6,HEAT_TRANSFER_COEFFICIENT=0,TMP_INNER=665.3/
alpart1 ID='AL DROPS',SURF_ID='AL
DROP',AGE=2.0,SAMPLING_FACTOR=10,MONODISPERSE=T,RGB=100,100,100/
alprop1 ID='DROPS',PART_ID='AL DROPS',FLOW_RAMP='RAMP
MF',MASS_FLOW_RATE=almfr,PARTICLES_PER_SECOND=20000,PARTICLE_VELOCITY=10,SPRAY_ANGLE=0
,60/

! The block below is for copper.

cumatl1 ID='MOLTEN
CU',DENSITY=8960,CONDUCTIVITY=340.,SPECIFIC_HEAT=0.517,EMISSIVITY=0,A=3.333,E=0,
N_REACTIONS=1,HEAT_OF_REACTION=0,HEAT_OF_COMBUSTION=0,MATL_ID(1,1)='MOLTEN
CU2',SPEC_ID(1,1)='COPPER',NU_MATL(1,1)=0.75,NU_SPEC(1,1)=0.25/
cumatl2 ID='MOLTEN
CU2',DENSITY=7168,CONDUCTIVITY=340.,SPECIFIC_HEAT=0.517,EMISSIVITY=0/

cusurf1 ID='CU DROP',MATL_ID='MOLTEN CU',GEOMETRY='SPHERICAL',THICKNESS=5.E-
6,HEAT_TRANSFER_COEFFICIENT=0,TMP_INNER=1084.85/
```

```
cupart1 ID='CU DROPS',SURF_ID='CU
DROP',AGE=2.0,SAMPLING_FACTOR=10,MONODISPERSE=T,RGB=184,115,51/
cuprop1 ID='DROPS',PART_ID='CU DROPS',FLOW_RAMP='RAMP
MF',MASS_FLOW_RATE=cumfr,PARTICLES_PER_SECOND=20000,PARTICLE_VELOCITY=10,SPRAY_ANGLE=0
,60/

! First INIT line is the volumetric source term where the RADAITIVE_FRACTION uses
Cressault's data interpolated based on power,. The HRRPUV is
! reduced based on energy needed to degrade the electrodes:
! Adjusted total energy = (Total arc energy - electrode mass loss * (vapor fraction *
energy to vaporize + liquid fraction * energy to melt))
!
! Cressault data:
!
! X_r,Al = 0.2275*Max_Power^0.3292
! X_r,Al = 0.1273*Max_Power^0.3859
!
! Phase  Energy (kJ/kg)
! Change    Al     Cu
! Melt    1063.4  695.2

&INIT XB=initx1,initx2,inity1,inity2,initz1,initz2,HRRPUV=hrrpuvval,RAMP_Q='RAMP
Q',RADIATIVE_FRACTION=radfrac/

! One spray nozzle device per electrode that inject liquid droplets

&DEVC
PROP_ID='DROPS',XYZ=nozx1,nozy1,nozz1,QUANTITY='TIME',SETPOINT=0.0,ORIENTATION=orient1
,orient2,orient3/
&DEVC
PROP_ID='DROPS',XYZ=nozx2,nozy2,nozz2,QUANTITY='TIME',SETPOINT=0.0,ORIENTATION=orient1
,orient2,orient3/
&DEVC
PROP_ID='DROPS',XYZ=nozx3,nozy3,nozz3,QUANTITY='TIME',SETPOINT=0.0,ORIENTATION=orient1
,orient2,orient3/

! An 0.1 s ramp up and down for the arc volumetric source term helps avoid numerical
instabilities

&RAMP ID='RAMP Q',T=0.0,F=0.0000/
&RAMP ID='RAMP Q',T=0.1,F=rampqf1/
&RAMP ID='RAMP Q',T=0.2,F=rampqf2/
&RAMP ID='RAMP Q',T=0.3,F=rampqf3/
&RAMP ID='RAMP Q',T=0.4,F=rampqf4/
&RAMP ID='RAMP Q',T=0.5,F=rampqf5/
&RAMP ID='RAMP Q',T=0.6,F=rampqf6/
&RAMP ID='RAMP Q',T=0.7,F=rampqf7/
&RAMP ID='RAMP Q',T=0.8,F=rampqf8/
&RAMP ID='RAMP Q',T=0.9,F=rampqf9/
&RAMP ID='RAMP Q',T=1.0,F=rampqf10/
&RAMP ID='RAMP Q',T=1.1,F=rampqf11/
&RAMP ID='RAMP Q',T=1.2,F=rampqf12/
&RAMP ID='RAMP Q',T=1.3,F=rampqf13/
&RAMP ID='RAMP Q',T=1.4,F=rampqf14/
&RAMP ID='RAMP Q',T=1.5,F=rampqf15/
&RAMP ID='RAMP Q',T=1.6,F=rampqf16/
&RAMP ID='RAMP Q',T=1.7,F=rampqf17/
&RAMP ID='RAMP Q',T=1.8,F=rampqf18/
&RAMP ID='RAMP Q',T=1.9,F=rampqf19/
&RAMP ID='RAMP Q',T=2.0,F=rampqf20/
&RAMP ID='RAMP Q',T=2.1,F=rampqf21/
&RAMP ID='RAMP Q',T=2.2,F=rampqf22/
&RAMP ID='RAMP Q',T=2.3,F=rampqf23/
&RAMP ID='RAMP Q',T=2.4,F=rampqf24/
```

```
&RAMP ID='RAMP Q',T=2.5,F=rampqf25/
&RAMP ID='RAMP Q',T=2.6,F=rampqf26/
&RAMP ID='RAMP Q',T=2.7,F=rampqf27/
&RAMP ID='RAMP Q',T=2.8,F=rampqf28/
&RAMP ID='RAMP Q',T=2.9,F=rampqf29/
&RAMP ID='RAMP Q',T=3.0,F=rampqf30/
&RAMP ID='RAMP Q',T=3.1,F=rampqf31/
&RAMP ID='RAMP Q',T=3.2,F=rampqf32/
&RAMP ID='RAMP Q',T=3.3,F=rampqf33/
&RAMP ID='RAMP Q',T=3.4,F=rampqf34/
&RAMP ID='RAMP Q',T=3.5,F=rampqf35/
&RAMP ID='RAMP Q',T=3.6,F=rampqf36/
&RAMP ID='RAMP Q',T=3.7,F=rampqf37/
&RAMP ID='RAMP Q',T=3.8,F=rampqf38/
&RAMP ID='RAMP Q',T=3.9,F=rampqf39/
&RAMP ID='RAMP Q',T=4.0,F=rampqf40/
&RAMP ID='RAMP Q',T=4.1,F=rampqf41/
&RAMP ID='RAMP Q',T=4.2,F=rampqf42/
&RAMP ID='RAMP Q',T=4.3,F=rampqf43/
&RAMP ID='RAMP Q',T=4.4,F=rampqf44/
&RAMP ID='RAMP Q',T=4.5,F=rampqf45/
&RAMP ID='RAMP Q',T=4.6,F=rampqf46/
&RAMP ID='RAMP Q',T=4.7,F=rampqf47/
&RAMP ID='RAMP Q',T=4.8,F=rampqf48/
&RAMP ID='RAMP Q',T=4.9,F=rampqf49/
&RAMP ID='RAMP Q',T=5.0,F=rampqf50/
&RAMP ID='RAMP Q',T=5.1,F=rampqf51/
&RAMP ID='RAMP Q',T=5.2,F=rampqf52/
&RAMP ID='RAMP Q',T=5.3,F=rampqf53/
&RAMP ID='RAMP Q',T=5.4,F=rampqf54/
&RAMP ID='RAMP Q',T=5.5,F=rampqf55/
&RAMP ID='RAMP Q',T=5.6,F=rampqf56/
&RAMP ID='RAMP Q',T=5.7,F=rampqf57/
&RAMP ID='RAMP Q',T=5.8,F=rampqf58/
&RAMP ID='RAMP Q',T=5.9,F=rampqf59/
&RAMP ID='RAMP Q',T=6.0,F=rampqf60/
&RAMP ID='RAMP Q',T=6.1,F=rampqf61/
&RAMP ID='RAMP Q',T=6.2,F=rampqf62/
&RAMP ID='RAMP Q',T=6.3,F=rampqf63/
&RAMP ID='RAMP Q',T=6.4,F=rampqf64/
&RAMP ID='RAMP Q',T=6.5,F=rampqf65/
&RAMP ID='RAMP Q',T=6.6,F=rampqf66/
&RAMP ID='RAMP Q',T=6.7,F=rampqf67/
&RAMP ID='RAMP Q',T=6.8,F=rampqf68/
&RAMP ID='RAMP Q',T=6.9,F=rampqf69/
&RAMP ID='RAMP Q',T=7.0,F=rampqf70/
&RAMP ID='RAMP Q',T=7.1,F=rampqf71/
&RAMP ID='RAMP Q',T=7.2,F=rampqf72/
&RAMP ID='RAMP Q',T=7.3,F=rampqf73/
&RAMP ID='RAMP Q',T=7.4,F=rampqf74/
&RAMP ID='RAMP Q',T=7.5,F=rampqf75/
&RAMP ID='RAMP Q',T=7.6,F=rampqf76/
&RAMP ID='RAMP Q',T=7.7,F=rampqf77/
&RAMP ID='RAMP Q',T=7.8,F=rampqf78/
&RAMP ID='RAMP Q',T=7.9,F=rampqf79/
&RAMP ID='RAMP Q',T=8.0,F=rampqf80/
&RAMP ID='RAMP Q',T=8.1,F=rampqf81/
&RAMP ID='RAMP Q',T=8.2,F=rampqf82/
&RAMP ID='RAMP Q',T=8.3,F=rampqf83/
&RAMP ID='RAMP Q',T=8.4,F=rampqf84/
&RAMP ID='RAMP Q',T=8.5,F=rampqf85/
&RAMP ID='RAMP Q',T=8.6,F=rampqf86/
&RAMP ID='RAMP Q',T=8.7,F=rampqf87/
&RAMP ID='RAMP Q',T=8.8,F=rampqf88/
```

```
&RAMP ID='RAMP Q',T=8.9,F=rampqf89/
&RAMP ID='RAMP Q',T=9.0,F=rampqf90/
&RAMP ID='RAMP Q',T=9.1,F=rampqf91/
&RAMP ID='RAMP Q',T=9.2,F=rampqf92/
&RAMP ID='RAMP Q',T=9.3,F=rampqf93/
&RAMP ID='RAMP Q',T=9.4,F=rampqf94/
&RAMP ID='RAMP Q',T=9.5,F=rampqf95/
&RAMP ID='RAMP Q',T=9.6,F=rampqf96/
&RAMP ID='RAMP Q',T=9.7,F=rampqf97/
&RAMP ID='RAMP Q',T=9.8,F=rampqf98/
&RAMP ID='RAMP Q',T=9.9,F=rampqf99/
&RAMP ID='RAMP Q',T=10.0,F=rampqf100/
&RAMP ID='RAMP Q',T=10.1,F=rampqf101/
&RAMP ID='RAMP Q',T=10.2,F=rampqf102/
&RAMP ID='RAMP Q',T=10.3,F=rampqf103/
&RAMP ID='RAMP Q',T=10.4,F=rampqf104/
&RAMP ID='RAMP Q',T=10.5,F=rampqf105/
&RAMP ID='RAMP Q',T=10.6,F=rampqf106/
&RAMP ID='RAMP Q',T=10.7,F=rampqf107/
&RAMP ID='RAMP Q',T=10.8,F=rampqf108/
&RAMP ID='RAMP Q',T=10.9,F=rampqf109/
&RAMP ID='RAMP Q',T=11.0,F=rampqf110/
&RAMP ID='RAMP Q',T=11.1,F=rampqf111/
&RAMP ID='RAMP Q',T=11.2,F=rampqf112/
&RAMP ID='RAMP Q',T=11.3,F=rampqf113/
&RAMP ID='RAMP Q',T=11.4,F=rampqf114/
&RAMP ID='RAMP Q',T=11.5,F=rampqf115/
&RAMP ID='RAMP Q',T=11.6,F=rampqf116/
&RAMP ID='RAMP Q',T=11.7,F=rampqf117/
&RAMP ID='RAMP Q',T=11.8,F=rampqf118/
&RAMP ID='RAMP Q',T=11.9,F=rampqf119/
&RAMP ID='RAMP Q',T=12.0,F=rampqf120/
&RAMP ID='RAMP Q',T=12.1,F=rampqf121/
&RAMP ID='RAMP Q',T=12.2,F=rampqf122/
&RAMP ID='RAMP Q',T=12.3,F=rampqf123/
&RAMP ID='RAMP Q',T=12.4,F=rampqf124/
&RAMP ID='RAMP Q',T=12.5,F=rampqf125/
&RAMP ID='RAMP Q',T=12.6,F=rampqf126/
&RAMP ID='RAMP Q',T=12.7,F=rampqf127/
&RAMP ID='RAMP Q',T=12.8,F=rampqf128/
&RAMP ID='RAMP Q',T=12.9,F=rampqf129/
&RAMP ID='RAMP Q',T=13.0,F=rampqf130/
&RAMP ID='RAMP Q',T=13.1,F=rampqf131/
&RAMP ID='RAMP Q',T=13.2,F=rampqf132/
&RAMP ID='RAMP Q',T=13.3,F=rampqf133/
&RAMP ID='RAMP Q',T=13.4,F=rampqf134/
&RAMP ID='RAMP Q',T=13.5,F=rampqf135/
&RAMP ID='RAMP Q',T=13.6,F=rampqf136/
&RAMP ID='RAMP Q',T=13.7,F=rampqf137/
&RAMP ID='RAMP Q',T=13.8,F=rampqf138/
&RAMP ID='RAMP Q',T=13.9,F=rampqf139/
&RAMP ID='RAMP Q',T=14.0,F=rampqf140/
&RAMP ID='RAMP Q',T=14.1,F=rampqf141/
&RAMP ID='RAMP Q',T=14.2,F=rampqf142/
&RAMP ID='RAMP Q',T=14.3,F=rampqf143/
&RAMP ID='RAMP Q',T=14.4,F=rampqf144/
&RAMP ID='RAMP Q',T=14.5,F=rampqf145/
&RAMP ID='RAMP Q',T=14.6,F=rampqf146/
&RAMP ID='RAMP Q',T=14.7,F=rampqf147/
&RAMP ID='RAMP Q',T=14.8,F=rampqf148/
&RAMP ID='RAMP Q',T=14.9,F=rampqf149/
&RAMP ID='RAMP Q',T=15.0,F=rampqf150/
&RAMP ID='RAMP Q',T=15.1,F=rampqf151/
&RAMP ID='RAMP Q',T=15.2,F=rampqf152/
```

```
&RAMP ID='RAMP Q',T=15.3,F=rampqf153/
&RAMP ID='RAMP Q',T=15.4,F=rampqf154/
&RAMP ID='RAMP Q',T=15.5,F=rampqf155/
&RAMP ID='RAMP Q',T=15.6,F=rampqf156/
&RAMP ID='RAMP Q',T=15.7,F=rampqf157/
&RAMP ID='RAMP Q',T=15.8,F=rampqf158/
&RAMP ID='RAMP Q',T=15.9,F=rampqf159/
&RAMP ID='RAMP Q',T=16.0,F=rampqf160/
&RAMP ID='RAMP Q',T=16.1,F=rampqf161/
&RAMP ID='RAMP Q',T=16.2,F=rampqf162/
&RAMP ID='RAMP Q',T=16.3,F=rampqf163/
&RAMP ID='RAMP Q',T=16.4,F=rampqf164/
&RAMP ID='RAMP Q',T=16.5,F=rampqf165/
&RAMP ID='RAMP Q',T=16.6,F=rampqf166/
&RAMP ID='RAMP Q',T=16.7,F=rampqf167/
&RAMP ID='RAMP Q',T=16.8,F=rampqf168/
&RAMP ID='RAMP Q',T=16.9,F=rampqf169/
&RAMP ID='RAMP Q',T=17.0,F=rampqf170/
&RAMP ID='RAMP Q',T=17.1,F=rampqf171/
&RAMP ID='RAMP Q',T=17.2,F=rampqf172/
&RAMP ID='RAMP Q',T=17.3,F=rampqf173/
&RAMP ID='RAMP Q',T=17.4,F=rampqf174/
&RAMP ID='RAMP Q',T=17.5,F=rampqf175/
&RAMP ID='RAMP Q',T=17.6,F=rampqf176/
&RAMP ID='RAMP Q',T=17.7,F=rampqf177/
&RAMP ID='RAMP Q',T=17.8,F=rampqf178/
&RAMP ID='RAMP Q',T=17.9,F=rampqf179/
&RAMP ID='RAMP Q',T=18.0,F=rampqf180/
&RAMP ID='RAMP Q',T=18.1,F=rampqf181/
&RAMP ID='RAMP Q',T=18.2,F=rampqf182/
&RAMP ID='RAMP Q',T=18.3,F=rampqf183/
&RAMP ID='RAMP Q',T=18.4,F=rampqf184/
&RAMP ID='RAMP Q',T=18.5,F=rampqf185/
&RAMP ID='RAMP Q',T=18.6,F=rampqf186/
&RAMP ID='RAMP Q',T=18.7,F=rampqf187/
&RAMP ID='RAMP Q',T=18.8,F=rampqf188/
&RAMP ID='RAMP Q',T=18.9,F=rampqf189/
&RAMP ID='RAMP Q',T=19.0,F=rampqf190/
&RAMP ID='RAMP Q',T=19.1,F=rampqf191/
&RAMP ID='RAMP Q',T=19.2,F=rampqf192/
&RAMP ID='RAMP Q',T=19.3,F=rampqf193/
&RAMP ID='RAMP Q',T=19.4,F=rampqf194/
&RAMP ID='RAMP Q',T=19.5,F=rampqf195/
&RAMP ID='RAMP Q',T=19.6,F=rampqf196/
&RAMP ID='RAMP Q',T=19.7,F=rampqf197/
&RAMP ID='RAMP Q',T=19.8,F=rampqf198/
&RAMP ID='RAMP Q',T=19.9,F=rampqf199/
&RAMP ID='RAMP Q',T=20.0,F=rampqf200/
&RAMP ID='RAMP Q',T=20.1,F=0.0000/

! RAMP for droplets

&RAMP ID='RAMP MF',T=0.00,F=0.0000/
&RAMP ID='RAMP MF',T=0.1,F=rampmff1/
&RAMP ID='RAMP MF',T=0.2,F=rampmff2/
&RAMP ID='RAMP MF',T=0.3,F=rampmff3/
&RAMP ID='RAMP MF',T=0.4,F=rampmff4/
&RAMP ID='RAMP MF',T=0.5,F=rampmff5/
&RAMP ID='RAMP MF',T=0.6,F=rampmff6/
&RAMP ID='RAMP MF',T=0.7,F=rampmff7/
&RAMP ID='RAMP MF',T=0.8,F=rampmff8/
&RAMP ID='RAMP MF',T=0.9,F=rampmff9/
&RAMP ID='RAMP MF',T=1.0,F=rampmff10/
&RAMP ID='RAMP MF',T=1.1,F=rampmff11/
```

```
&RAMP ID='RAMP MF',T=1.2,F=rampmff12/
&RAMP ID='RAMP MF',T=1.3,F=rampmff13/
&RAMP ID='RAMP MF',T=1.4,F=rampmff14/
&RAMP ID='RAMP MF',T=1.5,F=rampmff15/
&RAMP ID='RAMP MF',T=1.6,F=rampmff16/
&RAMP ID='RAMP MF',T=1.7,F=rampmff17/
&RAMP ID='RAMP MF',T=1.8,F=rampmff18/
&RAMP ID='RAMP MF',T=1.9,F=rampmff19/
&RAMP ID='RAMP MF',T=2.0,F=rampmff20/
&RAMP ID='RAMP MF',T=2.1,F=rampmff21/
&RAMP ID='RAMP MF',T=2.2,F=rampmff22/
&RAMP ID='RAMP MF',T=2.3,F=rampmff23/
&RAMP ID='RAMP MF',T=2.4,F=rampmff24/
&RAMP ID='RAMP MF',T=2.5,F=rampmff25/
&RAMP ID='RAMP MF',T=2.6,F=rampmff26/
&RAMP ID='RAMP MF',T=2.7,F=rampmff27/
&RAMP ID='RAMP MF',T=2.8,F=rampmff28/
&RAMP ID='RAMP MF',T=2.9,F=rampmff29/
&RAMP ID='RAMP MF',T=3.0,F=rampmff30/
&RAMP ID='RAMP MF',T=3.1,F=rampmff31/
&RAMP ID='RAMP MF',T=3.2,F=rampmff32/
&RAMP ID='RAMP MF',T=3.3,F=rampmff33/
&RAMP ID='RAMP MF',T=3.4,F=rampmff34/
&RAMP ID='RAMP MF',T=3.5,F=rampmff35/
&RAMP ID='RAMP MF',T=3.6,F=rampmff36/
&RAMP ID='RAMP MF',T=3.7,F=rampmff37/
&RAMP ID='RAMP MF',T=3.8,F=rampmff38/
&RAMP ID='RAMP MF',T=3.9,F=rampmff39/
&RAMP ID='RAMP MF',T=4.0,F=rampmff40/
&RAMP ID='RAMP MF',T=4.1,F=rampmff41/
&RAMP ID='RAMP MF',T=4.2,F=rampmff42/
&RAMP ID='RAMP MF',T=4.3,F=rampmff43/
&RAMP ID='RAMP MF',T=4.4,F=rampmff44/
&RAMP ID='RAMP MF',T=4.5,F=rampmff45/
&RAMP ID='RAMP MF',T=4.6,F=rampmff46/
&RAMP ID='RAMP MF',T=4.7,F=rampmff47/
&RAMP ID='RAMP MF',T=4.8,F=rampmff48/
&RAMP ID='RAMP MF',T=4.9,F=rampmff49/
&RAMP ID='RAMP MF',T=5.0,F=rampmff50/
&RAMP ID='RAMP MF',T=5.1,F=rampmff51/
&RAMP ID='RAMP MF',T=5.2,F=rampmff52/
&RAMP ID='RAMP MF',T=5.3,F=rampmff53/
&RAMP ID='RAMP MF',T=5.4,F=rampmff54/
&RAMP ID='RAMP MF',T=5.5,F=rampmff55/
&RAMP ID='RAMP MF',T=5.6,F=rampmff56/
&RAMP ID='RAMP MF',T=5.7,F=rampmff57/
&RAMP ID='RAMP MF',T=5.8,F=rampmff58/
&RAMP ID='RAMP MF',T=5.9,F=rampmff59/
&RAMP ID='RAMP MF',T=6.0,F=rampmff60/
&RAMP ID='RAMP MF',T=6.1,F=rampmff61/
&RAMP ID='RAMP MF',T=6.2,F=rampmff62/
&RAMP ID='RAMP MF',T=6.3,F=rampmff63/
&RAMP ID='RAMP MF',T=6.4,F=rampmff64/
&RAMP ID='RAMP MF',T=6.5,F=rampmff65/
&RAMP ID='RAMP MF',T=6.6,F=rampmff66/
&RAMP ID='RAMP MF',T=6.7,F=rampmff67/
&RAMP ID='RAMP MF',T=6.8,F=rampmff68/
&RAMP ID='RAMP MF',T=6.9,F=rampmff69/
&RAMP ID='RAMP MF',T=7.0,F=rampmff70/
&RAMP ID='RAMP MF',T=7.1,F=rampmff71/
&RAMP ID='RAMP MF',T=7.2,F=rampmff72/
&RAMP ID='RAMP MF',T=7.3,F=rampmff73/
&RAMP ID='RAMP MF',T=7.4,F=rampmff74/
&RAMP ID='RAMP MF',T=7.5,F=rampmff75/
```

```
&RAMP ID='RAMP MF',T=7.6,F=rampmff76/
&RAMP ID='RAMP MF',T=7.7,F=rampmff77/
&RAMP ID='RAMP MF',T=7.8,F=rampmff78/
&RAMP ID='RAMP MF',T=7.9,F=rampmff79/
&RAMP ID='RAMP MF',T=8.0,F=rampmff80/
&RAMP ID='RAMP MF',T=8.1,F=rampmff81/
&RAMP ID='RAMP MF',T=8.2,F=rampmff82/
&RAMP ID='RAMP MF',T=8.3,F=rampmff83/
&RAMP ID='RAMP MF',T=8.4,F=rampmff84/
&RAMP ID='RAMP MF',T=8.5,F=rampmff85/
&RAMP ID='RAMP MF',T=8.6,F=rampmff86/
&RAMP ID='RAMP MF',T=8.7,F=rampmff87/
&RAMP ID='RAMP MF',T=8.8,F=rampmff88/
&RAMP ID='RAMP MF',T=8.9,F=rampmff89/
&RAMP ID='RAMP MF',T=9.0,F=rampmff90/
&RAMP ID='RAMP MF',T=9.1,F=rampmff91/
&RAMP ID='RAMP MF',T=9.2,F=rampmff92/
&RAMP ID='RAMP MF',T=9.3,F=rampmff93/
&RAMP ID='RAMP MF',T=9.4,F=rampmff94/
&RAMP ID='RAMP MF',T=9.5,F=rampmff95/
&RAMP ID='RAMP MF',T=9.6,F=rampmff96/
&RAMP ID='RAMP MF',T=9.7,F=rampmff97/
&RAMP ID='RAMP MF',T=9.8,F=rampmff98/
&RAMP ID='RAMP MF',T=9.9,F=rampmff99/
&RAMP ID='RAMP MF',T=10.0,F=rampmff100/
&RAMP ID='RAMP MF',T=10.1,F=rampmff101/
&RAMP ID='RAMP MF',T=10.2,F=rampmff102/
&RAMP ID='RAMP MF',T=10.3,F=rampmff103/
&RAMP ID='RAMP MF',T=10.4,F=rampmff104/
&RAMP ID='RAMP MF',T=10.5,F=rampmff105/
&RAMP ID='RAMP MF',T=10.6,F=rampmff106/
&RAMP ID='RAMP MF',T=10.7,F=rampmff107/
&RAMP ID='RAMP MF',T=10.8,F=rampmff108/
&RAMP ID='RAMP MF',T=10.9,F=rampmff109/
&RAMP ID='RAMP MF',T=11.0,F=rampmff110/
&RAMP ID='RAMP MF',T=11.1,F=rampmff111/
&RAMP ID='RAMP MF',T=11.2,F=rampmff112/
&RAMP ID='RAMP MF',T=11.3,F=rampmff113/
&RAMP ID='RAMP MF',T=11.4,F=rampmff114/
&RAMP ID='RAMP MF',T=11.5,F=rampmff115/
&RAMP ID='RAMP MF',T=11.6,F=rampmff116/
&RAMP ID='RAMP MF',T=11.7,F=rampmff117/
&RAMP ID='RAMP MF',T=11.8,F=rampmff118/
&RAMP ID='RAMP MF',T=11.9,F=rampmff119/
&RAMP ID='RAMP MF',T=12.0,F=rampmff120/
&RAMP ID='RAMP MF',T=12.1,F=rampmff121/
&RAMP ID='RAMP MF',T=12.2,F=rampmff122/
&RAMP ID='RAMP MF',T=12.3,F=rampmff123/
&RAMP ID='RAMP MF',T=12.4,F=rampmff124/
&RAMP ID='RAMP MF',T=12.5,F=rampmff125/
&RAMP ID='RAMP MF',T=12.6,F=rampmff126/
&RAMP ID='RAMP MF',T=12.7,F=rampmff127/
&RAMP ID='RAMP MF',T=12.8,F=rampmff128/
&RAMP ID='RAMP MF',T=12.9,F=rampmff129/
&RAMP ID='RAMP MF',T=13.0,F=rampmff130/
&RAMP ID='RAMP MF',T=13.1,F=rampmff131/
&RAMP ID='RAMP MF',T=13.2,F=rampmff132/
&RAMP ID='RAMP MF',T=13.3,F=rampmff133/
&RAMP ID='RAMP MF',T=13.4,F=rampmff134/
&RAMP ID='RAMP MF',T=13.5,F=rampmff135/
&RAMP ID='RAMP MF',T=13.6,F=rampmff136/
&RAMP ID='RAMP MF',T=13.7,F=rampmff137/
&RAMP ID='RAMP MF',T=13.8,F=rampmff138/
&RAMP ID='RAMP MF',T=13.9,F=rampmff139/
```

```
&RAMP ID='RAMP MF',T=14.0,F=rampmff140/
&RAMP ID='RAMP MF',T=14.1,F=rampmff141/
&RAMP ID='RAMP MF',T=14.2,F=rampmff142/
&RAMP ID='RAMP MF',T=14.3,F=rampmff143/
&RAMP ID='RAMP MF',T=14.4,F=rampmff144/
&RAMP ID='RAMP MF',T=14.5,F=rampmff145/
&RAMP ID='RAMP MF',T=14.6,F=rampmff146/
&RAMP ID='RAMP MF',T=14.7,F=rampmff147/
&RAMP ID='RAMP MF',T=14.8,F=rampmff148/
&RAMP ID='RAMP MF',T=14.9,F=rampmff149/
&RAMP ID='RAMP MF',T=15.0,F=rampmff150/
&RAMP ID='RAMP MF',T=15.1,F=rampmff151/
&RAMP ID='RAMP MF',T=15.2,F=rampmff152/
&RAMP ID='RAMP MF',T=15.3,F=rampmff153/
&RAMP ID='RAMP MF',T=15.4,F=rampmff154/
&RAMP ID='RAMP MF',T=15.5,F=rampmff155/
&RAMP ID='RAMP MF',T=15.6,F=rampmff156/
&RAMP ID='RAMP MF',T=15.7,F=rampmff157/
&RAMP ID='RAMP MF',T=15.8,F=rampmff158/
&RAMP ID='RAMP MF',T=15.9,F=rampmff159/
&RAMP ID='RAMP MF',T=16.0,F=rampmff160/
&RAMP ID='RAMP MF',T=16.1,F=rampmff161/
&RAMP ID='RAMP MF',T=16.2,F=rampmff162/
&RAMP ID='RAMP MF',T=16.3,F=rampmff163/
&RAMP ID='RAMP MF',T=16.4,F=rampmff164/
&RAMP ID='RAMP MF',T=16.5,F=rampmff165/
&RAMP ID='RAMP MF',T=16.6,F=rampmff166/
&RAMP ID='RAMP MF',T=16.7,F=rampmff167/
&RAMP ID='RAMP MF',T=16.8,F=rampmff168/
&RAMP ID='RAMP MF',T=16.9,F=rampmff169/
&RAMP ID='RAMP MF',T=17.0,F=rampmff170/
&RAMP ID='RAMP MF',T=17.1,F=rampmff171/
&RAMP ID='RAMP MF',T=17.2,F=rampmff172/
&RAMP ID='RAMP MF',T=17.3,F=rampmff173/
&RAMP ID='RAMP MF',T=17.4,F=rampmff174/
&RAMP ID='RAMP MF',T=17.5,F=rampmff175/
&RAMP ID='RAMP MF',T=17.6,F=rampmff176/
&RAMP ID='RAMP MF',T=17.7,F=rampmff177/
&RAMP ID='RAMP MF',T=17.8,F=rampmff178/
&RAMP ID='RAMP MF',T=17.9,F=rampmff179/
&RAMP ID='RAMP MF',T=18.0,F=rampmff180/
&RAMP ID='RAMP MF',T=18.1,F=rampmff181/
&RAMP ID='RAMP MF',T=18.2,F=rampmff182/
&RAMP ID='RAMP MF',T=18.3,F=rampmff183/
&RAMP ID='RAMP MF',T=18.4,F=rampmff184/
&RAMP ID='RAMP MF',T=18.5,F=rampmff185/
&RAMP ID='RAMP MF',T=18.6,F=rampmff186/
&RAMP ID='RAMP MF',T=18.7,F=rampmff187/
&RAMP ID='RAMP MF',T=18.8,F=rampmff188/
&RAMP ID='RAMP MF',T=18.9,F=rampmff189/
&RAMP ID='RAMP MF',T=19.0,F=rampmff190/
&RAMP ID='RAMP MF',T=19.1,F=rampmff191/
&RAMP ID='RAMP MF',T=19.2,F=rampmff192/
&RAMP ID='RAMP MF',T=19.3,F=rampmff193/
&RAMP ID='RAMP MF',T=19.4,F=rampmff194/
&RAMP ID='RAMP MF',T=19.5,F=rampmff195/
&RAMP ID='RAMP MF',T=19.6,F=rampmff196/
&RAMP ID='RAMP MF',T=19.7,F=rampmff197/
&RAMP ID='RAMP MF',T=19.8,F=rampmff198/
&RAMP ID='RAMP MF',T=19.9,F=rampmff199/
&RAMP ID='RAMP MF',T=20.0,F=rampmff200/
&RAMP ID='RAMP MF',T=20.1,F=0.0000/
```

```
! Gas phase specific heats. FDS defaults for N2, O2, H2O, and CO2 replaced to extend
values to higher temperatures than present in FDS

&RAMP ID='AL2O3 C', T=-73, F=0.761/ NASA TP-2002-211556
&RAMP ID='AL2O3 C', T=127, F=0.921/
&RAMP ID='AL2O3 C', T=327, F=0.999/
&RAMP ID='AL2O3 C', T=527, F=1.038/
&RAMP ID='AL2O3 C', T=727, F=1.058/
&RAMP ID='AL2O3 C', T=1727, F=1.090/
&RAMP ID='AL2O3 C', T=2727, F=1.096/
&RAMP ID='AL2O3 C', T=3727, F=1.098/
&RAMP ID='AL2O3 C', T=4727, F=1.099/
&RAMP ID='AL2O3 C', T=5727, F=1.100/

&RAMP ID='AL C', T=-73, F=0.820/ NASA TP-2002-211556
&RAMP ID='AL C', T=127, F=0.783/
&RAMP ID='AL C', T=327, F=0.776/
&RAMP ID='AL C', T=527, F=0.773/
&RAMP ID='AL C', T=727, F=0.772/
&RAMP ID='AL C', T=1727, F=0.771/
&RAMP ID='AL C', T=2727, F=0.771/
&RAMP ID='AL C', T=3727, F=0.775/
&RAMP ID='AL C', T=4727, F=0.793/
&RAMP ID='AL C', T=5727, F=0.841/
&RAMP ID='AL C', T=6727, F=0.930/
&RAMP ID='AL C', T=7727, F=1.034/
&RAMP ID='AL C', T=8727, F=1.130/
&RAMP ID='AL C', T=9727, F=1.204/
&RAMP ID='AL C', T=10727, F=1.250/
&RAMP ID='AL C', T=11727, F=1.271/
&RAMP ID='AL C', T=12727, F=1.269/
&RAMP ID='AL C', T=13727, F=1.252/
&RAMP ID='AL C', T=14727, F=1.226/
&RAMP ID='AL C', T=15727, F=1.196/
&RAMP ID='AL C', T=16727, F=1.168/
&RAMP ID='AL C', T=17727, F=1.145/
&RAMP ID='AL C', T=18727, F=1.125/
&RAMP ID='AL C', T=19727, F=1.108/

&RAMP ID='CU C', T=-73, F=0.327/ NASA TP-2002-211556
&RAMP ID='CU C', T=127, F=0.327/
&RAMP ID='CU C', T=327, F=0.327/
&RAMP ID='CU C', T=527, F=0.327/
&RAMP ID='CU C', T=727, F=0.327/
&RAMP ID='CU C', T=1727, F=0.337/
&RAMP ID='CU C', T=2727, F=0.396/
&RAMP ID='CU C', T=3727, F=0.471/
&RAMP ID='CU C', T=4727, F=0.517/
&RAMP ID='CU C', T=5727, F=0.537/
&RAMP ID='CU C', T=6727, F=0.551/
&RAMP ID='CU C', T=7727, F=0.577/
&RAMP ID='CU C', T=8727, F=0.606/
&RAMP ID='CU C', T=9727, F=0.633/
&RAMP ID='CU C', T=10727, F=0.653/
&RAMP ID='CU C', T=11727, F=0.663/
&RAMP ID='CU C', T=12727, F=0.664/
&RAMP ID='CU C', T=13727, F=0.657/
&RAMP ID='CU C', T=14727, F=0.642/
&RAMP ID='CU C', T=15727, F=0.622/
&RAMP ID='CU C', T=16727, F=0.599/
&RAMP ID='CU C', T=17727, F=0.574/
&RAMP ID='CU C', T=18727, F=0.550/
&RAMP ID='CU C', T=19727, F=0.528/
```

```
&RAMP ID='N2 C', T=-73, F=1.039/ NASA TP-2002-211556
&RAMP ID='N2 C', T=127, F=1.044/
&RAMP ID='N2 C', T=327, F=1.075/
&RAMP ID='N2 C', T=527, F=1.122/
&RAMP ID='N2 C', T=727, F=1.167/
&RAMP ID='N2 C', T=1727, F=1.284/
&RAMP ID='N2 C', T=2727, F=1.322/
&RAMP ID='N2 C', T=3727, F=1.340/
&RAMP ID='N2 C', T=4727, F=1.354/
&RAMP ID='N2 C', T=5727, F=1.371/
&RAMP ID='N2 C', T=6727, F=1.402/
&RAMP ID='N2 C', T=7727, F=1.454/
&RAMP ID='N2 C', T=8727, F=1.544/
&RAMP ID='N2 C', T=9727, F=1.670/
&RAMP ID='N2 C', T=10727, F=1.822/
&RAMP ID='N2 C', T=11727, F=1.984/
&RAMP ID='N2 C', T=12727, F=2.136/
&RAMP ID='N2 C', T=13727, F=2.261/
&RAMP ID='N2 C', T=14727, F=2.346/
&RAMP ID='N2 C', T=15727, F=2.383/
&RAMP ID='N2 C', T=16727, F=2.372/
&RAMP ID='N2 C', T=17727, F=2.320/
&RAMP ID='N2 C', T=18727, F=2.241/
&RAMP ID='N2 C', T=19727, F=2.159/

&RAMP ID='O2 C', T=-73, F=0.910/ NASA TP-2002-211556
&RAMP ID='O2 C', T=127, F=0.941/
&RAMP ID='O2 C', T=327, F=1.003/
&RAMP ID='O2 C', T=527, F=1.055/
&RAMP ID='O2 C', T=727, F=1.090/
&RAMP ID='O2 C', T=1727, F=1.181/
&RAMP ID='O2 C', T=2727, F=1.249/
&RAMP ID='O2 C', T=3727, F=1.303/
&RAMP ID='O2 C', T=4727, F=1.344/
&RAMP ID='O2 C', T=5727, F=1.373/
&RAMP ID='O2 C', T=6727, F=1.386/
&RAMP ID='O2 C', T=7727, F=1.376/
&RAMP ID='O2 C', T=8727, F=1.344/
&RAMP ID='O2 C', T=9727, F=1.296/
&RAMP ID='O2 C', T=10727, F=1.241/
&RAMP ID='O2 C', T=11727, F=1.184/
&RAMP ID='O2 C', T=12727, F=1.128/
&RAMP ID='O2 C', T=13727, F=1.077/
&RAMP ID='O2 C', T=14727, F=1.030/
&RAMP ID='O2 C', T=15727, F=0.989/
&RAMP ID='O2 C', T=16727, F=0.953/
&RAMP ID='O2 C', T=17727, F=0.922/
&RAMP ID='O2 C', T=18727, F=0.894/
&RAMP ID='O2 C', T=19727, F=0.870/

&RAMP ID='CO2 C', T=-73, F=0.735/ NASA TP-2002-211556
&RAMP ID='CO2 C', T=127, F=0.939/
&RAMP ID='CO2 C', T=327, F=1.075/
&RAMP ID='CO2 C', T=527, F=1.169/
&RAMP ID='CO2 C', T=727, F=1.234/
&RAMP ID='CO2 C', T=1727, F=1.371/
&RAMP ID='CO2 C', T=2727, F=1.412/
&RAMP ID='CO2 C', T=3727, F=1.436/
&RAMP ID='CO2 C', T=4727, F=1.466/
&RAMP ID='CO2 C', T=5727, F=1.517/
&RAMP ID='CO2 C', T=6727, F=1.595/
&RAMP ID='CO2 C', T=7727, F=1.694/
&RAMP ID='CO2 C', T=8727, F=1.797/
&RAMP ID='CO2 C', T=9727, F=1.888/
```

```
&RAMP ID='CO2 C', T=10727, F=1.957/
&RAMP ID='CO2 C', T=11727, F=2.000/
&RAMP ID='CO2 C', T=12727, F=2.019/
&RAMP ID='CO2 C', T=13727, F=2.020/
&RAMP ID='CO2 C', T=14727, F=2.007/
&RAMP ID='CO2 C', T=15727, F=1.987/
&RAMP ID='CO2 C', T=16727, F=1.965/
&RAMP ID='CO2 C', T=17727, F=1.944/
&RAMP ID='CO2 C', T=18727, F=1.924/
&RAMP ID='CO2 C', T=19727, F=1.905/

!Smokeview Outputs. Adjust PBY and PBX for center of arc volume.

alslcf1 QUANTITY='MASS FRACTION',SPEC_ID='ALUMINUM',CELL_CENTERED=.TRUE.,PBY=0.0000/
alslcf2 QUANTITY='MASS FRACTION',SPEC_ID='ALUMINUM
OXIDE',CELL_CENTERED=.TRUE.,PBY=0.0000/
cuslcf1 QUANTITY='MASS FRACTION',SPEC_ID='COPPER',CELL_CENTERED=.TRUE.,PBY=0.0000/
cuslcf2 QUANTITY='MASS FRACTION',SPEC_ID='COPPER
OXIDE',CELL_CENTERED=.TRUE.,PBY=0.0000/
&SLCF QUANTITY='MASS FRACTION',SPEC_ID='OXYGEN',CELL_CENTERED=.TRUE.,PBY=0.0000/
&SLCF QUANTITY='HRRPUV',CELL_CENTERED=.TRUE.,PBY=0.0000/
&SLCF QUANTITY='HRRPUV',CELL_CENTERED=.TRUE.,PBX=slcfpbx/
&SLCF QUANTITY='TEMPERATURE',CELL_CENTERED=.TRUE.,PBY=0.0000/
&SLCF QUANTITY='TEMPERATURE',CELL_CENTERED=.TRUE.,PBX=slcfpbx/
&SLCF QUANTITY='INTEGRATED INTENSITY',CELL_CENTERED=.TRUE.,PBY=0.0000/
&SLCF QUANTITY='INTEGRATED INTENSITY',CELL_CENTERED=.TRUE.,PBX=slcfpbx/
&SLCF QUANTITY='VELOCITY',CELL_CENTERED=.TRUE.,PBY=0.0000/
&SLCF QUANTITY='U-VELOCITY',CELL_CENTERED=.TRUE.,PBY=0.0000/
&SLCF QUANTITY='VELOCITY',CELL_CENTERED=.TRUE.,PBX=slcfpbx/
&SLCF QUANTITY='V-VELOCITY',CELL_CENTERED=.TRUE.,PBX=slcfpbx/
&SLCF QUANTITY='PRESSURE',CELL_CENTERED=.TRUE.,PBY=0.0000/

&BNDF QUANTITY='WALL TEMPERATURE',CELL_CENTERED=.TRUE./
&BNDF QUANTITY='GAUGE HEAT FLUX',CELL_CENTERED=.TRUE./
&BNDF QUANTITY='WALL THICKNESS',CELL_CENTERED=.TRUE./
&BNDF QUANTITY='VELOCITY ERROR',CELL_CENTERED=.TRUE./

!Example DEVC for ZOI runs. Have planes of devices at a range of distances that look
at each face of the enclosure
!Plane should be large enough to see any permanent venting, plus any area heated by or
damaged by the arc, plus any bouyancy impacts
!Here the DEVC ID my means this is on the (m)inus (y) face at the given x,y,z location
!The orientation is the unit vector given by Arc Center - DEVC XYZ.  Pointing the DEVC
at the arc centroid will approximate the worst case view factor
!for the radiative component.
!These can easily be generated with Excel using CONCATENATE()

!&DEVC XYZ=4.3434,4.8514,2.9210, ORIENTATION=0.131,0.578,-0.805, QUANTITY='GAUGE HEAT
FLUX GAS', ID='my:x=4.34,y=4.85,z=2.92'/
```

C.2.2 Horizontal Draw-Out Style

```
&HEAD CHID='fileid'/

! 3 in. resolution. Approximately 2 m to each side, 2 m above, and 2.4 m front and
back.

&MESH ID='Cabinet',IJK=24,22,20,XB=-2.4384,-0.6096,-2.5146,-
0.8382,0.0000,1.5240,MULT_ID='M1'/ 3 in. resolution
&MULT ID='M1',I_UPPER=3,DX=1.8288,J_UPPER=2,DY=1.6764,K_UPPER=2,DZ=1.5240/

&VENT MB='ZMAX',SURF_ID='OPEN'/
&VENT MB='YMAX',SURF_ID='OPEN'/
```

```
&VENT MB='XMAX',SURF_ID='OPEN'/
&VENT MB='YMIN',SURF_ID='OPEN'/
&VENT MB='XMIN',SURF_ID='OPEN'/

! I_MAX_TEMP=35000 ensures property arrays are high enough for the CLIP vlaues.
! AEROSOL_AL2O3 replaces default SOOT radiative properties with those for AL2O3

&MISC AEROSOL_AL2O3=T,I_MAX_TEMP=35000 /

! SMOKE3D_SPEC_ID sets the species used by Smokeview to visualize smoke

&DUMP SMOKE3D_SPEC_ID='3dsmoke',SUPPRESS_DIAGNOSTICS=F,MASS_FILE=T/

! Turns off the extinction model. Default values in the model may not be appropriate
for metal oxidation
&COMB SUPPRESSION=F /

! 0.01 kg/m3 greatly limits clipping of density.
&CLIP MINIMUM_DENSITY=0.01, MAXIMUM_TEMPERATURE=35000.,CLIP_DT_RESTRICTIONS_MAX=0 /

! These cases a very challenging for the pressure solver. The selected values seem to
give enough pressure iterations to
! drop the velocity error down to a plateau value.

&PRES MAX_PRESSURE_ITERATIONS=30, VELOCITY_TOLERANCE=0.001,
SUSPEND_PRESSURE_ITERATIONS=F/

! For ZOI runs suggest T_END = arc time + 8 s

&TIME T_END=tend, DT=0.001,WALL_INCREMENT=1 /

&RADI NUMBER_RADIATION_ANGLES=500 /

! 1 cell thick OBST to help out pressure solver.

&OBST XB=0.0000,0.0762,-0.3810,0.3810,0.3048,2.2860,SURF_ID='CABINET'/ rear panel
&OBST XB=0.0000,0.0762,-0.3810,0.3810,0.0000,0.0762,SURF_ID='CABINET'/ thin strip of
rear panel below vent
&OBST XB =1.9812,2.0574 ,-0.3810,0.3810,1.6002,2.1336,SURF_ID='CABINET'/ front top
panel
&OBST XB=0.0000,1.2192,-0.3810,0.3810,2.2098,2.2860,SURF_ID='CABINET'/ top panel, rear
section
&OBST XB=1.3716,2.0574,-0.3810,0.3810,2.2098,2.2860,SURF_ID='CABINET'/ top panel,
front section
&OBST XB=0.0000,2.0574,-0.4572,-0.3810,0.0000,2.2860,SURF_ID='CABINET'/ right panel
&OBST XB=0.0000,2.0574,0.3810,0.4572,0.0000,2.2860,SURF_ID='CABINET'/ left panel
&OBST XB=1.0668,1.143,-0.3810,0.3810,0.0000,2.2098,SURF_ID='CABINET'/ center vertical
internal
&OBST XB=1.2192,1.3716,-0.3048,0.3048,1.9812,2.0574,SURF_ID='CABINET'/ hanging piece
below vent
&OBST XB=1.8288,2.0574,-0.3810,0.3810,1.524,1.6002,SURF_ID='CABINET'/ horizontal piece
above breaker
&OBST XB=1.524,1.6002,-0.3810,0.3810,1.8288,2.2860,SURF_ID='CABINET'/ vertical piece
above breaker
&OBST XB=1.6002,1.6764,-0.3810,0.3810,1.7526,1.8288,SURF_ID='CABINET'/ diagonal
&OBST XB=1.6764,1.7526,-0.3810,0.3810,1.6764,1.7526,SURF_ID='CABINET'/ diagonal
&OBST XB=1.7526,1.8288,-0.3810,0.3810,1.6002,1.6764,SURF_ID='CABINET'/ diagonal
&OBST XB=0.6858,1.0668,-0.3810,0.3810,0.6096,0.6858,SURF_ID='CABINET'/rear partition
shelf
&OBST XB=0.6096,0.7620,-0.3810,0.3810,0.8382,0.9144,SURF_ID='CABINET'/rear partition
shelf
&OBST XB=0.6858,0.7620,-0.3810,0.3810,0.6858,0.8382,SURF_ID='CABINET'/rear partition
shelf
```

```
&OBST XB=0.6096,0.6858,-0.3810,0.3810,0.9144,1.524,SURF_ID='CABINET'/rear partition
vertical lower (gap to prevent pressure compt)
&OBST XB=0.6096,0.6858,-0.3810,0.3810,1.6002,2.2098,SURF_ID='CABINET'/rear partition
vertical upper (gap to prevent pressure compt)
&OBST XB=1.524,2.0574,-0.3048,0.3048,0.0000,1.4478,SURF_ID='BREAKER'/

! RADCAL_ID='SOOT' makes the SPEC use the SOOT radiation properties which the MISC
line has changed to those for AL2O3
! RAMPs used instead of built in cp data for N2, CO2, and O2 to extend temperature to
20,000 K

&SPEC ID='WET NITROGEN',BACKGROUND=T,SPEC_ID='NITROGEN','CARBON DIOXIDE','WATER
VAPOR',MASS_FRACTION=1,0.000775,0.007792/FDS Default AIR without O2
&SPEC ID='NITROGEN', LUMPED_COMPONENT_ONLY=T,RAMP_CP='N2 C'/
&SPEC ID='CARBON DIOXIDE', LUMPED_COMPONENT_ONLY=T,RAMP_CP='CO2 C'/
&SPEC ID='WATER VAPOR', LUMPED_COMPONENT_ONLY=T /
&SPEC ID='OXYGEN', MASS_FRACTION_0=0.230997,RAMP_CP='O2 C' /
alspec1 ID='ALUMINUM',FORMULA='Al',RAMP_CP='AL
C',SIGMALJ=2.655,EPSILONKLJ=2750.,PR_GAS=1/
alspec2 ID='ALUMINUM
OXIDE',MASS_EXTINCTION_COEFFICIENT=3000,FORMULA='Al2O3',RAMP_CP='AL2O3
C',SIGMALJ=3.186,EPSILONKLJ=557.449,PR_GAS=1,RADCAL_ID='SOOT'/
cuspec1 ID='COPPER',FORMULA='Cu',RAMP_CP='CU
C',SIGMALJ=5.058,EPSILONKLJ=2983.,PR_GAS=1/
cuspec2 ID='COPPER
OXIDE',MASS_EXTINCTION_COEFFICIENT=3000,FORMULA='Cu2O',SPECIFIC_HEAT=0.7,SIGMALJ=5.403
,PR_GAS=1,RADCAL_ID='SOOT'/C from JANAF, LJ take as CuO

alreac FUEL='ALUMINUM', SPEC_ID_NU='ALUMINUM','OXYGEN','ALUMINUM OXIDE', NU=-2,-1.5,1,
HEAT_OF_COMBUSTION=31100. / Al -> AL2O3
cureac FUEL='COPPER',SPEC_ID_NU='COPPER','OXYGEN','COPPER OXIDE',NU=-2,-
0.5,1,HEAT_OF_COMBUSTION=1340./ Cu->Cu2O

&MATL ID='CONCRETE', DENSITY=2400, CONDUCTIVITY=1.6, SPECIFIC_HEAT=0.75,
EMISSIVITY=0.95 /

! Non-melting steel
&MATL ID='INERT STEEL', DENSITY=7800., SPECIFIC_HEAT_RAMP='STEEL C',
CONDUCTIVITY_RAMP='STEEL K', EMISSIVITY=0.85/

! Melting steel
&MATL ID='STEEL', DENSITY=7800., SPECIFIC_HEAT_RAMP='STEEL C',
CONDUCTIVITY_RAMP='STEEL K', EMISSIVITY=0.85,
      THRESHOLD_TEMPERATURE=1300., THRESHOLD_SIGN=1, HEAT_OF_REACTION(1)=250.,
PCR(1)=T, A(1)=0.6, E(1)=0., N_S(1)=0., N_T(1)=1. /

! Eurocode values
&RAMP ID='STEEL C',T=20,F=0.440/
&RAMP ID='STEEL C',T=600,F=0.760/
&RAMP ID='STEEL C',T=700,F=1.008/
&RAMP ID='STEEL C',T=720,F=1.388/
&RAMP ID='STEEL C',T=725,F=1.666/
&RAMP ID='STEEL C',T=730,F=2.291/
&RAMP ID='STEEL C',T=735,F=5.000/
&RAMP ID='STEEL C',T=740,F=2.525/ BCC -> FCC Transition
&RAMP ID='STEEL C',T=745,F=1.818/
&RAMP ID='STEEL C',T=750,F=1.483/
&RAMP ID='STEEL C',T=800,F=0.803/
&RAMP ID='STEEL C',T=900,F=0.650/

&RAMP ID='STEEL K',T=20,F=53.3/
&RAMP ID='STEEL K',T=800,F=27.3/
```

```
&SURF ID='BREAKER', MATL_ID='INERT STEEL', THICKNESS=0.02,
RGB=204,204,255,CELL_SIZE_FACTOR=0.05,STRETCH_FACTOR=1 /
&SURF ID='CABINET', MATL_ID='STEEL', THICKNESS=0.002381,  COLOR='GRAY 60',
BURN_AWAY=.TRUE.,CELL_SIZE_FACTOR=0.05,STRETCH_FACTOR=1 /
&SURF ID='FLOOR', MATL_ID='CONCRETE', THICKNESS=0.15, RGB=50,50,50, DEFAULT=T /

!The block below defines particles that emit vapor for aluminum.
!The particles are initialized at the melting point.
!The PROP MASS_FLOW_RATE is the maximum liquid production rate divided by the number
of electrodes
!NU_SPEC and NU_MATL are set to get the 75 % oxidation for Al and 25 % for Cu. The
second MOLTEN AL2 and CU2 species have a modified density to preserve diameter.
!A and E are set to give the vapor over 0.3 s.

almatl1 ID='MOLTEN
AL',DENSITY=2375,CONDUCTIVITY=100.,SPECIFIC_HEAT=1.177,EMISSIVITY=0,A=3.333,E=0,
N_REACTIONS=1,HEAT_OF_REACTION=0,HEAT_OF_COMBUSTION=0,MATL_ID(1,1)='MOLTEN
AL2',SPEC_ID(1,1)='ALUMINUM',NU_MATL(1,1)=0.25,NU_SPEC(1,1)=0.75/
almatl2 ID='MOLTEN
AL2',DENSITY=593.75,SPEC_ID='ALUMINUM',NU_SPEC=1,CONDUCTIVITY=100.,SPECIFIC_HEAT=1.177
/

alsurf1 ID='AL DROP',MATL_ID='MOLTEN AL',GEOMETRY='SPHERICAL',THICKNESS=5.E-
6,HEAT_TRANSFER_COEFFICIENT=0,TMP_INNER=665.3/
alpart1 ID='AL DROPS',SURF_ID='AL
DROP',AGE=2.0,SAMPLING_FACTOR=10,MONODISPERSE=T,RGB=100,100,100/
alprop1 ID='DROPS',PART_ID='AL DROPS',FLOW_RAMP='RAMP
MF',MASS_FLOW_RATE=almfr,PARTICLES_PER_SECOND=20000,PARTICLE_VELOCITY=10,SPRAY_ANGLE=0
,60/

! The block below is for copper.

cumatl1 ID='MOLTEN
CU',DENSITY=8960,CONDUCTIVITY=340.,SPECIFIC_HEAT=0.517,EMISSIVITY=0,A=3.333,E=0,
N_REACTIONS=1,HEAT_OF_REACTION=0,HEAT_OF_COMBUSTION=0,MATL_ID(1,1)='MOLTEN
CU2',SPEC_ID(1,1)='COPPER',NU_MATL(1,1)=0.75,NU_SPEC(1,1)=0.25/
cumatl2 ID='MOLTEN
CU2',DENSITY=7168,CONDUCTIVITY=340.,SPECIFIC_HEAT=0.517,EMISSIVITY=0/

cusurf1 ID='CU DROP',MATL_ID='MOLTEN CU',GEOMETRY='SPHERICAL',THICKNESS=5.E-
6,HEAT_TRANSFER_COEFFICIENT=0,TMP_INNER=1084.85/
cupart1 ID='CU DROPS',SURF_ID='CU
DROP',AGE=2.0,SAMPLING_FACTOR=10,MONODISPERSE=T,RGB=184,115,51/
cuprop1 ID='DROPS',PART_ID='CU DROPS',FLOW_RAMP='RAMP
MF',MASS_FLOW_RATE=cumfr,PARTICLES_PER_SECOND=20000,PARTICLE_VELOCITY=10,SPRAY_ANGLE=0
,60/

! First INIT line is the volumetric source term where the RADAITIVE_FRACTION uses
Cressault's data interpolated based on power,. The HRRPUV is
! reduced based on energy needed to degrade the electrodes:
! Adjusted total energy = (Total arc energy - electrode mass loss * (vapor fraction *
energy to vaporize + liquid fraction * energy to melt))
!
! Cressault data:
!
! X_r,Al = 0.2275*Max_Power^0.3292
! X_r,Al = 0.1273*Max_Power^0.3859
!
! Phase  Energy (kJ/kg)
! Change    Al     Cu
! Melt    1063.4  695.2

&INIT XB=initx1,initx2,inity1,inity2,initz1,initz2,HRRPUV=hrrpuvval,RAMP_Q='RAMP
Q',RADIATIVE_FRACTION=radfrac/
```

```
! One spray nozzle device per electrode that inject liquid droplets

&DEVC
PROP_ID='DROPS',XYZ=nozx1,nozy1,nozz1,QUANTITY='TIME',SETPOINT=0.0,ORIENTATION=orient1
,orient2,orient3/
&DEVC
PROP_ID='DROPS',XYZ=nozx2,nozy2,nozz2,QUANTITY='TIME',SETPOINT=0.0,ORIENTATION=orient1
,orient2,orient3/
&DEVC
PROP_ID='DROPS',XYZ=nozx3,nozy3,nozz3,QUANTITY='TIME',SETPOINT=0.0,ORIENTATION=orient1
,orient2,orient3/

! An 0.1 s ramp up and down for the arc volumetric source term helps avoid numerical
instabilities

&RAMP ID='RAMP Q',T=0.0,F=0.0000/
&RAMP ID='RAMP Q',T=0.1,F=rampqf1/
&RAMP ID='RAMP Q',T=0.2,F=rampqf2/
&RAMP ID='RAMP Q',T=0.3,F=rampqf3/
&RAMP ID='RAMP Q',T=0.4,F=rampqf4/
&RAMP ID='RAMP Q',T=0.5,F=rampqf5/
&RAMP ID='RAMP Q',T=0.6,F=rampqf6/
&RAMP ID='RAMP Q',T=0.7,F=rampqf7/
&RAMP ID='RAMP Q',T=0.8,F=rampqf8/
&RAMP ID='RAMP Q',T=0.9,F=rampqf9/
&RAMP ID='RAMP Q',T=1.0,F=rampqf10/
&RAMP ID='RAMP Q',T=1.1,F=rampqf11/
&RAMP ID='RAMP Q',T=1.2,F=rampqf12/
&RAMP ID='RAMP Q',T=1.3,F=rampqf13/
&RAMP ID='RAMP Q',T=1.4,F=rampqf14/
&RAMP ID='RAMP Q',T=1.5,F=rampqf15/
&RAMP ID='RAMP Q',T=1.6,F=rampqf16/
&RAMP ID='RAMP Q',T=1.7,F=rampqf17/
&RAMP ID='RAMP Q',T=1.8,F=rampqf18/
&RAMP ID='RAMP Q',T=1.9,F=rampqf19/
&RAMP ID='RAMP Q',T=2.0,F=rampqf20/
&RAMP ID='RAMP Q',T=2.1,F=rampqf21/
&RAMP ID='RAMP Q',T=2.2,F=rampqf22/
&RAMP ID='RAMP Q',T=2.3,F=rampqf23/
&RAMP ID='RAMP Q',T=2.4,F=rampqf24/
&RAMP ID='RAMP Q',T=2.5,F=rampqf25/
&RAMP ID='RAMP Q',T=2.6,F=rampqf26/
&RAMP ID='RAMP Q',T=2.7,F=rampqf27/
&RAMP ID='RAMP Q',T=2.8,F=rampqf28/
&RAMP ID='RAMP Q',T=2.9,F=rampqf29/
&RAMP ID='RAMP Q',T=3.0,F=rampqf30/
&RAMP ID='RAMP Q',T=3.1,F=rampqf31/
&RAMP ID='RAMP Q',T=3.2,F=rampqf32/
&RAMP ID='RAMP Q',T=3.3,F=rampqf33/
&RAMP ID='RAMP Q',T=3.4,F=rampqf34/
&RAMP ID='RAMP Q',T=3.5,F=rampqf35/
&RAMP ID='RAMP Q',T=3.6,F=rampqf36/
&RAMP ID='RAMP Q',T=3.7,F=rampqf37/
&RAMP ID='RAMP Q',T=3.8,F=rampqf38/
&RAMP ID='RAMP Q',T=3.9,F=rampqf39/
&RAMP ID='RAMP Q',T=4.0,F=rampqf40/
&RAMP ID='RAMP Q',T=4.1,F=rampqf41/
&RAMP ID='RAMP Q',T=4.2,F=rampqf42/
&RAMP ID='RAMP Q',T=4.3,F=rampqf43/
&RAMP ID='RAMP Q',T=4.4,F=rampqf44/
&RAMP ID='RAMP Q',T=4.5,F=rampqf45/
&RAMP ID='RAMP Q',T=4.6,F=rampqf46/
&RAMP ID='RAMP Q',T=4.7,F=rampqf47/
```

```
&RAMP ID='RAMP Q',T=4.8,F=rampqf48/
&RAMP ID='RAMP Q',T=4.9,F=rampqf49/
&RAMP ID='RAMP Q',T=5.0,F=rampqf50/
&RAMP ID='RAMP Q',T=5.1,F=rampqf51/
&RAMP ID='RAMP Q',T=5.2,F=rampqf52/
&RAMP ID='RAMP Q',T=5.3,F=rampqf53/
&RAMP ID='RAMP Q',T=5.4,F=rampqf54/
&RAMP ID='RAMP Q',T=5.5,F=rampqf55/
&RAMP ID='RAMP Q',T=5.6,F=rampqf56/
&RAMP ID='RAMP Q',T=5.7,F=rampqf57/
&RAMP ID='RAMP Q',T=5.8,F=rampqf58/
&RAMP ID='RAMP Q',T=5.9,F=rampqf59/
&RAMP ID='RAMP Q',T=6.0,F=rampqf60/
&RAMP ID='RAMP Q',T=6.1,F=rampqf61/
&RAMP ID='RAMP Q',T=6.2,F=rampqf62/
&RAMP ID='RAMP Q',T=6.3,F=rampqf63/
&RAMP ID='RAMP Q',T=6.4,F=rampqf64/
&RAMP ID='RAMP Q',T=6.5,F=rampqf65/
&RAMP ID='RAMP Q',T=6.6,F=rampqf66/
&RAMP ID='RAMP Q',T=6.7,F=rampqf67/
&RAMP ID='RAMP Q',T=6.8,F=rampqf68/
&RAMP ID='RAMP Q',T=6.9,F=rampqf69/
&RAMP ID='RAMP Q',T=7.0,F=rampqf70/
&RAMP ID='RAMP Q',T=7.1,F=rampqf71/
&RAMP ID='RAMP Q',T=7.2,F=rampqf72/
&RAMP ID='RAMP Q',T=7.3,F=rampqf73/
&RAMP ID='RAMP Q',T=7.4,F=rampqf74/
&RAMP ID='RAMP Q',T=7.5,F=rampqf75/
&RAMP ID='RAMP Q',T=7.6,F=rampqf76/
&RAMP ID='RAMP Q',T=7.7,F=rampqf77/
&RAMP ID='RAMP Q',T=7.8,F=rampqf78/
&RAMP ID='RAMP Q',T=7.9,F=rampqf79/
&RAMP ID='RAMP Q',T=8.0,F=rampqf80/
&RAMP ID='RAMP Q',T=8.1,F=rampqf81/
&RAMP ID='RAMP Q',T=8.2,F=rampqf82/
&RAMP ID='RAMP Q',T=8.3,F=rampqf83/
&RAMP ID='RAMP Q',T=8.4,F=rampqf84/
&RAMP ID='RAMP Q',T=8.5,F=rampqf85/
&RAMP ID='RAMP Q',T=8.6,F=rampqf86/
&RAMP ID='RAMP Q',T=8.7,F=rampqf87/
&RAMP ID='RAMP Q',T=8.8,F=rampqf88/
&RAMP ID='RAMP Q',T=8.9,F=rampqf89/
&RAMP ID='RAMP Q',T=9.0,F=rampqf90/
&RAMP ID='RAMP Q',T=9.1,F=rampqf91/
&RAMP ID='RAMP Q',T=9.2,F=rampqf92/
&RAMP ID='RAMP Q',T=9.3,F=rampqf93/
&RAMP ID='RAMP Q',T=9.4,F=rampqf94/
&RAMP ID='RAMP Q',T=9.5,F=rampqf95/
&RAMP ID='RAMP Q',T=9.6,F=rampqf96/
&RAMP ID='RAMP Q',T=9.7,F=rampqf97/
&RAMP ID='RAMP Q',T=9.8,F=rampqf98/
&RAMP ID='RAMP Q',T=9.9,F=rampqf99/
&RAMP ID='RAMP Q',T=10.0,F=rampqf100/
&RAMP ID='RAMP Q',T=10.1,F=rampqf101/
&RAMP ID='RAMP Q',T=10.2,F=rampqf102/
&RAMP ID='RAMP Q',T=10.3,F=rampqf103/
&RAMP ID='RAMP Q',T=10.4,F=rampqf104/
&RAMP ID='RAMP Q',T=10.5,F=rampqf105/
&RAMP ID='RAMP Q',T=10.6,F=rampqf106/
&RAMP ID='RAMP Q',T=10.7,F=rampqf107/
&RAMP ID='RAMP Q',T=10.8,F=rampqf108/
&RAMP ID='RAMP Q',T=10.9,F=rampqf109/
&RAMP ID='RAMP Q',T=11.0,F=rampqf110/
&RAMP ID='RAMP Q',T=11.1,F=rampqf111/
```

```
&RAMP ID='RAMP Q',T=11.2,F=rampqf112/
&RAMP ID='RAMP Q',T=11.3,F=rampqf113/
&RAMP ID='RAMP Q',T=11.4,F=rampqf114/
&RAMP ID='RAMP Q',T=11.5,F=rampqf115/
&RAMP ID='RAMP Q',T=11.6,F=rampqf116/
&RAMP ID='RAMP Q',T=11.7,F=rampqf117/
&RAMP ID='RAMP Q',T=11.8,F=rampqf118/
&RAMP ID='RAMP Q',T=11.9,F=rampqf119/
&RAMP ID='RAMP Q',T=12.0,F=rampqf120/
&RAMP ID='RAMP Q',T=12.1,F=rampqf121/
&RAMP ID='RAMP Q',T=12.2,F=rampqf122/
&RAMP ID='RAMP Q',T=12.3,F=rampqf123/
&RAMP ID='RAMP Q',T=12.4,F=rampqf124/
&RAMP ID='RAMP Q',T=12.5,F=rampqf125/
&RAMP ID='RAMP Q',T=12.6,F=rampqf126/
&RAMP ID='RAMP Q',T=12.7,F=rampqf127/
&RAMP ID='RAMP Q',T=12.8,F=rampqf128/
&RAMP ID='RAMP Q',T=12.9,F=rampqf129/
&RAMP ID='RAMP Q',T=13.0,F=rampqf130/
&RAMP ID='RAMP Q',T=13.1,F=rampqf131/
&RAMP ID='RAMP Q',T=13.2,F=rampqf132/
&RAMP ID='RAMP Q',T=13.3,F=rampqf133/
&RAMP ID='RAMP Q',T=13.4,F=rampqf134/
&RAMP ID='RAMP Q',T=13.5,F=rampqf135/
&RAMP ID='RAMP Q',T=13.6,F=rampqf136/
&RAMP ID='RAMP Q',T=13.7,F=rampqf137/
&RAMP ID='RAMP Q',T=13.8,F=rampqf138/
&RAMP ID='RAMP Q',T=13.9,F=rampqf139/
&RAMP ID='RAMP Q',T=14.0,F=rampqf140/
&RAMP ID='RAMP Q',T=14.1,F=rampqf141/
&RAMP ID='RAMP Q',T=14.2,F=rampqf142/
&RAMP ID='RAMP Q',T=14.3,F=rampqf143/
&RAMP ID='RAMP Q',T=14.4,F=rampqf144/
&RAMP ID='RAMP Q',T=14.5,F=rampqf145/
&RAMP ID='RAMP Q',T=14.6,F=rampqf146/
&RAMP ID='RAMP Q',T=14.7,F=rampqf147/
&RAMP ID='RAMP Q',T=14.8,F=rampqf148/
&RAMP ID='RAMP Q',T=14.9,F=rampqf149/
&RAMP ID='RAMP Q',T=15.0,F=rampqf150/
&RAMP ID='RAMP Q',T=15.1,F=rampqf151/
&RAMP ID='RAMP Q',T=15.2,F=rampqf152/
&RAMP ID='RAMP Q',T=15.3,F=rampqf153/
&RAMP ID='RAMP Q',T=15.4,F=rampqf154/
&RAMP ID='RAMP Q',T=15.5,F=rampqf155/
&RAMP ID='RAMP Q',T=15.6,F=rampqf156/
&RAMP ID='RAMP Q',T=15.7,F=rampqf157/
&RAMP ID='RAMP Q',T=15.8,F=rampqf158/
&RAMP ID='RAMP Q',T=15.9,F=rampqf159/
&RAMP ID='RAMP Q',T=16.0,F=rampqf160/
&RAMP ID='RAMP Q',T=16.1,F=rampqf161/
&RAMP ID='RAMP Q',T=16.2,F=rampqf162/
&RAMP ID='RAMP Q',T=16.3,F=rampqf163/
&RAMP ID='RAMP Q',T=16.4,F=rampqf164/
&RAMP ID='RAMP Q',T=16.5,F=rampqf165/
&RAMP ID='RAMP Q',T=16.6,F=rampqf166/
&RAMP ID='RAMP Q',T=16.7,F=rampqf167/
&RAMP ID='RAMP Q',T=16.8,F=rampqf168/
&RAMP ID='RAMP Q',T=16.9,F=rampqf169/
&RAMP ID='RAMP Q',T=17.0,F=rampqf170/
&RAMP ID='RAMP Q',T=17.1,F=rampqf171/
&RAMP ID='RAMP Q',T=17.2,F=rampqf172/
&RAMP ID='RAMP Q',T=17.3,F=rampqf173/
&RAMP ID='RAMP Q',T=17.4,F=rampqf174/
&RAMP ID='RAMP Q',T=17.5,F=rampqf175/
```

```
&RAMP ID='RAMP Q',T=17.6,F=rampqf176/
&RAMP ID='RAMP Q',T=17.7,F=rampqf177/
&RAMP ID='RAMP Q',T=17.8,F=rampqf178/
&RAMP ID='RAMP Q',T=17.9,F=rampqf179/
&RAMP ID='RAMP Q',T=18.0,F=rampqf180/
&RAMP ID='RAMP Q',T=18.1,F=rampqf181/
&RAMP ID='RAMP Q',T=18.2,F=rampqf182/
&RAMP ID='RAMP Q',T=18.3,F=rampqf183/
&RAMP ID='RAMP Q',T=18.4,F=rampqf184/
&RAMP ID='RAMP Q',T=18.5,F=rampqf185/
&RAMP ID='RAMP Q',T=18.6,F=rampqf186/
&RAMP ID='RAMP Q',T=18.7,F=rampqf187/
&RAMP ID='RAMP Q',T=18.8,F=rampqf188/
&RAMP ID='RAMP Q',T=18.9,F=rampqf189/
&RAMP ID='RAMP Q',T=19.0,F=rampqf190/
&RAMP ID='RAMP Q',T=19.1,F=rampqf191/
&RAMP ID='RAMP Q',T=19.2,F=rampqf192/
&RAMP ID='RAMP Q',T=19.3,F=rampqf193/
&RAMP ID='RAMP Q',T=19.4,F=rampqf194/
&RAMP ID='RAMP Q',T=19.5,F=rampqf195/
&RAMP ID='RAMP Q',T=19.6,F=rampqf196/
&RAMP ID='RAMP Q',T=19.7,F=rampqf197/
&RAMP ID='RAMP Q',T=19.8,F=rampqf198/
&RAMP ID='RAMP Q',T=19.9,F=rampqf199/
&RAMP ID='RAMP Q',T=20.0,F=rampqf200/
&RAMP ID='RAMP Q',T=20.1,F=0.0000/

! RAMP for droplets

&RAMP ID='RAMP MF',T=0.00,F=0.0000/
&RAMP ID='RAMP MF',T=0.1,F=rampmff1/
&RAMP ID='RAMP MF',T=0.2,F=rampmff2/
&RAMP ID='RAMP MF',T=0.3,F=rampmff3/
&RAMP ID='RAMP MF',T=0.4,F=rampmff4/
&RAMP ID='RAMP MF',T=0.5,F=rampmff5/
&RAMP ID='RAMP MF',T=0.6,F=rampmff6/
&RAMP ID='RAMP MF',T=0.7,F=rampmff7/
&RAMP ID='RAMP MF',T=0.8,F=rampmff8/
&RAMP ID='RAMP MF',T=0.9,F=rampmff9/
&RAMP ID='RAMP MF',T=1.0,F=rampmff10/
&RAMP ID='RAMP MF',T=1.1,F=rampmff11/
&RAMP ID='RAMP MF',T=1.2,F=rampmff12/
&RAMP ID='RAMP MF',T=1.3,F=rampmff13/
&RAMP ID='RAMP MF',T=1.4,F=rampmff14/
&RAMP ID='RAMP MF',T=1.5,F=rampmff15/
&RAMP ID='RAMP MF',T=1.6,F=rampmff16/
&RAMP ID='RAMP MF',T=1.7,F=rampmff17/
&RAMP ID='RAMP MF',T=1.8,F=rampmff18/
&RAMP ID='RAMP MF',T=1.9,F=rampmff19/
&RAMP ID='RAMP MF',T=2.0,F=rampmff20/
&RAMP ID='RAMP MF',T=2.1,F=rampmff21/
&RAMP ID='RAMP MF',T=2.2,F=rampmff22/
&RAMP ID='RAMP MF',T=2.3,F=rampmff23/
&RAMP ID='RAMP MF',T=2.4,F=rampmff24/
&RAMP ID='RAMP MF',T=2.5,F=rampmff25/
&RAMP ID='RAMP MF',T=2.6,F=rampmff26/
&RAMP ID='RAMP MF',T=2.7,F=rampmff27/
&RAMP ID='RAMP MF',T=2.8,F=rampmff28/
&RAMP ID='RAMP MF',T=2.9,F=rampmff29/
&RAMP ID='RAMP MF',T=3.0,F=rampmff30/
&RAMP ID='RAMP MF',T=3.1,F=rampmff31/
&RAMP ID='RAMP MF',T=3.2,F=rampmff32/
&RAMP ID='RAMP MF',T=3.3,F=rampmff33/
&RAMP ID='RAMP MF',T=3.4,F=rampmff34/
```

```
&RAMP ID='RAMP MF',T=3.5,F=rampmff35/
&RAMP ID='RAMP MF',T=3.6,F=rampmff36/
&RAMP ID='RAMP MF',T=3.7,F=rampmff37/
&RAMP ID='RAMP MF',T=3.8,F=rampmff38/
&RAMP ID='RAMP MF',T=3.9,F=rampmff39/
&RAMP ID='RAMP MF',T=4.0,F=rampmff40/
&RAMP ID='RAMP MF',T=4.1,F=rampmff41/
&RAMP ID='RAMP MF',T=4.2,F=rampmff42/
&RAMP ID='RAMP MF',T=4.3,F=rampmff43/
&RAMP ID='RAMP MF',T=4.4,F=rampmff44/
&RAMP ID='RAMP MF',T=4.5,F=rampmff45/
&RAMP ID='RAMP MF',T=4.6,F=rampmff46/
&RAMP ID='RAMP MF',T=4.7,F=rampmff47/
&RAMP ID='RAMP MF',T=4.8,F=rampmff48/
&RAMP ID='RAMP MF',T=4.9,F=rampmff49/
&RAMP ID='RAMP MF',T=5.0,F=rampmff50/
&RAMP ID='RAMP MF',T=5.1,F=rampmff51/
&RAMP ID='RAMP MF',T=5.2,F=rampmff52/
&RAMP ID='RAMP MF',T=5.3,F=rampmff53/
&RAMP ID='RAMP MF',T=5.4,F=rampmff54/
&RAMP ID='RAMP MF',T=5.5,F=rampmff55/
&RAMP ID='RAMP MF',T=5.6,F=rampmff56/
&RAMP ID='RAMP MF',T=5.7,F=rampmff57/
&RAMP ID='RAMP MF',T=5.8,F=rampmff58/
&RAMP ID='RAMP MF',T=5.9,F=rampmff59/
&RAMP ID='RAMP MF',T=6.0,F=rampmff60/
&RAMP ID='RAMP MF',T=6.1,F=rampmff61/
&RAMP ID='RAMP MF',T=6.2,F=rampmff62/
&RAMP ID='RAMP MF',T=6.3,F=rampmff63/
&RAMP ID='RAMP MF',T=6.4,F=rampmff64/
&RAMP ID='RAMP MF',T=6.5,F=rampmff65/
&RAMP ID='RAMP MF',T=6.6,F=rampmff66/
&RAMP ID='RAMP MF',T=6.7,F=rampmff67/
&RAMP ID='RAMP MF',T=6.8,F=rampmff68/
&RAMP ID='RAMP MF',T=6.9,F=rampmff69/
&RAMP ID='RAMP MF',T=7.0,F=rampmff70/
&RAMP ID='RAMP MF',T=7.1,F=rampmff71/
&RAMP ID='RAMP MF',T=7.2,F=rampmff72/
&RAMP ID='RAMP MF',T=7.3,F=rampmff73/
&RAMP ID='RAMP MF',T=7.4,F=rampmff74/
&RAMP ID='RAMP MF',T=7.5,F=rampmff75/
&RAMP ID='RAMP MF',T=7.6,F=rampmff76/
&RAMP ID='RAMP MF',T=7.7,F=rampmff77/
&RAMP ID='RAMP MF',T=7.8,F=rampmff78/
&RAMP ID='RAMP MF',T=7.9,F=rampmff79/
&RAMP ID='RAMP MF',T=8.0,F=rampmff80/
&RAMP ID='RAMP MF',T=8.1,F=rampmff81/
&RAMP ID='RAMP MF',T=8.2,F=rampmff82/
&RAMP ID='RAMP MF',T=8.3,F=rampmff83/
&RAMP ID='RAMP MF',T=8.4,F=rampmff84/
&RAMP ID='RAMP MF',T=8.5,F=rampmff85/
&RAMP ID='RAMP MF',T=8.6,F=rampmff86/
&RAMP ID='RAMP MF',T=8.7,F=rampmff87/
&RAMP ID='RAMP MF',T=8.8,F=rampmff88/
&RAMP ID='RAMP MF',T=8.9,F=rampmff89/
&RAMP ID='RAMP MF',T=9.0,F=rampmff90/
&RAMP ID='RAMP MF',T=9.1,F=rampmff91/
&RAMP ID='RAMP MF',T=9.2,F=rampmff92/
&RAMP ID='RAMP MF',T=9.3,F=rampmff93/
&RAMP ID='RAMP MF',T=9.4,F=rampmff94/
&RAMP ID='RAMP MF',T=9.5,F=rampmff95/
&RAMP ID='RAMP MF',T=9.6,F=rampmff96/
&RAMP ID='RAMP MF',T=9.7,F=rampmff97/
&RAMP ID='RAMP MF',T=9.8,F=rampmff98/
```

```
&RAMP ID='RAMP MF',T=9.9,F=rampmff99/
&RAMP ID='RAMP MF',T=10.0,F=rampmff100/
&RAMP ID='RAMP MF',T=10.1,F=rampmff101/
&RAMP ID='RAMP MF',T=10.2,F=rampmff102/
&RAMP ID='RAMP MF',T=10.3,F=rampmff103/
&RAMP ID='RAMP MF',T=10.4,F=rampmff104/
&RAMP ID='RAMP MF',T=10.5,F=rampmff105/
&RAMP ID='RAMP MF',T=10.6,F=rampmff106/
&RAMP ID='RAMP MF',T=10.7,F=rampmff107/
&RAMP ID='RAMP MF',T=10.8,F=rampmff108/
&RAMP ID='RAMP MF',T=10.9,F=rampmff109/
&RAMP ID='RAMP MF',T=11.0,F=rampmff110/
&RAMP ID='RAMP MF',T=11.1,F=rampmff111/
&RAMP ID='RAMP MF',T=11.2,F=rampmff112/
&RAMP ID='RAMP MF',T=11.3,F=rampmff113/
&RAMP ID='RAMP MF',T=11.4,F=rampmff114/
&RAMP ID='RAMP MF',T=11.5,F=rampmff115/
&RAMP ID='RAMP MF',T=11.6,F=rampmff116/
&RAMP ID='RAMP MF',T=11.7,F=rampmff117/
&RAMP ID='RAMP MF',T=11.8,F=rampmff118/
&RAMP ID='RAMP MF',T=11.9,F=rampmff119/
&RAMP ID='RAMP MF',T=12.0,F=rampmff120/
&RAMP ID='RAMP MF',T=12.1,F=rampmff121/
&RAMP ID='RAMP MF',T=12.2,F=rampmff122/
&RAMP ID='RAMP MF',T=12.3,F=rampmff123/
&RAMP ID='RAMP MF',T=12.4,F=rampmff124/
&RAMP ID='RAMP MF',T=12.5,F=rampmff125/
&RAMP ID='RAMP MF',T=12.6,F=rampmff126/
&RAMP ID='RAMP MF',T=12.7,F=rampmff127/
&RAMP ID='RAMP MF',T=12.8,F=rampmff128/
&RAMP ID='RAMP MF',T=12.9,F=rampmff129/
&RAMP ID='RAMP MF',T=13.0,F=rampmff130/
&RAMP ID='RAMP MF',T=13.1,F=rampmff131/
&RAMP ID='RAMP MF',T=13.2,F=rampmff132/
&RAMP ID='RAMP MF',T=13.3,F=rampmff133/
&RAMP ID='RAMP MF',T=13.4,F=rampmff134/
&RAMP ID='RAMP MF',T=13.5,F=rampmff135/
&RAMP ID='RAMP MF',T=13.6,F=rampmff136/
&RAMP ID='RAMP MF',T=13.7,F=rampmff137/
&RAMP ID='RAMP MF',T=13.8,F=rampmff138/
&RAMP ID='RAMP MF',T=13.9,F=rampmff139/
&RAMP ID='RAMP MF',T=14.0,F=rampmff140/
&RAMP ID='RAMP MF',T=14.1,F=rampmff141/
&RAMP ID='RAMP MF',T=14.2,F=rampmff142/
&RAMP ID='RAMP MF',T=14.3,F=rampmff143/
&RAMP ID='RAMP MF',T=14.4,F=rampmff144/
&RAMP ID='RAMP MF',T=14.5,F=rampmff145/
&RAMP ID='RAMP MF',T=14.6,F=rampmff146/
&RAMP ID='RAMP MF',T=14.7,F=rampmff147/
&RAMP ID='RAMP MF',T=14.8,F=rampmff148/
&RAMP ID='RAMP MF',T=14.9,F=rampmff149/
&RAMP ID='RAMP MF',T=15.0,F=rampmff150/
&RAMP ID='RAMP MF',T=15.1,F=rampmff151/
&RAMP ID='RAMP MF',T=15.2,F=rampmff152/
&RAMP ID='RAMP MF',T=15.3,F=rampmff153/
&RAMP ID='RAMP MF',T=15.4,F=rampmff154/
&RAMP ID='RAMP MF',T=15.5,F=rampmff155/
&RAMP ID='RAMP MF',T=15.6,F=rampmff156/
&RAMP ID='RAMP MF',T=15.7,F=rampmff157/
&RAMP ID='RAMP MF',T=15.8,F=rampmff158/
&RAMP ID='RAMP MF',T=15.9,F=rampmff159/
&RAMP ID='RAMP MF',T=16.0,F=rampmff160/
&RAMP ID='RAMP MF',T=16.1,F=rampmff161/
&RAMP ID='RAMP MF',T=16.2,F=rampmff162/
```

```
&RAMP ID='RAMP MF',T=16.3,F=rampmff163/
&RAMP ID='RAMP MF',T=16.4,F=rampmff164/
&RAMP ID='RAMP MF',T=16.5,F=rampmff165/
&RAMP ID='RAMP MF',T=16.6,F=rampmff166/
&RAMP ID='RAMP MF',T=16.7,F=rampmff167/
&RAMP ID='RAMP MF',T=16.8,F=rampmff168/
&RAMP ID='RAMP MF',T=16.9,F=rampmff169/
&RAMP ID='RAMP MF',T=17.0,F=rampmff170/
&RAMP ID='RAMP MF',T=17.1,F=rampmff171/
&RAMP ID='RAMP MF',T=17.2,F=rampmff172/
&RAMP ID='RAMP MF',T=17.3,F=rampmff173/
&RAMP ID='RAMP MF',T=17.4,F=rampmff174/
&RAMP ID='RAMP MF',T=17.5,F=rampmff175/
&RAMP ID='RAMP MF',T=17.6,F=rampmff176/
&RAMP ID='RAMP MF',T=17.7,F=rampmff177/
&RAMP ID='RAMP MF',T=17.8,F=rampmff178/
&RAMP ID='RAMP MF',T=17.9,F=rampmff179/
&RAMP ID='RAMP MF',T=18.0,F=rampmff180/
&RAMP ID='RAMP MF',T=18.1,F=rampmff181/
&RAMP ID='RAMP MF',T=18.2,F=rampmff182/
&RAMP ID='RAMP MF',T=18.3,F=rampmff183/
&RAMP ID='RAMP MF',T=18.4,F=rampmff184/
&RAMP ID='RAMP MF',T=18.5,F=rampmff185/
&RAMP ID='RAMP MF',T=18.6,F=rampmff186/
&RAMP ID='RAMP MF',T=18.7,F=rampmff187/
&RAMP ID='RAMP MF',T=18.8,F=rampmff188/
&RAMP ID='RAMP MF',T=18.9,F=rampmff189/
&RAMP ID='RAMP MF',T=19.0,F=rampmff190/
&RAMP ID='RAMP MF',T=19.1,F=rampmff191/
&RAMP ID='RAMP MF',T=19.2,F=rampmff192/
&RAMP ID='RAMP MF',T=19.3,F=rampmff193/
&RAMP ID='RAMP MF',T=19.4,F=rampmff194/
&RAMP ID='RAMP MF',T=19.5,F=rampmff195/
&RAMP ID='RAMP MF',T=19.6,F=rampmff196/
&RAMP ID='RAMP MF',T=19.7,F=rampmff197/
&RAMP ID='RAMP MF',T=19.8,F=rampmff198/
&RAMP ID='RAMP MF',T=19.9,F=rampmff199/
&RAMP ID='RAMP MF',T=20.0,F=rampmff200/
&RAMP ID='RAMP MF',T=20.1,F=0.0000/

! Gas phase specific heats. FDS defaults for N2, O2, H2O, and CO2 replaced to extend
values to higher temperatures than present in FDS

&RAMP ID='AL2O3 C', T=-73, F=0.761/ NASA TP-2002-211556
&RAMP ID='AL2O3 C', T=127, F=0.921/
&RAMP ID='AL2O3 C', T=327, F=0.999/
&RAMP ID='AL2O3 C', T=527, F=1.038/
&RAMP ID='AL2O3 C', T=727, F=1.058/
&RAMP ID='AL2O3 C', T=1727, F=1.090/
&RAMP ID='AL2O3 C', T=2727, F=1.096/
&RAMP ID='AL2O3 C', T=3727, F=1.098/
&RAMP ID='AL2O3 C', T=4727, F=1.099/
&RAMP ID='AL2O3 C', T=5727, F=1.100/

&RAMP ID='AL C', T=-73, F=0.820/ NASA TP-2002-211556
&RAMP ID='AL C', T=127, F=0.783/
&RAMP ID='AL C', T=327, F=0.776/
&RAMP ID='AL C', T=527, F=0.773/
&RAMP ID='AL C', T=727, F=0.772/
&RAMP ID='AL C', T=1727, F=0.771/
&RAMP ID='AL C', T=2727, F=0.771/
&RAMP ID='AL C', T=3727, F=0.775/
&RAMP ID='AL C', T=4727, F=0.793/
&RAMP ID='AL C', T=5727, F=0.841/
```

```
&RAMP ID='AL C', T=6727, F=0.930/
&RAMP ID='AL C', T=7727, F=1.034/
&RAMP ID='AL C', T=8727, F=1.130/
&RAMP ID='AL C', T=9727, F=1.204/
&RAMP ID='AL C', T=10727, F=1.250/
&RAMP ID='AL C', T=11727, F=1.271/
&RAMP ID='AL C', T=12727, F=1.269/
&RAMP ID='AL C', T=13727, F=1.252/
&RAMP ID='AL C', T=14727, F=1.226/
&RAMP ID='AL C', T=15727, F=1.196/
&RAMP ID='AL C', T=16727, F=1.168/
&RAMP ID='AL C', T=17727, F=1.145/
&RAMP ID='AL C', T=18727, F=1.125/
&RAMP ID='AL C', T=19727, F=1.108/

&RAMP ID='CU C', T=-73, F=0.327/ NASA TP-2002-211556
&RAMP ID='CU C', T=127, F=0.327/
&RAMP ID='CU C', T=327, F=0.327/
&RAMP ID='CU C', T=527, F=0.327/
&RAMP ID='CU C', T=727, F=0.327/
&RAMP ID='CU C', T=1727, F=0.337/
&RAMP ID='CU C', T=2727, F=0.396/
&RAMP ID='CU C', T=3727, F=0.471/
&RAMP ID='CU C', T=4727, F=0.517/
&RAMP ID='CU C', T=5727, F=0.537/
&RAMP ID='CU C', T=6727, F=0.551/
&RAMP ID='CU C', T=7727, F=0.577/
&RAMP ID='CU C', T=8727, F=0.606/
&RAMP ID='CU C', T=9727, F=0.633/
&RAMP ID='CU C', T=10727, F=0.653/
&RAMP ID='CU C', T=11727, F=0.663/
&RAMP ID='CU C', T=12727, F=0.664/
&RAMP ID='CU C', T=13727, F=0.657/
&RAMP ID='CU C', T=14727, F=0.642/
&RAMP ID='CU C', T=15727, F=0.622/
&RAMP ID='CU C', T=16727, F=0.599/
&RAMP ID='CU C', T=17727, F=0.574/
&RAMP ID='CU C', T=18727, F=0.550/
&RAMP ID='CU C', T=19727, F=0.528/

&RAMP ID='N2 C', T=-73, F=1.039/ NASA TP-2002-211556
&RAMP ID='N2 C', T=127, F=1.044/
&RAMP ID='N2 C', T=327, F=1.075/
&RAMP ID='N2 C', T=527, F=1.122/
&RAMP ID='N2 C', T=727, F=1.167/
&RAMP ID='N2 C', T=1727, F=1.284/
&RAMP ID='N2 C', T=2727, F=1.322/
&RAMP ID='N2 C', T=3727, F=1.340/
&RAMP ID='N2 C', T=4727, F=1.354/
&RAMP ID='N2 C', T=5727, F=1.371/
&RAMP ID='N2 C', T=6727, F=1.402/
&RAMP ID='N2 C', T=7727, F=1.454/
&RAMP ID='N2 C', T=8727, F=1.544/
&RAMP ID='N2 C', T=9727, F=1.670/
&RAMP ID='N2 C', T=10727, F=1.822/
&RAMP ID='N2 C', T=11727, F=1.984/
&RAMP ID='N2 C', T=12727, F=2.136/
&RAMP ID='N2 C', T=13727, F=2.261/
&RAMP ID='N2 C', T=14727, F=2.346/
&RAMP ID='N2 C', T=15727, F=2.383/
&RAMP ID='N2 C', T=16727, F=2.372/
&RAMP ID='N2 C', T=17727, F=2.320/
&RAMP ID='N2 C', T=18727, F=2.241/
&RAMP ID='N2 C', T=19727, F=2.159/
```

```
&RAMP ID='O2 C', T=-73, F=0.910/ NASA TP-2002-211556
&RAMP ID='O2 C', T=127, F=0.941/
&RAMP ID='O2 C', T=327, F=1.003/
&RAMP ID='O2 C', T=527, F=1.055/
&RAMP ID='O2 C', T=727, F=1.090/
&RAMP ID='O2 C', T=1727, F=1.181/
&RAMP ID='O2 C', T=2727, F=1.249/
&RAMP ID='O2 C', T=3727, F=1.303/
&RAMP ID='O2 C', T=4727, F=1.344/
&RAMP ID='O2 C', T=5727, F=1.373/
&RAMP ID='O2 C', T=6727, F=1.386/
&RAMP ID='O2 C', T=7727, F=1.376/
&RAMP ID='O2 C', T=8727, F=1.344/
&RAMP ID='O2 C', T=9727, F=1.296/
&RAMP ID='O2 C', T=10727, F=1.241/
&RAMP ID='O2 C', T=11727, F=1.184/
&RAMP ID='O2 C', T=12727, F=1.128/
&RAMP ID='O2 C', T=13727, F=1.077/
&RAMP ID='O2 C', T=14727, F=1.030/
&RAMP ID='O2 C', T=15727, F=0.989/
&RAMP ID='O2 C', T=16727, F=0.953/
&RAMP ID='O2 C', T=17727, F=0.922/
&RAMP ID='O2 C', T=18727, F=0.894/
&RAMP ID='O2 C', T=19727, F=0.870/

&RAMP ID='CO2 C', T=-73, F=0.735/ NASA TP-2002-211556
&RAMP ID='CO2 C', T=127, F=0.939/
&RAMP ID='CO2 C', T=327, F=1.075/
&RAMP ID='CO2 C', T=527, F=1.169/
&RAMP ID='CO2 C', T=727, F=1.234/
&RAMP ID='CO2 C', T=1727, F=1.371/
&RAMP ID='CO2 C', T=2727, F=1.412/
&RAMP ID='CO2 C', T=3727, F=1.436/
&RAMP ID='CO2 C', T=4727, F=1.466/
&RAMP ID='CO2 C', T=5727, F=1.517/
&RAMP ID='CO2 C', T=6727, F=1.595/
&RAMP ID='CO2 C', T=7727, F=1.694/
&RAMP ID='CO2 C', T=8727, F=1.797/
&RAMP ID='CO2 C', T=9727, F=1.888/
&RAMP ID='CO2 C', T=10727, F=1.957/
&RAMP ID='CO2 C', T=11727, F=2.000/
&RAMP ID='CO2 C', T=12727, F=2.019/
&RAMP ID='CO2 C', T=13727, F=2.020/
&RAMP ID='CO2 C', T=14727, F=2.007/
&RAMP ID='CO2 C', T=15727, F=1.987/
&RAMP ID='CO2 C', T=16727, F=1.965/
&RAMP ID='CO2 C', T=17727, F=1.944/
&RAMP ID='CO2 C', T=18727, F=1.924/
&RAMP ID='CO2 C', T=19727, F=1.905/

!Smokeview Outputs. Adjust PBY and PBX for center of arc volume.

alslcf1 QUANTITY='MASS FRACTION',SPEC_ID='ALUMINUM',CELL_CENTERED=.TRUE.,PBY=0.0000/
alslcf2 QUANTITY='MASS FRACTION',SPEC_ID='ALUMINUM
OXIDE',CELL_CENTERED=.TRUE.,PBY=0.0000/
cuslcf1 QUANTITY='MASS FRACTION',SPEC_ID='COPPER',CELL_CENTERED=.TRUE.,PBY=0.0000/
cuslcf2 QUANTITY='MASS FRACTION',SPEC_ID='COPPER
OXIDE',CELL_CENTERED=.TRUE.,PBY=0.0000/
&SLCF QUANTITY='MASS FRACTION',SPEC_ID='OXYGEN',CELL_CENTERED=.TRUE.,PBY=0.0000/
&SLCF QUANTITY='HRRPUV',CELL_CENTERED=.TRUE.,PBY=0.0000/
&SLCF QUANTITY='HRRPUV',CELL_CENTERED=.TRUE.,PBX=slcfpbx/
&SLCF QUANTITY='TEMPERATURE',CELL_CENTERED=.TRUE.,PBY=0.0000/
&SLCF QUANTITY='TEMPERATURE',CELL_CENTERED=.TRUE.,PBX=slcfpbx/
```

```
&SLCF QUANTITY='INTEGRATED INTENSITY',CELL_CENTERED=.TRUE.,PBY=0.0000/
&SLCF QUANTITY='INTEGRATED INTENSITY',CELL_CENTERED=.TRUE.,PBX=slcfpbx/
&SLCF QUANTITY='VELOCITY',CELL_CENTERED=.TRUE.,PBY=0.0000/
&SLCF QUANTITY='U-VELOCITY',CELL_CENTERED=.TRUE.,PBY=0.0000/
&SLCF QUANTITY='VELOCITY',CELL_CENTERED=.TRUE.,PBX=slcfpbx/
&SLCF QUANTITY='V-VELOCITY',CELL_CENTERED=.TRUE.,PBX=slcfpbx/
&SLCF QUANTITY='PRESSURE',CELL_CENTERED=.TRUE.,PBY=0.0000/

&BNDF QUANTITY='WALL TEMPERATURE',CELL_CENTERED=.TRUE./
&BNDF QUANTITY='GAUGE HEAT FLUX',CELL_CENTERED=.TRUE./
&BNDF QUANTITY='WALL THICKNESS',CELL_CENTERED=.TRUE./
&BNDF QUANTITY='VELOCITY ERROR',CELL_CENTERED=.TRUE./

!Example DEVC for ZOI runs. Have planes of devices at a range of distances that look
at each face of the enclosure
!Plane should be large enough to see any permanent venting, plus any area heated by or
damaged by the arc, plus any bouyancy impacts
!Here the DEVC ID my means this is on the (m)inus (y) face at the given x,y,z location
!The orientation is the unit vector given by Arc Center - DEVC XYZ.  Pointing the DEVC
at the arc centroid will approximate the worst case view factor
!for the radiative component.
!These can easily be generated with Excel using CONCATENATE()

&DEVC XB=-0.0381,-2.4003,-0.1905,-
0.1905,0.0381,0.0381,POINTS=31,ORIENTATION=1,0,0,ID='BL y:-0.1905
z:0.0381',QUANTITY='GAUGE HEAT FLUX GAS',STATISTICS_START=0,TEMPORAL_STATISTIC='TIME
INTEGRAL'/
&DEVC XB=-0.0381,-2.4003,-0.1905,-
0.1905,0.1143,0.1143,POINTS=31,ORIENTATION=1,0,0,ID='BL y:-0.1905
z:0.1143',QUANTITY='GAUGE HEAT FLUX GAS',STATISTICS_START=0,TEMPORAL_STATISTIC='TIME
INTEGRAL'/
&DEVC XB=-0.0381,-2.4003,-0.1905,-
0.1905,0.1905,0.1905,POINTS=31,ORIENTATION=1,0,0,ID='BL y:-0.1905
z:0.1905',QUANTITY='GAUGE HEAT FLUX GAS',STATISTICS_START=0,TEMPORAL_STATISTIC='TIME
INTEGRAL'/
&DEVC XB=-0.0381,-2.4003,-0.1905,-
0.1905,0.2667,0.2667,POINTS=31,ORIENTATION=1,0,0,ID='BL y:-0.1905
z:0.2667',QUANTITY='GAUGE HEAT FLUX GAS',STATISTICS_START=0,TEMPORAL_STATISTIC='TIME
INTEGRAL'/
&DEVC XB=-0.0381,-2.4003,-0.1905,-
0.1905,0.3429,0.3429,POINTS=31,ORIENTATION=1,0,0,ID='BL y:-0.1905
z:0.3429',QUANTITY='GAUGE HEAT FLUX GAS',STATISTICS_START=0,TEMPORAL_STATISTIC='TIME
INTEGRAL'/
&DEVC XB=-0.0381,-2.4003,-0.1905,-
0.1905,0.4191,0.4191,POINTS=31,ORIENTATION=1,0,0,ID='BL y:-0.1905
z:0.4191',QUANTITY='GAUGE HEAT FLUX GAS',STATISTICS_START=0,TEMPORAL_STATISTIC='TIME
INTEGRAL'/
&DEVC XB=-0.0381,-2.4003,-0.1143,-
0.1143,0.0381,0.0381,POINTS=31,ORIENTATION=1,0,0,ID='BL y:-0.1143
z:0.0381',QUANTITY='GAUGE HEAT FLUX GAS',STATISTICS_START=0,TEMPORAL_STATISTIC='TIME
INTEGRAL'/
&DEVC XB=-0.0381,-2.4003,-0.1143,-
0.1143,0.1143,0.1143,POINTS=31,ORIENTATION=1,0,0,ID='BL y:-0.1143
z:0.1143',QUANTITY='GAUGE HEAT FLUX GAS',STATISTICS_START=0,TEMPORAL_STATISTIC='TIME
INTEGRAL'/
&DEVC XB=-0.0381,-2.4003,-0.1143,-
0.1143,0.1905,0.1905,POINTS=31,ORIENTATION=1,0,0,ID='BL y:-0.1143
z:0.1905',QUANTITY='GAUGE HEAT FLUX GAS',STATISTICS_START=0,TEMPORAL_STATISTIC='TIME
INTEGRAL'/
&DEVC XB=-0.0381,-2.4003,-0.1143,-
0.1143,0.2667,0.2667,POINTS=31,ORIENTATION=1,0,0,ID='BL y:-0.1143
z:0.2667',QUANTITY='GAUGE HEAT FLUX GAS',STATISTICS_START=0,TEMPORAL_STATISTIC='TIME
INTEGRAL'/
```

```
&DEVC XB=-0.0381,-2.4003,-0.1143,-
0.1143,0.3429,0.3429,POINTS=31,ORIENTATION=1,0,0,ID='BL y:-0.1143
z:0.3429',QUANTITY='GAUGE HEAT FLUX GAS',STATISTICS_START=0,TEMPORAL_STATISTIC='TIME
INTEGRAL'/
&DEVC XB=-0.0381,-2.4003,-0.1143,-
0.1143,0.4191,0.4191,POINTS=31,ORIENTATION=1,0,0,ID='BL y:-0.1143
z:0.4191',QUANTITY='GAUGE HEAT FLUX GAS',STATISTICS_START=0,TEMPORAL_STATISTIC='TIME
INTEGRAL'/
&DEVC XB=-0.0381,-2.4003,-0.0381,-
0.0381,0.0381,0.0381,POINTS=31,ORIENTATION=1,0,0,ID='BL y:-0.0381
z:0.0381',QUANTITY='GAUGE HEAT FLUX GAS',STATISTICS_START=0,TEMPORAL_STATISTIC='TIME
INTEGRAL'/
&DEVC XB=-0.0381,-2.4003,-0.0381,-
0.0381,0.1143,0.1143,POINTS=31,ORIENTATION=1,0,0,ID='BL y:-0.0381
z:0.1143',QUANTITY='GAUGE HEAT FLUX GAS',STATISTICS_START=0,TEMPORAL_STATISTIC='TIME
INTEGRAL'/
&DEVC XB=-0.0381,-2.4003,-0.0381,-
0.0381,0.1905,0.1905,POINTS=31,ORIENTATION=1,0,0,ID='BL y:-0.0381
z:0.1905',QUANTITY='GAUGE HEAT FLUX GAS',STATISTICS_START=0,TEMPORAL_STATISTIC='TIME
INTEGRAL'/
&DEVC XB=-0.0381,-2.4003,-0.0381,-
0.0381,0.2667,0.2667,POINTS=31,ORIENTATION=1,0,0,ID='BL y:-0.0381
z:0.2667',QUANTITY='GAUGE HEAT FLUX GAS',STATISTICS_START=0,TEMPORAL_STATISTIC='TIME
INTEGRAL'/
&DEVC XB=-0.0381,-2.4003,-0.0381,-
0.0381,0.3429,0.3429,POINTS=31,ORIENTATION=1,0,0,ID='BL y:-0.0381
z:0.3429',QUANTITY='GAUGE HEAT FLUX GAS',STATISTICS_START=0,TEMPORAL_STATISTIC='TIME
INTEGRAL'/
&DEVC XB=-0.0381,-2.4003,-0.0381,-
0.0381,0.4191,0.4191,POINTS=31,ORIENTATION=1,0,0,ID='BL y:-0.0381
z:0.4191',QUANTITY='GAUGE HEAT FLUX GAS',STATISTICS_START=0,TEMPORAL_STATISTIC='TIME
INTEGRAL'/
&DEVC XB=-0.0381,-
2.4003,0.0381,0.0381,0.0381,0.0381,POINTS=31,ORIENTATION=1,0,0,ID='BL y:0.0381
z:0.0381',QUANTITY='GAUGE HEAT FLUX GAS',STATISTICS_START=0,TEMPORAL_STATISTIC='TIME
INTEGRAL'/
&DEVC XB=-0.0381,-
2.4003,0.0381,0.0381,0.1143,0.1143,POINTS=31,ORIENTATION=1,0,0,ID='BL y:0.0381
z:0.1143',QUANTITY='GAUGE HEAT FLUX GAS',STATISTICS_START=0,TEMPORAL_STATISTIC='TIME
INTEGRAL'/
&DEVC XB=-0.0381,-
2.4003,0.0381,0.0381,0.1905,0.1905,POINTS=31,ORIENTATION=1,0,0,ID='BL y:0.0381
z:0.1905',QUANTITY='GAUGE HEAT FLUX GAS',STATISTICS_START=0,TEMPORAL_STATISTIC='TIME
INTEGRAL'/
&DEVC XB=-0.0381,-
2.4003,0.0381,0.0381,0.2667,0.2667,POINTS=31,ORIENTATION=1,0,0,ID='BL y:0.0381
z:0.2667',QUANTITY='GAUGE HEAT FLUX GAS',STATISTICS_START=0,TEMPORAL_STATISTIC='TIME
INTEGRAL'/
&DEVC XB=-0.0381,-
2.4003,0.0381,0.0381,0.3429,0.3429,POINTS=31,ORIENTATION=1,0,0,ID='BL y:0.0381
z:0.3429',QUANTITY='GAUGE HEAT FLUX GAS',STATISTICS_START=0,TEMPORAL_STATISTIC='TIME
INTEGRAL'/
&DEVC XB=-0.0381,-
2.4003,0.0381,0.0381,0.4191,0.4191,POINTS=31,ORIENTATION=1,0,0,ID='BL y:0.0381
z:0.4191',QUANTITY='GAUGE HEAT FLUX GAS',STATISTICS_START=0,TEMPORAL_STATISTIC='TIME
INTEGRAL'/
&DEVC XB=-0.0381,-
2.4003,0.1143,0.1143,0.0381,0.0381,POINTS=31,ORIENTATION=1,0,0,ID='BL y:0.1143
z:0.0381',QUANTITY='GAUGE HEAT FLUX GAS',STATISTICS_START=0,TEMPORAL_STATISTIC='TIME
INTEGRAL'/
&DEVC XB=-0.0381,-
2.4003,0.1143,0.1143,0.1143,0.1143,POINTS=31,ORIENTATION=1,0,0,ID='BL y:0.1143
z:0.1143',QUANTITY='GAUGE HEAT FLUX GAS',STATISTICS_START=0,TEMPORAL_STATISTIC='TIME
INTEGRAL'/
```

```
&DEVC XB=-0.0381,-
2.4003,0.1143,0.1143,0.1905,0.1905,POINTS=31,ORIENTATION=1,0,0,ID='BL y:0.1143
z:0.1905',QUANTITY='GAUGE HEAT FLUX GAS',STATISTICS_START=0,TEMPORAL_STATISTIC='TIME
INTEGRAL'/
&DEVC XB=-0.0381,-
2.4003,0.1143,0.1143,0.2667,0.2667,POINTS=31,ORIENTATION=1,0,0,ID='BL y:0.1143
z:0.2667',QUANTITY='GAUGE HEAT FLUX GAS',STATISTICS_START=0,TEMPORAL_STATISTIC='TIME
INTEGRAL'/
&DEVC XB=-0.0381,-
2.4003,0.1143,0.1143,0.3429,0.3429,POINTS=31,ORIENTATION=1,0,0,ID='BL y:0.1143
z:0.3429',QUANTITY='GAUGE HEAT FLUX GAS',STATISTICS_START=0,TEMPORAL_STATISTIC='TIME
INTEGRAL'/
&DEVC XB=-0.0381,-
2.4003,0.1143,0.1143,0.4191,0.4191,POINTS=31,ORIENTATION=1,0,0,ID='BL y:0.1143
z:0.4191',QUANTITY='GAUGE HEAT FLUX GAS',STATISTICS_START=0,TEMPORAL_STATISTIC='TIME
INTEGRAL'/
&DEVC XB=-0.0381,-
2.4003,0.1905,0.1905,0.0381,0.0381,POINTS=31,ORIENTATION=1,0,0,ID='BL y:0.1905
z:0.0381',QUANTITY='GAUGE HEAT FLUX GAS',STATISTICS_START=0,TEMPORAL_STATISTIC='TIME
INTEGRAL'/
&DEVC XB=-0.0381,-
2.4003,0.1905,0.1905,0.1143,0.1143,POINTS=31,ORIENTATION=1,0,0,ID='BL y:0.1905
z:0.1143',QUANTITY='GAUGE HEAT FLUX GAS',STATISTICS_START=0,TEMPORAL_STATISTIC='TIME
INTEGRAL'/
&DEVC XB=-0.0381,-
2.4003,0.1905,0.1905,0.1905,0.1905,POINTS=31,ORIENTATION=1,0,0,ID='BL y:0.1905
z:0.1905',QUANTITY='GAUGE HEAT FLUX GAS',STATISTICS_START=0,TEMPORAL_STATISTIC='TIME
INTEGRAL'/
&DEVC XB=-0.0381,-
2.4003,0.1905,0.1905,0.2667,0.2667,POINTS=31,ORIENTATION=1,0,0,ID='BL y:0.1905
z:0.2667',QUANTITY='GAUGE HEAT FLUX GAS',STATISTICS_START=0,TEMPORAL_STATISTIC='TIME
INTEGRAL'/
&DEVC XB=-0.0381,-
2.4003,0.1905,0.1905,0.3429,0.3429,POINTS=31,ORIENTATION=1,0,0,ID='BL y:0.1905
z:0.3429',QUANTITY='GAUGE HEAT FLUX GAS',STATISTICS_START=0,TEMPORAL_STATISTIC='TIME
INTEGRAL'/
&DEVC XB=-0.0381,-
2.4003,0.1905,0.1905,0.4191,0.4191,POINTS=31,ORIENTATION=1,0,0,ID='BL y:0.1905
z:0.4191',QUANTITY='GAUGE HEAT FLUX GAS',STATISTICS_START=0,TEMPORAL_STATISTIC='TIME
INTEGRAL'/



&DEVC XB=1.1811,1.1811,-2.4765,-
0.4953,0.3429,0.3429,POINTS=26,ORIENTATION=0,1,0,ID='SL x:1.1811
z:0.3429',QUANTITY='GAUGE HEAT FLUX GAS',STATISTICS_START=0,TEMPORAL_STATISTIC='TIME
INTEGRAL'/
&DEVC XB=1.1811,1.1811,-2.4765,-
0.4953,0.4191,0.4191,POINTS=26,ORIENTATION=0,1,0,ID='SL x:1.1811
z:0.4191',QUANTITY='GAUGE HEAT FLUX GAS',STATISTICS_START=0,TEMPORAL_STATISTIC='TIME
INTEGRAL'/
&DEVC XB=1.1811,1.1811,-2.4765,-
0.4953,0.4953,0.4953,POINTS=26,ORIENTATION=0,1,0,ID='SL x:1.1811
z:0.4953',QUANTITY='GAUGE HEAT FLUX GAS',STATISTICS_START=0,TEMPORAL_STATISTIC='TIME
INTEGRAL'/
&DEVC XB=1.1811,1.1811,-2.4765,-
0.4953,0.5715,0.5715,POINTS=26,ORIENTATION=0,1,0,ID='SL x:1.1811
z:0.5715',QUANTITY='GAUGE HEAT FLUX GAS',STATISTICS_START=0,TEMPORAL_STATISTIC='TIME
INTEGRAL'/
&DEVC XB=1.1811,1.1811,-2.4765,-
0.4953,0.6477,0.6477,POINTS=26,ORIENTATION=0,1,0,ID='SL x:1.1811
z:0.6477',QUANTITY='GAUGE HEAT FLUX GAS',STATISTICS_START=0,TEMPORAL_STATISTIC='TIME
INTEGRAL'/
```

```
&DEVC XB=1.1811,1.1811,-2.4765,-
0.4953,0.7239,0.7239,POINTS=26,ORIENTATION=0,1,0,ID='SL x:1.1811
z:0.7239',QUANTITY='GAUGE HEAT FLUX GAS',STATISTICS_START=0,TEMPORAL_STATISTIC='TIME
INTEGRAL'/
&DEVC XB=1.2573,1.2573,-2.4765,-
0.4953,0.3429,0.3429,POINTS=26,ORIENTATION=0,1,0,ID='SL x:1.2573
z:0.3429',QUANTITY='GAUGE HEAT FLUX GAS',STATISTICS_START=0,TEMPORAL_STATISTIC='TIME
INTEGRAL'/
&DEVC XB=1.2573,1.2573,-2.4765,-
0.4953,0.4191,0.4191,POINTS=26,ORIENTATION=0,1,0,ID='SL x:1.2573
z:0.4191',QUANTITY='GAUGE HEAT FLUX GAS',STATISTICS_START=0,TEMPORAL_STATISTIC='TIME
INTEGRAL'/
&DEVC XB=1.2573,1.2573,-2.4765,-
0.4953,0.4953,0.4953,POINTS=26,ORIENTATION=0,1,0,ID='SL x:1.2573
z:0.4953',QUANTITY='GAUGE HEAT FLUX GAS',STATISTICS_START=0,TEMPORAL_STATISTIC='TIME
INTEGRAL'/
&DEVC XB=1.2573,1.2573,-2.4765,-
0.4953,0.5715,0.5715,POINTS=26,ORIENTATION=0,1,0,ID='SL x:1.2573
z:0.5715',QUANTITY='GAUGE HEAT FLUX GAS',STATISTICS_START=0,TEMPORAL_STATISTIC='TIME
INTEGRAL'/
&DEVC XB=1.2573,1.2573,-2.4765,-
0.4953,0.6477,0.6477,POINTS=26,ORIENTATION=0,1,0,ID='SL x:1.2573
z:0.6477',QUANTITY='GAUGE HEAT FLUX GAS',STATISTICS_START=0,TEMPORAL_STATISTIC='TIME
INTEGRAL'/
&DEVC XB=1.2573,1.2573,-2.4765,-
0.4953,0.7239,0.7239,POINTS=26,ORIENTATION=0,1,0,ID='SL x:1.2573
z:0.7239',QUANTITY='GAUGE HEAT FLUX GAS',STATISTICS_START=0,TEMPORAL_STATISTIC='TIME
INTEGRAL'/
&DEVC XB=1.3335,1.3335,-2.4765,-
0.4953,0.3429,0.3429,POINTS=26,ORIENTATION=0,1,0,ID='SL x:1.3335
z:0.3429',QUANTITY='GAUGE HEAT FLUX GAS',STATISTICS_START=0,TEMPORAL_STATISTIC='TIME
INTEGRAL'/
&DEVC XB=1.3335,1.3335,-2.4765,-
0.4953,0.4191,0.4191,POINTS=26,ORIENTATION=0,1,0,ID='SL x:1.3335
z:0.4191',QUANTITY='GAUGE HEAT FLUX GAS',STATISTICS_START=0,TEMPORAL_STATISTIC='TIME
INTEGRAL'/
&DEVC XB=1.3335,1.3335,-2.4765,-
0.4953,0.4953,0.4953,POINTS=26,ORIENTATION=0,1,0,ID='SL x:1.3335
z:0.4953',QUANTITY='GAUGE HEAT FLUX GAS',STATISTICS_START=0,TEMPORAL_STATISTIC='TIME
INTEGRAL'/
&DEVC XB=1.3335,1.3335,-2.4765,-
0.4953,0.5715,0.5715,POINTS=26,ORIENTATION=0,1,0,ID='SL x:1.3335
z:0.5715',QUANTITY='GAUGE HEAT FLUX GAS',STATISTICS_START=0,TEMPORAL_STATISTIC='TIME
INTEGRAL'/
&DEVC XB=1.3335,1.3335,-2.4765,-
0.4953,0.6477,0.6477,POINTS=26,ORIENTATION=0,1,0,ID='SL x:1.3335
z:0.6477',QUANTITY='GAUGE HEAT FLUX GAS',STATISTICS_START=0,TEMPORAL_STATISTIC='TIME
INTEGRAL'/
&DEVC XB=1.3335,1.3335,-2.4765,-
0.4953,0.7239,0.7239,POINTS=26,ORIENTATION=0,1,0,ID='SL x:1.3335
z:0.7239',QUANTITY='GAUGE HEAT FLUX GAS',STATISTICS_START=0,TEMPORAL_STATISTIC='TIME
INTEGRAL'/
&DEVC XB=1.4097,1.4097,-2.4765,-
0.4953,0.3429,0.3429,POINTS=26,ORIENTATION=0,1,0,ID='SL x:1.4097
z:0.3429',QUANTITY='GAUGE HEAT FLUX GAS',STATISTICS_START=0,TEMPORAL_STATISTIC='TIME
INTEGRAL'/
&DEVC XB=1.4097,1.4097,-2.4765,-
0.4953,0.4191,0.4191,POINTS=26,ORIENTATION=0,1,0,ID='SL x:1.4097
z:0.4191',QUANTITY='GAUGE HEAT FLUX GAS',STATISTICS_START=0,TEMPORAL_STATISTIC='TIME
INTEGRAL'/
&DEVC XB=1.4097,1.4097,-2.4765,-
0.4953,0.4953,0.4953,POINTS=26,ORIENTATION=0,1,0,ID='SL x:1.4097
z:0.4953',QUANTITY='GAUGE HEAT FLUX GAS',STATISTICS_START=0,TEMPORAL_STATISTIC='TIME
INTEGRAL'/
```

```
&DEVC XB=1.4097,1.4097,-2.4765,-
0.4953,0.5715,0.5715,POINTS=26,ORIENTATION=0,1,0,ID='SL x:1.4097
z:0.5715',QUANTITY='GAUGE HEAT FLUX GAS',STATISTICS_START=0,TEMPORAL_STATISTIC='TIME
INTEGRAL'/
&DEVC XB=1.4097,1.4097,-2.4765,-
0.4953,0.6477,0.6477,POINTS=26,ORIENTATION=0,1,0,ID='SL x:1.4097
z:0.6477',QUANTITY='GAUGE HEAT FLUX GAS',STATISTICS_START=0,TEMPORAL_STATISTIC='TIME
INTEGRAL'/
&DEVC XB=1.4097,1.4097,-2.4765,-
0.4953,0.7239,0.7239,POINTS=26,ORIENTATION=0,1,0,ID='SL x:1.4097
z:0.7239',QUANTITY='GAUGE HEAT FLUX GAS',STATISTICS_START=0,TEMPORAL_STATISTIC='TIME
INTEGRAL'/
&DEVC XB=1.4859,1.4859,-2.4765,-
0.4953,0.3429,0.3429,POINTS=26,ORIENTATION=0,1,0,ID='SL x:1.4859
z:0.3429',QUANTITY='GAUGE HEAT FLUX GAS',STATISTICS_START=0,TEMPORAL_STATISTIC='TIME
INTEGRAL'/
&DEVC XB=1.4859,1.4859,-2.4765,-
0.4953,0.4191,0.4191,POINTS=26,ORIENTATION=0,1,0,ID='SL x:1.4859
z:0.4191',QUANTITY='GAUGE HEAT FLUX GAS',STATISTICS_START=0,TEMPORAL_STATISTIC='TIME
INTEGRAL'/
&DEVC XB=1.4859,1.4859,-2.4765,-
0.4953,0.4953,0.4953,POINTS=26,ORIENTATION=0,1,0,ID='SL x:1.4859
z:0.4953',QUANTITY='GAUGE HEAT FLUX GAS',STATISTICS_START=0,TEMPORAL_STATISTIC='TIME
INTEGRAL'/
&DEVC XB=1.4859,1.4859,-2.4765,-
0.4953,0.5715,0.5715,POINTS=26,ORIENTATION=0,1,0,ID='SL x:1.4859
z:0.5715',QUANTITY='GAUGE HEAT FLUX GAS',STATISTICS_START=0,TEMPORAL_STATISTIC='TIME
INTEGRAL'/
&DEVC XB=1.4859,1.4859,-2.4765,-
0.4953,0.6477,0.6477,POINTS=26,ORIENTATION=0,1,0,ID='SL x:1.4859
z:0.6477',QUANTITY='GAUGE HEAT FLUX GAS',STATISTICS_START=0,TEMPORAL_STATISTIC='TIME
INTEGRAL'/
&DEVC XB=1.4859,1.4859,-2.4765,-
0.4953,0.7239,0.7239,POINTS=26,ORIENTATION=0,1,0,ID='SL x:1.4859
z:0.7239',QUANTITY='GAUGE HEAT FLUX GAS',STATISTICS_START=0,TEMPORAL_STATISTIC='TIME
INTEGRAL'/
&DEVC XB=1.5621,1.5621,-2.4765,-
0.4953,0.3429,0.3429,POINTS=26,ORIENTATION=0,1,0,ID='SL x:1.5621
z:0.3429',QUANTITY='GAUGE HEAT FLUX GAS',STATISTICS_START=0,TEMPORAL_STATISTIC='TIME
INTEGRAL'/
&DEVC XB=1.5621,1.5621,-2.4765,-
0.4953,0.4191,0.4191,POINTS=26,ORIENTATION=0,1,0,ID='SL x:1.5621
z:0.4191',QUANTITY='GAUGE HEAT FLUX GAS',STATISTICS_START=0,TEMPORAL_STATISTIC='TIME
INTEGRAL'/
&DEVC XB=1.5621,1.5621,-2.4765,-
0.4953,0.4953,0.4953,POINTS=26,ORIENTATION=0,1,0,ID='SL x:1.5621
z:0.4953',QUANTITY='GAUGE HEAT FLUX GAS',STATISTICS_START=0,TEMPORAL_STATISTIC='TIME
INTEGRAL'/
&DEVC XB=1.5621,1.5621,-2.4765,-
0.4953,0.5715,0.5715,POINTS=26,ORIENTATION=0,1,0,ID='SL x:1.5621
z:0.5715',QUANTITY='GAUGE HEAT FLUX GAS',STATISTICS_START=0,TEMPORAL_STATISTIC='TIME
INTEGRAL'/
&DEVC XB=1.5621,1.5621,-2.4765,-
0.4953,0.6477,0.6477,POINTS=26,ORIENTATION=0,1,0,ID='SL x:1.5621
z:0.6477',QUANTITY='GAUGE HEAT FLUX GAS',STATISTICS_START=0,TEMPORAL_STATISTIC='TIME
INTEGRAL'/
&DEVC XB=1.5621,1.5621,-2.4765,-
0.4953,0.7239,0.7239,POINTS=26,ORIENTATION=0,1,0,ID='SL x:1.5621
z:0.7239',QUANTITY='GAUGE HEAT FLUX GAS',STATISTICS_START=0,TEMPORAL_STATISTIC='TIME
INTEGRAL'/
```

```
&DEVC XB=1.1811,1.1811,0.4953,2.4765,0.3429,0.3429,POINTS=26,ORIENTATION=0,-1,0,ID='SR
x:1.1811 z:0.3429',QUANTITY='GAUGE HEAT FLUX
GAS',STATISTICS_START=0,TEMPORAL_STATISTIC='TIME INTEGRAL'/
&DEVC XB=1.1811,1.1811,0.4953,2.4765,0.4191,0.4191,POINTS=26,ORIENTATION=0,-1,0,ID='SR
x:1.1811 z:0.4191',QUANTITY='GAUGE HEAT FLUX
GAS',STATISTICS_START=0,TEMPORAL_STATISTIC='TIME INTEGRAL'/
&DEVC XB=1.1811,1.1811,0.4953,2.4765,0.4953,0.4953,POINTS=26,ORIENTATION=0,-1,0,ID='SR
x:1.1811 z:0.4953',QUANTITY='GAUGE HEAT FLUX
GAS',STATISTICS_START=0,TEMPORAL_STATISTIC='TIME INTEGRAL'/
&DEVC XB=1.1811,1.1811,0.4953,2.4765,0.5715,0.5715,POINTS=26,ORIENTATION=0,-1,0,ID='SR
x:1.1811 z:0.5715',QUANTITY='GAUGE HEAT FLUX
GAS',STATISTICS_START=0,TEMPORAL_STATISTIC='TIME INTEGRAL'/
&DEVC XB=1.1811,1.1811,0.4953,2.4765,0.6477,0.6477,POINTS=26,ORIENTATION=0,-1,0,ID='SR
x:1.1811 z:0.6477',QUANTITY='GAUGE HEAT FLUX
GAS',STATISTICS_START=0,TEMPORAL_STATISTIC='TIME INTEGRAL'/
&DEVC XB=1.1811,1.1811,0.4953,2.4765,0.7239,0.7239,POINTS=26,ORIENTATION=0,-1,0,ID='SR
x:1.1811 z:0.7239',QUANTITY='GAUGE HEAT FLUX
GAS',STATISTICS_START=0,TEMPORAL_STATISTIC='TIME INTEGRAL'/
&DEVC XB=1.2573,1.2573,0.4953,2.4765,0.3429,0.3429,POINTS=26,ORIENTATION=0,-1,0,ID='SR
x:1.2573 z:0.3429',QUANTITY='GAUGE HEAT FLUX
GAS',STATISTICS_START=0,TEMPORAL_STATISTIC='TIME INTEGRAL'/
&DEVC XB=1.2573,1.2573,0.4953,2.4765,0.4191,0.4191,POINTS=26,ORIENTATION=0,-1,0,ID='SR
x:1.2573 z:0.4191',QUANTITY='GAUGE HEAT FLUX
GAS',STATISTICS_START=0,TEMPORAL_STATISTIC='TIME INTEGRAL'/
&DEVC XB=1.2573,1.2573,0.4953,2.4765,0.4953,0.4953,POINTS=26,ORIENTATION=0,-1,0,ID='SR
x:1.2573 z:0.4953',QUANTITY='GAUGE HEAT FLUX
GAS',STATISTICS_START=0,TEMPORAL_STATISTIC='TIME INTEGRAL'/
&DEVC XB=1.2573,1.2573,0.4953,2.4765,0.5715,0.5715,POINTS=26,ORIENTATION=0,-1,0,ID='SR
x:1.2573 z:0.5715',QUANTITY='GAUGE HEAT FLUX
GAS',STATISTICS_START=0,TEMPORAL_STATISTIC='TIME INTEGRAL'/
&DEVC XB=1.2573,1.2573,0.4953,2.4765,0.6477,0.6477,POINTS=26,ORIENTATION=0,-1,0,ID='SR
x:1.2573 z:0.6477',QUANTITY='GAUGE HEAT FLUX
GAS',STATISTICS_START=0,TEMPORAL_STATISTIC='TIME INTEGRAL'/
&DEVC XB=1.2573,1.2573,0.4953,2.4765,0.7239,0.7239,POINTS=26,ORIENTATION=0,-1,0,ID='SR
x:1.2573 z:0.7239',QUANTITY='GAUGE HEAT FLUX
GAS',STATISTICS_START=0,TEMPORAL_STATISTIC='TIME INTEGRAL'/
&DEVC XB=1.3335,1.3335,0.4953,2.4765,0.3429,0.3429,POINTS=26,ORIENTATION=0,-1,0,ID='SR
x:1.3335 z:0.3429',QUANTITY='GAUGE HEAT FLUX
GAS',STATISTICS_START=0,TEMPORAL_STATISTIC='TIME INTEGRAL'/
&DEVC XB=1.3335,1.3335,0.4953,2.4765,0.4191,0.4191,POINTS=26,ORIENTATION=0,-1,0,ID='SR
x:1.3335 z:0.4191',QUANTITY='GAUGE HEAT FLUX
GAS',STATISTICS_START=0,TEMPORAL_STATISTIC='TIME INTEGRAL'/
&DEVC XB=1.3335,1.3335,0.4953,2.4765,0.4953,0.4953,POINTS=26,ORIENTATION=0,-1,0,ID='SR
x:1.3335 z:0.4953',QUANTITY='GAUGE HEAT FLUX
GAS',STATISTICS_START=0,TEMPORAL_STATISTIC='TIME INTEGRAL'/
&DEVC XB=1.3335,1.3335,0.4953,2.4765,0.5715,0.5715,POINTS=26,ORIENTATION=0,-1,0,ID='SR
x:1.3335 z:0.5715',QUANTITY='GAUGE HEAT FLUX
GAS',STATISTICS_START=0,TEMPORAL_STATISTIC='TIME INTEGRAL'/
&DEVC XB=1.3335,1.3335,0.4953,2.4765,0.6477,0.6477,POINTS=26,ORIENTATION=0,-1,0,ID='SR
x:1.3335 z:0.6477',QUANTITY='GAUGE HEAT FLUX
GAS',STATISTICS_START=0,TEMPORAL_STATISTIC='TIME INTEGRAL'/
&DEVC XB=1.3335,1.3335,0.4953,2.4765,0.7239,0.7239,POINTS=26,ORIENTATION=0,-1,0,ID='SR
x:1.3335 z:0.7239',QUANTITY='GAUGE HEAT FLUX
GAS',STATISTICS_START=0,TEMPORAL_STATISTIC='TIME INTEGRAL'/
&DEVC XB=1.4097,1.4097,0.4953,2.4765,0.3429,0.3429,POINTS=26,ORIENTATION=0,-1,0,ID='SR
x:1.4097 z:0.3429',QUANTITY='GAUGE HEAT FLUX
GAS',STATISTICS_START=0,TEMPORAL_STATISTIC='TIME INTEGRAL'/
&DEVC XB=1.4097,1.4097,0.4953,2.4765,0.4191,0.4191,POINTS=26,ORIENTATION=0,-1,0,ID='SR
x:1.4097 z:0.4191',QUANTITY='GAUGE HEAT FLUX
GAS',STATISTICS_START=0,TEMPORAL_STATISTIC='TIME INTEGRAL'/
&DEVC XB=1.4097,1.4097,0.4953,2.4765,0.4953,0.4953,POINTS=26,ORIENTATION=0,-1,0,ID='SR
x:1.4097 z:0.4953',QUANTITY='GAUGE HEAT FLUX
GAS',STATISTICS_START=0,TEMPORAL_STATISTIC='TIME INTEGRAL'/
```

```
&DEVC XB=1.4097,1.4097,0.4953,2.4765,0.5715,0.5715,POINTS=26,ORIENTATION=0,-1,0,ID='SR
x:1.4097 z:0.5715',QUANTITY='GAUGE HEAT FLUX
GAS',STATISTICS_START=0,TEMPORAL_STATISTIC='TIME INTEGRAL'/
&DEVC XB=1.4097,1.4097,0.4953,2.4765,0.6477,0.6477,POINTS=26,ORIENTATION=0,-1,0,ID='SR
x:1.4097 z:0.6477',QUANTITY='GAUGE HEAT FLUX
GAS',STATISTICS_START=0,TEMPORAL_STATISTIC='TIME INTEGRAL'/
&DEVC XB=1.4097,1.4097,0.4953,2.4765,0.7239,0.7239,POINTS=26,ORIENTATION=0,-1,0,ID='SR
x:1.4097 z:0.7239',QUANTITY='GAUGE HEAT FLUX
GAS',STATISTICS_START=0,TEMPORAL_STATISTIC='TIME INTEGRAL'/
&DEVC XB=1.4859,1.4859,0.4953,2.4765,0.3429,0.3429,POINTS=26,ORIENTATION=0,-1,0,ID='SR
x:1.4859 z:0.3429',QUANTITY='GAUGE HEAT FLUX
GAS',STATISTICS_START=0,TEMPORAL_STATISTIC='TIME INTEGRAL'/
&DEVC XB=1.4859,1.4859,0.4953,2.4765,0.4191,0.4191,POINTS=26,ORIENTATION=0,-1,0,ID='SR
x:1.4859 z:0.4191',QUANTITY='GAUGE HEAT FLUX
GAS',STATISTICS_START=0,TEMPORAL_STATISTIC='TIME INTEGRAL'/
&DEVC XB=1.4859,1.4859,0.4953,2.4765,0.4953,0.4953,POINTS=26,ORIENTATION=0,-1,0,ID='SR
x:1.4859 z:0.4953',QUANTITY='GAUGE HEAT FLUX
GAS',STATISTICS_START=0,TEMPORAL_STATISTIC='TIME INTEGRAL'/
&DEVC XB=1.4859,1.4859,0.4953,2.4765,0.5715,0.5715,POINTS=26,ORIENTATION=0,-1,0,ID='SR
x:1.4859 z:0.5715',QUANTITY='GAUGE HEAT FLUX
GAS',STATISTICS_START=0,TEMPORAL_STATISTIC='TIME INTEGRAL'/
&DEVC XB=1.4859,1.4859,0.4953,2.4765,0.6477,0.6477,POINTS=26,ORIENTATION=0,-1,0,ID='SR
x:1.4859 z:0.6477',QUANTITY='GAUGE HEAT FLUX
GAS',STATISTICS_START=0,TEMPORAL_STATISTIC='TIME INTEGRAL'/
&DEVC XB=1.4859,1.4859,0.4953,2.4765,0.7239,0.7239,POINTS=26,ORIENTATION=0,-1,0,ID='SR
x:1.4859 z:0.7239',QUANTITY='GAUGE HEAT FLUX
GAS',STATISTICS_START=0,TEMPORAL_STATISTIC='TIME INTEGRAL'/
&DEVC XB=1.5621,1.5621,0.4953,2.4765,0.3429,0.3429,POINTS=26,ORIENTATION=0,-1,0,ID='SR
x:1.5621 z:0.3429',QUANTITY='GAUGE HEAT FLUX
GAS',STATISTICS_START=0,TEMPORAL_STATISTIC='TIME INTEGRAL'/
&DEVC XB=1.5621,1.5621,0.4953,2.4765,0.4191,0.4191,POINTS=26,ORIENTATION=0,-1,0,ID='SR
x:1.5621 z:0.4191',QUANTITY='GAUGE HEAT FLUX
GAS',STATISTICS_START=0,TEMPORAL_STATISTIC='TIME INTEGRAL'/
&DEVC XB=1.5621,1.5621,0.4953,2.4765,0.4953,0.4953,POINTS=26,ORIENTATION=0,-1,0,ID='SR
x:1.5621 z:0.4953',QUANTITY='GAUGE HEAT FLUX
GAS',STATISTICS_START=0,TEMPORAL_STATISTIC='TIME INTEGRAL'/
&DEVC XB=1.5621,1.5621,0.4953,2.4765,0.5715,0.5715,POINTS=26,ORIENTATION=0,-1,0,ID='SR
x:1.5621 z:0.5715',QUANTITY='GAUGE HEAT FLUX
GAS',STATISTICS_START=0,TEMPORAL_STATISTIC='TIME INTEGRAL'/
&DEVC XB=1.5621,1.5621,0.4953,2.4765,0.6477,0.6477,POINTS=26,ORIENTATION=0,-1,0,ID='SR
x:1.5621 z:0.6477',QUANTITY='GAUGE HEAT FLUX
GAS',STATISTICS_START=0,TEMPORAL_STATISTIC='TIME INTEGRAL'/
&DEVC XB=1.5621,1.5621,0.4953,2.4765,0.7239,0.7239,POINTS=26,ORIENTATION=0,-1,0,ID='SR
x:1.5621 z:0.7239',QUANTITY='GAUGE HEAT FLUX
GAS',STATISTICS_START=0,TEMPORAL_STATISTIC='TIME INTEGRAL'/

&DEVC XB=1.1811,1.1811,-0.1143,-0.1143,2.3241,4.4577,POINTS=28,ORIENTATION=0,0,-
1,ID='TF x:1.1811 y:-0.1143',QUANTITY='GAUGE HEAT FLUX
GAS',STATISTICS_START=0,TEMPORAL_STATISTIC='TIME INTEGRAL'/
&DEVC XB=1.1811,1.1811,-0.0381,-0.0381,2.3241,4.4577,POINTS=28,ORIENTATION=0,0,-
1,ID='TF x:1.1811 y:-0.0381',QUANTITY='GAUGE HEAT FLUX
GAS',STATISTICS_START=0,TEMPORAL_STATISTIC='TIME INTEGRAL'/
&DEVC XB=1.1811,1.1811,0.0381,0.0381,2.3241,4.4577,POINTS=28,ORIENTATION=0,0,-1,ID='TF
x:1.1811 y:0.0381',QUANTITY='GAUGE HEAT FLUX
GAS',STATISTICS_START=0,TEMPORAL_STATISTIC='TIME INTEGRAL'/
&DEVC XB=1.1811,1.1811,0.1143,0.1143,2.3241,4.4577,POINTS=28,ORIENTATION=0,0,-1,ID='TF
x:1.1811 y:0.1143',QUANTITY='GAUGE HEAT FLUX
GAS',STATISTICS_START=0,TEMPORAL_STATISTIC='TIME INTEGRAL'/
&DEVC XB=1.2573,1.2573,-0.1143,-0.1143,2.3241,4.4577,POINTS=28,ORIENTATION=0,0,-
1,ID='TF x:1.2573 y:-0.1143',QUANTITY='GAUGE HEAT FLUX
GAS',STATISTICS_START=0,TEMPORAL_STATISTIC='TIME INTEGRAL'/
&DEVC XB=1.2573,1.2573,-0.0381,-0.0381,2.3241,4.4577,POINTS=28,ORIENTATION=0,0,-
1,ID='TF x:1.2573 y:-0.0381',QUANTITY='GAUGE HEAT FLUX
GAS',STATISTICS_START=0,TEMPORAL_STATISTIC='TIME INTEGRAL'/
```

```
&DEVC XB=1.2573,1.2573,0.0381,0.0381,2.3241,4.4577,POINTS=28,ORIENTATION=0,0,-1,ID='TF
x:1.2573 y:0.0381',QUANTITY='GAUGE HEAT FLUX
GAS',STATISTICS_START=0,TEMPORAL_STATISTIC='TIME INTEGRAL'/
&DEVC XB=1.2573,1.2573,0.1143,0.1143,2.3241,4.4577,POINTS=28,ORIENTATION=0,0,-1,ID='TF
x:1.2573 y:0.1143',QUANTITY='GAUGE HEAT FLUX
GAS',STATISTICS_START=0,TEMPORAL_STATISTIC='TIME INTEGRAL'/
&DEVC XB=1.3335,1.3335,-0.1143,-0.1143,2.3241,4.4577,POINTS=28,ORIENTATION=0,0,-
1,ID='TF x:1.3335 y:-0.1143',QUANTITY='GAUGE HEAT FLUX
GAS',STATISTICS_START=0,TEMPORAL_STATISTIC='TIME INTEGRAL'/
&DEVC XB=1.3335,1.3335,-0.0381,-0.0381,2.3241,4.4577,POINTS=28,ORIENTATION=0,0,-
1,ID='TF x:1.3335 y:-0.0381',QUANTITY='GAUGE HEAT FLUX
GAS',STATISTICS_START=0,TEMPORAL_STATISTIC='TIME INTEGRAL'/
&DEVC XB=1.3335,1.3335,0.0381,0.0381,2.3241,4.4577,POINTS=28,ORIENTATION=0,0,-1,ID='TF
x:1.3335 y:0.0381',QUANTITY='GAUGE HEAT FLUX
GAS',STATISTICS_START=0,TEMPORAL_STATISTIC='TIME INTEGRAL'/
&DEVC XB=1.3335,1.3335,0.1143,0.1143,2.3241,4.4577,POINTS=28,ORIENTATION=0,0,-1,ID='TF
x:1.3335 y:0.1143',QUANTITY='GAUGE HEAT FLUX
GAS',STATISTICS_START=0,TEMPORAL_STATISTIC='TIME INTEGRAL'/
&DEVC XB=1.4097,1.4097,-0.1143,-0.1143,2.3241,4.4577,POINTS=28,ORIENTATION=0,0,-
1,ID='TF x:1.4097 y:-0.1143',QUANTITY='GAUGE HEAT FLUX
GAS',STATISTICS_START=0,TEMPORAL_STATISTIC='TIME INTEGRAL'/
&DEVC XB=1.4097,1.4097,-0.0381,-0.0381,2.3241,4.4577,POINTS=28,ORIENTATION=0,0,-
1,ID='TF x:1.4097 y:-0.0381',QUANTITY='GAUGE HEAT FLUX
GAS',STATISTICS_START=0,TEMPORAL_STATISTIC='TIME INTEGRAL'/
&DEVC XB=1.4097,1.4097,0.0381,0.0381,2.3241,4.4577,POINTS=28,ORIENTATION=0,0,-1,ID='TF
x:1.4097 y:0.0381',QUANTITY='GAUGE HEAT FLUX
GAS',STATISTICS_START=0,TEMPORAL_STATISTIC='TIME INTEGRAL'/
&DEVC XB=1.4097,1.4097,0.1143,0.1143,2.3241,4.4577,POINTS=28,ORIENTATION=0,0,-1,ID='TF
x:1.4097 y:0.1143',QUANTITY='GAUGE HEAT FLUX
GAS',STATISTICS_START=0,TEMPORAL_STATISTIC='TIME INTEGRAL'/


&DEVC XB=2.0955,4.5339,-0.4191,-0.4191,0.0381,0.0381,POINTS=32,ORIENTATION=-
1,0,0,ID='F y:-0.4191 z:0.0381',QUANTITY='GAUGE HEAT FLUX
GAS',STATISTICS_START=0,TEMPORAL_STATISTIC='TIME INTEGRAL'/
&DEVC XB=2.0955,4.5339,-0.3429,-0.3429,0.0381,0.0381,POINTS=32,ORIENTATION=-
1,0,0,ID='F y:-0.3429 z:0.0381',QUANTITY='GAUGE HEAT FLUX
GAS',STATISTICS_START=0,TEMPORAL_STATISTIC='TIME INTEGRAL'/
&DEVC XB=2.0955,4.5339,-0.2667,-0.2667,0.0381,0.0381,POINTS=32,ORIENTATION=-
1,0,0,ID='F y:-0.2667 z:0.0381',QUANTITY='GAUGE HEAT FLUX
GAS',STATISTICS_START=0,TEMPORAL_STATISTIC='TIME INTEGRAL'/
&DEVC XB=2.0955,4.5339,0.4191,0.4191,0.0381,0.0381,POINTS=32,ORIENTATION=-1,0,0,ID='F
y:0.4191 z:0.0381',QUANTITY='GAUGE HEAT FLUX
GAS',STATISTICS_START=0,TEMPORAL_STATISTIC='TIME INTEGRAL'/
&DEVC XB=2.0955,4.5339,0.3429,0.3429,0.0381,0.0381,POINTS=32,ORIENTATION=-1,0,0,ID='F
y:0.3429 z:0.0381',QUANTITY='GAUGE HEAT FLUX
GAS',STATISTICS_START=0,TEMPORAL_STATISTIC='TIME INTEGRAL'/
&DEVC XB=2.0955,4.5339,0.2667,0.2667,0.0381,0.0381,POINTS=32,ORIENTATION=-1,0,0,ID='F
y:0.2667 z:0.0381',QUANTITY='GAUGE HEAT FLUX
GAS',STATISTICS_START=0,TEMPORAL_STATISTIC='TIME INTEGRAL'/
&DEVC XB=2.0955,4.5339,-0.4191,-0.4191,0.1143,0.1143,POINTS=32,ORIENTATION=-
1,0,0,ID='F y:-0.4191 z:0.1143',QUANTITY='GAUGE HEAT FLUX
GAS',STATISTICS_START=0,TEMPORAL_STATISTIC='TIME INTEGRAL'/
&DEVC XB=2.0955,4.5339,-0.3429,-0.3429,0.1143,0.1143,POINTS=32,ORIENTATION=-
1,0,0,ID='F y:-0.3429 z:0.1143',QUANTITY='GAUGE HEAT FLUX
GAS',STATISTICS_START=0,TEMPORAL_STATISTIC='TIME INTEGRAL'/
&DEVC XB=2.0955,4.5339,-0.2667,-0.2667,0.1143,0.1143,POINTS=32,ORIENTATION=-
1,0,0,ID='F y:-0.2667 z:0.1143',QUANTITY='GAUGE HEAT FLUX
GAS',STATISTICS_START=0,TEMPORAL_STATISTIC='TIME INTEGRAL'/
&DEVC XB=2.0955,4.5339,0.4191,0.4191,0.1143,0.1143,POINTS=32,ORIENTATION=-1,0,0,ID='F
y:0.4191 z:0.1143',QUANTITY='GAUGE HEAT FLUX
GAS',STATISTICS_START=0,TEMPORAL_STATISTIC='TIME INTEGRAL'/
```

```
&DEVC XB=2.0955,4.5339,0.3429,0.3429,0.1143,0.1143,POINTS=32,ORIENTATION=-1,0,0,ID='F
y:0.3429 z:0.1143',QUANTITY='GAUGE HEAT FLUX
GAS',STATISTICS_START=0,TEMPORAL_STATISTIC='TIME INTEGRAL'/
&DEVC XB=2.0955,4.5339,0.2667,0.2667,0.1143,0.1143,POINTS=32,ORIENTATION=-1,0,0,ID='F
y:0.2667 z:0.1143',QUANTITY='GAUGE HEAT FLUX
GAS',STATISTICS_START=0,TEMPORAL_STATISTIC='TIME INTEGRAL'/
&DEVC XB=2.0955,4.5339,-0.4191,-0.4191,0.1905,0.1905,POINTS=32,ORIENTATION=-
1,0,0,ID='F y:-0.4191 z:0.1905',QUANTITY='GAUGE HEAT FLUX
GAS',STATISTICS_START=0,TEMPORAL_STATISTIC='TIME INTEGRAL'/
&DEVC XB=2.0955,4.5339,-0.3429,-0.3429,0.1905,0.1905,POINTS=32,ORIENTATION=-
1,0,0,ID='F y:-0.3429 z:0.1905',QUANTITY='GAUGE HEAT FLUX
GAS',STATISTICS_START=0,TEMPORAL_STATISTIC='TIME INTEGRAL'/
&DEVC XB=2.0955,4.5339,-0.2667,-0.2667,0.1905,0.1905,POINTS=32,ORIENTATION=-
1,0,0,ID='F y:-0.2667 z:0.1905',QUANTITY='GAUGE HEAT FLUX
GAS',STATISTICS_START=0,TEMPORAL_STATISTIC='TIME INTEGRAL'/
&DEVC XB=2.0955,4.5339,0.4191,0.4191,0.1905,0.1905,POINTS=32,ORIENTATION=-1,0,0,ID='F
y:0.4191 z:0.1905',QUANTITY='GAUGE HEAT FLUX
GAS',STATISTICS_START=0,TEMPORAL_STATISTIC='TIME INTEGRAL'/
&DEVC XB=2.0955,4.5339,0.3429,0.3429,0.1905,0.1905,POINTS=32,ORIENTATION=-1,0,0,ID='F
y:0.3429 z:0.1905',QUANTITY='GAUGE HEAT FLUX
GAS',STATISTICS_START=0,TEMPORAL_STATISTIC='TIME INTEGRAL'/
&DEVC XB=2.0955,4.5339,0.2667,0.2667,0.1905,0.1905,POINTS=32,ORIENTATION=-1,0,0,ID='F
y:0.2667 z:0.1905',QUANTITY='GAUGE HEAT FLUX
GAS',STATISTICS_START=0,TEMPORAL_STATISTIC='TIME INTEGRAL'/
&DEVC XB=2.0955,4.5339,-0.4191,-0.4191,0.2667,0.2667,POINTS=32,ORIENTATION=-
1,0,0,ID='F y:-0.4191 z:0.2667',QUANTITY='GAUGE HEAT FLUX
GAS',STATISTICS_START=0,TEMPORAL_STATISTIC='TIME INTEGRAL'/
&DEVC XB=2.0955,4.5339,-0.3429,-0.3429,0.2667,0.2667,POINTS=32,ORIENTATION=-
1,0,0,ID='F y:-0.3429 z:0.2667',QUANTITY='GAUGE HEAT FLUX
GAS',STATISTICS_START=0,TEMPORAL_STATISTIC='TIME INTEGRAL'/
&DEVC XB=2.0955,4.5339,-0.2667,-0.2667,0.2667,0.2667,POINTS=32,ORIENTATION=-
1,0,0,ID='F y:-0.2667 z:0.2667',QUANTITY='GAUGE HEAT FLUX
GAS',STATISTICS_START=0,TEMPORAL_STATISTIC='TIME INTEGRAL'/
&DEVC XB=2.0955,4.5339,0.4191,0.4191,0.2667,0.2667,POINTS=32,ORIENTATION=-1,0,0,ID='F
y:0.4191 z:0.2667',QUANTITY='GAUGE HEAT FLUX
GAS',STATISTICS_START=0,TEMPORAL_STATISTIC='TIME INTEGRAL'/
&DEVC XB=2.0955,4.5339,0.3429,0.3429,0.2667,0.2667,POINTS=32,ORIENTATION=-1,0,0,ID='F
y:0.3429 z:0.2667',QUANTITY='GAUGE HEAT FLUX
GAS',STATISTICS_START=0,TEMPORAL_STATISTIC='TIME INTEGRAL'/
&DEVC XB=2.0955,4.5339,0.2667,0.2667,0.2667,0.2667,POINTS=32,ORIENTATION=-1,0,0,ID='F
y:0.2667 z:0.2667',QUANTITY='GAUGE HEAT FLUX
GAS',STATISTICS_START=0,TEMPORAL_STATISTIC='TIME INTEGRAL'/
&DEVC XB=2.0955,4.5339,-0.4191,-0.4191,0.3429,0.3429,POINTS=32,ORIENTATION=-
1,0,0,ID='F y:-0.4191 z:0.3429',QUANTITY='GAUGE HEAT FLUX
GAS',STATISTICS_START=0,TEMPORAL_STATISTIC='TIME INTEGRAL'/
&DEVC XB=2.0955,4.5339,-0.3429,-0.3429,0.3429,0.3429,POINTS=32,ORIENTATION=-
1,0,0,ID='F y:-0.3429 z:0.3429',QUANTITY='GAUGE HEAT FLUX
GAS',STATISTICS_START=0,TEMPORAL_STATISTIC='TIME INTEGRAL'/
&DEVC XB=2.0955,4.5339,-0.2667,-0.2667,0.3429,0.3429,POINTS=32,ORIENTATION=-
1,0,0,ID='F y:-0.2667 z:0.3429',QUANTITY='GAUGE HEAT FLUX
GAS',STATISTICS_START=0,TEMPORAL_STATISTIC='TIME INTEGRAL'/
&DEVC XB=2.0955,4.5339,0.4191,0.4191,0.3429,0.3429,POINTS=32,ORIENTATION=-1,0,0,ID='F
y:0.4191 z:0.3429',QUANTITY='GAUGE HEAT FLUX
GAS',STATISTICS_START=0,TEMPORAL_STATISTIC='TIME INTEGRAL'/
&DEVC XB=2.0955,4.5339,0.3429,0.3429,0.3429,0.3429,POINTS=32,ORIENTATION=-1,0,0,ID='F
y:0.3429 z:0.3429',QUANTITY='GAUGE HEAT FLUX
GAS',STATISTICS_START=0,TEMPORAL_STATISTIC='TIME INTEGRAL'/
&DEVC XB=2.0955,4.5339,0.2667,0.2667,0.3429,0.3429,POINTS=32,ORIENTATION=-1,0,0,ID='F
y:0.2667 z:0.3429',QUANTITY='GAUGE HEAT FLUX
GAS',STATISTICS_START=0,TEMPORAL_STATISTIC='TIME INTEGRAL'/
&DEVC XB=2.0955,4.5339,-0.4191,-0.4191,0.4191,0.4191,POINTS=32,ORIENTATION=-
1,0,0,ID='F y:-0.4191 z:0.4191',QUANTITY='GAUGE HEAT FLUX
GAS',STATISTICS_START=0,TEMPORAL_STATISTIC='TIME INTEGRAL'/
```

```
&DEVC XB=2.0955,4.5339,-0.3429,-0.3429,0.4191,0.4191,POINTS=32,ORIENTATION=-
1,0,0,ID='F y:-0.3429 z:0.4191',QUANTITY='GAUGE HEAT FLUX
GAS',STATISTICS_START=0,TEMPORAL_STATISTIC='TIME INTEGRAL'/
&DEVC XB=2.0955,4.5339,-0.2667,-0.2667,0.4191,0.4191,POINTS=32,ORIENTATION=-
1,0,0,ID='F y:-0.2667 z:0.4191',QUANTITY='GAUGE HEAT FLUX
GAS',STATISTICS_START=0,TEMPORAL_STATISTIC='TIME INTEGRAL'/
&DEVC XB=2.0955,4.5339,0.4191,0.4191,0.4191,0.4191,POINTS=32,ORIENTATION=-1,0,0,ID='F
y:0.4191 z:0.4191',QUANTITY='GAUGE HEAT FLUX
GAS',STATISTICS_START=0,TEMPORAL_STATISTIC='TIME INTEGRAL'/
&DEVC XB=2.0955,4.5339,0.3429,0.3429,0.4191,0.4191,POINTS=32,ORIENTATION=-1,0,0,ID='F
y:0.3429 z:0.4191',QUANTITY='GAUGE HEAT FLUX
GAS',STATISTICS_START=0,TEMPORAL_STATISTIC='TIME INTEGRAL'/
&DEVC XB=2.0955,4.5339,0.2667,0.2667,0.4191,0.4191,POINTS=32,ORIENTATION=-1,0,0,ID='F
y:0.2667 z:0.4191',QUANTITY='GAUGE HEAT FLUX
GAS',STATISTICS_START=0,TEMPORAL_STATISTIC='TIME INTEGRAL'/
&DEVC XB=2.0955,4.5339,-0.4191,-0.4191,0.4953,0.4953,POINTS=32,ORIENTATION=-
1,0,0,ID='F y:-0.4191 z:0.4953',QUANTITY='GAUGE HEAT FLUX
GAS',STATISTICS_START=0,TEMPORAL_STATISTIC='TIME INTEGRAL'/
&DEVC XB=2.0955,4.5339,-0.3429,-0.3429,0.4953,0.4953,POINTS=32,ORIENTATION=-
1,0,0,ID='F y:-0.3429 z:0.4953',QUANTITY='GAUGE HEAT FLUX
GAS',STATISTICS_START=0,TEMPORAL_STATISTIC='TIME INTEGRAL'/
&DEVC XB=2.0955,4.5339,-0.2667,-0.2667,0.4953,0.4953,POINTS=32,ORIENTATION=-
1,0,0,ID='F y:-0.2667 z:0.4953',QUANTITY='GAUGE HEAT FLUX
GAS',STATISTICS_START=0,TEMPORAL_STATISTIC='TIME INTEGRAL'/
&DEVC XB=2.0955,4.5339,0.4191,0.4191,0.4953,0.4953,POINTS=32,ORIENTATION=-1,0,0,ID='F
y:0.4191 z:0.4953',QUANTITY='GAUGE HEAT FLUX
GAS',STATISTICS_START=0,TEMPORAL_STATISTIC='TIME INTEGRAL'/
&DEVC XB=2.0955,4.5339,0.3429,0.3429,0.4953,0.4953,POINTS=32,ORIENTATION=-1,0,0,ID='F
y:0.3429 z:0.4953',QUANTITY='GAUGE HEAT FLUX
GAS',STATISTICS_START=0,TEMPORAL_STATISTIC='TIME INTEGRAL'/
&DEVC XB=2.0955,4.5339,0.2667,0.2667,0.4953,0.4953,POINTS=32,ORIENTATION=-1,0,0,ID='F
y:0.2667 z:0.4953',QUANTITY='GAUGE HEAT FLUX
GAS',STATISTICS_START=0,TEMPORAL_STATISTIC='TIME INTEGRAL'/
&DEVC XB=2.0955,4.5339,-0.4191,-0.4191,0.5715,0.5715,POINTS=32,ORIENTATION=-
1,0,0,ID='F y:-0.4191 z:0.5715',QUANTITY='GAUGE HEAT FLUX
GAS',STATISTICS_START=0,TEMPORAL_STATISTIC='TIME INTEGRAL'/
&DEVC XB=2.0955,4.5339,-0.3429,-0.3429,0.5715,0.5715,POINTS=32,ORIENTATION=-
1,0,0,ID='F y:-0.3429 z:0.5715',QUANTITY='GAUGE HEAT FLUX
GAS',STATISTICS_START=0,TEMPORAL_STATISTIC='TIME INTEGRAL'/
&DEVC XB=2.0955,4.5339,-0.2667,-0.2667,0.5715,0.5715,POINTS=32,ORIENTATION=-
1,0,0,ID='F y:-0.2667 z:0.5715',QUANTITY='GAUGE HEAT FLUX
GAS',STATISTICS_START=0,TEMPORAL_STATISTIC='TIME INTEGRAL'/
&DEVC XB=2.0955,4.5339,0.4191,0.4191,0.5715,0.5715,POINTS=32,ORIENTATION=-1,0,0,ID='F
y:0.4191 z:0.5715',QUANTITY='GAUGE HEAT FLUX
GAS',STATISTICS_START=0,TEMPORAL_STATISTIC='TIME INTEGRAL'/
&DEVC XB=2.0955,4.5339,0.3429,0.3429,0.5715,0.5715,POINTS=32,ORIENTATION=-1,0,0,ID='F
y:0.3429 z:0.5715',QUANTITY='GAUGE HEAT FLUX
GAS',STATISTICS_START=0,TEMPORAL_STATISTIC='TIME INTEGRAL'/
&DEVC XB=2.0955,4.5339,0.2667,0.2667,0.5715,0.5715,POINTS=32,ORIENTATION=-1,0,0,ID='F
y:0.2667 z:0.5715',QUANTITY='GAUGE HEAT FLUX
GAS',STATISTICS_START=0,TEMPORAL_STATISTIC='TIME INTEGRAL'/
&DEVC XB=2.0955,4.5339,-0.4191,-0.4191,0.6477,0.6477,POINTS=32,ORIENTATION=-
1,0,0,ID='F y:-0.4191 z:0.6477',QUANTITY='GAUGE HEAT FLUX
GAS',STATISTICS_START=0,TEMPORAL_STATISTIC='TIME INTEGRAL'/
&DEVC XB=2.0955,4.5339,-0.3429,-0.3429,0.6477,0.6477,POINTS=32,ORIENTATION=-
1,0,0,ID='F y:-0.3429 z:0.6477',QUANTITY='GAUGE HEAT FLUX
GAS',STATISTICS_START=0,TEMPORAL_STATISTIC='TIME INTEGRAL'/
&DEVC XB=2.0955,4.5339,-0.2667,-0.2667,0.6477,0.6477,POINTS=32,ORIENTATION=-
1,0,0,ID='F y:-0.2667 z:0.6477',QUANTITY='GAUGE HEAT FLUX
GAS',STATISTICS_START=0,TEMPORAL_STATISTIC='TIME INTEGRAL'/
&DEVC XB=2.0955,4.5339,0.4191,0.4191,0.6477,0.6477,POINTS=32,ORIENTATION=-1,0,0,ID='F
y:0.4191 z:0.6477',QUANTITY='GAUGE HEAT FLUX
GAS',STATISTICS_START=0,TEMPORAL_STATISTIC='TIME INTEGRAL'/
```

```
&DEVC XB=2.0955,4.5339,0.3429,0.3429,0.6477,0.6477,POINTS=32,ORIENTATION=-1,0,0,ID='F
y:0.3429 z:0.6477',QUANTITY='GAUGE HEAT FLUX
GAS',STATISTICS_START=0,TEMPORAL_STATISTIC='TIME INTEGRAL'/
&DEVC XB=2.0955,4.5339,0.2667,0.2667,0.6477,0.6477,POINTS=32,ORIENTATION=-1,0,0,ID='F
y:0.2667 z:0.6477',QUANTITY='GAUGE HEAT FLUX
GAS',STATISTICS_START=0,TEMPORAL_STATISTIC='TIME INTEGRAL'/
&DEVC XB=2.0955,4.5339,-0.4191,-0.4191,0.7239,0.7239,POINTS=32,ORIENTATION=-
1,0,0,ID='F y:-0.4191 z:0.7239',QUANTITY='GAUGE HEAT FLUX
GAS',STATISTICS_START=0,TEMPORAL_STATISTIC='TIME INTEGRAL'/
&DEVC XB=2.0955,4.5339,-0.3429,-0.3429,0.7239,0.7239,POINTS=32,ORIENTATION=-
1,0,0,ID='F y:-0.3429 z:0.7239',QUANTITY='GAUGE HEAT FLUX
GAS',STATISTICS_START=0,TEMPORAL_STATISTIC='TIME INTEGRAL'/
&DEVC XB=2.0955,4.5339,-0.2667,-0.2667,0.7239,0.7239,POINTS=32,ORIENTATION=-
1,0,0,ID='F y:-0.2667 z:0.7239',QUANTITY='GAUGE HEAT FLUX
GAS',STATISTICS_START=0,TEMPORAL_STATISTIC='TIME INTEGRAL'/
&DEVC XB=2.0955,4.5339,0.4191,0.4191,0.7239,0.7239,POINTS=32,ORIENTATION=-1,0,0,ID='F
y:0.4191 z:0.7239',QUANTITY='GAUGE HEAT FLUX
GAS',STATISTICS_START=0,TEMPORAL_STATISTIC='TIME INTEGRAL'/
&DEVC XB=2.0955,4.5339,0.3429,0.3429,0.7239,0.7239,POINTS=32,ORIENTATION=-1,0,0,ID='F
y:0.3429 z:0.7239',QUANTITY='GAUGE HEAT FLUX
GAS',STATISTICS_START=0,TEMPORAL_STATISTIC='TIME INTEGRAL'/
&DEVC XB=2.0955,4.5339,0.2667,0.2667,0.7239,0.7239,POINTS=32,ORIENTATION=-1,0,0,ID='F
y:0.2667 z:0.7239',QUANTITY='GAUGE HEAT FLUX
GAS',STATISTICS_START=0,TEMPORAL_STATISTIC='TIME INTEGRAL'/
&DEVC XB=2.0955,4.5339,-0.4191,-0.4191,0.8001,0.8001,POINTS=32,ORIENTATION=-
1,0,0,ID='F y:-0.4191 z:0.8001',QUANTITY='GAUGE HEAT FLUX
GAS',STATISTICS_START=0,TEMPORAL_STATISTIC='TIME INTEGRAL'/
&DEVC XB=2.0955,4.5339,-0.3429,-0.3429,0.8001,0.8001,POINTS=32,ORIENTATION=-
1,0,0,ID='F y:-0.3429 z:0.8001',QUANTITY='GAUGE HEAT FLUX
GAS',STATISTICS_START=0,TEMPORAL_STATISTIC='TIME INTEGRAL'/
&DEVC XB=2.0955,4.5339,-0.2667,-0.2667,0.8001,0.8001,POINTS=32,ORIENTATION=-
1,0,0,ID='F y:-0.2667 z:0.8001',QUANTITY='GAUGE HEAT FLUX
GAS',STATISTICS_START=0,TEMPORAL_STATISTIC='TIME INTEGRAL'/
&DEVC XB=2.0955,4.5339,0.4191,0.4191,0.8001,0.8001,POINTS=32,ORIENTATION=-1,0,0,ID='F
y:0.4191 z:0.8001',QUANTITY='GAUGE HEAT FLUX
GAS',STATISTICS_START=0,TEMPORAL_STATISTIC='TIME INTEGRAL'/
&DEVC XB=2.0955,4.5339,0.3429,0.3429,0.8001,0.8001,POINTS=32,ORIENTATION=-1,0,0,ID='F
y:0.3429 z:0.8001',QUANTITY='GAUGE HEAT FLUX
GAS',STATISTICS_START=0,TEMPORAL_STATISTIC='TIME INTEGRAL'/
&DEVC XB=2.0955,4.5339,0.2667,0.2667,0.8001,0.8001,POINTS=32,ORIENTATION=-1,0,0,ID='F
y:0.2667 z:0.8001',QUANTITY='GAUGE HEAT FLUX
GAS',STATISTICS_START=0,TEMPORAL_STATISTIC='TIME INTEGRAL'/
&DEVC XB=2.0955,4.5339,-0.4191,-0.4191,0.8763,0.8763,POINTS=32,ORIENTATION=-
1,0,0,ID='F y:-0.4191 z:0.8763',QUANTITY='GAUGE HEAT FLUX
GAS',STATISTICS_START=0,TEMPORAL_STATISTIC='TIME INTEGRAL'/
&DEVC XB=2.0955,4.5339,-0.3429,-0.3429,0.8763,0.8763,POINTS=32,ORIENTATION=-
1,0,0,ID='F y:-0.3429 z:0.8763',QUANTITY='GAUGE HEAT FLUX
GAS',STATISTICS_START=0,TEMPORAL_STATISTIC='TIME INTEGRAL'/
&DEVC XB=2.0955,4.5339,-0.2667,-0.2667,0.8763,0.8763,POINTS=32,ORIENTATION=-
1,0,0,ID='F y:-0.2667 z:0.8763',QUANTITY='GAUGE HEAT FLUX
GAS',STATISTICS_START=0,TEMPORAL_STATISTIC='TIME INTEGRAL'/
&DEVC XB=2.0955,4.5339,0.4191,0.4191,0.8763,0.8763,POINTS=32,ORIENTATION=-1,0,0,ID='F
y:0.4191 z:0.8763',QUANTITY='GAUGE HEAT FLUX
GAS',STATISTICS_START=0,TEMPORAL_STATISTIC='TIME INTEGRAL'/
&DEVC XB=2.0955,4.5339,0.3429,0.3429,0.8763,0.8763,POINTS=32,ORIENTATION=-1,0,0,ID='F
y:0.3429 z:0.8763',QUANTITY='GAUGE HEAT FLUX
GAS',STATISTICS_START=0,TEMPORAL_STATISTIC='TIME INTEGRAL'/
&DEVC XB=2.0955,4.5339,0.2667,0.2667,0.8763,0.8763,POINTS=32,ORIENTATION=-1,0,0,ID='F
y:0.2667 z:0.8763',QUANTITY='GAUGE HEAT FLUX
GAS',STATISTICS_START=0,TEMPORAL_STATISTIC='TIME INTEGRAL'/
&DEVC XB=2.0955,4.5339,-0.4191,-0.4191,0.9525,0.9525,POINTS=32,ORIENTATION=-
1,0,0,ID='F y:-0.4191 z:0.9525',QUANTITY='GAUGE HEAT FLUX
GAS',STATISTICS_START=0,TEMPORAL_STATISTIC='TIME INTEGRAL'/
```

```
&DEVC XB=2.0955,4.5339,-0.3429,-0.3429,0.9525,0.9525,POINTS=32,ORIENTATION=-
1,0,0,ID='F y:-0.3429 z:0.9525',QUANTITY='GAUGE HEAT FLUX
GAS',STATISTICS_START=0,TEMPORAL_STATISTIC='TIME INTEGRAL'/
&DEVC XB=2.0955,4.5339,-0.2667,-0.2667,0.9525,0.9525,POINTS=32,ORIENTATION=-
1,0,0,ID='F y:-0.2667 z:0.9525',QUANTITY='GAUGE HEAT FLUX
GAS',STATISTICS_START=0,TEMPORAL_STATISTIC='TIME INTEGRAL'/
&DEVC XB=2.0955,4.5339,0.4191,0.4191,0.9525,0.9525,POINTS=32,ORIENTATION=-1,0,0,ID='F
y:0.4191 z:0.9525',QUANTITY='GAUGE HEAT FLUX
GAS',STATISTICS_START=0,TEMPORAL_STATISTIC='TIME INTEGRAL'/
&DEVC XB=2.0955,4.5339,0.3429,0.3429,0.9525,0.9525,POINTS=32,ORIENTATION=-1,0,0,ID='F
y:0.3429 z:0.9525',QUANTITY='GAUGE HEAT FLUX
GAS',STATISTICS_START=0,TEMPORAL_STATISTIC='TIME INTEGRAL'/
&DEVC XB=2.0955,4.5339,0.2667,0.2667,0.9525,0.9525,POINTS=32,ORIENTATION=-1,0,0,ID='F
y:0.2667 z:0.9525',QUANTITY='GAUGE HEAT FLUX
GAS',STATISTICS_START=0,TEMPORAL_STATISTIC='TIME INTEGRAL'/
&DEVC XB=2.0955,4.5339,-0.4191,-0.4191,1.0287,1.0287,POINTS=32,ORIENTATION=-
1,0,0,ID='F y:-0.4191 z:1.0287',QUANTITY='GAUGE HEAT FLUX
GAS',STATISTICS_START=0,TEMPORAL_STATISTIC='TIME INTEGRAL'/
&DEVC XB=2.0955,4.5339,-0.3429,-0.3429,1.0287,1.0287,POINTS=32,ORIENTATION=-
1,0,0,ID='F y:-0.3429 z:1.0287',QUANTITY='GAUGE HEAT FLUX
GAS',STATISTICS_START=0,TEMPORAL_STATISTIC='TIME INTEGRAL'/
&DEVC XB=2.0955,4.5339,-0.2667,-0.2667,1.0287,1.0287,POINTS=32,ORIENTATION=-
1,0,0,ID='F y:-0.2667 z:1.0287',QUANTITY='GAUGE HEAT FLUX
GAS',STATISTICS_START=0,TEMPORAL_STATISTIC='TIME INTEGRAL'/
&DEVC XB=2.0955,4.5339,0.4191,0.4191,1.0287,1.0287,POINTS=32,ORIENTATION=-1,0,0,ID='F
y:0.4191 z:1.0287',QUANTITY='GAUGE HEAT FLUX
GAS',STATISTICS_START=0,TEMPORAL_STATISTIC='TIME INTEGRAL'/
&DEVC XB=2.0955,4.5339,0.3429,0.3429,1.0287,1.0287,POINTS=32,ORIENTATION=-1,0,0,ID='F
y:0.3429 z:1.0287',QUANTITY='GAUGE HEAT FLUX
GAS',STATISTICS_START=0,TEMPORAL_STATISTIC='TIME INTEGRAL'/
&DEVC XB=2.0955,4.5339,0.2667,0.2667,1.0287,1.0287,POINTS=32,ORIENTATION=-1,0,0,ID='F
y:0.2667 z:1.0287',QUANTITY='GAUGE HEAT FLUX
GAS',STATISTICS_START=0,TEMPORAL_STATISTIC='TIME INTEGRAL'/
&DEVC XB=2.0955,4.5339,-0.4191,-0.4191,1.1049,1.1049,POINTS=32,ORIENTATION=-
1,0,0,ID='F y:-0.4191 z:1.1049',QUANTITY='GAUGE HEAT FLUX
GAS',STATISTICS_START=0,TEMPORAL_STATISTIC='TIME INTEGRAL'/
&DEVC XB=2.0955,4.5339,-0.3429,-0.3429,1.1049,1.1049,POINTS=32,ORIENTATION=-
1,0,0,ID='F y:-0.3429 z:1.1049',QUANTITY='GAUGE HEAT FLUX
GAS',STATISTICS_START=0,TEMPORAL_STATISTIC='TIME INTEGRAL'/
&DEVC XB=2.0955,4.5339,-0.2667,-0.2667,1.1049,1.1049,POINTS=32,ORIENTATION=-
1,0,0,ID='F y:-0.2667 z:1.1049',QUANTITY='GAUGE HEAT FLUX
GAS',STATISTICS_START=0,TEMPORAL_STATISTIC='TIME INTEGRAL'/
&DEVC XB=2.0955,4.5339,0.4191,0.4191,1.1049,1.1049,POINTS=32,ORIENTATION=-1,0,0,ID='F
y:0.4191 z:1.1049',QUANTITY='GAUGE HEAT FLUX
GAS',STATISTICS_START=0,TEMPORAL_STATISTIC='TIME INTEGRAL'/
&DEVC XB=2.0955,4.5339,0.3429,0.3429,1.1049,1.1049,POINTS=32,ORIENTATION=-1,0,0,ID='F
y:0.3429 z:1.1049',QUANTITY='GAUGE HEAT FLUX
GAS',STATISTICS_START=0,TEMPORAL_STATISTIC='TIME INTEGRAL'/
&DEVC XB=2.0955,4.5339,0.2667,0.2667,1.1049,1.1049,POINTS=32,ORIENTATION=-1,0,0,ID='F
y:0.2667 z:1.1049',QUANTITY='GAUGE HEAT FLUX
GAS',STATISTICS_START=0,TEMPORAL_STATISTIC='TIME INTEGRAL'/
&DEVC XB=2.0955,4.5339,-0.4191,-0.4191,1.1811,1.1811,POINTS=32,ORIENTATION=-
1,0,0,ID='F y:-0.4191 z:1.1811',QUANTITY='GAUGE HEAT FLUX
GAS',STATISTICS_START=0,TEMPORAL_STATISTIC='TIME INTEGRAL'/
&DEVC XB=2.0955,4.5339,-0.3429,-0.3429,1.1811,1.1811,POINTS=32,ORIENTATION=-
1,0,0,ID='F y:-0.3429 z:1.1811',QUANTITY='GAUGE HEAT FLUX
GAS',STATISTICS_START=0,TEMPORAL_STATISTIC='TIME INTEGRAL'/
&DEVC XB=2.0955,4.5339,-0.2667,-0.2667,1.1811,1.1811,POINTS=32,ORIENTATION=-
1,0,0,ID='F y:-0.2667 z:1.1811',QUANTITY='GAUGE HEAT FLUX
GAS',STATISTICS_START=0,TEMPORAL_STATISTIC='TIME INTEGRAL'/
&DEVC XB=2.0955,4.5339,0.4191,0.4191,1.1811,1.1811,POINTS=32,ORIENTATION=-1,0,0,ID='F
y:0.4191 z:1.1811',QUANTITY='GAUGE HEAT FLUX
GAS',STATISTICS_START=0,TEMPORAL_STATISTIC='TIME INTEGRAL'/
```

```
&DEVC XB=2.0955,4.5339,0.3429,0.3429,1.1811,1.1811,POINTS=32,ORIENTATION=-1,0,0,ID='F
y:0.3429 z:1.1811',QUANTITY='GAUGE HEAT FLUX
GAS',STATISTICS_START=0,TEMPORAL_STATISTIC='TIME INTEGRAL'/
&DEVC XB=2.0955,4.5339,0.2667,0.2667,1.1811,1.1811,POINTS=32,ORIENTATION=-1,0,0,ID='F
y:0.2667 z:1.1811',QUANTITY='GAUGE HEAT FLUX
GAS',STATISTICS_START=0,TEMPORAL_STATISTIC='TIME INTEGRAL'/
&DEVC XB=2.0955,4.5339,-0.4191,-0.4191,1.2573,1.2573,POINTS=32,ORIENTATION=-
1,0,0,ID='F y:-0.4191 z:1.2573',QUANTITY='GAUGE HEAT FLUX
GAS',STATISTICS_START=0,TEMPORAL_STATISTIC='TIME INTEGRAL'/
&DEVC XB=2.0955,4.5339,-0.3429,-0.3429,1.2573,1.2573,POINTS=32,ORIENTATION=-
1,0,0,ID='F y:-0.3429 z:1.2573',QUANTITY='GAUGE HEAT FLUX
GAS',STATISTICS_START=0,TEMPORAL_STATISTIC='TIME INTEGRAL'/
&DEVC XB=2.0955,4.5339,-0.2667,-0.2667,1.2573,1.2573,POINTS=32,ORIENTATION=-
1,0,0,ID='F y:-0.2667 z:1.2573',QUANTITY='GAUGE HEAT FLUX
GAS',STATISTICS_START=0,TEMPORAL_STATISTIC='TIME INTEGRAL'/
&DEVC XB=2.0955,4.5339,0.4191,0.4191,1.2573,1.2573,POINTS=32,ORIENTATION=-1,0,0,ID='F
y:0.4191 z:1.2573',QUANTITY='GAUGE HEAT FLUX
GAS',STATISTICS_START=0,TEMPORAL_STATISTIC='TIME INTEGRAL'/
&DEVC XB=2.0955,4.5339,0.3429,0.3429,1.2573,1.2573,POINTS=32,ORIENTATION=-1,0,0,ID='F
y:0.3429 z:1.2573',QUANTITY='GAUGE HEAT FLUX
GAS',STATISTICS_START=0,TEMPORAL_STATISTIC='TIME INTEGRAL'/
&DEVC XB=2.0955,4.5339,0.2667,0.2667,1.2573,1.2573,POINTS=32,ORIENTATION=-1,0,0,ID='F
y:0.2667 z:1.2573',QUANTITY='GAUGE HEAT FLUX
GAS',STATISTICS_START=0,TEMPORAL_STATISTIC='TIME INTEGRAL'/
&DEVC XB=2.0955,4.5339,-0.4191,-0.4191,1.3335,1.3335,POINTS=32,ORIENTATION=-
1,0,0,ID='F y:-0.4191 z:1.3335',QUANTITY='GAUGE HEAT FLUX
GAS',STATISTICS_START=0,TEMPORAL_STATISTIC='TIME INTEGRAL'/
&DEVC XB=2.0955,4.5339,-0.3429,-0.3429,1.3335,1.3335,POINTS=32,ORIENTATION=-
1,0,0,ID='F y:-0.3429 z:1.3335',QUANTITY='GAUGE HEAT FLUX
GAS',STATISTICS_START=0,TEMPORAL_STATISTIC='TIME INTEGRAL'/
&DEVC XB=2.0955,4.5339,-0.2667,-0.2667,1.3335,1.3335,POINTS=32,ORIENTATION=-
1,0,0,ID='F y:-0.2667 z:1.3335',QUANTITY='GAUGE HEAT FLUX
GAS',STATISTICS_START=0,TEMPORAL_STATISTIC='TIME INTEGRAL'/
&DEVC XB=2.0955,4.5339,0.4191,0.4191,1.3335,1.3335,POINTS=32,ORIENTATION=-1,0,0,ID='F
y:0.4191 z:1.3335',QUANTITY='GAUGE HEAT FLUX
GAS',STATISTICS_START=0,TEMPORAL_STATISTIC='TIME INTEGRAL'/
&DEVC XB=2.0955,4.5339,0.3429,0.3429,1.3335,1.3335,POINTS=32,ORIENTATION=-1,0,0,ID='F
y:0.3429 z:1.3335',QUANTITY='GAUGE HEAT FLUX
GAS',STATISTICS_START=0,TEMPORAL_STATISTIC='TIME INTEGRAL'/
&DEVC XB=2.0955,4.5339,0.2667,0.2667,1.3335,1.3335,POINTS=32,ORIENTATION=-1,0,0,ID='F
y:0.2667 z:1.3335',QUANTITY='GAUGE HEAT FLUX
GAS',STATISTICS_START=0,TEMPORAL_STATISTIC='TIME INTEGRAL'/
&DEVC XB=2.0955,4.5339,-0.4191,-0.4191,1.4097,1.4097,POINTS=32,ORIENTATION=-
1,0,0,ID='F y:-0.4191 z:1.4097',QUANTITY='GAUGE HEAT FLUX
GAS',STATISTICS_START=0,TEMPORAL_STATISTIC='TIME INTEGRAL'/
&DEVC XB=2.0955,4.5339,-0.3429,-0.3429,1.4097,1.4097,POINTS=32,ORIENTATION=-
1,0,0,ID='F y:-0.3429 z:1.4097',QUANTITY='GAUGE HEAT FLUX
GAS',STATISTICS_START=0,TEMPORAL_STATISTIC='TIME INTEGRAL'/
&DEVC XB=2.0955,4.5339,-0.2667,-0.2667,1.4097,1.4097,POINTS=32,ORIENTATION=-
1,0,0,ID='F y:-0.2667 z:1.4097',QUANTITY='GAUGE HEAT FLUX
GAS',STATISTICS_START=0,TEMPORAL_STATISTIC='TIME INTEGRAL'/
&DEVC XB=2.0955,4.5339,0.4191,0.4191,1.4097,1.4097,POINTS=32,ORIENTATION=-1,0,0,ID='F
y:0.4191 z:1.4097',QUANTITY='GAUGE HEAT FLUX
GAS',STATISTICS_START=0,TEMPORAL_STATISTIC='TIME INTEGRAL'/
&DEVC XB=2.0955,4.5339,0.3429,0.3429,1.4097,1.4097,POINTS=32,ORIENTATION=-1,0,0,ID='F
y:0.3429 z:1.4097',QUANTITY='GAUGE HEAT FLUX
GAS',STATISTICS_START=0,TEMPORAL_STATISTIC='TIME INTEGRAL'/
&DEVC XB=2.0955,4.5339,0.2667,0.2667,1.4097,1.4097,POINTS=32,ORIENTATION=-1,0,0,ID='F
y:0.2667 z:1.4097',QUANTITY='GAUGE HEAT FLUX
GAS',STATISTICS_START=0,TEMPORAL_STATISTIC='TIME INTEGRAL'/
&DEVC XB=2.0955,4.5339,-0.4191,-0.4191,1.4859,1.4859,POINTS=32,ORIENTATION=-
1,0,0,ID='F y:-0.4191 z:1.4859',QUANTITY='GAUGE HEAT FLUX
GAS',STATISTICS_START=0,TEMPORAL_STATISTIC='TIME INTEGRAL'/
```

```
&DEVC XB=2.0955,4.5339,-0.3429,-0.3429,1.4859,1.4859,POINTS=32,ORIENTATION=-
1,0,0,ID='F y:-0.3429 z:1.4859',QUANTITY='GAUGE HEAT FLUX
GAS',STATISTICS_START=0,TEMPORAL_STATISTIC='TIME INTEGRAL'/
&DEVC XB=2.0955,4.5339,-0.2667,-0.2667,1.4859,1.4859,POINTS=32,ORIENTATION=-
1,0,0,ID='F y:-0.2667 z:1.4859',QUANTITY='GAUGE HEAT FLUX
GAS',STATISTICS_START=0,TEMPORAL_STATISTIC='TIME INTEGRAL'/
&DEVC XB=2.0955,4.5339,0.4191,0.4191,1.4859,1.4859,POINTS=32,ORIENTATION=-1,0,0,ID='F
y:0.4191 z:1.4859',QUANTITY='GAUGE HEAT FLUX
GAS',STATISTICS_START=0,TEMPORAL_STATISTIC='TIME INTEGRAL'/
&DEVC XB=2.0955,4.5339,0.3429,0.3429,1.4859,1.4859,POINTS=32,ORIENTATION=-1,0,0,ID='F
y:0.3429 z:1.4859',QUANTITY='GAUGE HEAT FLUX
GAS',STATISTICS_START=0,TEMPORAL_STATISTIC='TIME INTEGRAL'/
&DEVC XB=2.0955,4.5339,0.2667,0.2667,1.4859,1.4859,POINTS=32,ORIENTATION=-1,0,0,ID='F
y:0.2667 z:1.4859',QUANTITY='GAUGE HEAT FLUX
GAS',STATISTICS_START=0,TEMPORAL_STATISTIC='TIME INTEGRAL'/
&DEVC XB=2.0955,4.5339,-0.4191,-0.4191,1.5621,1.5621,POINTS=32,ORIENTATION=-
1,0,0,ID='F y:-0.4191 z:1.5621',QUANTITY='GAUGE HEAT FLUX
GAS',STATISTICS_START=0,TEMPORAL_STATISTIC='TIME INTEGRAL'/
&DEVC XB=2.0955,4.5339,-0.3429,-0.3429,1.5621,1.5621,POINTS=32,ORIENTATION=-
1,0,0,ID='F y:-0.3429 z:1.5621',QUANTITY='GAUGE HEAT FLUX
GAS',STATISTICS_START=0,TEMPORAL_STATISTIC='TIME INTEGRAL'/
&DEVC XB=2.0955,4.5339,-0.2667,-0.2667,1.5621,1.5621,POINTS=32,ORIENTATION=-
1,0,0,ID='F y:-0.2667 z:1.5621',QUANTITY='GAUGE HEAT FLUX
GAS',STATISTICS_START=0,TEMPORAL_STATISTIC='TIME INTEGRAL'/
&DEVC XB=2.0955,4.5339,0.4191,0.4191,1.5621,1.5621,POINTS=32,ORIENTATION=-1,0,0,ID='F
y:0.4191 z:1.5621',QUANTITY='GAUGE HEAT FLUX
GAS',STATISTICS_START=0,TEMPORAL_STATISTIC='TIME INTEGRAL'/
&DEVC XB=2.0955,4.5339,0.3429,0.3429,1.5621,1.5621,POINTS=32,ORIENTATION=-1,0,0,ID='F
y:0.3429 z:1.5621',QUANTITY='GAUGE HEAT FLUX
GAS',STATISTICS_START=0,TEMPORAL_STATISTIC='TIME INTEGRAL'/
&DEVC XB=2.0955,4.5339,0.2667,0.2667,1.5621,1.5621,POINTS=32,ORIENTATION=-1,0,0,ID='F
y:0.2667 z:1.5621',QUANTITY='GAUGE HEAT FLUX
GAS',STATISTICS_START=0,TEMPORAL_STATISTIC='TIME INTEGRAL'/
&DEVC XB=2.0955,4.5339,-0.4191,-0.4191,1.6383,1.6383,POINTS=32,ORIENTATION=-
1,0,0,ID='F y:-0.4191 z:1.6383',QUANTITY='GAUGE HEAT FLUX
GAS',STATISTICS_START=0,TEMPORAL_STATISTIC='TIME INTEGRAL'/
&DEVC XB=2.0955,4.5339,-0.3429,-0.3429,1.6383,1.6383,POINTS=32,ORIENTATION=-
1,0,0,ID='F y:-0.3429 z:1.6383',QUANTITY='GAUGE HEAT FLUX
GAS',STATISTICS_START=0,TEMPORAL_STATISTIC='TIME INTEGRAL'/
&DEVC XB=2.0955,4.5339,-0.2667,-0.2667,1.6383,1.6383,POINTS=32,ORIENTATION=-
1,0,0,ID='F y:-0.2667 z:1.6383',QUANTITY='GAUGE HEAT FLUX
GAS',STATISTICS_START=0,TEMPORAL_STATISTIC='TIME INTEGRAL'/
&DEVC XB=2.0955,4.5339,0.4191,0.4191,1.6383,1.6383,POINTS=32,ORIENTATION=-1,0,0,ID='F
y:0.4191 z:1.6383',QUANTITY='GAUGE HEAT FLUX
GAS',STATISTICS_START=0,TEMPORAL_STATISTIC='TIME INTEGRAL'/
&DEVC XB=2.0955,4.5339,0.3429,0.3429,1.6383,1.6383,POINTS=32,ORIENTATION=-1,0,0,ID='F
y:0.3429 z:1.6383',QUANTITY='GAUGE HEAT FLUX
GAS',STATISTICS_START=0,TEMPORAL_STATISTIC='TIME INTEGRAL'/
&DEVC XB=2.0955,4.5339,0.2667,0.2667,1.6383,1.6383,POINTS=32,ORIENTATION=-1,0,0,ID='F
y:0.2667 z:1.6383',QUANTITY='GAUGE HEAT FLUX
GAS',STATISTICS_START=0,TEMPORAL_STATISTIC='TIME INTEGRAL'/
&DEVC XB=2.0955,4.5339,-0.4191,-0.4191,1.7145,1.7145,POINTS=32,ORIENTATION=-
1,0,0,ID='F y:-0.4191 z:1.7145',QUANTITY='GAUGE HEAT FLUX
GAS',STATISTICS_START=0,TEMPORAL_STATISTIC='TIME INTEGRAL'/
&DEVC XB=2.0955,4.5339,-0.3429,-0.3429,1.7145,1.7145,POINTS=32,ORIENTATION=-
1,0,0,ID='F y:-0.3429 z:1.7145',QUANTITY='GAUGE HEAT FLUX
GAS',STATISTICS_START=0,TEMPORAL_STATISTIC='TIME INTEGRAL'/
&DEVC XB=2.0955,4.5339,-0.2667,-0.2667,1.7145,1.7145,POINTS=32,ORIENTATION=-
1,0,0,ID='F y:-0.2667 z:1.7145',QUANTITY='GAUGE HEAT FLUX
GAS',STATISTICS_START=0,TEMPORAL_STATISTIC='TIME INTEGRAL'/
&DEVC XB=2.0955,4.5339,0.4191,0.4191,1.7145,1.7145,POINTS=32,ORIENTATION=-1,0,0,ID='F
y:0.4191 z:1.7145',QUANTITY='GAUGE HEAT FLUX
GAS',STATISTICS_START=0,TEMPORAL_STATISTIC='TIME INTEGRAL'/
```

```
&DEVC XB=2.0955,4.5339,0.3429,0.3429,1.7145,1.7145,POINTS=32,ORIENTATION=-1,0,0,ID='F
y:0.3429 z:1.7145',QUANTITY='GAUGE HEAT FLUX
GAS',STATISTICS_START=0,TEMPORAL_STATISTIC='TIME INTEGRAL'/
&DEVC XB=2.0955,4.5339,0.2667,0.2667,1.7145,1.7145,POINTS=32,ORIENTATION=-1,0,0,ID='F
y:0.2667 z:1.7145',QUANTITY='GAUGE HEAT FLUX
GAS',STATISTICS_START=0,TEMPORAL_STATISTIC='TIME INTEGRAL'/
&DEVC XB=2.0955,4.5339,-0.4191,-0.4191,1.7907,1.7907,POINTS=32,ORIENTATION=-
1,0,0,ID='F y:-0.4191 z:1.7907',QUANTITY='GAUGE HEAT FLUX
GAS',STATISTICS_START=0,TEMPORAL_STATISTIC='TIME INTEGRAL'/
&DEVC XB=2.0955,4.5339,-0.3429,-0.3429,1.7907,1.7907,POINTS=32,ORIENTATION=-
1,0,0,ID='F y:-0.3429 z:1.7907',QUANTITY='GAUGE HEAT FLUX
GAS',STATISTICS_START=0,TEMPORAL_STATISTIC='TIME INTEGRAL'/
&DEVC XB=2.0955,4.5339,-0.2667,-0.2667,1.7907,1.7907,POINTS=32,ORIENTATION=-
1,0,0,ID='F y:-0.2667 z:1.7907',QUANTITY='GAUGE HEAT FLUX
GAS',STATISTICS_START=0,TEMPORAL_STATISTIC='TIME INTEGRAL'/
&DEVC XB=2.0955,4.5339,0.4191,0.4191,1.7907,1.7907,POINTS=32,ORIENTATION=-1,0,0,ID='F
y:0.4191 z:1.7907',QUANTITY='GAUGE HEAT FLUX
GAS',STATISTICS_START=0,TEMPORAL_STATISTIC='TIME INTEGRAL'/
&DEVC XB=2.0955,4.5339,0.3429,0.3429,1.7907,1.7907,POINTS=32,ORIENTATION=-1,0,0,ID='F
y:0.3429 z:1.7907',QUANTITY='GAUGE HEAT FLUX
GAS',STATISTICS_START=0,TEMPORAL_STATISTIC='TIME INTEGRAL'/
&DEVC XB=2.0955,4.5339,0.2667,0.2667,1.7907,1.7907,POINTS=32,ORIENTATION=-1,0,0,ID='F
y:0.2667 z:1.7907',QUANTITY='GAUGE HEAT FLUX
GAS',STATISTICS_START=0,TEMPORAL_STATISTIC='TIME INTEGRAL'/
&DEVC XB=2.0955,4.5339,-0.1905,-0.1905,1.3335,1.3335,POINTS=32,ORIENTATION=-
1,0,0,ID='F y:-0.1905 z:1.3335',QUANTITY='GAUGE HEAT FLUX
GAS',STATISTICS_START=0,TEMPORAL_STATISTIC='TIME INTEGRAL'/
&DEVC XB=2.0955,4.5339,-0.1143,-0.1143,1.3335,1.3335,POINTS=32,ORIENTATION=-
1,0,0,ID='F y:-0.1143 z:1.3335',QUANTITY='GAUGE HEAT FLUX
GAS',STATISTICS_START=0,TEMPORAL_STATISTIC='TIME INTEGRAL'/
&DEVC XB=2.0955,4.5339,-0.0381,-0.0381,1.3335,1.3335,POINTS=32,ORIENTATION=-
1,0,0,ID='F y:-0.0381 z:1.3335',QUANTITY='GAUGE HEAT FLUX
GAS',STATISTICS_START=0,TEMPORAL_STATISTIC='TIME INTEGRAL'/
&DEVC XB=2.0955,4.5339,0.0381,0.0381,1.3335,1.3335,POINTS=32,ORIENTATION=-1,0,0,ID='F
y:0.0381 z:1.3335',QUANTITY='GAUGE HEAT FLUX
GAS',STATISTICS_START=0,TEMPORAL_STATISTIC='TIME INTEGRAL'/
&DEVC XB=2.0955,4.5339,0.1143,0.1143,1.3335,1.3335,POINTS=32,ORIENTATION=-1,0,0,ID='F
y:0.1143 z:1.3335',QUANTITY='GAUGE HEAT FLUX
GAS',STATISTICS_START=0,TEMPORAL_STATISTIC='TIME INTEGRAL'/
&DEVC XB=2.0955,4.5339,0.1905,0.1905,1.3335,1.3335,POINTS=32,ORIENTATION=-1,0,0,ID='F
y:0.1905 z:1.3335',QUANTITY='GAUGE HEAT FLUX
GAS',STATISTICS_START=0,TEMPORAL_STATISTIC='TIME INTEGRAL'/
&DEVC XB=2.0955,4.5339,-0.1905,-0.1905,1.4097,1.4097,POINTS=32,ORIENTATION=-
1,0,0,ID='F y:-0.1905 z:1.4097',QUANTITY='GAUGE HEAT FLUX
GAS',STATISTICS_START=0,TEMPORAL_STATISTIC='TIME INTEGRAL'/
&DEVC XB=2.0955,4.5339,-0.1143,-0.1143,1.4097,1.4097,POINTS=32,ORIENTATION=-
1,0,0,ID='F y:-0.1143 z:1.4097',QUANTITY='GAUGE HEAT FLUX
GAS',STATISTICS_START=0,TEMPORAL_STATISTIC='TIME INTEGRAL'/
&DEVC XB=2.0955,4.5339,-0.0381,-0.0381,1.4097,1.4097,POINTS=32,ORIENTATION=-
1,0,0,ID='F y:-0.0381 z:1.4097',QUANTITY='GAUGE HEAT FLUX
GAS',STATISTICS_START=0,TEMPORAL_STATISTIC='TIME INTEGRAL'/
&DEVC XB=2.0955,4.5339,0.0381,0.0381,1.4097,1.4097,POINTS=32,ORIENTATION=-1,0,0,ID='F
y:0.0381 z:1.4097',QUANTITY='GAUGE HEAT FLUX
GAS',STATISTICS_START=0,TEMPORAL_STATISTIC='TIME INTEGRAL'/
&DEVC XB=2.0955,4.5339,0.1143,0.1143,1.4097,1.4097,POINTS=32,ORIENTATION=-1,0,0,ID='F
y:0.1143 z:1.4097',QUANTITY='GAUGE HEAT FLUX
GAS',STATISTICS_START=0,TEMPORAL_STATISTIC='TIME INTEGRAL'/
&DEVC XB=2.0955,4.5339,0.1905,0.1905,1.4097,1.4097,POINTS=32,ORIENTATION=-1,0,0,ID='F
y:0.1905 z:1.4097',QUANTITY='GAUGE HEAT FLUX
GAS',STATISTICS_START=0,TEMPORAL_STATISTIC='TIME INTEGRAL'/
&DEVC XB=2.0955,4.5339,-0.1905,-0.1905,1.4859,1.4859,POINTS=32,ORIENTATION=-
1,0,0,ID='F y:-0.1905 z:1.4859',QUANTITY='GAUGE HEAT FLUX
GAS',STATISTICS_START=0,TEMPORAL_STATISTIC='TIME INTEGRAL'/
```

```
&DEVC XB=2.0955,4.5339,-0.1143,-0.1143,1.4859,1.4859,POINTS=32,ORIENTATION=-
1,0,0,ID='F y:-0.1143 z:1.4859',QUANTITY='GAUGE HEAT FLUX
GAS',STATISTICS_START=0,TEMPORAL_STATISTIC='TIME INTEGRAL'/
&DEVC XB=2.0955,4.5339,-0.0381,-0.0381,1.4859,1.4859,POINTS=32,ORIENTATION=-
1,0,0,ID='F y:-0.0381 z:1.4859',QUANTITY='GAUGE HEAT FLUX
GAS',STATISTICS_START=0,TEMPORAL_STATISTIC='TIME INTEGRAL'/
&DEVC XB=2.0955,4.5339,0.0381,0.0381,1.4859,1.4859,POINTS=32,ORIENTATION=-1,0,0,ID='F
y:0.0381 z:1.4859',QUANTITY='GAUGE HEAT FLUX
GAS',STATISTICS_START=0,TEMPORAL_STATISTIC='TIME INTEGRAL'/
&DEVC XB=2.0955,4.5339,0.1143,0.1143,1.4859,1.4859,POINTS=32,ORIENTATION=-1,0,0,ID='F
y:0.1143 z:1.4859',QUANTITY='GAUGE HEAT FLUX
GAS',STATISTICS_START=0,TEMPORAL_STATISTIC='TIME INTEGRAL'/
&DEVC XB=2.0955,4.5339,0.1905,0.1905,1.4859,1.4859,POINTS=32,ORIENTATION=-1,0,0,ID='F
y:0.1905 z:1.4859',QUANTITY='GAUGE HEAT FLUX
GAS',STATISTICS_START=0,TEMPORAL_STATISTIC='TIME INTEGRAL'/
&DEVC XB=2.0955,4.5339,-0.1905,-0.1905,1.5621,1.5621,POINTS=32,ORIENTATION=-
1,0,0,ID='F y:-0.1905 z:1.5621',QUANTITY='GAUGE HEAT FLUX
GAS',STATISTICS_START=0,TEMPORAL_STATISTIC='TIME INTEGRAL'/
&DEVC XB=2.0955,4.5339,-0.1143,-0.1143,1.5621,1.5621,POINTS=32,ORIENTATION=-
1,0,0,ID='F y:-0.1143 z:1.5621',QUANTITY='GAUGE HEAT FLUX
GAS',STATISTICS_START=0,TEMPORAL_STATISTIC='TIME INTEGRAL'/
&DEVC XB=2.0955,4.5339,-0.0381,-0.0381,1.5621,1.5621,POINTS=32,ORIENTATION=-
1,0,0,ID='F y:-0.0381 z:1.5621',QUANTITY='GAUGE HEAT FLUX
GAS',STATISTICS_START=0,TEMPORAL_STATISTIC='TIME INTEGRAL'/
&DEVC XB=2.0955,4.5339,0.0381,0.0381,1.5621,1.5621,POINTS=32,ORIENTATION=-1,0,0,ID='F
y:0.0381 z:1.5621',QUANTITY='GAUGE HEAT FLUX
GAS',STATISTICS_START=0,TEMPORAL_STATISTIC='TIME INTEGRAL'/
&DEVC XB=2.0955,4.5339,0.1143,0.1143,1.5621,1.5621,POINTS=32,ORIENTATION=-1,0,0,ID='F
y:0.1143 z:1.5621',QUANTITY='GAUGE HEAT FLUX
GAS',STATISTICS_START=0,TEMPORAL_STATISTIC='TIME INTEGRAL'/
&DEVC XB=2.0955,4.5339,0.1905,0.1905,1.5621,1.5621,POINTS=32,ORIENTATION=-1,0,0,ID='F
y:0.1905 z:1.5621',QUANTITY='GAUGE HEAT FLUX
GAS',STATISTICS_START=0,TEMPORAL_STATISTIC='TIME INTEGRAL'/
&DEVC XB=2.0955,4.5339,-0.1905,-0.1905,1.6383,1.6383,POINTS=32,ORIENTATION=-
1,0,0,ID='F y:-0.1905 z:1.6383',QUANTITY='GAUGE HEAT FLUX
GAS',STATISTICS_START=0,TEMPORAL_STATISTIC='TIME INTEGRAL'/
&DEVC XB=2.0955,4.5339,-0.1143,-0.1143,1.6383,1.6383,POINTS=32,ORIENTATION=-
1,0,0,ID='F y:-0.1143 z:1.6383',QUANTITY='GAUGE HEAT FLUX
GAS',STATISTICS_START=0,TEMPORAL_STATISTIC='TIME INTEGRAL'/
&DEVC XB=2.0955,4.5339,-0.0381,-0.0381,1.6383,1.6383,POINTS=32,ORIENTATION=-
1,0,0,ID='F y:-0.0381 z:1.6383',QUANTITY='GAUGE HEAT FLUX
GAS',STATISTICS_START=0,TEMPORAL_STATISTIC='TIME INTEGRAL'/
&DEVC XB=2.0955,4.5339,0.0381,0.0381,1.6383,1.6383,POINTS=32,ORIENTATION=-1,0,0,ID='F
y:0.0381 z:1.6383',QUANTITY='GAUGE HEAT FLUX
GAS',STATISTICS_START=0,TEMPORAL_STATISTIC='TIME INTEGRAL'/
&DEVC XB=2.0955,4.5339,0.1143,0.1143,1.6383,1.6383,POINTS=32,ORIENTATION=-1,0,0,ID='F
y:0.1143 z:1.6383',QUANTITY='GAUGE HEAT FLUX
GAS',STATISTICS_START=0,TEMPORAL_STATISTIC='TIME INTEGRAL'/
&DEVC XB=2.0955,4.5339,0.1905,0.1905,1.6383,1.6383,POINTS=32,ORIENTATION=-1,0,0,ID='F
y:0.1905 z:1.6383',QUANTITY='GAUGE HEAT FLUX
GAS',STATISTICS_START=0,TEMPORAL_STATISTIC='TIME INTEGRAL'/
&DEVC XB=2.0955,4.5339,-0.1905,-0.1905,1.7145,1.7145,POINTS=32,ORIENTATION=-
1,0,0,ID='F y:-0.1905 z:1.7145',QUANTITY='GAUGE HEAT FLUX
GAS',STATISTICS_START=0,TEMPORAL_STATISTIC='TIME INTEGRAL'/
&DEVC XB=2.0955,4.5339,-0.1143,-0.1143,1.7145,1.7145,POINTS=32,ORIENTATION=-
1,0,0,ID='F y:-0.1143 z:1.7145',QUANTITY='GAUGE HEAT FLUX
GAS',STATISTICS_START=0,TEMPORAL_STATISTIC='TIME INTEGRAL'/
&DEVC XB=2.0955,4.5339,-0.0381,-0.0381,1.7145,1.7145,POINTS=32,ORIENTATION=-
1,0,0,ID='F y:-0.0381 z:1.7145',QUANTITY='GAUGE HEAT FLUX
GAS',STATISTICS_START=0,TEMPORAL_STATISTIC='TIME INTEGRAL'/
&DEVC XB=2.0955,4.5339,0.0381,0.0381,1.7145,1.7145,POINTS=32,ORIENTATION=-1,0,0,ID='F
y:0.0381 z:1.7145',QUANTITY='GAUGE HEAT FLUX
GAS',STATISTICS_START=0,TEMPORAL_STATISTIC='TIME INTEGRAL'/
```

```
&DEVC XB=2.0955,4.5339,0.1143,0.1143,1.7145,1.7145,POINTS=32,ORIENTATION=-1,0,0,ID='F
y:0.1143 z:1.7145',QUANTITY='GAUGE HEAT FLUX
GAS',STATISTICS_START=0,TEMPORAL_STATISTIC='TIME INTEGRAL'/
&DEVC XB=2.0955,4.5339,0.1905,0.1905,1.7145,1.7145,POINTS=32,ORIENTATION=-1,0,0,ID='F
y:0.1905 z:1.7145',QUANTITY='GAUGE HEAT FLUX
GAS',STATISTICS_START=0,TEMPORAL_STATISTIC='TIME INTEGRAL'/

&TAIL/
```

C.3 Low Voltage Switchgear

Since only a small number of LV SWGR simulations were run, the python tool for generating input files was not used. FDS inputs to define the electrode metal and arc location were edited by hand.

```
&HEAD CHID='LV_FC_Mid_Mid_Al'/

! 3 in. resolution. Approximately 2 m to each side, 2 m above, and 2.4 m front and
back.

&MESH ID='Cabinet',IJK=23,22,20,XB=-2.3622,-0.6096,-2.5146,-
0.8382,0.0000,1.5240,MULT_ID='M1'/ 3 in. resolution
&MULT ID='M1',I_LOWER=-1,I_UPPER=2,DX=1.7526,J_UPPER=2,DY=1.6764,K_UPPER=2,DZ=1.5240/

&VENT MB='ZMAX',SURF_ID='OPEN'/
&VENT PBZ=0,SURF_ID='FLOOR'/
&VENT MB='YMAX',SURF_ID='OPEN'/
&VENT MB='XMAX',SURF_ID='OPEN'/
&VENT MB='YMIN',SURF_ID='OPEN'/
&VENT MB='XMIN',SURF_ID='OPEN'/

&MISC AEROSOL_AL2O3=T,I_MAX_TEMP=35000 /

! SMOKE3D_SPEC_ID sets the species used by Smokeview to visualize smoke

&DUMP SMOKE3D_SPEC_ID='ALUMINUM OXIDE',SUPPRESS_DIAGNOSTICS=F,MASS_FILE=T/

! Turns off the extinction model. Default values in the model may not be appropriate
for metal oxidation
&COMB SUPPRESSION=F /

! 0.01 kg/m3 greatly limits clipping of density.
&CLIP MINIMUM_DENSITY=0.01, MAXIMUM_TEMPERATURE=35000.,CLIP_DT_RESTRICTIONS_MAX=0 /

! These cases a very challenging for the pressure solver. The selected values seem to
give enough pressure iterations to
! drop the velocity error down to a plateau value.

&PRES MAX_PRESSURE_ITERATIONS=30, VELOCITY_TOLERANCE=0.001,
SUSPEND_PRESSURE_ITERATIONS=F/

! For ZOI runs suggest T_END = arc time + 8 s

&TIME T_END=0., DT=0.001,WALL_INCREMENT=1 /

&RADI NUMBER_RADIATION_ANGLES=500 /

! 1 cell thick OBST to help out pressure solver.

&OBST XB=-0.6858,0.0000,-0.6096,0.6096,2.3622,2.4384,SURF_ID='CABINET'/
&OBST XB=-1.6764,-0.6858,-0.6096,0.6096,2.2098,2.2860,SURF_ID='CABINET'/
```

```
&OBST XB=-1.6764,0.0000,-0.6096,-0.5334,0.0000,2.2098,SURF_ID='CABINET'/
&OBST XB=-0.6858,0.0000,-0.6096,-0.5334,2.2098,2.3622,SURF_ID='CABINET'/
&OBST XB=-1.1430,-0.6858,-0.6096,-0.5334,2.2098,2.2860,SURF_ID='CABINET'/
&OBST XB=-1.6764,0.0000,0.5334,0.6096,0.0000,2.2098,SURF_ID='CABINET'/
&OBST XB=-0.6858,0.0000,0.5334,0.6096,2.2098,2.3622,SURF_ID='CABINET'/
&OBST XB=-1.1430,-0.6858,0.5334,0.6096,2.2098,2.2860,SURF_ID='CABINET'/

&OBST XB=-1.7526,-1.6764,-0.6096,0.6096,0.0000,2.2860,SURF_ID='CABINET'/

&OBST XB=-0.0762,0.0000,-0.6096,0.6096,0.0000,2.3622,SURF_ID='CABINET'/

&OBST XB=-0.6858,0.0000,-0.0762,0.0000,0.0000,2.3622,SURF_ID='CABINET'/
&OBST XB=-1.6764,-0.6858,-0.0762,0.0000,0.0000,2.2098,SURF_ID='CABINET'/
&OBST XB=-0.7620,-0.6858,-0.6096,0.6096,0.0000,2.4384,SURF_ID='CABINET'/
&OBST XB=-1.2192,-1.1430,-0.6096,0.6096,0.0000,2.2098,SURF_ID='CABINET'/
&OBST XB=-0.6096,-0.0762,-0.4572,-0.1524,0.0000,0.5334,SURF_ID='BREAKER'/
&OBST XB=-0.6096,-0.0762,0.0762,0.4572,0.0000,0.5334,SURF_ID='BREAKER'/
&OBST XB=-0.6096,-0.0762,-0.4572,-0.1524,0.6096,1.1430,SURF_ID='BREAKER'/
&OBST XB=-0.6096,-0.0762,-0.4572,-0.1524,1.2192,1.7526,SURF_ID='BREAKER'/
&OBST XB=-0.6096,-0.0762,-0.4572,-0.1524,1.8288,2.2860,SURF_ID='BREAKER'/
&OBST XB=-0.6096,-0.0762,0.0762,0.4572,0.6096,1.1430,SURF_ID='BREAKER'/
&OBST XB=-0.6096,-0.0762,0.0762,0.4572,1.2192,1.7526,SURF_ID='BREAKER'/
&OBST XB=-0.6096,-0.0762,0.0762,0.4572,1.8288,2.2860,SURF_ID='BREAKER'/
&OBST XB=-0.0762,0.0000,-0.5334,0.5334,0.6096,0.6858,SURF_ID='CABINET'/
&OBST XB=-0.0762,0.0000,-0.5334,0.5334,1.2192,1.2954,SURF_ID='CABINET'/
&OBST XB=-0.0762,0.0000,-0.5334,0.5334,1.8288,1.9050,SURF_ID='CABINET'/
&HOLE XB=-1.2202,-1.1420,0.2286,0.3048,2.1336,2.2098/
&HOLE XB=-1.2202,-1.1420,-0.3048,-0.2286,2.1336,2.2098/

&HOLE XB=-0.6096,-0.5334,0.3810,0.4572,2.3612,2.4394/
&HOLE XB=-0.3810,-0.2286,0.3810,0.4572,2.3612,2.4394/
&HOLE XB=-0.6096,-0.5334,-0.4572,-0.3810,2.3612,2.4394/
&HOLE XB=-0.3810,-0.2286,-0.4572,-0.3810,2.3612,2.4394/
&HOLE XB=-0.6096,-0.5334,0.2286,0.3048,2.3612,2.4394/
&HOLE XB=-0.3810,-0.2286,0.2286,0.3048,2.3612,2.4394/
&HOLE XB=-0.6096,-0.5334,-0.3048,-0.2286,2.3612,2.4394/
&HOLE XB=-0.3810,-0.2286,-0.3048,-0.2286,2.3612,2.4394/
&HOLE XB=-0.6096,-0.5334,0.0762,0.1524,2.3612,2.4394/
&HOLE XB=-0.3810,-0.2286,0.0762,0.1524,2.3612,2.4394/
&HOLE XB=-0.6096,-0.5334,-0.1524,-0.0762,2.3612,2.4394/
&HOLE XB=-0.3810,-0.2286,-0.1524,-0.0762,2.3612,2.4394/

&HOLE XB=-1.7536,-1.6754,-0.4572,-0.0762,0.0762,0.1524/
&HOLE XB=-1.7536,-1.6754,-0.4572,-0.0762,0.2286,0.3048/
&HOLE XB=-1.7536,-1.6754,-0.4572,-0.0762,1.9050,1.9812/
&HOLE XB=-1.7536,-1.6754,-0.4572,-0.0762,2.0574,2.1336/
&HOLE XB=-1.7536,-1.6754,0.0762,0.4572,0.0762,0.1524/
&HOLE XB=-1.7536,-1.6754,0.0762,0.4572,0.2286,0.3048/
&HOLE XB=-1.7536,-1.6754,0.0762,0.4572,1.9050,1.9812/
&HOLE XB=-1.7536,-1.6754,0.0762,0.4572,2.0574,2.1336/

&HOLE XB=-0.0772,0.0010,0.0000,0.5334,0.6858,1.2192/Door
&HOLE XB=-0.7630,-0.6848,0.0000,0.5334,0.7620,0.8382/ ARC

! RADCAL_ID='SOOT' makes the SPEC use the SOOT radiation properties which the MISC
line has changed to those for AL2O3
! RAMPs used instead of built in cp data for N2, CO2, and O2 to extend temperature to
20,000 K

&SPEC ID='WET NITROGEN',BACKGROUND=T,SPEC_ID='NITROGEN','CARBON DIOXIDE','WATER
VAPOR',MASS_FRACTION=1,0.000775,0.007792/FDS Default AIR without O2
&SPEC ID='NITROGEN', LUMPED_COMPONENT_ONLY=T,RAMP_CP='N2 C'/
&SPEC ID='CARBON DIOXIDE', LUMPED_COMPONENT_ONLY=T,RAMP_CP='CO2 C'/
&SPEC ID='WATER VAPOR', LUMPED_COMPONENT_ONLY=T /
```

```
&SPEC ID='OXYGEN', MASS_FRACTION_0=0.230997,RAMP_CP='O2 C' /
&SPEC ID='ALUMINUM',FORMULA='Al',RAMP_CP='AL
C',SIGMALJ=2.655,EPSILONKLJ=2750.,PR_GAS=1/
&SPEC ID='ALUMINUM OXIDE',FORMULA='Al2O3',RAMP_CP='AL2O3
C',SIGMALJ=3.186,EPSILONKLJ=557.449,PR_GAS=1,RADCAL_ID='SOOT'/

&REAC FUEL='ALUMINUM', SPEC_ID_NU='ALUMINUM','OXYGEN','ALUMINUM OXIDE', NU=-2,-1.5,1,
HEAT_OF_COMBUSTION=31100. / Al -> AL2O3

&MATL ID='CONCRETE', DENSITY=2400, CONDUCTIVITY=1.6, SPECIFIC_HEAT=0.75,
EMISSIVITY=0.95 /

! Non-melting steel
&MATL ID='INERT STEEL', DENSITY=7800., SPECIFIC_HEAT_RAMP='STEEL C',
CONDUCTIVITY_RAMP='STEEL K', EMISSIVITY=0.85/

! Melting steel
&MATL ID='STEEL', DENSITY=7800., SPECIFIC_HEAT_RAMP='STEEL C',
CONDUCTIVITY_RAMP='STEEL K', EMISSIVITY=0.85,
      THRESHOLD_TEMPERATURE=1300., THRESHOLD_SIGN=1, HEAT_OF_REACTION(1)=250.,
PCR(1)=T, A(1)=0.6, E(1)=0., N_S(1)=0., N_T(1)=1. /

! Eurocode values
&RAMP ID='STEEL C',T=20,F=0.440/
&RAMP ID='STEEL C',T=600,F=0.760/
&RAMP ID='STEEL C',T=700,F=1.008/
&RAMP ID='STEEL C',T=720,F=1.388/
&RAMP ID='STEEL C',T=725,F=1.666/
&RAMP ID='STEEL C',T=730,F=2.291/
&RAMP ID='STEEL C',T=735,F=5.000/
&RAMP ID='STEEL C',T=740,F=2.525/ BCC -> FCC Transition
&RAMP ID='STEEL C',T=745,F=1.818/
&RAMP ID='STEEL C',T=750,F=1.483/
&RAMP ID='STEEL C',T=800,F=0.803/
&RAMP ID='STEEL C',T=900,F=0.650/

&RAMP ID='STEEL K',T=20,F=53.3/
&RAMP ID='STEEL K',T=800,F=27.3/

&SURF ID='BREAKER', MATL_ID='INERT STEEL', THICKNESS=0.02,
RGB=204,204,255,CELL_SIZE_FACTOR=0.05,STRETCH_FACTOR=1 /
&SURF ID='CABINET', MATL_ID='STEEL', THICKNESS=0.002381,  COLOR='GRAY 60',
BURN_AWAY=.TRUE.,CELL_SIZE_FACTOR=0.05,STRETCH_FACTOR=1 /
&SURF ID='FLOOR', MATL_ID='CONCRETE', THICKNESS=0.15, RGB=50,50,50, DEFAULT=T /

&MATL ID='MOLTEN
AL',DENSITY=2375,CONDUCTIVITY=100.,SPECIFIC_HEAT=1.177,EMISSIVITY=0,A=3.333,E=0,
N_REACTIONS=1,HEAT_OF_REACTION=0,HEAT_OF_COMBUSTION=0,MATL_ID(1,1)='MOLTEN
AL2',SPEC_ID(1,1)='ALUMINUM',NU_MATL(1,1)=0.25,NU_SPEC(1,1)=0.75/
&MATL ID='MOLTEN
AL2',DENSITY=593.75,SPEC_ID='ALUMINUM',NU_SPEC=1,CONDUCTIVITY=100.,SPECIFIC_HEAT=1.177
/

&SURF ID='AL DROP',MATL_ID='MOLTEN AL',GEOMETRY='SPHERICAL',THICKNESS=5.E-
6,HEAT_TRANSFER_COEFFICIENT=0,TMP_INNER=665.3/
&PART ID='AL DROPS',SURF_ID='AL
DROP',AGE=2.0,SAMPLING_FACTOR=10,MONODISPERSE=T,RGB=100,100,100/
&PROP ID='DROPS',PART_ID='AL DROPS',FLOW_RAMP='RAMP
MF',MASS_FLOW_RATE=0.00181,PARTICLES_PER_SECOND=20000,PARTICLE_VELOCITY=10,SPRAY_ANGLE
=0,60,OFFSET=0.05/

&INIT XB=-0.9906,-0.9144,0.0762,0.4572,0.7620,0.8382,HRRPUV=859124,RAMP_Q='RAMP
Q',RADIATIVE_FRACTION=0.316/
```

```
! One spray nozzle device per electrode that inject liquid droplets

&DEVC PROP_ID='DROPS',XYZ=-0.9525,
0.1143,0.8001,QUANTITY='TIME',SETPOINT=0.0,ORIENTATION=0,0,1/
&DEVC PROP_ID='DROPS',XYZ=-0.9525,
0.2667,0.8001,QUANTITY='TIME',SETPOINT=0.0,ORIENTATION=0,0,1/
&DEVC PROP_ID='DROPS',XYZ=-0.9525,
0.4191,0.8001,QUANTITY='TIME',SETPOINT=0.0,ORIENTATION=0,0,1/

&RAMP ID='RAMP Q',T=0.00,F=0.0000/
&RAMP ID='RAMP Q',T=0.10,F=1.0000/
&RAMP ID='RAMP Q',T=20.0,F=1.0000/
&RAMP ID='RAMP Q',T=20.1,F=0.6058/
&RAMP ID='RAMP Q',T=41.0,F=0.6058/
&RAMP ID='RAMP Q',T=41.1,F=0.0000/

&RAMP ID='RAMP MF', T= 0.00, F=0.0000/
&RAMP ID='RAMP MF', T=0.10, F=1.0000/
&RAMP ID='RAMP MF', T=20.00, F=1.0000/
&RAMP ID='RAMP MF', T=20.10, F=0.4681/
&RAMP ID='RAMP MF', T=41.00, F=0.4681/
&RAMP ID='RAMP MF', T=41.01, F=0.0000/

! Gas phase specific heats. FDS defaults for N2, O2, H2O, and CO2 replaced to extend
values to higher temperatures than present in FDS

&RAMP ID='AL2O3 C', T=-73, F=0.761/ NASA TP-2002-211556
&RAMP ID='AL2O3 C', T=127, F=0.921/
&RAMP ID='AL2O3 C', T=327, F=0.999/
&RAMP ID='AL2O3 C', T=527, F=1.038/
&RAMP ID='AL2O3 C', T=727, F=1.058/
&RAMP ID='AL2O3 C', T=1727, F=1.090/
&RAMP ID='AL2O3 C', T=2727, F=1.096/
&RAMP ID='AL2O3 C', T=3727, F=1.098/
&RAMP ID='AL2O3 C', T=4727, F=1.099/
&RAMP ID='AL2O3 C', T=5727, F=1.100/

&RAMP ID='AL C', T=-73, F=0.820/ NASA TP-2002-211556
&RAMP ID='AL C', T=127, F=0.783/
&RAMP ID='AL C', T=327, F=0.776/
&RAMP ID='AL C', T=527, F=0.773/
&RAMP ID='AL C', T=727, F=0.772/
&RAMP ID='AL C', T=1727, F=0.771/
&RAMP ID='AL C', T=2727, F=0.771/
&RAMP ID='AL C', T=3727, F=0.775/
&RAMP ID='AL C', T=4727, F=0.793/
&RAMP ID='AL C', T=5727, F=0.841/
&RAMP ID='AL C', T=6727, F=0.930/
&RAMP ID='AL C', T=7727, F=1.034/
&RAMP ID='AL C', T=8727, F=1.130/
&RAMP ID='AL C', T=9727, F=1.204/
&RAMP ID='AL C', T=10727, F=1.250/
&RAMP ID='AL C', T=11727, F=1.271/
&RAMP ID='AL C', T=12727, F=1.269/
&RAMP ID='AL C', T=13727, F=1.252/
&RAMP ID='AL C', T=14727, F=1.226/
&RAMP ID='AL C', T=15727, F=1.196/
&RAMP ID='AL C', T=16727, F=1.168/
&RAMP ID='AL C', T=17727, F=1.145/
&RAMP ID='AL C', T=18727, F=1.125/
&RAMP ID='AL C', T=19727, F=1.108/

&RAMP ID='CU C', T=-73, F=0.327/ NASA TP-2002-211556
&RAMP ID='CU C', T=127, F=0.327/
```

```
&RAMP ID='CU C', T=327, F=0.327/
&RAMP ID='CU C', T=527, F=0.327/
&RAMP ID='CU C', T=727, F=0.327/
&RAMP ID='CU C', T=1727, F=0.337/
&RAMP ID='CU C', T=2727, F=0.396/
&RAMP ID='CU C', T=3727, F=0.471/
&RAMP ID='CU C', T=4727, F=0.517/
&RAMP ID='CU C', T=5727, F=0.537/
&RAMP ID='CU C', T=6727, F=0.551/
&RAMP ID='CU C', T=7727, F=0.577/
&RAMP ID='CU C', T=8727, F=0.606/
&RAMP ID='CU C', T=9727, F=0.633/
&RAMP ID='CU C', T=10727, F=0.653/
&RAMP ID='CU C', T=11727, F=0.663/
&RAMP ID='CU C', T=12727, F=0.664/
&RAMP ID='CU C', T=13727, F=0.657/
&RAMP ID='CU C', T=14727, F=0.642/
&RAMP ID='CU C', T=15727, F=0.622/
&RAMP ID='CU C', T=16727, F=0.599/
&RAMP ID='CU C', T=17727, F=0.574/
&RAMP ID='CU C', T=18727, F=0.550/
&RAMP ID='CU C', T=19727, F=0.528/

&RAMP ID='N2 C', T=-73, F=1.039/ NASA TP-2002-211556
&RAMP ID='N2 C', T=127, F=1.044/
&RAMP ID='N2 C', T=327, F=1.075/
&RAMP ID='N2 C', T=527, F=1.122/
&RAMP ID='N2 C', T=727, F=1.167/
&RAMP ID='N2 C', T=1727, F=1.284/
&RAMP ID='N2 C', T=2727, F=1.322/
&RAMP ID='N2 C', T=3727, F=1.340/
&RAMP ID='N2 C', T=4727, F=1.354/
&RAMP ID='N2 C', T=5727, F=1.371/
&RAMP ID='N2 C', T=6727, F=1.402/
&RAMP ID='N2 C', T=7727, F=1.454/
&RAMP ID='N2 C', T=8727, F=1.544/
&RAMP ID='N2 C', T=9727, F=1.670/
&RAMP ID='N2 C', T=10727, F=1.822/
&RAMP ID='N2 C', T=11727, F=1.984/
&RAMP ID='N2 C', T=12727, F=2.136/
&RAMP ID='N2 C', T=13727, F=2.261/
&RAMP ID='N2 C', T=14727, F=2.346/
&RAMP ID='N2 C', T=15727, F=2.383/
&RAMP ID='N2 C', T=16727, F=2.372/
&RAMP ID='N2 C', T=17727, F=2.320/
&RAMP ID='N2 C', T=18727, F=2.241/
&RAMP ID='N2 C', T=19727, F=2.159/

&RAMP ID='O2 C', T=-73, F=0.910/ NASA TP-2002-211556
&RAMP ID='O2 C', T=127, F=0.941/
&RAMP ID='O2 C', T=327, F=1.003/
&RAMP ID='O2 C', T=527, F=1.055/
&RAMP ID='O2 C', T=727, F=1.090/
&RAMP ID='O2 C', T=1727, F=1.181/
&RAMP ID='O2 C', T=2727, F=1.249/
&RAMP ID='O2 C', T=3727, F=1.303/
&RAMP ID='O2 C', T=4727, F=1.344/
&RAMP ID='O2 C', T=5727, F=1.373/
&RAMP ID='O2 C', T=6727, F=1.386/
&RAMP ID='O2 C', T=7727, F=1.376/
&RAMP ID='O2 C', T=8727, F=1.344/
&RAMP ID='O2 C', T=9727, F=1.296/
&RAMP ID='O2 C', T=10727, F=1.241/
&RAMP ID='O2 C', T=11727, F=1.184/
```

```
&RAMP ID='O2 C', T=12727, F=1.128/
&RAMP ID='O2 C', T=13727, F=1.077/
&RAMP ID='O2 C', T=14727, F=1.030/
&RAMP ID='O2 C', T=15727, F=0.989/
&RAMP ID='O2 C', T=16727, F=0.953/
&RAMP ID='O2 C', T=17727, F=0.922/
&RAMP ID='O2 C', T=18727, F=0.894/
&RAMP ID='O2 C', T=19727, F=0.870/

&RAMP ID='CO2 C', T=-73, F=0.735/ NASA TP-2002-211556
&RAMP ID='CO2 C', T=127, F=0.939/
&RAMP ID='CO2 C', T=327, F=1.075/
&RAMP ID='CO2 C', T=527, F=1.169/
&RAMP ID='CO2 C', T=727, F=1.234/
&RAMP ID='CO2 C', T=1727, F=1.371/
&RAMP ID='CO2 C', T=2727, F=1.412/
&RAMP ID='CO2 C', T=3727, F=1.436/
&RAMP ID='CO2 C', T=4727, F=1.466/
&RAMP ID='CO2 C', T=5727, F=1.517/
&RAMP ID='CO2 C', T=6727, F=1.595/
&RAMP ID='CO2 C', T=7727, F=1.694/
&RAMP ID='CO2 C', T=8727, F=1.797/
&RAMP ID='CO2 C', T=9727, F=1.888/
&RAMP ID='CO2 C', T=10727, F=1.957/
&RAMP ID='CO2 C', T=11727, F=2.000/
&RAMP ID='CO2 C', T=12727, F=2.019/
&RAMP ID='CO2 C', T=13727, F=2.020/
&RAMP ID='CO2 C', T=14727, F=2.007/
&RAMP ID='CO2 C', T=15727, F=1.987/
&RAMP ID='CO2 C', T=16727, F=1.965/
&RAMP ID='CO2 C', T=17727, F=1.944/
&RAMP ID='CO2 C', T=18727, F=1.924/
&RAMP ID='CO2 C', T=19727, F=1.905/

!Smokeview Outputs. Adjust PBY and PBX for center of arc volume.

&SLCF QUANTITY='MASS FRACTION',SPEC_ID='ALUMINUM',CELL_CENTERED=.TRUE.,PBY=0.2668/
&SLCF QUANTITY='MASS FRACTION',SPEC_ID='ALUMINUM
OXIDE',CELL_CENTERED=.TRUE.,PBY=0.2668/
&SLCF QUANTITY='MASS FRACTION',SPEC_ID='OXYGEN',CELL_CENTERED=.TRUE.,PBY=0.2668/
&SLCF QUANTITY='HRRPUV',CELL_CENTERED=.TRUE.,PBY=0.2668/
&SLCF QUANTITY='HRRPUV',CELL_CENTERED=.TRUE.,PBX=-0.9525/
&SLCF QUANTITY='TEMPERATURE',CELL_CENTERED=.TRUE.,PBY=0.2668/
&SLCF QUANTITY='TEMPERATURE',CELL_CENTERED=.TRUE.,PBX=-0.9525/
&SLCF QUANTITY='INTEGRATED INTENSITY',CELL_CENTERED=.TRUE.,PBY=0.2668/
&SLCF QUANTITY='INTEGRATED INTENSITY',CELL_CENTERED=.TRUE.,PBX=-0.9525/
&SLCF QUANTITY='VELOCITY',CELL_CENTERED=.TRUE.,PBY=0.2668/
&SLCF QUANTITY='U-VELOCITY',CELL_CENTERED=.TRUE.,PBY=0.2668/
&SLCF QUANTITY='VELOCITY',CELL_CENTERED=.TRUE.,PBX=-0.9525/
&SLCF QUANTITY='V-VELOCITY',CELL_CENTERED=.TRUE.,PBX=-0.9525/
&SLCF QUANTITY='PRESSURE',CELL_CENTERED=.TRUE.,PBY=0.2668/

&BNDF QUANTITY='WALL TEMPERATURE',CELL_CENTERED=.TRUE./
&BNDF QUANTITY='GAUGE HEAT FLUX',CELL_CENTERED=.TRUE./
&BNDF QUANTITY='WALL THICKNESS',CELL_CENTERED=.TRUE./

&TAIL /
```

C.4 Non-Segregated Bus Ducts

For the NSBDs, a single template was created that contained all three bus duct geometries. To obtain the elbow, tee, or straight run configuration the FDS mesh was limited to just that specific portion of the overall geometry.

```
&HEAD CHID='fileid', TITLE='Bus Duct fileid' /

&MESH XB=-1.0,1.0,-1.0,1.0,-0.6,0.6, IJK=50,50,30, MULT_ID='mesh' /

!For T, use I_LOWER=-3, I_Upper=-1
!For straight, use I_LOWER=-1, I_Upper=1
!For elbow, use I_LOWER=1, I_Upper=3
&MULT ID='mesh', DX=2.0, DY=2.0, DZ=1.2, I_LOWER=imeshlower, I_UPPER=imeshupper,
J_LOWER=-1, J_UPPER=1, K_LOWER=-2, K_UPPER=2 /

&VENT MB='XMIN',SURF_ID='OPEN'/
&VENT MB='XMAX',SURF_ID='OPEN'/
&VENT MB='YMIN',SURF_ID='OPEN'/
&VENT MB='YMAX',SURF_ID='OPEN'/
&VENT MB='ZMIN',SURF_ID='OPEN'/
&VENT MB='ZMAX',SURF_ID='OPEN'/

! I_MAX_TEMP=35000 ensures property arrays are high enough for the CLIP vlaues.
! AEROSOL_AL2O3 replaces default SOOT radiative properties with those for AL2O3

&MISC AEROSOL_AL2O3=T,I_MAX_TEMP=35000 /

! SMOKE3D_SPEC_ID sets the species used by Smokeview to visualize smoke

&DUMP SMOKE3D_SPEC_ID='3dsmoke',SUPPRESS_DIAGNOSTICS=F,MASS_FILE=T, DT_RESTART=0.1/

! Turns off the extinction model. Default values in the model may not be appropriate
for metal oxidation
&COMB SUPPRESSION=F /

! 0.01 kg/m3 greatly limits clipping of density.
&CLIP MINIMUM_DENSITY=0.01, MAXIMUM_TEMPERATURE=35000.,CLIP_DT_RESTRICTIONS_MAX=0 /

! These cases a very challenging for the pressure solver. The selected values seem to
give enough pressure iterations to
! drop the velocity error down to a plateau value.

&PRES MAX_PRESSURE_ITERATIONS=30, VELOCITY_TOLERANCE=0.001,
SUSPEND_PRESSURE_ITERATIONS=F/

! For ZOI runs suggest T_END = arc time + 8 s

&TIME T_END=tend, DT=0.001, WALL_INCREMENT=1 /

&RADI NUMBER_RADIATION_ANGLES=500 /

!Geometry for the straight duct
&OBST XB=-7.00, 4.24,-0.28, 0.28, -0.24, -0.20, SURF_ID='ductsurf' /  Straight duct
bottom
&OBST XB=-3.72, 3.76,-0.28, 0.28, 0.20, 0.24, SURF_ID='ductsurf' /  Straight duct top
&OBST XB=-7.00, 4.24,-0.32, -0.28, -0.24, 0.24, SURF_ID='ductsurf' /  Straight duct
front
&OBST XB=-7.00, 4.24, 0.28, 0.32, -0.24, 0.24, SURF_ID='ductsurf' /  Straight duct
back

!Geometry for the Tee
&OBST XB=-3.72, -3.68, -0.28, 3.00, 0.24, 0.72, SURF_ID='ductsurf' /  Tee right
```

```
&OBST XB=-4.32, -4.28, -0.28, 3.00, 0.24, 0.72, SURF_ID='ductsurf' /  Tee left
&OBST XB=-4.28, -3.72, -0.28, 3.00, 0.68, 0.72, SURF_ID='ductsurf' /  Tee top
&OBST XB=-4.32, -3.68, 0.28, 3.00, 0.24, 0.28, SURF_ID='ductsurf' /  Tee bottom
&OBST XB=-4.32, -3.68, -0.32, -0.28, 0.24, 0.72, SURF_ID='ductsurf' /  Tee upper cap
&OBST XB=-7.00, -4.28, -0.28, 0.28, 0.20, 0.24, SURF_ID='ductsurf' /  Remaining top
panel


&OBST XB=3.76, 3.80, -0.28, 0.28, 0.24, 3.00, SURF_ID='ductsurf' /  Elbow left
&OBST XB=4.20, 4.24, -0.28, 0.28, -0.24, 3.00, SURF_ID='ductsurf' /  Elbow right
&OBST XB=3.76, 4.24, -0.32, -0.28, 0.24, 3.00, SURF_ID='ductsurf' /  Elbow front
&OBST XB=3.76, 4.24, 0.28, 0.32, 0.24, 3.00, SURF_ID='ductsurf' /  Elbow back

&SPEC ID='WET NITROGEN',BACKGROUND=T,SPEC_ID='NITROGEN','CARBON DIOXIDE','WATER
VAPOR',MASS_FRACTION=1,0.000775,0.007792/FDS Default AIR without O2
&SPEC ID='NITROGEN', LUMPED_COMPONENT_ONLY=T,RAMP_CP='N2 C'/
&SPEC ID='CARBON DIOXIDE', LUMPED_COMPONENT_ONLY=T,RAMP_CP='CO2 C'/
&SPEC ID='WATER VAPOR', LUMPED_COMPONENT_ONLY=T /
&SPEC ID='OXYGEN', MASS_FRACTION_0=0.230997,RAMP_CP='O2 C' /
alspec1 ID='ALUMINUM',FORMULA='Al',RAMP_CP='AL
C',SIGMALJ=2.655,EPSILONKLJ=2750.,PR_GAS=1/
alspec2 ID='ALUMINUM
OXIDE',MASS_EXTINCTION_COEFFICIENT=3000,FORMULA='Al2O3',RAMP_CP='AL2O3
C',SIGMALJ=3.186,EPSILONKLJ=557.449,PR_GAS=1,RADCAL_ID='SOOT'/
cuspec1 ID='COPPER',FORMULA='Cu',RAMP_CP='CU
C',SIGMALJ=5.058,EPSILONKLJ=2983.,PR_GAS=1/
cuspec2 ID='COPPER
OXIDE',MASS_EXTINCTION_COEFFICIENT=3000,FORMULA='Cu2O',SPECIFIC_HEAT=0.7,SIGMALJ=5.403
,PR_GAS=1,RADCAL_ID='SOOT'/C from JANAF, LJ take as CuO

alreac FUEL='ALUMINUM', SPEC_ID_NU='ALUMINUM','OXYGEN','ALUMINUM OXIDE', NU=-2,-1.5,1,
HEAT_OF_COMBUSTION=31100. / Al -> AL2O3
cureac FUEL='COPPER',SPEC_ID_NU='COPPER','OXYGEN','COPPER OXIDE',NU=-2,-
0.5,1,HEAT_OF_COMBUSTION=1340./ Cu->Cu2O

&MATL ID='CONCRETE', DENSITY=2400, CONDUCTIVITY=1.6, SPECIFIC_HEAT=0.75,
EMISSIVITY=0.95 /

&MATL ID='STEEL DUCT', DENSITY=7800., SPECIFIC_HEAT_RAMP='STEEL C',
CONDUCTIVITY_RAMP='STEEL K', EMISSIVITY=0.85,
      THRESHOLD_TEMPERATURE=1300., THRESHOLD_SIGN=1, HEAT_OF_REACTION(1)=250.,
PCR(1)=T, A(1)=0.6, E(1)=0., N_S(1)=0., N_T(1)=1. /

&MATL ID='ALUMINUM DUCT', DENSITY=2700, CONDUCTIVITY_RAMP='ALUMINUM K',
SPECIFIC_HEAT_RAMP='ALUMINUM C', EMISSIVITY=0.35,
       THRESHOLD_TEMPERATURE=650., THRESHOLD_SIGN=1, HEAT_OF_REACTION(1)=320.,
PCR(1)=T, A(1)=1.2, E(1)=0., N_S(1)=0., N_T(1) = 1. /


! Eurocode values
&RAMP ID='STEEL C',T=20,F=0.440/
&RAMP ID='STEEL C',T=600,F=0.760/
&RAMP ID='STEEL C',T=700,F=1.008/
&RAMP ID='STEEL C',T=720,F=1.388/
&RAMP ID='STEEL C',T=725,F=1.666/
&RAMP ID='STEEL C',T=730,F=2.291/
&RAMP ID='STEEL C',T=735,F=5.000/
&RAMP ID='STEEL C',T=740,F=2.525/ BCC -> FCC Transition
&RAMP ID='STEEL C',T=745,F=1.818/
&RAMP ID='STEEL C',T=750,F=1.483/
&RAMP ID='STEEL C',T=800,F=0.803/
&RAMP ID='STEEL C',T=900,F=0.650/

&RAMP ID='STEEL K',T=20,F=53.3/
```

```
&RAMP ID='STEEL K',T=800,F=27.3/

&RAMP ID='ALUMINUM C',T=27,F=0.898/
&RAMP ID='ALUMINUM C',T=127,F=0.955/
&RAMP ID='ALUMINUM C',T=227,F=0.994/
&RAMP ID='ALUMINUM C',T=327,F=1.033/
&RAMP ID='ALUMINUM C',T=427,F=1.078/
&RAMP ID='ALUMINUM C',T=527,F=1.132/
&RAMP ID='ALUMINUM C',T=627,F=1.197/

&RAMP ID='ALUMINUM K',T=0,F=236/
&RAMP ID='ALUMINUM K',T=127,F=240/
&RAMP ID='ALUMINUM K',T=327,F=232/
&RAMP ID='ALUMINUM K',T=527,F=220/

&SURF ID='ALUMINUM DUCT', MATL_ID='ALUMINUM DUCT', THICKNESS=0.003175, COLOR='GRAY
80', BURN_AWAY=T /
&SURF ID='STEEL DUCT', MATL_ID='STEEL DUCT', THICKNESS=0.003175, COLOR='GRAY 70',
BURN_AWAY=T /
&SURF ID='FLOOR', MATL_ID='CONCRETE', THICKNESS=0.15, RGB=50,50,50, DEFAULT=T /

!The block below defines particles that emit vapor for aluminum.
!The particles are initialized at the melting point.
!The PROP MASS_FLOW_RATE is the maximum liquid production rate divided by the number
of electrodes
!NU_SPEC and NU_MATL are set to get the 75 % oxidation for Al and 25 % for Cu. The
second MOLTEN AL2 and CU2 species have a modified density to preserve diameter.
!A and E are set to give the vapor over 0.3 s.

almatl1 ID='MOLTEN
AL',DENSITY=2375,CONDUCTIVITY=100.,SPECIFIC_HEAT=1.177,EMISSIVITY=0,A=3.333,E=0,
N_REACTIONS=1,HEAT_OF_REACTION=0,HEAT_OF_COMBUSTION=0,MATL_ID(1,1)='MOLTEN
AL2',SPEC_ID(1,1)='ALUMINUM',NU_MATL(1,1)=0.25,NU_SPEC(1,1)=0.75/
almatl2 ID='MOLTEN
AL2',DENSITY=593.75,SPEC_ID='ALUMINUM',NU_SPEC=1,CONDUCTIVITY=100.,SPECIFIC_HEAT=1.177
/

alsurf1 ID='AL DROP',MATL_ID='MOLTEN AL',GEOMETRY='SPHERICAL',THICKNESS=5.E-
6,HEAT_TRANSFER_COEFFICIENT=0,TMP_INNER=665.3/
alpart1 ID='AL DROPS',SURF_ID='AL
DROP',AGE=2.0,SAMPLING_FACTOR=10,MONODISPERSE=T,RGB=100,100,100/
alprop1 ID='DROPS',PART_ID='AL DROPS',FLOW_RAMP='RAMP
MF',MASS_FLOW_RATE=almfr,PARTICLES_PER_SECOND=20000,PARTICLE_VELOCITY=10,SPRAY_ANGLE=0
,60/

! The block below is for copper.

cumatl1 ID='MOLTEN
CU',DENSITY=8960,CONDUCTIVITY=340.,SPECIFIC_HEAT=0.517,EMISSIVITY=0,A=3.333,E=0,
N_REACTIONS=1,HEAT_OF_REACTION=0,HEAT_OF_COMBUSTION=0,MATL_ID(1,1)='MOLTEN
CU2',SPEC_ID(1,1)='COPPER',NU_MATL(1,1)=0.75,NU_SPEC(1,1)=0.25/
cumatl2 ID='MOLTEN
CU2',DENSITY=7168,CONDUCTIVITY=340.,SPECIFIC_HEAT=0.517,EMISSIVITY=0/

cusurf1 ID='CU DROP',MATL_ID='MOLTEN CU',GEOMETRY='SPHERICAL',THICKNESS=5.E-
6,HEAT_TRANSFER_COEFFICIENT=0,TMP_INNER=1084.85/
cupart1 ID='CU DROPS',SURF_ID='CU
DROP',AGE=2.0,SAMPLING_FACTOR=10,MONODISPERSE=T,RGB=184,115,51/
cuprop1 ID='DROPS',PART_ID='CU DROPS',FLOW_RAMP='RAMP
MF',MASS_FLOW_RATE=cumfr,PARTICLES_PER_SECOND=20000,PARTICLE_VELOCITY=10,SPRAY_ANGLE=0
,60/
```

```
! First INIT line is the volumetric source term where the RADAITIVE_FRACTION uses
Cressault's data interpolated based on power,. The HRRPUV is
! reduced based on energy needed to degrade the electrodes:
! Adjusted total energy = (Total arc energy - electrode mass loss * (vapor fraction *
energy to vaporize + liquid fraction * energy to melt))
!
! Cressault data:
!
! X_r,Al = 0.2275*Max_Power^0.3292
! X_r,Al = 0.1273*Max_Power^0.3859
!
! Phase  Energy (kJ/kg)
! Change    Al     Cu
! Melt    1063.4  695.2

&INIT XB=initx1,initx2,inity1,inity2,initz1,initz2,HRRPUV=hrrpuvval,RAMP_Q='RAMP
Q',RADIATIVE_FRACTION=radfrac/

! One spray nozzle device per electrode that inject liquid droplets

&DEVC
PROP_ID='DROPS',XYZ=nozx1,nozy1,nozz1,QUANTITY='TIME',SETPOINT=0.0,ORIENTATION=orient1
,orient2,orient3/
&DEVC
PROP_ID='DROPS',XYZ=nozx2,nozy2,nozz2,QUANTITY='TIME',SETPOINT=0.0,ORIENTATION=orient1
,orient2,orient3/
&DEVC
PROP_ID='DROPS',XYZ=nozx3,nozy3,nozz3,QUANTITY='TIME',SETPOINT=0.0,ORIENTATION=orient1
,orient2,orient3/

! An 0.1 s ramp up and down for the arc volumetric source term helps avoid numerical
instabilities

&RAMP ID='RAMP Q',T=0.0,F=0.0000/
&RAMP ID='RAMP Q',T=0.1,F=rampqf1/
&RAMP ID='RAMP Q',T=0.2,F=rampqf2/
&RAMP ID='RAMP Q',T=0.3,F=rampqf3/
&RAMP ID='RAMP Q',T=0.4,F=rampqf4/
&RAMP ID='RAMP Q',T=0.5,F=rampqf5/
&RAMP ID='RAMP Q',T=0.6,F=rampqf6/
&RAMP ID='RAMP Q',T=0.7,F=rampqf7/
&RAMP ID='RAMP Q',T=0.8,F=rampqf8/
&RAMP ID='RAMP Q',T=0.9,F=rampqf9/
&RAMP ID='RAMP Q',T=1.0,F=rampqf10/
&RAMP ID='RAMP Q',T=1.1,F=rampqf11/
&RAMP ID='RAMP Q',T=1.2,F=rampqf12/
&RAMP ID='RAMP Q',T=1.3,F=rampqf13/
&RAMP ID='RAMP Q',T=1.4,F=rampqf14/
&RAMP ID='RAMP Q',T=1.5,F=rampqf15/
&RAMP ID='RAMP Q',T=1.6,F=rampqf16/
&RAMP ID='RAMP Q',T=1.7,F=rampqf17/
&RAMP ID='RAMP Q',T=1.8,F=rampqf18/
&RAMP ID='RAMP Q',T=1.9,F=rampqf19/
&RAMP ID='RAMP Q',T=2.0,F=rampqf20/
&RAMP ID='RAMP Q',T=2.1,F=rampqf21/
&RAMP ID='RAMP Q',T=2.2,F=rampqf22/
&RAMP ID='RAMP Q',T=2.3,F=rampqf23/
&RAMP ID='RAMP Q',T=2.4,F=rampqf24/
&RAMP ID='RAMP Q',T=2.5,F=rampqf25/
&RAMP ID='RAMP Q',T=2.6,F=rampqf26/
&RAMP ID='RAMP Q',T=2.7,F=rampqf27/
&RAMP ID='RAMP Q',T=2.8,F=rampqf28/
&RAMP ID='RAMP Q',T=2.9,F=rampqf29/
&RAMP ID='RAMP Q',T=3.0,F=rampqf30/
```

```
&RAMP ID='RAMP Q',T=3.1,F=rampqf31/
&RAMP ID='RAMP Q',T=3.2,F=rampqf32/
&RAMP ID='RAMP Q',T=3.3,F=rampqf33/
&RAMP ID='RAMP Q',T=3.4,F=rampqf34/
&RAMP ID='RAMP Q',T=3.5,F=rampqf35/
&RAMP ID='RAMP Q',T=3.6,F=rampqf36/
&RAMP ID='RAMP Q',T=3.7,F=rampqf37/
&RAMP ID='RAMP Q',T=3.8,F=rampqf38/
&RAMP ID='RAMP Q',T=3.9,F=rampqf39/
&RAMP ID='RAMP Q',T=4.0,F=rampqf40/
&RAMP ID='RAMP Q',T=4.1,F=rampqf41/
&RAMP ID='RAMP Q',T=4.2,F=rampqf42/
&RAMP ID='RAMP Q',T=4.3,F=rampqf43/
&RAMP ID='RAMP Q',T=4.4,F=rampqf44/
&RAMP ID='RAMP Q',T=4.5,F=rampqf45/
&RAMP ID='RAMP Q',T=4.6,F=rampqf46/
&RAMP ID='RAMP Q',T=4.7,F=rampqf47/
&RAMP ID='RAMP Q',T=4.8,F=rampqf48/
&RAMP ID='RAMP Q',T=4.9,F=rampqf49/
&RAMP ID='RAMP Q',T=5.0,F=rampqf50/
&RAMP ID='RAMP Q',T=5.1,F=rampqf51/
&RAMP ID='RAMP Q',T=5.2,F=rampqf52/
&RAMP ID='RAMP Q',T=5.3,F=rampqf53/
&RAMP ID='RAMP Q',T=5.4,F=rampqf54/
&RAMP ID='RAMP Q',T=5.5,F=rampqf55/
&RAMP ID='RAMP Q',T=5.6,F=rampqf56/
&RAMP ID='RAMP Q',T=5.7,F=rampqf57/
&RAMP ID='RAMP Q',T=5.8,F=rampqf58/
&RAMP ID='RAMP Q',T=5.9,F=rampqf59/
&RAMP ID='RAMP Q',T=6.0,F=rampqf60/
&RAMP ID='RAMP Q',T=6.1,F=rampqf61/
&RAMP ID='RAMP Q',T=6.2,F=rampqf62/
&RAMP ID='RAMP Q',T=6.3,F=rampqf63/
&RAMP ID='RAMP Q',T=6.4,F=rampqf64/
&RAMP ID='RAMP Q',T=6.5,F=rampqf65/
&RAMP ID='RAMP Q',T=6.6,F=rampqf66/
&RAMP ID='RAMP Q',T=6.7,F=rampqf67/
&RAMP ID='RAMP Q',T=6.8,F=rampqf68/
&RAMP ID='RAMP Q',T=6.9,F=rampqf69/
&RAMP ID='RAMP Q',T=7.0,F=rampqf70/
&RAMP ID='RAMP Q',T=7.1,F=rampqf71/
&RAMP ID='RAMP Q',T=7.2,F=rampqf72/
&RAMP ID='RAMP Q',T=7.3,F=rampqf73/
&RAMP ID='RAMP Q',T=7.4,F=rampqf74/
&RAMP ID='RAMP Q',T=7.5,F=rampqf75/
&RAMP ID='RAMP Q',T=7.6,F=rampqf76/
&RAMP ID='RAMP Q',T=7.7,F=rampqf77/
&RAMP ID='RAMP Q',T=7.8,F=rampqf78/
&RAMP ID='RAMP Q',T=7.9,F=rampqf79/
&RAMP ID='RAMP Q',T=8.0,F=rampqf80/
&RAMP ID='RAMP Q',T=8.1,F=rampqf81/
&RAMP ID='RAMP Q',T=8.2,F=rampqf82/
&RAMP ID='RAMP Q',T=8.3,F=rampqf83/
&RAMP ID='RAMP Q',T=8.4,F=rampqf84/
&RAMP ID='RAMP Q',T=8.5,F=rampqf85/
&RAMP ID='RAMP Q',T=8.6,F=rampqf86/
&RAMP ID='RAMP Q',T=8.7,F=rampqf87/
&RAMP ID='RAMP Q',T=8.8,F=rampqf88/
&RAMP ID='RAMP Q',T=8.9,F=rampqf89/
&RAMP ID='RAMP Q',T=9.0,F=rampqf90/
&RAMP ID='RAMP Q',T=9.1,F=rampqf91/
&RAMP ID='RAMP Q',T=9.2,F=rampqf92/
&RAMP ID='RAMP Q',T=9.3,F=rampqf93/
&RAMP ID='RAMP Q',T=9.4,F=rampqf94/
```

```
&RAMP ID='RAMP Q',T=9.5,F=rampqf95/
&RAMP ID='RAMP Q',T=9.6,F=rampqf96/
&RAMP ID='RAMP Q',T=9.7,F=rampqf97/
&RAMP ID='RAMP Q',T=9.8,F=rampqf98/
&RAMP ID='RAMP Q',T=9.9,F=rampqf99/
&RAMP ID='RAMP Q',T=10.0,F=rampqf100/
&RAMP ID='RAMP Q',T=10.1,F=rampqf101/
&RAMP ID='RAMP Q',T=10.2,F=rampqf102/
&RAMP ID='RAMP Q',T=10.3,F=rampqf103/
&RAMP ID='RAMP Q',T=10.4,F=rampqf104/
&RAMP ID='RAMP Q',T=10.5,F=rampqf105/
&RAMP ID='RAMP Q',T=10.6,F=rampqf106/
&RAMP ID='RAMP Q',T=10.7,F=rampqf107/
&RAMP ID='RAMP Q',T=10.8,F=rampqf108/
&RAMP ID='RAMP Q',T=10.9,F=rampqf109/
&RAMP ID='RAMP Q',T=11.0,F=rampqf110/
&RAMP ID='RAMP Q',T=11.1,F=rampqf111/
&RAMP ID='RAMP Q',T=11.2,F=rampqf112/
&RAMP ID='RAMP Q',T=11.3,F=rampqf113/
&RAMP ID='RAMP Q',T=11.4,F=rampqf114/
&RAMP ID='RAMP Q',T=11.5,F=rampqf115/
&RAMP ID='RAMP Q',T=11.6,F=rampqf116/
&RAMP ID='RAMP Q',T=11.7,F=rampqf117/
&RAMP ID='RAMP Q',T=11.8,F=rampqf118/
&RAMP ID='RAMP Q',T=11.9,F=rampqf119/
&RAMP ID='RAMP Q',T=12.0,F=rampqf120/
&RAMP ID='RAMP Q',T=12.1,F=rampqf121/
&RAMP ID='RAMP Q',T=12.2,F=rampqf122/
&RAMP ID='RAMP Q',T=12.3,F=rampqf123/
&RAMP ID='RAMP Q',T=12.4,F=rampqf124/
&RAMP ID='RAMP Q',T=12.5,F=rampqf125/
&RAMP ID='RAMP Q',T=12.6,F=rampqf126/
&RAMP ID='RAMP Q',T=12.7,F=rampqf127/
&RAMP ID='RAMP Q',T=12.8,F=rampqf128/
&RAMP ID='RAMP Q',T=12.9,F=rampqf129/
&RAMP ID='RAMP Q',T=13.0,F=rampqf130/
&RAMP ID='RAMP Q',T=13.1,F=rampqf131/
&RAMP ID='RAMP Q',T=13.2,F=rampqf132/
&RAMP ID='RAMP Q',T=13.3,F=rampqf133/
&RAMP ID='RAMP Q',T=13.4,F=rampqf134/
&RAMP ID='RAMP Q',T=13.5,F=rampqf135/
&RAMP ID='RAMP Q',T=13.6,F=rampqf136/
&RAMP ID='RAMP Q',T=13.7,F=rampqf137/
&RAMP ID='RAMP Q',T=13.8,F=rampqf138/
&RAMP ID='RAMP Q',T=13.9,F=rampqf139/
&RAMP ID='RAMP Q',T=14.0,F=rampqf140/
&RAMP ID='RAMP Q',T=14.1,F=rampqf141/
&RAMP ID='RAMP Q',T=14.2,F=rampqf142/
&RAMP ID='RAMP Q',T=14.3,F=rampqf143/
&RAMP ID='RAMP Q',T=14.4,F=rampqf144/
&RAMP ID='RAMP Q',T=14.5,F=rampqf145/
&RAMP ID='RAMP Q',T=14.6,F=rampqf146/
&RAMP ID='RAMP Q',T=14.7,F=rampqf147/
&RAMP ID='RAMP Q',T=14.8,F=rampqf148/
&RAMP ID='RAMP Q',T=14.9,F=rampqf149/
&RAMP ID='RAMP Q',T=15.0,F=rampqf150/
&RAMP ID='RAMP Q',T=15.1,F=rampqf151/
&RAMP ID='RAMP Q',T=15.2,F=rampqf152/
&RAMP ID='RAMP Q',T=15.3,F=rampqf153/
&RAMP ID='RAMP Q',T=15.4,F=rampqf154/
&RAMP ID='RAMP Q',T=15.5,F=rampqf155/
&RAMP ID='RAMP Q',T=15.6,F=rampqf156/
&RAMP ID='RAMP Q',T=15.7,F=rampqf157/
&RAMP ID='RAMP Q',T=15.8,F=rampqf158/
```

```
&RAMP ID='RAMP Q',T=15.9,F=rampqf159/
&RAMP ID='RAMP Q',T=16.0,F=rampqf160/
&RAMP ID='RAMP Q',T=16.1,F=rampqf161/
&RAMP ID='RAMP Q',T=16.2,F=rampqf162/
&RAMP ID='RAMP Q',T=16.3,F=rampqf163/
&RAMP ID='RAMP Q',T=16.4,F=rampqf164/
&RAMP ID='RAMP Q',T=16.5,F=rampqf165/
&RAMP ID='RAMP Q',T=16.6,F=rampqf166/
&RAMP ID='RAMP Q',T=16.7,F=rampqf167/
&RAMP ID='RAMP Q',T=16.8,F=rampqf168/
&RAMP ID='RAMP Q',T=16.9,F=rampqf169/
&RAMP ID='RAMP Q',T=17.0,F=rampqf170/
&RAMP ID='RAMP Q',T=17.1,F=rampqf171/
&RAMP ID='RAMP Q',T=17.2,F=rampqf172/
&RAMP ID='RAMP Q',T=17.3,F=rampqf173/
&RAMP ID='RAMP Q',T=17.4,F=rampqf174/
&RAMP ID='RAMP Q',T=17.5,F=rampqf175/
&RAMP ID='RAMP Q',T=17.6,F=rampqf176/
&RAMP ID='RAMP Q',T=17.7,F=rampqf177/
&RAMP ID='RAMP Q',T=17.8,F=rampqf178/
&RAMP ID='RAMP Q',T=17.9,F=rampqf179/
&RAMP ID='RAMP Q',T=18.0,F=rampqf180/
&RAMP ID='RAMP Q',T=18.1,F=rampqf181/
&RAMP ID='RAMP Q',T=18.2,F=rampqf182/
&RAMP ID='RAMP Q',T=18.3,F=rampqf183/
&RAMP ID='RAMP Q',T=18.4,F=rampqf184/
&RAMP ID='RAMP Q',T=18.5,F=rampqf185/
&RAMP ID='RAMP Q',T=18.6,F=rampqf186/
&RAMP ID='RAMP Q',T=18.7,F=rampqf187/
&RAMP ID='RAMP Q',T=18.8,F=rampqf188/
&RAMP ID='RAMP Q',T=18.9,F=rampqf189/
&RAMP ID='RAMP Q',T=19.0,F=rampqf190/
&RAMP ID='RAMP Q',T=19.1,F=rampqf191/
&RAMP ID='RAMP Q',T=19.2,F=rampqf192/
&RAMP ID='RAMP Q',T=19.3,F=rampqf193/
&RAMP ID='RAMP Q',T=19.4,F=rampqf194/
&RAMP ID='RAMP Q',T=19.5,F=rampqf195/
&RAMP ID='RAMP Q',T=19.6,F=rampqf196/
&RAMP ID='RAMP Q',T=19.7,F=rampqf197/
&RAMP ID='RAMP Q',T=19.8,F=rampqf198/
&RAMP ID='RAMP Q',T=19.9,F=rampqf199/
&RAMP ID='RAMP Q',T=20.0,F=rampqf200/
&RAMP ID='RAMP Q',T=20.1,F=0.0000/

! RAMP for droplets

&RAMP ID='RAMP MF',T=0.00,F=0.0000/
&RAMP ID='RAMP MF',T=0.1,F=rampmff1/
&RAMP ID='RAMP MF',T=0.2,F=rampmff2/
&RAMP ID='RAMP MF',T=0.3,F=rampmff3/
&RAMP ID='RAMP MF',T=0.4,F=rampmff4/
&RAMP ID='RAMP MF',T=0.5,F=rampmff5/
&RAMP ID='RAMP MF',T=0.6,F=rampmff6/
&RAMP ID='RAMP MF',T=0.7,F=rampmff7/
&RAMP ID='RAMP MF',T=0.8,F=rampmff8/
&RAMP ID='RAMP MF',T=0.9,F=rampmff9/
&RAMP ID='RAMP MF',T=1.0,F=rampmff10/
&RAMP ID='RAMP MF',T=1.1,F=rampmff11/
&RAMP ID='RAMP MF',T=1.2,F=rampmff12/
&RAMP ID='RAMP MF',T=1.3,F=rampmff13/
&RAMP ID='RAMP MF',T=1.4,F=rampmff14/
&RAMP ID='RAMP MF',T=1.5,F=rampmff15/
&RAMP ID='RAMP MF',T=1.6,F=rampmff16/
&RAMP ID='RAMP MF',T=1.7,F=rampmff17/
```

```
&RAMP ID='RAMP MF',T=1.8,F=rampmff18/
&RAMP ID='RAMP MF',T=1.9,F=rampmff19/
&RAMP ID='RAMP MF',T=2.0,F=rampmff20/
&RAMP ID='RAMP MF',T=2.1,F=rampmff21/
&RAMP ID='RAMP MF',T=2.2,F=rampmff22/
&RAMP ID='RAMP MF',T=2.3,F=rampmff23/
&RAMP ID='RAMP MF',T=2.4,F=rampmff24/
&RAMP ID='RAMP MF',T=2.5,F=rampmff25/
&RAMP ID='RAMP MF',T=2.6,F=rampmff26/
&RAMP ID='RAMP MF',T=2.7,F=rampmff27/
&RAMP ID='RAMP MF',T=2.8,F=rampmff28/
&RAMP ID='RAMP MF',T=2.9,F=rampmff29/
&RAMP ID='RAMP MF',T=3.0,F=rampmff30/
&RAMP ID='RAMP MF',T=3.1,F=rampmff31/
&RAMP ID='RAMP MF',T=3.2,F=rampmff32/
&RAMP ID='RAMP MF',T=3.3,F=rampmff33/
&RAMP ID='RAMP MF',T=3.4,F=rampmff34/
&RAMP ID='RAMP MF',T=3.5,F=rampmff35/
&RAMP ID='RAMP MF',T=3.6,F=rampmff36/
&RAMP ID='RAMP MF',T=3.7,F=rampmff37/
&RAMP ID='RAMP MF',T=3.8,F=rampmff38/
&RAMP ID='RAMP MF',T=3.9,F=rampmff39/
&RAMP ID='RAMP MF',T=4.0,F=rampmff40/
&RAMP ID='RAMP MF',T=4.1,F=rampmff41/
&RAMP ID='RAMP MF',T=4.2,F=rampmff42/
&RAMP ID='RAMP MF',T=4.3,F=rampmff43/
&RAMP ID='RAMP MF',T=4.4,F=rampmff44/
&RAMP ID='RAMP MF',T=4.5,F=rampmff45/
&RAMP ID='RAMP MF',T=4.6,F=rampmff46/
&RAMP ID='RAMP MF',T=4.7,F=rampmff47/
&RAMP ID='RAMP MF',T=4.8,F=rampmff48/
&RAMP ID='RAMP MF',T=4.9,F=rampmff49/
&RAMP ID='RAMP MF',T=5.0,F=rampmff50/
&RAMP ID='RAMP MF',T=5.1,F=rampmff51/
&RAMP ID='RAMP MF',T=5.2,F=rampmff52/
&RAMP ID='RAMP MF',T=5.3,F=rampmff53/
&RAMP ID='RAMP MF',T=5.4,F=rampmff54/
&RAMP ID='RAMP MF',T=5.5,F=rampmff55/
&RAMP ID='RAMP MF',T=5.6,F=rampmff56/
&RAMP ID='RAMP MF',T=5.7,F=rampmff57/
&RAMP ID='RAMP MF',T=5.8,F=rampmff58/
&RAMP ID='RAMP MF',T=5.9,F=rampmff59/
&RAMP ID='RAMP MF',T=6.0,F=rampmff60/
&RAMP ID='RAMP MF',T=6.1,F=rampmff61/
&RAMP ID='RAMP MF',T=6.2,F=rampmff62/
&RAMP ID='RAMP MF',T=6.3,F=rampmff63/
&RAMP ID='RAMP MF',T=6.4,F=rampmff64/
&RAMP ID='RAMP MF',T=6.5,F=rampmff65/
&RAMP ID='RAMP MF',T=6.6,F=rampmff66/
&RAMP ID='RAMP MF',T=6.7,F=rampmff67/
&RAMP ID='RAMP MF',T=6.8,F=rampmff68/
&RAMP ID='RAMP MF',T=6.9,F=rampmff69/
&RAMP ID='RAMP MF',T=7.0,F=rampmff70/
&RAMP ID='RAMP MF',T=7.1,F=rampmff71/
&RAMP ID='RAMP MF',T=7.2,F=rampmff72/
&RAMP ID='RAMP MF',T=7.3,F=rampmff73/
&RAMP ID='RAMP MF',T=7.4,F=rampmff74/
&RAMP ID='RAMP MF',T=7.5,F=rampmff75/
&RAMP ID='RAMP MF',T=7.6,F=rampmff76/
&RAMP ID='RAMP MF',T=7.7,F=rampmff77/
&RAMP ID='RAMP MF',T=7.8,F=rampmff78/
&RAMP ID='RAMP MF',T=7.9,F=rampmff79/
&RAMP ID='RAMP MF',T=8.0,F=rampmff80/
&RAMP ID='RAMP MF',T=8.1,F=rampmff81/
```

```
&RAMP ID='RAMP MF',T=8.2,F=rampmff82/
&RAMP ID='RAMP MF',T=8.3,F=rampmff83/
&RAMP ID='RAMP MF',T=8.4,F=rampmff84/
&RAMP ID='RAMP MF',T=8.5,F=rampmff85/
&RAMP ID='RAMP MF',T=8.6,F=rampmff86/
&RAMP ID='RAMP MF',T=8.7,F=rampmff87/
&RAMP ID='RAMP MF',T=8.8,F=rampmff88/
&RAMP ID='RAMP MF',T=8.9,F=rampmff89/
&RAMP ID='RAMP MF',T=9.0,F=rampmff90/
&RAMP ID='RAMP MF',T=9.1,F=rampmff91/
&RAMP ID='RAMP MF',T=9.2,F=rampmff92/
&RAMP ID='RAMP MF',T=9.3,F=rampmff93/
&RAMP ID='RAMP MF',T=9.4,F=rampmff94/
&RAMP ID='RAMP MF',T=9.5,F=rampmff95/
&RAMP ID='RAMP MF',T=9.6,F=rampmff96/
&RAMP ID='RAMP MF',T=9.7,F=rampmff97/
&RAMP ID='RAMP MF',T=9.8,F=rampmff98/
&RAMP ID='RAMP MF',T=9.9,F=rampmff99/
&RAMP ID='RAMP MF',T=10.0,F=rampmff100/
&RAMP ID='RAMP MF',T=10.1,F=rampmff101/
&RAMP ID='RAMP MF',T=10.2,F=rampmff102/
&RAMP ID='RAMP MF',T=10.3,F=rampmff103/
&RAMP ID='RAMP MF',T=10.4,F=rampmff104/
&RAMP ID='RAMP MF',T=10.5,F=rampmff105/
&RAMP ID='RAMP MF',T=10.6,F=rampmff106/
&RAMP ID='RAMP MF',T=10.7,F=rampmff107/
&RAMP ID='RAMP MF',T=10.8,F=rampmff108/
&RAMP ID='RAMP MF',T=10.9,F=rampmff109/
&RAMP ID='RAMP MF',T=11.0,F=rampmff110/
&RAMP ID='RAMP MF',T=11.1,F=rampmff111/
&RAMP ID='RAMP MF',T=11.2,F=rampmff112/
&RAMP ID='RAMP MF',T=11.3,F=rampmff113/
&RAMP ID='RAMP MF',T=11.4,F=rampmff114/
&RAMP ID='RAMP MF',T=11.5,F=rampmff115/
&RAMP ID='RAMP MF',T=11.6,F=rampmff116/
&RAMP ID='RAMP MF',T=11.7,F=rampmff117/
&RAMP ID='RAMP MF',T=11.8,F=rampmff118/
&RAMP ID='RAMP MF',T=11.9,F=rampmff119/
&RAMP ID='RAMP MF',T=12.0,F=rampmff120/
&RAMP ID='RAMP MF',T=12.1,F=rampmff121/
&RAMP ID='RAMP MF',T=12.2,F=rampmff122/
&RAMP ID='RAMP MF',T=12.3,F=rampmff123/
&RAMP ID='RAMP MF',T=12.4,F=rampmff124/
&RAMP ID='RAMP MF',T=12.5,F=rampmff125/
&RAMP ID='RAMP MF',T=12.6,F=rampmff126/
&RAMP ID='RAMP MF',T=12.7,F=rampmff127/
&RAMP ID='RAMP MF',T=12.8,F=rampmff128/
&RAMP ID='RAMP MF',T=12.9,F=rampmff129/
&RAMP ID='RAMP MF',T=13.0,F=rampmff130/
&RAMP ID='RAMP MF',T=13.1,F=rampmff131/
&RAMP ID='RAMP MF',T=13.2,F=rampmff132/
&RAMP ID='RAMP MF',T=13.3,F=rampmff133/
&RAMP ID='RAMP MF',T=13.4,F=rampmff134/
&RAMP ID='RAMP MF',T=13.5,F=rampmff135/
&RAMP ID='RAMP MF',T=13.6,F=rampmff136/
&RAMP ID='RAMP MF',T=13.7,F=rampmff137/
&RAMP ID='RAMP MF',T=13.8,F=rampmff138/
&RAMP ID='RAMP MF',T=13.9,F=rampmff139/
&RAMP ID='RAMP MF',T=14.0,F=rampmff140/
&RAMP ID='RAMP MF',T=14.1,F=rampmff141/
&RAMP ID='RAMP MF',T=14.2,F=rampmff142/
&RAMP ID='RAMP MF',T=14.3,F=rampmff143/
&RAMP ID='RAMP MF',T=14.4,F=rampmff144/
&RAMP ID='RAMP MF',T=14.5,F=rampmff145/
```

```
&RAMP ID='RAMP MF',T=14.6,F=rampmff146/
&RAMP ID='RAMP MF',T=14.7,F=rampmff147/
&RAMP ID='RAMP MF',T=14.8,F=rampmff148/
&RAMP ID='RAMP MF',T=14.9,F=rampmff149/
&RAMP ID='RAMP MF',T=15.0,F=rampmff150/
&RAMP ID='RAMP MF',T=15.1,F=rampmff151/
&RAMP ID='RAMP MF',T=15.2,F=rampmff152/
&RAMP ID='RAMP MF',T=15.3,F=rampmff153/
&RAMP ID='RAMP MF',T=15.4,F=rampmff154/
&RAMP ID='RAMP MF',T=15.5,F=rampmff155/
&RAMP ID='RAMP MF',T=15.6,F=rampmff156/
&RAMP ID='RAMP MF',T=15.7,F=rampmff157/
&RAMP ID='RAMP MF',T=15.8,F=rampmff158/
&RAMP ID='RAMP MF',T=15.9,F=rampmff159/
&RAMP ID='RAMP MF',T=16.0,F=rampmff160/
&RAMP ID='RAMP MF',T=16.1,F=rampmff161/
&RAMP ID='RAMP MF',T=16.2,F=rampmff162/
&RAMP ID='RAMP MF',T=16.3,F=rampmff163/
&RAMP ID='RAMP MF',T=16.4,F=rampmff164/
&RAMP ID='RAMP MF',T=16.5,F=rampmff165/
&RAMP ID='RAMP MF',T=16.6,F=rampmff166/
&RAMP ID='RAMP MF',T=16.7,F=rampmff167/
&RAMP ID='RAMP MF',T=16.8,F=rampmff168/
&RAMP ID='RAMP MF',T=16.9,F=rampmff169/
&RAMP ID='RAMP MF',T=17.0,F=rampmff170/
&RAMP ID='RAMP MF',T=17.1,F=rampmff171/
&RAMP ID='RAMP MF',T=17.2,F=rampmff172/
&RAMP ID='RAMP MF',T=17.3,F=rampmff173/
&RAMP ID='RAMP MF',T=17.4,F=rampmff174/
&RAMP ID='RAMP MF',T=17.5,F=rampmff175/
&RAMP ID='RAMP MF',T=17.6,F=rampmff176/
&RAMP ID='RAMP MF',T=17.7,F=rampmff177/
&RAMP ID='RAMP MF',T=17.8,F=rampmff178/
&RAMP ID='RAMP MF',T=17.9,F=rampmff179/
&RAMP ID='RAMP MF',T=18.0,F=rampmff180/
&RAMP ID='RAMP MF',T=18.1,F=rampmff181/
&RAMP ID='RAMP MF',T=18.2,F=rampmff182/
&RAMP ID='RAMP MF',T=18.3,F=rampmff183/
&RAMP ID='RAMP MF',T=18.4,F=rampmff184/
&RAMP ID='RAMP MF',T=18.5,F=rampmff185/
&RAMP ID='RAMP MF',T=18.6,F=rampmff186/
&RAMP ID='RAMP MF',T=18.7,F=rampmff187/
&RAMP ID='RAMP MF',T=18.8,F=rampmff188/
&RAMP ID='RAMP MF',T=18.9,F=rampmff189/
&RAMP ID='RAMP MF',T=19.0,F=rampmff190/
&RAMP ID='RAMP MF',T=19.1,F=rampmff191/
&RAMP ID='RAMP MF',T=19.2,F=rampmff192/
&RAMP ID='RAMP MF',T=19.3,F=rampmff193/
&RAMP ID='RAMP MF',T=19.4,F=rampmff194/
&RAMP ID='RAMP MF',T=19.5,F=rampmff195/
&RAMP ID='RAMP MF',T=19.6,F=rampmff196/
&RAMP ID='RAMP MF',T=19.7,F=rampmff197/
&RAMP ID='RAMP MF',T=19.8,F=rampmff198/
&RAMP ID='RAMP MF',T=19.9,F=rampmff199/
&RAMP ID='RAMP MF',T=20.0,F=rampmff200/
&RAMP ID='RAMP MF',T=20.1,F=0.0000/

! Gas phase specific heats. FDS defaults for N2, O2, H2O, and CO2 replaced to extend
values to higher temperatures than present in FDS

&RAMP ID='AL2O3 C', T=-73, F=0.761/ NASA TP-2002-211556
&RAMP ID='AL2O3 C', T=127, F=0.921/
&RAMP ID='AL2O3 C', T=327, F=0.999/
&RAMP ID='AL2O3 C', T=527, F=1.038/
```

```
&RAMP ID='AL2O3 C', T=727, F=1.058/
&RAMP ID='AL2O3 C', T=1727, F=1.090/
&RAMP ID='AL2O3 C', T=2727, F=1.096/
&RAMP ID='AL2O3 C', T=3727, F=1.098/
&RAMP ID='AL2O3 C', T=4727, F=1.099/
&RAMP ID='AL2O3 C', T=5727, F=1.100/

&RAMP ID='AL C', T=-73, F=0.820/ NASA TP-2002-211556
&RAMP ID='AL C', T=127, F=0.783/
&RAMP ID='AL C', T=327, F=0.776/
&RAMP ID='AL C', T=527, F=0.773/
&RAMP ID='AL C', T=727, F=0.772/
&RAMP ID='AL C', T=1727, F=0.771/
&RAMP ID='AL C', T=2727, F=0.771/
&RAMP ID='AL C', T=3727, F=0.775/
&RAMP ID='AL C', T=4727, F=0.793/
&RAMP ID='AL C', T=5727, F=0.841/
&RAMP ID='AL C', T=6727, F=0.930/
&RAMP ID='AL C', T=7727, F=1.034/
&RAMP ID='AL C', T=8727, F=1.130/
&RAMP ID='AL C', T=9727, F=1.204/
&RAMP ID='AL C', T=10727, F=1.250/
&RAMP ID='AL C', T=11727, F=1.271/
&RAMP ID='AL C', T=12727, F=1.269/
&RAMP ID='AL C', T=13727, F=1.252/
&RAMP ID='AL C', T=14727, F=1.226/
&RAMP ID='AL C', T=15727, F=1.196/
&RAMP ID='AL C', T=16727, F=1.168/
&RAMP ID='AL C', T=17727, F=1.145/
&RAMP ID='AL C', T=18727, F=1.125/
&RAMP ID='AL C', T=19727, F=1.108/

&RAMP ID='CU C', T=-73, F=0.327/ NASA TP-2002-211556
&RAMP ID='CU C', T=127, F=0.327/
&RAMP ID='CU C', T=327, F=0.327/
&RAMP ID='CU C', T=527, F=0.327/
&RAMP ID='CU C', T=727, F=0.327/
&RAMP ID='CU C', T=1727, F=0.337/
&RAMP ID='CU C', T=2727, F=0.396/
&RAMP ID='CU C', T=3727, F=0.471/
&RAMP ID='CU C', T=4727, F=0.517/
&RAMP ID='CU C', T=5727, F=0.537/
&RAMP ID='CU C', T=6727, F=0.551/
&RAMP ID='CU C', T=7727, F=0.577/
&RAMP ID='CU C', T=8727, F=0.606/
&RAMP ID='CU C', T=9727, F=0.633/
&RAMP ID='CU C', T=10727, F=0.653/
&RAMP ID='CU C', T=11727, F=0.663/
&RAMP ID='CU C', T=12727, F=0.664/
&RAMP ID='CU C', T=13727, F=0.657/
&RAMP ID='CU C', T=14727, F=0.642/
&RAMP ID='CU C', T=15727, F=0.622/
&RAMP ID='CU C', T=16727, F=0.599/
&RAMP ID='CU C', T=17727, F=0.574/
&RAMP ID='CU C', T=18727, F=0.550/
&RAMP ID='CU C', T=19727, F=0.528/

&RAMP ID='N2 C', T=-73, F=1.039/ NASA TP-2002-211556
&RAMP ID='N2 C', T=127, F=1.044/
&RAMP ID='N2 C', T=327, F=1.075/
&RAMP ID='N2 C', T=527, F=1.122/
&RAMP ID='N2 C', T=727, F=1.167/
&RAMP ID='N2 C', T=1727, F=1.284/
&RAMP ID='N2 C', T=2727, F=1.322/
```

```
&RAMP ID='N2 C', T=3727, F=1.340/
&RAMP ID='N2 C', T=4727, F=1.354/
&RAMP ID='N2 C', T=5727, F=1.371/
&RAMP ID='N2 C', T=6727, F=1.402/
&RAMP ID='N2 C', T=7727, F=1.454/
&RAMP ID='N2 C', T=8727, F=1.544/
&RAMP ID='N2 C', T=9727, F=1.670/
&RAMP ID='N2 C', T=10727, F=1.822/
&RAMP ID='N2 C', T=11727, F=1.984/
&RAMP ID='N2 C', T=12727, F=2.136/
&RAMP ID='N2 C', T=13727, F=2.261/
&RAMP ID='N2 C', T=14727, F=2.346/
&RAMP ID='N2 C', T=15727, F=2.383/
&RAMP ID='N2 C', T=16727, F=2.372/
&RAMP ID='N2 C', T=17727, F=2.320/
&RAMP ID='N2 C', T=18727, F=2.241/
&RAMP ID='N2 C', T=19727, F=2.159/

&RAMP ID='O2 C', T=-73, F=0.910/ NASA TP-2002-211556
&RAMP ID='O2 C', T=127, F=0.941/
&RAMP ID='O2 C', T=327, F=1.003/
&RAMP ID='O2 C', T=527, F=1.055/
&RAMP ID='O2 C', T=727, F=1.090/
&RAMP ID='O2 C', T=1727, F=1.181/
&RAMP ID='O2 C', T=2727, F=1.249/
&RAMP ID='O2 C', T=3727, F=1.303/
&RAMP ID='O2 C', T=4727, F=1.344/
&RAMP ID='O2 C', T=5727, F=1.373/
&RAMP ID='O2 C', T=6727, F=1.386/
&RAMP ID='O2 C', T=7727, F=1.376/
&RAMP ID='O2 C', T=8727, F=1.344/
&RAMP ID='O2 C', T=9727, F=1.296/
&RAMP ID='O2 C', T=10727, F=1.241/
&RAMP ID='O2 C', T=11727, F=1.184/
&RAMP ID='O2 C', T=12727, F=1.128/
&RAMP ID='O2 C', T=13727, F=1.077/
&RAMP ID='O2 C', T=14727, F=1.030/
&RAMP ID='O2 C', T=15727, F=0.989/
&RAMP ID='O2 C', T=16727, F=0.953/
&RAMP ID='O2 C', T=17727, F=0.922/
&RAMP ID='O2 C', T=18727, F=0.894/
&RAMP ID='O2 C', T=19727, F=0.870/

&RAMP ID='CO2 C', T=-73, F=0.735/ NASA TP-2002-211556
&RAMP ID='CO2 C', T=127, F=0.939/
&RAMP ID='CO2 C', T=327, F=1.075/
&RAMP ID='CO2 C', T=527, F=1.169/
&RAMP ID='CO2 C', T=727, F=1.234/
&RAMP ID='CO2 C', T=1727, F=1.371/
&RAMP ID='CO2 C', T=2727, F=1.412/
&RAMP ID='CO2 C', T=3727, F=1.436/
&RAMP ID='CO2 C', T=4727, F=1.466/
&RAMP ID='CO2 C', T=5727, F=1.517/
&RAMP ID='CO2 C', T=6727, F=1.595/
&RAMP ID='CO2 C', T=7727, F=1.694/
&RAMP ID='CO2 C', T=8727, F=1.797/
&RAMP ID='CO2 C', T=9727, F=1.888/
&RAMP ID='CO2 C', T=10727, F=1.957/
&RAMP ID='CO2 C', T=11727, F=2.000/
&RAMP ID='CO2 C', T=12727, F=2.019/
&RAMP ID='CO2 C', T=13727, F=2.020/
&RAMP ID='CO2 C', T=14727, F=2.007/
&RAMP ID='CO2 C', T=15727, F=1.987/
&RAMP ID='CO2 C', T=16727, F=1.965/
```

```
&RAMP ID='CO2 C', T=17727, F=1.944/
&RAMP ID='CO2 C', T=18727, F=1.924/
&RAMP ID='CO2 C', T=19727, F=1.905/

!Smokeview Outputs. Adjust PBY and PBX for center of arc volume.

alslcf1 QUANTITY='MASS FRACTION',SPEC_ID='ALUMINUM',CELL_CENTERED=.TRUE.,PBY=0.0000/
alslcf2 QUANTITY='MASS FRACTION',SPEC_ID='ALUMINUM
OXIDE',CELL_CENTERED=.TRUE.,PBY=0.0000/
cuslcf1 QUANTITY='MASS FRACTION',SPEC_ID='COPPER',CELL_CENTERED=.TRUE.,PBY=0.0000/
cuslcf2 QUANTITY='MASS FRACTION',SPEC_ID='COPPER
OXIDE',CELL_CENTERED=.TRUE.,PBY=0.0000/
&SLCF QUANTITY='MASS FRACTION',SPEC_ID='OXYGEN',CELL_CENTERED=.TRUE.,PBY=0.0000/
&SLCF QUANTITY='HRRPUV',CELL_CENTERED=.TRUE.,PBY=0.0000/
&SLCF QUANTITY='HRRPUV',CELL_CENTERED=.TRUE.,PBX=slcfpbx/
&SLCF QUANTITY='TEMPERATURE',CELL_CENTERED=.TRUE.,PBY=0.0000/
&SLCF QUANTITY='TEMPERATURE',CELL_CENTERED=.TRUE.,PBX=slcfpbx/
&SLCF QUANTITY='INTEGRATED INTENSITY',CELL_CENTERED=.TRUE.,PBY=0.0000/
&SLCF QUANTITY='INTEGRATED INTENSITY',CELL_CENTERED=.TRUE.,PBX=slcfpbx/
&SLCF QUANTITY='VELOCITY',CELL_CENTERED=.TRUE.,PBY=0.0000/
&SLCF QUANTITY='U-VELOCITY',CELL_CENTERED=.TRUE.,PBY=0.0000/
&SLCF QUANTITY='VELOCITY',CELL_CENTERED=.TRUE.,PBX=slcfpbx/
&SLCF QUANTITY='V-VELOCITY',CELL_CENTERED=.TRUE.,PBX=slcfpbx/
&SLCF QUANTITY='PRESSURE',CELL_CENTERED=.TRUE.,PBY=0.0000/

&BNDF QUANTITY='WALL TEMPERATURE',CELL_CENTERED=.TRUE./
&BNDF QUANTITY='GAUGE HEAT FLUX',CELL_CENTERED=.TRUE./
&BNDF QUANTITY='WALL THICKNESS',CELL_CENTERED=.TRUE./
&BNDF QUANTITY='VELOCITY ERROR',CELL_CENTERED=.TRUE./

!Example DEVC for ZOI runs. Have planes of devices at a range of distances that look
at each face of the enclosure
!Plane should be large enough to see any permanent venting, plus any area heated by or
damaged by the arc, plus any bouyancy impacts
!Here the DEVC ID my means this is on the (m)inus (y) face at the given x,y,z location
!The orientation is the unit vector given by Arc Center - DEVC XYZ.  Pointing the DEVC
at the arc centroid will approximate the worst case view factor
!for the radiative component.
!These can easily be generated with Excel using CONCATENATE()


&DEVC XB=-4.1800,-4.1800,-0.1800,-0.1800,-2.7000,-
0.3000,POINTS=31,ORIENTATION=0,0,1,ID='BL x:-4.18 y:-0.18',QUANTITY='GAUGE HEAT FLUX
GAS',STATISTICS_START=0,TEMPORAL_STATISTIC='TIME INTEGRAL'/
&DEVC XB=-4.1800,-4.1800,-0.1000,-0.1000,-2.7000,-
0.3000,POINTS=31,ORIENTATION=0,0,1,ID='BL x:-4.18 y:-0.10',QUANTITY='GAUGE HEAT FLUX
GAS',STATISTICS_START=0,TEMPORAL_STATISTIC='TIME INTEGRAL'/
&DEVC XB=-4.1800,-4.1800,-0.0200,-0.0200,-2.7000,-
0.3000,POINTS=31,ORIENTATION=0,0,1,ID='BL x:-4.18 y:-0.02',QUANTITY='GAUGE HEAT FLUX
GAS',STATISTICS_START=0,TEMPORAL_STATISTIC='TIME INTEGRAL'/
&DEVC XB=-4.1800,-4.1800,0.0200,0.0200,-2.7000,-
0.3000,POINTS=31,ORIENTATION=0,0,1,ID='BL x:-4.18 y:0.02',QUANTITY='GAUGE HEAT FLUX
GAS',STATISTICS_START=0,TEMPORAL_STATISTIC='TIME INTEGRAL'/
&DEVC XB=-4.1800,-4.1800,0.1000,0.1000,-2.7000,-
0.3000,POINTS=31,ORIENTATION=0,0,1,ID='BL x:-4.18 y:0.10',QUANTITY='GAUGE HEAT FLUX
GAS',STATISTICS_START=0,TEMPORAL_STATISTIC='TIME INTEGRAL'/
&DEVC XB=-4.1800,-4.1800,0.1800,0.1800,-2.7000,-
0.3000,POINTS=31,ORIENTATION=0,0,1,ID='BL x:-4.18 y:0.18',QUANTITY='GAUGE HEAT FLUX
GAS',STATISTICS_START=0,TEMPORAL_STATISTIC='TIME INTEGRAL'/
&DEVC XB=-4.1000,-4.1000,-0.1800,-0.1800,-2.7000,-
0.3000,POINTS=31,ORIENTATION=0,0,1,ID='BL x:-4.10 y:-0.18',QUANTITY='GAUGE HEAT FLUX
GAS',STATISTICS_START=0,TEMPORAL_STATISTIC='TIME INTEGRAL'/
```

```
&DEVC XB=-4.1000,-4.1000,-0.1000,-0.1000,-2.7000,-
0.3000,POINTS=31,ORIENTATION=0,0,1,ID='BL x:-4.10 y:-0.10',QUANTITY='GAUGE HEAT FLUX
GAS',STATISTICS_START=0,TEMPORAL_STATISTIC='TIME INTEGRAL'/
&DEVC XB=-4.1000,-4.1000,-0.0200,-0.0200,-2.7000,-
0.3000,POINTS=31,ORIENTATION=0,0,1,ID='BL x:-4.10 y:-0.02',QUANTITY='GAUGE HEAT FLUX
GAS',STATISTICS_START=0,TEMPORAL_STATISTIC='TIME INTEGRAL'/
&DEVC XB=-4.1000,-4.1000,0.0200,0.0200,-2.7000,-
0.3000,POINTS=31,ORIENTATION=0,0,1,ID='BL x:-4.10 y:0.02',QUANTITY='GAUGE HEAT FLUX
GAS',STATISTICS_START=0,TEMPORAL_STATISTIC='TIME INTEGRAL'/
&DEVC XB=-4.1000,-4.1000,0.1000,0.1000,-2.7000,-
0.3000,POINTS=31,ORIENTATION=0,0,1,ID='BL x:-4.10 y:0.10',QUANTITY='GAUGE HEAT FLUX
GAS',STATISTICS_START=0,TEMPORAL_STATISTIC='TIME INTEGRAL'/
&DEVC XB=-4.1000,-4.1000,0.1800,0.1800,-2.7000,-
0.3000,POINTS=31,ORIENTATION=0,0,1,ID='BL x:-4.10 y:0.18',QUANTITY='GAUGE HEAT FLUX
GAS',STATISTICS_START=0,TEMPORAL_STATISTIC='TIME INTEGRAL'/
&DEVC XB=-4.0200,-4.0200,-0.1800,-0.1800,-2.7000,-
0.3000,POINTS=31,ORIENTATION=0,0,1,ID='BL x:-4.02 y:-0.18',QUANTITY='GAUGE HEAT FLUX
GAS',STATISTICS_START=0,TEMPORAL_STATISTIC='TIME INTEGRAL'/
&DEVC XB=-4.0200,-4.0200,-0.1000,-0.1000,-2.7000,-
0.3000,POINTS=31,ORIENTATION=0,0,1,ID='BL x:-4.02 y:-0.10',QUANTITY='GAUGE HEAT FLUX
GAS',STATISTICS_START=0,TEMPORAL_STATISTIC='TIME INTEGRAL'/
&DEVC XB=-4.0200,-4.0200,-0.0200,-0.0200,-2.7000,-
0.3000,POINTS=31,ORIENTATION=0,0,1,ID='BL x:-4.02 y:-0.02',QUANTITY='GAUGE HEAT FLUX
GAS',STATISTICS_START=0,TEMPORAL_STATISTIC='TIME INTEGRAL'/
&DEVC XB=-4.0200,-4.0200,0.0200,0.0200,-2.7000,-
0.3000,POINTS=31,ORIENTATION=0,0,1,ID='BL x:-4.02 y:0.02',QUANTITY='GAUGE HEAT FLUX
GAS',STATISTICS_START=0,TEMPORAL_STATISTIC='TIME INTEGRAL'/
&DEVC XB=-4.0200,-4.0200,0.1000,0.1000,-2.7000,-
0.3000,POINTS=31,ORIENTATION=0,0,1,ID='BL x:-4.02 y:0.10',QUANTITY='GAUGE HEAT FLUX
GAS',STATISTICS_START=0,TEMPORAL_STATISTIC='TIME INTEGRAL'/
&DEVC XB=-4.0200,-4.0200,0.1800,0.1800,-2.7000,-
0.3000,POINTS=31,ORIENTATION=0,0,1,ID='BL x:-4.02 y:0.18',QUANTITY='GAUGE HEAT FLUX
GAS',STATISTICS_START=0,TEMPORAL_STATISTIC='TIME INTEGRAL'/
&DEVC XB=-3.9800,-3.9800,-0.1800,-0.1800,-2.7000,-
0.3000,POINTS=31,ORIENTATION=0,0,1,ID='BL x:-3.98 y:-0.18',QUANTITY='GAUGE HEAT FLUX
GAS',STATISTICS_START=0,TEMPORAL_STATISTIC='TIME INTEGRAL'/
&DEVC XB=-3.9800,-3.9800,-0.1000,-0.1000,-2.7000,-
0.3000,POINTS=31,ORIENTATION=0,0,1,ID='BL x:-3.98 y:-0.10',QUANTITY='GAUGE HEAT FLUX
GAS',STATISTICS_START=0,TEMPORAL_STATISTIC='TIME INTEGRAL'/
&DEVC XB=-3.9800,-3.9800,-0.0200,-0.0200,-2.7000,-
0.3000,POINTS=31,ORIENTATION=0,0,1,ID='BL x:-3.98 y:-0.02',QUANTITY='GAUGE HEAT FLUX
GAS',STATISTICS_START=0,TEMPORAL_STATISTIC='TIME INTEGRAL'/
&DEVC XB=-3.9800,-3.9800,0.0200,0.0200,-2.7000,-
0.3000,POINTS=31,ORIENTATION=0,0,1,ID='BL x:-3.98 y:0.02',QUANTITY='GAUGE HEAT FLUX
GAS',STATISTICS_START=0,TEMPORAL_STATISTIC='TIME INTEGRAL'/
&DEVC XB=-3.9800,-3.9800,0.1000,0.1000,-2.7000,-
0.3000,POINTS=31,ORIENTATION=0,0,1,ID='BL x:-3.98 y:0.10',QUANTITY='GAUGE HEAT FLUX
GAS',STATISTICS_START=0,TEMPORAL_STATISTIC='TIME INTEGRAL'/
&DEVC XB=-3.9800,-3.9800,0.1800,0.1800,-2.7000,-
0.3000,POINTS=31,ORIENTATION=0,0,1,ID='BL x:-3.98 y:0.18',QUANTITY='GAUGE HEAT FLUX
GAS',STATISTICS_START=0,TEMPORAL_STATISTIC='TIME INTEGRAL'/
&DEVC XB=-3.9000,-3.9000,-0.1800,-0.1800,-2.7000,-
0.3000,POINTS=31,ORIENTATION=0,0,1,ID='BL x:-3.90 y:-0.18',QUANTITY='GAUGE HEAT FLUX
GAS',STATISTICS_START=0,TEMPORAL_STATISTIC='TIME INTEGRAL'/
&DEVC XB=-3.9000,-3.9000,-0.1000,-0.1000,-2.7000,-
0.3000,POINTS=31,ORIENTATION=0,0,1,ID='BL x:-3.90 y:-0.10',QUANTITY='GAUGE HEAT FLUX
GAS',STATISTICS_START=0,TEMPORAL_STATISTIC='TIME INTEGRAL'/
&DEVC XB=-3.9000,-3.9000,-0.0200,-0.0200,-2.7000,-
0.3000,POINTS=31,ORIENTATION=0,0,1,ID='BL x:-3.90 y:-0.02',QUANTITY='GAUGE HEAT FLUX
GAS',STATISTICS_START=0,TEMPORAL_STATISTIC='TIME INTEGRAL'/
&DEVC XB=-3.9000,-3.9000,0.0200,0.0200,-2.7000,-
0.3000,POINTS=31,ORIENTATION=0,0,1,ID='BL x:-3.90 y:0.02',QUANTITY='GAUGE HEAT FLUX
GAS',STATISTICS_START=0,TEMPORAL_STATISTIC='TIME INTEGRAL'/
```

```
&DEVC XB=-3.9000,-3.9000,0.1000,0.1000,-2.7000,-
0.3000,POINTS=31,ORIENTATION=0,0,1,ID='BL x:-3.90 y:0.10',QUANTITY='GAUGE HEAT FLUX
GAS',STATISTICS_START=0,TEMPORAL_STATISTIC='TIME INTEGRAL'/
&DEVC XB=-3.9000,-3.9000,0.1800,0.1800,-2.7000,-
0.3000,POINTS=31,ORIENTATION=0,0,1,ID='BL x:-3.90 y:0.18',QUANTITY='GAUGE HEAT FLUX
GAS',STATISTICS_START=0,TEMPORAL_STATISTIC='TIME INTEGRAL'/
&DEVC XB=-3.8200,-3.8200,-0.1800,-0.1800,-2.7000,-
0.3000,POINTS=31,ORIENTATION=0,0,1,ID='BL x:-3.82 y:-0.18',QUANTITY='GAUGE HEAT FLUX
GAS',STATISTICS_START=0,TEMPORAL_STATISTIC='TIME INTEGRAL'/
&DEVC XB=-3.8200,-3.8200,-0.1000,-0.1000,-2.7000,-
0.3000,POINTS=31,ORIENTATION=0,0,1,ID='BL x:-3.82 y:-0.10',QUANTITY='GAUGE HEAT FLUX
GAS',STATISTICS_START=0,TEMPORAL_STATISTIC='TIME INTEGRAL'/
&DEVC XB=-3.8200,-3.8200,-0.0200,-0.0200,-2.7000,-
0.3000,POINTS=31,ORIENTATION=0,0,1,ID='BL x:-3.82 y:-0.02',QUANTITY='GAUGE HEAT FLUX
GAS',STATISTICS_START=0,TEMPORAL_STATISTIC='TIME INTEGRAL'/
&DEVC XB=-3.8200,-3.8200,0.0200,0.0200,-2.7000,-
0.3000,POINTS=31,ORIENTATION=0,0,1,ID='BL x:-3.82 y:0.02',QUANTITY='GAUGE HEAT FLUX
GAS',STATISTICS_START=0,TEMPORAL_STATISTIC='TIME INTEGRAL'/
&DEVC XB=-3.8200,-3.8200,0.1000,0.1000,-2.7000,-
0.3000,POINTS=31,ORIENTATION=0,0,1,ID='BL x:-3.82 y:0.10',QUANTITY='GAUGE HEAT FLUX
GAS',STATISTICS_START=0,TEMPORAL_STATISTIC='TIME INTEGRAL'/
&DEVC XB=-3.8200,-3.8200,0.1800,0.1800,-2.7000,-
0.3000,POINTS=31,ORIENTATION=0,0,1,ID='BL x:-3.82 y:0.18',QUANTITY='GAUGE HEAT FLUX
GAS',STATISTICS_START=0,TEMPORAL_STATISTIC='TIME INTEGRAL'/


&DEVC XB=-4.1800,-4.1800,-0.1800,-0.1800,0.7800,2.9400,POINTS=28,ORIENTATION=0,0,-
1,ID='AB x:-4.18 y:-0.18',QUANTITY='GAUGE HEAT FLUX
GAS',STATISTICS_START=0,TEMPORAL_STATISTIC='TIME INTEGRAL'/
&DEVC XB=-4.1800,-4.1800,-0.1000,-0.1000,0.7800,2.9400,POINTS=28,ORIENTATION=0,0,-
1,ID='AB x:-4.18 y:-0.10',QUANTITY='GAUGE HEAT FLUX
GAS',STATISTICS_START=0,TEMPORAL_STATISTIC='TIME INTEGRAL'/
&DEVC XB=-4.1800,-4.1800,-0.0200,-0.0200,0.7800,2.9400,POINTS=28,ORIENTATION=0,0,-
1,ID='AB x:-4.18 y:-0.02',QUANTITY='GAUGE HEAT FLUX
GAS',STATISTICS_START=0,TEMPORAL_STATISTIC='TIME INTEGRAL'/
&DEVC XB=-4.1800,-4.1800,0.0200,0.0200,0.7800,2.9400,POINTS=28,ORIENTATION=0,0,-
1,ID='AB x:-4.18 y:0.02',QUANTITY='GAUGE HEAT FLUX
GAS',STATISTICS_START=0,TEMPORAL_STATISTIC='TIME INTEGRAL'/
&DEVC XB=-4.1800,-4.1800,0.1000,0.1000,0.7800,2.9400,POINTS=28,ORIENTATION=0,0,-
1,ID='AB x:-4.18 y:0.10',QUANTITY='GAUGE HEAT FLUX
GAS',STATISTICS_START=0,TEMPORAL_STATISTIC='TIME INTEGRAL'/
&DEVC XB=-4.1800,-4.1800,0.1800,0.1800,0.7800,2.9400,POINTS=28,ORIENTATION=0,0,-
1,ID='AB x:-4.18 y:0.18',QUANTITY='GAUGE HEAT FLUX
GAS',STATISTICS_START=0,TEMPORAL_STATISTIC='TIME INTEGRAL'/
&DEVC XB=-4.1000,-4.1000,-0.1800,-0.1800,0.7800,2.9400,POINTS=28,ORIENTATION=0,0,-
1,ID='AB x:-4.10 y:-0.18',QUANTITY='GAUGE HEAT FLUX
GAS',STATISTICS_START=0,TEMPORAL_STATISTIC='TIME INTEGRAL'/
&DEVC XB=-4.1000,-4.1000,-0.1000,-0.1000,0.7800,2.9400,POINTS=28,ORIENTATION=0,0,-
1,ID='AB x:-4.10 y:-0.10',QUANTITY='GAUGE HEAT FLUX
GAS',STATISTICS_START=0,TEMPORAL_STATISTIC='TIME INTEGRAL'/
&DEVC XB=-4.1000,-4.1000,-0.0200,-0.0200,0.7800,2.9400,POINTS=28,ORIENTATION=0,0,-
1,ID='AB x:-4.10 y:-0.02',QUANTITY='GAUGE HEAT FLUX
GAS',STATISTICS_START=0,TEMPORAL_STATISTIC='TIME INTEGRAL'/
&DEVC XB=-4.1000,-4.1000,0.0200,0.0200,0.7800,2.9400,POINTS=28,ORIENTATION=0,0,-
1,ID='AB x:-4.10 y:0.02',QUANTITY='GAUGE HEAT FLUX
GAS',STATISTICS_START=0,TEMPORAL_STATISTIC='TIME INTEGRAL'/
&DEVC XB=-4.1000,-4.1000,0.1000,0.1000,0.7800,2.9400,POINTS=28,ORIENTATION=0,0,-
1,ID='AB x:-4.10 y:0.10',QUANTITY='GAUGE HEAT FLUX
GAS',STATISTICS_START=0,TEMPORAL_STATISTIC='TIME INTEGRAL'/
&DEVC XB=-4.1000,-4.1000,0.1800,0.1800,0.7800,2.9400,POINTS=28,ORIENTATION=0,0,-
1,ID='AB x:-4.10 y:0.18',QUANTITY='GAUGE HEAT FLUX
GAS',STATISTICS_START=0,TEMPORAL_STATISTIC='TIME INTEGRAL'/
```

```
&DEVC XB=-4.0200,-4.0200,-0.1800,-0.1800,0.7800,2.9400,POINTS=28,ORIENTATION=0,0,-
1,ID='AB x:-4.02 y:-0.18',QUANTITY='GAUGE HEAT FLUX
GAS',STATISTICS_START=0,TEMPORAL_STATISTIC='TIME INTEGRAL'/
&DEVC XB=-4.0200,-4.0200,-0.1000,-0.1000,0.7800,2.9400,POINTS=28,ORIENTATION=0,0,-
1,ID='AB x:-4.02 y:-0.10',QUANTITY='GAUGE HEAT FLUX
GAS',STATISTICS_START=0,TEMPORAL_STATISTIC='TIME INTEGRAL'/
&DEVC XB=-4.0200,-4.0200,-0.0200,-0.0200,0.7800,2.9400,POINTS=28,ORIENTATION=0,0,-
1,ID='AB x:-4.02 y:-0.02',QUANTITY='GAUGE HEAT FLUX
GAS',STATISTICS_START=0,TEMPORAL_STATISTIC='TIME INTEGRAL'/
&DEVC XB=-4.0200,-4.0200,0.0200,0.0200,0.7800,2.9400,POINTS=28,ORIENTATION=0,0,-
1,ID='AB x:-4.02 y:0.02',QUANTITY='GAUGE HEAT FLUX
GAS',STATISTICS_START=0,TEMPORAL_STATISTIC='TIME INTEGRAL'/
&DEVC XB=-4.0200,-4.0200,0.1000,0.1000,0.7800,2.9400,POINTS=28,ORIENTATION=0,0,-
1,ID='AB x:-4.02 y:0.10',QUANTITY='GAUGE HEAT FLUX
GAS',STATISTICS_START=0,TEMPORAL_STATISTIC='TIME INTEGRAL'/
&DEVC XB=-4.0200,-4.0200,0.1800,0.1800,0.7800,2.9400,POINTS=28,ORIENTATION=0,0,-
1,ID='AB x:-4.02 y:0.18',QUANTITY='GAUGE HEAT FLUX
GAS',STATISTICS_START=0,TEMPORAL_STATISTIC='TIME INTEGRAL'/
&DEVC XB=-3.9800,-3.9800,-0.1800,-0.1800,0.7800,2.9400,POINTS=28,ORIENTATION=0,0,-
1,ID='AB x:-3.98 y:-0.18',QUANTITY='GAUGE HEAT FLUX
GAS',STATISTICS_START=0,TEMPORAL_STATISTIC='TIME INTEGRAL'/
&DEVC XB=-3.9800,-3.9800,-0.1000,-0.1000,0.7800,2.9400,POINTS=28,ORIENTATION=0,0,-
1,ID='AB x:-3.98 y:-0.10',QUANTITY='GAUGE HEAT FLUX
GAS',STATISTICS_START=0,TEMPORAL_STATISTIC='TIME INTEGRAL'/
&DEVC XB=-3.9800,-3.9800,-0.0200,-0.0200,0.7800,2.9400,POINTS=28,ORIENTATION=0,0,-
1,ID='AB x:-3.98 y:-0.02',QUANTITY='GAUGE HEAT FLUX
GAS',STATISTICS_START=0,TEMPORAL_STATISTIC='TIME INTEGRAL'/
&DEVC XB=-3.9800,-3.9800,0.0200,0.0200,0.7800,2.9400,POINTS=28,ORIENTATION=0,0,-
1,ID='AB x:-3.98 y:0.02',QUANTITY='GAUGE HEAT FLUX
GAS',STATISTICS_START=0,TEMPORAL_STATISTIC='TIME INTEGRAL'/
&DEVC XB=-3.9800,-3.9800,0.1000,0.1000,0.7800,2.9400,POINTS=28,ORIENTATION=0,0,-
1,ID='AB x:-3.98 y:0.10',QUANTITY='GAUGE HEAT FLUX
GAS',STATISTICS_START=0,TEMPORAL_STATISTIC='TIME INTEGRAL'/
&DEVC XB=-3.9800,-3.9800,0.1800,0.1800,0.7800,2.9400,POINTS=28,ORIENTATION=0,0,-
1,ID='AB x:-3.98 y:0.18',QUANTITY='GAUGE HEAT FLUX
GAS',STATISTICS_START=0,TEMPORAL_STATISTIC='TIME INTEGRAL'/
&DEVC XB=-3.9000,-3.9000,-0.1800,-0.1800,0.7800,2.9400,POINTS=28,ORIENTATION=0,0,-
1,ID='AB x:-3.90 y:-0.18',QUANTITY='GAUGE HEAT FLUX
GAS',STATISTICS_START=0,TEMPORAL_STATISTIC='TIME INTEGRAL'/
&DEVC XB=-3.9000,-3.9000,-0.1000,-0.1000,0.7800,2.9400,POINTS=28,ORIENTATION=0,0,-
1,ID='AB x:-3.90 y:-0.10',QUANTITY='GAUGE HEAT FLUX
GAS',STATISTICS_START=0,TEMPORAL_STATISTIC='TIME INTEGRAL'/
&DEVC XB=-3.9000,-3.9000,-0.0200,-0.0200,0.7800,2.9400,POINTS=28,ORIENTATION=0,0,-
1,ID='AB x:-3.90 y:-0.02',QUANTITY='GAUGE HEAT FLUX
GAS',STATISTICS_START=0,TEMPORAL_STATISTIC='TIME INTEGRAL'/
&DEVC XB=-3.9000,-3.9000,0.0200,0.0200,0.7800,2.9400,POINTS=28,ORIENTATION=0,0,-
1,ID='AB x:-3.90 y:0.02',QUANTITY='GAUGE HEAT FLUX
GAS',STATISTICS_START=0,TEMPORAL_STATISTIC='TIME INTEGRAL'/
&DEVC XB=-3.9000,-3.9000,0.1000,0.1000,0.7800,2.9400,POINTS=28,ORIENTATION=0,0,-
1,ID='AB x:-3.90 y:0.10',QUANTITY='GAUGE HEAT FLUX
GAS',STATISTICS_START=0,TEMPORAL_STATISTIC='TIME INTEGRAL'/
&DEVC XB=-3.9000,-3.9000,0.1800,0.1800,0.7800,2.9400,POINTS=28,ORIENTATION=0,0,-
1,ID='AB x:-3.90 y:0.18',QUANTITY='GAUGE HEAT FLUX
GAS',STATISTICS_START=0,TEMPORAL_STATISTIC='TIME INTEGRAL'/
&DEVC XB=-3.8200,-3.8200,-0.1800,-0.1800,0.7800,2.9400,POINTS=28,ORIENTATION=0,0,-
1,ID='AB x:-3.82 y:-0.18',QUANTITY='GAUGE HEAT FLUX
GAS',STATISTICS_START=0,TEMPORAL_STATISTIC='TIME INTEGRAL'/
&DEVC XB=-3.8200,-3.8200,-0.1000,-0.1000,0.7800,2.9400,POINTS=28,ORIENTATION=0,0,-
1,ID='AB x:-3.82 y:-0.10',QUANTITY='GAUGE HEAT FLUX
GAS',STATISTICS_START=0,TEMPORAL_STATISTIC='TIME INTEGRAL'/
&DEVC XB=-3.8200,-3.8200,-0.0200,-0.0200,0.7800,2.9400,POINTS=28,ORIENTATION=0,0,-
1,ID='AB x:-3.82 y:-0.02',QUANTITY='GAUGE HEAT FLUX
GAS',STATISTICS_START=0,TEMPORAL_STATISTIC='TIME INTEGRAL'/
```

```
&DEVC XB=-3.8200,-3.8200,0.0200,0.0200,0.7800,2.9400,POINTS=28,ORIENTATION=0,0,-
1,ID='AB x:-3.82 y:0.02',QUANTITY='GAUGE HEAT FLUX
GAS',STATISTICS_START=0,TEMPORAL_STATISTIC='TIME INTEGRAL'/
&DEVC XB=-3.8200,-3.8200,0.1000,0.1000,0.7800,2.9400,POINTS=28,ORIENTATION=0,0,-
1,ID='AB x:-3.82 y:0.10',QUANTITY='GAUGE HEAT FLUX
GAS',STATISTICS_START=0,TEMPORAL_STATISTIC='TIME INTEGRAL'/
&DEVC XB=-3.8200,-3.8200,0.1800,0.1800,0.7800,2.9400,POINTS=28,ORIENTATION=0,0,-
1,ID='AB x:-3.82 y:0.18',QUANTITY='GAUGE HEAT FLUX
GAS',STATISTICS_START=0,TEMPORAL_STATISTIC='TIME INTEGRAL'/


&DEVC XB=-4.1800,-4.1800,-2.7800,-0.3800,-0.1800,-
0.1800,POINTS=31,ORIENTATION=0,1,0,ID='FL x:-4.18 z:-0.18',QUANTITY='GAUGE HEAT FLUX
GAS',STATISTICS_START=0,TEMPORAL_STATISTIC='TIME INTEGRAL'/
&DEVC XB=-4.1800,-4.1800,-2.7800,-0.3800,-0.1000,-
0.1000,POINTS=31,ORIENTATION=0,1,0,ID='FL x:-4.18 z:-0.10',QUANTITY='GAUGE HEAT FLUX
GAS',STATISTICS_START=0,TEMPORAL_STATISTIC='TIME INTEGRAL'/
&DEVC XB=-4.1800,-4.1800,-2.7800,-0.3800,-0.0200,-
0.0200,POINTS=31,ORIENTATION=0,1,0,ID='FL x:-4.18 z:-0.02',QUANTITY='GAUGE HEAT FLUX
GAS',STATISTICS_START=0,TEMPORAL_STATISTIC='TIME INTEGRAL'/
&DEVC XB=-4.1800,-4.1800,-2.7800,-
0.3800,0.0200,0.0200,POINTS=31,ORIENTATION=0,1,0,ID='FL x:-4.18
z:0.02',QUANTITY='GAUGE HEAT FLUX GAS',STATISTICS_START=0,TEMPORAL_STATISTIC='TIME
INTEGRAL'/
&DEVC XB=-4.1800,-4.1800,-2.7800,-
0.3800,0.1000,0.1000,POINTS=31,ORIENTATION=0,1,0,ID='FL x:-4.18
z:0.10',QUANTITY='GAUGE HEAT FLUX GAS',STATISTICS_START=0,TEMPORAL_STATISTIC='TIME
INTEGRAL'/
&DEVC XB=-4.1800,-4.1800,-2.7800,-
0.3800,0.1800,0.1800,POINTS=31,ORIENTATION=0,1,0,ID='FL x:-4.18
z:0.18',QUANTITY='GAUGE HEAT FLUX GAS',STATISTICS_START=0,TEMPORAL_STATISTIC='TIME
INTEGRAL'/
&DEVC XB=-4.1000,-4.1000,-2.7800,-0.3800,-0.1800,-
0.1800,POINTS=31,ORIENTATION=0,1,0,ID='FL x:-4.10 z:-0.18',QUANTITY='GAUGE HEAT FLUX
GAS',STATISTICS_START=0,TEMPORAL_STATISTIC='TIME INTEGRAL'/
&DEVC XB=-4.1000,-4.1000,-2.7800,-0.3800,-0.1000,-
0.1000,POINTS=31,ORIENTATION=0,1,0,ID='FL x:-4.10 z:-0.10',QUANTITY='GAUGE HEAT FLUX
GAS',STATISTICS_START=0,TEMPORAL_STATISTIC='TIME INTEGRAL'/
&DEVC XB=-4.1000,-4.1000,-2.7800,-0.3800,-0.0200,-
0.0200,POINTS=31,ORIENTATION=0,1,0,ID='FL x:-4.10 z:-0.02',QUANTITY='GAUGE HEAT FLUX
GAS',STATISTICS_START=0,TEMPORAL_STATISTIC='TIME INTEGRAL'/
&DEVC XB=-4.1000,-4.1000,-2.7800,-
0.3800,0.0200,0.0200,POINTS=31,ORIENTATION=0,1,0,ID='FL x:-4.10
z:0.02',QUANTITY='GAUGE HEAT FLUX GAS',STATISTICS_START=0,TEMPORAL_STATISTIC='TIME
INTEGRAL'/
&DEVC XB=-4.1000,-4.1000,-2.7800,-
0.3800,0.1000,0.1000,POINTS=31,ORIENTATION=0,1,0,ID='FL x:-4.10
z:0.10',QUANTITY='GAUGE HEAT FLUX GAS',STATISTICS_START=0,TEMPORAL_STATISTIC='TIME
INTEGRAL'/
&DEVC XB=-4.1000,-4.1000,-2.7800,-
0.3800,0.1800,0.1800,POINTS=31,ORIENTATION=0,1,0,ID='FL x:-4.10
z:0.18',QUANTITY='GAUGE HEAT FLUX GAS',STATISTICS_START=0,TEMPORAL_STATISTIC='TIME
INTEGRAL'/
&DEVC XB=-4.0200,-4.0200,-2.7800,-0.3800,-0.1800,-
0.1800,POINTS=31,ORIENTATION=0,1,0,ID='FL x:-4.02 z:-0.18',QUANTITY='GAUGE HEAT FLUX
GAS',STATISTICS_START=0,TEMPORAL_STATISTIC='TIME INTEGRAL'/
&DEVC XB=-4.0200,-4.0200,-2.7800,-0.3800,-0.1000,-
0.1000,POINTS=31,ORIENTATION=0,1,0,ID='FL x:-4.02 z:-0.10',QUANTITY='GAUGE HEAT FLUX
GAS',STATISTICS_START=0,TEMPORAL_STATISTIC='TIME INTEGRAL'/
&DEVC XB=-4.0200,-4.0200,-2.7800,-0.3800,-0.0200,-
0.0200,POINTS=31,ORIENTATION=0,1,0,ID='FL x:-4.02 z:-0.02',QUANTITY='GAUGE HEAT FLUX
GAS',STATISTICS_START=0,TEMPORAL_STATISTIC='TIME INTEGRAL'/
&DEVC XB=-4.0200,-4.0200,-2.7800,-
0.3800,0.0200,0.0200,POINTS=31,ORIENTATION=0,1,0,ID='FL x:-4.02
```

```
z:0.02',QUANTITY='GAUGE HEAT FLUX GAS',STATISTICS_START=0,TEMPORAL_STATISTIC='TIME
INTEGRAL'/
&DEVC XB=-4.0200,-4.0200,-2.7800,-
0.3800,0.1000,0.1000,POINTS=31,ORIENTATION=0,1,0,ID='FL x:-4.02
z:0.10',QUANTITY='GAUGE HEAT FLUX GAS',STATISTICS_START=0,TEMPORAL_STATISTIC='TIME
INTEGRAL'/
&DEVC XB=-4.0200,-4.0200,-2.7800,-
0.3800,0.1800,0.1800,POINTS=31,ORIENTATION=0,1,0,ID='FL x:-4.02
z:0.18',QUANTITY='GAUGE HEAT FLUX GAS',STATISTICS_START=0,TEMPORAL_STATISTIC='TIME
INTEGRAL'/
&DEVC XB=-3.9800,-3.9800,-2.7800,-0.3800,-0.1800,-
0.1800,POINTS=31,ORIENTATION=0,1,0,ID='FL x:-3.98 z:-0.18',QUANTITY='GAUGE HEAT FLUX
GAS',STATISTICS_START=0,TEMPORAL_STATISTIC='TIME INTEGRAL'/
&DEVC XB=-3.9800,-3.9800,-2.7800,-0.3800,-0.1000,-
0.1000,POINTS=31,ORIENTATION=0,1,0,ID='FL x:-3.98 z:-0.10',QUANTITY='GAUGE HEAT FLUX
GAS',STATISTICS_START=0,TEMPORAL_STATISTIC='TIME INTEGRAL'/
&DEVC XB=-3.9800,-3.9800,-2.7800,-0.3800,-0.0200,-
0.0200,POINTS=31,ORIENTATION=0,1,0,ID='FL x:-3.98 z:-0.02',QUANTITY='GAUGE HEAT FLUX
GAS',STATISTICS_START=0,TEMPORAL_STATISTIC='TIME INTEGRAL'/
&DEVC XB=-3.9800,-3.9800,-2.7800,-
0.3800,0.0200,0.0200,POINTS=31,ORIENTATION=0,1,0,ID='FL x:-3.98
z:0.02',QUANTITY='GAUGE HEAT FLUX GAS',STATISTICS_START=0,TEMPORAL_STATISTIC='TIME
INTEGRAL'/
&DEVC XB=-3.9800,-3.9800,-2.7800,-
0.3800,0.1000,0.1000,POINTS=31,ORIENTATION=0,1,0,ID='FL x:-3.98
z:0.10',QUANTITY='GAUGE HEAT FLUX GAS',STATISTICS_START=0,TEMPORAL_STATISTIC='TIME
INTEGRAL'/
&DEVC XB=-3.9800,-3.9800,-2.7800,-
0.3800,0.1800,0.1800,POINTS=31,ORIENTATION=0,1,0,ID='FL x:-3.98
z:0.18',QUANTITY='GAUGE HEAT FLUX GAS',STATISTICS_START=0,TEMPORAL_STATISTIC='TIME
INTEGRAL'/
&DEVC XB=-3.9000,-3.9000,-2.7800,-0.3800,-0.1800,-
0.1800,POINTS=31,ORIENTATION=0,1,0,ID='FL x:-3.90 z:-0.18',QUANTITY='GAUGE HEAT FLUX
GAS',STATISTICS_START=0,TEMPORAL_STATISTIC='TIME INTEGRAL'/
&DEVC XB=-3.9000,-3.9000,-2.7800,-0.3800,-0.1000,-
0.1000,POINTS=31,ORIENTATION=0,1,0,ID='FL x:-3.90 z:-0.10',QUANTITY='GAUGE HEAT FLUX
GAS',STATISTICS_START=0,TEMPORAL_STATISTIC='TIME INTEGRAL'/
&DEVC XB=-3.9000,-3.9000,-2.7800,-0.3800,-0.0200,-
0.0200,POINTS=31,ORIENTATION=0,1,0,ID='FL x:-3.90 z:-0.02',QUANTITY='GAUGE HEAT FLUX
GAS',STATISTICS_START=0,TEMPORAL_STATISTIC='TIME INTEGRAL'/
&DEVC XB=-3.9000,-3.9000,-2.7800,-
0.3800,0.0200,0.0200,POINTS=31,ORIENTATION=0,1,0,ID='FL x:-3.90
z:0.02',QUANTITY='GAUGE HEAT FLUX GAS',STATISTICS_START=0,TEMPORAL_STATISTIC='TIME
INTEGRAL'/
&DEVC XB=-3.9000,-3.9000,-2.7800,-
0.3800,0.1000,0.1000,POINTS=31,ORIENTATION=0,1,0,ID='FL x:-3.90
z:0.10',QUANTITY='GAUGE HEAT FLUX GAS',STATISTICS_START=0,TEMPORAL_STATISTIC='TIME
INTEGRAL'/
&DEVC XB=-3.9000,-3.9000,-2.7800,-
0.3800,0.1800,0.1800,POINTS=31,ORIENTATION=0,1,0,ID='FL x:-3.90
z:0.18',QUANTITY='GAUGE HEAT FLUX GAS',STATISTICS_START=0,TEMPORAL_STATISTIC='TIME
INTEGRAL'/
&DEVC XB=-3.8200,-3.8200,-2.7800,-0.3800,-0.1800,-
0.1800,POINTS=31,ORIENTATION=0,1,0,ID='FL x:-3.82 z:-0.18',QUANTITY='GAUGE HEAT FLUX
GAS',STATISTICS_START=0,TEMPORAL_STATISTIC='TIME INTEGRAL'/
&DEVC XB=-3.8200,-3.8200,-2.7800,-0.3800,-0.1000,-
0.1000,POINTS=31,ORIENTATION=0,1,0,ID='FL x:-3.82 z:-0.10',QUANTITY='GAUGE HEAT FLUX
GAS',STATISTICS_START=0,TEMPORAL_STATISTIC='TIME INTEGRAL'/
&DEVC XB=-3.8200,-3.8200,-2.7800,-0.3800,-0.0200,-
0.0200,POINTS=31,ORIENTATION=0,1,0,ID='FL x:-3.82 z:-0.02',QUANTITY='GAUGE HEAT FLUX
GAS',STATISTICS_START=0,TEMPORAL_STATISTIC='TIME INTEGRAL'/
&DEVC XB=-3.8200,-3.8200,-2.7800,-
0.3800,0.0200,0.0200,POINTS=31,ORIENTATION=0,1,0,ID='FL x:-3.82
```

```
z:0.02',QUANTITY='GAUGE HEAT FLUX GAS',STATISTICS_START=0,TEMPORAL_STATISTIC='TIME
INTEGRAL'/
&DEVC XB=-3.8200,-3.8200,-2.7800,-
0.3800,0.1000,0.1000,POINTS=31,ORIENTATION=0,1,0,ID='FL x:-3.82
z:0.10',QUANTITY='GAUGE HEAT FLUX GAS',STATISTICS_START=0,TEMPORAL_STATISTIC='TIME
INTEGRAL'/
&DEVC XB=-3.8200,-3.8200,-2.7800,-
0.3800,0.1800,0.1800,POINTS=31,ORIENTATION=0,1,0,ID='FL x:-3.82
z:0.18',QUANTITY='GAUGE HEAT FLUX GAS',STATISTICS_START=0,TEMPORAL_STATISTIC='TIME
INTEGRAL'/


&DEVC XB=-4.1800,-4.1800,-2.7800,-
0.3800,0.3000,0.3000,POINTS=31,ORIENTATION=0,1,0,ID='FU x:-4.18
z:0.30',QUANTITY='GAUGE HEAT FLUX GAS',STATISTICS_START=0,TEMPORAL_STATISTIC='TIME
INTEGRAL'/
&DEVC XB=-4.1800,-4.1800,-2.7800,-
0.3800,0.3800,0.3800,POINTS=31,ORIENTATION=0,1,0,ID='FU x:-4.18
z:0.38',QUANTITY='GAUGE HEAT FLUX GAS',STATISTICS_START=0,TEMPORAL_STATISTIC='TIME
INTEGRAL'/
&DEVC XB=-4.1800,-4.1800,-2.7800,-
0.3800,0.4600,0.4600,POINTS=31,ORIENTATION=0,1,0,ID='FU x:-4.18
z:0.46',QUANTITY='GAUGE HEAT FLUX GAS',STATISTICS_START=0,TEMPORAL_STATISTIC='TIME
INTEGRAL'/
&DEVC XB=-4.1800,-4.1800,-2.7800,-
0.3800,0.5000,0.5000,POINTS=31,ORIENTATION=0,1,0,ID='FU x:-4.18
z:0.50',QUANTITY='GAUGE HEAT FLUX GAS',STATISTICS_START=0,TEMPORAL_STATISTIC='TIME
INTEGRAL'/
&DEVC XB=-4.1800,-4.1800,-2.7800,-
0.3800,0.5800,0.5800,POINTS=31,ORIENTATION=0,1,0,ID='FU x:-4.18
z:0.58',QUANTITY='GAUGE HEAT FLUX GAS',STATISTICS_START=0,TEMPORAL_STATISTIC='TIME
INTEGRAL'/
&DEVC XB=-4.1800,-4.1800,-2.7800,-
0.3800,0.6600,0.6600,POINTS=31,ORIENTATION=0,1,0,ID='FU x:-4.18
z:0.66',QUANTITY='GAUGE HEAT FLUX GAS',STATISTICS_START=0,TEMPORAL_STATISTIC='TIME
INTEGRAL'/
&DEVC XB=-4.1000,-4.1000,-2.7800,-
0.3800,0.3000,0.3000,POINTS=31,ORIENTATION=0,1,0,ID='FU x:-4.10
z:0.30',QUANTITY='GAUGE HEAT FLUX GAS',STATISTICS_START=0,TEMPORAL_STATISTIC='TIME
INTEGRAL'/
&DEVC XB=-4.1000,-4.1000,-2.7800,-
0.3800,0.3800,0.3800,POINTS=31,ORIENTATION=0,1,0,ID='FU x:-4.10
z:0.38',QUANTITY='GAUGE HEAT FLUX GAS',STATISTICS_START=0,TEMPORAL_STATISTIC='TIME
INTEGRAL'/
&DEVC XB=-4.1000,-4.1000,-2.7800,-
0.3800,0.4600,0.4600,POINTS=31,ORIENTATION=0,1,0,ID='FU x:-4.10
z:0.46',QUANTITY='GAUGE HEAT FLUX GAS',STATISTICS_START=0,TEMPORAL_STATISTIC='TIME
INTEGRAL'/
&DEVC XB=-4.1000,-4.1000,-2.7800,-
0.3800,0.5000,0.5000,POINTS=31,ORIENTATION=0,1,0,ID='FU x:-4.10
z:0.50',QUANTITY='GAUGE HEAT FLUX GAS',STATISTICS_START=0,TEMPORAL_STATISTIC='TIME
INTEGRAL'/
&DEVC XB=-4.1000,-4.1000,-2.7800,-
0.3800,0.5800,0.5800,POINTS=31,ORIENTATION=0,1,0,ID='FU x:-4.10
z:0.58',QUANTITY='GAUGE HEAT FLUX GAS',STATISTICS_START=0,TEMPORAL_STATISTIC='TIME
INTEGRAL'/
&DEVC XB=-4.1000,-4.1000,-2.7800,-
0.3800,0.6600,0.6600,POINTS=31,ORIENTATION=0,1,0,ID='FU x:-4.10
z:0.66',QUANTITY='GAUGE HEAT FLUX GAS',STATISTICS_START=0,TEMPORAL_STATISTIC='TIME
INTEGRAL'/
&DEVC XB=-4.0200,-4.0200,-2.7800,-
0.3800,0.3000,0.3000,POINTS=31,ORIENTATION=0,1,0,ID='FU x:-4.02
z:0.30',QUANTITY='GAUGE HEAT FLUX GAS',STATISTICS_START=0,TEMPORAL_STATISTIC='TIME
INTEGRAL'/
```

```
&DEVC XB=-4.0200,-4.0200,-2.7800,-
0.3800,0.3800,0.3800,POINTS=31,ORIENTATION=0,1,0,ID='FU x:-4.02
z:0.38',QUANTITY='GAUGE HEAT FLUX GAS',STATISTICS_START=0,TEMPORAL_STATISTIC='TIME
INTEGRAL'/
&DEVC XB=-4.0200,-4.0200,-2.7800,-
0.3800,0.4600,0.4600,POINTS=31,ORIENTATION=0,1,0,ID='FU x:-4.02
z:0.46',QUANTITY='GAUGE HEAT FLUX GAS',STATISTICS_START=0,TEMPORAL_STATISTIC='TIME
INTEGRAL'/
&DEVC XB=-4.0200,-4.0200,-2.7800,-
0.3800,0.5000,0.5000,POINTS=31,ORIENTATION=0,1,0,ID='FU x:-4.02
z:0.50',QUANTITY='GAUGE HEAT FLUX GAS',STATISTICS_START=0,TEMPORAL_STATISTIC='TIME
INTEGRAL'/
&DEVC XB=-4.0200,-4.0200,-2.7800,-
0.3800,0.5800,0.5800,POINTS=31,ORIENTATION=0,1,0,ID='FU x:-4.02
z:0.58',QUANTITY='GAUGE HEAT FLUX GAS',STATISTICS_START=0,TEMPORAL_STATISTIC='TIME
INTEGRAL'/
&DEVC XB=-4.0200,-4.0200,-2.7800,-
0.3800,0.6600,0.6600,POINTS=31,ORIENTATION=0,1,0,ID='FU x:-4.02
z:0.66',QUANTITY='GAUGE HEAT FLUX GAS',STATISTICS_START=0,TEMPORAL_STATISTIC='TIME
INTEGRAL'/
&DEVC XB=-3.9800,-3.9800,-2.7800,-
0.3800,0.3000,0.3000,POINTS=31,ORIENTATION=0,1,0,ID='FU x:-3.98
z:0.30',QUANTITY='GAUGE HEAT FLUX GAS',STATISTICS_START=0,TEMPORAL_STATISTIC='TIME
INTEGRAL'/
&DEVC XB=-3.9800,-3.9800,-2.7800,-
0.3800,0.3800,0.3800,POINTS=31,ORIENTATION=0,1,0,ID='FU x:-3.98
z:0.38',QUANTITY='GAUGE HEAT FLUX GAS',STATISTICS_START=0,TEMPORAL_STATISTIC='TIME
INTEGRAL'/
&DEVC XB=-3.9800,-3.9800,-2.7800,-
0.3800,0.4600,0.4600,POINTS=31,ORIENTATION=0,1,0,ID='FU x:-3.98
z:0.46',QUANTITY='GAUGE HEAT FLUX GAS',STATISTICS_START=0,TEMPORAL_STATISTIC='TIME
INTEGRAL'/
&DEVC XB=-3.9800,-3.9800,-2.7800,-
0.3800,0.5000,0.5000,POINTS=31,ORIENTATION=0,1,0,ID='FU x:-3.98
z:0.50',QUANTITY='GAUGE HEAT FLUX GAS',STATISTICS_START=0,TEMPORAL_STATISTIC='TIME
INTEGRAL'/
&DEVC XB=-3.9800,-3.9800,-2.7800,-
0.3800,0.5800,0.5800,POINTS=31,ORIENTATION=0,1,0,ID='FU x:-3.98
z:0.58',QUANTITY='GAUGE HEAT FLUX GAS',STATISTICS_START=0,TEMPORAL_STATISTIC='TIME
INTEGRAL'/
&DEVC XB=-3.9800,-3.9800,-2.7800,-
0.3800,0.6600,0.6600,POINTS=31,ORIENTATION=0,1,0,ID='FU x:-3.98
z:0.66',QUANTITY='GAUGE HEAT FLUX GAS',STATISTICS_START=0,TEMPORAL_STATISTIC='TIME
INTEGRAL'/
&DEVC XB=-3.9000,-3.9000,-2.7800,-
0.3800,0.3000,0.3000,POINTS=31,ORIENTATION=0,1,0,ID='FU x:-3.90
z:0.30',QUANTITY='GAUGE HEAT FLUX GAS',STATISTICS_START=0,TEMPORAL_STATISTIC='TIME
INTEGRAL'/
&DEVC XB=-3.9000,-3.9000,-2.7800,-
0.3800,0.3800,0.3800,POINTS=31,ORIENTATION=0,1,0,ID='FU x:-3.90
z:0.38',QUANTITY='GAUGE HEAT FLUX GAS',STATISTICS_START=0,TEMPORAL_STATISTIC='TIME
INTEGRAL'/
&DEVC XB=-3.9000,-3.9000,-2.7800,-
0.3800,0.4600,0.4600,POINTS=31,ORIENTATION=0,1,0,ID='FU x:-3.90
z:0.46',QUANTITY='GAUGE HEAT FLUX GAS',STATISTICS_START=0,TEMPORAL_STATISTIC='TIME
INTEGRAL'/
&DEVC XB=-3.9000,-3.9000,-2.7800,-
0.3800,0.5000,0.5000,POINTS=31,ORIENTATION=0,1,0,ID='FU x:-3.90
z:0.50',QUANTITY='GAUGE HEAT FLUX GAS',STATISTICS_START=0,TEMPORAL_STATISTIC='TIME
INTEGRAL'/
&DEVC XB=-3.9000,-3.9000,-2.7800,-
0.3800,0.5800,0.5800,POINTS=31,ORIENTATION=0,1,0,ID='FU x:-3.90
z:0.58',QUANTITY='GAUGE HEAT FLUX GAS',STATISTICS_START=0,TEMPORAL_STATISTIC='TIME
INTEGRAL'/
```

```
&DEVC XB=-3.9000,-3.9000,-2.7800,-
0.3800,0.6600,0.6600,POINTS=31,ORIENTATION=0,1,0,ID='FU x:-3.90
z:0.66',QUANTITY='GAUGE HEAT FLUX GAS',STATISTICS_START=0,TEMPORAL_STATISTIC='TIME
INTEGRAL'/
&DEVC XB=-3.8200,-3.8200,-2.7800,-
0.3800,0.3000,0.3000,POINTS=31,ORIENTATION=0,1,0,ID='FU x:-3.82
z:0.30',QUANTITY='GAUGE HEAT FLUX GAS',STATISTICS_START=0,TEMPORAL_STATISTIC='TIME
INTEGRAL'/
&DEVC XB=-3.8200,-3.8200,-2.7800,-
0.3800,0.3800,0.3800,POINTS=31,ORIENTATION=0,1,0,ID='FU x:-3.82
z:0.38',QUANTITY='GAUGE HEAT FLUX GAS',STATISTICS_START=0,TEMPORAL_STATISTIC='TIME
INTEGRAL'/
&DEVC XB=-3.8200,-3.8200,-2.7800,-
0.3800,0.4600,0.4600,POINTS=31,ORIENTATION=0,1,0,ID='FU x:-3.82
z:0.46',QUANTITY='GAUGE HEAT FLUX GAS',STATISTICS_START=0,TEMPORAL_STATISTIC='TIME
INTEGRAL'/
&DEVC XB=-3.8200,-3.8200,-2.7800,-
0.3800,0.5000,0.5000,POINTS=31,ORIENTATION=0,1,0,ID='FU x:-3.82
z:0.50',QUANTITY='GAUGE HEAT FLUX GAS',STATISTICS_START=0,TEMPORAL_STATISTIC='TIME
INTEGRAL'/
&DEVC XB=-3.8200,-3.8200,-2.7800,-
0.3800,0.5800,0.5800,POINTS=31,ORIENTATION=0,1,0,ID='FU x:-3.82
z:0.58',QUANTITY='GAUGE HEAT FLUX GAS',STATISTICS_START=0,TEMPORAL_STATISTIC='TIME
INTEGRAL'/
&DEVC XB=-3.8200,-3.8200,-2.7800,-
0.3800,0.6600,0.6600,POINTS=31,ORIENTATION=0,1,0,ID='FU x:-3.82
z:0.66',QUANTITY='GAUGE HEAT FLUX GAS',STATISTICS_START=0,TEMPORAL_STATISTIC='TIME
INTEGRAL'/

&DEVC XB=-0.1800,-0.1800,-0.1800,-0.1800,-2.7000,-
0.3000,POINTS=31,ORIENTATION=0,0,1,ID='BL x:-0.18 y:-0.18',QUANTITY='GAUGE HEAT FLUX
GAS',STATISTICS_START=0,TEMPORAL_STATISTIC='TIME INTEGRAL'/
&DEVC XB=-0.1800,-0.1800,-0.1000,-0.1000,-2.7000,-
0.3000,POINTS=31,ORIENTATION=0,0,1,ID='BL x:-0.18 y:-0.10',QUANTITY='GAUGE HEAT FLUX
GAS',STATISTICS_START=0,TEMPORAL_STATISTIC='TIME INTEGRAL'/
&DEVC XB=-0.1800,-0.1800,-0.0200,-0.0200,-2.7000,-
0.3000,POINTS=31,ORIENTATION=0,0,1,ID='BL x:-0.18 y:-0.02',QUANTITY='GAUGE HEAT FLUX
GAS',STATISTICS_START=0,TEMPORAL_STATISTIC='TIME INTEGRAL'/
&DEVC XB=-0.1800,-0.1800,0.0200,0.0200,-2.7000,-
0.3000,POINTS=31,ORIENTATION=0,0,1,ID='BL x:-0.18 y:0.02',QUANTITY='GAUGE HEAT FLUX
GAS',STATISTICS_START=0,TEMPORAL_STATISTIC='TIME INTEGRAL'/
&DEVC XB=-0.1800,-0.1800,0.1000,0.1000,-2.7000,-
0.3000,POINTS=31,ORIENTATION=0,0,1,ID='BL x:-0.18 y:0.10',QUANTITY='GAUGE HEAT FLUX
GAS',STATISTICS_START=0,TEMPORAL_STATISTIC='TIME INTEGRAL'/
&DEVC XB=-0.1800,-0.1800,0.1800,0.1800,-2.7000,-
0.3000,POINTS=31,ORIENTATION=0,0,1,ID='BL x:-0.18 y:0.18',QUANTITY='GAUGE HEAT FLUX
GAS',STATISTICS_START=0,TEMPORAL_STATISTIC='TIME INTEGRAL'/
&DEVC XB=-0.1000,-0.1000,-0.1800,-0.1800,-2.7000,-
0.3000,POINTS=31,ORIENTATION=0,0,1,ID='BL x:-0.10 y:-0.18',QUANTITY='GAUGE HEAT FLUX
GAS',STATISTICS_START=0,TEMPORAL_STATISTIC='TIME INTEGRAL'/
&DEVC XB=-0.1000,-0.1000,-0.1000,-0.1000,-2.7000,-
0.3000,POINTS=31,ORIENTATION=0,0,1,ID='BL x:-0.10 y:-0.10',QUANTITY='GAUGE HEAT FLUX
GAS',STATISTICS_START=0,TEMPORAL_STATISTIC='TIME INTEGRAL'/
&DEVC XB=-0.1000,-0.1000,-0.0200,-0.0200,-2.7000,-
0.3000,POINTS=31,ORIENTATION=0,0,1,ID='BL x:-0.10 y:-0.02',QUANTITY='GAUGE HEAT FLUX
GAS',STATISTICS_START=0,TEMPORAL_STATISTIC='TIME INTEGRAL'/
&DEVC XB=-0.1000,-0.1000,0.0200,0.0200,-2.7000,-
0.3000,POINTS=31,ORIENTATION=0,0,1,ID='BL x:-0.10 y:0.02',QUANTITY='GAUGE HEAT FLUX
GAS',STATISTICS_START=0,TEMPORAL_STATISTIC='TIME INTEGRAL'/
&DEVC XB=-0.1000,-0.1000,0.1000,0.1000,-2.7000,-
0.3000,POINTS=31,ORIENTATION=0,0,1,ID='BL x:-0.10 y:0.10',QUANTITY='GAUGE HEAT FLUX
GAS',STATISTICS_START=0,TEMPORAL_STATISTIC='TIME INTEGRAL'/
```

```
&DEVC XB=-0.1000,-0.1000,0.1800,0.1800,-2.7000,-
0.3000,POINTS=31,ORIENTATION=0,0,1,ID='BL x:-0.10 y:0.18',QUANTITY='GAUGE HEAT FLUX
GAS',STATISTICS_START=0,TEMPORAL_STATISTIC='TIME INTEGRAL'/
&DEVC XB=-0.0200,-0.0200,-0.1800,-0.1800,-2.7000,-
0.3000,POINTS=31,ORIENTATION=0,0,1,ID='BL x:-0.02 y:-0.18',QUANTITY='GAUGE HEAT FLUX
GAS',STATISTICS_START=0,TEMPORAL_STATISTIC='TIME INTEGRAL'/
&DEVC XB=-0.0200,-0.0200,-0.1000,-0.1000,-2.7000,-
0.3000,POINTS=31,ORIENTATION=0,0,1,ID='BL x:-0.02 y:-0.10',QUANTITY='GAUGE HEAT FLUX
GAS',STATISTICS_START=0,TEMPORAL_STATISTIC='TIME INTEGRAL'/
&DEVC XB=-0.0200,-0.0200,-0.0200,-0.0200,-2.7000,-
0.3000,POINTS=31,ORIENTATION=0,0,1,ID='BL x:-0.02 y:-0.02',QUANTITY='GAUGE HEAT FLUX
GAS',STATISTICS_START=0,TEMPORAL_STATISTIC='TIME INTEGRAL'/
&DEVC XB=-0.0200,-0.0200,0.0200,0.0200,-2.7000,-
0.3000,POINTS=31,ORIENTATION=0,0,1,ID='BL x:-0.02 y:0.02',QUANTITY='GAUGE HEAT FLUX
GAS',STATISTICS_START=0,TEMPORAL_STATISTIC='TIME INTEGRAL'/
&DEVC XB=-0.0200,-0.0200,0.1000,0.1000,-2.7000,-
0.3000,POINTS=31,ORIENTATION=0,0,1,ID='BL x:-0.02 y:0.10',QUANTITY='GAUGE HEAT FLUX
GAS',STATISTICS_START=0,TEMPORAL_STATISTIC='TIME INTEGRAL'/
&DEVC XB=-0.0200,-0.0200,0.1800,0.1800,-2.7000,-
0.3000,POINTS=31,ORIENTATION=0,0,1,ID='BL x:-0.02 y:0.18',QUANTITY='GAUGE HEAT FLUX
GAS',STATISTICS_START=0,TEMPORAL_STATISTIC='TIME INTEGRAL'/
&DEVC XB=0.0200,0.0200,-0.1800,-0.1800,-2.7000,-
0.3000,POINTS=31,ORIENTATION=0,0,1,ID='BL x:0.02 y:-0.18',QUANTITY='GAUGE HEAT FLUX
GAS',STATISTICS_START=0,TEMPORAL_STATISTIC='TIME INTEGRAL'/
&DEVC XB=0.0200,0.0200,-0.1000,-0.1000,-2.7000,-
0.3000,POINTS=31,ORIENTATION=0,0,1,ID='BL x:0.02 y:-0.10',QUANTITY='GAUGE HEAT FLUX
GAS',STATISTICS_START=0,TEMPORAL_STATISTIC='TIME INTEGRAL'/
&DEVC XB=0.0200,0.0200,-0.0200,-0.0200,-2.7000,-
0.3000,POINTS=31,ORIENTATION=0,0,1,ID='BL x:0.02 y:-0.02',QUANTITY='GAUGE HEAT FLUX
GAS',STATISTICS_START=0,TEMPORAL_STATISTIC='TIME INTEGRAL'/
&DEVC XB=0.0200,0.0200,0.0200,0.0200,-2.7000,-
0.3000,POINTS=31,ORIENTATION=0,0,1,ID='BL x:0.02 y:0.02',QUANTITY='GAUGE HEAT FLUX
GAS',STATISTICS_START=0,TEMPORAL_STATISTIC='TIME INTEGRAL'/
&DEVC XB=0.0200,0.0200,0.1000,0.1000,-2.7000,-
0.3000,POINTS=31,ORIENTATION=0,0,1,ID='BL x:0.02 y:0.10',QUANTITY='GAUGE HEAT FLUX
GAS',STATISTICS_START=0,TEMPORAL_STATISTIC='TIME INTEGRAL'/
&DEVC XB=0.0200,0.0200,0.1800,0.1800,-2.7000,-
0.3000,POINTS=31,ORIENTATION=0,0,1,ID='BL x:0.02 y:0.18',QUANTITY='GAUGE HEAT FLUX
GAS',STATISTICS_START=0,TEMPORAL_STATISTIC='TIME INTEGRAL'/
&DEVC XB=0.1000,0.1000,-0.1800,-0.1800,-2.7000,-
0.3000,POINTS=31,ORIENTATION=0,0,1,ID='BL x:0.10 y:-0.18',QUANTITY='GAUGE HEAT FLUX
GAS',STATISTICS_START=0,TEMPORAL_STATISTIC='TIME INTEGRAL'/
&DEVC XB=0.1000,0.1000,-0.1000,-0.1000,-2.7000,-
0.3000,POINTS=31,ORIENTATION=0,0,1,ID='BL x:0.10 y:-0.10',QUANTITY='GAUGE HEAT FLUX
GAS',STATISTICS_START=0,TEMPORAL_STATISTIC='TIME INTEGRAL'/
&DEVC XB=0.1000,0.1000,-0.0200,-0.0200,-2.7000,-
0.3000,POINTS=31,ORIENTATION=0,0,1,ID='BL x:0.10 y:-0.02',QUANTITY='GAUGE HEAT FLUX
GAS',STATISTICS_START=0,TEMPORAL_STATISTIC='TIME INTEGRAL'/
&DEVC XB=0.1000,0.1000,0.0200,0.0200,-2.7000,-
0.3000,POINTS=31,ORIENTATION=0,0,1,ID='BL x:0.10 y:0.02',QUANTITY='GAUGE HEAT FLUX
GAS',STATISTICS_START=0,TEMPORAL_STATISTIC='TIME INTEGRAL'/
&DEVC XB=0.1000,0.1000,0.1000,0.1000,-2.7000,-
0.3000,POINTS=31,ORIENTATION=0,0,1,ID='BL x:0.10 y:0.10',QUANTITY='GAUGE HEAT FLUX
GAS',STATISTICS_START=0,TEMPORAL_STATISTIC='TIME INTEGRAL'/
&DEVC XB=0.1000,0.1000,0.1800,0.1800,-2.7000,-
0.3000,POINTS=31,ORIENTATION=0,0,1,ID='BL x:0.10 y:0.18',QUANTITY='GAUGE HEAT FLUX
GAS',STATISTICS_START=0,TEMPORAL_STATISTIC='TIME INTEGRAL'/
&DEVC XB=0.1800,0.1800,-0.1800,-0.1800,-2.7000,-
0.3000,POINTS=31,ORIENTATION=0,0,1,ID='BL x:0.18 y:-0.18',QUANTITY='GAUGE HEAT FLUX
GAS',STATISTICS_START=0,TEMPORAL_STATISTIC='TIME INTEGRAL'/
&DEVC XB=0.1800,0.1800,-0.1000,-0.1000,-2.7000,-
0.3000,POINTS=31,ORIENTATION=0,0,1,ID='BL x:0.18 y:-0.10',QUANTITY='GAUGE HEAT FLUX
GAS',STATISTICS_START=0,TEMPORAL_STATISTIC='TIME INTEGRAL'/
```

```
&DEVC XB=0.1800,0.1800,-0.0200,-0.0200,-2.7000,-
0.3000,POINTS=31,ORIENTATION=0,0,1,ID='BL x:0.18 y:-0.02',QUANTITY='GAUGE HEAT FLUX
GAS',STATISTICS_START=0,TEMPORAL_STATISTIC='TIME INTEGRAL'/
&DEVC XB=0.1800,0.1800,0.0200,0.0200,-2.7000,-
0.3000,POINTS=31,ORIENTATION=0,0,1,ID='BL x:0.18 y:0.02',QUANTITY='GAUGE HEAT FLUX
GAS',STATISTICS_START=0,TEMPORAL_STATISTIC='TIME INTEGRAL'/
&DEVC XB=0.1800,0.1800,0.1000,0.1000,-2.7000,-
0.3000,POINTS=31,ORIENTATION=0,0,1,ID='BL x:0.18 y:0.10',QUANTITY='GAUGE HEAT FLUX
GAS',STATISTICS_START=0,TEMPORAL_STATISTIC='TIME INTEGRAL'/
&DEVC XB=0.1800,0.1800,0.1800,0.1800,-2.7000,-
0.3000,POINTS=31,ORIENTATION=0,0,1,ID='BL x:0.18 y:0.18',QUANTITY='GAUGE HEAT FLUX
GAS',STATISTICS_START=0,TEMPORAL_STATISTIC='TIME INTEGRAL'/


&DEVC XB=-0.1800,-0.1800,-0.1800,-0.1800,0.3000,2.7000,POINTS=31,ORIENTATION=0,0,-
1,ID='AB x:-0.18 y:-0.18',QUANTITY='GAUGE HEAT FLUX
GAS',STATISTICS_START=0,TEMPORAL_STATISTIC='TIME INTEGRAL'/
&DEVC XB=-0.1800,-0.1800,-0.1000,-0.1000,0.3000,2.7000,POINTS=31,ORIENTATION=0,0,-
1,ID='AB x:-0.18 y:-0.10',QUANTITY='GAUGE HEAT FLUX
GAS',STATISTICS_START=0,TEMPORAL_STATISTIC='TIME INTEGRAL'/
&DEVC XB=-0.1800,-0.1800,-0.0200,-0.0200,0.3000,2.7000,POINTS=31,ORIENTATION=0,0,-
1,ID='AB x:-0.18 y:-0.02',QUANTITY='GAUGE HEAT FLUX
GAS',STATISTICS_START=0,TEMPORAL_STATISTIC='TIME INTEGRAL'/
&DEVC XB=-0.1800,-0.1800,0.0200,0.0200,0.3000,2.7000,POINTS=31,ORIENTATION=0,0,-
1,ID='AB x:-0.18 y:0.02',QUANTITY='GAUGE HEAT FLUX
GAS',STATISTICS_START=0,TEMPORAL_STATISTIC='TIME INTEGRAL'/
&DEVC XB=-0.1800,-0.1800,0.1000,0.1000,0.3000,2.7000,POINTS=31,ORIENTATION=0,0,-
1,ID='AB x:-0.18 y:0.10',QUANTITY='GAUGE HEAT FLUX
GAS',STATISTICS_START=0,TEMPORAL_STATISTIC='TIME INTEGRAL'/
&DEVC XB=-0.1800,-0.1800,0.1800,0.1800,0.3000,2.7000,POINTS=31,ORIENTATION=0,0,-
1,ID='AB x:-0.18 y:0.18',QUANTITY='GAUGE HEAT FLUX
GAS',STATISTICS_START=0,TEMPORAL_STATISTIC='TIME INTEGRAL'/
&DEVC XB=-0.1000,-0.1000,-0.1800,-0.1800,0.3000,2.7000,POINTS=31,ORIENTATION=0,0,-
1,ID='AB x:-0.10 y:-0.18',QUANTITY='GAUGE HEAT FLUX
GAS',STATISTICS_START=0,TEMPORAL_STATISTIC='TIME INTEGRAL'/
&DEVC XB=-0.1000,-0.1000,-0.1000,-0.1000,0.3000,2.7000,POINTS=31,ORIENTATION=0,0,-
1,ID='AB x:-0.10 y:-0.10',QUANTITY='GAUGE HEAT FLUX
GAS',STATISTICS_START=0,TEMPORAL_STATISTIC='TIME INTEGRAL'/
&DEVC XB=-0.1000,-0.1000,-0.0200,-0.0200,0.3000,2.7000,POINTS=31,ORIENTATION=0,0,-
1,ID='AB x:-0.10 y:-0.02',QUANTITY='GAUGE HEAT FLUX
GAS',STATISTICS_START=0,TEMPORAL_STATISTIC='TIME INTEGRAL'/
&DEVC XB=-0.1000,-0.1000,0.0200,0.0200,0.3000,2.7000,POINTS=31,ORIENTATION=0,0,-
1,ID='AB x:-0.10 y:0.02',QUANTITY='GAUGE HEAT FLUX
GAS',STATISTICS_START=0,TEMPORAL_STATISTIC='TIME INTEGRAL'/
&DEVC XB=-0.1000,-0.1000,0.1000,0.1000,0.3000,2.7000,POINTS=31,ORIENTATION=0,0,-
1,ID='AB x:-0.10 y:0.10',QUANTITY='GAUGE HEAT FLUX
GAS',STATISTICS_START=0,TEMPORAL_STATISTIC='TIME INTEGRAL'/
&DEVC XB=-0.1000,-0.1000,0.1800,0.1800,0.3000,2.7000,POINTS=31,ORIENTATION=0,0,-
1,ID='AB x:-0.10 y:0.18',QUANTITY='GAUGE HEAT FLUX
GAS',STATISTICS_START=0,TEMPORAL_STATISTIC='TIME INTEGRAL'/
&DEVC XB=-0.0200,-0.0200,-0.1800,-0.1800,0.3000,2.7000,POINTS=31,ORIENTATION=0,0,-
1,ID='AB x:-0.02 y:-0.18',QUANTITY='GAUGE HEAT FLUX
GAS',STATISTICS_START=0,TEMPORAL_STATISTIC='TIME INTEGRAL'/
&DEVC XB=-0.0200,-0.0200,-0.1000,-0.1000,0.3000,2.7000,POINTS=31,ORIENTATION=0,0,-
1,ID='AB x:-0.02 y:-0.10',QUANTITY='GAUGE HEAT FLUX
GAS',STATISTICS_START=0,TEMPORAL_STATISTIC='TIME INTEGRAL'/
&DEVC XB=-0.0200,-0.0200,-0.0200,-0.0200,0.3000,2.7000,POINTS=31,ORIENTATION=0,0,-
1,ID='AB x:-0.02 y:-0.02',QUANTITY='GAUGE HEAT FLUX
GAS',STATISTICS_START=0,TEMPORAL_STATISTIC='TIME INTEGRAL'/
&DEVC XB=-0.0200,-0.0200,0.0200,0.0200,0.3000,2.7000,POINTS=31,ORIENTATION=0,0,-
1,ID='AB x:-0.02 y:0.02',QUANTITY='GAUGE HEAT FLUX
GAS',STATISTICS_START=0,TEMPORAL_STATISTIC='TIME INTEGRAL'/
```

```
&DEVC XB=-0.0200,-0.0200,0.1000,0.1000,0.3000,2.7000,POINTS=31,ORIENTATION=0,0,-
1,ID='AB x:-0.02 y:0.10',QUANTITY='GAUGE HEAT FLUX
GAS',STATISTICS_START=0,TEMPORAL_STATISTIC='TIME INTEGRAL'/
&DEVC XB=-0.0200,-0.0200,0.1800,0.1800,0.3000,2.7000,POINTS=31,ORIENTATION=0,0,-
1,ID='AB x:-0.02 y:0.18',QUANTITY='GAUGE HEAT FLUX
GAS',STATISTICS_START=0,TEMPORAL_STATISTIC='TIME INTEGRAL'/
&DEVC XB=0.0200,0.0200,-0.1800,-0.1800,0.3000,2.7000,POINTS=31,ORIENTATION=0,0,-
1,ID='AB x:0.02 y:-0.18',QUANTITY='GAUGE HEAT FLUX
GAS',STATISTICS_START=0,TEMPORAL_STATISTIC='TIME INTEGRAL'/
&DEVC XB=0.0200,0.0200,-0.1000,-0.1000,0.3000,2.7000,POINTS=31,ORIENTATION=0,0,-
1,ID='AB x:0.02 y:-0.10',QUANTITY='GAUGE HEAT FLUX
GAS',STATISTICS_START=0,TEMPORAL_STATISTIC='TIME INTEGRAL'/
&DEVC XB=0.0200,0.0200,-0.0200,-0.0200,0.3000,2.7000,POINTS=31,ORIENTATION=0,0,-
1,ID='AB x:0.02 y:-0.02',QUANTITY='GAUGE HEAT FLUX
GAS',STATISTICS_START=0,TEMPORAL_STATISTIC='TIME INTEGRAL'/
&DEVC XB=0.0200,0.0200,0.0200,0.0200,0.3000,2.7000,POINTS=31,ORIENTATION=0,0,-1,ID='AB
x:0.02 y:0.02',QUANTITY='GAUGE HEAT FLUX
GAS',STATISTICS_START=0,TEMPORAL_STATISTIC='TIME INTEGRAL'/
&DEVC XB=0.0200,0.0200,0.1000,0.1000,0.3000,2.7000,POINTS=31,ORIENTATION=0,0,-1,ID='AB
x:0.02 y:0.10',QUANTITY='GAUGE HEAT FLUX
GAS',STATISTICS_START=0,TEMPORAL_STATISTIC='TIME INTEGRAL'/
&DEVC XB=0.0200,0.0200,0.1800,0.1800,0.3000,2.7000,POINTS=31,ORIENTATION=0,0,-1,ID='AB
x:0.02 y:0.18',QUANTITY='GAUGE HEAT FLUX
GAS',STATISTICS_START=0,TEMPORAL_STATISTIC='TIME INTEGRAL'/
&DEVC XB=0.1000,0.1000,-0.1800,-0.1800,0.3000,2.7000,POINTS=31,ORIENTATION=0,0,-
1,ID='AB x:0.10 y:-0.18',QUANTITY='GAUGE HEAT FLUX
GAS',STATISTICS_START=0,TEMPORAL_STATISTIC='TIME INTEGRAL'/
&DEVC XB=0.1000,0.1000,-0.1000,-0.1000,0.3000,2.7000,POINTS=31,ORIENTATION=0,0,-
1,ID='AB x:0.10 y:-0.10',QUANTITY='GAUGE HEAT FLUX
GAS',STATISTICS_START=0,TEMPORAL_STATISTIC='TIME INTEGRAL'/
&DEVC XB=0.1000,0.1000,-0.0200,-0.0200,0.3000,2.7000,POINTS=31,ORIENTATION=0,0,-
1,ID='AB x:0.10 y:-0.02',QUANTITY='GAUGE HEAT FLUX
GAS',STATISTICS_START=0,TEMPORAL_STATISTIC='TIME INTEGRAL'/
&DEVC XB=0.1000,0.1000,0.0200,0.0200,0.3000,2.7000,POINTS=31,ORIENTATION=0,0,-1,ID='AB
x:0.10 y:0.02',QUANTITY='GAUGE HEAT FLUX
GAS',STATISTICS_START=0,TEMPORAL_STATISTIC='TIME INTEGRAL'/
&DEVC XB=0.1000,0.1000,0.1000,0.1000,0.3000,2.7000,POINTS=31,ORIENTATION=0,0,-1,ID='AB
x:0.10 y:0.10',QUANTITY='GAUGE HEAT FLUX
GAS',STATISTICS_START=0,TEMPORAL_STATISTIC='TIME INTEGRAL'/
&DEVC XB=0.1000,0.1000,0.1800,0.1800,0.3000,2.7000,POINTS=31,ORIENTATION=0,0,-1,ID='AB
x:0.10 y:0.18',QUANTITY='GAUGE HEAT FLUX
GAS',STATISTICS_START=0,TEMPORAL_STATISTIC='TIME INTEGRAL'/
&DEVC XB=0.1800,0.1800,-0.1800,-0.1800,0.3000,2.7000,POINTS=31,ORIENTATION=0,0,-
1,ID='AB x:0.18 y:-0.18',QUANTITY='GAUGE HEAT FLUX
GAS',STATISTICS_START=0,TEMPORAL_STATISTIC='TIME INTEGRAL'/
&DEVC XB=0.1800,0.1800,-0.1000,-0.1000,0.3000,2.7000,POINTS=31,ORIENTATION=0,0,-
1,ID='AB x:0.18 y:-0.10',QUANTITY='GAUGE HEAT FLUX
GAS',STATISTICS_START=0,TEMPORAL_STATISTIC='TIME INTEGRAL'/
&DEVC XB=0.1800,0.1800,-0.0200,-0.0200,0.3000,2.7000,POINTS=31,ORIENTATION=0,0,-
1,ID='AB x:0.18 y:-0.02',QUANTITY='GAUGE HEAT FLUX
GAS',STATISTICS_START=0,TEMPORAL_STATISTIC='TIME INTEGRAL'/
&DEVC XB=0.1800,0.1800,0.0200,0.0200,0.3000,2.7000,POINTS=31,ORIENTATION=0,0,-1,ID='AB
x:0.18 y:0.02',QUANTITY='GAUGE HEAT FLUX
GAS',STATISTICS_START=0,TEMPORAL_STATISTIC='TIME INTEGRAL'/
&DEVC XB=0.1800,0.1800,0.1000,0.1000,0.3000,2.7000,POINTS=31,ORIENTATION=0,0,-1,ID='AB
x:0.18 y:0.10',QUANTITY='GAUGE HEAT FLUX
GAS',STATISTICS_START=0,TEMPORAL_STATISTIC='TIME INTEGRAL'/
&DEVC XB=0.1800,0.1800,0.1800,0.1800,0.3000,2.7000,POINTS=31,ORIENTATION=0,0,-1,ID='AB
x:0.18 y:0.18',QUANTITY='GAUGE HEAT FLUX
GAS',STATISTICS_START=0,TEMPORAL_STATISTIC='TIME INTEGRAL'/
```

```
&DEVC XB=-0.1800,-0.1800,-2.7800,-0.3800,-0.1800,-
0.1800,POINTS=31,ORIENTATION=0,1,0,ID='FR x:-0.18 z:-0.18',QUANTITY='GAUGE HEAT FLUX
GAS',STATISTICS_START=0,TEMPORAL_STATISTIC='TIME INTEGRAL'/
&DEVC XB=-0.1800,-0.1800,-2.7800,-0.3800,-0.1000,-
0.1000,POINTS=31,ORIENTATION=0,1,0,ID='FR x:-0.18 z:-0.10',QUANTITY='GAUGE HEAT FLUX
GAS',STATISTICS_START=0,TEMPORAL_STATISTIC='TIME INTEGRAL'/
&DEVC XB=-0.1800,-0.1800,-2.7800,-0.3800,-0.0200,-
0.0200,POINTS=31,ORIENTATION=0,1,0,ID='FR x:-0.18 z:-0.02',QUANTITY='GAUGE HEAT FLUX
GAS',STATISTICS_START=0,TEMPORAL_STATISTIC='TIME INTEGRAL'/
&DEVC XB=-0.1800,-0.1800,-2.7800,-
0.3800,0.0200,0.0200,POINTS=31,ORIENTATION=0,1,0,ID='FR x:-0.18
z:0.02',QUANTITY='GAUGE HEAT FLUX GAS',STATISTICS_START=0,TEMPORAL_STATISTIC='TIME
INTEGRAL'/
&DEVC XB=-0.1800,-0.1800,-2.7800,-
0.3800,0.1000,0.1000,POINTS=31,ORIENTATION=0,1,0,ID='FR x:-0.18
z:0.10',QUANTITY='GAUGE HEAT FLUX GAS',STATISTICS_START=0,TEMPORAL_STATISTIC='TIME
INTEGRAL'/
&DEVC XB=-0.1800,-0.1800,-2.7800,-
0.3800,0.1800,0.1800,POINTS=31,ORIENTATION=0,1,0,ID='FR x:-0.18
z:0.18',QUANTITY='GAUGE HEAT FLUX GAS',STATISTICS_START=0,TEMPORAL_STATISTIC='TIME
INTEGRAL'/
&DEVC XB=-0.1000,-0.1000,-2.7800,-0.3800,-0.1800,-
0.1800,POINTS=31,ORIENTATION=0,1,0,ID='FR x:-0.10 z:-0.18',QUANTITY='GAUGE HEAT FLUX
GAS',STATISTICS_START=0,TEMPORAL_STATISTIC='TIME INTEGRAL'/
&DEVC XB=-0.1000,-0.1000,-2.7800,-0.3800,-0.1000,-
0.1000,POINTS=31,ORIENTATION=0,1,0,ID='FR x:-0.10 z:-0.10',QUANTITY='GAUGE HEAT FLUX
GAS',STATISTICS_START=0,TEMPORAL_STATISTIC='TIME INTEGRAL'/
&DEVC XB=-0.1000,-0.1000,-2.7800,-0.3800,-0.0200,-
0.0200,POINTS=31,ORIENTATION=0,1,0,ID='FR x:-0.10 z:-0.02',QUANTITY='GAUGE HEAT FLUX
GAS',STATISTICS_START=0,TEMPORAL_STATISTIC='TIME INTEGRAL'/
&DEVC XB=-0.1000,-0.1000,-2.7800,-
0.3800,0.0200,0.0200,POINTS=31,ORIENTATION=0,1,0,ID='FR x:-0.10
z:0.02',QUANTITY='GAUGE HEAT FLUX GAS',STATISTICS_START=0,TEMPORAL_STATISTIC='TIME
INTEGRAL'/
&DEVC XB=-0.1000,-0.1000,-2.7800,-
0.3800,0.1000,0.1000,POINTS=31,ORIENTATION=0,1,0,ID='FR x:-0.10
z:0.10',QUANTITY='GAUGE HEAT FLUX GAS',STATISTICS_START=0,TEMPORAL_STATISTIC='TIME
INTEGRAL'/
&DEVC XB=-0.1000,-0.1000,-2.7800,-
0.3800,0.1800,0.1800,POINTS=31,ORIENTATION=0,1,0,ID='FR x:-0.10
z:0.18',QUANTITY='GAUGE HEAT FLUX GAS',STATISTICS_START=0,TEMPORAL_STATISTIC='TIME
INTEGRAL'/
&DEVC XB=-0.0200,-0.0200,-2.7800,-0.3800,-0.1800,-
0.1800,POINTS=31,ORIENTATION=0,1,0,ID='FR x:-0.02 z:-0.18',QUANTITY='GAUGE HEAT FLUX
GAS',STATISTICS_START=0,TEMPORAL_STATISTIC='TIME INTEGRAL'/
&DEVC XB=-0.0200,-0.0200,-2.7800,-0.3800,-0.1000,-
0.1000,POINTS=31,ORIENTATION=0,1,0,ID='FR x:-0.02 z:-0.10',QUANTITY='GAUGE HEAT FLUX
GAS',STATISTICS_START=0,TEMPORAL_STATISTIC='TIME INTEGRAL'/
&DEVC XB=-0.0200,-0.0200,-2.7800,-0.3800,-0.0200,-
0.0200,POINTS=31,ORIENTATION=0,1,0,ID='FR x:-0.02 z:-0.02',QUANTITY='GAUGE HEAT FLUX
GAS',STATISTICS_START=0,TEMPORAL_STATISTIC='TIME INTEGRAL'/
&DEVC XB=-0.0200,-0.0200,-2.7800,-
0.3800,0.0200,0.0200,POINTS=31,ORIENTATION=0,1,0,ID='FR x:-0.02
z:0.02',QUANTITY='GAUGE HEAT FLUX GAS',STATISTICS_START=0,TEMPORAL_STATISTIC='TIME
INTEGRAL'/
&DEVC XB=-0.0200,-0.0200,-2.7800,-
0.3800,0.1000,0.1000,POINTS=31,ORIENTATION=0,1,0,ID='FR x:-0.02
z:0.10',QUANTITY='GAUGE HEAT FLUX GAS',STATISTICS_START=0,TEMPORAL_STATISTIC='TIME
INTEGRAL'/
&DEVC XB=-0.0200,-0.0200,-2.7800,-
0.3800,0.1800,0.1800,POINTS=31,ORIENTATION=0,1,0,ID='FR x:-0.02
z:0.18',QUANTITY='GAUGE HEAT FLUX GAS',STATISTICS_START=0,TEMPORAL_STATISTIC='TIME
INTEGRAL'/
```

```
&DEVC XB=0.0200,0.0200,-2.7800,-0.3800,-0.1800,-
0.1800,POINTS=31,ORIENTATION=0,1,0,ID='FR x:0.02 z:-0.18',QUANTITY='GAUGE HEAT FLUX
GAS',STATISTICS_START=0,TEMPORAL_STATISTIC='TIME INTEGRAL'/
&DEVC XB=0.0200,0.0200,-2.7800,-0.3800,-0.1000,-
0.1000,POINTS=31,ORIENTATION=0,1,0,ID='FR x:0.02 z:-0.10',QUANTITY='GAUGE HEAT FLUX
GAS',STATISTICS_START=0,TEMPORAL_STATISTIC='TIME INTEGRAL'/
&DEVC XB=0.0200,0.0200,-2.7800,-0.3800,-0.0200,-
0.0200,POINTS=31,ORIENTATION=0,1,0,ID='FR x:0.02 z:-0.02',QUANTITY='GAUGE HEAT FLUX
GAS',STATISTICS_START=0,TEMPORAL_STATISTIC='TIME INTEGRAL'/
&DEVC XB=0.0200,0.0200,-2.7800,-
0.3800,0.0200,0.0200,POINTS=31,ORIENTATION=0,1,0,ID='FR x:0.02 z:0.02',QUANTITY='GAUGE
HEAT FLUX GAS',STATISTICS_START=0,TEMPORAL_STATISTIC='TIME INTEGRAL'/
&DEVC XB=0.0200,0.0200,-2.7800,-
0.3800,0.1000,0.1000,POINTS=31,ORIENTATION=0,1,0,ID='FR x:0.02 z:0.10',QUANTITY='GAUGE
HEAT FLUX GAS',STATISTICS_START=0,TEMPORAL_STATISTIC='TIME INTEGRAL'/
&DEVC XB=0.0200,0.0200,-2.7800,-
0.3800,0.1800,0.1800,POINTS=31,ORIENTATION=0,1,0,ID='FR x:0.02 z:0.18',QUANTITY='GAUGE
HEAT FLUX GAS',STATISTICS_START=0,TEMPORAL_STATISTIC='TIME INTEGRAL'/
&DEVC XB=0.1000,0.1000,-2.7800,-0.3800,-0.1800,-
0.1800,POINTS=31,ORIENTATION=0,1,0,ID='FR x:0.10 z:-0.18',QUANTITY='GAUGE HEAT FLUX
GAS',STATISTICS_START=0,TEMPORAL_STATISTIC='TIME INTEGRAL'/
&DEVC XB=0.1000,0.1000,-2.7800,-0.3800,-0.1000,-
0.1000,POINTS=31,ORIENTATION=0,1,0,ID='FR x:0.10 z:-0.10',QUANTITY='GAUGE HEAT FLUX
GAS',STATISTICS_START=0,TEMPORAL_STATISTIC='TIME INTEGRAL'/
&DEVC XB=0.1000,0.1000,-2.7800,-0.3800,-0.0200,-
0.0200,POINTS=31,ORIENTATION=0,1,0,ID='FR x:0.10 z:-0.02',QUANTITY='GAUGE HEAT FLUX
GAS',STATISTICS_START=0,TEMPORAL_STATISTIC='TIME INTEGRAL'/
&DEVC XB=0.1000,0.1000,-2.7800,-
0.3800,0.0200,0.0200,POINTS=31,ORIENTATION=0,1,0,ID='FR x:0.10 z:0.02',QUANTITY='GAUGE
HEAT FLUX GAS',STATISTICS_START=0,TEMPORAL_STATISTIC='TIME INTEGRAL'/
&DEVC XB=0.1000,0.1000,-2.7800,-
0.3800,0.1000,0.1000,POINTS=31,ORIENTATION=0,1,0,ID='FR x:0.10 z:0.10',QUANTITY='GAUGE
HEAT FLUX GAS',STATISTICS_START=0,TEMPORAL_STATISTIC='TIME INTEGRAL'/
&DEVC XB=0.1000,0.1000,-2.7800,-
0.3800,0.1800,0.1800,POINTS=31,ORIENTATION=0,1,0,ID='FR x:0.10 z:0.18',QUANTITY='GAUGE
HEAT FLUX GAS',STATISTICS_START=0,TEMPORAL_STATISTIC='TIME INTEGRAL'/
&DEVC XB=0.1800,0.1800,-2.7800,-0.3800,-0.1800,-
0.1800,POINTS=31,ORIENTATION=0,1,0,ID='FR x:0.18 z:-0.18',QUANTITY='GAUGE HEAT FLUX
GAS',STATISTICS_START=0,TEMPORAL_STATISTIC='TIME INTEGRAL'/
&DEVC XB=0.1800,0.1800,-2.7800,-0.3800,-0.1000,-
0.1000,POINTS=31,ORIENTATION=0,1,0,ID='FR x:0.18 z:-0.10',QUANTITY='GAUGE HEAT FLUX
GAS',STATISTICS_START=0,TEMPORAL_STATISTIC='TIME INTEGRAL'/
&DEVC XB=0.1800,0.1800,-2.7800,-0.3800,-0.0200,-
0.0200,POINTS=31,ORIENTATION=0,1,0,ID='FR x:0.18 z:-0.02',QUANTITY='GAUGE HEAT FLUX
GAS',STATISTICS_START=0,TEMPORAL_STATISTIC='TIME INTEGRAL'/
&DEVC XB=0.1800,0.1800,-2.7800,-
0.3800,0.0200,0.0200,POINTS=31,ORIENTATION=0,1,0,ID='FR x:0.18 z:0.02',QUANTITY='GAUGE
HEAT FLUX GAS',STATISTICS_START=0,TEMPORAL_STATISTIC='TIME INTEGRAL'/
&DEVC XB=0.1800,0.1800,-2.7800,-
0.3800,0.1000,0.1000,POINTS=31,ORIENTATION=0,1,0,ID='FR x:0.18 z:0.10',QUANTITY='GAUGE
HEAT FLUX GAS',STATISTICS_START=0,TEMPORAL_STATISTIC='TIME INTEGRAL'/
&DEVC XB=0.1800,0.1800,-2.7800,-
0.3800,0.1800,0.1800,POINTS=31,ORIENTATION=0,1,0,ID='FR x:0.18 z:0.18',QUANTITY='GAUGE
HEAT FLUX GAS',STATISTICS_START=0,TEMPORAL_STATISTIC='TIME INTEGRAL'/


&DEVC XB=-0.1800,-0.1800,0.3800,2.7800,-0.1800,-0.1800,POINTS=31,ORIENTATION=0,-
1,0,ID='BK x:-0.18 z:-0.18',QUANTITY='GAUGE HEAT FLUX
GAS',STATISTICS_START=0,TEMPORAL_STATISTIC='TIME INTEGRAL'/
&DEVC XB=-0.1800,-0.1800,0.3800,2.7800,-0.1000,-0.1000,POINTS=31,ORIENTATION=0,-
1,0,ID='BK x:-0.18 z:-0.10',QUANTITY='GAUGE HEAT FLUX
GAS',STATISTICS_START=0,TEMPORAL_STATISTIC='TIME INTEGRAL'/
```

```
&DEVC XB=-0.1800,-0.1800,0.3800,2.7800,-0.0200,-0.0200,POINTS=31,ORIENTATION=0,-
1,0,ID='BK x:-0.18 z:-0.02',QUANTITY='GAUGE HEAT FLUX
GAS',STATISTICS_START=0,TEMPORAL_STATISTIC='TIME INTEGRAL'/
&DEVC XB=-0.1800,-0.1800,0.3800,2.7800,0.0200,0.0200,POINTS=31,ORIENTATION=0,-
1,0,ID='BK x:-0.18 z:0.02',QUANTITY='GAUGE HEAT FLUX
GAS',STATISTICS_START=0,TEMPORAL_STATISTIC='TIME INTEGRAL'/
&DEVC XB=-0.1800,-0.1800,0.3800,2.7800,0.1000,0.1000,POINTS=31,ORIENTATION=0,-
1,0,ID='BK x:-0.18 z:0.10',QUANTITY='GAUGE HEAT FLUX
GAS',STATISTICS_START=0,TEMPORAL_STATISTIC='TIME INTEGRAL'/
&DEVC XB=-0.1800,-0.1800,0.3800,2.7800,0.1800,0.1800,POINTS=31,ORIENTATION=0,-
1,0,ID='BK x:-0.18 z:0.18',QUANTITY='GAUGE HEAT FLUX
GAS',STATISTICS_START=0,TEMPORAL_STATISTIC='TIME INTEGRAL'/
&DEVC XB=-0.1000,-0.1000,0.3800,2.7800,-0.1800,-0.1800,POINTS=31,ORIENTATION=0,-
1,0,ID='BK x:-0.10 z:-0.18',QUANTITY='GAUGE HEAT FLUX
GAS',STATISTICS_START=0,TEMPORAL_STATISTIC='TIME INTEGRAL'/
&DEVC XB=-0.1000,-0.1000,0.3800,2.7800,-0.1000,-0.1000,POINTS=31,ORIENTATION=0,-
1,0,ID='BK x:-0.10 z:-0.10',QUANTITY='GAUGE HEAT FLUX
GAS',STATISTICS_START=0,TEMPORAL_STATISTIC='TIME INTEGRAL'/
&DEVC XB=-0.1000,-0.1000,0.3800,2.7800,-0.0200,-0.0200,POINTS=31,ORIENTATION=0,-
1,0,ID='BK x:-0.10 z:-0.02',QUANTITY='GAUGE HEAT FLUX
GAS',STATISTICS_START=0,TEMPORAL_STATISTIC='TIME INTEGRAL'/
&DEVC XB=-0.1000,-0.1000,0.3800,2.7800,0.0200,0.0200,POINTS=31,ORIENTATION=0,-
1,0,ID='BK x:-0.10 z:0.02',QUANTITY='GAUGE HEAT FLUX
GAS',STATISTICS_START=0,TEMPORAL_STATISTIC='TIME INTEGRAL'/
&DEVC XB=-0.1000,-0.1000,0.3800,2.7800,0.1000,0.1000,POINTS=31,ORIENTATION=0,-
1,0,ID='BK x:-0.10 z:0.10',QUANTITY='GAUGE HEAT FLUX
GAS',STATISTICS_START=0,TEMPORAL_STATISTIC='TIME INTEGRAL'/
&DEVC XB=-0.1000,-0.1000,0.3800,2.7800,0.1800,0.1800,POINTS=31,ORIENTATION=0,-
1,0,ID='BK x:-0.10 z:0.18',QUANTITY='GAUGE HEAT FLUX
GAS',STATISTICS_START=0,TEMPORAL_STATISTIC='TIME INTEGRAL'/
&DEVC XB=-0.0200,-0.0200,0.3800,2.7800,-0.1800,-0.1800,POINTS=31,ORIENTATION=0,-
1,0,ID='BK x:-0.02 z:-0.18',QUANTITY='GAUGE HEAT FLUX
GAS',STATISTICS_START=0,TEMPORAL_STATISTIC='TIME INTEGRAL'/
&DEVC XB=-0.0200,-0.0200,0.3800,2.7800,-0.1000,-0.1000,POINTS=31,ORIENTATION=0,-
1,0,ID='BK x:-0.02 z:-0.10',QUANTITY='GAUGE HEAT FLUX
GAS',STATISTICS_START=0,TEMPORAL_STATISTIC='TIME INTEGRAL'/
&DEVC XB=-0.0200,-0.0200,0.3800,2.7800,-0.0200,-0.0200,POINTS=31,ORIENTATION=0,-
1,0,ID='BK x:-0.02 z:-0.02',QUANTITY='GAUGE HEAT FLUX
GAS',STATISTICS_START=0,TEMPORAL_STATISTIC='TIME INTEGRAL'/
&DEVC XB=-0.0200,-0.0200,0.3800,2.7800,0.0200,0.0200,POINTS=31,ORIENTATION=0,-
1,0,ID='BK x:-0.02 z:0.02',QUANTITY='GAUGE HEAT FLUX
GAS',STATISTICS_START=0,TEMPORAL_STATISTIC='TIME INTEGRAL'/
&DEVC XB=-0.0200,-0.0200,0.3800,2.7800,0.1000,0.1000,POINTS=31,ORIENTATION=0,-
1,0,ID='BK x:-0.02 z:0.10',QUANTITY='GAUGE HEAT FLUX
GAS',STATISTICS_START=0,TEMPORAL_STATISTIC='TIME INTEGRAL'/
&DEVC XB=-0.0200,-0.0200,0.3800,2.7800,0.1800,0.1800,POINTS=31,ORIENTATION=0,-
1,0,ID='BK x:-0.02 z:0.18',QUANTITY='GAUGE HEAT FLUX
GAS',STATISTICS_START=0,TEMPORAL_STATISTIC='TIME INTEGRAL'/
&DEVC XB=0.0200,0.0200,0.3800,2.7800,-0.1800,-0.1800,POINTS=31,ORIENTATION=0,-
1,0,ID='BK x:0.02 z:-0.18',QUANTITY='GAUGE HEAT FLUX
GAS',STATISTICS_START=0,TEMPORAL_STATISTIC='TIME INTEGRAL'/
&DEVC XB=0.0200,0.0200,0.3800,2.7800,-0.1000,-0.1000,POINTS=31,ORIENTATION=0,-
1,0,ID='BK x:0.02 z:-0.10',QUANTITY='GAUGE HEAT FLUX
GAS',STATISTICS_START=0,TEMPORAL_STATISTIC='TIME INTEGRAL'/
&DEVC XB=0.0200,0.0200,0.3800,2.7800,-0.0200,-0.0200,POINTS=31,ORIENTATION=0,-
1,0,ID='BK x:0.02 z:-0.02',QUANTITY='GAUGE HEAT FLUX
GAS',STATISTICS_START=0,TEMPORAL_STATISTIC='TIME INTEGRAL'/
&DEVC XB=0.0200,0.0200,0.3800,2.7800,0.0200,0.0200,POINTS=31,ORIENTATION=0,-1,0,ID='BK
x:0.02 z:0.02',QUANTITY='GAUGE HEAT FLUX
GAS',STATISTICS_START=0,TEMPORAL_STATISTIC='TIME INTEGRAL'/
&DEVC XB=0.0200,0.0200,0.3800,2.7800,0.1000,0.1000,POINTS=31,ORIENTATION=0,-1,0,ID='BK
x:0.02 z:0.10',QUANTITY='GAUGE HEAT FLUX
GAS',STATISTICS_START=0,TEMPORAL_STATISTIC='TIME INTEGRAL'/
```

```
&DEVC XB=0.0200,0.0200,0.3800,2.7800,0.1800,0.1800,POINTS=31,ORIENTATION=0,-1,0,ID='BK
x:0.02 z:0.18',QUANTITY='GAUGE HEAT FLUX
GAS',STATISTICS_START=0,TEMPORAL_STATISTIC='TIME INTEGRAL'/
&DEVC XB=0.1000,0.1000,0.3800,2.7800,-0.1800,-0.1800,POINTS=31,ORIENTATION=0,-
1,0,ID='BK x:0.10 z:-0.18',QUANTITY='GAUGE HEAT FLUX
GAS',STATISTICS_START=0,TEMPORAL_STATISTIC='TIME INTEGRAL'/
&DEVC XB=0.1000,0.1000,0.3800,2.7800,-0.1000,-0.1000,POINTS=31,ORIENTATION=0,-
1,0,ID='BK x:0.10 z:-0.10',QUANTITY='GAUGE HEAT FLUX
GAS',STATISTICS_START=0,TEMPORAL_STATISTIC='TIME INTEGRAL'/
&DEVC XB=0.1000,0.1000,0.3800,2.7800,-0.0200,-0.0200,POINTS=31,ORIENTATION=0,-
1,0,ID='BK x:0.10 z:-0.02',QUANTITY='GAUGE HEAT FLUX
GAS',STATISTICS_START=0,TEMPORAL_STATISTIC='TIME INTEGRAL'/
&DEVC XB=0.1000,0.1000,0.3800,2.7800,0.0200,0.0200,POINTS=31,ORIENTATION=0,-1,0,ID='BK
x:0.10 z:0.02',QUANTITY='GAUGE HEAT FLUX
GAS',STATISTICS_START=0,TEMPORAL_STATISTIC='TIME INTEGRAL'/
&DEVC XB=0.1000,0.1000,0.3800,2.7800,0.1000,0.1000,POINTS=31,ORIENTATION=0,-1,0,ID='BK
x:0.10 z:0.10',QUANTITY='GAUGE HEAT FLUX
GAS',STATISTICS_START=0,TEMPORAL_STATISTIC='TIME INTEGRAL'/
&DEVC XB=0.1000,0.1000,0.3800,2.7800,0.1800,0.1800,POINTS=31,ORIENTATION=0,-1,0,ID='BK
x:0.10 z:0.18',QUANTITY='GAUGE HEAT FLUX
GAS',STATISTICS_START=0,TEMPORAL_STATISTIC='TIME INTEGRAL'/
&DEVC XB=0.1800,0.1800,0.3800,2.7800,-0.1800,-0.1800,POINTS=31,ORIENTATION=0,-
1,0,ID='BK x:0.18 z:-0.18',QUANTITY='GAUGE HEAT FLUX
GAS',STATISTICS_START=0,TEMPORAL_STATISTIC='TIME INTEGRAL'/
&DEVC XB=0.1800,0.1800,0.3800,2.7800,-0.1000,-0.1000,POINTS=31,ORIENTATION=0,-
1,0,ID='BK x:0.18 z:-0.10',QUANTITY='GAUGE HEAT FLUX
GAS',STATISTICS_START=0,TEMPORAL_STATISTIC='TIME INTEGRAL'/
&DEVC XB=0.1800,0.1800,0.3800,2.7800,-0.0200,-0.0200,POINTS=31,ORIENTATION=0,-
1,0,ID='BK x:0.18 z:-0.02',QUANTITY='GAUGE HEAT FLUX
GAS',STATISTICS_START=0,TEMPORAL_STATISTIC='TIME INTEGRAL'/
&DEVC XB=0.1800,0.1800,0.3800,2.7800,0.0200,0.0200,POINTS=31,ORIENTATION=0,-1,0,ID='BK
x:0.18 z:0.02',QUANTITY='GAUGE HEAT FLUX
GAS',STATISTICS_START=0,TEMPORAL_STATISTIC='TIME INTEGRAL'/
&DEVC XB=0.1800,0.1800,0.3800,2.7800,0.1000,0.1000,POINTS=31,ORIENTATION=0,-1,0,ID='BK
x:0.18 z:0.10',QUANTITY='GAUGE HEAT FLUX
GAS',STATISTICS_START=0,TEMPORAL_STATISTIC='TIME INTEGRAL'/
&DEVC XB=0.1800,0.1800,0.3800,2.7800,0.1800,0.1800,POINTS=31,ORIENTATION=0,-1,0,ID='BK
x:0.18 z:0.18',QUANTITY='GAUGE HEAT FLUX
GAS',STATISTICS_START=0,TEMPORAL_STATISTIC='TIME INTEGRAL'/

&DEVC XB=3.8200,3.8200,-0.1800,-0.1800,-2.7000,-
0.3000,POINTS=31,ORIENTATION=0,0,1,ID='BL x:3.82 y:-0.18',QUANTITY='GAUGE HEAT FLUX
GAS',STATISTICS_START=0,TEMPORAL_STATISTIC='TIME INTEGRAL'/
&DEVC XB=3.8200,3.8200,-0.1000,-0.1000,-2.7000,-
0.3000,POINTS=31,ORIENTATION=0,0,1,ID='BL x:3.82 y:-0.10',QUANTITY='GAUGE HEAT FLUX
GAS',STATISTICS_START=0,TEMPORAL_STATISTIC='TIME INTEGRAL'/
&DEVC XB=3.8200,3.8200,-0.0200,-0.0200,-2.7000,-
0.3000,POINTS=31,ORIENTATION=0,0,1,ID='BL x:3.82 y:-0.02',QUANTITY='GAUGE HEAT FLUX
GAS',STATISTICS_START=0,TEMPORAL_STATISTIC='TIME INTEGRAL'/
&DEVC XB=3.8200,3.8200,0.0200,0.0200,-2.7000,-
0.3000,POINTS=31,ORIENTATION=0,0,1,ID='BL x:3.82 y:0.02',QUANTITY='GAUGE HEAT FLUX
GAS',STATISTICS_START=0,TEMPORAL_STATISTIC='TIME INTEGRAL'/
&DEVC XB=3.8200,3.8200,0.1000,0.1000,-2.7000,-
0.3000,POINTS=31,ORIENTATION=0,0,1,ID='BL x:3.82 y:0.10',QUANTITY='GAUGE HEAT FLUX
GAS',STATISTICS_START=0,TEMPORAL_STATISTIC='TIME INTEGRAL'/
&DEVC XB=3.8200,3.8200,0.1800,0.1800,-2.7000,-
0.3000,POINTS=31,ORIENTATION=0,0,1,ID='BL x:3.82 y:0.18',QUANTITY='GAUGE HEAT FLUX
GAS',STATISTICS_START=0,TEMPORAL_STATISTIC='TIME INTEGRAL'/
&DEVC XB=3.9000,3.9000,-0.1800,-0.1800,-2.7000,-
0.3000,POINTS=31,ORIENTATION=0,0,1,ID='BL x:3.90 y:-0.18',QUANTITY='GAUGE HEAT FLUX
GAS',STATISTICS_START=0,TEMPORAL_STATISTIC='TIME INTEGRAL'/
&DEVC XB=3.9000,3.9000,-0.1000,-0.1000,-2.7000,-
0.3000,POINTS=31,ORIENTATION=0,0,1,ID='BL x:3.90 y:-0.10',QUANTITY='GAUGE HEAT FLUX
GAS',STATISTICS_START=0,TEMPORAL_STATISTIC='TIME INTEGRAL'/
```

```
&DEVC XB=3.9000,3.9000,-0.0200,-0.0200,-2.7000,-
0.3000,POINTS=31,ORIENTATION=0,0,1,ID='BL x:3.90 y:-0.02',QUANTITY='GAUGE HEAT FLUX
GAS',STATISTICS_START=0,TEMPORAL_STATISTIC='TIME INTEGRAL'/
&DEVC XB=3.9000,3.9000,0.0200,0.0200,-2.7000,-
0.3000,POINTS=31,ORIENTATION=0,0,1,ID='BL x:3.90 y:0.02',QUANTITY='GAUGE HEAT FLUX
GAS',STATISTICS_START=0,TEMPORAL_STATISTIC='TIME INTEGRAL'/
&DEVC XB=3.9000,3.9000,0.1000,0.1000,-2.7000,-
0.3000,POINTS=31,ORIENTATION=0,0,1,ID='BL x:3.90 y:0.10',QUANTITY='GAUGE HEAT FLUX
GAS',STATISTICS_START=0,TEMPORAL_STATISTIC='TIME INTEGRAL'/
&DEVC XB=3.9000,3.9000,0.1800,0.1800,-2.7000,-
0.3000,POINTS=31,ORIENTATION=0,0,1,ID='BL x:3.90 y:0.18',QUANTITY='GAUGE HEAT FLUX
GAS',STATISTICS_START=0,TEMPORAL_STATISTIC='TIME INTEGRAL'/
&DEVC XB=3.9800,3.9800,-0.1800,-0.1800,-2.7000,-
0.3000,POINTS=31,ORIENTATION=0,0,1,ID='BL x:3.98 y:-0.18',QUANTITY='GAUGE HEAT FLUX
GAS',STATISTICS_START=0,TEMPORAL_STATISTIC='TIME INTEGRAL'/
&DEVC XB=3.9800,3.9800,-0.1000,-0.1000,-2.7000,-
0.3000,POINTS=31,ORIENTATION=0,0,1,ID='BL x:3.98 y:-0.10',QUANTITY='GAUGE HEAT FLUX
GAS',STATISTICS_START=0,TEMPORAL_STATISTIC='TIME INTEGRAL'/
&DEVC XB=3.9800,3.9800,-0.0200,-0.0200,-2.7000,-
0.3000,POINTS=31,ORIENTATION=0,0,1,ID='BL x:3.98 y:-0.02',QUANTITY='GAUGE HEAT FLUX
GAS',STATISTICS_START=0,TEMPORAL_STATISTIC='TIME INTEGRAL'/
&DEVC XB=3.9800,3.9800,0.0200,0.0200,-2.7000,-
0.3000,POINTS=31,ORIENTATION=0,0,1,ID='BL x:3.98 y:0.02',QUANTITY='GAUGE HEAT FLUX
GAS',STATISTICS_START=0,TEMPORAL_STATISTIC='TIME INTEGRAL'/
&DEVC XB=3.9800,3.9800,0.1000,0.1000,-2.7000,-
0.3000,POINTS=31,ORIENTATION=0,0,1,ID='BL x:3.98 y:0.10',QUANTITY='GAUGE HEAT FLUX
GAS',STATISTICS_START=0,TEMPORAL_STATISTIC='TIME INTEGRAL'/
&DEVC XB=3.9800,3.9800,0.1800,0.1800,-2.7000,-
0.3000,POINTS=31,ORIENTATION=0,0,1,ID='BL x:3.98 y:0.18',QUANTITY='GAUGE HEAT FLUX
GAS',STATISTICS_START=0,TEMPORAL_STATISTIC='TIME INTEGRAL'/
&DEVC XB=4.0200,4.0200,-0.1800,-0.1800,-2.7000,-
0.3000,POINTS=31,ORIENTATION=0,0,1,ID='BL x:4.02 y:-0.18',QUANTITY='GAUGE HEAT FLUX
GAS',STATISTICS_START=0,TEMPORAL_STATISTIC='TIME INTEGRAL'/
&DEVC XB=4.0200,4.0200,-0.1000,-0.1000,-2.7000,-
0.3000,POINTS=31,ORIENTATION=0,0,1,ID='BL x:4.02 y:-0.10',QUANTITY='GAUGE HEAT FLUX
GAS',STATISTICS_START=0,TEMPORAL_STATISTIC='TIME INTEGRAL'/
&DEVC XB=4.0200,4.0200,-0.0200,-0.0200,-2.7000,-
0.3000,POINTS=31,ORIENTATION=0,0,1,ID='BL x:4.02 y:-0.02',QUANTITY='GAUGE HEAT FLUX
GAS',STATISTICS_START=0,TEMPORAL_STATISTIC='TIME INTEGRAL'/
&DEVC XB=4.0200,4.0200,0.0200,0.0200,-2.7000,-
0.3000,POINTS=31,ORIENTATION=0,0,1,ID='BL x:4.02 y:0.02',QUANTITY='GAUGE HEAT FLUX
GAS',STATISTICS_START=0,TEMPORAL_STATISTIC='TIME INTEGRAL'/
&DEVC XB=4.0200,4.0200,0.1000,0.1000,-2.7000,-
0.3000,POINTS=31,ORIENTATION=0,0,1,ID='BL x:4.02 y:0.10',QUANTITY='GAUGE HEAT FLUX
GAS',STATISTICS_START=0,TEMPORAL_STATISTIC='TIME INTEGRAL'/
&DEVC XB=4.0200,4.0200,0.1800,0.1800,-2.7000,-
0.3000,POINTS=31,ORIENTATION=0,0,1,ID='BL x:4.02 y:0.18',QUANTITY='GAUGE HEAT FLUX
GAS',STATISTICS_START=0,TEMPORAL_STATISTIC='TIME INTEGRAL'/
&DEVC XB=4.1000,4.1000,-0.1800,-0.1800,-2.7000,-
0.3000,POINTS=31,ORIENTATION=0,0,1,ID='BL x:4.10 y:-0.18',QUANTITY='GAUGE HEAT FLUX
GAS',STATISTICS_START=0,TEMPORAL_STATISTIC='TIME INTEGRAL'/
&DEVC XB=4.1000,4.1000,-0.1000,-0.1000,-2.7000,-
0.3000,POINTS=31,ORIENTATION=0,0,1,ID='BL x:4.10 y:-0.10',QUANTITY='GAUGE HEAT FLUX
GAS',STATISTICS_START=0,TEMPORAL_STATISTIC='TIME INTEGRAL'/
&DEVC XB=4.1000,4.1000,-0.0200,-0.0200,-2.7000,-
0.3000,POINTS=31,ORIENTATION=0,0,1,ID='BL x:4.10 y:-0.02',QUANTITY='GAUGE HEAT FLUX
GAS',STATISTICS_START=0,TEMPORAL_STATISTIC='TIME INTEGRAL'/
&DEVC XB=4.1000,4.1000,0.0200,0.0200,-2.7000,-
0.3000,POINTS=31,ORIENTATION=0,0,1,ID='BL x:4.10 y:0.02',QUANTITY='GAUGE HEAT FLUX
GAS',STATISTICS_START=0,TEMPORAL_STATISTIC='TIME INTEGRAL'/
&DEVC XB=4.1000,4.1000,0.1000,0.1000,-2.7000,-
0.3000,POINTS=31,ORIENTATION=0,0,1,ID='BL x:4.10 y:0.10',QUANTITY='GAUGE HEAT FLUX
GAS',STATISTICS_START=0,TEMPORAL_STATISTIC='TIME INTEGRAL'/
```

```
&DEVC XB=4.1000,4.1000,0.1800,0.1800,-2.7000,-
0.3000,POINTS=31,ORIENTATION=0,0,1,ID='BL x:4.10 y:0.18',QUANTITY='GAUGE HEAT FLUX
GAS',STATISTICS_START=0,TEMPORAL_STATISTIC='TIME INTEGRAL'/
&DEVC XB=4.1800,4.1800,-0.1800,-0.1800,-2.7000,-
0.3000,POINTS=31,ORIENTATION=0,0,1,ID='BL x:4.18 y:-0.18',QUANTITY='GAUGE HEAT FLUX
GAS',STATISTICS_START=0,TEMPORAL_STATISTIC='TIME INTEGRAL'/
&DEVC XB=4.1800,4.1800,-0.1000,-0.1000,-2.7000,-
0.3000,POINTS=31,ORIENTATION=0,0,1,ID='BL x:4.18 y:-0.10',QUANTITY='GAUGE HEAT FLUX
GAS',STATISTICS_START=0,TEMPORAL_STATISTIC='TIME INTEGRAL'/
&DEVC XB=4.1800,4.1800,-0.0200,-0.0200,-2.7000,-
0.3000,POINTS=31,ORIENTATION=0,0,1,ID='BL x:4.18 y:-0.02',QUANTITY='GAUGE HEAT FLUX
GAS',STATISTICS_START=0,TEMPORAL_STATISTIC='TIME INTEGRAL'/
&DEVC XB=4.1800,4.1800,0.0200,0.0200,-2.7000,-
0.3000,POINTS=31,ORIENTATION=0,0,1,ID='BL x:4.18 y:0.02',QUANTITY='GAUGE HEAT FLUX
GAS',STATISTICS_START=0,TEMPORAL_STATISTIC='TIME INTEGRAL'/
&DEVC XB=4.1800,4.1800,0.1000,0.1000,-2.7000,-
0.3000,POINTS=31,ORIENTATION=0,0,1,ID='BL x:4.18 y:0.10',QUANTITY='GAUGE HEAT FLUX
GAS',STATISTICS_START=0,TEMPORAL_STATISTIC='TIME INTEGRAL'/
&DEVC XB=4.1800,4.1800,0.1800,0.1800,-2.7000,-
0.3000,POINTS=31,ORIENTATION=0,0,1,ID='BL x:4.18 y:0.18',QUANTITY='GAUGE HEAT FLUX
GAS',STATISTICS_START=0,TEMPORAL_STATISTIC='TIME INTEGRAL'/


&DEVC XB=3.8200,3.8200,-2.7800,-0.3800,-0.1800,-
0.1800,POINTS=31,ORIENTATION=0,1,0,ID='FR x:3.82 z:-0.18',QUANTITY='GAUGE HEAT FLUX
GAS',STATISTICS_START=0,TEMPORAL_STATISTIC='TIME INTEGRAL'/
&DEVC XB=3.8200,3.8200,-2.7800,-0.3800,-0.1000,-
0.1000,POINTS=31,ORIENTATION=0,1,0,ID='FR x:3.82 z:-0.10',QUANTITY='GAUGE HEAT FLUX
GAS',STATISTICS_START=0,TEMPORAL_STATISTIC='TIME INTEGRAL'/
&DEVC XB=3.8200,3.8200,-2.7800,-0.3800,-0.0200,-
0.0200,POINTS=31,ORIENTATION=0,1,0,ID='FR x:3.82 z:-0.02',QUANTITY='GAUGE HEAT FLUX
GAS',STATISTICS_START=0,TEMPORAL_STATISTIC='TIME INTEGRAL'/
&DEVC XB=3.8200,3.8200,-2.7800,-
0.3800,0.0200,0.0200,POINTS=31,ORIENTATION=0,1,0,ID='FR x:3.82 z:0.02',QUANTITY='GAUGE
HEAT FLUX GAS',STATISTICS_START=0,TEMPORAL_STATISTIC='TIME INTEGRAL'/
&DEVC XB=3.8200,3.8200,-2.7800,-
0.3800,0.1000,0.1000,POINTS=31,ORIENTATION=0,1,0,ID='FR x:3.82 z:0.10',QUANTITY='GAUGE
HEAT FLUX GAS',STATISTICS_START=0,TEMPORAL_STATISTIC='TIME INTEGRAL'/
&DEVC XB=3.8200,3.8200,-2.7800,-
0.3800,0.1800,0.1800,POINTS=31,ORIENTATION=0,1,0,ID='FR x:3.82 z:0.18',QUANTITY='GAUGE
HEAT FLUX GAS',STATISTICS_START=0,TEMPORAL_STATISTIC='TIME INTEGRAL'/
&DEVC XB=3.9000,3.9000,-2.7800,-0.3800,-0.1800,-
0.1800,POINTS=31,ORIENTATION=0,1,0,ID='FR x:3.90 z:-0.18',QUANTITY='GAUGE HEAT FLUX
GAS',STATISTICS_START=0,TEMPORAL_STATISTIC='TIME INTEGRAL'/
&DEVC XB=3.9000,3.9000,-2.7800,-0.3800,-0.1000,-
0.1000,POINTS=31,ORIENTATION=0,1,0,ID='FR x:3.90 z:-0.10',QUANTITY='GAUGE HEAT FLUX
GAS',STATISTICS_START=0,TEMPORAL_STATISTIC='TIME INTEGRAL'/
&DEVC XB=3.9000,3.9000,-2.7800,-0.3800,-0.0200,-
0.0200,POINTS=31,ORIENTATION=0,1,0,ID='FR x:3.90 z:-0.02',QUANTITY='GAUGE HEAT FLUX
GAS',STATISTICS_START=0,TEMPORAL_STATISTIC='TIME INTEGRAL'/
&DEVC XB=3.9000,3.9000,-2.7800,-
0.3800,0.0200,0.0200,POINTS=31,ORIENTATION=0,1,0,ID='FR x:3.90 z:0.02',QUANTITY='GAUGE
HEAT FLUX GAS',STATISTICS_START=0,TEMPORAL_STATISTIC='TIME INTEGRAL'/
&DEVC XB=3.9000,3.9000,-2.7800,-
0.3800,0.1000,0.1000,POINTS=31,ORIENTATION=0,1,0,ID='FR x:3.90 z:0.10',QUANTITY='GAUGE
HEAT FLUX GAS',STATISTICS_START=0,TEMPORAL_STATISTIC='TIME INTEGRAL'/
&DEVC XB=3.9000,3.9000,-2.7800,-
0.3800,0.1800,0.1800,POINTS=31,ORIENTATION=0,1,0,ID='FR x:3.90 z:0.18',QUANTITY='GAUGE
HEAT FLUX GAS',STATISTICS_START=0,TEMPORAL_STATISTIC='TIME INTEGRAL'/
&DEVC XB=3.9800,3.9800,-2.7800,-0.3800,-0.1800,-
0.1800,POINTS=31,ORIENTATION=0,1,0,ID='FR x:3.98 z:-0.18',QUANTITY='GAUGE HEAT FLUX
GAS',STATISTICS_START=0,TEMPORAL_STATISTIC='TIME INTEGRAL'/
```

```
&DEVC XB=3.9800,3.9800,-2.7800,-0.3800,-0.1000,-
0.1000,POINTS=31,ORIENTATION=0,1,0,ID='FR x:3.98 z:-0.10',QUANTITY='GAUGE HEAT FLUX
GAS',STATISTICS_START=0,TEMPORAL_STATISTIC='TIME INTEGRAL'/
&DEVC XB=3.9800,3.9800,-2.7800,-0.3800,-0.0200,-
0.0200,POINTS=31,ORIENTATION=0,1,0,ID='FR x:3.98 z:-0.02',QUANTITY='GAUGE HEAT FLUX
GAS',STATISTICS_START=0,TEMPORAL_STATISTIC='TIME INTEGRAL'/
&DEVC XB=3.9800,3.9800,-2.7800,-
0.3800,0.0200,0.0200,POINTS=31,ORIENTATION=0,1,0,ID='FR x:3.98 z:0.02',QUANTITY='GAUGE
HEAT FLUX GAS',STATISTICS_START=0,TEMPORAL_STATISTIC='TIME INTEGRAL'/
&DEVC XB=3.9800,3.9800,-2.7800,-
0.3800,0.1000,0.1000,POINTS=31,ORIENTATION=0,1,0,ID='FR x:3.98 z:0.10',QUANTITY='GAUGE
HEAT FLUX GAS',STATISTICS_START=0,TEMPORAL_STATISTIC='TIME INTEGRAL'/
&DEVC XB=3.9800,3.9800,-2.7800,-
0.3800,0.1800,0.1800,POINTS=31,ORIENTATION=0,1,0,ID='FR x:3.98 z:0.18',QUANTITY='GAUGE
HEAT FLUX GAS',STATISTICS_START=0,TEMPORAL_STATISTIC='TIME INTEGRAL'/
&DEVC XB=4.0200,4.0200,-2.7800,-0.3800,-0.1800,-
0.1800,POINTS=31,ORIENTATION=0,1,0,ID='FR x:4.02 z:-0.18',QUANTITY='GAUGE HEAT FLUX
GAS',STATISTICS_START=0,TEMPORAL_STATISTIC='TIME INTEGRAL'/
&DEVC XB=4.0200,4.0200,-2.7800,-0.3800,-0.1000,-
0.1000,POINTS=31,ORIENTATION=0,1,0,ID='FR x:4.02 z:-0.10',QUANTITY='GAUGE HEAT FLUX
GAS',STATISTICS_START=0,TEMPORAL_STATISTIC='TIME INTEGRAL'/
&DEVC XB=4.0200,4.0200,-2.7800,-0.3800,-0.0200,-
0.0200,POINTS=31,ORIENTATION=0,1,0,ID='FR x:4.02 z:-0.02',QUANTITY='GAUGE HEAT FLUX
GAS',STATISTICS_START=0,TEMPORAL_STATISTIC='TIME INTEGRAL'/
&DEVC XB=4.0200,4.0200,-2.7800,-
0.3800,0.0200,0.0200,POINTS=31,ORIENTATION=0,1,0,ID='FR x:4.02 z:0.02',QUANTITY='GAUGE
HEAT FLUX GAS',STATISTICS_START=0,TEMPORAL_STATISTIC='TIME INTEGRAL'/
&DEVC XB=4.0200,4.0200,-2.7800,-
0.3800,0.1000,0.1000,POINTS=31,ORIENTATION=0,1,0,ID='FR x:4.02 z:0.10',QUANTITY='GAUGE
HEAT FLUX GAS',STATISTICS_START=0,TEMPORAL_STATISTIC='TIME INTEGRAL'/
&DEVC XB=4.0200,4.0200,-2.7800,-
0.3800,0.1800,0.1800,POINTS=31,ORIENTATION=0,1,0,ID='FR x:4.02 z:0.18',QUANTITY='GAUGE
HEAT FLUX GAS',STATISTICS_START=0,TEMPORAL_STATISTIC='TIME INTEGRAL'/
&DEVC XB=4.1000,4.1000,-2.7800,-0.3800,-0.1800,-
0.1800,POINTS=31,ORIENTATION=0,1,0,ID='FR x:4.10 z:-0.18',QUANTITY='GAUGE HEAT FLUX
GAS',STATISTICS_START=0,TEMPORAL_STATISTIC='TIME INTEGRAL'/
&DEVC XB=4.1000,4.1000,-2.7800,-0.3800,-0.1000,-
0.1000,POINTS=31,ORIENTATION=0,1,0,ID='FR x:4.10 z:-0.10',QUANTITY='GAUGE HEAT FLUX
GAS',STATISTICS_START=0,TEMPORAL_STATISTIC='TIME INTEGRAL'/
&DEVC XB=4.1000,4.1000,-2.7800,-0.3800,-0.0200,-
0.0200,POINTS=31,ORIENTATION=0,1,0,ID='FR x:4.10 z:-0.02',QUANTITY='GAUGE HEAT FLUX
GAS',STATISTICS_START=0,TEMPORAL_STATISTIC='TIME INTEGRAL'/
&DEVC XB=4.1000,4.1000,-2.7800,-
0.3800,0.0200,0.0200,POINTS=31,ORIENTATION=0,1,0,ID='FR x:4.10 z:0.02',QUANTITY='GAUGE
HEAT FLUX GAS',STATISTICS_START=0,TEMPORAL_STATISTIC='TIME INTEGRAL'/
&DEVC XB=4.1000,4.1000,-2.7800,-
0.3800,0.1000,0.1000,POINTS=31,ORIENTATION=0,1,0,ID='FR x:4.10 z:0.10',QUANTITY='GAUGE
HEAT FLUX GAS',STATISTICS_START=0,TEMPORAL_STATISTIC='TIME INTEGRAL'/
&DEVC XB=4.1000,4.1000,-2.7800,-
0.3800,0.1800,0.1800,POINTS=31,ORIENTATION=0,1,0,ID='FR x:4.10 z:0.18',QUANTITY='GAUGE
HEAT FLUX GAS',STATISTICS_START=0,TEMPORAL_STATISTIC='TIME INTEGRAL'/
&DEVC XB=4.1800,4.1800,-2.7800,-0.3800,-0.1800,-
0.1800,POINTS=31,ORIENTATION=0,1,0,ID='FR x:4.18 z:-0.18',QUANTITY='GAUGE HEAT FLUX
GAS',STATISTICS_START=0,TEMPORAL_STATISTIC='TIME INTEGRAL'/
&DEVC XB=4.1800,4.1800,-2.7800,-0.3800,-0.1000,-
0.1000,POINTS=31,ORIENTATION=0,1,0,ID='FR x:4.18 z:-0.10',QUANTITY='GAUGE HEAT FLUX
GAS',STATISTICS_START=0,TEMPORAL_STATISTIC='TIME INTEGRAL'/
&DEVC XB=4.1800,4.1800,-2.7800,-0.3800,-0.0200,-
0.0200,POINTS=31,ORIENTATION=0,1,0,ID='FR x:4.18 z:-0.02',QUANTITY='GAUGE HEAT FLUX
GAS',STATISTICS_START=0,TEMPORAL_STATISTIC='TIME INTEGRAL'/
&DEVC XB=4.1800,4.1800,-2.7800,-
0.3800,0.0200,0.0200,POINTS=31,ORIENTATION=0,1,0,ID='FR x:4.18 z:0.02',QUANTITY='GAUGE
HEAT FLUX GAS',STATISTICS_START=0,TEMPORAL_STATISTIC='TIME INTEGRAL'/
```

```
&DEVC XB=4.1800,4.1800,-2.7800,-
0.3800,0.1000,0.1000,POINTS=31,ORIENTATION=0,1,0,ID='FR x:4.18 z:0.10',QUANTITY='GAUGE
HEAT FLUX GAS',STATISTICS_START=0,TEMPORAL_STATISTIC='TIME INTEGRAL'/
&DEVC XB=4.1800,4.1800,-2.7800,-
0.3800,0.1800,0.1800,POINTS=31,ORIENTATION=0,1,0,ID='FR x:4.18 z:0.18',QUANTITY='GAUGE
HEAT FLUX GAS',STATISTICS_START=0,TEMPORAL_STATISTIC='TIME INTEGRAL'/


&DEVC XB=3.8200,3.8200,0.3800,2.7800,-0.1800,-0.1800,POINTS=31,ORIENTATION=0,-
1,0,ID='BK x:3.82 z:-0.18',QUANTITY='GAUGE HEAT FLUX
GAS',STATISTICS_START=0,TEMPORAL_STATISTIC='TIME INTEGRAL'/
&DEVC XB=3.8200,3.8200,0.3800,2.7800,-0.1000,-0.1000,POINTS=31,ORIENTATION=0,-
1,0,ID='BK x:3.82 z:-0.10',QUANTITY='GAUGE HEAT FLUX
GAS',STATISTICS_START=0,TEMPORAL_STATISTIC='TIME INTEGRAL'/
&DEVC XB=3.8200,3.8200,0.3800,2.7800,-0.0200,-0.0200,POINTS=31,ORIENTATION=0,-
1,0,ID='BK x:3.82 z:-0.02',QUANTITY='GAUGE HEAT FLUX
GAS',STATISTICS_START=0,TEMPORAL_STATISTIC='TIME INTEGRAL'/
&DEVC XB=3.8200,3.8200,0.3800,2.7800,0.0200,0.0200,POINTS=31,ORIENTATION=0,-1,0,ID='BK
x:3.82 z:0.02',QUANTITY='GAUGE HEAT FLUX
GAS',STATISTICS_START=0,TEMPORAL_STATISTIC='TIME INTEGRAL'/
&DEVC XB=3.8200,3.8200,0.3800,2.7800,0.1000,0.1000,POINTS=31,ORIENTATION=0,-1,0,ID='BK
x:3.82 z:0.10',QUANTITY='GAUGE HEAT FLUX
GAS',STATISTICS_START=0,TEMPORAL_STATISTIC='TIME INTEGRAL'/
&DEVC XB=3.8200,3.8200,0.3800,2.7800,0.1800,0.1800,POINTS=31,ORIENTATION=0,-1,0,ID='BK
x:3.82 z:0.18',QUANTITY='GAUGE HEAT FLUX
GAS',STATISTICS_START=0,TEMPORAL_STATISTIC='TIME INTEGRAL'/
&DEVC XB=3.9000,3.9000,0.3800,2.7800,-0.1800,-0.1800,POINTS=31,ORIENTATION=0,-
1,0,ID='BK x:3.90 z:-0.18',QUANTITY='GAUGE HEAT FLUX
GAS',STATISTICS_START=0,TEMPORAL_STATISTIC='TIME INTEGRAL'/
&DEVC XB=3.9000,3.9000,0.3800,2.7800,-0.1000,-0.1000,POINTS=31,ORIENTATION=0,-
1,0,ID='BK x:3.90 z:-0.10',QUANTITY='GAUGE HEAT FLUX
GAS',STATISTICS_START=0,TEMPORAL_STATISTIC='TIME INTEGRAL'/
&DEVC XB=3.9000,3.9000,0.3800,2.7800,-0.0200,-0.0200,POINTS=31,ORIENTATION=0,-
1,0,ID='BK x:3.90 z:-0.02',QUANTITY='GAUGE HEAT FLUX
GAS',STATISTICS_START=0,TEMPORAL_STATISTIC='TIME INTEGRAL'/
&DEVC XB=3.9000,3.9000,0.3800,2.7800,0.0200,0.0200,POINTS=31,ORIENTATION=0,-1,0,ID='BK
x:3.90 z:0.02',QUANTITY='GAUGE HEAT FLUX
GAS',STATISTICS_START=0,TEMPORAL_STATISTIC='TIME INTEGRAL'/
&DEVC XB=3.9000,3.9000,0.3800,2.7800,0.1000,0.1000,POINTS=31,ORIENTATION=0,-1,0,ID='BK
x:3.90 z:0.10',QUANTITY='GAUGE HEAT FLUX
GAS',STATISTICS_START=0,TEMPORAL_STATISTIC='TIME INTEGRAL'/
&DEVC XB=3.9000,3.9000,0.3800,2.7800,0.1800,0.1800,POINTS=31,ORIENTATION=0,-1,0,ID='BK
x:3.90 z:0.18',QUANTITY='GAUGE HEAT FLUX
GAS',STATISTICS_START=0,TEMPORAL_STATISTIC='TIME INTEGRAL'/
&DEVC XB=3.9800,3.9800,0.3800,2.7800,-0.1800,-0.1800,POINTS=31,ORIENTATION=0,-
1,0,ID='BK x:3.98 z:-0.18',QUANTITY='GAUGE HEAT FLUX
GAS',STATISTICS_START=0,TEMPORAL_STATISTIC='TIME INTEGRAL'/
&DEVC XB=3.9800,3.9800,0.3800,2.7800,-0.1000,-0.1000,POINTS=31,ORIENTATION=0,-
1,0,ID='BK x:3.98 z:-0.10',QUANTITY='GAUGE HEAT FLUX
GAS',STATISTICS_START=0,TEMPORAL_STATISTIC='TIME INTEGRAL'/
&DEVC XB=3.9800,3.9800,0.3800,2.7800,-0.0200,-0.0200,POINTS=31,ORIENTATION=0,-
1,0,ID='BK x:3.98 z:-0.02',QUANTITY='GAUGE HEAT FLUX
GAS',STATISTICS_START=0,TEMPORAL_STATISTIC='TIME INTEGRAL'/
&DEVC XB=3.9800,3.9800,0.3800,2.7800,0.0200,0.0200,POINTS=31,ORIENTATION=0,-1,0,ID='BK
x:3.98 z:0.02',QUANTITY='GAUGE HEAT FLUX
GAS',STATISTICS_START=0,TEMPORAL_STATISTIC='TIME INTEGRAL'/
&DEVC XB=3.9800,3.9800,0.3800,2.7800,0.1000,0.1000,POINTS=31,ORIENTATION=0,-1,0,ID='BK
x:3.98 z:0.10',QUANTITY='GAUGE HEAT FLUX
GAS',STATISTICS_START=0,TEMPORAL_STATISTIC='TIME INTEGRAL'/
&DEVC XB=3.9800,3.9800,0.3800,2.7800,0.1800,0.1800,POINTS=31,ORIENTATION=0,-1,0,ID='BK
x:3.98 z:0.18',QUANTITY='GAUGE HEAT FLUX
GAS',STATISTICS_START=0,TEMPORAL_STATISTIC='TIME INTEGRAL'/
```

```
&DEVC XB=4.0200,4.0200,0.3800,2.7800,-0.1800,-0.1800,POINTS=31,ORIENTATION=0,-
1,0,ID='BK x:4.02 z:-0.18',QUANTITY='GAUGE HEAT FLUX
GAS',STATISTICS_START=0,TEMPORAL_STATISTIC='TIME INTEGRAL'/
&DEVC XB=4.0200,4.0200,0.3800,2.7800,-0.1000,-0.1000,POINTS=31,ORIENTATION=0,-
1,0,ID='BK x:4.02 z:-0.10',QUANTITY='GAUGE HEAT FLUX
GAS',STATISTICS_START=0,TEMPORAL_STATISTIC='TIME INTEGRAL'/
&DEVC XB=4.0200,4.0200,0.3800,2.7800,-0.0200,-0.0200,POINTS=31,ORIENTATION=0,-
1,0,ID='BK x:4.02 z:-0.02',QUANTITY='GAUGE HEAT FLUX
GAS',STATISTICS_START=0,TEMPORAL_STATISTIC='TIME INTEGRAL'/
&DEVC XB=4.0200,4.0200,0.3800,2.7800,0.0200,0.0200,POINTS=31,ORIENTATION=0,-1,0,ID='BK
x:4.02 z:0.02',QUANTITY='GAUGE HEAT FLUX
GAS',STATISTICS_START=0,TEMPORAL_STATISTIC='TIME INTEGRAL'/
&DEVC XB=4.0200,4.0200,0.3800,2.7800,0.1000,0.1000,POINTS=31,ORIENTATION=0,-1,0,ID='BK
x:4.02 z:0.10',QUANTITY='GAUGE HEAT FLUX
GAS',STATISTICS_START=0,TEMPORAL_STATISTIC='TIME INTEGRAL'/
&DEVC XB=4.0200,4.0200,0.3800,2.7800,0.1800,0.1800,POINTS=31,ORIENTATION=0,-1,0,ID='BK
x:4.02 z:0.18',QUANTITY='GAUGE HEAT FLUX
GAS',STATISTICS_START=0,TEMPORAL_STATISTIC='TIME INTEGRAL'/
&DEVC XB=4.1000,4.1000,0.3800,2.7800,-0.1800,-0.1800,POINTS=31,ORIENTATION=0,-
1,0,ID='BK x:4.10 z:-0.18',QUANTITY='GAUGE HEAT FLUX
GAS',STATISTICS_START=0,TEMPORAL_STATISTIC='TIME INTEGRAL'/
&DEVC XB=4.1000,4.1000,0.3800,2.7800,-0.1000,-0.1000,POINTS=31,ORIENTATION=0,-
1,0,ID='BK x:4.10 z:-0.10',QUANTITY='GAUGE HEAT FLUX
GAS',STATISTICS_START=0,TEMPORAL_STATISTIC='TIME INTEGRAL'/
&DEVC XB=4.1000,4.1000,0.3800,2.7800,-0.0200,-0.0200,POINTS=31,ORIENTATION=0,-
1,0,ID='BK x:4.10 z:-0.02',QUANTITY='GAUGE HEAT FLUX
GAS',STATISTICS_START=0,TEMPORAL_STATISTIC='TIME INTEGRAL'/
&DEVC XB=4.1000,4.1000,0.3800,2.7800,0.0200,0.0200,POINTS=31,ORIENTATION=0,-1,0,ID='BK
x:4.10 z:0.02',QUANTITY='GAUGE HEAT FLUX
GAS',STATISTICS_START=0,TEMPORAL_STATISTIC='TIME INTEGRAL'/
&DEVC XB=4.1000,4.1000,0.3800,2.7800,0.1000,0.1000,POINTS=31,ORIENTATION=0,-1,0,ID='BK
x:4.10 z:0.10',QUANTITY='GAUGE HEAT FLUX
GAS',STATISTICS_START=0,TEMPORAL_STATISTIC='TIME INTEGRAL'/
&DEVC XB=4.1000,4.1000,0.3800,2.7800,0.1800,0.1800,POINTS=31,ORIENTATION=0,-1,0,ID='BK
x:4.10 z:0.18',QUANTITY='GAUGE HEAT FLUX
GAS',STATISTICS_START=0,TEMPORAL_STATISTIC='TIME INTEGRAL'/
&DEVC XB=4.1800,4.1800,0.3800,2.7800,-0.1800,-0.1800,POINTS=31,ORIENTATION=0,-
1,0,ID='BK x:4.18 z:-0.18',QUANTITY='GAUGE HEAT FLUX
GAS',STATISTICS_START=0,TEMPORAL_STATISTIC='TIME INTEGRAL'/
&DEVC XB=4.1800,4.1800,0.3800,2.7800,-0.1000,-0.1000,POINTS=31,ORIENTATION=0,-
1,0,ID='BK x:4.18 z:-0.10',QUANTITY='GAUGE HEAT FLUX
GAS',STATISTICS_START=0,TEMPORAL_STATISTIC='TIME INTEGRAL'/
&DEVC XB=4.1800,4.1800,0.3800,2.7800,-0.0200,-0.0200,POINTS=31,ORIENTATION=0,-
1,0,ID='BK x:4.18 z:-0.02',QUANTITY='GAUGE HEAT FLUX
GAS',STATISTICS_START=0,TEMPORAL_STATISTIC='TIME INTEGRAL'/
&DEVC XB=4.1800,4.1800,0.3800,2.7800,0.0200,0.0200,POINTS=31,ORIENTATION=0,-1,0,ID='BK
x:4.18 z:0.02',QUANTITY='GAUGE HEAT FLUX
GAS',STATISTICS_START=0,TEMPORAL_STATISTIC='TIME INTEGRAL'/
&DEVC XB=4.1800,4.1800,0.3800,2.7800,0.1000,0.1000,POINTS=31,ORIENTATION=0,-1,0,ID='BK
x:4.18 z:0.10',QUANTITY='GAUGE HEAT FLUX
GAS',STATISTICS_START=0,TEMPORAL_STATISTIC='TIME INTEGRAL'/
&DEVC XB=4.1800,4.1800,0.3800,2.7800,0.1800,0.1800,POINTS=31,ORIENTATION=0,-1,0,ID='BK
x:4.18 z:0.18',QUANTITY='GAUGE HEAT FLUX
GAS',STATISTICS_START=0,TEMPORAL_STATISTIC='TIME INTEGRAL'/


&DEVC XB=4.3000,6.7000,-0.1800,-0.1800,-0.1800,-0.1800,POINTS=31,ORIENTATION=-
1,0,0,ID='RT y:-0.18 z:-0.18',QUANTITY='GAUGE HEAT FLUX
GAS',STATISTICS_START=0,TEMPORAL_STATISTIC='TIME INTEGRAL'/
&DEVC XB=4.3000,6.7000,-0.1800,-0.1800,-0.1000,-0.1000,POINTS=31,ORIENTATION=-
1,0,0,ID='RT y:-0.18 z:-0.10',QUANTITY='GAUGE HEAT FLUX
GAS',STATISTICS_START=0,TEMPORAL_STATISTIC='TIME INTEGRAL'/
```

```
&DEVC XB=4.3000,6.7000,-0.1800,-0.1800,-0.0200,-0.0200,POINTS=31,ORIENTATION=-
1,0,0,ID='RT y:-0.18 z:-0.02',QUANTITY='GAUGE HEAT FLUX
GAS',STATISTICS_START=0,TEMPORAL_STATISTIC='TIME INTEGRAL'/
&DEVC XB=4.3000,6.7000,-0.1800,-0.1800,0.0200,0.0200,POINTS=31,ORIENTATION=-
1,0,0,ID='RT y:-0.18 z:0.02',QUANTITY='GAUGE HEAT FLUX
GAS',STATISTICS_START=0,TEMPORAL_STATISTIC='TIME INTEGRAL'/
&DEVC XB=4.3000,6.7000,-0.1800,-0.1800,0.1000,0.1000,POINTS=31,ORIENTATION=-
1,0,0,ID='RT y:-0.18 z:0.10',QUANTITY='GAUGE HEAT FLUX
GAS',STATISTICS_START=0,TEMPORAL_STATISTIC='TIME INTEGRAL'/
&DEVC XB=4.3000,6.7000,-0.1800,-0.1800,0.1800,0.1800,POINTS=31,ORIENTATION=-
1,0,0,ID='RT y:-0.18 z:0.18',QUANTITY='GAUGE HEAT FLUX
GAS',STATISTICS_START=0,TEMPORAL_STATISTIC='TIME INTEGRAL'/
&DEVC XB=4.3000,6.7000,-0.1000,-0.1000,-0.1800,-0.1800,POINTS=31,ORIENTATION=-
1,0,0,ID='RT y:-0.10 z:-0.18',QUANTITY='GAUGE HEAT FLUX
GAS',STATISTICS_START=0,TEMPORAL_STATISTIC='TIME INTEGRAL'/
&DEVC XB=4.3000,6.7000,-0.1000,-0.1000,-0.1000,-0.1000,POINTS=31,ORIENTATION=-
1,0,0,ID='RT y:-0.10 z:-0.10',QUANTITY='GAUGE HEAT FLUX
GAS',STATISTICS_START=0,TEMPORAL_STATISTIC='TIME INTEGRAL'/
&DEVC XB=4.3000,6.7000,-0.1000,-0.1000,-0.0200,-0.0200,POINTS=31,ORIENTATION=-
1,0,0,ID='RT y:-0.10 z:-0.02',QUANTITY='GAUGE HEAT FLUX
GAS',STATISTICS_START=0,TEMPORAL_STATISTIC='TIME INTEGRAL'/
&DEVC XB=4.3000,6.7000,-0.1000,-0.1000,0.0200,0.0200,POINTS=31,ORIENTATION=-
1,0,0,ID='RT y:-0.10 z:0.02',QUANTITY='GAUGE HEAT FLUX
GAS',STATISTICS_START=0,TEMPORAL_STATISTIC='TIME INTEGRAL'/
&DEVC XB=4.3000,6.7000,-0.1000,-0.1000,0.1000,0.1000,POINTS=31,ORIENTATION=-
1,0,0,ID='RT y:-0.10 z:0.10',QUANTITY='GAUGE HEAT FLUX
GAS',STATISTICS_START=0,TEMPORAL_STATISTIC='TIME INTEGRAL'/
&DEVC XB=4.3000,6.7000,-0.1000,-0.1000,0.1800,0.1800,POINTS=31,ORIENTATION=-
1,0,0,ID='RT y:-0.10 z:0.18',QUANTITY='GAUGE HEAT FLUX
GAS',STATISTICS_START=0,TEMPORAL_STATISTIC='TIME INTEGRAL'/
&DEVC XB=4.3000,6.7000,-0.0200,-0.0200,-0.1800,-0.1800,POINTS=31,ORIENTATION=-
1,0,0,ID='RT y:-0.02 z:-0.18',QUANTITY='GAUGE HEAT FLUX
GAS',STATISTICS_START=0,TEMPORAL_STATISTIC='TIME INTEGRAL'/
&DEVC XB=4.3000,6.7000,-0.0200,-0.0200,-0.1000,-0.1000,POINTS=31,ORIENTATION=-
1,0,0,ID='RT y:-0.02 z:-0.10',QUANTITY='GAUGE HEAT FLUX
GAS',STATISTICS_START=0,TEMPORAL_STATISTIC='TIME INTEGRAL'/
&DEVC XB=4.3000,6.7000,-0.0200,-0.0200,-0.0200,-0.0200,POINTS=31,ORIENTATION=-
1,0,0,ID='RT y:-0.02 z:-0.02',QUANTITY='GAUGE HEAT FLUX
GAS',STATISTICS_START=0,TEMPORAL_STATISTIC='TIME INTEGRAL'/
&DEVC XB=4.3000,6.7000,-0.0200,-0.0200,0.0200,0.0200,POINTS=31,ORIENTATION=-
1,0,0,ID='RT y:-0.02 z:0.02',QUANTITY='GAUGE HEAT FLUX
GAS',STATISTICS_START=0,TEMPORAL_STATISTIC='TIME INTEGRAL'/
&DEVC XB=4.3000,6.7000,-0.0200,-0.0200,0.1000,0.1000,POINTS=31,ORIENTATION=-
1,0,0,ID='RT y:-0.02 z:0.10',QUANTITY='GAUGE HEAT FLUX
GAS',STATISTICS_START=0,TEMPORAL_STATISTIC='TIME INTEGRAL'/
&DEVC XB=4.3000,6.7000,-0.0200,-0.0200,0.1800,0.1800,POINTS=31,ORIENTATION=-
1,0,0,ID='RT y:-0.02 z:0.18',QUANTITY='GAUGE HEAT FLUX
GAS',STATISTICS_START=0,TEMPORAL_STATISTIC='TIME INTEGRAL'/
&DEVC XB=4.3000,6.7000,0.0200,0.0200,-0.1800,-0.1800,POINTS=31,ORIENTATION=-
1,0,0,ID='RT y:0.02 z:-0.18',QUANTITY='GAUGE HEAT FLUX
GAS',STATISTICS_START=0,TEMPORAL_STATISTIC='TIME INTEGRAL'/
&DEVC XB=4.3000,6.7000,0.0200,0.0200,-0.1000,-0.1000,POINTS=31,ORIENTATION=-
1,0,0,ID='RT y:0.02 z:-0.10',QUANTITY='GAUGE HEAT FLUX
GAS',STATISTICS_START=0,TEMPORAL_STATISTIC='TIME INTEGRAL'/
&DEVC XB=4.3000,6.7000,0.0200,0.0200,-0.0200,-0.0200,POINTS=31,ORIENTATION=-
1,0,0,ID='RT y:0.02 z:-0.02',QUANTITY='GAUGE HEAT FLUX
GAS',STATISTICS_START=0,TEMPORAL_STATISTIC='TIME INTEGRAL'/
&DEVC XB=4.3000,6.7000,0.0200,0.0200,0.0200,0.0200,POINTS=31,ORIENTATION=-1,0,0,ID='RT
y:0.02 z:0.02',QUANTITY='GAUGE HEAT FLUX
GAS',STATISTICS_START=0,TEMPORAL_STATISTIC='TIME INTEGRAL'/
&DEVC XB=4.3000,6.7000,0.0200,0.0200,0.1000,0.1000,POINTS=31,ORIENTATION=-1,0,0,ID='RT
y:0.02 z:0.10',QUANTITY='GAUGE HEAT FLUX
GAS',STATISTICS_START=0,TEMPORAL_STATISTIC='TIME INTEGRAL'/
```

```
&DEVC XB=4.3000,6.7000,0.0200,0.0200,0.1800,0.1800,POINTS=31,ORIENTATION=-1,0,0,ID='RT
y:0.02 z:0.18',QUANTITY='GAUGE HEAT FLUX
GAS',STATISTICS_START=0,TEMPORAL_STATISTIC='TIME INTEGRAL'/
&DEVC XB=4.3000,6.7000,0.1000,0.1000,-0.1800,-0.1800,POINTS=31,ORIENTATION=-
1,0,0,ID='RT y:0.10 z:-0.18',QUANTITY='GAUGE HEAT FLUX
GAS',STATISTICS_START=0,TEMPORAL_STATISTIC='TIME INTEGRAL'/
&DEVC XB=4.3000,6.7000,0.1000,0.1000,-0.1000,-0.1000,POINTS=31,ORIENTATION=-
1,0,0,ID='RT y:0.10 z:-0.10',QUANTITY='GAUGE HEAT FLUX
GAS',STATISTICS_START=0,TEMPORAL_STATISTIC='TIME INTEGRAL'/
&DEVC XB=4.3000,6.7000,0.1000,0.1000,-0.0200,-0.0200,POINTS=31,ORIENTATION=-
1,0,0,ID='RT y:0.10 z:-0.02',QUANTITY='GAUGE HEAT FLUX
GAS',STATISTICS_START=0,TEMPORAL_STATISTIC='TIME INTEGRAL'/
&DEVC XB=4.3000,6.7000,0.1000,0.1000,0.0200,0.0200,POINTS=31,ORIENTATION=-1,0,0,ID='RT
y:0.10 z:0.02',QUANTITY='GAUGE HEAT FLUX
GAS',STATISTICS_START=0,TEMPORAL_STATISTIC='TIME INTEGRAL'/
&DEVC XB=4.3000,6.7000,0.1000,0.1000,0.1000,0.1000,POINTS=31,ORIENTATION=-1,0,0,ID='RT
y:0.10 z:0.10',QUANTITY='GAUGE HEAT FLUX
GAS',STATISTICS_START=0,TEMPORAL_STATISTIC='TIME INTEGRAL'/
&DEVC XB=4.3000,6.7000,0.1000,0.1000,0.1800,0.1800,POINTS=31,ORIENTATION=-1,0,0,ID='RT
y:0.10 z:0.18',QUANTITY='GAUGE HEAT FLUX
GAS',STATISTICS_START=0,TEMPORAL_STATISTIC='TIME INTEGRAL'/
&DEVC XB=4.3000,6.7000,0.1800,0.1800,-0.1800,-0.1800,POINTS=31,ORIENTATION=-
1,0,0,ID='RT y:0.18 z:-0.18',QUANTITY='GAUGE HEAT FLUX
GAS',STATISTICS_START=0,TEMPORAL_STATISTIC='TIME INTEGRAL'/
&DEVC XB=4.3000,6.7000,0.1800,0.1800,-0.1000,-0.1000,POINTS=31,ORIENTATION=-
1,0,0,ID='RT y:0.18 z:-0.10',QUANTITY='GAUGE HEAT FLUX
GAS',STATISTICS_START=0,TEMPORAL_STATISTIC='TIME INTEGRAL'/
&DEVC XB=4.3000,6.7000,0.1800,0.1800,-0.0200,-0.0200,POINTS=31,ORIENTATION=-
1,0,0,ID='RT y:0.18 z:-0.02',QUANTITY='GAUGE HEAT FLUX
GAS',STATISTICS_START=0,TEMPORAL_STATISTIC='TIME INTEGRAL'/
&DEVC XB=4.3000,6.7000,0.1800,0.1800,0.0200,0.0200,POINTS=31,ORIENTATION=-1,0,0,ID='RT
y:0.18 z:0.02',QUANTITY='GAUGE HEAT FLUX
GAS',STATISTICS_START=0,TEMPORAL_STATISTIC='TIME INTEGRAL'/
&DEVC XB=4.3000,6.7000,0.1800,0.1800,0.1000,0.1000,POINTS=31,ORIENTATION=-1,0,0,ID='RT
y:0.18 z:0.10',QUANTITY='GAUGE HEAT FLUX
GAS',STATISTICS_START=0,TEMPORAL_STATISTIC='TIME INTEGRAL'/
&DEVC XB=4.3000,6.7000,0.1800,0.1800,0.1800,0.1800,POINTS=31,ORIENTATION=-1,0,0,ID='RT
y:0.18 z:0.18',QUANTITY='GAUGE HEAT FLUX
GAS',STATISTICS_START=0,TEMPORAL_STATISTIC='TIME INTEGRAL'/


&TAIL /
```

D
SANDIA PARTICLE TESTING

This appendix contains a summary of the scaled aluminum and copper 3-phase alternating current arc testing that was conducted at Sandia National Laboratories.

D.1 Summary of Testing Approach and Parameters

D.1.1 Experimental Aims for Scaled Arc Testing and Outputs

In August 2021, three phase arc experiments were conducted with the purpose of providing inputs for FDS modeling of aluminum and copper bus bar effects on high energy arc fault (HEAF) incident energy. The purpose of these tests was to provide input regarding HEAF-evolved metal particle characteristics, including particle size, degree of oxidation, and percentage of bus bar metal melted and vaporized. These tests were designed to be scaled (similar current density) three phase arcs based on a series of full scale open box electrical arc tests performed in August and September of 2019. The purpose of those prior tests was to 1) generate data to support model development and refinement, 2) evaluate existing models' ability to predict material loss and arc voltages and 3) deploy sensors to evaluate the impact of non-thermal hazards. The tests were performed at DNV GL KEMA Powertest facility located in Chalfont, PA. The tests were supported by a team of testing and measurement experts from the National Institute of Standards and Technology (NIST) and Sandia National Laboratories (SNL). In the open box experiments, input electrical energy and evolved thermal energy were characterized but particle capture was not conducted.

In these prior open box HEAF tests, for the same electrical input energy, the measured evolved thermal energy measured on plate calorimeters appeared to differ between aluminum and copper bus bars of the same dimension (1.3 – 2.5 cm diameter bus bars). This effect was most notable for higher currents (over 15 kA) and current densities (over 30 A/mm²) as shown in Figure D-1.

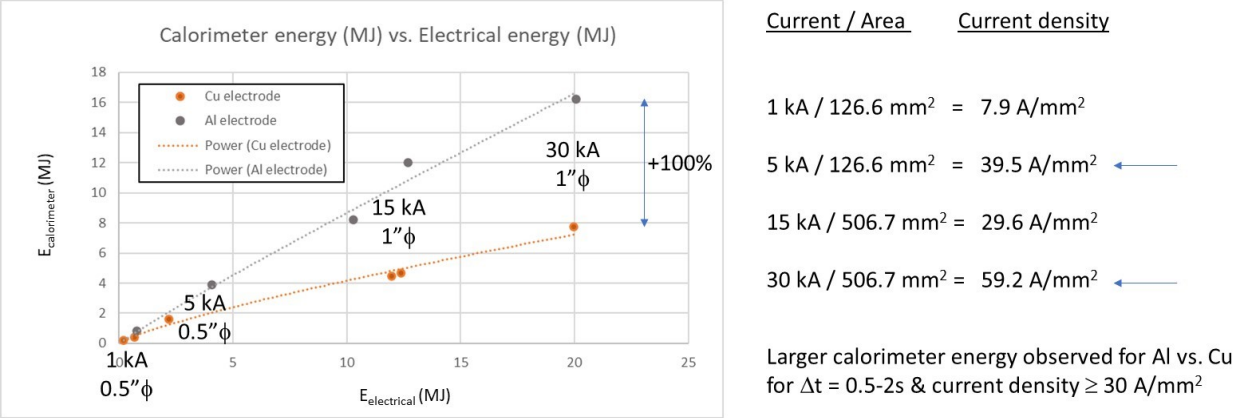

Figure D-1
Summary of open box calorimeter energy vs. electrical energy for 1-30 kA, 0.5 inch and 1 inch diameter copper and aluminum bus bars

Since particle capture was not conducted for these tests, the aim of the present scaled HEAF experiments was to provide inputs for FDS arc fault modeling at 60 A/mm² current density for 1 mm × 1 mm electrodes.

- Particular details were requested by modeling experts to guide appropriate FDS modeling, including:
- What particle drop size distribution should be applied?
- What fraction of bus bars is initially vapor?
- To calculate potential added energy due to metal combustion, what is the initial vapor mass fraction, droplet size distribution, and observed droplet oxidation?

The scaled experiments were designed to measure differences in behavior between scaled size copper and aluminum electrodes of equivalent current density (60 A/mm²) to the prior open box high energy arc fault testing and quantification of:

- Heat rise, ΔT
- Particle size distribution
- Oxidation degree
- Bus bar mass percent melted, and maximum mass percent vaporized
- Voltage/current/arc resistance

D.1.2 Scaled Arc Fault Experimental Approach

Analysis of three-phase AC arcing was conducted using a Pacific Power Model M2288 AC source, shown in Figure D-2, at a voltage of 600 V, current of 60 – 100 A and conducted for 0.1 – 2 s duration, until the bus bar electrodes were fully consumed, or the AC arc extinguished. For these experiments, 1 mm × 1mm × 10 cm length aluminum and copper rods were used to achieve high current densities of 60-100 A/mm², for comparison to similar current density (29.6 – 59.2 A/mm²), previous 5 – 30 kA open box HEAF test data using full scale aluminum and copper bus bars.

Figure D-2
Pacific Power 3-phase continuous AC power source for scaled arc testing

Based on prior open box testing, three phase arcs were observed to be sustained at AC voltage of 600 V and above. The aims of this experiment were to strike and sustain stable three phase arcs within a closed copper cylinder calorimeter volume for 0.1 – 2 s durations, and to measure the voltage, current, and temperature rise (to enable calorimetry) of copper and aluminum scaled bus bars of the same dimension (see Figure D-3, Figure D-4, and Figure D-5).

The mass of the copper cylinder was measured, and the steady state post-arc temperature rise of the cylinder were measured using calibrated thermocouples to measure temperature rise ΔT and enable quantification of evolved thermal energy. To quantify the possible mass of bus bars vaporized, the masses of the bus bars were measured before experiments, and masses of remaining post-arc bus bars and collected macroscopic (0.1 – 3 mm diameter) evolved droplets were measured.

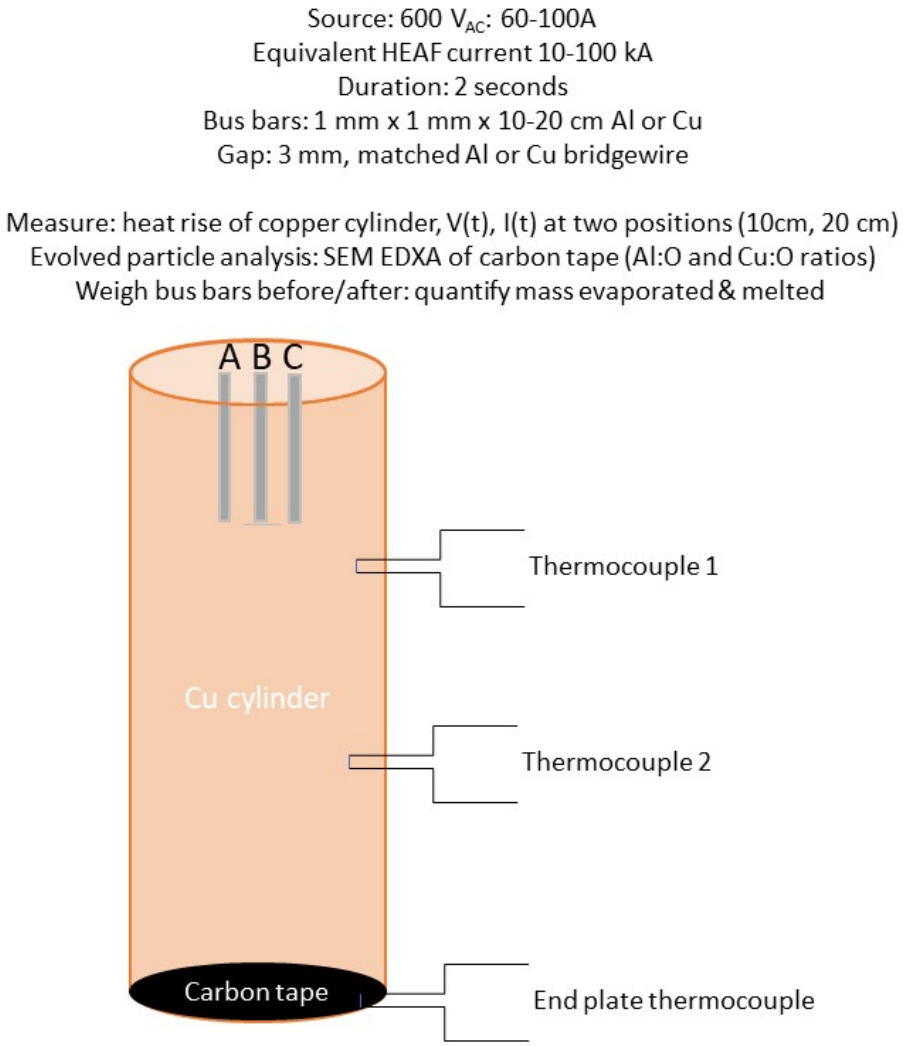

Figure D-3
Schematic of scaled test method

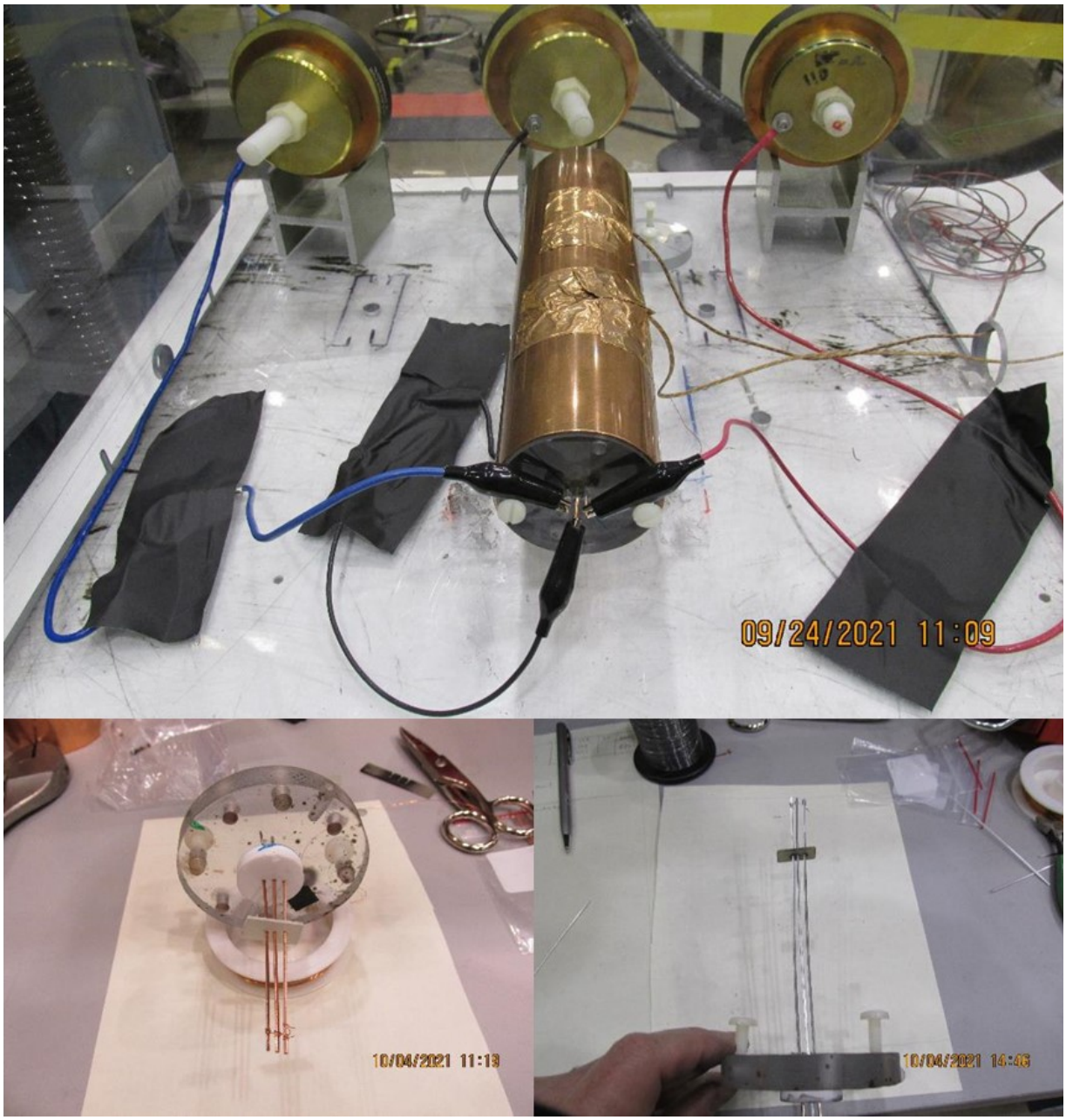

Figure D-4
Images of copper calorimeter enclosure and scaled three-phase bus bars

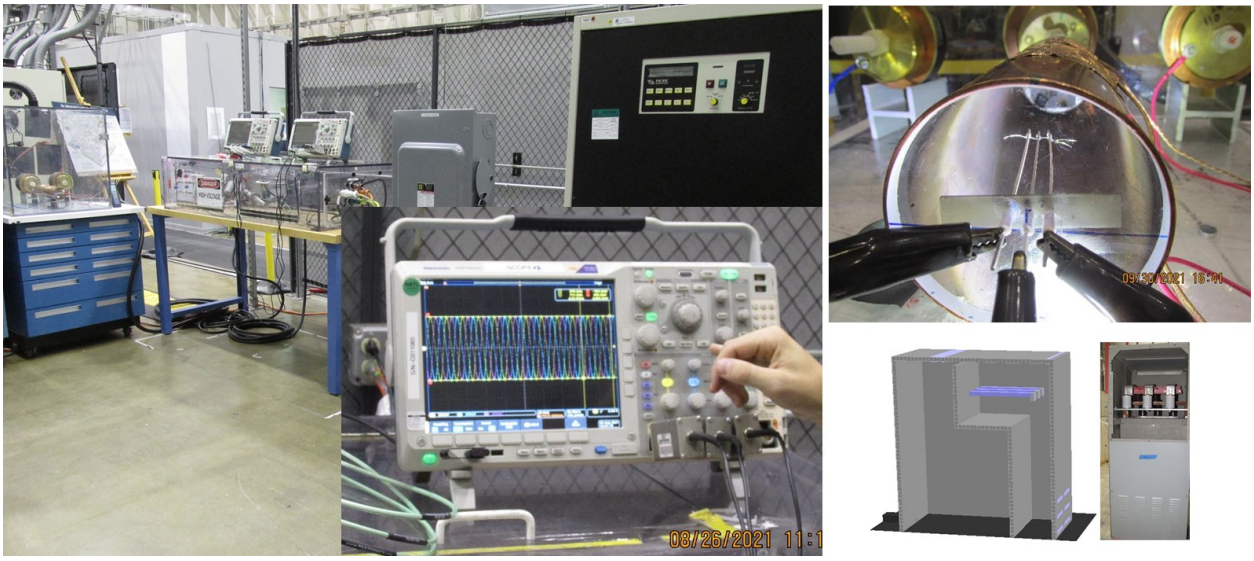

Figure D-5
Oscilloscope collection of three-phase voltage and current (left), internal view of scaled three phase copper and aluminum bus bars within copper calorimeter (upper right) and schematic of commercial three phase switchgear bus bar configuration (lower right)

D.1.3 Particle Capture and Analysis Method

To collect arc-generated particles for analysis of particle size, composition and state of oxidation, strips of carbon tape attached to scanning electron microscope mounting stubs were mounted on the opposite end of the calorimeter from the scaled bus bars and utilized as particle collectors. The carbon tape coated stubs faced the end of the three parallel electrodes. This enabled collection of airborne molten and/or vaporized particles with minimal change in collected particle morphology and strong chemical contrast between the collected particles and the carbon mounting tape.

Evolved airborne particles (all below 0.1 mm) from the three phase arcs were collected and analyzed using scanning electron microscopy (SEM) for particle size and SEM energy dispersive spectroscopy (SEM EDS) to analyze copper to oxygen ratio and aluminum to oxygen ratio to evaluate degree of evolved particle oxidation. Hitachi Galileo and FEI Magellan electron microscopes with 2 nanometer resolution were used to determine particle sizes of evolved particles, analyze surface morphology to determine their origin (melted or vaporized), and analyze the chemical composition via EDS at 5 kV acceleration voltage.

High-magnification analysis using SEM enables the physical and chemical characterization of evolved particle sizes, geometries, and chemical composition (see Figure D-6). Energy dispersive X-ray analysis enables specific identification of particle composition (e.g., aluminum, copper, or specific alloys) as well as degree of particle oxidation (ratio of aluminum to oxygen X-ray intensity, normalized to an Al2O3 or CuO standard). This assists determination whether evolved particles are simply resolidified molten droplets of metallic copper or aluminum, or have exothermically oxidized, a potential source of added energy during arc flash.

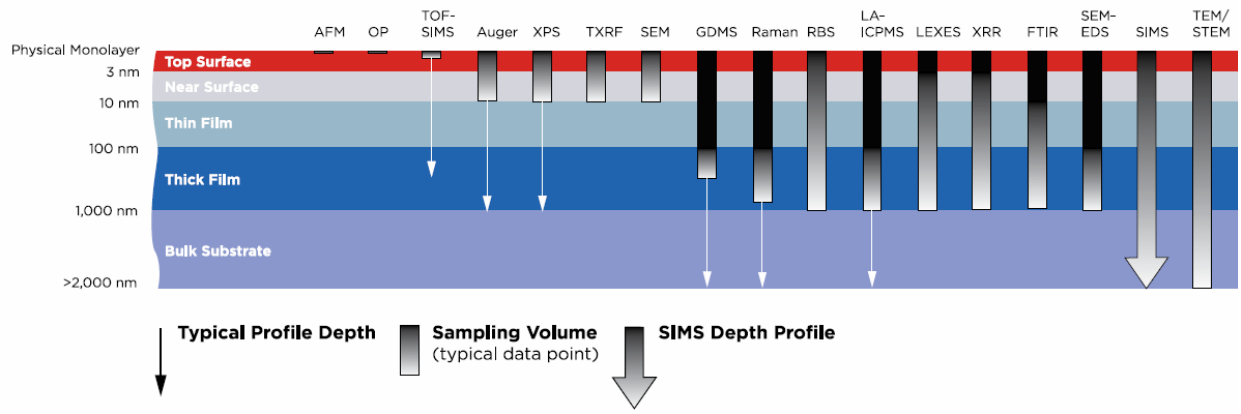

Figure D-6
Typical analytical depth range based on technique

D.2 Scaled Three-Phase Arc Fault Experimental Results

D.2.1 Aluminum and Copper 1 to 2 s Arcs: 600 VAC, 3 Phase, 100 A/mm²

During the arc experiments, the three phase AC voltage and current were measured using calibrated Tektronix P6015 voltage monitors and Pearson 110 current voltage transformers (CVTs). Bus bars were shorted together using a thin 10 mil diameter wire of the same composition metal (copper or aluminum) as the bus bars, and voltage was applied using the Pacific Power source, as shown in Figure D-7 to initiate three phase arcs. A sustained arc is indicated by both continuous voltage and current on all three phases. Arc duration was measured as the time during which all three phases conducted current; sustained arc durations ranged from 0.11 s to 1.49 s.

Figure D-7 illustrates a stable three phase arc which had a duration of 858 ms before extinguishing. Aluminum bus bars typically extinguished when the full exposed length was consumed; copper bus bars melted roughly three times slower, consistent with the threefold higher density and volumetric heat capacity of copper.

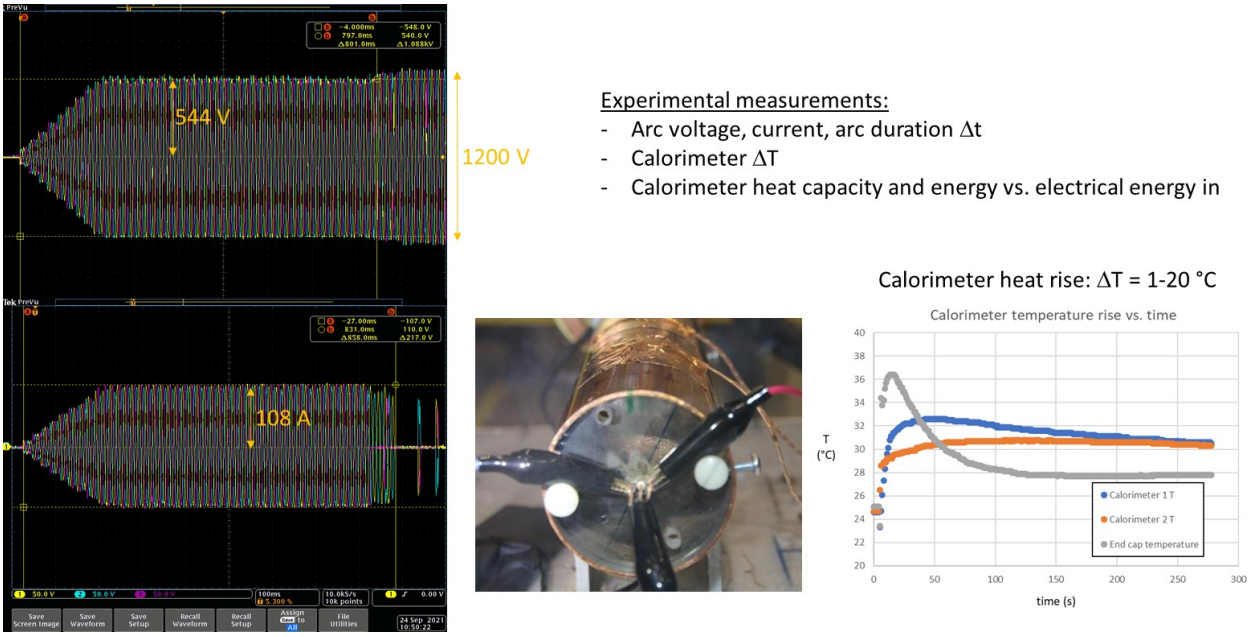

Figure D-7
A three phase, 544 VAC, 858 ms duration arc shown on oscilloscope produced a sustained 108 A arc current on all phases (left), image of three phase electrical connections (center) and measured heat rise versus time for calorimeter thermocouples (blue and orange traces) and at end cap (gray). The temperature rise ΔT is taken as the average of the blue and orange temperatures

Following testing, post-arc analysis was conducted, including both calorimeter thermal analysis and mass analysis of the bus bar and evolved materials. Characteristics of typical aluminum and copper mass analysis are shown below in Figure D-8. As discussed above, bus bars were measured individually prior to experiments as well as afterward. Additionally, all free evolved particles from within the calorimeter were collected and weighed; these were primarily large millimeter-scale droplets below the original bus bar locations. Remaining “missing” bus bar mass consisted of fine under 100 micron size particles which appeared to have vaporized and condensed on the calorimeter walls and carbon tape collector.

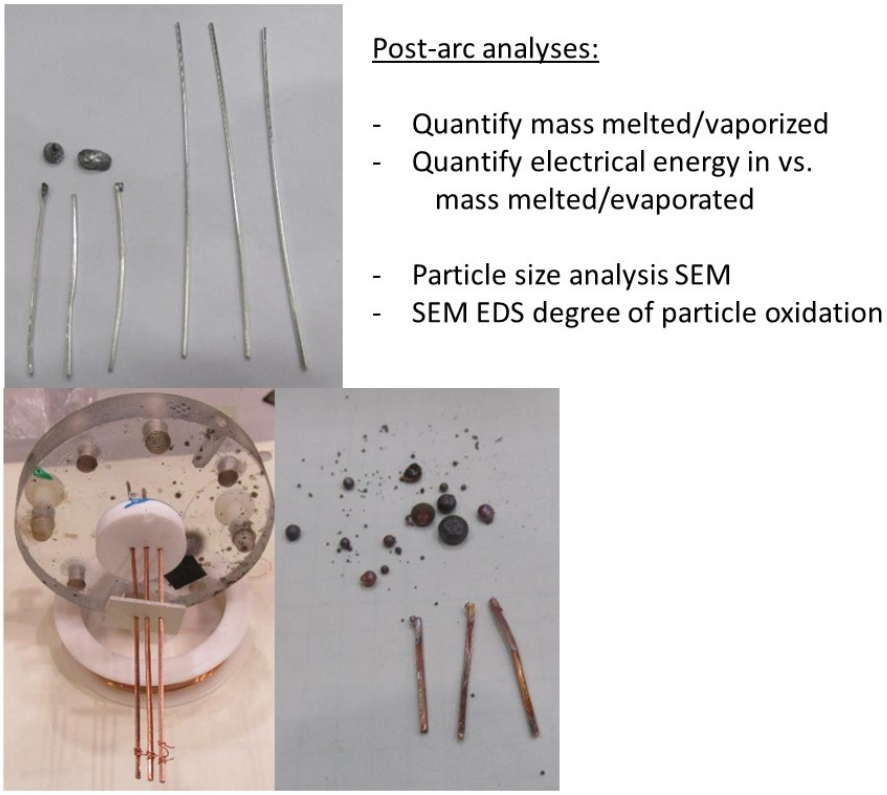

Figure D-8
Images of scaled aluminum bus bar before and after sustained three phase arc, including collected molten particles (top); copper bus bar samples before (bottom left) and after a sustained arc, including collected droplets (bottom right)

D.2.2 Heat Rise versus Arc Duration for Aluminum and Copper

As noted above, two calorimeters were mounted on the copper calorimeter chamber in which the arc experiments were conducted and used to measure the copper temperature rise ΔT as well as a measurement of calorimetric energy deposited in the copper as a function of arc duration and electrode type. The calorimeter ends were capped with 1 cm thick plexiglass, containing the heated air inside the chamber, and the calorimeter was supported on thermally insulating fiberglass supports. The temperature rise of the calibrated K-type thermocouples was measured as a function of time by a calibrated Omega measurement unit, with an uncertainty of 0.2°C. The temperature rise ΔT was taken as the peak of the average temperature of the two thermocouples, which were located at 1/3 and 2/3 of the length of the copper cylinder. The thermocouple nearest the arc location initially read higher but equilibrated with the second thermocouple, as shown in Figure D-7; the calorimeter temperature remained within 1 degree of this average for over 5 minutes.

The peak temperature rise values for all experiments were calculated and are plotted in Figure D-9. Among the observations in the experiments were:

1) Heat rise was generally larger for aluminum than copper for the same electrical input and duration.

2) Aluminum electrodes achieved full melting (7.6 – 15 cm) much earlier in time than copper electrodes.

As noted, the volumetric heat capacity of aluminum (2.42 J/(cm³·K)) is lower than copper (3.45 J/(cm³·K)), and the resistivity and expected Joule heating effect larger, consistent with a greater linear consumption for the same cross section electrodes.

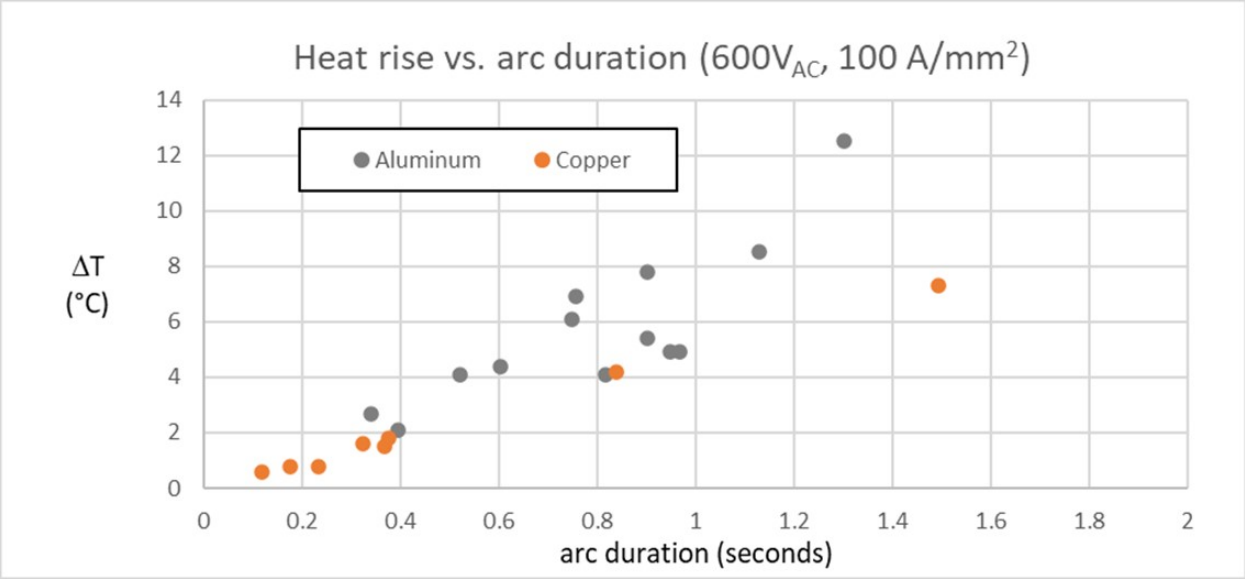

Figure D-9
Summary of measured temperature rise ΔT versus arc duration for all aluminum and copper arc experiments

D.2.3 Heat Rise versus Arc Duration for Aluminum and Copper

The above copper calorimeter heat rise data was combined with the mass and heat capacity of the copper calorimeter to establish the calorimeter energy increase in Joules. The electrical energy input using the RMS AC voltage and current, and time duration was used to calculate the electrical energy input, and these are plotted in Figure D-10.

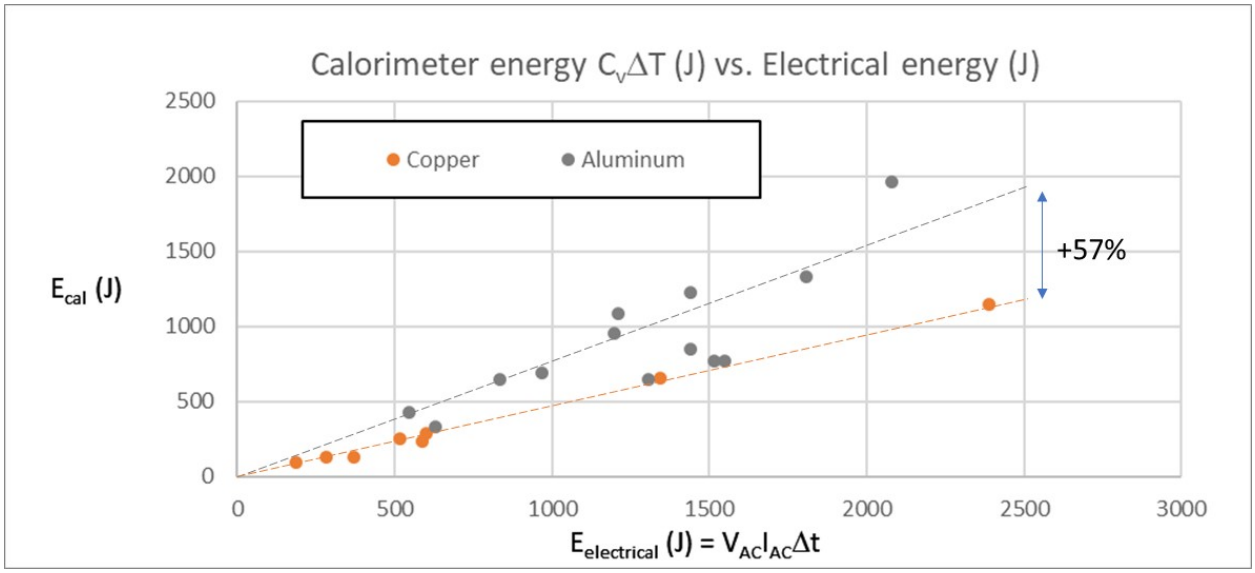

Figure D-10
Calculated calorimeter heat rise plotted vs. electrical energy input

For the collected arc experiments, observations included that the calorimeter energy was generally larger for aluminum than copper for the same electrical input and duration. A linear curve fit to the data suggests an average 57% increase in calorimeter energy increase for the same dimension and electrical energy input aluminum electrodes vs. copper electrodes.

D.2.4 Analysis of Mass Percent Melted versus Potential Vaporized

For FDS modeling, key input questions included estimation of the percentage of bus bar that should be treated as melted and vaporized for calculations. Mass analysis of pre- and post-arc samples was used to calculate the percent of mass melted (mass of remaining bus bar and mass of collected macroscopic particles, shown in Figure D-11 center). An estimation of the maximum percent of vaporized material was calculated by subtracting the remaining post-arc bus mass and collected particle mass from the mass of the bus bars and initiating shorting wire prior to each arc experiment. A fine powdered debris condensed with vaporized material collected on the walls of the calorimeter and carbon tape collector and is described below in Section D.2.5. The results showing percent melted and maximum percent vaporized are shown in Figure D-11.

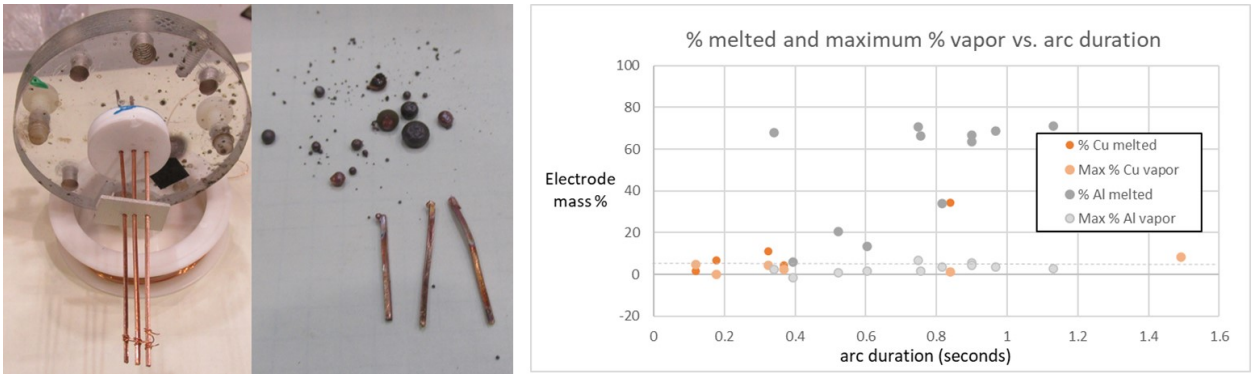

Figure D-11
Image of pre-arc copper bus bar and shorting wire (left), representative collection of post-arc bus bars and collected spherical particles (center) and tabulation of % metal melted and maximum % vaporized particles (right)

Arcs typically extinguished when reaching the white ceramic insulator sample holder shown at left in Figure D-11, limiting the percent melted to that percent of length beyond the insulator. As shown above, aluminum bus bars often completely consumed the full available length, while copper percent consumed showed a more linear time dependence. Observations from the data above included:

1) Aluminum electrodes achieve full melting (7.6 to15 cm) much earlier in time than copper electrodes.
2) For longer duration arcs, up to 60 to 80% of electrode length was melted and recovered as large 0.1 mm or larger diameter spheres consistent with melted and resolidified metal.
3) In most cases, less than 5% of electrode material was not recovered either as remaining bus bars or large 0.1 to 5 mm solidified molten spheres; this supported setting a bound that 3.5% metal is vaporized (Cu: 2.6%, Al 3.5%).

D.2.5 Differences between Aluminum and Copper Melt Rates

The differences in aluminum and copper melting behavior (Figure D-12) were considered in light of two possible explanations for the much greater percentage of aluminum melted versus time.

1) Aluminum density is three times lower than copper, the aluminum melting point is much lower (660°C versus 1,085°C) and volumetric heat capacity is 42% lower than that of copper; these are consistent with a significantly higher aluminum volume loss than copper for the same arc duration.
2) Using the Preece equation to predict wire fusing currents suggests that fusing current densities for aluminum are lower than copper (Preece equation: $I_{\text{fusing}} = Ad^{1.5}$; where $A_{\text{Al}} = 59$ and $A_{\text{Cu}} = 80$ for d in mm):
    - Aluminum fusing current density: 46.6 A/mm²
    - Copper fusing current density: 62.8 A/mm²

In certain current density regimes (46 – 63 A/mm²), melting of aluminum would be expected when it would not for copper.

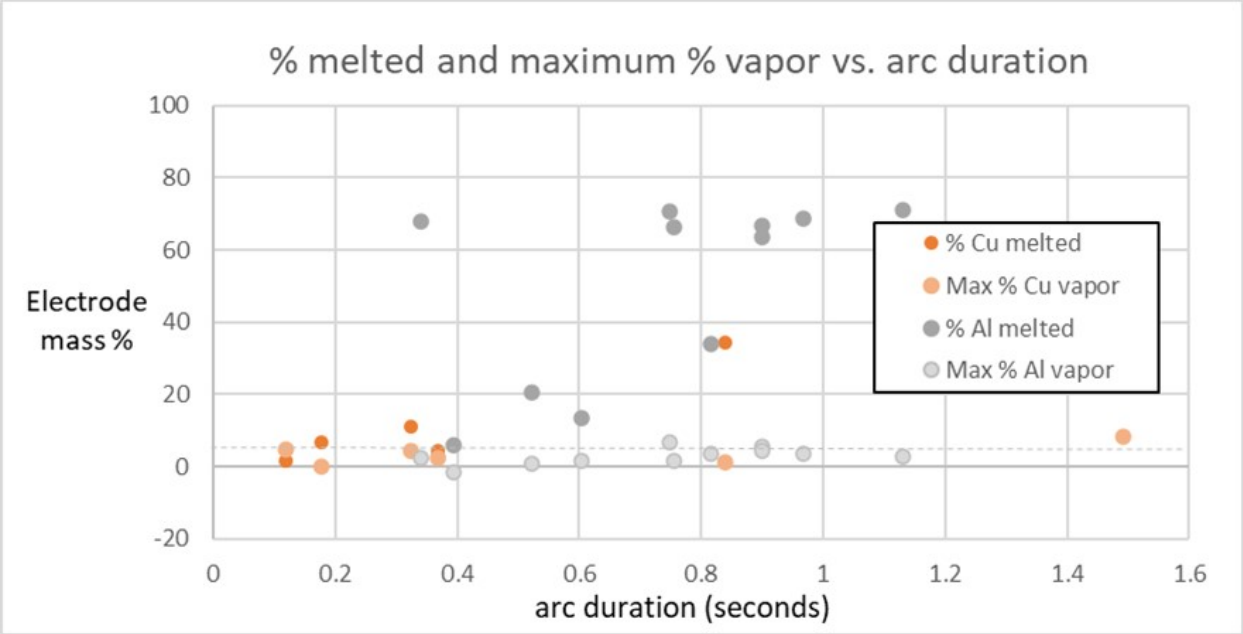

Figure D-12
Plot of percent melted and maximum percent metal vaporized versus arc duration

D.3 Evolved Particle Oxidation Analysis

D.3.1 Electron Microscope Analysis of Evolved Aluminum Particles

As described above, particles were collected on carbon tape from the back end of the calorimeter and characterized via scanning electron microscopy and EDS analysis using Hitachi Galileo and FEI Magellan electron microscopes. A fully oxidized standard of aluminum oxide ceramic was utilized for calculation of the degree of oxidation from the oxygen to aluminum EDS peak ratios.

Evolved particles from the Pacific Power three-phase 600 VAC testing of aluminum scaled bus bars again demonstrated particle sizes of 2.4 – 28 microns in size. From an SEM analysis of 50 particles, average particle size was 8.96 microns and average particle volume was 880 mm^3, as shown below in Figure D-13 through Figure D-16.

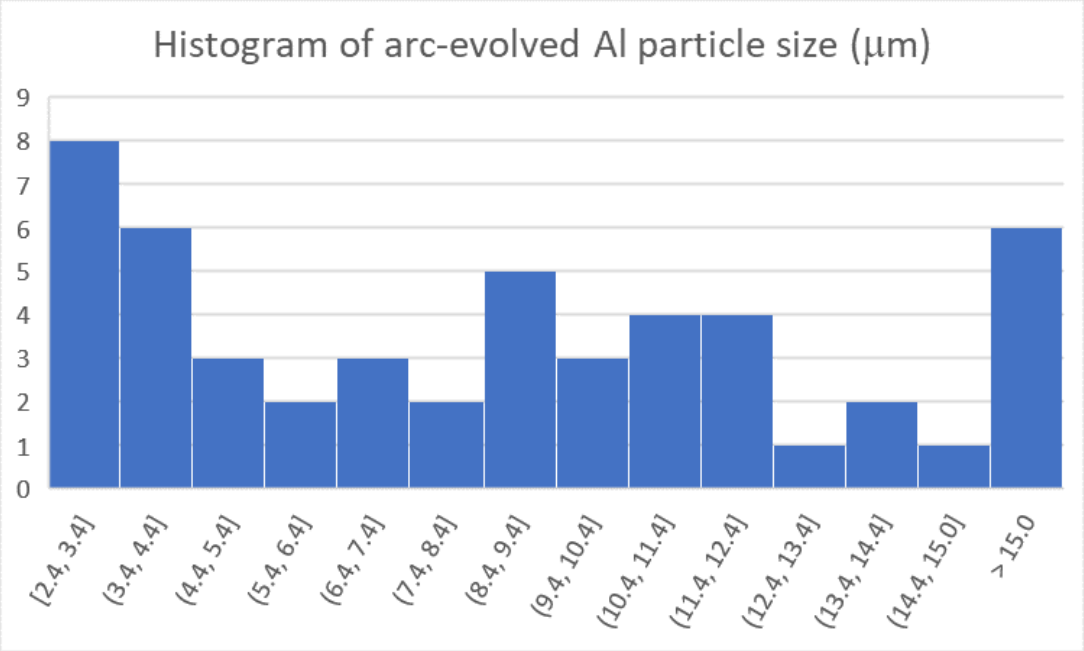

Figure D-13
Histogram of size in microns of 50 aluminum bus bar-evolved particles; the average particle size of these evolved aluminum particles was 8.96 microns

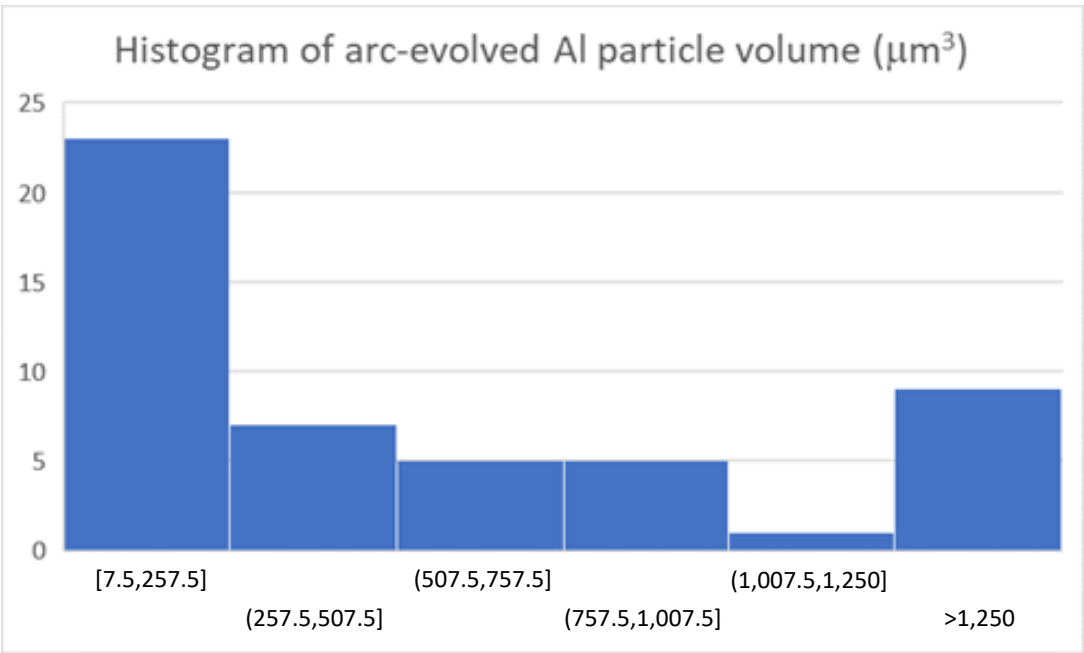

Figure D-14
Histogram of volume in cubic microns of 50 aluminum bus bar-evolved particles; the average particle volume calculated for evolved aluminum particles was 880 cubic microns

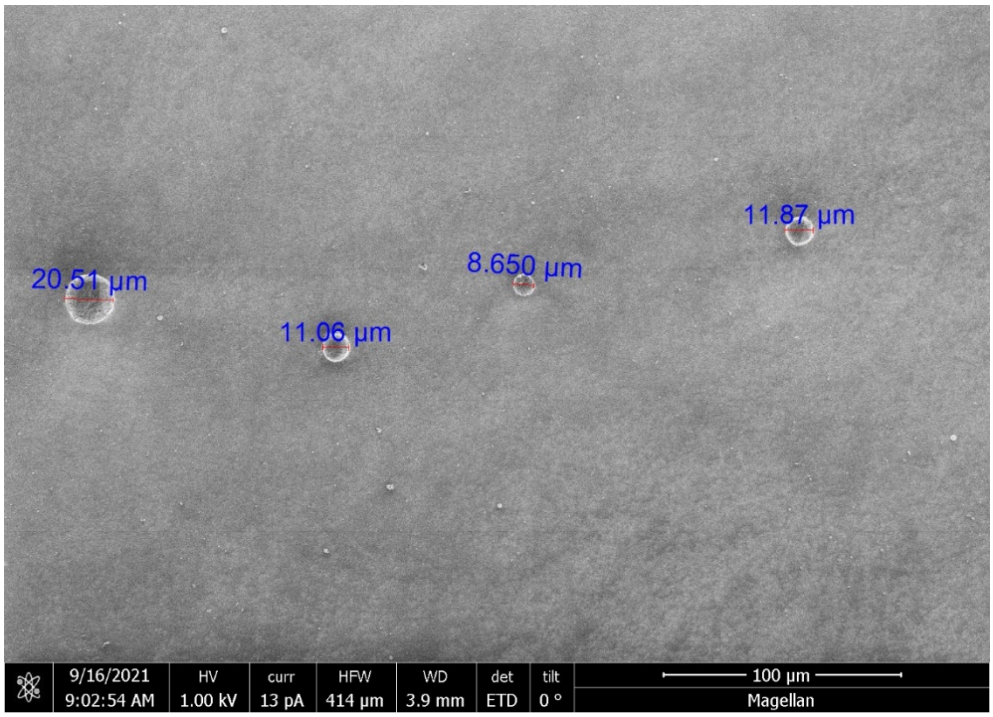

Figure D-15
Representative SEM image and size measurements of aluminum bus bar-evolved particles; the average particle size for these evolved aluminum particles was 8.96 microns

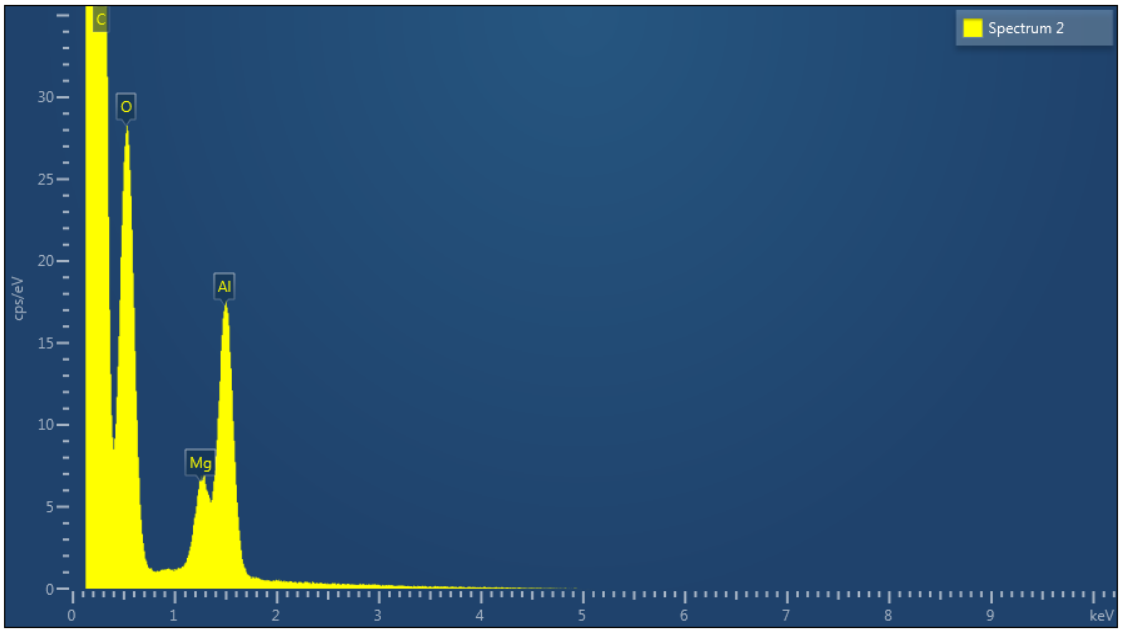

Figure D-16
Representative EDS analysis of a three-phase arc-evolved aluminum particle; from the peak ratios of aluminum, magnesium, and oxygen, an estimated degree of oxidation of 73% was calculated

D.3.2 Electron Microscope Analysis of Evolved Copper Particles

Analysis of 3 phase AC arc-evolved particles was conducted on particles collected from 600 V arcs of 0.5 second to 2 second duration between 1 mm² cross section copper bus bars. Image analysis was conducted on 50 particles to provide a statistical distribution of particle sizes and volumes, and EDS was conducted to quantify oxygen to copper ratio.

Compared to the prior aluminum particle size analysis, the copper particles displayed a broad particle size distribution and were notably finer, with a median particle size of 0.225 microns and median particle volume of 0.056 mm³ (median volume radius ~0.383 mm, since the volume average is biased toward larger particles). Examples of the particle size distribution and shape are shown in Figure D-17, and a histogram of particle sizes are shown in Figure D-18.

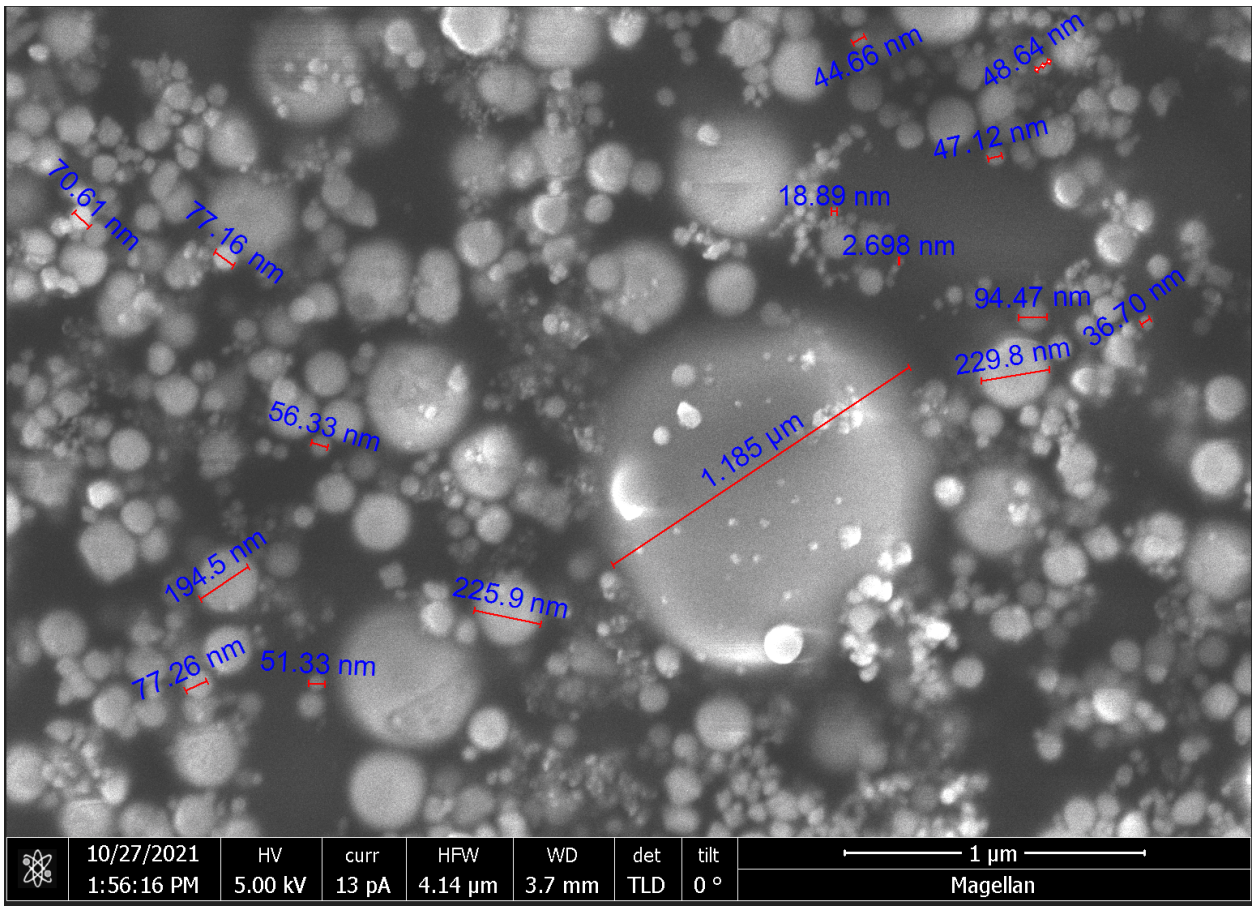

Figure D-17
SEM of 600 VAC arc-evolved, 0.02 – 1.2 micron copper particles

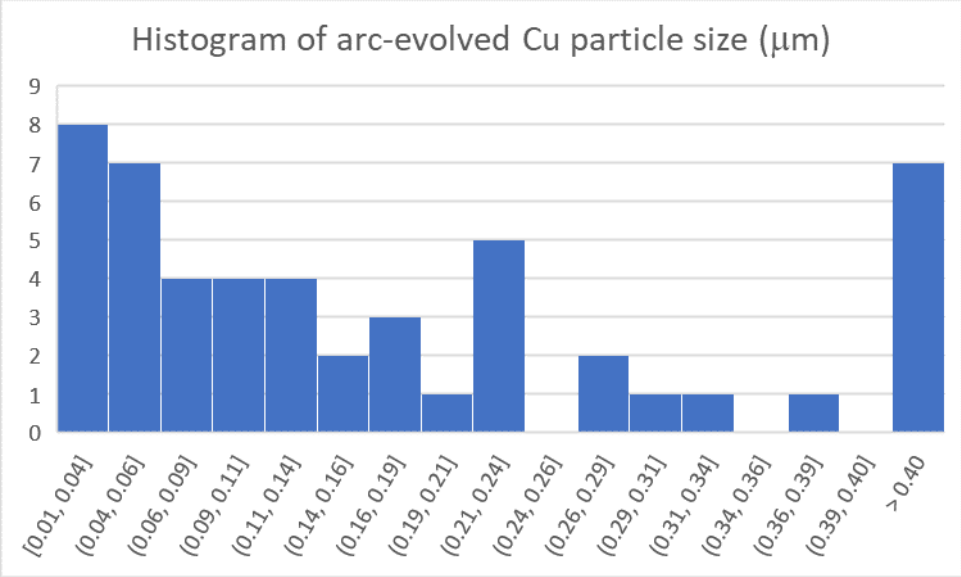

Figure D-18
Histogram of particle sizes of 50 particles evolved from 600 VAC arcs, displaying a median particle size of 0.225 microns and median particle volume of 0.056 mm³

Energy dispersive spectroscopy was conducted on these collected particles. The majority of particles indicated an oxygen to copper ratios of 13 – 28%, with one outlier particle with a 51% degree of oxidation, shown in Figure D-19 and Figure D-20.

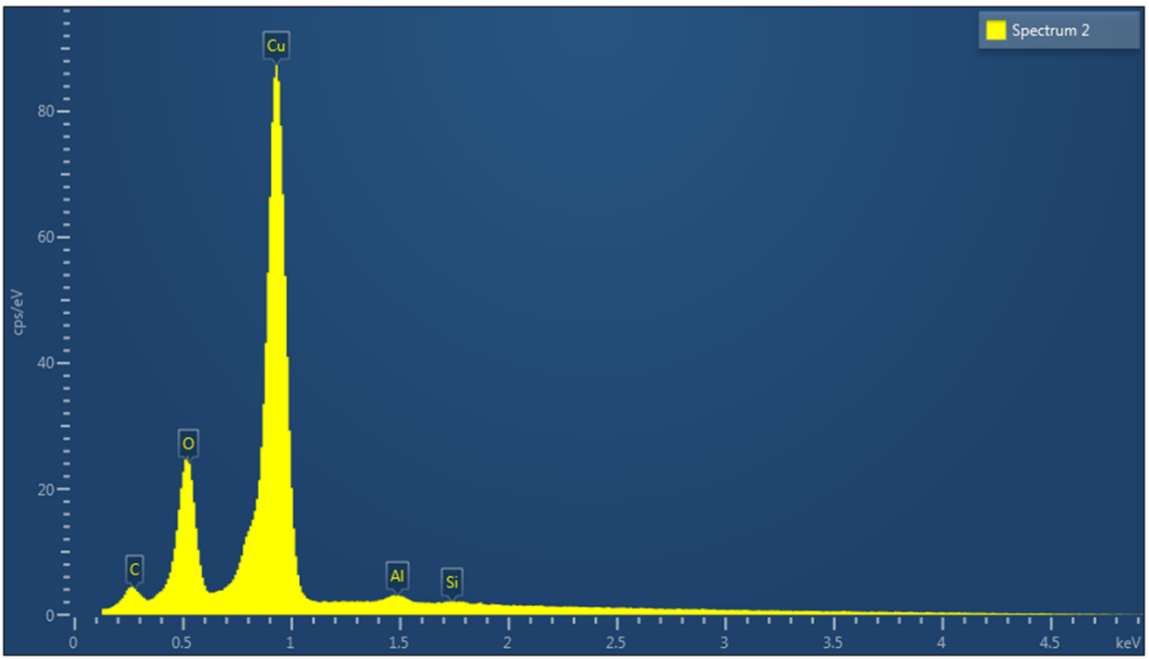

Figure D-19
EDS spectrum of 600 VAC arc-evolved, 0.02-2 micron copper particles, displaying oxygen and copper peaks, with an oxygen to copper ratio of 0.28

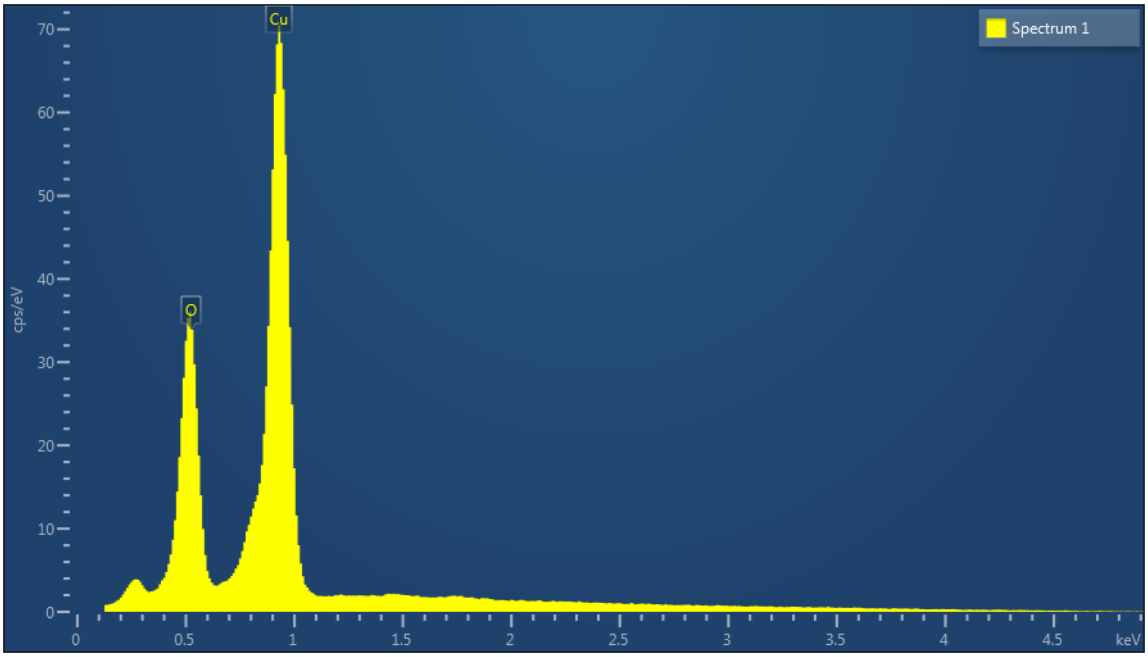

Figure D-20
EDS spectrum of 600 VAC arc-evolved, 0.02 – 2 micron copper particles, displaying oxygen and copper peaks, with an oxygen to copper ratio of 0.51

D.3.3 Summary of Particle Collection Data for FDS Modeling Input

FDS modeling questions posed from the working group included:

- Working group question 1: Is it important to track droplets from the melting enclosure and allow them to combust? What drop size distribution should be applied and does that distribution change over metal type?
- Working group question 2: what fraction is initially vapor and the time dependent functional form?
- FDS modeling limitations note: The added energy due to metal combustion is based on many unverified assumptions (initial vapor mass fraction 10%, droplet size distribution, droplet initial temperature, arc radiant fraction, and others).

Experimental results as input for FDS modeling:

- Calorimeter energy output for aluminum appeared larger than for copper.
    - Small copper data set: linear curve fit shows 57% more energy from vaporized aluminum than vaporized copper.
- Aluminum median droplet size was 9 micons, and median volume 880 micons^3.
- Copper droplet size displayed a broad range of particle sizes, with a median particle size of 0.225 microns and median particle volume of 0.056 microns^3.
- Vapor mass fraction was less than 5% (copper: 2.6%, aluminum 3.5%).
- Estimated upper limit of evolved particle droplet oxidation were aluminum 73%, and copper 51%.